ROBIN DAVIDSON-ARNOTT

Nilanjana Ray
Department of Geography (Faculty),
Vidyasagar Metropolitan College,
University of Calcutta

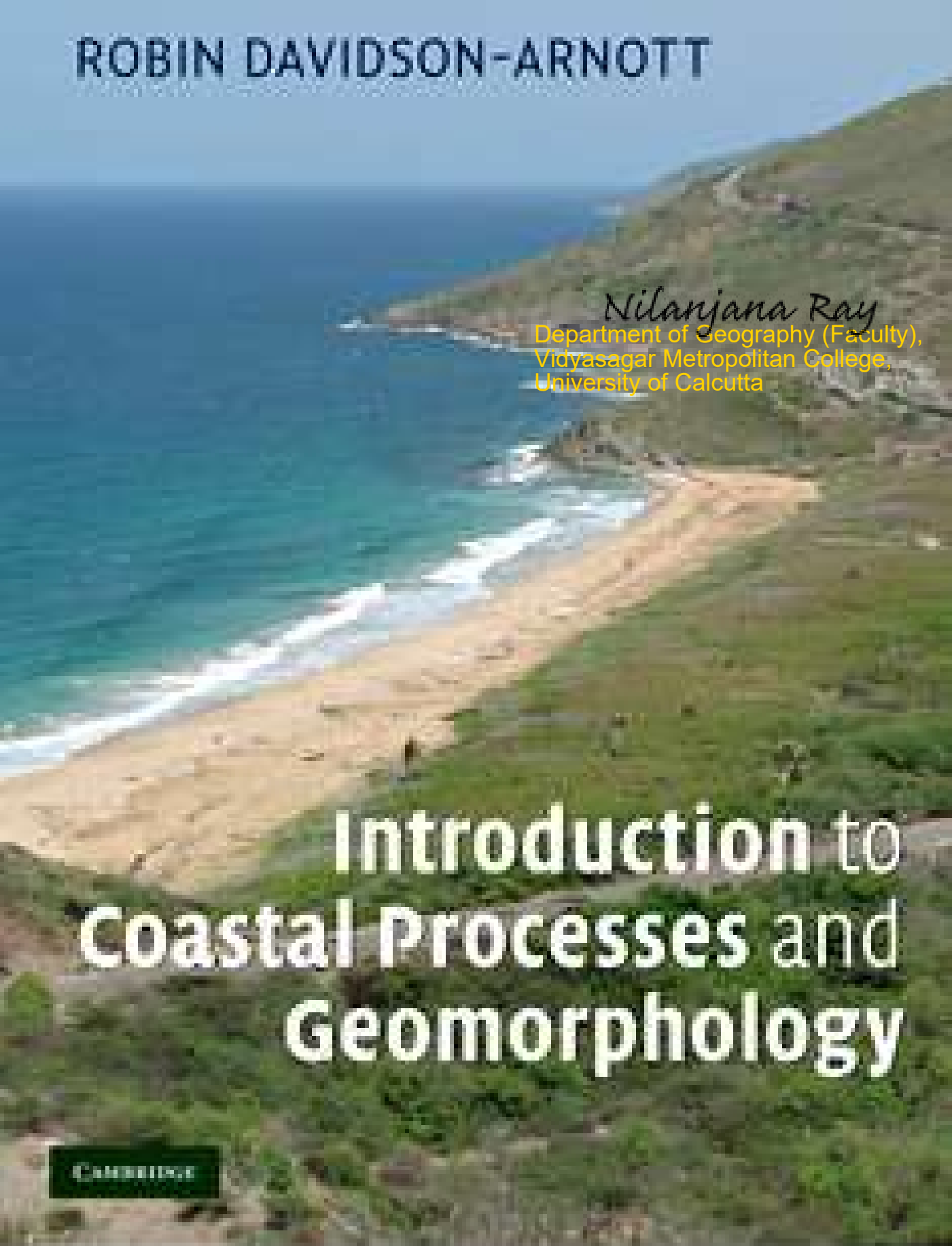

Introduction to Coastal Processes and Geomorphology

CAMBRIDGE

CAMBRIDGE www.cambridge.org/9780521874458

This page intentionally left blank

Introduction to Coastal Processes and Geomorphology

Written for undergraduate students studying coastal geomorphology, this is the complete guide to the processes at work on our coastlines and the features that we see in coastal systems across the world. Accessible to students from a range of disciplines, the quantitative approach helps to build a solid understanding of wave and current processes that shape coastlines globally. The resulting processes of erosion, transport and deposition and the features they create are clearly explained, with a strong illustration and photo programme. From sandy beaches to coral reefs, the major coastal features are related to contemporary processes and to sea-level changes over the past 25 000 years. Key equations that describe or predict measurements from the instruments used to map these processes are all presented in this wide-ranging overview. Robin Davidson-Arnott completes the teaching package with online material that brings the subject to life, including videos of coastal processes and virtual field trips.

Robin Davidson-Arnott completed his Ph.D. in 1975 from the Department of Geography at the University of Toronto. He was appointed Assistant Professor at the University of Guelph in 1976, Associate Professor in 1980, and has served as Professor from 1988 onwards. He has been a member of the Task Force of the International Joint Commission (Canada/USA) Great Lakes Water Levels Reference Study Phase 1 (1987–89), and has seconded as a Scientist to the Ontario Ministry of Natural Resources Development of Ontario Shoreline Management Policy and Technical Guideline (1992–95), and to the International Joint Commission (Canada/USA) Upper Great Lakes Water Level Regulation Study (2007–11). He has worked as a consultant for a number of studies for Ontario Conservation Authorities and Parks, Canada, and been awarded the R. J. Russell Award from the Coastal and Marine Specialty Group of the Association of American Geographers in 2000. His research interests are in coastal geomorphology – on beach and nearshore processes on sandy coasts, nearshore erosion of cohesive coasts, coastal saltmarshes, aeolian sediment transport and coastal dunes – and he has received continuous support in this from the Natural Sciences and Engineering Research Council of Canada for over 30 years. He has authored and co-authored many books and papers on the subject, including a contribution to *Geomorphology and Global Environmental Change* (Cambridge University Press, 2009).

An Introduction to Coastal Processes and Geomorphology

Robin Davidson-Arnott

CAMBRIDGE
UNIVERSITY PRESS

CAMBRIDGE UNIVERSITY PRESS
Cambridge, New York, Melbourne, Madrid, Cape Town, Singapore,
São Paulo, Delhi, Dubai, Tokyo

Cambridge University Press
The Edinburgh Building, Cambridge CB2 8RU, UK

Published in the United States of America by Cambridge University Press, New York

www.cambridge.org
Information on this title: www.cambridge.org/9780521874458

First published in print format 2009

ISBN-13 978-0-511-69133-1 eBook (NetLibrary)

ISBN-13 978-0-521-87445-8 Hardback

ISBN-13 978-0-521-69671-5 Paperback

Contents

Preface

This book is designed primarily as a textbook for an upper-level undergraduate course in coastal processes and geomorphology and it stems from a fourth-year course that I have taught for twenty-five years at the University of Guelph. Its primary objective is to provide students with a description of processes acting to erode, transport and deposit sediments in the coastal zone, and of the factors that act in concert with these to produce the infinite variety of features that characterise marine and freshwater coasts around the world. The intent is to provide sufficient information for the reader to be able to then tackle more detailed material available in primary sources such as refereed journal articles, monographs and the World Wide Web.

The students in the course I teach are primarily in the BSc programme in Physical Geography or Earth Surface Science, with a focus on geomorphology and hydrology, but students from a number of other disciplines, including Engineering, Marine Biology and the BA programme in Geography also take the course. In writing this book I have assumed some background in geomorphology or earth sciences and some level of comfort with mathematical equations and basic physics. However, it should still be readable for those who do not have these. It is my hope that the book will also provide a useful reference source for coastal managers and for other scientists and social scientists interested in the coastal zone.

While I have tried to be broad in my coverage and in the examples used, the book invariably reflects my own experiences and approach. This is biased somewhat towards field studies rather than numerical modelling, and to research carried out in Canada, the USA, the Caribbean and Western Europe, as well as travels to Australia and New Zealand. As much as possible I have drawn on the literature in peer-reviewed journals and some monographs, while acknowledging that there is now a wealth of information available on the web. The expectation is that material presented here will make it easier to find and interpret these sources.

Following the introductory two chapters, the book is divided into two roughly equal parts, the first intended to provide an understanding of coastal processes operating on all oceans and large lakes. The second deals with the geomorphology and morphodynamics of a number of coastal environments including beaches, barrier systems, cliffs, coral coasts and saltmarsh and mangrove coasts. A more comprehensive coverage might also include estuaries and deltas, but to treat them in the same level of detail as the other environments would have made the book too long and I was easily persuaded that these could equally be covered in a book dealing with fluvial geomorphology.

The intense media coverage of natural disasters in the coastal zone such as the December 2004 tsunami in the Pacific and Indian oceans, and Hurricane Katrina in the USA have served to focus attention on vulnerability and adaptation to these and other coastal hazards. This is reinforced by the ongoing debate over human-induced climate change and particularly the predicted increase in the rate of sea level rise and the threat this may pose to populations living in the coastal zone. At the same time there is growing acknowledgement of the need for some comprehensive system of coastal zone management to facilitate adaptation to natural hazards and to reduce human impact on natural coastal systems. This book does deal explicitly with future sea level scenarios in the chapter on sea level and in Part III there is consideration of the potential impact of increasing rates of sea level rise in each of the coastal environments treated there. There are a multitude of good texts and monographs dealing with coastal management so, rather than treating it cursorily in a separate chapter, I have chosen to give some examples of application to specific problems for each coastal environment. It is hoped that the material presented here can be used to provide coastal managers with background on the physical processes and features of the coastal zone which need to be considered in developing management strategies and plans.

A variety of material is available online to supplement the material presented in the book. This includes colour versions of all photographs and diagrams and a consolidated list of references. Virtual field trips providing examples of the coastal environments described in Part III include supplementary photographs, maps diagrams and short videos. A number of key coastal processes are also illustrated with short videos. Finally, data from field experiments that can be used in laboratory exercises for students are included in separate spreadsheets. It is my intention to try to add to this list over the next two years.

Acknowledgements

This book is the outcome of my experience of many years of research and teaching on coasts. I have been fortunate in that time to have the support of many colleagues and friends who have contributed to this. Numbered among these are more than thirty graduate students who have cheerfully shared long days (and some nights) on beaches, in the water, and underwater. They have endured without complaint the tribulations of weather, equipment malfunctions and the shear physical labour required to carry out a successful field experiment. Their contributions are evident throughout this book in references to published papers. I have also benefited over the years from working with colleagues on field experiments and sharing ideas and experiences, many of which have found their way into this book. Included among them are: Brian Greenwood, Doug Sherman, Bernie Bauer, Karl Nordstrom, Patrick Hesp, Jeff Ollerhead, Troels Aagaard, Ian Walker, Danika van Proosdij, and the late Brian McCann and Bill Carter.

I have been fortunate to have been able to teach a fourth year course in coastal processes, which ultimately spawned this book, and the students who have taken that course have continuously renewed my interest in finding new ways to stimulate their interest in all things coastal. I am indebted to my colleagues in the Geography Department at the University of Guelph who have provided such a great environment to work and teach in. I would like to thank especially Bill Nickling, Ray Kostaschuk and Mike Moss for sharing ideas over many years and Mario Finoro for building and maintaining much of the research equipment. Special thanks go to Marie Puddister who has worked cheerfully for more than a year to produce all the figures for this book and for the web resources and who has been able to turn some of my illegible scratchings into recognisable diagrams.

Thanks to Anne Lamb for pushing me to do this. Thanks also to Frances who was there at the beginning and to my daughters Julia and Alison who have of necessity spent more time on beaches than they might otherwise have cared to do.

Finally, I could not have written this without the support of my wife Sharon who has cheerfully put up with all the trials of putting this book together over the past 18 months. Her reward will likely be a bit more time together on a beach in the Caribbean.

A number of colleagues have kindly let me use photographs from their own collection and these are acknowledged within the text. I would like to thank the following for permission to reproduce figures used in the text:

Academic Press

Figure 10.19: from *Barrier Islands: from the Gulf of St Lawrence to the Gulf of Mexico*

American Geophysical Union

Figure 5.13, 5.25: from *Journal of. Geophysical Research*, 73; figure 6.10: from *Journal of Geophysical Research*, 74; figure 7.15: from *Journal of Geophysical Research*, 75; figure 8.18: from *Journal of Geophysical Research*, 76; figure 11.30: from *Tropical Mangrove Ecosystems*

American Society of Civil Engineers

Figure 5.15: from *Proceedings 16th Coastal Engineering Conference*; figures 5.16, 5.17: from *Journal of Waterway, Port, Coastal and Ocean Engineering*, 111; figure 5.26; from *Proceedings 19th Coastal Engineering Conference*; figure 7.5: from *Proceedings 8th Conference on Coastal Engineering*; figure 7.16: from *Proceedings 18th Coastal Engineering Conference*; figure 8.17: from *Journal of Waterway, Harbors and Coastal Engineering*

Association of American Geographers

Figure 8.12: from *Geographical Review*, 78

Blackwell

Figures 3.1 and 3.7: from Institute of British Geographers Special Publication #20; figure 3.3: from Institute of British Geographers Special Publication #2; figures 7.18, 9.10: from *Sedimentology*, 50; figure 10.26: from *Transactions*

Institute of British Geographers, 34; figure 11.12: from *Earth Surface Processes and Landforms*, 17; figures 13.15a, b: from *Earth Surface Processes and Landforms*, 11; figure 13.26: from *Earth Surface Processes and Landforms*, 23

Cambridge University Press

Figures 4.2, 4.10, 4.11, 4.13, 4.14: from *Waves in Oceanic and Coastal Waters*; figure 9.24: from *Landscape Changes in the 21st Century*; figure 12.9: from *The Geomorphology of the Great Barrier Reef*

Coastal Education Research Foundation

Figure 3.22: from *Journal of Coastal Research*, SI 8; figure 3.25: *Journal of Coastal Research*, 24; figures 5.22; 7.7b: from *Journal of Coastal Research*, SI 36; figure 7.23: from *Journal of Coastal Research*, 13; figure 8.15: from *Journal of Coastal Research*, 8; figure 8.22: from *Journal of Coastal Research*, 9; figure 9.7: from *Journal of Coastal Research*, 12; figure 9.16: from *Journal of Coastal Research*, 21; figure 9.27a: from *Journal of Coastal Research*, SI 8; figure 10.6: from *Journal of Coastal Research*, 22; figure 10.17: from *Journal of Coastal Research*, SI 23; figure 11.16: from *Journal of Coastal Research*, SI 36; figure 11.21: from *Journal of Coastal Research*, 9; figure 12.14: from *Journal of Coastal Research*, 22

Elsevier Scientific

Figure 3.5: from *Journal of Great Lakes Research*; figure 3.21: from *Marine Geology*, 210; figure 3.26: from *Global and Planetary Change*, 55; figure 5.11: from *Applied Geography*, 5; figure 6.2a: from *Coastal Engineering*, 8; figure 6.2b: from *Coastal Engineering*, 10; figures 6.4, 6.5, 6.6: from *Marine Geology*, 86; figure 6.13: from *Coastal Engineering*, 10; figure 7.6: from *Marine Geology*, 131; figure 7.7a: from *Marine Geology*, 106; figure 7.8: from *Continental Shelf Research*, 15; figure 7.9: from *Marine Geology*, 118; figure 7.17: from *Coastal Engineering*, 54; figure 8.6: from *Marine Geology*, 182; figure 8.10b: from *Marine Geology*, 60; figure 8.10e: from *Marine Geology*, 244; figure 9.20a: from *Geomorphology*, 49; figure 9.25: from *Geomorphology*, 48; figure 9.28: from *Geomorphology*, 60; figure 10.11: from *Marine Geology*, 24; figure 10.18: from *Sedimentary Geology*, 28; figure 10.21: from *Marine Geology*, 63; figure 10.28: from *Marine Geology*, 200; figure 11.5: from *Geomorphology*, 48; figures 11.22a, 11.24: from *Marine Geology*, 225; figure 11.23: from *Estuaries*, 12; figure 11.26: from *Estuarine, Coastal and Shelf Science*, 76; figure 11.28: from *Quaternary Science Reviews*, 19; figure 11.32: from *Fluid Dynamics Research*, 24; figure 12.3, 12.6: from *Earth-Science Reviews*, 71; figure 12.5: from *Earth and Planetary Science Letters*, 141; figure 12.8: from *Earth-Science Reviews*, 57; figure 12.12: from *Global and Planetary Change*, 62; figure 12.13: from Earth-Science Reviews, 64; figure 13.10, 13.20: from *Marine Geology*, 122; figure 13.21: from *Marine Geology*, 166

The Geological Society, London

Figures 11.17a, 11.20: from *Coastal and Estuarine Environments*

International Association for Great Lakes Research

Figure 3.6: from *Proceedings of the 12th Conference on Great Lakes Research*

Kluwer Academic Publishers

Figure 13.23: from *Encyclopedia of Coastal Sciences*

Morrow

Figure 9.12: from *The Physics of Blown Sand and Desert Dunes*

Macmillan

Figure 3.8: from *Physical Oceanography*

National Research Council of Canada

Figure 3.2: from *Canadian Journal of Earth Sciences*, 35; figures 10.15, 10.16: from *Canadian Journal of Earth Sciences*, 29

Oliver and Boyd

Figures 3.9, 3.11,12.4: from *Geographical Variation in Coastal Development*

Prentice-Hall, New Jersey

Figures 5.1, 5.3, 5.6, 7.11: from *Beach Processes and Sedimentation*

SEPM Society for Sedimentary Research

Figures 3.18, 3.19: from SEPM Special Publication, #41; figures 5.18, 5.19, 7.3b: from SEPM Special

Publication, #24; figure 7.3a: from *Journal of Sedimentary Petrology*, 41; figure 10.27: from *Journal of Sedimentary Petrology*, 58; figure 11.7: from *Journal of Sedimentary Petrology*, 51

SpringerLink
Figure 11.33: from *Mangroves and Saltmarshes*, 1

John Wiley and Sons
Figure 3.4: from *Earth Rheology, Isostacy and Eustacy*; figure 5.2: from *Geomorphology of Rocky Coasts*; figures 5.27, 8.19, 8.20: from *Handbook of Beach and Shoreface Morphodynamics*; figures 8.2, 8.10c: from *Nearshore Sediment Dynamics and Sedimentation: An Interdisciplinary Review*; figure 9.20b: from *Coastal Dunes: Form and Process*; figure 11.3: from *Canadian Geographer*, 43

World Scientific, Singapore
Figure 5.20: from *Mechanics of Coastal Sediment Transport*

Mark Donelan
Figures 4.15, 4.16, 4.17: from *Proceedings Canadian Coastal Conference*, 1980

Rob Holman
Figure 5.28, 5.29: from *Edge Waves and the Configuration of the Shoreline*

Gary Parkes
Figure 3.23: from *Storm Surge Events in the Maritimes*

Tsuguo Sunamura
Figure 13.5: from *Processes of Sea Cliff and Platform Erosion*

Danika van Proosdij
Figure 11.18: from *Spatial and Temporal Controls on the Sediment Budget of a Macrotidal Saltmarsh*

Part I

Introduction

1

Introduction

1.1 Humans and the coastal zone

Beaches and, more generally, the coastal zone occur at the interface between the three major natural systems at the earth's surface – atmosphere, ocean and land surface. Processes operating in all three of these systems are responsible for shaping the coastal zone, and the interaction between the three different sets of processes makes the coastal zone an extremely dynamic one. The coastal zone is also a zone of transfer of material from the land surface to the ocean system, with sediments eroded by rivers, glaciers, etc., being moved to the beach and nearshore, and ultimately some to the ocean floor. In some areas accumulation of sediments may add to the land mass.

The focus of this book is on describing the physical processes that act to shape the coast and the landforms that make up the coast. As in any other branch of applied science, we can study these for their own interest, without the need to justify it in terms of potential benefits. However, in addition to its geomorphological significance, the coastal zone is particularly important from a human perspective. A large proportion of the world population is concentrated in the coastal zone, including almost all of the major cities. The coastal zone is used for fishing, transportation, recreation, waste disposal, cooling and drinking water and is potentially a source of energy from tidal and wave power. Many of these activities pose an environmental threat to coastal systems, both physical and biological, through pollution, siltation, dredging, infilling and a host of other activities that alter the way natural systems operate. In recent years there has been increasing pressure from leisure activities focused on water sports, and recreation at the seashore (Figure 1.1). In addition, natural processes often pose a hazard to human occupation and utilisation of the coastal zone through wave action, flooding, storm surge, and through coastal erosion and sedimentation. Because of the threats to human life and activities posed by both environmental impact and natural hazards, there is a strong economic incentive to improve our understanding of processes operating in the coastal zone so that we can minimise their effects, and use this knowledge in the development of comprehensive coastal zone management planning.

Each maritime country has a unique perspective of their coastline, shaped by history and culture, and by the physical and biological nature of the coast itself. There are commonalities among great differences; for example, the people of the Netherlands and of the Maldives both face a similar threat posed by a dense coastal population and rising sea level even though one nation is situated on a large delta that has largely been reclaimed by dyking and the other sits on a small coral atoll. In the United States a Federal Agency, the US Army Corps of Engineers has played a key role in coastal development and the management of coastal hazards and they have been in the forefront of applied research on coastal processes and engineering. In Canada there is no equivalent federal agency

Figure 1.1 Examples of recreational pressures on the coast: (A) beach, promenade and sea front shops and apartments, Malo les Bains, Dunkerque, France. Development of the seafront in many coastal towns in Britain, France and Western Europe began in the late nineteenth century with the advent of cheap rail travel. Small seafront guest houses are being replaced by apartments that are used for weekends and holidays; (B) resort development, Frigate Bay, St Kitts, West Indies in June, 2008. The advent of cheap air fares from northern parts of the USA, Canada and Western Europe has fuelled resort development on a massive scale in Florida and much of the Caribbean. Developments here include a large five star hotel and golf course, other smaller hotels, time share and condominium apartments and individual houses that are privately owned or rented.

and the relatively small population and limited resources has left a much greater proportion of the coast relatively pristine.

My own experience has been shaped by living in Canada and by carrying out much of my research here. Canada has one of the longest marine coastlines in the world, totalling nearly 250 000 km and bordering on three oceans (Figure 1.2). It has an additional 15 000 km of coastline in the Great Lakes and tens of thousands more along smaller, but still significant lakes. There is a great variety of coastal environments. The Pacific coast is dominated by swell waves and is generally ice free, while the Arctic coast is dominated by the presence of ice year round and, in the eastern Arctic by ongoing post-glacial isostatic uplift. The East coast experiences strong mid-latitude storms as well as the effects of one or two hurricanes a year, and much of it is influenced by a seasonal ice cover. On this coast the tidal

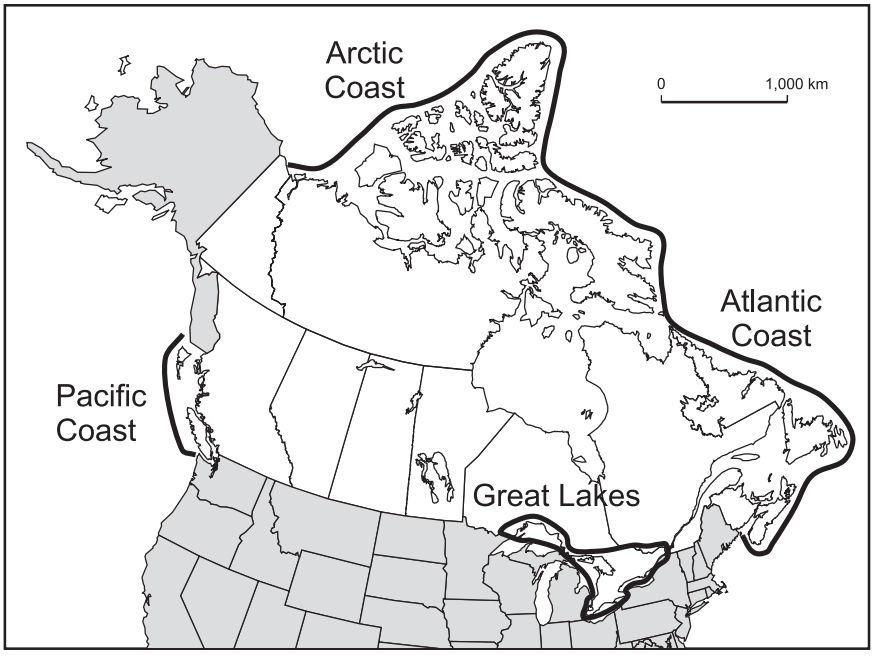

Figure 1.2 Primary divisions of the coasts of Canada (Owens, 1977)

range is <1 m in parts of the Gulf of St Lawrence and may be over 15 m in the Bay of Fundy. Finally, the Great Lakes are freshwater, but act as small seas, with tides being replaced by seasonal and long-term water level fluctuations. Like the Atlantic coast, seasonal ice foot development occurs in all the lakes and there is considerable surface ice cover on Lakes Erie and Huron.

Almost all of the population of Canada lives within 50 km of one of these coasts, and more than half along the Great Lakes-St Lawrence system. All of the activities noted above are carried out on the coast and thus the coastal zone is as significant for Canada as it is for any other country. The potential impact of oil exploration and exploitation off the Arctic and Atlantic coasts, destruction of coastal wetlands and interference with longshore sediment transport, as well as the effects of coastal erosion and storm wave damage are examples of some of the conflicts that exist in the Canadian coastal zone and that provide a stimulus for developing an improved knowledge and understanding of the features and processes. There is also recognition that human-induced climate change will have a significant impact on many of the coastal areas of Canada, as it will in many other parts of the world.

1.2 Approaches to the study of coasts

Geomorphology encompasses the study of the landforms of the earth and the processes that form them, especially those that lead to the erosion, transport and deposition of sediments. The focus of coastal geomorphology is therefore on the morphology of the coastal zone and on processes such as waves, tides and currents that act to shape features as disparate as high rock cliffs, low coral atolls, and sandy beach and dune systems. Research in coastal geomorphology is greatly influenced by other fields of geomorphology, especially fluvial and aeolian geomorphology, and there is a common set of paradigms, instrumentation and methodology.

The coastal zone and coastal processes are also the subject of study by a number of other disciplines, each of which brings a different focus or

approach. In particular there is considerable overlap of interest between coastal geomorphologists and sedimentologists, coastal oceanographers and coastal engineers in the study of waves and currents, and coastal erosion and deposition. While the ultimate objectives of the different disciplinary groups may be somewhat different, they share a common interest in expanding our understanding of these physical processes. In the past few decades many of the artificial barriers that often separated these groups have disappeared. This is evident in the range of disciplines represented at international coastal conferences, in the groups of collaborators carrying out large projects, and in the contributors to most of the journals that appear in the reference lists at the end of each chapter in this book.

There are also areas of overlap between coastal geomorphologists and biologists studying plant and animal life in coastal waters, beaches, estuaries and marshes. Waves and currents may place stresses on plants and animals on the coast and in shallow water and they may also be important for dispersal of organisms. An understanding of processes of erosion and deposition may be helpful in the study, for example, of shellfish and a variety of other organisms that live in surface sediments of the sandy beach and nearshore environment. The interaction between plants and wave and current action is important in the study of sea grass beds and coastal marshes. On the one hand, waves and currents impose stresses on plants, and on plant establishment, and on the other hand the presence of the vegetation serves to modify flow conditions near the bed and to stabilise the substrate. A similar relationship exists for coral reef systems. The coastal zone provides a habitat for many species of fish and shellfish, and some open water species may breed in coastal waters. Estuaries and marshes may play a significant role as nurseries for juvenile fish and so Fisheries Biologists have an interest in the functioning and conservation of these systems.

1.3 Information sources

There is a long history of the study of coastal processes and landforms and in the past 50 years or so there have been a number of textbooks, published in English, aimed at various levels of undergraduate and graduate instruction, and as resources for researchers of all kinds. Two books by D.W. Johnson (Johnson, 1919, 1925) provide a wealth of information about the coast of the United States and approaches to the study of coasts in the early twentieth Century. After 1950 there was a rapid growth in studies of coastal geomorphology, marked by the appearance of the first edition of *Beaches and Coasts* by Cuchlaine King (King, 1959) and a popular book by Willard Bascom (Bascom, 1964). Both of these highlighted research experiences that began in the Second World War. An English translation of a text by Zenkovitch (1967) provided access to a considerable body of literature from what was then the Soviet Union. The US Army Corps of Engineers through the Beach Erosion Board and later the Coastal Engineering Research Centre published the *Coastal Engineering Manual* which provided background on coastal processes, particularly waves, wave hindcasting and sediment transport as well as engineering applications. While designed primarily to support practising coastal engineers, it proved a useful source for people interested in physical processes in the coastal zone. The last paper edition was published in 1984 and updated versions are now available in PDF format on the web. Finally, an eclectic book by Jack Davies (1972) emphasised the importance of climate, tidal range and wave climate in controlling coastal processes and coastal evolution.

The past thirty years have seen a number of textbooks that provide a variety of different perspectives and many of these still provide a good source for information and insights on both processes and coastal landforms. Included in these are books by Komar (1998); Davis (1984); Carter (1988); Carter and Woodroffe (1994); Bird (2000); Trenhaile (1997); Short (1999) and Woodroffe (2002) which were all generally aimed at senior undergraduates, graduates and researchers. There are also a number of texts that are devoted to one aspect of coastal geomorphology, such as Sunamura (1992), Trenhaile (1987), Nordstrom (2000), and to Coastal Engineering (Kamphuis, 2000). Books by Pethick (1984), Masselink and

Hughes (2003) and Davis and FitzGerald (2004) were aimed at providing an introduction to the subject that was accessible to undergraduates, both in terms of content and affordability.

In addition to the specialist texts in coastal processes and geomorphology, much of the material in this book is drawn from articles published in journals and conference proceedings. While the material in this book can be read on its own, one of its aims is to provide sufficient basic information on vocabulary, methods and processes to make exploring this literature much easier. Almost all the journals are now available online. Many provide access to back issues that go back twenty years or more and, increasingly, they provide a number of routes to access related publications. The *Journal of Coastal Research* provides broad coverage of all the material covered in this book and includes physical and biological processes, aspects of coastal management and case studies from around the world. There is also considerable coverage in *Marine Geology*, *Continental Shelf Research*, *Coastal Engineering* and the *Journal of Estuarine, Coastal and Shelf Science*. Both *Geomorphology* and *Earth Surface Processes and Landforms* encourage papers on coastal geomorphology. Useful updates can be found in *Progress in Physical Geography* and substantial reviews often appear in *Annual Review of Fluid Mechanics* and *Annual Review of Earth and Planetary Sciences*.

Conferences provide a major forum for the exchange of information and ideas and published conference proceedings still provide a useful source of new information. The Coastal Engineering Conferences sponsored by the American Society of Civil Engineers (ASCE) which began just after World War II are held every two years and more specialised ones such as Coastal Sediments and Coastal Dynamics every four years. The Coastal Education Research Foundation, which sponsors the *Journal of Coastal Research*, also sponsors an international Coastal Symposium which is held every two or three years in countries around the world. In Canada the first coastal conference was held in Halifax in 1978 (McCann, 1980) under the auspices of the Geological Survey of Canada. Beginning in 1980, Canadian Coastal Conferences were held every two or three years, sponsored initially through a committee of the National Research Council and later by its successor the Canadian Coastal Science and Engineering Association (CCSEA). They brought together scientists from a range of disciplines as well as coastal engineers and some people working in coastal management. They also sponsored several specialist conferences, including one on cohesive shores and another on coastal dunes.

There is of course a vast amount of material available on the web from real time access to data from wave buoys and cameras set up at various beaches, to data and information provided by a host of Government departments and agencies and from web sites of individual organisations and researchers. A good search engine will open up a huge range of possibilities and the problem is to determine what is relevant and what is not.

1.4 Approach and organisation

The book is organised into three sections. In Part I, following this introductory chapter, Chapter 2 provides some background on the scope of coastal geomorphology, some basic definitions and terminology, and an overview of the major factors controlling the appearance and development of coasts worldwide.

Part II, Coastal Processes, has five chapters which cover sea level changes and processes associated with waves and currents that together act to transform the coast on a range of timescales. An understanding of these processes is also important for managing coastal hazards and human impacts on the coastal zone. It begins in Chapter 3 with an examination of the processes controlling sea level at temporal scales ranging from seconds to thousands and millions of years. Following this, Chapters 4 and 5 cover waves and wave processes. The first of these provides a general description of waves and the factors that control their formation, as well as the range of wave conditions that can be experienced at any location. The second makes use of wave theory to describe wave oscillatory motion and the processes involved in wave

shoaling and breaking as waves move from open water to the coast. Chapter 6 examines wave-generated currents and circulation patterns in the nearshore. Finally, Chapter 7 draws on the water motion described in the previous three chapters to describe the processes of sediment transport, both onshore–offshore and alongshore.

Part III, Coastal Systems, contains six chapters that describe the geomorphology, sedimentology and processes that are characteristic of major coastal systems. Chapter 8 begins by examining the characteristics of beaches and the response of beach form to varying wave, tide and water level conditions. Chapter 9 covers aeolian sediment transport on beaches and the development of coastal dune systems. Chapter 10 describes coastal barriers such as spits and barrier islands and their associated lagoon. Saltmarshes and mangroves, which are both formed in the intertidal zone in sheltered areas, are covered in Chapter 11. Chapter 12 deals with coral reef coasts which are a significant element of coasts within the tropics. Finally, Chapter 13 covers coastal cliff systems.

A more comprehensive coverage might also include treatment of coastal systems such as estuaries, fiords, deltas and muddy coasts (including intertidal mudflats), but to describe them in the same level of detail as the other coastal systems would have made the book too long. Rather surprisingly, given the Canadian content, there is no detailed treatment of the role of ice in the coastal zone. This is justified partly in the interest of length and partly because the role of ice is primarily a passive one, restricting the operation of wave and current processes for some period of the year.

Each chapter after Chapter 2 begins with a synopsis. Also included are Boxes which expand on some aspect covered in the chapter but are not essential to understanding it. I have chosen to include a reference list for each chapter, rather than consolidating all the references at the end of the book. This is done to provide a sense of where published material from which the chapter is drawn is located, as well as to highlight the people who are actively involved in research in that field or fields. A consolidated reference list is available on the web site for the book.

Diagrams and photographs for the book were all prepared in both grey scale and colour. The book of necessity only uses grey scale figures but all of them are available on the web site for the book in full colour. Additional materials are provided on the web site and these can be used to supplement the text and as an aid to teaching.

References

Bascom, W. 1964. *Waves and Beaches: the Dynamics of the Ocean Surface*. Anchor Books, Garden City, 267 pp.

Bird, E. C. F. 2000. *Coastal Geomorphology: An Introduction*. Wiley, Chichester, 332 pp.

Carter, R. W. G. 1988. *Coastal Environments*. Academic Press, 617 pp.

Carter , R. W. G. and Woodroffe, C. D. (eds) 1994. *Coastal Evolution: Late Quaternary Shoreline Morphodynamics*. Cambridge University Press, Cambridge, 517 pp.

Clark, J. R. 1996. *Coastal Zone Management Handbook*. CRC Press, Boca Raton, FL, 694 pp.

Davies, J. L. 1972. *Geographical Variation in Coastal Development*. Oliver & Boyd, Edinburgh, 2nd edn., 204 pp.

Davis, R. A., Jr. (ed.) 1984. *Coastal Sedimentary Environments*, 2nd edn., Springer, Berlin, 716 pp.

Davis, R. A., Jr. and FitzGerald, D. M. 2004. *Beaches and Coasts*. Blackwell, Oxford, 419 pp.

Johnson, D. W. 1919. *Shore Processes and Shoreline Development*. Prentice Hall, New York, 584 pp.

Johnson, D. W. 1925. *The New England-Acadian Shoreline*. Wiley, New York, 608 pp.

Kamphuis, J. W. 2000. *Introduction to Coastal Engineering and Management*. World Scientific, Singapore, 437 pp.

King, C. A. M. 1959. *Beaches and Coasts*. Arnold, New York, 403 pp.

Komar, P. D. 1998. *Beach Processes and Sedimentation*. 2nd edn., Prentice-Hall, Englewood Cliffs, NJ, 544 pp.

Masselink, G. and Hughes, M. G. 2003. *Introduction to Coastal Processes and Geomorphology*. Edward Arnold, London, 354 pp.

McCann, S. B. (ed.) 1980. *The Coastline of Canada*. Paper 80–10. Geological Survey of Canada, 439 pp.

Nordstrom, K. F. 2000. *Beaches and Dunes of Developed Coasts*. Cambridge University Press, Cambridge, 338 pp.

Owens, E. H. 1977. Coastal Environments of Canada: The impact and cleanup of oil spills. *Fisheries and Environment Canada, EPS-3-EC-77–13 Report*, 413 pp.

Pethick, J. 1984. *An Introduction to Coastal Geomorphology*, Edward Arnold, London, 260 pp.

Short, A. D. (ed.) 1999. *Handbook of Beach and Shoreface Morphodynamics*. Wiley, Chichester, 379 pp.

Sunamura, T. 1992. *Geomorphology of Rocky Coasts*. Wiley, Chichester, 302 pp.

Trenhaile, A. S. 1987. *The Geomorphology of Rock Coasts*. Oxford University Press, Oxford, 384 pp.

Trenhaile, A. S. 1997. *Coastal Dynamics and Landforms*. Oxford, Clarendon Press, 366p.

Woodroffe, C. D. 2002. *Coasts: Form, Process and Evolution*. Cambridge University Press, Cambridge, 623 pp.

Zenkovitch, V. P. 1967. *Processes of Coastal Development*, Oliver and Boyd, Edinburgh, 738 pp.

2

Coastal geomorphology

2.1 Definition and scope of coastal geomorphology

Coastal geomorphology is a branch of geomorphology in which the focus is on the area influenced by large bodies of water, including seas and oceans, and large lakes such as the Great Lakes in North America. It is perhaps best viewed as an applied science and overlaps with other applied sciences such as geology, meteorology, oceanography, coastal engineering and elements of biology.

Prior to 1950, coastal geomorphology was highly descriptive and much of it was influenced by concepts related to the Davisian Cycle of Erosion. Coastal classification and description paid considerable attention to the effects of sea level change and especially the role of the Holocene sea level rise in producing drowned coastal features such as fjords (drowned glaciated valleys) and rias (drowned river valleys). Waves and currents were seen to operate to straighten and simplify the coastline by trimming headlands and building barriers across bay mouths (Woodroffe, 2002). Coastal evolution was therefore directed towards a simple, relatively static equilibrium. One branch of coastal geomorphology also followed the paradigm of denudation chronology, which attempted to reconstruct the detailed geological evolution of coastal landscapes. Much of this was guided by concepts of erosion cycles and interpretation based primarily on landforms rather than stratigraphy. The advent of a range of methodologies for coring and geophysical remote sensing, combined with new methods for dating sediments, has transformed this branch of coastal geomorphology/sedimentology. In particular, it has allowed the building of detailed histories of the glacial and post-glacial evolution of coasts worldwide.

Much of the research in coastal geomorphology in the past four decades has been concentrated on the zone influenced by waves and tides, wave-generated currents, and tidal currents, and on the erosional and depositional features associated with these. There has been a rapid change in the instrumentation available for measuring fluid motion and sediment transport, as well as for measuring morphological change (Davidson-Arnott, 2005) and this has permitted a focus on studies of morphodynamics – simultaneous measurements of process and morphological change, especially in the sandy nearshore. As is the case in other areas of geomorphology, the reductionist paradigm guided much of the field and laboratory experimentation. The ultimate goal of this approach is to build models from an understanding of how the system functions at the smallest scale – time scales of a second or less and spatial scales of millimetres to tens of centimetres – and then to upscale these to simulate or make predictions at larger spatial and temporal scales.

There is no doubt that improved technology and the efforts of a large number of scientists and engineers, working in the field and in the laboratory, have greatly expanded our understanding of coastal processes in this period. This has been accompanied by similar improvements

in numerical modelling and in the development of theory. At the same time there has been a recognition that modelling large-scale coastal evolution (defined as temporal scale of decades and spatial scale of tens to hundreds of kilometres) may require a different approach than simply running the small-scale models for larger areas and over longer periods of time (Cowell *et al.*, 1995; Ashton *et al.*, 2001; Harvey, 2007; Baquerizo and Losada, 2008; Kroon *et al.*, 2008.). Some of this is driven by consideration of the potential impacts of global climate change and especially of an increase in the rate of eustatic sea level rise (Stive, 2004; Cowell *et al.*, 2006; Slott *et al.*, 2006).

Coastal systems vary greatly in their dynamic range and in their response to changing controls. At one end of the continuum, the beach foreshore morphology can respond at a temporal scale of seconds and minutes to changes in incident wave conditions and tidal elevation. At the other end of the continuum, cliffs in resistant rock such as dolomite or granite may show no observable morphological change over hundreds of years. Concepts of systems interrelationships, feedback paths, dynamic equilibrium and thresholds that have been part of geomorphology for the past 40 years (Chorley and Kennedy, 1971) are a part of the current paradigm of coastal geomorphology. Above all, there is a firm belief among coastal geomorphologists and, perhaps especially among coastal engineers, that dynamic coastal systems can be modelled deterministically as long as we have sufficient understanding of processes and the data needed to carry out the modelling. Furthermore, much of the research is guided by a belief that coastal systems tend towards dynamic equilibrium and that a change in the incident conditions will rapidly be reflected in a predictable change in morphology towards another dynamic equilibrium. This is perhaps best seen in describing beach profile response to a change from steep, short period storm waves, to low, long period swell waves (see Section 8.3.3). Another example is the persistence of the so-called Bruun rule (Schwartz, 1967) for predicting the response of sandy shorelines to sea level rise.

While uncertainty and the stochastic nature of many events are increasingly being acknowledged, coastal geomorphologists have perhaps been less willing to let go of their vision of an orderly and predictable universe than in other branches of the discipline and to embrace, for example, non-linear dynamics (Phillips, 1995). We may, however, see more examples of the concept of self-organisation (Werner, 2003; Baas, 2007), perhaps because this produces some form of recognisable order.

2.2 The coastal zone: definition and nomenclature

As is the case in most areas of geomorphology, there are many terms used to describe coastal features and processes that are poorly defined and occasionally subject to misuse. Differences in meaning are also common between the different disciplines working in the coastal zone – e.g. biologists, engineers, geologists and geomorphologists. Features associated with a general coastal profile as used in this book are illustrated in Figure 2.1. Other definitions related to waves and to specific coastal environments are defined in the relevant chapters.

Coastal zone broad term for the area influenced by proximity to the coast; both the onshore and offshore limits are (deliberately) imprecisely defined. The limit on land may be a few hundred metres inland from a cliff top or several kilometres where there are extensive sand dunes, or along tidal estuaries (Figure 2.2). The seaward limit may be the edge of the continental shelf and is usually at least several kilometres.

Offshore zone portion of the profile where there is no significant transport of sediment by wave action. The landward boundary can be defined precisely as the transition to water depths less than one-half the wave length of large storm waves. Note that the landward boundary is often defined (especially by coastal engineers) as the outer limit of the breaker zone. It is also occasionally used simply to include everything seaward of the low-tide line.

Littoral zone portion of the coastal profile where sediment can be transported by

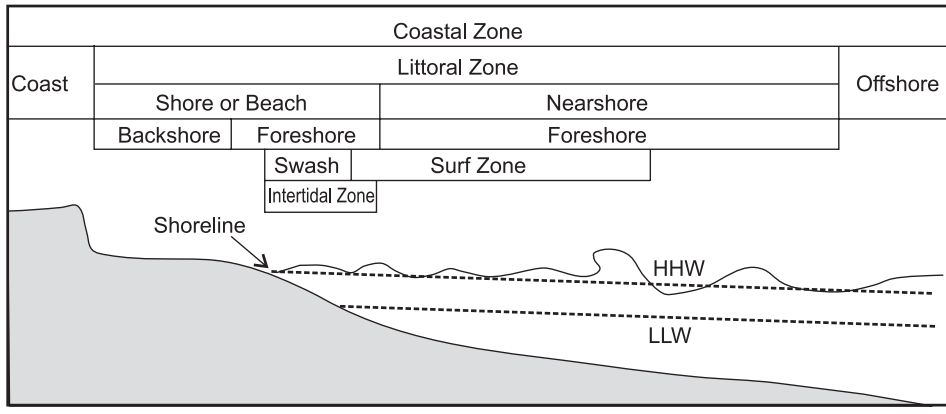

Figure 2.1 Sketch of the coastal zone and terminology used in this book.

Figure 2.2 The coastal zone. Oblique aerial photograph looking offshore along a shallow estuary, Buctouche, New Brunswick, Canada. The marine influence extends inland along the estuary to the tidal limit. The estuary connects to Buctouche Bay in the middle of the photograph, which is formed behind Buctouche spit which is visible towards the top of the photograph. The coastal zone extends beyond this into the waters of the Gulf of St Lawrence.

wave action. The seaward limit is defined by the water depth at which significant sediment transport by wave action ceases (it can be equated with the boundary between the offshore and the nearshore) and the landward limit is the limit of (normal) wave action.

Nearshore zone portion of the profile extending from the limit of significant sediment transport by waves to the low tide line. Note that where the offshore is defined as beginning at the seaward edge of the breaker line, then this will also mark the seaward limit of the nearshore.

Shoreface zone dominated by wave action from the offshore landward to the low tide line – synonymous with the definition of nearshore used in this book. It is used

primarily by geologists/sedimentologists and may be divided into an upper and lower shoreface marked by a distinct change in slope on sandy coasts at a depth of around 6–10 m (Cowell, 1999).

Shore or beach portion of the profile subject to wave action and which is exposed subaerially at least some of the time. The seaward limit is defined by the spring low tide line and the landward limit by the limit of swash uprush during 'normal' storms. The landward limit is often taken as the vegetation line.

Foreshore portion of the beach subject to wave action during non-storm conditions.

Backshore portion of the beach subject to wave action only during storms. During non-storm conditions sand may be reworked by aeolian action. This is 'the beach' for recreational purposes.

Surf zone zone of broken waves (surf bores) extending from the breaker zone to the foreshore. Varies with beach slope and wave conditions and will only be present when waves break some distance offshore.

Swash zone zone of wave run-up on the beach and return of water in the form of backwash. It varies with wave and slope conditions.

Intertidal zone zone between high and low water (tide).

Shoreline can be defined instantaneously as the intercept of the mean water level along the beach, but it is often used loosely as the swash limit or the landward edge of the backshore.

2.3 Factors influencing coastal morphology and processes

The characteristics of the coastal zone vary considerably world-wide, and they may do so over even fairly short distances. The outstanding feature of any particular coastline may result from large-scale geologic factors, local geology, surface processes and the effects of recent changes in the relative level of the land and the sea. The complexity of these factors has given rise to a number of different ways of classifying coasts and a brief examination of a couple of these will serve to illustrate the nature of this complexity. We will also consider a list of the major controlling factors and how they influence coastal development.

2.3.1 Controls on coastal development

Coastal classification

The drive for simplification and order in all sciences inevitably leads to the generation of classification schemes, and the coast has received its fair share. Finkl (2004) provides a thorough review of these in the lead-up to presenting his own classification based on a project to classify coasts in terms of their suitability for amphibious landings. Most of the early classifications attempted to group similar landforms based on some major control or controls, such as tectonic history, processes shaping coastal evolution, or sea level history.

Sheppard (1963) produced a comprehensive classification (modified from several earlier versions – e.g. Sheppard, 1937) in which coasts are divided into primary (youthful) and secondary coasts. Primary coasts are those that have been shaped primarily by terrestrial agents (including those associated with plate tectonics as we know them today) and are subdivided into land erosion coasts (rias, fjords, etc.), subaerial deposition coasts (deltas and alluvial plains, glacial deposition, etc.), volcanic coasts, and tectonic coasts (faulted and folded coasts). Secondary coasts are those in which wave action and other coastal processes are the dominant control on the form of the coast and these are subdivided into wave erosion coasts, marine deposition coasts (barriers, salt marsh, etc.), and coasts built by organisms (coral coasts, mangrove coasts).

Inman and Nordstrom (1971) devised a two-tier classification in which the first-order features are related to continental scales and are based on plate tectonics. They consider lengths on the order of 1000 km, widths of 100 km and heights of 10 km, and divide coasts into three major groups. These are:

(1) Collision coasts: (a) continental margin, characterised by cliffed shorelines, narrow coastal plains and deep ocean trenches, with high mountains just inland; (b) island arc collision coasts, which are similar to (a) in general form but lack the major mountain ranges and large rivers associated with the continental margin.

(2) Trailing edge coasts: (a) neo-trailing edge formed near the beginning of plate separation (e.g., the Red Sea) with little or no continental shelf development; (b) Afro trailing edge characterised by hilly or plateau coasts; and (c) Amero- trailing edge coasts with wide continental shelf and large rivers draining the interior of the continent.

(3) Marginal sea coasts: coasts fronting on marginal seas and protected from the open ocean (Mediterranean, China).

They then go on to consider second-order features which are based on morphology and processes.

Valentin (1952) produced a classification that focused on the direction of movement of the shoreline. He distinguishes first between coasts that have advanced and those that have retreated. Within each of these distinction is made between changes due to relative sea level rise or fall and those related to coastal progradation or erosion.

Two factors that complicate the success of any coastal classification scheme are the recent history of sea level change due to the growth and retreat of glaciers over the past 100 000 years, and the time scales over which different coastal features evolve. As is described in greater detail in the next chapter, sea level in the previous interglacial was roughly the same as that today. Over the last glacial period sea level fluctuated generally downward with the growth and retreat of continental ice sheets, culminating in a low stand about 30 000 to 25 000 BP when sea level was about 130 m lower than present. This was followed by a relatively rapid melting and retreat that produced submergence of most of the shorelines in tropical and mid-latitude and somewhat more complicated histories in glaciated coastal areas due to isostatic uplift. The result is that coastal processes have only been operating at the present sea level for a few thousand years and the character of most shorelines still reflects the impact of the transgression produced by rising sea level.

Where attempts are made to incorporate coastal processes into coastal classification schemes complications also arise because different coastal landforms evolve at quite different rates. Sandy coasts, and especially dynamic features such as spits and barrier islands, respond to storms that may recur more than once a decade and they may grow and disappear on a time scale of decades to a few thousand years. On the other hand, erosion of hard bedrock coasts occurs very slowly and erosional platforms associated with most modern coasts could not have formed during the 5000–6000 years that sea level has been close to its present level. They must therefore be inherited from a previous interglacial sea level (or more likely are the complex product of sea level fluctuations over several million years).

GIS and coastal classification

With the rapid development and adoption of Geographic Information System (GIS) software packages in the late 1980s, their utility for coastal management was quickly recognised.

The classification schemes described in the previous section are not particularly useful when it comes to providing information for coastal management at a scale of hundreds of metres to hundreds of kilometres. The databases that are associated with GIS operations are capable of holding information on many more variables than can be incorporated in the coastal classifications and the spatial unit for the shoreline is often a reach which may be a few hundred metres to a few kilometres in length, within which key geomorphic and geologic factors (e.g., beach sediments, nearshore slope, bedrock geology, longshore sediment transport direction; recession rate) are assumed to be uniform. Within the reach, information can be stored on natural features and processes as well as attributes associated with human activities (property values, property type, shore protection). In the Great Lakes Shoreline mapping and classification for a GIS was carried out for the whole

Table 2.1 | *Factors controlling coastal development (modified after Davies, 1972).*

Factors of the Land	
Geological structure	Plate tectonics, mountain ranges, continental shelf width, relief
Local geology	Local structure, rock type
Geomorphic processes	River valleys, deltas, sediment supply
Isostatic sea level change	tectonic isostacy, glacial isostacy
Factors of the Land	
Eustatic sea level change	glacial eustacy; geoidal changes
Wave climate	Water body size, orientation of the coast, wind and storm climatology
Tides	Tidal range, tidal type, tidal currents
Ice effects	shorefast ice, winter ice cover
Local erosion and deposition	coastal erosion, transport and deposition processes
Biological effects	mangroves, saltmarshes, coral reefs, sea grass beds, coastal dune vegetation

shoreline in the USA and Canada as early as 1991 as part of an International Joint Commission study of the impacts of high lake levels and storm events on coastal properties. Similar GIS databases are available for coasts along many parts of the world and are proving to be invaluable for local authorities charged with coastal management. They can be adapted to address a whole range of issues from modelling the potential impact of oil spills to addressing some of the challenges posed by global climate change and sea level rise (McFadden *et al.*, 2007).

Factors controlling coastal development

These three examples above give an indication of the range of factors that may be used to produce a general classification of coastal types. They are all valid approaches but it is not obvious that much can be done with them beyond the simple descriptive organisation. A somewhat different approach and one that still provides some useful insights was that provided by Davies (1972). The focus here is on the controls on coastal development and Davies provided several dynamic coastal classifications which were then mapped on a world scale. He recognised three broad groups of factors that influence coastal development, termed (1) physical factors of the land; (2) physical factors of the sea; and (3) biological factors (Table 2.1). Within chapters examining each of these in turn are maps showing worldwide coastal variation based on a number of different criteria (Davies, 1972). Among these are classifications based on wave climate and tidal range which have turned out to be very useful in a variety of applications and textbooks. Several maps taken from Davies (1972) appear in other chapters in this book.

References

Ashton, A., Murray, A. B. and Arnault, O. 2001. Formation of coastal features by large-scale instabilities induced by high angle waves. *Nature*, **414**, 296–300.

Baas, A. C. W. 2007. Complex systems in aeolian geomorphology. *Geomorphology*, **91**, 311–331.

Baquerizo, A. and Losada, M. A. 2008. Human interaction with large scale coastal morphological evolution. An assessment of the uncertainty. *Coastal Engineering*, **55**, 569–580.

Chorley, R. J. and Kennedy, B. A. 1971. *Physical Geography: a Systems Approach*. Prentice-Hall, London, 370 pp.

Cowell, P. J. 1999. The shoreface. In Short, A. D. (ed.), *Handbook of Beach and Shoreface Morphodynamics*. Wiley, Chichester, pp. 39–71.

Cowell, P. J., Roy, P. S. and Jones, R. A. 1995. Simulation of LSCB using a morphological behaviour model. *Marine Geology*, **126**, 45–61.

Cowell, P. J., Thom, B. G., Jones, R. A., Everts, C. H. and Simanovic, D. 2006. Management of uncertainty in predicting climate-change impacts on beaches. *Journal of Coastal Research*, **22**, 232–245.

Davidson-Arnott, R. G. D. 2005. Beach and nearshore instrumentation. In M. L. Schwartz (ed.), *Encyclopedia of Coastal Science*, Springer, Dordrecht, pp. 130–138.

Davies, J. L. 1972. *Geographical Variation in Coastal Development*. Oliver and Boyd, Edinburgh, 204 pp.

Finkl, C. W. 2004. Coastal classification: Systematic approaches to consider in the development of a

comprehensive system. *Journal of Coastal Research*, **20**, 166–213.

Harvey, A. M. 2007. Geomorphic instability and change – Introduction: Implications of temporal and spatial scales. *Geomorphology*, **84**, 153–158.

Inman D. L. and Nordstrom, C. E. 1971. On the tectonic and morphologic classification of coasts. *Journal of Geology*, **79**, 1–21.

Kroon, A., Larson, M., Möller, I., Yukoki, H., Rozynski, G., Cox, J. and Larroude, P. 2008. Statistical analysis of coastal morphological data sets over seasonal to decadal time scales. *Coastal Engineering*, **55**, 581–600.

McFadden, L., Nicholls, R. J., Vafeidis, A. and Tol, R. S. J. 2007. A methodology for modeling coastal space for global assessment. *Journal of Coastal Research*, **23**, 911–920.

Phillips, J. D. 1995. Nonlinear dynamics and the evolution of relief. *Geomorphology*, **14**, 57–64.

Schwartz, M. L. 1967. The Bruun theory of sea-level rise as a cause of shore erosion. *Journal of Geology*, **75**, 76–92.

Sheppard, F. P. 1937. Revised classification of marine shorelines. *Journal of Geology*, **45**, 602–624.

Sheppard, F. P. 1963. *Submarine Geology*. 2nd edn., Harper and Rowe, New York, 412 pp.

Slott, J. M., Murray, A. B., Ashton, A. D. and Crowley, T. J. 2006. Coastline responses to changing storm patterns. *Geophysical Research Letters*, **33**, L18404, doi: 10.1029/2006GL027445, 6 pp.

Stive, M. J. F. 2004. How important is global warming for coastal erosion? *Climatic Change*, **64**, 27–39.

Valentin, H. 1952. Die Küsten der Erde. Petermanns Geographisches Mitteilungen Ergänzsungheft, **246**, 118 pp.

Werner, B. T. 2003. Modeling landforms as self-organised, hierarchical dynamic systems. In Wilcock, P. R. and Iverson, R. M. (eds.), *Prediction in Geomorphology*, American Geophysical Union, Washington, DC, Geophysical Monograph 135, pp. 133–150.

Woodroffe, C. D.. 2002. *Coasts: Form, Process and Evolution*. Cambridge University Press, Cambridge, 623 pp.

Part II

Coastal Processes

3

Sea level fluctuations and changes

3.1 Synopsis

While the incident wave climate is the dominant process variable controlling changes in coastal form and evolution, changes in the relative level of the land and the water body, on a variety of time scales, can greatly influence the effect of these processes and the way in which coastal; evolution occurs. Dynamic changes in sea level on the order of hours to a few decades reflect response of the water surface to meteorological and oceanographic processes as well as tides and can be thought of as periodic or episodic deviations about mean sea level. They affect the level at which wave action occurs and may also lead to horizontal movements of water in tidal and other currents. They thus have an effect on coastal erosion, transportation and deposition. In addition to tides produced by the gravitational force of the moon and the sun, short-term fluctuation in sea level occur as a result of storm surge, seasonal variations in pressure and wind patterns and changes in weather patterns on a scale of years to decades such as the El Niño Southern Oscillation (ENSO) cycle in the Pacific. These fluctuations are also extremely significant ecologically, both directly through exposure and coverage of the intertidal zone and indirectly because of the movements of water and nutrients associated with the water level fluctuations.

Changes in the relative position of the land and sea on a time scale of thousands to millions of years lead to inundation (transgression) or exposure (regression) of the land. Eustatic changes result from changes in the volume of water in the ocean basins with the most significant of these being the effects of ice sheet growth and decay during the Pleistocene. During the last glacial period sea level reached its lowest point around 25 000 BP at an elevation of about 130 m below the present level. The succeeding Holocene transgression produced a rapid rise in sea level to something close to its present level about 5000 BP. Isostatic loading and unloading due to the growth and decay of the ice sheets complicates the response of the coast in mid- and high latitudes. Over longer time periods tectonic forces lead to relative changes in the elevation of the coast locally and to changes in the ocean basins as a result of continental drift.

One consequence of human-induced global warming is the potential for increased melting of glaciers and snow fields, particularly in Greenland and Antarctica where the largest reservoirs of fresh water are located. This in turn is leading to an increase in the eustatic sea level worldwide, though locally the magnitude will vary because of other factors.

3.2 Mean sea level, the geoid, and changes in mean sea level

In examining sea level changes it is convenient to think of them on three time scales (Fairbridge, 1983): (1) long-term changes on the order of 10^6–10^9 years where interest is focused on eustatic cycles of a few million years and sequence stratigraphy of deposition in coastal areas and deltas

(e.g. Wilgus *et al.*, 1988) and on large-scale plate tectonics; (2) medium-term changes on the order of 10^3 to 10^6 years where interest is primarily on the effects of Quaternary glaciation through crustal loading and unloading, and through eustatic changes associated with exchanges of water between the oceans and glaciers; local change in elevation of the land due to tectonic forces also occurs on this time scale; and (3) short-term changes on the order of hours to 10^3 years where attention is focused on astronomical tides, residual effects of the Wisconsinan glaciation, and on changes due to meteorological, oceanographic and climatic factors. Modern coastal features and processes are most affected by short-term sea level changes and by medium-term changes related primarily to the last 25 000 years, from the time of the last glacial maximum during the Wisconsinan glacial period through melting of the continental ice sheets and the Holocene transgression.

3.2.1 Mean sea level and the geoid

There are a large number of causes of changes in sea level which vary in their magnitude and on the time scale over which they operate (Table 3.1). This chapter focuses on describing each of these

Table 3.1 | *Major causes of sea level change and characteristic magnitude and time history. The magnitudes of change and time period are general and in some cases may fall outside the ranges indicated. Periodic and episodic changes result in a temporary deviation from mean sea level whereas continuous changes result in a change in the relative position of the sea and land.*

Name	Cause	Magnitude (m)	Time scale	Time history
surf beat	wave groups	0.05–0.5	30–300 seconds	periodic
seiche	oscillations in basin	0.02–0.75	seconds to hours	episodic periodic
tides	gravitational force of moon and sun	0.05–15	semi-diurnal or diurnal	periodic
wave set up (and set down)	wave momentum flux	0.05–0.75	hours-days	episodic
wind set up and storm surge	wind stress barometric pressure	0.05–3.0	hours-days	episodic
dynamic ocean temperature, currents	expansion and contraction due to temperature changes	0.05–0.5	days to months seasonal	episodic
astronomical cycle effects on tidal range	sun, moon and earth alignment, orbit, axis	0.05–5.0 m	14 days to 10^3 years	periodic
eustatic – changes in volume of ocean water – glacial eustasy	growth and decay of glaciers, lake and groundwater storage	metres to 10^2	10^2–10^4 years	continuous episodic (periodic?)
isostasy – glacio-isostasy, hydroisostasy	loading and unloading of crust	up to 150 m	10^3–10^4 years	continuous
geoidal	earth revolution, gravity changes	metres	10^3–10^6 years	continuous
eustatic – changes in ocean basin volume	plate tectonics	up to 10^2 metres	10^4–10^6 years	continuous
tectonic uplift and downwarping	local tectonics, plate tectonics, volcanism	metres to 10^3 metres	10^1–10^6 years	continuous

causes and their significance, with most attention being paid to those factors which have the greatest effect on modern coastal processes. Conceptually we can think of mean sea level as the average level of the sea at a point along the coastline, or in the open ocean, and thus fluctuations due to tides, meteorological conditions and short-term variations in ocean temperature and currents can be seen as departures above and below this level. Over the medium and long term changes in mean sea level relative to the adjacent land mass can occur because of uplift or subsidence of the land or because of changes in the height of the ocean itself, for example due to changes in the volume of water in the oceans. Practically, however, it is not easy to define or measure sea level accurately because fluctuations in sea level occur on a range of time scales which extend beyond the time over which we can average readings. Thus, if we measure sea level over a period of a year at a tide gauge we will get a value for the average sea level over that period. However, if measurements continue over a period of several years we will see that there are fluctuations due to changes in atmospheric pressure, winds, ocean currents and sea surface temperature that can extend over years, decades or longer and that mean sea level can therefore only be defined for the period over which the observations are made. This makes things a bit difficult for tasks such as national surveys which are often tied to a datum known as mean sea level. Sea level will change over time, and of course mean sea level at two points along the coastline may also vary.

If there were no differences resulting from tides, oceanic currents or meteorological factors then the height of the oceans would adjust so there were no horizontal forces to cause movement of the water, leading to the formation of an equipotential surface. The water elevation at any point on the earth's surface would be controlled solely by gravitational forces, which in turn depend on the distribution of mass within the earth, and the rotation of the earth on its axis. This ideal, undisturbed equipotential surface is called the geoid, and measured mean sea level can depart from this by as much as a metre as a result of the processes noted above (Pugh, 1987). The geoid itself is always deforming or adjusting to gravitational and rotational changes so that changes in mean sea level over time cannot be thought of as a simple worldwide linear shift (Figure 3.1). Instead, sea level change at a point on a coastline over a long period of time reflects changes in the geoid as well as eustatic and isostatic changes on local, regional and global scales.

3.2.2 Modern sea level measurement

Changes in sea level can be measured directly at locations along the coast using some form of stilling well or pressure transducer and recording device (Pugh, 1987). These have been in operation at major harbours around the world for over 100 years and they provide a relatively long record of sea level history at one location. The first gauges all used a stilling well and float connected to a chart recorder and later to data loggers. Float systems are mechanical and require constant maintenance. In recent years they have largely been replaced by acoustic transducers which measure the travel time of an acoustic signal. The major limitation of these is that the travel time of the acoustic pulse is highly sensitive to the temperature gradient in the air between the sensor and the water surface. This can be overcome by replacing the acoustic sensors with radar sensors (Miguez *et al.*, 2008). Both sensors are usually deployed within a stilling well so as to filter out high-frequency wave motion and to provide a better reflective surface. All gauges require a local datum to which they can be tied elevationally and there are a number of restrictions or limitations to their accuracy due to inherent limitations in the instrumentation and to the effects of local hydraulic conditions. One problem is to correct the gauges for any local vertical motion of the land at the site and this is now being partially overcome through the use of GPS (Wöppelmann *et al.*, 2007). Tide gauges provide a data base for assessing sea level rise over the last century and a comparison with data obtained from satellite altimetry (Douglas, 2001; Church *et al.*, 2006; Walton, 2007; Berge-Nguyen *et al.*, 2008). The Global Sea Level Observing System (GLOSS) provides a common set of criteria for installation of tide gauges and standards of accuracy, as well as a repository for tide gauge

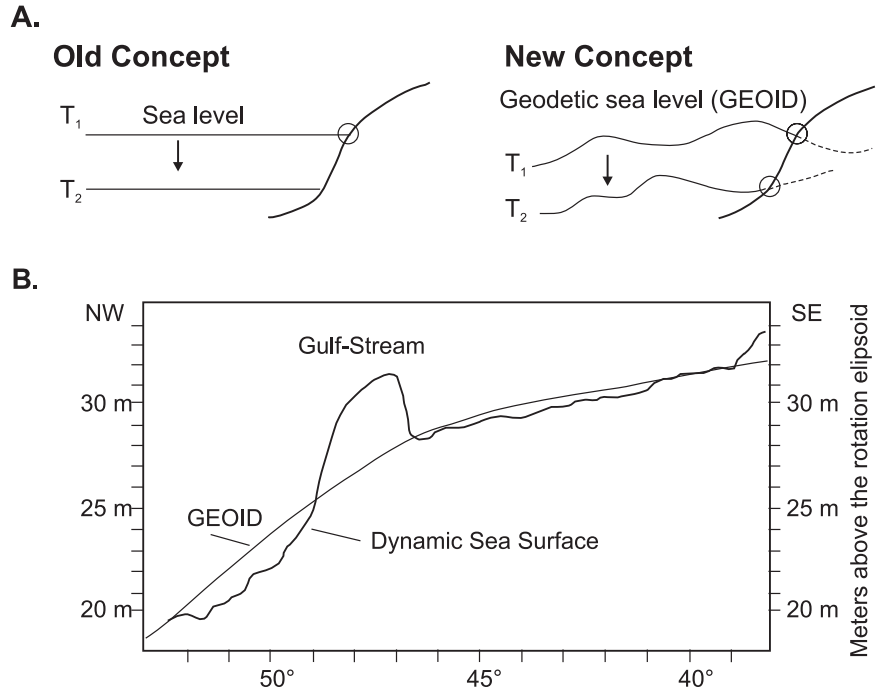

Figure 3.1 Static and dynamic concepts of sea level: (a) sketch of old concept of sea level as a simple uniform surface and sea level change expressed as a movement of this up or down versus the new concept of a dynamic geodetic surface; (b) profile across the Gulf Stream showing dynamical deviations in the sea surface from the geodetic sea surface resulting from surface water temperature (after Morner, 1987)

data from all over the world. Elevations can now be transmitted in real time and are available for some sites over the World Wide Web.

In the last three decades measurement of the elevation of the ocean surface from satellite altimetry has provided large spatial coverage of the elevation of the oceans and in particular the response to changing temperature, winds and pressure. The joint USA/France TOPEX/Poseidon and Jason-1 and Jason-2 satellites, first launched in 1992, are dedicated solely to altimetry (Pugh, 2004). They orbit the earth every 112 minutes at an altitude of 1336 km and provide continuous coverage every 9.9 days of the area equatorward of 66° latitude. They transmit a short radar pulse and measure the return pulse which, with corrections and averaging, can provide elevation with an accuracy of 2–4 cm. The radar reflections come from portions of the wave that are perpendicular to the target line and characteristic wave shapes result in a greater proportion of these occurring in the trough. The effect of this increases with increasing wave height and therefore corrections have to be made in order to get an accurate estimate of the still water level. Satellite altimetry provides a wealth of data on just how variable the sea surface is (and how difficult it is to define mean sea level).

3.2.3 Measurement of past sea level

Determination of past sea level change, locally or regionally, requires two major components: (1) the identification of some indicator or proxy that can be tied to sea level; and (2) the dating of that indicator directly or indirectly (Sutherland, 1983). Common indicators are *in situ* shells of organisms such as clams and barnacles, salt marsh diatoms, coral microatolls in lagoons, shore platforms, the base of beach ridges and coastal sand dunes, and salt marshes (e.g. Horton *et al.*, 2006; Goodwin and Harvey, 2008). In each case the relationship of the indicator to mean sea level should be known and care must be taken to account for factors such as tidal range and the

effect of exposure on the height of wave run-up. There are numerous methods available for dating sediments and organic materials (e.g. Rutter and Catto, 1995; Walker, 2005; Lamb *et al.*, 2006) In the past, dune and beach sand have been dated primarily by dating shells or driftwood thought to have been emplaced at the time of deposition of the sediments. Recent developments in thermoluminescence and optically stimulated luminescence dating now permit the sediments themselves to be dated. Once the age and elevation of the indicator has been determined, these can be compared to modern sea level. Determination of the age and elevation of a sequence of such indicators, for example a series of beach ridges or uplifted coral reefs, allows for a local sea level curve to be plotted. This approach can work reasonably well for Holocene and even Quaternary shorelines where the evidence is still relatively intact and where assumptions can be made about the stability of the land surface. It becomes increasingly problematic, except in a stratigraphic sense, beyond the Quaternary (Moucha *et al.*, 2008).

3.3 Changes in mean sea level

It is convenient to conceive of changes in the relative mean sea level at a point on the coastline as arising from two principal causes: (1) tectonic changes in the relative elevation of the land, such as those arising from plate tectonics, isostacy, deformation of the geoid and compaction of sediments; and (2) eustatic changes in the relative elevation of the ocean, caused by growth and decay of ice sheets, changes in the volume of ocean basins, changes in the geoid and changes in dynamic controls such as atmospheric pressure, winds and ocean currents. However, both sets of processes operate simultaneously and it is not always possible to separate the causes of a measured change in sea level. This becomes particularly important as we try to determine the potential effects of human-induced climatic change.

3.3.1 Tectonic changes in sea level

Tectonic changes in sea level occur because of crustal movements related to local, regional and global tectonic activity. Over long periods of geologic time uplift or subsidence can occur, particularly along plate margins. In areas of active plate tectonics changes in the elevation of the land occur along earthquake zones leading to uplift in some areas and subsidence in others. One area where this is currently occurring is in the eastern Mediterranean along the Hellenic Arc (Pirazzoli, 1987). Along the western part of the island of Crete periods of rapid subsidence between 4000 and 1700 BP led to the formation of a series of stepped shorelines. Around 1530 BP sudden uplift of about 10 m occurred in a single event leading to emergence of all of the older Holocene shorelines (Pirazzoli, 1987). On the Pacific coast of central and south-western Japan, which is located on the subduction zone at the contact between the Philippine Sea plate and the Asian plate, the maximum height of the last interglacial shoreline dated around 125 000 BP is about 200 m and that of the post-glacial shoreline dated at 6000 BP is around 30 m (Ota and Machida, 1987). In active tectonic zones rapid uplift or subsidence can occur along relatively short segments of fault lines associated with individual earthquake events. Thus, Ota and Machida note uplifts of 2 m for an earthquake in 1923 and 6 m for an earthquake in 1703 in one region of the Pacific Coast. The highest rates of uplift have been recorded for the Huon Peninsula in New Guinea where a series of raised reefs have been dated (Chappell, 1974; Bloom *et al.*, 1974). Uplift rates here range from 0.07–0.33 m per century.

Of particular interest in areas that have been glaciated or are close to them is the effect of isostatic adjustment of the crust to loading and unloading. The basic concept of isostatic adjustment to loading and unloading is well known, particularly with respect to the growth and melting of Pleistocene ice sheets. In the simplest sense, the weight of ice in a large glacier or ice sheet depresses the crust locally causing material in the upper mantle to flow outward away from it. When the ice melts and the weight is removed material in the mantle flows in and uplift of the crust occurs. The amount of depression is related directly to the thickness of the overlying ice and the rate of rebound can be predicted from models based on the rheological properties of the upper mantle.

In a sort of circular argument, models of the rheology of the upper mantle can be tested against rates of uplift and estimated ice thickness, rates of crustal uplift or subsidence can be predicted based on ice thickness and rheology, and estimate of ice thickness can be estimated from the models and known rates of uplift (e.g., Tushingham and Peltier, 1991; Tushingham, 1991; Dyke, 1998; Hagendoorn *et al.*, 2007). Associated with crustal loading and depression under an ice sheet is a marginal bulge or uplift around the margins of the ice sheets resulting from the inflow of material displaced from under the ice sheet. This bulge may have extended 800–1000 km south of the main glacial limit along the east coast of North America and the west coast of Europe. When the ice sheets melted and retreated, this bulge collapsed leading to subsidence along the margins. The east coast of Nova Scotia and the Scotian Shelf is one such area (Quinlan and Beaumont, 1981; Scott *et al.*, 1987) and this probably accounts for a large part of the relatively high (0.37 mm a year) present rate of sea level rise recorded at Halifax Harbour.

The rate of rebound associated with unloading of the crust as the ice melts is typically very rapid in the first few thousand years, with very little rebound occurring beyond 10 000 years. Plots of uplift versus time for shorelines on Devon Island in the eastern Arctic (Dyke, 1998) generally show an exponential form , though in areas where there were major fluctuations in the rate of ice sheet melting, or even periods of significant advance, the curves are more complex (Lohne *et al.*, 2007).

In areas near the southern limits of the continental ice sheets in North America and Western Europe isostatic uplift occurred simultaneously with the most rapid phase of sea level rise during the Holocene transgression. As a result, there was a rough balance between uplift and drowning and thus little evidence of the isostatic rebound in the form of raised beaches. However, in northern areas such as the Canadian Arctic and northern Scandinavia, where major ice cover persisted past 10 000 BP, much of the isostatic uplift occurred near the end of the Holocene transgression, resulting in the preservation of shorelines at altitudes >100 m above the present shoreline. In these areas

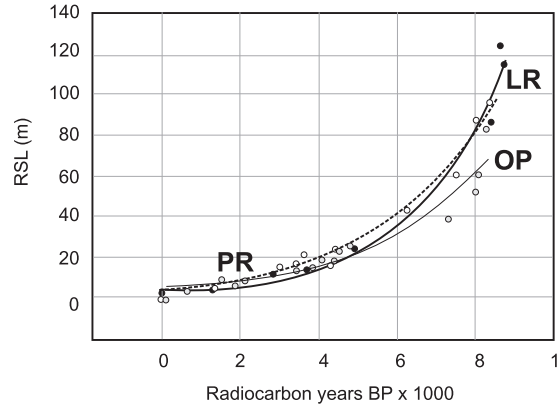

Figure 3.2 Relative sea level data for three sites on Devon Island, eastern Arctic Canada showing exponential decrease in the rate of isostatic uplift: Lyell River (LR), Port Refuge (PR) and Owen Point (OP) (Dyke, 1998).

isostatic uplift is still occurring at rates >0.25 m a century (e.g., Dyke, 1998). Isobase maps for eastern North America (Andrews, 1970) show the extent of uplift that has occurred in the area around Hudson Bay and the Canadian Arctic Archipelago over the past 6000 years (Fig. 3.3). The effects of these differences on shoreline positions in eastern Canada is shown in Figure 3.4 where it can be seen that areas such as the Scotian Shelf and Halifax have experienced submergence, with the 10 000 BP shoreline being underwater, while emergence has occurred in the northern Gulf of St Lawrence (Grant, 1980).

The presence of numerous dated lake shorelines and a network of lake level gauging stations have provided a data base for assessment of rheological response of the earth to deglaciation (Tushingham, 1991). Present rates of uplift in the Great Lakes area (Tushingham, 1992 – Figure 3.5) show an increase to the north and east, reflecting decreasing time for unloading since the retreat of the Wisconsinan ice. A key factor for ongoing shoreline evolution in the lakes is the relationship between the present rate of isostatic uplift of a point on the shoreline relative to the rate of uplift at the exit to the lake. On Lake Erie present isostatic uplift is negligible, but on Lake Ontario uplift near the exit to the St Lawrence River east of Kingston is higher than at the west end of the lake, leading to a slow transgression of the shoreline

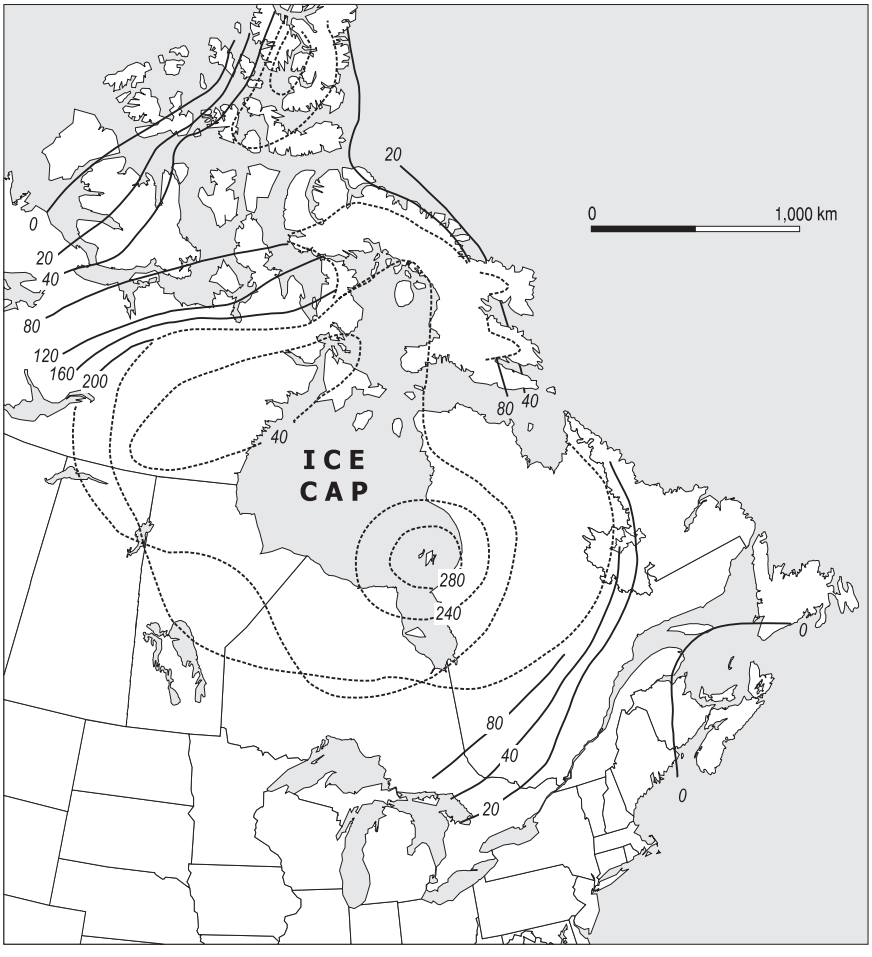

Figure 3.3 Isobase map for the region around Hudson Bay showing emergence since 6000 BP (m). The dashed line indicates the extent of ice cover (Andrews, 1970).

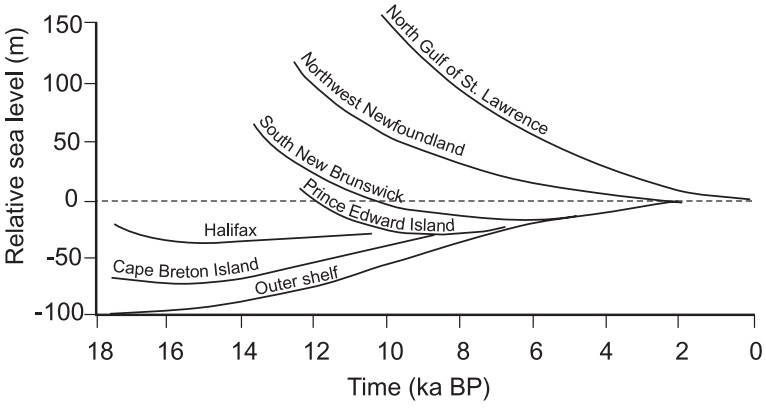

Figure 3.4 Changes in relative sea level in eastern Canada reflecting differences in the rate and amount of isostatic uplift and the timing of deglaciation (Grant, 1980).

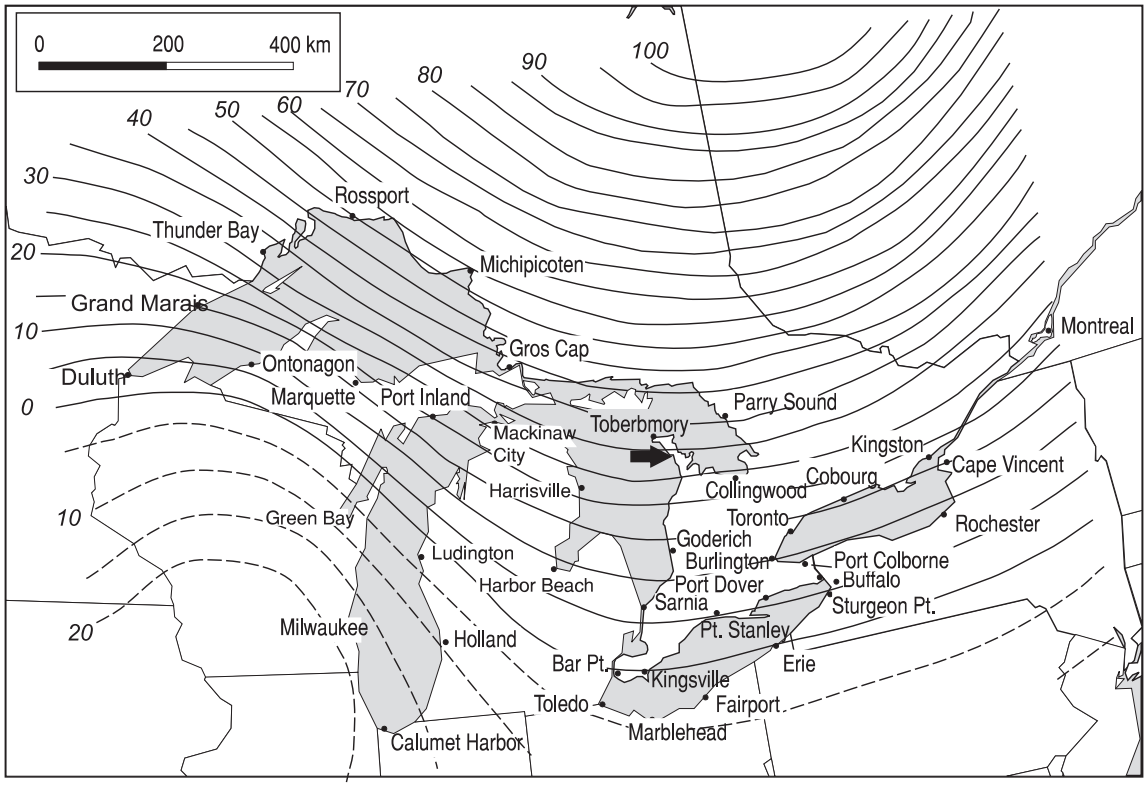

Figure 3.5 Present-day postglacial uplift (cm/century) for the Great Lakes region as predicted by the model ICE-3G (Tushingham, 1992). The arrow marks the location for the point graphed in Figure 3.6.

around Toronto and the mouth of the Niagara River (Figure 3.5). On Lake Huron and Georgian Bay almost all areas are rising relative to the outlet at Sarnia, but southern Lake Michigan is experiencing some drowning. On Lake Superior the contours of isostatic uplift are aligned northwest–southeast so that areas west of Thunder Bay, including most of the US shoreline, are rising more slowly than the exit at Port Iroquois and thus are experiencing drowning (Figure 3.5). These differences help to explain why cottage owners along some of the shorelines are experiencing increased flooding and erosion and are calling on governments to reduce lake levels while others are having difficulty accessing their boat docks and would like to see the levels raised.

The effects of isostatic adjustment as well as the timing of exposure of drainage outlets to the lakes during retreat of the last ice sheet has produced a complex series of lakes and lake levels in the basins over the past 14 000 years. The lake level curve for Lake Huron and Georgian Bay (Figure 3.6) shows initial inundation associated with glacial Lake Algonquin as ice to the north and east blocked flow to the Ottawa Valley area, while the southern exit was relatively high because isostatic uplift had already been underway there for some time (Lewis, 1969). Once retreat of the ice from the Ottawa Valley occurred these areas were still isostatically depressed so water flowed eastward into the Ottawa area and thence to the St Lawrence River leading to a rapid drop in lake level to the low stands of Lake Hough. As isostatic uplift occurred, the elevation of the eastern outlets increased leading to an increase in the lake level during the Nipissing transgression, reaching a high stand at the Lake Nipissing stage about 5500 BP (Figure 3.6). At

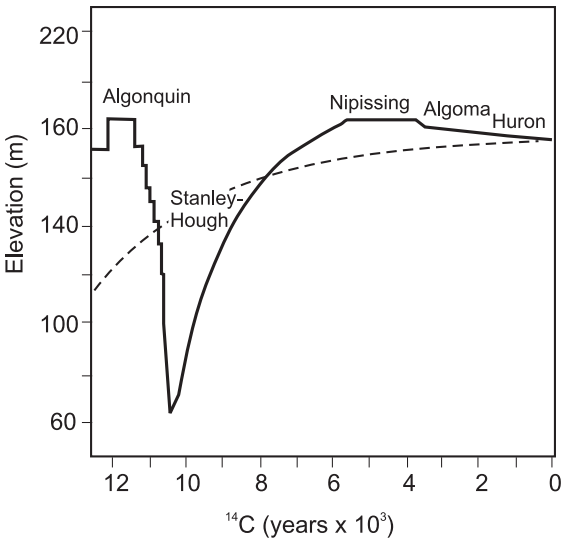

Figure 3.6 Postglacial lake levels in the Huron Basin (after Lewis, 1969). The dashed line shows the elevation of the modern shoreline near Red Bay on the west coast of the Bruce Peninsula in Ontario – see Figure 3.5 for location.

this time flow to the east ceased, and the exit through the St Clair River to Lake Erie and on to the St Lawrence River was restored. Since then lake levels have fallen slowly due to erosion of the outlet. Interestingly, the magnitude of the Nipissing transgression in lakes Michigan and Huron is similar to that on ocean coasts and the high stand is marked by transgressive barriers and high dune systems along many parts of southern Georgian Bay, southern Lake Huron and Lake Michigan (Davidson-Arnott and Pyskir, 1989; Hansen *et al.*, 2006).

Also associated with the growth and decay of continental ice sheets is the process of hydro-isostacy. The loading of the ocean basins by the increased water depth coming from ice sheet melting should result in a depression of the ocean floor by about 4 m. However, in areas with a wide continental shelf the effect is more noticeable, and this may account for a small portion of the high RSL rise noted for Halifax, Nova Scotia.

Local depression of the crust along the coast can also occur as a result of the accumulation of large amounts of sediment such as occurs in deltaic areas. Evidence from the Mississippi Delta (Fairbridge, 1983) suggests that the much of the subsidence here is due to isostatic loading of the sediments deposited onto the continental shelf, but in all deltaic environments the effects of compaction of the sediments must be taken into account as well. Recent estimates of sea level rise in the Mississippi Delta complex based on tide gauge analysis give values >1 m per century (Penland and Ramsey, 1990), of which three-quarters is probably due to subsidence.

3.3.2 Eustatic changes in the level of the sea

The term eustacy is applied to all changes of sea level resulting from changes in the volume and distribution of water in the ocean basins. These changes can arise from: (1) changes resulting from the growth and decay of ice sheets (glacial eustacy); (2) changes in the volume of the ocean basins (tectono-eustacy) arising from plate tectonics and continental drift as well as sediment infill and hydroisostacy; and (3) changes in ocean mass/level distribution arising from changes in the earth's rotation, tilt, gravitational distribution, etc. (geoidal eustacy).

The greatest impact on modern shorelines has come from fluctuations during the Quaternary associated with the growth and decay of ice sheets. Throughout the Quaternary sea level fell during the time that continental ice sheets grew in size and it rose during interglacial periods when the ice sheets melted (Figure 3.7a). During the warmest part of the last interglacial sea level was about 2–3 m above the present level (Hearty *et al.*, 2007). At the height of the Wisconsinan glacial period, sea level averaged over all the ocean basins was on the order of 110–130 m below its present level (Peltier and Fairbanks, 2006). The impact of this was particularly important in areas beyond the glacial limits where large areas of the continental shelves were exposed. Melting of the ice sheets, which began about 20 000–25 000 BP, led to an increase in the volume of water in the oceans and produced the Holocene transgression in many parts of the world (Figure 3.7b). The actual sea level history along any specific coast will vary from this because of other factors such as isostatic uplift and local tectonic factors examined in the

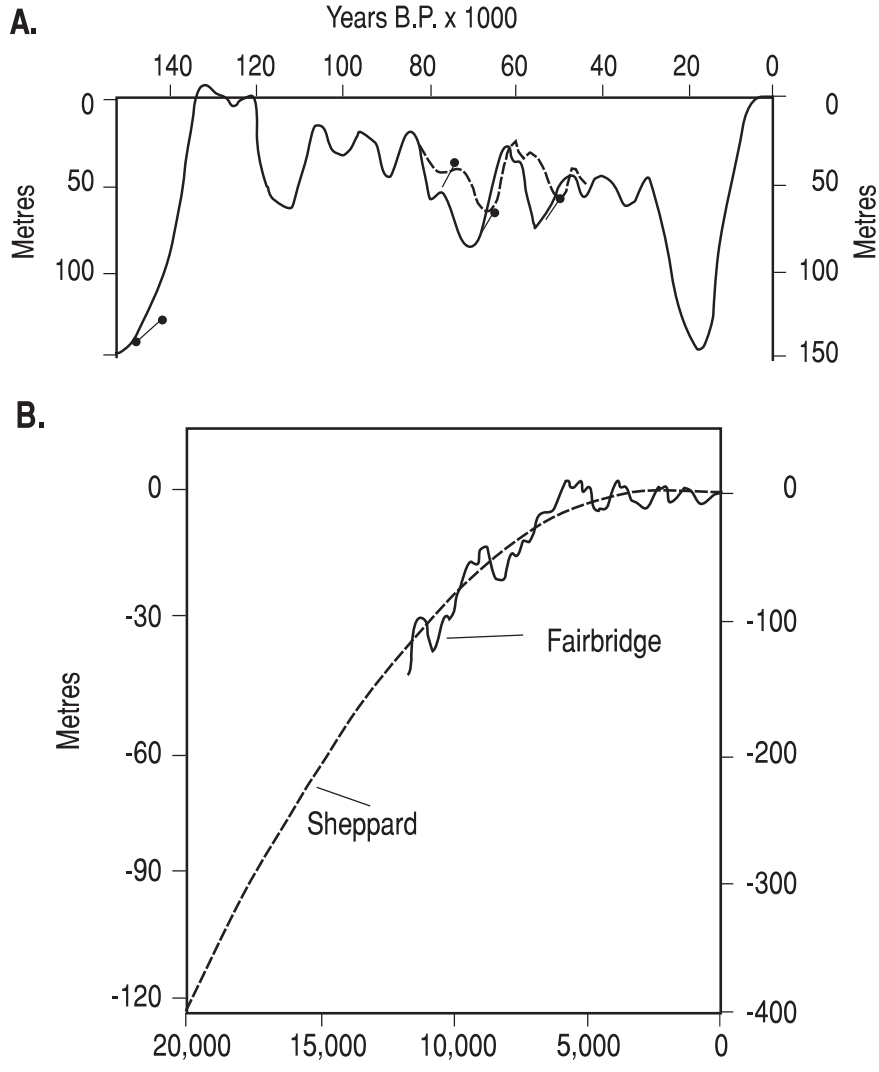

Figure 3.7 Changes in sea level. (A) Sea level changes over the past 15 000 years in the Australian region based on New Guinea shoreline data and deep sea cores (Chappel, 1987); (B) generalised postglacial eustatic sea level curves put forward by Fairbridge (1961) and Sheppard (1963) (Fairbridge, 1983).

previous section as well as changes in the geoid. However, most modern shorelines in the middle and low latitude reflect the impact of a large rise in sea level which brought with it transgression of the shoreline accompanied by a reworking of sediments deposited on the exposed shelf. These sediments are often stored in large barrier and dune systems such as those found along much of the east coast of North America and Australia. The evidence suggests that this transgression came to an end in most areas between 4000 and 6000 BP, or at least that the rate of RSL rise decreased markedly (Figure 3.7b). Evidence from a number of coasts suggests that sea level at the end of the transgression may have been 1–2 m above the present MSL. Hesp *et al.* (1996) suggest that sea level in Singapore peaked about 5000–6000 BP at a level 2–3 m above the present and they attribute the subsequent fall in sea level to hydroisostatic response of the shallow surrounding continental shelf to loading by the rising water.

It is likely that there were fluctuations on several time scales in the rate of sea level rise as a result of climatic cycles which tended to speed up or reduce the amount of melting, so that the curve should show oscillations as suggested by Fairbridge rather than the smooth form of the Sheppard curve (Figure 3.7b). In particular, large pulses of water leading to rapid sea level rise may have played a significant role in the drowning of coral reefs and barrier islands on the outer edge of continental shelves (Chappell *et al.*, 1996). However, at specific sites it is often difficult to separate fluctuations at this time scale from local isostatic or geoidal effects.

The rapid rise in sea level to about 5000 BP must have had an impact on Palaeolithic humans living along the coast over much of the tropical and temperate world. Some of the impacts of rapid transgression and the separation of Britain from the continental mass of Europe are now quite well documented (e.g. Coles, 2000; Turney and Brown, 2007). Recent unravelling of the sea level history of the Sea of Marmara (Eriş *et al.*, 2007) and the Black Sea (Ryan *et al.*, 1997; Ballard *et al.*, 2000) and the discovery of drowned settlements along the paleoshoreline have provided exciting opportunities for linking coastal processes and human history, and may provide a plausible origin for legends of the Great Flood.

The landward displacement of the shoreline associated with the Holocene transgression means that most coastlines world-wide are relatively young and adjustments to the transgression are still taking place. There is now evidence of a decrease in the amount of sediment in the littoral system as it becomes locked up in dunes and barriers. River deltas have changed locations and estuaries are gradually infilling, while in tropical areas coral reef growth has now largely stabilised.

3.4 Astronomical tides

3.4.1 Tides and coastal processes

Along ocean coasts tides produce a regular daily rise and fall of sea level that may range from a few decimetres to as much as 15 m in a few places. These fluctuations are termed astronomical tides because they are produced by the gravitational influence of the moon and sun, and this distinguishes them from other short-term changes in sea level produced, for example, by strong winds or changes in barometric pressure which are sometimes termed meteorological tides. Tidal fluctuations are very important in all aspects of the coastal zone and they affect physical processes such as the shoreward extent of wave action and the flushing of waters in estuaries, lagoons and bays; biological activities such as the zonation of plants and the feeding activities of birds, fish and other marine organisms; and chemical processes such as those associated with the wetting and drying of intertidal rock surfaces. The intertidal zone – the zone located between the high and low tide lines – may be only a few metres wide on steep coasts with a low tidal range, and hundreds of metres wide on gently sloping coasts with a high tidal range. The tidal range greatly affects the form and width of sandy beaches, and thus the source area for coastal sand dunes. The flow of water into and out of inlets connecting lagoons and bays to the open ocean maintains the openings and permits the exchange of water and nutrients. The rise and fall of the tides across the intertidal zone creates stresses for some organisms but at the same time the variability creates a variety of rich and diverse habitats such as intertidal pools and saltmarshes.

The tides ultimately owe their origin to the gravitational forces of the moon and the sun. These affect all objects on earth, but the response is most easily seen in the oceans because the deformation of the surface is large enough to be seen (tides can be measured in large lakes but the response is only a matter of a few millimetres up to a couple of centimetres for large lakes such as Lake Superior). The association of the regular rise and fall of the tides with the moon has long been recognised – Pytheas, a Greek navigator and astronomer, wrote about the relationship between the position of the moon and the height of the tide around 300 BC. In Western Europe tidal predictions for the time of high tide at particular ports were available as early as the thirteenth century (Macmillan, 1966). In

the seventeenth century Isaac Newton, building on developments in astronomy and his own development of gravitational theory, developed the equilibrium theory of tides which related the tide generating forces to the gravitational pull of the moon and the sun.

The equilibrium theory of tides provides a rough explanation of tides and the ability to predict their timing and height. Some of the observed discrepancies between observations and predictions can be attributed to the effects of land masses and the shape and slope of the coastline. However, some of the discrepancies arise from the need to account for the forces involved in the actual movement of the fluid mass of water in the tidal waves – i.e. the dynamical movement of the ocean – and accounting for this as well as the initiating gravitational forces gives rise to the modern dynamic theory of tides.

We will look first at some examples of the characteristics of tides before coming back to a description of the forces that give rise to those characteristics.

3.4.2 Characteristics of tides

Tides are simply a regular oscillation in water level on a daily basis with the highest level being termed high tide and the lowest level low tide. However, the range of that oscillation varies both spatially over the world and temporally at one location on the coast, as is evident from a comparison of the predicted tides for four locations over a one month period (Figure 3.8). At each station the key characteristics are: (1) the number of cycles in a day – the tidal type; (2) the variation in tidal elevation over a two week period – the spring-neap cycle; and (3) the difference in elevation between high and low tide – the tidal range.

The relative motion of the moon and the earth, the lunar day, takes 24 hours and 50 minutes so that the moon rises 50 minutes later every day. Because the moon is the most

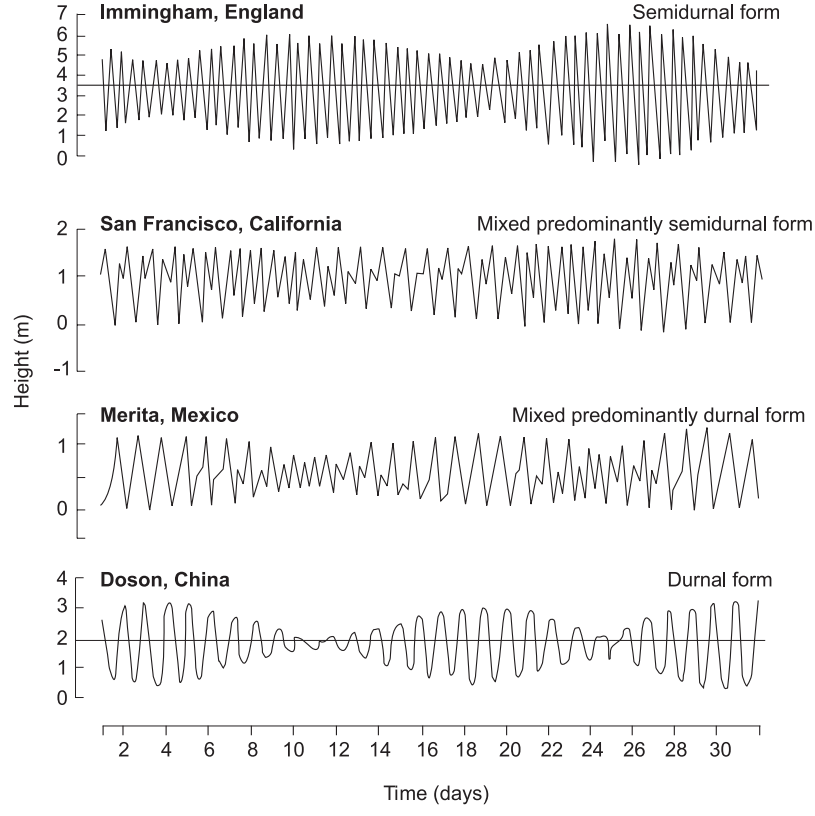

Figure 3.8 Examples of tidal curves for one month showing each of the major tidal patterns (after Defant, 1962).

important of the tide-generating controls, it is the lunar day that is the primary control on the tidal cycle (Figure 3.8). In some locations there is a single tidal cycle over the lunar day giving rise to a diurnal tide. In other locations there are two such cycles every day, giving rise to a semi-diurnal tide. In other areas elements of both the diurnal and semi-diurnal are present, producing a mixed tidal form which may be mixed semi-diurnal where the semi-diurnal component is dominant or a mixed diurnal where the diurnal component dominates. Diurnal tides occur primarily along the coast of Antarctica and the Indian Ocean and in parts of the eastern Arctic Archipelago (Figure 3.9). Semi-diurnal tides are common along much of the Atlantic and Arctic coasts and mixed tides are common in the northern Pacific.

All of the tidal curves in Figure 3.8 show a distinct variation in the amplitude of the tidal fluctuation that occurs over a period of a fortnight (two weeks). This is related to the relative positions of the two tide generating forces of the sun and the moon. As we will see later, the moon and the sun each produce two tidal waves. When the sun and the moon are aligned in a straight line as they are at the full and new moons (Figure 3.10) then these two waves are in phase and reinforce each other, producing higher high tides and lower low tides. When the sun and moon are aligned at right angles to each other, as they are at the first and third quarter, then the tidal waves are out of phase and tend to cancel each other. Because the solar component is much smaller than that of the lunar component it does not fully cancel it, leaving a diminished lunar tide. Tides with the largest range, which occur at the full and new moons, are termed spring tides while those with a lower range associated with the first and third quarters of the moon are termed neap tides. The neap tidal range is on average about 40% lower than that of the spring tide.

The difference between the elevation of high and low tide is the tidal range and it controls the excursion of the water level on the coastline. The average tidal range at spring tides can be used as an important shoreline descriptor and it ranges from <0.5 m in enclosed seas to over 15 m in a few elongate estuaries and embayments. On the basis of the spring tidal range, Davies (1964) classified shorelines into:

Microtidal, <2 m; Mesotidal, 2–4 m; Macrotidal, >4 m.

Figure 3.11 shows the worldwide distribution of tidal range. Microtidal and mesotidal ranges

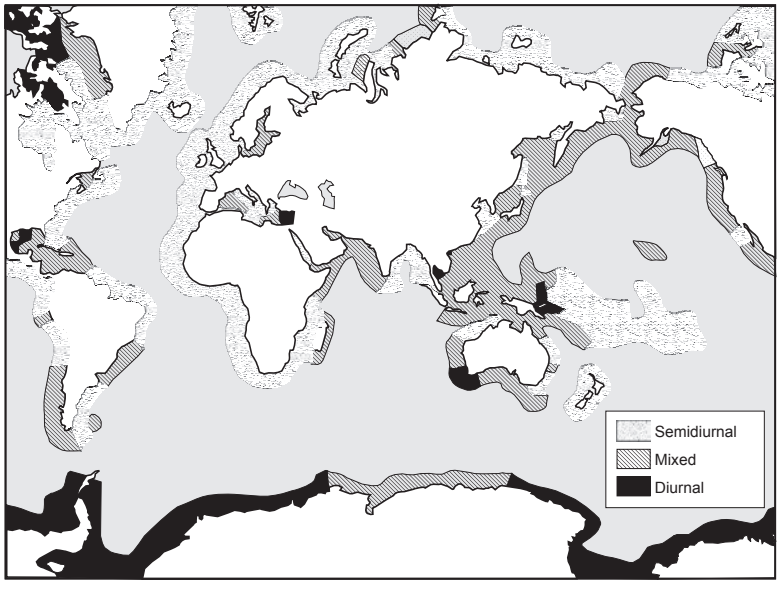

Figure 3.9 The distribution of tidal types around the world (Davies, 1972).

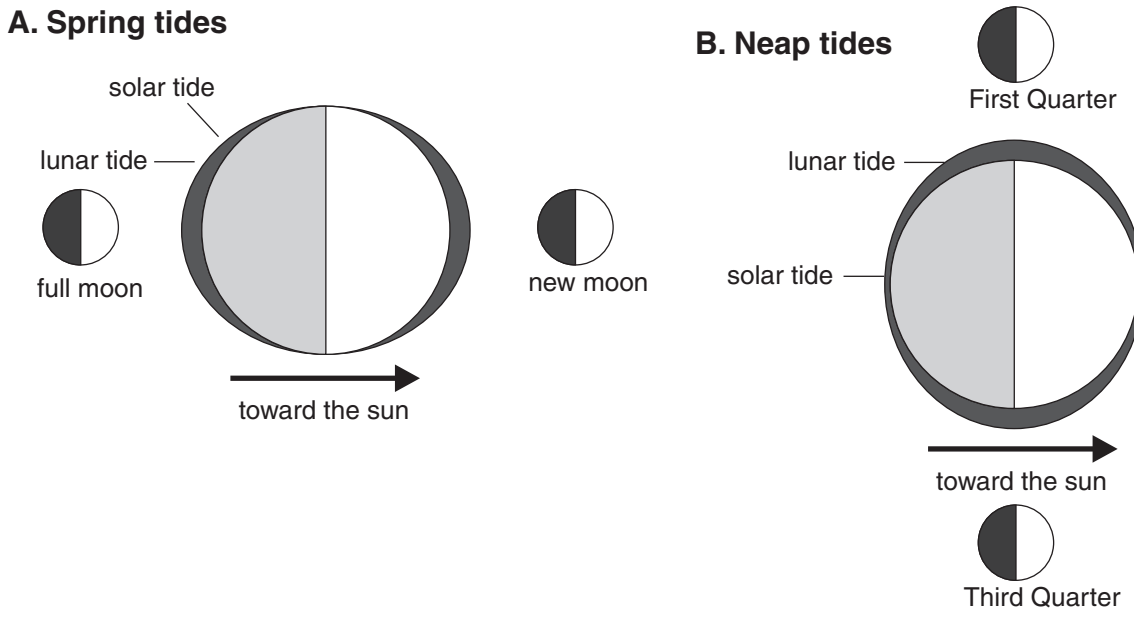

Figure 3.10 Relative positions of the sun, moon and earth during spring and neap tides.

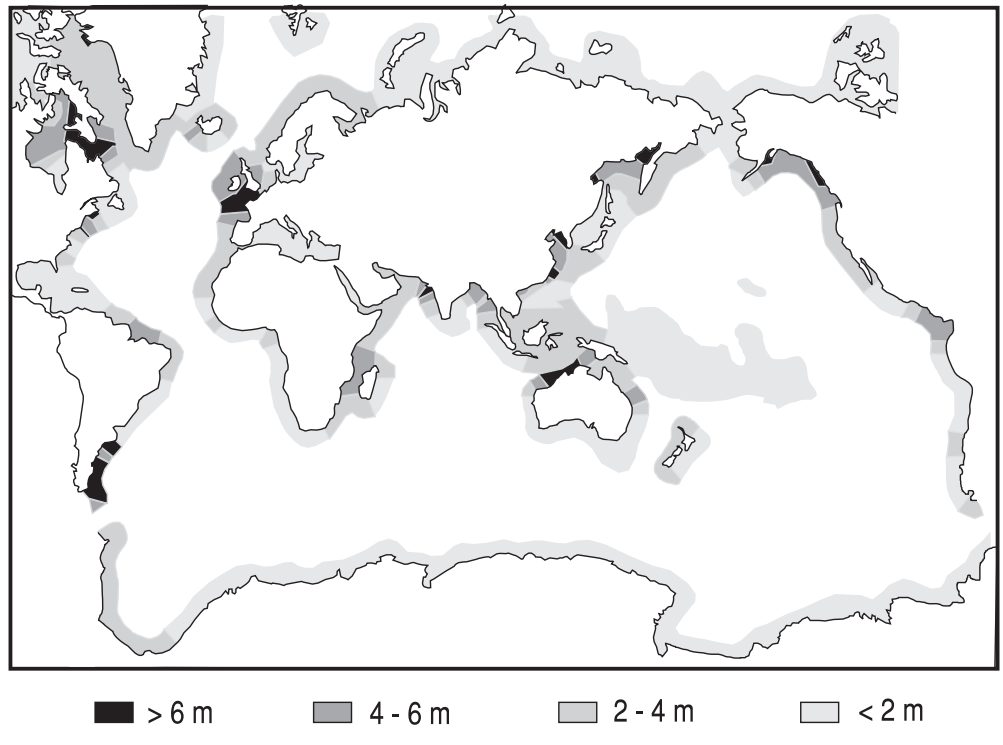

Figure 3.11 World distribution of tidal range (Davies, 1964).

generally occur on the open coasts of the world oceans as well as the enclosed seas such as the Mediterranean, Baltic and Gulf of St Lawrence. Macrotidal areas occur primarily in embayments and areas with shallow continental shelves such as around the British Isles, parts of the Canadian Eastern Arctic Archipelago and north-west Australia. In a few locations such as the Severn estuary in England and the Bay of Fundy, spring tidal range can exceed 12 m. Because the macrotidal designation encompasses such a wide range it may be useful to distinguish between macrotidal areas with a range of 4–8 m and high macrotidal areas with a range >8 m (e.g. Schostak *et al.*, 2000). Alternatively, Leroy *et al.* (2000) suggest the term megatidal, but this may be confusing because mega has a specific meaning as a numeric prefix.

3.4.3 Equilibrium theory of tidal generation

Newton's theory of gravity predicts that gravitational force is a function of the mass of the two bodies and inversely proportional to the distance between them:

$$F = \frac{Gm_1m_2}{R^2} \tag{3.1}$$

where F is the gravitational force; G is the universal gravitational constant; m_1, m_2 are the masses of the two bodies respectively; and R is the distance between the two bodies.

Thus, while the mass of the sun is very much larger than that of the moon, this is offset by the closer proximity of the moon to the earth. According to Newton's predictions the influence of the sun should be a bit less than half that of the moon and it is actually about 0.46. The gravitational effects of the sun and moon on tide generation will vary with astronomical factors that control the phase relationships between the sun and the moon, variations in their distance from the earth, and variations in their declination or position over the earth. Thus, the equilibrium theory of tides is based on a complete understanding of these astronomical factors controlling the gravitational forces.

If we consider an earth covered entirely by water then the water particles everywhere on the surface will be acted on by the combination of the earth's gravitational force, the gravitational force of the moon, and the centripetal or inertial force generated by the rotation of the earth–moon system. The earth–moon system rotates about a common centre of mass which, because of the much greater mass of the earth, is actually located within the earth (Figure 3.12). The small inequality of the vertical gravitational pull of the moon is opposed by the gravitational pull of the earth and would have only a negligible effect on the water surface. However, the tangential force is not opposed by any counterbalancing force and thus tends to accelerate the water surface towards a point directly opposite the moon. This generates a sloping water surface that would tend to grow until the pressure gradient associated with the sloping surface of the tidal wave balances the tangential acceleration (Figure 3.13). This accounts for the bulge facing the moon. On the side of the earth opposite to that of the moon there is a similar tangential stress produced because the gravitational pull of the moon is slightly smaller, thus giving rise to an excess tangential centripetal force which produces the second bulge in the water surface.

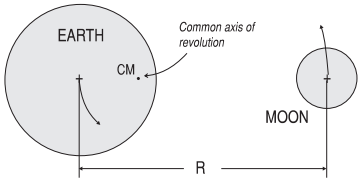

Figure 3.12 The earth/moon system and centre of rotation.

Rotation of the earth on its axis leads to the movement of the tidal bulges around the earth in the form of ('true') tidal waves (Figure 3.13). Similar reasoning can be applied to the gravitational effect of the sun but the tidal wave formed by the sun is much smaller than that of the moon because of its smaller gravitational force. Thus, on an earth uniformly covered with water, both the moon and the sun will generate tidal waves which travel around the world from east to west. As the position of the moon relative to the equator changes, the orientation of the tidal bulges is no longer centred on the equator but at an angle

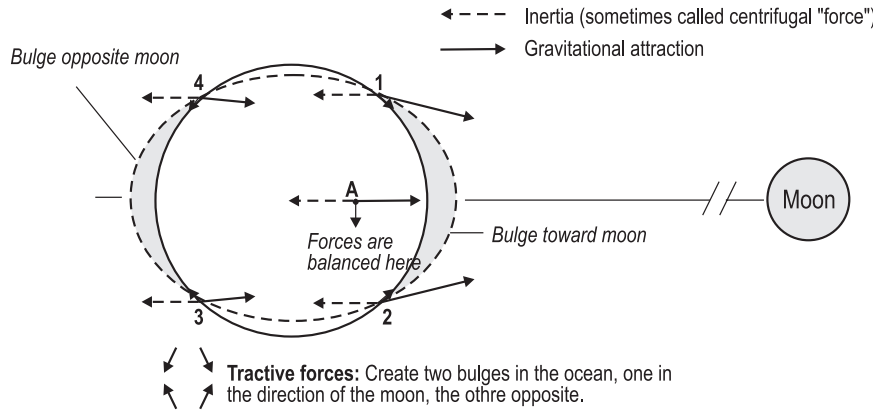

Figure 3.13 Inertial and gravitational forces acting on the earth surface to produce tides. On the side facing the moon the tangential gravitational forces exceed the inertial forces resulting in a convergence of water to a in line with the moon. On the opposite side of the earth the gravitational forces are slightly weaker than the inertial forces resulting in a convergence to a point opposite the moon. Rotation of the earth results in the rotation of these two 'bulges' producing two high and two low tides every sidereal day of 24 hours and 50.47 minutes.

to it and the result is to produce an inequality in the range of the two diurnal tides which depends on the latitude of the point of observation. An example of this can be seen in a plot of the forecast high tide level for Peck's Point located at the entrance to the Cumberland Basin, Bay of Fundy, Canada over a period of several days around spring tide (Figure 3.14). In this case forecast high tides at night are about 0.4 m higher than those occurring during the day.

Any other factors which affect the relative position of the sun and moon with respect to the earth's surface or the distance from the two bodies will result in variations in the gravitational force and thus in the tidal range. Thus, the spring tidal range tends to be greatest around the equinoxes (March 21 and September 21). Variations in the distance between the earth and the moon or sun also produce variations in the tides. The distance between the earth and the moon varies by about 25 000 km between their closest point (perigee) and their farthest point (apogee), producing a 30% variation in the lunar component of the semi-diurnal tide (Figure 3.15). Because one complete cycle from perigee to succeeding perigee takes 27.6 days the heights of the two sets of spring tides within one month will usually be different. Over an 18.6 year nodal period the maximum lunar monthly declination

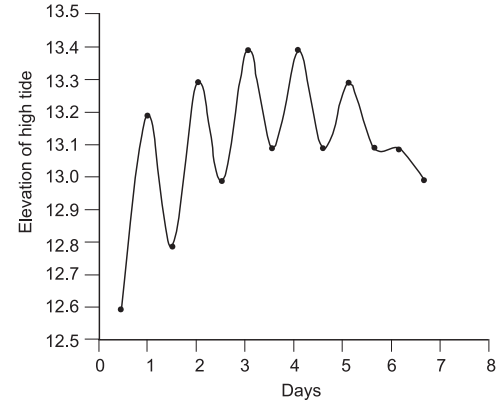

Figure 3.14 Plot of forecast high tides for several days around spring tide at Peck's Point, Bay of Fundy showing a diurnal variation of about 0.4 m between higher high tide and lower high tide.

varies from 18.3° to 28.6°. Minimum and maximum values occurred in March, 1996 and June 2006 respectively and the next ones are forecast for October 2014 and January 2022. The effect of this is proportional to tidal range and its effect is generally small except in macrotidal areas. Over a period of time there are occasions when extreme tidal forces occur as a result of the coincidence of several factors that produce large tides – when the sun and moon are in line with the earth and

Table 3.2 *Name, notation, period and relative amplitude of the main periodic contributions to tidal generation (Carter, 1988).*

Species	Notation	Period (hours)	Relative amplitude (%)	Description
Semi-diurnal	M2	12.42	100	Main lunar
	S2	12	46.6	Main solar
	N2	12.66	19.1	Moon's distance
	K2	11.97	12.7	Moon and sun relative distance
Diurnal	K1	23.93	58.4	Soli-lunar
	O1	25.82	41.5	Lunar diurnal
	P1	24.07	19.3	Solar diurnal
Fortnightly	Mf	330	17.2	Lunar phase
Monthly	Mm	661	9.1	Lunar monthly
Solar semi-annual	Ssa	4385	8	Seasonal solar
Solar annual	Sa	8759	1.3	Annual solar
Nodal		163 024	0.1	Moon orbital

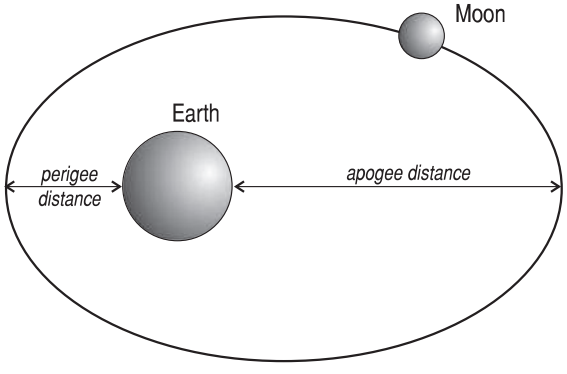

Figure 3.15 The effect of changes in the distance of the moon from the earth on tidal forces.

at their closest respective distances (Pugh, 1987). For maximum semi-diurnal tides the moon and the sun should have zero declination.

Each of the astronomical factors described above produces a periodic variation in tidal forces and thus in tidal amplitude. The period or frequency is determined by return frequency of the particular condition and the amplitude will vary with the strength of the force and with location on the earth's surface. The equilibrium tide at any point on the earth surface can therefore be predicted by summing all of the periodic components. In practice, the phase and amplitude of each will vary over the earth's surface but can be extracted from harmonic analysis of tide gauge records at a station and then used for future predictions. The most important harmonic tide generating components are given in Table 3.2.

3.4.4 Dynamic theory of tidal generation

There will be differences between the time and amplitude of measured tides at a location from those predicted solely from consideration of astronomical factors. Leaving aside sea level changes due to meteorological factors, these differences arise from a number of factors that influence the propagation of the tidal waves around the oceans, including the irregular distribution and shape of land masses on the earth's surface, the interaction of the tidal waves with the ocean bed and the land margins, the effects of inertia of the water mass and the coriolis 'force' produced by rotation of the earth.

In the open ocean the tidal waves would have a wave length on the order of 20 000 km and a period of a bit over 12 hours – these waves are thus shallow water waves everywhere on the earth's surface (depth of the ocean is <0.5 of the wavelength – see Section 5.2.2). Frictional drag on the bed leads to loss of energy, and shoaling and refraction affects the speed and direction of propagation. This becomes particularly important when the tidal wave travels over extensive continental shelves.

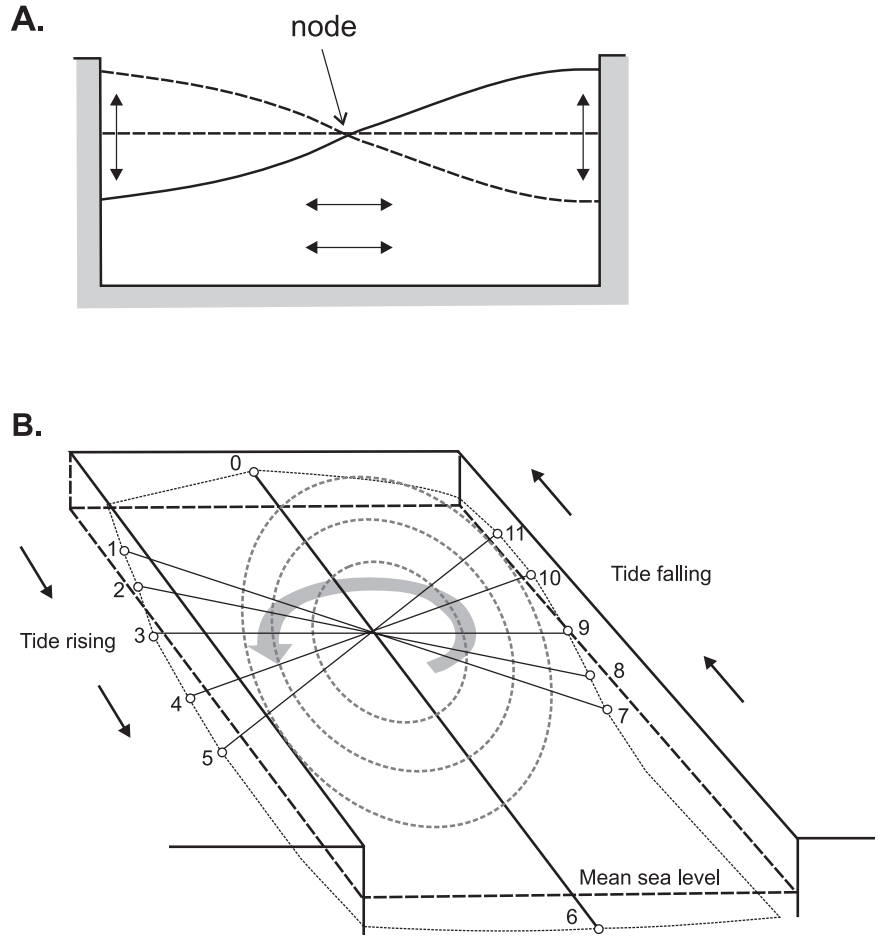

Figure 3.16 (A) Vertical and horizontal motions associated with a standing wave in a closed basin; (B) sketch of the progression of a tidal wave anticlockwise around an amphidrome in the northern hemisphere. The radial lines are co-phase lines which mark equal arrival times while the circles are co-range lines which mark areas with equal amplitude. The crest of the tidal wave (high tide) is at 0 and so at points 1–5 the tide is rising and conversely the trough of the wave is at 6 and at points 7–11 the tide is falling.

In practice ideal tidal waves racing freely around the earth do not occur. Instead, standing waves are generated within ocean basins and semi-enclosed seas and this leads to the formation of amphidromic points around which the tidal waves rotate. If we consider a tidal wave within a closed rectangular basin (Figure 3.16a), the wave will travel across the basin, reflect off the far wall and then interact with other advancing tidal waves. The result is to produce a standing wave with the highest vertical motion, or amplitudes of oscillation, at the boundaries and a nodal point where there is no vertical movement. Also associated with the standing wave is a horizontal movement of water which has its maximum excursion at the nodal point and minimum at the boundaries. Because of the coriolis effect, the water motion is deflected towards the left in the northern hemisphere, producing an anticlockwise rotation about the nodal point or amphidrome (Figure 3.16b). The movement and amplitude of the wave are depicted by co-phase or co-tidal lines which radiate outward from the centre of the amphidrome and by co-range lines which form concentric circles around it. The co-phase lines mark points of equal arrival time of the tidal stage and they can be depicted in terms of time or degrees around a circle. The co-range lines

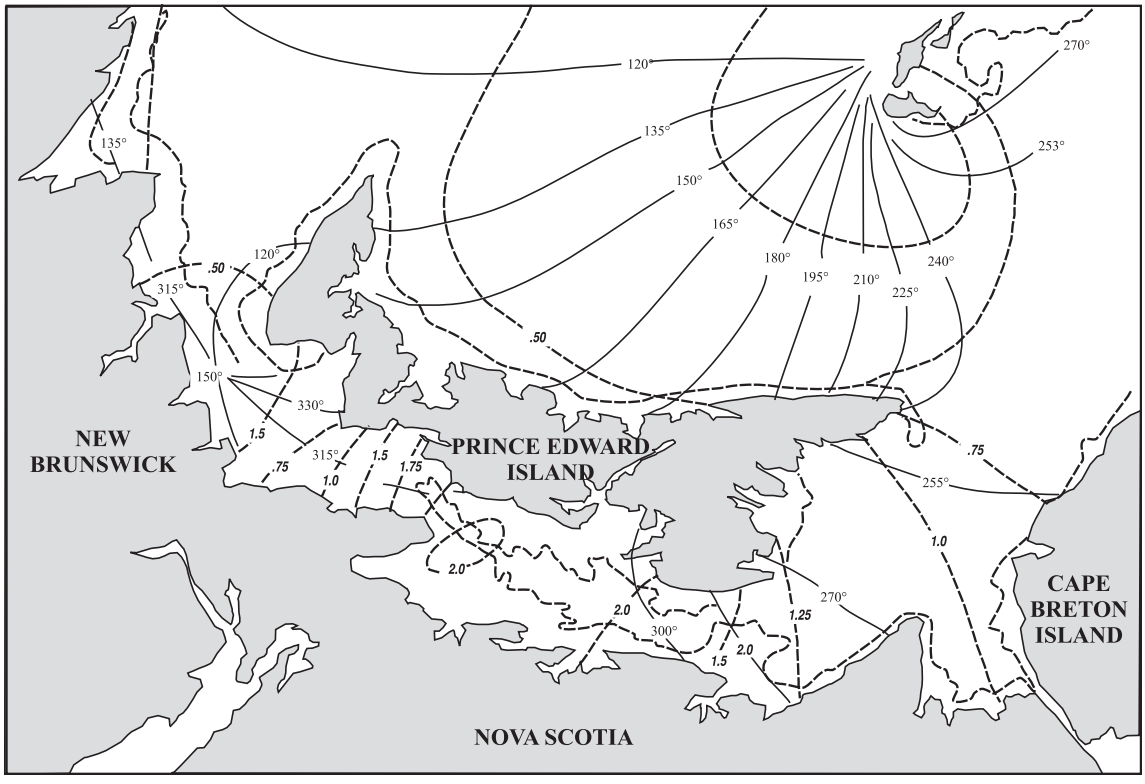

Figure 3.17 Amphidromic points and co-tidal lines for the southern Gulf of St Lawrence. The main amphidromic point off the Magdalen Islands is produced by the tidal wave which enters the Gulf through the Cabot Strait between Cape Breton and Newfoundland. A secondary amphidromic point occurs at the eastern end of the Northumberland Strait where the tide propagating around Prince Edward Island and eastward through the strait is out of phase with the next tide propagating westward through the straight (Farquharson, 1970).

join places having the same tidal amplitude and they increase in magnitude away from the centre.

There are a number of amphidromic points in the world oceans that control large-scale tidal motion and on the continental margins smaller amphidromic systems come into existence as a result of the complex interaction of tidal waves associated with these large systems and coastal topography. Examples of the smaller amphidromic systems can be seen in the Gulf of St Lawrence on the east coast of Canada (Farquharson, 1970). The tidal wave from the Atlantic Ocean enters the Gulf through the Cabot Strait, and moves anticlockwise around the coast leading to the generation of an amphidromic point near the Magdalen Islands (Figure 3.17). The tidal range increases from <0.25 m around the islands to about 2 m at the eastern end of the Northumberland Strait. A further example of the complexity of the tides in many coastal situations can be seen in the Northumberland Strait (Figure 3.17). Here the crest of the tidal wave (high tide) propagating through the eastern entrance to the strait meets the succeeding trough (low tide) propagating through the western entrance and produces a quasi-amphidromic point just off West Point, Prince Edward Island. Water motion here is not completely dampened, but the tidal range in the vicinity is <1 m and the tidal type is mixed semi-diurnal.

In elongate embayments the effects of constriction of the tidal wave, shoaling and harmonic amplification can produce extremely large tidal ranges. The Bay of Fundy is one such location and it has the highest measured spring tidal range in the world (over 16 m). The tide at the entrance to

the bay is already quite high (>3 m) because of amplification over the wide continental shelf. The bay itself is about 270 km long with an average depth of about 60 m, giving rise to a natural period of oscillation around 12.5 hours. This is very close to the semi-diurnal tide and thus resonance results in an increase in the tidal range up the basin to extreme spring tidal ranges over 15 m in the Minas Basin and Cumberland Basin. However, some portion of the increase in tidal range is due to the narrowing of the bay which results in a convergence of wave energy and thus in the height of the tidal wave.

In estuaries, and river mouths entering bays with a large tidal range a tidal bore may develop on the rising tide. The bore appears as a breaking wave that travels upstream at speeds of 20–25 km h^{-1} and is accompanied by a rapid increase in water level following its passage. Bores occur on the Petticodiac river and several other rivers draining into the upper Bay of Fundy as well as on the Severn River in England and a number of other rivers worldwide (Pugh, 1987).

3.5 Short-term dynamic changes in sea level

Changes in sea level on a time scale of hours to years or decades can result from changes in sea surface temperature, reflecting seasonal patterns of heating and cooling, as well as decadal scale changes in global pressure and wind systems such as ENSO events. Changes in the strength and/or position of major ocean currents can shift the position of areas of elevated or depressed sea level (Figure 3.1b). Finally, meteorological processes such as winds and pressure changes can produce elevated or depressed water levels along coasts. Changes in sea level close to the shoreline also result from the effects of wave shoaling and breaking – these changes are dealt with in Chapter 5.

3.5.1 Temperature, pressure and ocean current effects

There are a number of factors that contribute to dynamic fluctuations in sea level over a period of months to a decade or so (Komar and Enfield, 1987). These fluctuations are generally about 0.1–0.3 m but in some cases may range up to 1 m. Seasonal cycles occur as a result of fluctuations in barometric pressure, sea surface temperatures and changes in location of ocean currents. There is a change in sea level of about 1 cm for every 1 millibar (roughly 0.1 kPa) in atmospheric pressure. As a result, sea level responds not only to pressure changes associated with weather systems but also to seasonal changes in pressure such as those associated with the movement of the Azores High and the shifting of the Intertropical Convergence Zone (Figure 3.18).

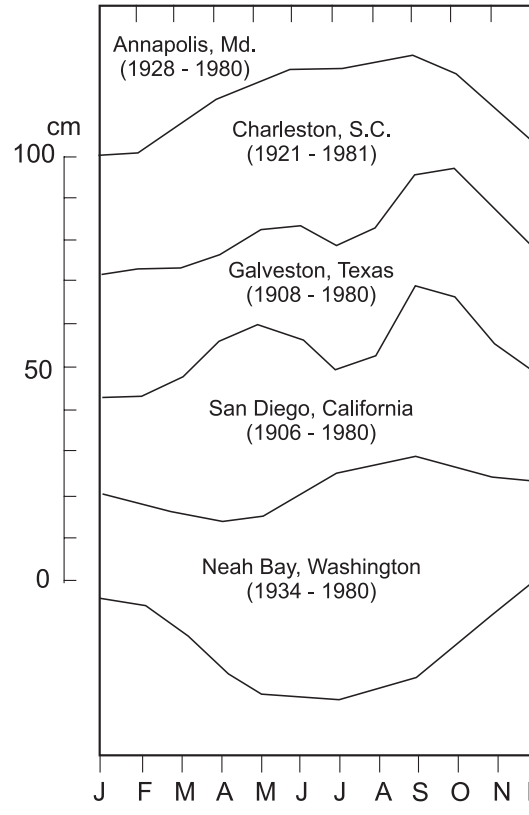

Figure 3.18 Examples of annual cycles of sea-level changes determined from tide gauges. The dates in brackets give the period over which the data were averaged. (Komar and Enfield, 1987).

Sea level changes in the Pacific occur as a result of changes in pressure, winds and ocean currents collectively associated with El Niño events. The 1982–83 El Niño event produced a wave of higher sea level 0.4–0.5 m high which travelled from west to east across the Pacific and affected many coastal areas of North, Central

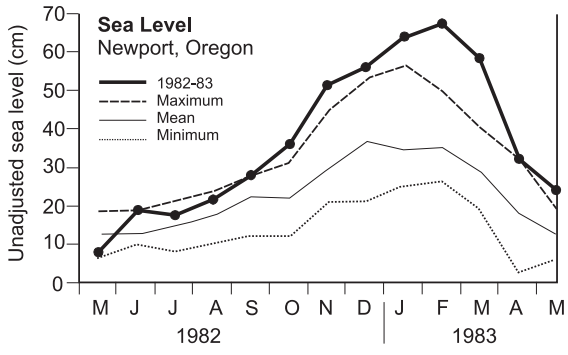

Figure 3.19 Monthly average sea level at Newport, Oregon, during the 1982–83 El Niño event compared to the maxima, average and minima previously measured. (Komar and Enfield, 1987).

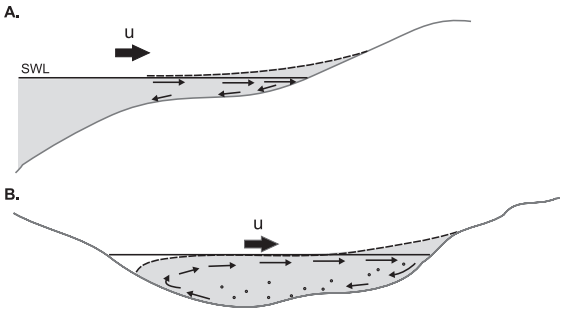

Figure 3.20 Storm surge generated by onshore winds: (A) surge effects on an open coast; (B) positive and negative surge in a lagoon or lake.

and South America. Typically El Niño events result in a rise of 0.1–0.2 m in sea level along the California coast and northward into Oregon (Komar and Enfield, 1987 – see Figure 3.19).

Much of the early work on these effects relied on data from tide gauges which are primarily located on the coast in harbours. Over the past few decades, satellite imagery of sea surface temperatures and sea levels have given us a much more complete picture of the dynamics of the ocean surface and regional variations that can persist for up to a decade or more. Changes in mean sea level over the period 1993–2007 from Topex and Jason-1 satellite altimetry show decadal scale dynamic variation superimposed on a long-term trend of sea level rise. During this period a large increase in height in the western Pacific reflects the warm phase of the Pacific Decadal Oscillation with increased sea surface temperature in this region producing expansion and the observed increase in sea level. Likewise, sea level rise in the North Atlantic south of Greenland may reflect a weakening of the cold current which flows south off the south-east coast and thus an increase in sea surface temperatures there. The only significant area of sea level decrease over the period is in the mid-Atlantic off the east coast of the USA, and this probably reflects a shift in the position of the Gulf Stream.

3.5.2 Storm surge

During storms changes in sea level occur as a result of wind stress on the water surface and changes in atmospheric pressure leading to positive displacement of the water level (storm surge or set-up) and negative displacement (negative surge or set-down). Wind stress on the water surface results in wind drift, a flow of surface water in the direction of the wind. Close to the shoreline the nearshore slope and beach provide a barrier to the surface drift, resulting in a set-up of water at the shoreline and a compensating return flow offshore below the surface (Figure 3.20a). The return flow will be retarded by frictional forces, and the greater this retardation the greater will be the equilibrium set-up. The highest storm surges thus tend to occur in shallow, gently sloping coastal areas and in semi-enclosed bays and estuaries where local wind set-up is superimposed on the general coastal one. Displacement below the mean water level with offshore winds on open coasts tends to be much smaller than a corresponding surge because the effects are dissipated into the open ocean. However, in shallow, enclosed water bodies such as lagoons and lakes, set-down on the upwind coast can be of the same order as the surge on the downwind coast (Figure 3.20b). Storm surge may be referred to as a meteorological tide, as in high tide, accompanying the storm. However, it should be thought of as being superimposed on the existing water level and the predicted water level changes associated with astronomical tides are usually subtracted from tide gauge records in order to separate out the storm surge effect. Because of

the potential impact on shoreline features and on human activities, most attention is focused on surges rather than set-down.

Storm surge elevation is determined primarily by the wind speed and wind direction relative to the shoreline, by the duration and fetch over which the wind blows, barometric pressure, the nearshore slope and coastal configuration, and by the track and speed of movement of the storm. Wave set-up at the shoreline is also included in the overall storm surge elevation. Actual circulation is complicated by the Coriolis effect which results in a deflection of the current with depth below the surface (Eckman spiral).

It is useful to distinguish between storm surge events associated with tropical cyclones (hurricanes, typhoons) and those generated by mid-latitude cyclones (Pugh 1987; Dolan and Davis, 1994). Tropical cyclones are relatively small in extent and originate at sea. They are generated and driven by the energy released by condensation of moisture evaporated from a warm ocean surface and thus they decay as they move into higher latitudes over cooler ocean waters and die out rapidly over land (Emanuel, 2003). They have a pressure gradient of about 20 mb per100 km and this produces intense winds which exceed 32 m s^{-1} for the least intense hurricane. When they reach land they can produce very high surges but these are usually confined to a few tens of kilometres of shoreline and occur over a time period of one or two tidal cycles or less. Because cyclonic rotation is generated by the coriolis effect they are usually absent from regions between 5° north and south of the equator. In the northern hemisphere they form in the Caribbean and off the Pacific coast of Mexico and in a broad zone across the Indian and Pacific oceans affecting the mainland coast of Asia from India to China as well as the islands of Indonesia and Japan. In the southern hemisphere they are generally absent from the Atlantic, but in the Pacific they are formed in a broad zone from west of Australia and New Guinea to the south west coast of Africa. The effects of wind dominate over those of pressure, though the extreme low pressure at the centre of the storm can account for a rise in sea level of up to 1 m.

Extra-tropical storms are formed largely along the boundary between warm and cold air masses and their track is controlled by large-scale pressure systems and by waves in the upper atmosphere jet stream. They extend over many hundreds of kilometres and the pressure gradient is about 5 mb per 100 km. They affect large areas of the coastline and their effects may take place over a number of tidal cycles. Pressure and wind effects may be equally important. The east coasts of the USA and Canada are affected particularly by depressions which track north-eastward off the coast and produce northeasters which commonly occur from late autumn through the winter (Dolan and Davis, 1994; Forbes *et al.*, 2004). These systems often track eastward across the north Atlantic, together with others generated off Labrador, and affect the coast of western Europe (Betts *et al.*, 2004 – see Figure 3.21).

The surge produced by hurricanes in general increases with increasing hurricane intensity (Xia *et al.*, 2008). Hurricane Hugo, which came ashore near Charleston, North Carolina on September 21, 1989 (Figure 3.22a) as one of the most intense Caribbean hurricanes of the last century, produced a maximum surge estimated at over 6.1 m just to the right of the eye (Coch and Wolfe, 1991; Brennan, 1991). However, at Kiwah Island just 24 km to the south (left) of the eye the surge was only 1.3 m. and the major impact of the surge only extended along about 100 km of the shoreline (Figure 3.22b). This illustrates a key feature of storm surge, and to a lesser extent wave heights, associated with tropical cyclones when they approach land. Because of the small diameter of the centre around which the winds move, the winds are onshore to the right of the eye (in the northern hemisphere) and they generate large waves moving onshore. Winds to the left of the path blow alongshore or offshore and thus the surge is greatly reduced and the effect of waves generated by the storm out to sea tends to be reduced by the winds blowing offshore just before it makes landfall. Thus while the height of the surge tends to increase with increasing intensity, the track of the storm, angle of approach to the shoreline trend and configuration of the coastline greatly influence the actual surge level at a point on the coast (Xia *et al.*, 2008).

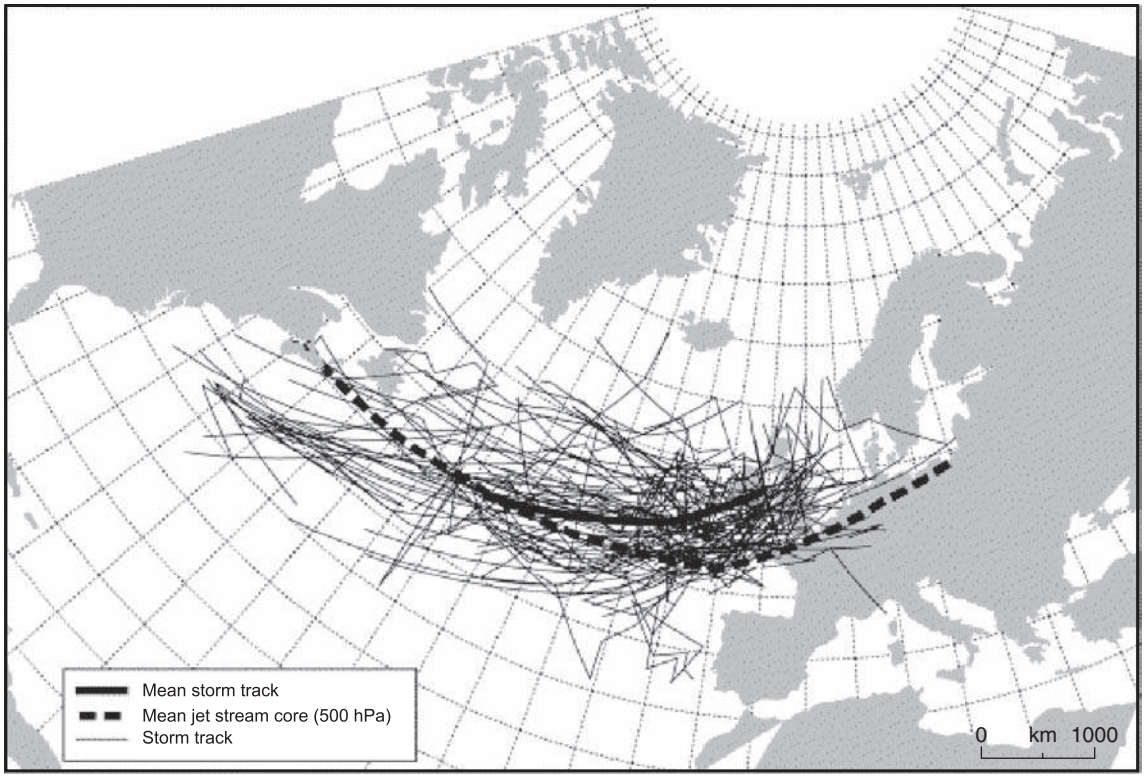

Figure 3.21 Position of individual storm tracks promoting extreme surge events (top 1%) at Brest for the period 1950–92. The mean jet stream core (500 hPa level) and mean storm track position are also shown (Betts *et al.*, 2004).

Cyclones in the Bay of Bengal affect low-lying coasts in India, Bangladesh and Burma. They can produce very high surges because of the configuration of the bay, low coastal gradients and the intensity of the storms (Murty and Flather, 1994). The impacts of surges are felt particularly along the low-lying areas of the Ganges River delta. A severe cyclone in November, 1970 produced a storm surge of more than 9 m on the coast north of Chittagong (Pugh, 1987) and one in 1990 generated a storm surge ranging from 5–10 m, leading to the loss of over 100 000 lives.

Two or three hurricanes and post-tropical storms bring large waves to the Atlantic coast of Canada every year, and on average one crosses the coast every two or three years. Hurricane Hortense tracked along the Nova Scotia coast on September 14–15, 1996 and produced a storm surge of about 1 m at Halifax (Parkes *et al.*, 1997 – see Figure 3.23a). Note the small negative surge associated with the rapid passage of the storm and offshore winds. Significant wave heights measured by a wave rider buoy off Halifax Harbour peaked at 8.7 m and the combined wave action and storm surge had a major impact on the gravel barrier systems north of Halifax (Taylor *et al.*, 1997). However, the frequency and magnitude of storm surges associated with mid-latitude cyclones is much greater (Jones and Davis, 1995; Forbes *et al.*, 2004) and they are a major control on the dynamics of barrier systems along the Atlantic and Gulf of St Lawrence coasts. The Point du Chene storm of January 4, 1986 produced a surge of 1.94 m at Halifax (Figure 3.23b), but its impact on the coast was reduced because it occurred at low tide during a period of neap tides (Parkes *et al.*, 1997).

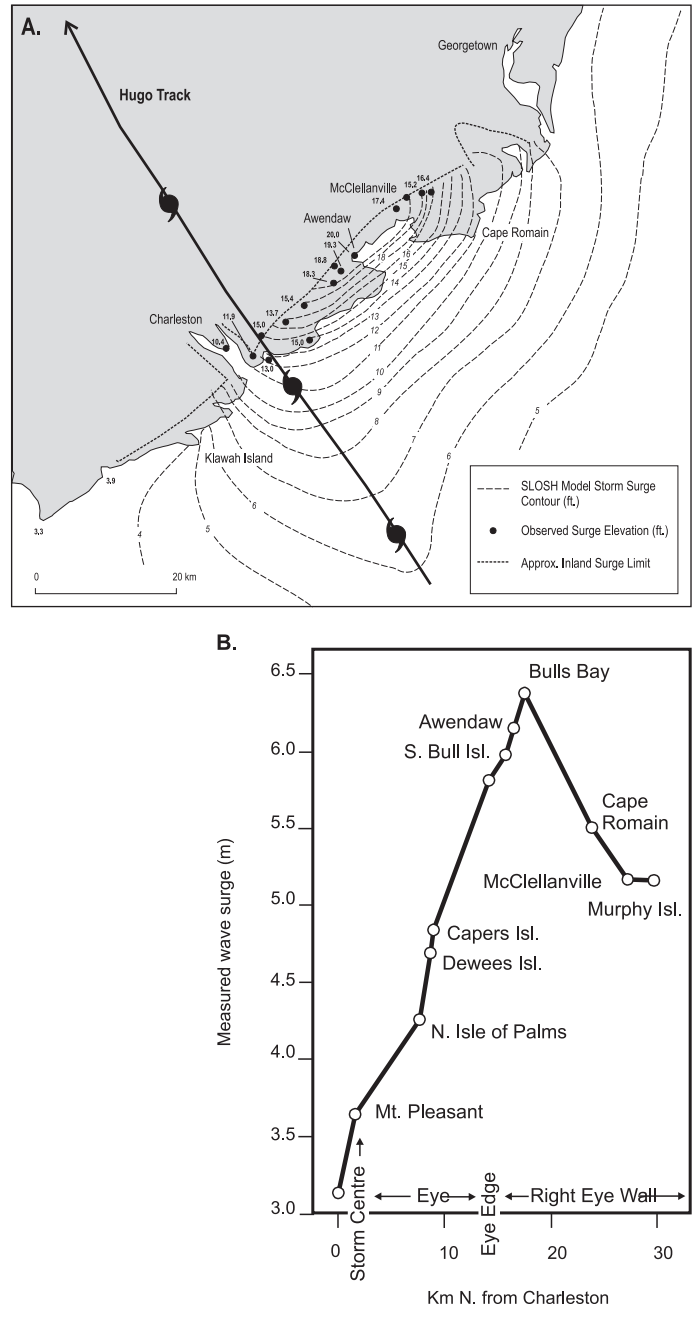

Figure 3.22 Storm surge associated with Hurricane Hugo September 22, 1989: (A) hurricane path, and storm surge values predicted by SLOSH (Sea, Land and Overland Surge from Hurricanes); (B) plot of observed surge values on the South Carolina coast (Coch and Wolff, 1991).

Extra-tropical storms are also responsible for most periods of significant wave action and storm surge generation in the Great Lakes. An intense storm on December 2, 1985 resulted in extensive overwash and damage to property along much of the coastline of Lake Erie and over 80 cottages were destroyed at Long Point alone (see Figure 10.34). The maximum surge recorded at Port Colborne near the east end of the lake was just over 2 m and the set down at Kingsville towards the western end was over 1.5 m (Figure 3.24). At Port Stanley, near the centre of the lake, water level fluctuations were <0.5 m.

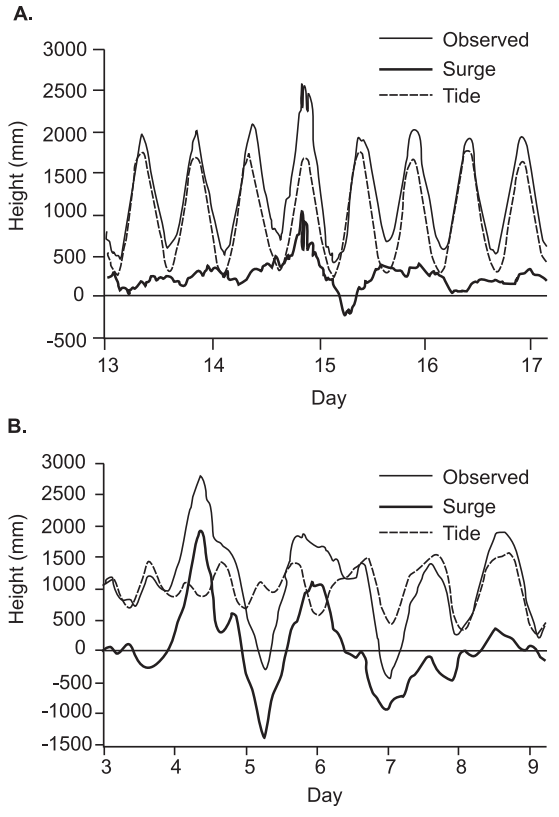

Figure 3.23 Storm surges measured off Halifax harbour: (A) during the passage of Hurricane Hortense, September 15, 1996; (B) during the passage of the Point du Chene storm, January 4, 1986. (Parkes *et al.*,1997).

Another area of notable storm surges is the North Sea where the coastal geometry and shallow water often enhance storm effects. A storm surge in 1953, which coincided with spring tides, breached dykes along much of the coast of Holland and did extensive damage to low-lying areas in other coastal communities, including the east coast of England.

3.5.3 Seiches and other long waves

In enclosed bodies of water such as lakes, lagoons, bays and harbours, long period standing waves termed seiches (pronounced sayshh) can be generated by processes such as changes in atmospheric pressure and winds, and by the release of a storm surge following a change in wind direction (Miles, 1974). Seiches in Lake Erie as an example are generated by storm surge set up on one shoreline and the matching surge set down at the opposite shoreline. As the storm system that generated the surge passes on, and the wind direction shifts, the water level differential is no longer maintained and the water is released from the high side towards the low side. As a result a series of water level oscillations with decreasing amplitude are generated as the water 'sloshes' back and forth. The longest natural period of oscillation T_0 depends on the length of the water body and its depth, and is given by

$$T_0 = \frac{2L}{\sqrt{gD}} \tag{3.2}$$

where T_0 is the period of oscillation, L is the length of the basin, D is the average depth of basin.

Note that the term $(gD)^{0.5}$ is the formula for the speed of a shallow water wave and $2L$ is the distance from one shore to the opposite shore and back again. The period of a seiche along the length of Lake Erie (about 350 km) is just over 9 hours. On the open ocean release of a storm surge will produce long waves that can propagate both offshore and along the coast (Yankovsky, 2008).

3.5.4 Water levels in lakes and inland seas

The North American Great Lakes and other large lakes and inland seas such as the Black Sea, Caspian Sea and Lake Baikal in central Asia, and the lakes of the rift valley in east Africa experience wave action and littoral processes that are similar in magnitude to those of many coastal areas of limited fetch such as the Baltic, the Mediterranean and the Gulf of St Lawrence. Because they are cut off from the oceans, tidal changes are negligible, but water level fluctuations due to meteorological forcing and isostatic effects are similar to those on ocean coasts. In addition, fluctuations in water level on a time scale of days to years occur as a result of variations in inflows and outflows of water to and from the basins, water temperature change and, for high latitude lakes, ice formation in winter. These fluctuations are of great significance for both natural processes associated with wetlands, bluff erosion, and beach

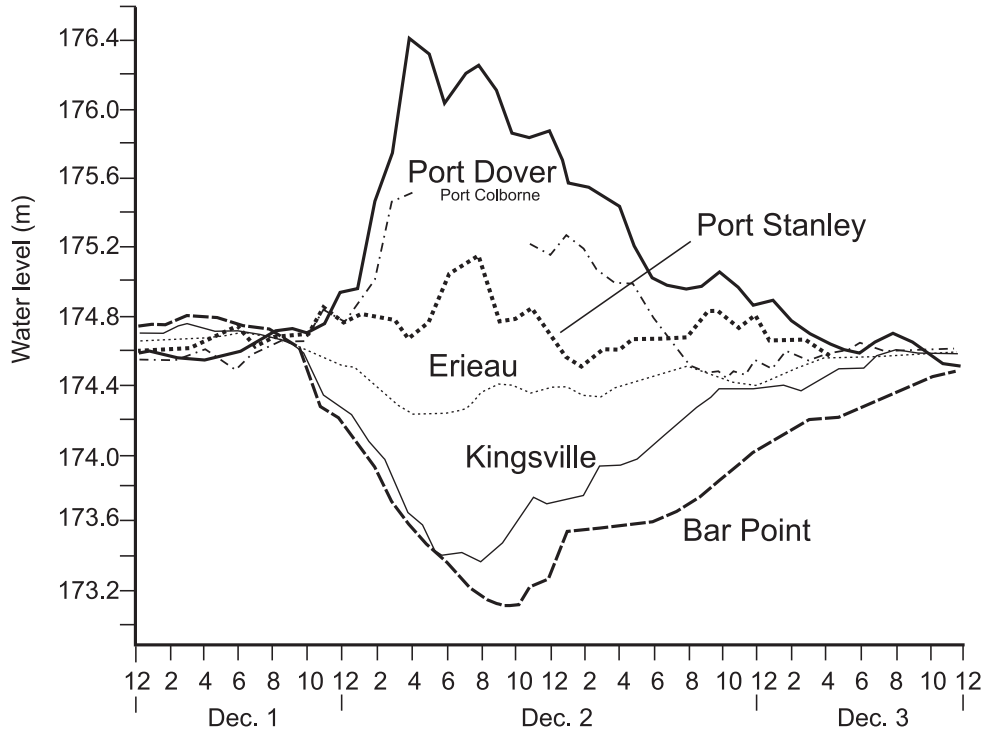

Figure 3.24 Water levels recorded at several gauges on Lake Erie during the December 2, 1985 storm. Note the positive surge at the eastern end of the lake (Port Colborne) and corresponding negative surge at the upwind (western) end (Kingville, Bar Point). Source, Environment Canada.

and dune development as well as for human activities such as hydro power generation, navigation and depth of channel for shipping, and marina operations.

In the Great Lakes the response of individual lakes varies somewhat because of their size and depth, and where they are located on the system (Table 3.3). All of the lakes except Lake Erie have deep basins that lie below sea level and the volume of water in storage means that the response to changes in input or output may take several years to work through the system. Lake Superior, because of its large volume has the smallest long-term fluctuation in lake level of just over a metre while the other three lakes have had long term fluctuations of nearly 2 m. Lake Superior at the head of the system receives its inputs only from surface runoff and from direct precipitation on the lake. The outflows from the lakes further down the system become increasingly large compared to supply from local surface runoff, because of the supply from the lakes higher up the system. Lake level fluctuations on them reflect basin-wide trends in precipitation, evaporation and snow melt as well as local watershed conditions. All the lakes experience a marked annual cycle of lake level that reflects seasonal variations in runoff and evaporation. Levels are generally lowest in mid to late winter when evaporation is low because of ice cover and/or low lake temperatures and when runoff from rivers is much reduced. Lake levels increase rapidly in the spring as a result of snow melt so that water levels tend to increase and reach a maximum in late May or June. Because of the time it takes for snow melt from the Lake Superior basin to pass down the system, peak levels in Lakes Erie and Ontario may not occur until late June or July and these two lakes will often experience two or more peaks, reflecting local snow melt followed by the arrival of the snow melt from the upper lakes.

Table 3.3 *Characteristics of the Great Lakes System water levels and flows (source: Environment Canada).*

Lake	Average elevation (m)	Volume (km^3)	Long-term range (m)	Seasonal range (m)	Outflow ($m^3\ s^{-1}$)
Superior	183.1	12 100	1.1	0.3	2,150
Michigan–Huron	176.3	8460	1.8	0.35	5,130
Erie	173.9	484	1.9	0.35	5,860
Ontario	74.6	1640	2	0.45	6,880

3.6 Climate change and sea level rise

The results of a large number of studies worldwide suggest that over the past one thousand years sea level averaged globally rose at a rate of <2 mm a^{-1} (Gornitz, 1995; Flemming *et al.*, 1998). There are a number of components which control changes in sea level and various models can estimate the likely contribution of each of these components over the past century (Table 3.4). The two major contributors to present sea level rise are: (1) steric height variations produced by the expansion or contraction of the water in the oceans as a result of changing temperature and density; and (2) variations in the mass of water in the oceans. In this case the major process is melting of glaciers and snow packs worldwide, and particularly melting of the Greenland and Antarctic ice sheets. We can use measured trends in global sea level to extrapolate future sea levels (e.g. Wake *et al.*, 2006) but, because melting of ice sheets and warming of the oceans tends to lag behind increases in atmospheric temperature, present trends may not be a good predictor of future levels. In particular, there is still considerable uncertainty about the present contribution from the two major ice sheets of Greenland and Antarctica (Cazenave, 2006). Thus models of sea level change due to projected global warming scenarios attempt to account for each of the components identified in Table 3.4.

3.6.1 Measured rates of mean sea level rise

Most data on rates of sea level rise for periods prior to the twentieth century come from a variety of proxy measures, with considerable limits on their precision and accuracy. In the past century tide gauge data are available for an increasing number of stations worldwide and these provide measurements with a precision on the order of 2 cm. Gauges with a record of more than 50 years offer an opportunity to filter out annual- and decadal-scale dynamic variations as well as cyclic variations associated with the 18.6 year tidal oscillation, and thus to determine recent trends in sea level. An example of this is the record for Newlyn on the southwest coast of Britain (Arújo and Pugh, 2008) where a linear trend through the annual mean sea level (MSL) values shows sea level increasing at a rate of 1.77 ± 0.12 mm a^{-1} (Figure 3.25). This is consistent with a computed value of 1.8 ± 0.3 mm a^{-1} for the period 1950–2000 using a global combined tide gauge and satellite altimetry data base (Church *et al.*, 2004) and a value of 1.74 ± 0.16 mm a^{-1} for nine tide gauges worldwide for the 100 year period from 1904–2003 (Holgate, 2007). Use of the tide gauge data requires considerable effort to identify and remove errors from the data recording system, as well as the tidal components and the nottidal residuals (Arújo and Pugh, 2008). It also requires that corrections be made for any vertical changes in the elevation of the land at the location of the tide gauge. This can be done through use of a model of glacial isostatic adjustment (e.g. Hagedoorn *et al.*, 2007) but increasingly it is possible to do this through continuous GPS monitoring of positions and height (Wöppelmann *et al.*, 2007). Caution also has to be exercised in using tide gauge

Table 3.4 *Minimum, central and maximum estimates for the contribution of various components of sea level change 1910–90. (from IPCC Report, 2001).*

Component	Minimum (mm/yr)	Central (mm/yr)	Maximum (mm/yr)
Thermal expansion	0.3	0.5	0.7
Glaciers and ice caps	0.2	0.3	0.4
Greenland 20th C effects	0	0.1	0.1
Antarctica 20th C effects	–0.2	–0.1	0
Long-term ice sheet adjustments	0	0.25	0.5
Permafrost	0	0.03	0.05
Sediment deposition	0	–0.35	0.05
Terrestrial storage	–1.1	0.7	0.4
TOTAL	–0.8	0.7	2.2
Estimated from observations	1	1.5	2

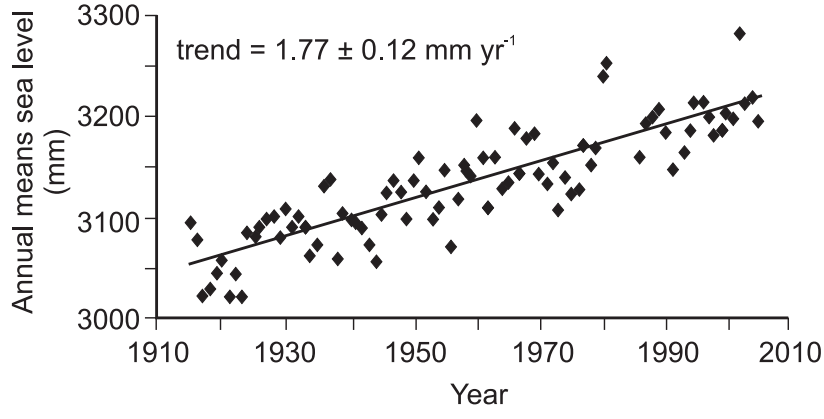

Figure 3.25 Annual mean sea level values for Newlyn, England from 1915–2005 (Arujo and Pugh, 2008).

measurements to estimate sea level rise globally because of the uneven distribution of gauges world-wide (Pugh, 1987).

Satellite altimetry now provides a high precision record of sea level over the world oceans below 66° latitude, and the launch of Jason-2 in June 2008 will improve estimates still further. However, continued analysis and updating of the altimetry data has shown the need for calibration against established gauge sites, and to make corrections for atmospheric conditions and small variations in satellite orbits (Nerem *et al.*, 2007). The data collected to date after calibration and corrections for glacial isostatic adjustment are consistent with tide gauge curves and show sea level rising at an average of 3 mm ± 0.4 mm a^{-1} (Figure 3.26). The wealth of new data from the oceans paradoxically have shown the dynamic variability of the ocean surface due to decadal scale atmospheric and ocean current changes, particularly in the tropical Pacific and Indian oceans (Church *et al.*, 2006), and thus the need to acquire longer records in order to smooth these dynamic changes and provide a robust estimate of long-term trends.

3.6.2 Future rates of sea level rise

There is still considerable uncertainty as to forecasts of global temperature change and consequently even greater uncertainty in how fast the oceans will respond to this. The IPCC (Intergovernmental Panel on Climate Change)

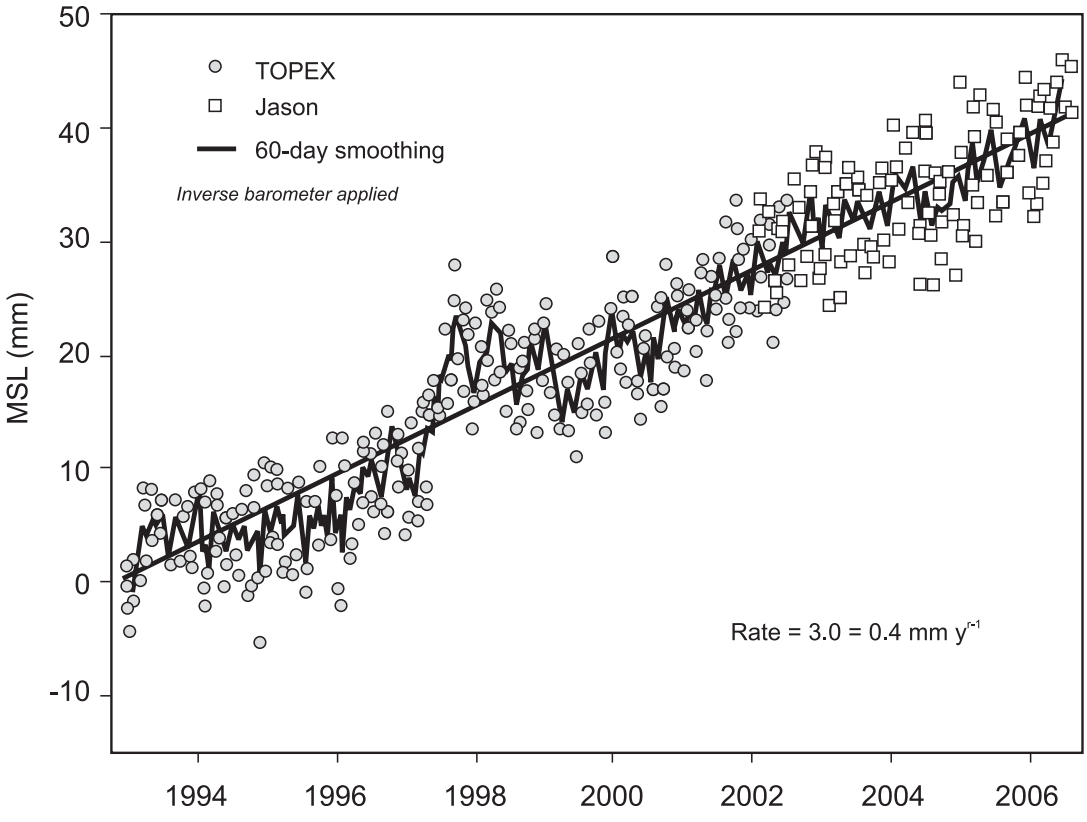

Figure 3.26 Global mean sea level variations from TOPEX and Jason altimeter measurements showing sea level rising at a rate of 3.0 mm a^{-1}. The rate increases to 3.3 mm a^{-1} after correction for the effects of glacial isostatic adjustment (Nerem *et al.*, 2007).

best estimate scenario predicts sea level rise from a base of 1990 of about 0.5 m by 2100 with a range of 0.11 to 0.77. This estimate is much more conservative than the estimates made in the early 1980s which ranged above 3 m (French et *al.*, 1995).

Clearly, rising sea level and the potential for an acceleration of this rate have implications for natural coastal systems as well as human economic activities (e.g. McLean *et al.*, 2001; Nichols *et al.*, 2007; Walton, 2007). Early scenarios focused on the extent of inundation of low-lying areas such as Florida and Bangladesh and the threat to Pacific island atoll nations, where most of the land base is only a few metres above present sea-level. Some of these simply took the highest projected sea level and spread this over the present land mass without any allowance for dynamic coastal processes, with the result that most low-lying regions simply disappeared. This approach is still to be found in some assessments of vulnerability (McGranahan *et al.*, 2007) However, with the continued downward revision in the 'best guess' estimates of the amount of the rise, more attention is now being focused on the response of different shoreline geomorphic types and ecological communities to the change in sea level, and to assessing the impact of the rise on coastal zone management strategies (French *et al.*, 1995; Nicholls and Leatherman, 1996; Bray *et al.*, 1997; Shaw *et al.*, 1998; Vafeidis *et al.*, 2008). The hysteria of the early projections is now calming down and we need to focus on sea level rise as simply one factor to be considered within an integrated coastal management plan. The significance of sea level rise needs to be assessed locally in comparison with other factors and especially with a whole range of other human

impacts. We will examine the potential impacts of sea level rise further in chapters dealing with beaches, barriers, dunes, saltmarshes and cliffed coasts.

3.6.3 Forecasting extreme events

An important element in coastal management plans is the forecasting of extreme sea level events. This will be used in the design of shore protection structures, especially the height of seawalls and dykes, marina design, and the designation of flood-prone zones. The starting point for this is an analysis of historical water levels and the determination of return frequencies for particular events/elevations. This can be coupled with GIS mapping of hazard lands and the use of LiDAR to develop very precise Digital Elevation Maps to facilitate identification of areas subject to flooding at particular water levels (e.g. Webster *et al.*, 2004). Historical data provide a starting point for this, but forecasting future events must include consideration of changing environmental conditions. Climate change may bring increased storm intensity, while reduced ice cover in high latitudes will extend the open water season and increase fetch lengths for storms. Changing tidal components and sea level rise will also be added to the factors that need to be taken into account (Bernier *et al.*, 2007; Arújo and Pugh, 2008; Tomasin and Pirazzoli, 2008).

References

Andrews, J.T. 1970. *A Geomorphological Study of Postglacial Uplift with Particular Reference to Arctic Canada*. Institute of British Geographers Special Publication #2, London, 156 pp.

Arújo, I.B. and Pugh, D.T. 2008. Sea levels at Newlyn 1915–2005: Analysis of trends for future floooding risk. *Journal of Coastal Research*, **24**, **4c**, 203–312.

Ballard, R.D., Coleman, D.F. and Rosenberg, G.D. 2000. Further evidence of abrupt Holocene drowning of the Black Sea Shelf. *Marine Geology*, **170**, 253–261.

Berge-Nguyen, M., Cazenave, A., Lombard, A., Llovel, W., Viarre, J. and Cretaux, J.F. 2008. Reconstruction of past decades sea level using thermosteric sea level, tide gauge, satellite altimetry and ocean reanalysis data, *Global and Planetary Change*, **62**, 1–13.

Bernier, N.B., Thompson, K.R., Ou, J. and Ritchie, H. 2007. Mapping the return periods of extreme sea levels: Allowing for short sea level records, seasonality, and climate change, *Global and Planetary Change*, **57**, 139–150.

Betts, N.L, Orford, J.D., White, D. and Graham, C.J. 2004. Storminess and surges in the South-Western Approaches of the eastern North Atlantic: the synoptic climatology of recent extreme coastal storms. *Marine Geology*, **210**, 227–246.

Bloom, A.L., Broeker, W.S., Chappell, J., Mathews, R.K. and Mesolella, K.J. 1974. Quaternary sea-level fluctuations on a tectonic coast: New ^{230}Th ^{234}U dates from New Guinea. *Quaternary Research*, **4**, 185–205.

Bray, M., Hooke, J. and Carter, D. 1997. Planning for sea-level rise on the south coast of England: advising the decision-makers. *Transactions of the Institute of British Geographers NS*, **22**, 13–30.

Brennan, J.W 1991. Meteorological summary of Hurrican Hugo. *Journal of Coastal Research*, **SI 8**, 1–12.

Carter, R.W.G., 1988. *Coastal Environments*. Academic, New York, 617 pp.

Cazenave, A. 2006. How fast are the ice sheets melting? *Science*, **314**, 1250–1252.

Chappell, J. 1974. Geology of coral terraces, Huon Peninsula, New Guinea: a study of Quaternary tectonic movements and sea-level changes. *Geological Society of America Bulletin*, **85**, 553–570.

Chappell, J. 1987. Late Quaternary sea-level changes in the Australian region. In Tooley, M.J. and Shennan, I. (eds.), *Sea Level Changes*. Institute of British Geographers Special Publication #20, Blackwell, Oxford, 296–331.

Chappell, J., Omura, A., Esat, T., McCulloch, M., Pandolfi, J., Ota, Y. and Pillans, B. 1996. Reconciliation of late Quaternary sea levels derived from coastal terraces at Huon Peninsula with deep sea oxygen isotope records. *Earth and Planetary Science Letters*, **141**, 227–236.

Church, J.A., White, N.J., Coleman, R., Lambeck, K. and Mitrivica, J.X. 2004. Estimates of the regional distribution of sea level rise over the 1950–2000 period. *Journal of Climate*, **17**, 2609–2625.

Church, J.A., White, N.J. and Hunter, J.R. 2006. Sea-level rise at tropical Pacific and Indian Ocean islands. *Global and Planetary Change*, **53**, 155–168.

Coch, N.K. and Wolff, M.P. 1991. Effects of Hurricane Hugo storm surge in coastal South Carolina. *Journal of Coastal Research*, **SI 8**, 201–226.

Coles, B. J. 2000. Doggerland: the cultural dynamics of a shifting coastline. In Pye, K. and Allen, J. R. L. (eds.), Coastal and Estuarine Environments. *Journal of The Geological Society*, Special Publication, **175**, 59–73.

Davidson-Arnott, R. G. D. and Pyskir, N. M. 1989. Morphology and formation of an holocene coastal dune field, Bruce Peninsula, Ontario. *Geographie Physique et Quaternaire*, **42**, 163–170.

Davies, J. L. 1964. A morphogenetic approach to world shorelines. *Zeitschrift fur Geomorphologie*, **8**, 127–142.

Davies, J. L. 1972. *Geographical Variation in Coastal Development*. Oliver and Boyd, Edinburgh, 204 pp.

Defant, A. 1962. *Physical Oceanography*. MacMillan, New York, vol. **2**, 598 pp.

Dolan, R. and Davis, R. E. 1994. Coastal storm hazards. *Journal of Coastal Research*, **SI 12**, 103–114.

Douglas, B. C. 2001. Sea level change in the era of the recording tide gauge. In Douglas, B. C., Kearney, M. S. and Leatherman, S. P. (editors), *Sea Level Rise*. Academic, New York, pp. 37–64.

Dyke, A. S. 1998. Holocene delevelling of Devon Island, Arctic Canada: implications for ice sheet geometry and crustal response. *Canadian Journal of Earth Sciences*, **35**, 885–904.

Emanuel, K. 2003. Tropical cyclones. *Annual Review of Earth and Planetary Science*, **31**, 75–104.

Eriş, K. K., Ryan, W. B. F., Çağatay, M. N., Sancar, U., Lericolais, G., Ménot, G., and Bard, E. 2007. The timing and evolution of the post-glacial transgression across the Sea of Marmara Shelf south of Istanbul. *Marine Geology*, **243**, 57–76.

Fairbridge, R. W. 1961. Eustatic changes in sea level. *Physics and Chemistry of the Earth*, **4**, 88–185.

Greenwood, B. and Davidson-Arnott, R. G. D. 1975. Marine bars and nearshore sedimentary processes, Kouchibouguac Bay, New Brunswick, Canada. In Hails, J. and Carr, A. (eds.), *Nearshore Sediment Dynamics and Sedimentation: An Interdisciplinary Review*. Wiley, Chichester, pp. 123–150.

Fairbridge, R. W. 1983. Isostacy and eustasy. In Smith, D. E. and Dawson, A. G. (eds.), *Shorelines and Isostacy*. Institute of British Geographers Special Publication #16, Academic, London, pp. 3–25.

Farquharson, W. I. 1970. Tides and tidal currents in the Gulf of St Lawrence. Canada Department of Energy, Mines and Resources, Surveys and Mapping Branch, Ottawa.

Fleming, K., Johnston, P., Zwartz, D., Yokoyama, Y., Lambeck, K. and Chappell, J. 1998. Refining the eustatic sea-level curve since the last glacial maximum using far- and intermediate-field sites. *Earth and Planetary Science Letters*, **163**, 327–342.

Forbes, D. L., Parkes, G. S., Manson, G. K. and Ketch, L. A. 2004. Storms and shoreline retreat in the southern Gulf of St Lawrence. *Marine Geology*, **210**, 169–204.

French, J. R., Spencer, T. and Reed, D. 1995. Editorial – Geomorphic response to sea-level rise: existing evidence and future impacts. *Earth Surface Processes and Landforms*, **20**, 1–6.

Gornitz, V. 1995. Sea-level rise: a review of recent past and near-future trends. *Earth Surface Processes and Landforms*, **20**, 7–20.

Goodwin, I. D. and Harvey, N. 2008. Subtropical sea-level history from coral microatolls in the southern Cook Islands, since 300 AD. *Marine Geology*, **253**, 14–25.

Grant, D. R., 1980. Quaternary sea-level change in Atlantic Canada as an indicator of crustal delevelling. In Morner, N-A., (ed.), *Earth Rheology, Isostacy and Eustacy*. Wiley, Chichester, pp. 201–214.

Hagedoorn, J. M., Wolf, D. and Martinec, Z. 2007. An estimate of global mean sea-level rise inferred from tide-gauge measurements using glacial-isostatic models consistent with the relative sea-level record. *Pure and Applied Geophysics*, **164**, 791–818.

Hansen, E. C., Arbogast A. F., van Dijk, D. and Yurk, B. 2006. Growth and migration of parabolic dunes along the southeastern Coast of Lake Michigan. *Journal of Coastal Research*, **SI 39**, 209–214.

Hearty, P., Hollin, J., Neumann, A. C., O'Leary, M. and McCulloch, M. 2007. Global sea-level fluctuations during the last interglaciation (MIS 5e). *Quaternary Science Reviews*, **26**, 2090–2112.

Hesp, P. A., Chang, C. H., Hilton, M., Ming, C. L. and Turner, I. M. 1996. A first tentative holocene sea-level curve for Singapore. *Journal of Coastal Research*, **14**, 308–314.

Holgate, S. J. 2007. On the decadal rates of sea level change during the twentieth century. *Geophysical Research Letters*, **34**, L01602, doi:1029/2006GL028492, 4 pp.

Horton, B. P., Corbett, R., Culver, S. J., Edwards, R. J. and Hillier, C. 2006. Modern saltmarsh diatom distributions of the outer banks, North Carolina, and the development of a transfer function for high resolution reconstructions of sea level. *Estuarine, Coastal and Shelf Science*, **69**, 381–394.

Jones, G. V. and Davis, R. E., 1995. Climatology of Nor'easters and the 30 kPa jet. *Journal of Coastal Research*, **11**, 1210–1220.

Komar, P. D. and Enfield, D. B. 1987. Short-term sea-level changes and coastal erosion. In: Nummedal, D., Pilkey, O. H. and Howard, J. D. (eds.), *Sea-Level Fluctuations and Coastal Evolution*. SEPM Special Publication #41, 17–27.

Lamb, A. L., Wilson, G. P., and Leng, M. J. 2006. A review of coastal palaeoclimate and relative sea-level reconstructions using $\delta^{13}C$ and C/N ratios in organic material, *Earth-Science Reviews*, **75**, 29–57.

Leroy, F., Anthony, E. J., Monfort, O. and Larsonneur, C. 2000. The morphodynamics of megatidal beaches in Normandy, France. *Marine Geology*, **171**, 39–59.

Lewis, C. F. M. 1969. Late Quaternary history of lake levels in the Huron and Erie basins. *Proceedings of the 12th Conference on Great Lakes Research*, International Association for Great Lakes Research, pp. 250–270.

Lohne, Ø, Bondevik, S., Mangerud, J. and Svendsen, J. 2007. Sea-level fluctuations imply that the Younger Dryas ice-sheet expansion in western Norway commenced during the Allerød. *Quaternary Science Reviews*, **26**, 2128–2151.

McGranahan, G., Balk, D. and Anderson, B. 2007. The rising tide: assessing the risks of climate change and human settlements in low elevation coastal zones. *Environment and Urbanisation*, **19**, 17–37.

Macmillan, D. H. 1966. *Tides*. Elsevier, New York, 240 pp.

McLean, R. F., Tsyban, A., Burkett, A., Codign, J. O., Forbes, D. L., Mimura, N., Beamish, R. J. and Itterkkot, V. 2001. Coastal zones and marine ecosystems. In McCarthy, J. J., Canziani, O. F., Leary, N. A., Dokken, D. J. and White, K. S. (eds.), *Climate Change 2001: Impacts, Adaptations and Vulnerability*. Cambridge University Press, Cambridge, pp. 343–380.

Miguez, B. M., Le Roy, R. and Wöpelmann, G. 2008. The use of radar tide gauges to measure variations in sea level along the French coast. *Journal of Coastal Research*, **24**, 61–68.

Miles, J. W. 1974. Harbor seiching. *Annual Review of Fluid Mechanics*, **6**, 17–34.

Moucha, R., Forte, A. M., Mitrovica, J. X., Rowley, D. B., Quéré, S., Simmons, N. A. and Grand, S. P. 2008. Dynamic topography and long-term sea-level variations: There is no such thing as a stable continental platform. *Earth and Planetary Science Letters*, **271**, 101–108.

Morner, N-A. 1987. Models of sea-level changes. In: Tooley, M. J. and Shennan, I (editors) *Sea Level Changes*. Institute of British Geographers Special Publication #20, Blackwell, Oxford, 332–355.

Murty, T. S., and Flather, R. A. 1994. Impact of storm surges in the Bay of Bengal. *Journal of Coastal Research*, **SI 12**, 149–161.

Nerem R. S., Cazenave, A., Chambers, D. P., Fu e, L. L., Leuliette, E. W. and Mitchum, G. T. 2007. Comment on 'estimating future sea level changes from past records' by Nils-Axel Morner. *Global and Planetary Change*, **55**, 358–360.

Nicholls, R. J. and Leatherman, S. P. 1996. Adapting to sea-level rise: relative sea-level trends to 2100 for the United States. *Coastal Management*, **24**, 301–324.

Nicholls, R. J., Klein, R. J. T. and Tol, R. S. J. 2007. Managing coastal vulnerability and climate change: a nation to global perspective. In McFadden, L., Nicholls, R. J. and Pennington-Rowsell, E. C. (eds.), *Managing Coastal Vulnerability: An Integrated Approach*. Elsevier, Amsterdam, 221–240.

Ota, Y. and Machida, H., 1987. Quaternary sea level changes in Japan. In Tooley, M. J. and Shennan, I. (eds.), *Sea Level Changes*. Institute of British Geographers Special Publication #20, Blackwell, Oxford, pp. 182–224.

Parkes, G. S., Ketch, L. A. and O'Reilly, C. T. 1997. Storm surge events in the Maritimes. *Proceedings of the Canadian Coastal Conference (CCSEA)*, 115–129.

Peltier, W. R. and Fairbanks, R. G. 2006. Global glacial ice volume and Last Glacial Maximum duration from an extended Barbados sea level record. *Quaternary Science Reviews*, **25**, 3322–3337.

Penland, S. and Ramsey, K. E. 1990. Relative sea-level rise in Louisiana and the Gulf of Mexico:1908–1988. *Journal of Coastal Research*, **6**, 323–342.

Pirazzoli, P. A., 1987. Sea level changes in the Mediterranean. In: Tooley, M. J. and Shennan, I. (editors) *Sea Level Changes*. Institute of British Geographers Special Publication #20, Blackwell, Oxford, pp. 154–181.

Pugh, D. T., 1987. *Tides, Surges and Mean Sea-Level*. Wiley, Chichester, 472 pp.

Pugh, D. T., 2004. *Changing Sea Levels*. Cambridge University Press, Cambridge, 265 pp.

Quinlan G. and Beaumont, C. 1981. A comparison of observed and theoretical postglacial relative sea-level in Atlantic Canada. *Canadian Journal of Earth Sciences*, **8**, 1146–1163.

Ryan W. B. F., Pittman, W. C. L., Major, C. O., and 7 others 1997. An abrupt drowning of the Black Sea Shelf. *Marine Geology*, **138**, 119–126.

Rutter, N. W. and Catto, N. R. (eds.), 1995. *Dating Methods for Quaternary Deposits*. Geological Association of Canada, GEOtext2, St. John's, Newfoundland, Canada, 308 pp.

Scott, D. B., Boyd, R. and Medioli, F. S. 1987. Relative sea-level changes in Atlantic Canada: observed level and sedimentological changes vs. theoretical models. In Nummedal, D., Pilkey, O. H. and Howard, J. D. (eds.), *Sea-Level Fluctuations and Coastal Evolution*. SEPM Special Publication #41, pp. 87–96.

Shaw, J., Taylor, R.B., Forbes, D.L., Ruz, M-H. and Solomon, S., 1998. Sensitivity of the coasts of Canada to sea-level rise. *Geological Survey of Canada Bulletin*, **505**, 79 pp.

Sheppard, F.P. 1963. *Submarine Geology*. 2nd edn., Harper and Rowe, New York, 412 pp.

Sutherland, D.G. 1983. The dating of former shorelines. In Smith, D.E. and Dawson, A.G. (eds.), *Shorelines and Isostacy*. Institute of British Geographers Special Publication #16, Academic, London, 129–157.

Taylor, R.B., Forbes, D.L., Frobel, D., Shaw, J. and Parkes, G. 1997. Hurricane Hortense strikes Atlantic Nova Scotia: An examination of beach response and recovery. *Proceedings of the Canadian Coastal Conference (CCSEA)*, pp. 375–386.

Tomasin, A. and Pirazzoli, A. 2008. Extreme sea levels in the English Channel: Calibration of the Joint Probability method. *Journal of Coastal Research*, **24**, **4c**, 1–13.

Turney, C.M. and Brown, H. 2007. Catastrophic early holocene sea level rise, human migration and the neolithic transition in Europe. *Quaternary Science Reviews*, **26**, 2036–2041.

Tushingham, A.M. 1991. On the extent and thickness of the Innuitian ice sheet: a postglacial-adjustment approach. *Canadian Journal of Earth Sciences*, **28**, 231–239.

Tushingham, A.M., 1992. Postglacial uplift predictions and historical water levels of the Great Lakes. *Journal of Great Lakes Research*, **18**, 440–455.

Tushingham, A.M. and Peltier, W.R. 1991. ICE-3G: a new global model of late Pleistocene deglaciation based upon geophysical predictions of post-glacial relative sea level change. *Journal of Geophysical Research*, **96**, 4497–4523.

Vafeidis, A.T., Nicholls, R.J., McFadden, L. and six others, 2008. A new global coastal database for impact and vulnerability. *Journal of Coastal Research*, **24**, 917–924.

Wake, L., Milne, G. and Leuliette, E. 2006. 20th century sea-level change along the eastern US: Unravelling the contributions from steric changes, Greenland ice sheet mass balance and late Pleistocene glacial loading. *Earth and Planetary Science Letters*, **250**, 572–580.

Walker, M. 2005. *Quaternary Dating Methods*. Wiley, Chichester, 286 pp.

Walton, T.L., Jr. 2007. Projected sea level rise in Florida. *Ocean Engineering*, **34**, 1832–1840.

Webster, T.L., Forbes, D.L., Dickie, S. and Shreenan, R. 2004. Using topographic Lidar to map flood risk from storm-surge events for Charlottetown, Prince Edward Island, Canada. *Canadian Journal of Remote Sensing*, **30**, 64–76.

Wilgus, C.K., Hastings, B.S., Kendall, C.G.St C., Pasamentier, H.W., Ross, C.A. and van Wagoner, J. (eds.), 1988. *Sea-level Changes: an Integrated Approach*. SEPM Special Publication #42, Tulsa, Oklahoma, 407 pp.

Wöppelmann, G., Martin M.B., Bouin, M-N. and Altamimi, Z. 2007. Geocentric sea-level trend estimates from GPS analyses at relevant tide gauges world-wide, *Global and Planetary Change*, **57**, 396–406.

Xia, M, Xie, L., Pietrafesa, L.J. and Peng, M. 2008. A numerical study of storm surge in the Cape Fear River estuary and adjacent coast. *Journal of Coastal Research*, **24**, **4C**, 159–167.

Yankovsky, A.E., 2008. Long wave response of the West Florida shelf to the landfall of Hurricane Wilma. *Journal of Coastal Research*, **24**, **4C**, 33–39.

4

Wind-generated waves

4.1 Synopsis

Wind-generated waves are the most important energy input into the littoral zone and, together with wave-generated currents, they are responsible for coastal erosion and sediment transport. They are thus the primary force leading to modification of the coast and the creation of erosional and depositional landforms

A wind wave is simply a vertical displacement of the surface of a body of water that results from the transfer of energy from the wind to the water surface. Wind-generated waves are periodic, in that they appear as undulations on the water surface characterised by a high point, or crest, followed by a low point, or trough. They are also progressive in that the wave form travels across the water surface in the direction that the generating wind blows. The energy transferred from the wind is expressed in the potential energy resulting from the displacement of the crest and trough of the wave above and below the original still-water surface, and in the kinetic energy of the circular motion of water particles within the wave. In addition to waves generated by winds, a variety of other waves are found in oceans and lakes ranging from very long period waves, such as the tidal waves generated by the gravitational force of the moon and sun, to waves with much shorter periods, such as the standing waves produced by reflection of wind waves from seawalls.

The height, length and period of waves increase with increasing wind speed and with the length of time and distance over water that the wind blows. While the exact mechanism of energy transfer is still not fully understood, there are now computer models that permit forecasting of wave conditions based on knowledge of wind conditions and the subsequent transformation of the waves as they travel across a lake or ocean. These models also permit us to hindcast wave conditions from past weather data and thus to construct the wave climate for a particular coast. This provides critical data for input into coastal zone management and the construction of sea defences and harbours.

4.2 Definition and characteristics of waves

The form and water motion associated with an individual wave are illustrated in Figure 4.1 and the nomenclature for the wave form, water particle orbits and the direction of movement of the wave is given in Table 4.1. The wave form appears as a periodic undulation of the water surface above and below the still-water level (swl) – the level the water surface would assume in the absence of waves. The form of a simple wave in deep water is very close to that of a harmonic wave and as shown is symmetric above and below the swl (Figure 4.1a). Indeed, the mathematical descriptions of the surface form of wind waves all make use of the sine or cosine function. The height H of the wave is equal to the distance from the trough to the

Table 4.1 *Notation for waves*

Symbol	Name	Description
	Crest	peak or highest part of wave
	Trough	lowest part of wave
swl	Still water level	water surface in the absence of waves
H	Height	vertical distance between crest and trough
a	Amplitude	vertical distance from crest or trough to swl
L	Length	distance between successive crests
T	Period	time between successive crests
f	Frequency	$1/T$
σ	Radian frequency	$2\pi/T$
C	Celerity	speed of movement of individual wave form
C_G	Wave group velocity	speed of movement of a group of waves
k	Wave angular number	$2\pi/L$
η	Water surface elevation	water surface elevation defined with respect to time (t) and distance (x)
h	Water depth	vertical distance from swl to bed
z	Distance below swl	$z = -h$ at the bed
o	(subscript) Deep water	$h > 0.5L_o$
s	(subscript) Shallow water	$H < 0.05L_o$
b	(subscript) Break point	breaking conditions

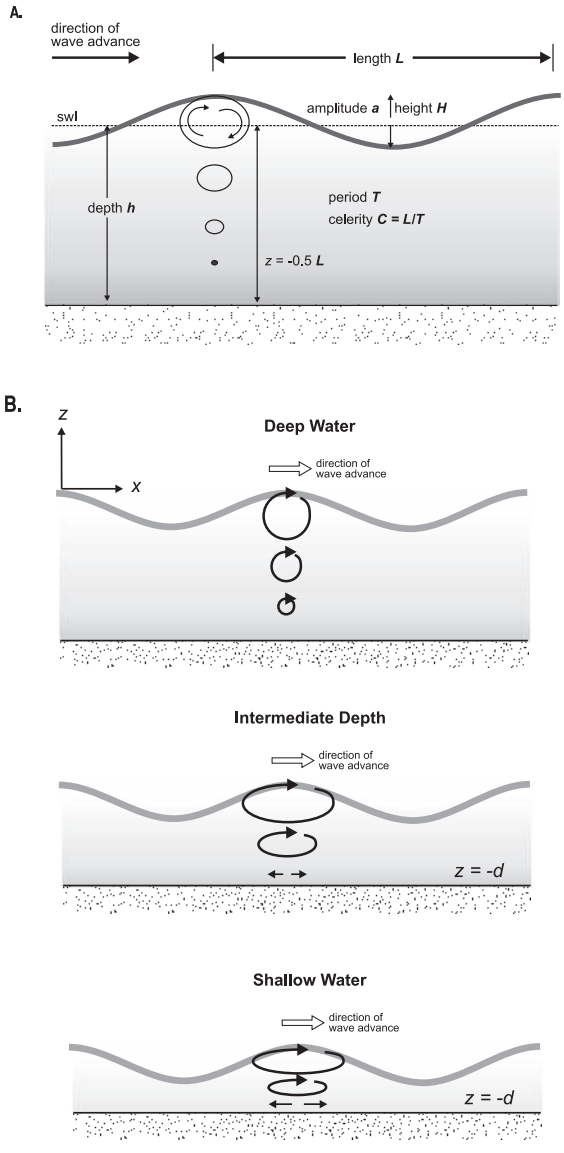

Figure 4.1 Wave characteristics: (A) definition sketch of the characteristics of a simple progressive wind wave in deep water; (B) wave orbital motion in deep, intermediate and shallow water.

crest and the amplitude a of the displacement of the water surface above the swl is the same as that for the displacement below it; this is not quite true for real waves, especially as they approach land. The wave length L is the distance between successive wave crests, or between two similar points such as the wave troughs, and the wave period T is the time taken for the passage of

two such points. When we describe properties of more than one wave it is more useful to use the wave frequency rather than the period: this is defined as $1/T$ and is expressed in Hz. These basic descriptors can be used to characterise a variety of wave types on the ocean surface.

A wind wave is a progressive wave in which the wave form advances across the water surface and the speed at which it travels is the wave celerity C. The wave form advances one wave length in the period T and thus celerity can be defined as

$$C = \frac{L}{T}. \tag{4.1}$$

Equation (4.1) is very useful since any one of the properties can be obtained if the other two are known. Since for most practical purposes T does not change as waves approach the coast, changes in C directly control changes in L.

Within the wave water particles move in an orbit that is circular, with a diameter at the surface equal to the height of the wave. As the wave crest approaches the water moves upwards and forwards, and it moves downward and backwards through the trough. The orbital diameter decreases exponentially with depth and becomes negligible at a distance $z = 0.5L$ below the swl (Figure 4.1b). We can thus define deep water for a wave as a depth $h > 0.5L_0$, where L_0 is the longest wave length predicted for a particular period T. The decrease in orbital diameter with depth can be described by a hyperbolic function and, as we will see in the mathematical description of waves in Chapter 5, description of wave orbital motion makes use of the hyperbolic functions sinh, cosh and tanh to determine the orbital motion with depth below the swl.

There is a direct relationship in deep water between wave period and wave length, with L increasing as a function of T^2. From equation (4.1) it can be seen that C must also increase with increasing wave period – thus, long-period waves travel across the water surface faster than short-period waves. When waves move into a water depth $<0.5L_0$ the bottom begins to affect the shape of the wave form and the orbital motion; and the wave celerity and wave length both decrease. In particular, the wave orbits become compressed vertically into an elliptical shape so that the vertical diameter is smaller than the horizontal diameter. By the time a wave enters shallow water (defined as $h < 0.05L_0$ – see Table 4.1) the wave form and orbital motion are greatly changed compared to deep-water conditions, Figure 4.1b).

Surface waves on the ocean, seas and lakes can be generated by several mechanisms, including the wind, earthquakes, the gravitational force of the sun and moon (tides) and pressure fluctuations. It is useful to identify the characteristics of waves generated by each of these mechanisms in terms of their characteristic period or frequency and relative energy and restoring force (Figure 4.2). Wind-generated waves generally have the shortest period, ranging from < 0.25 seconds for capillary waves to a maximum of about 30 seconds for the longest swell waves in the open ocean. Capillary waves are the little ripples, with a wave length <10 cm which can be seen on the surface as a gust of wind passes over a still body of water (Figure 4.3) and they can be found on the surface of much larger waves when the wind is strong and blowing continuously. They are affected by surface tension and quickly diminish if the wind dies down. Waves with a period longer than about 0.25 s are too large to be greatly affected by surface tension and the main restoring force is gravity; hence they are termed ordinary gravity waves. In the area where waves are being actively generated by winds they are confused, irregular, short-crested, and often characterised by the appearance of white caps where there is local wave breaking. Such conditions are termed 'sea' and they result from the fact that new waves are constantly being generated by the wind. Waves continue to grow in height and period as the wind blows, giving rise to the superposition of waves with a wide range of period, height, and length. Conditions within the area of wave generation contrast with the much more regular, long-crested swell waves that propogate outward from the area of wave generation and may travel thousands of kilometres across the ocean. Because of the dependence of celerity on wave period, the long-period waves travel away from the area of generation

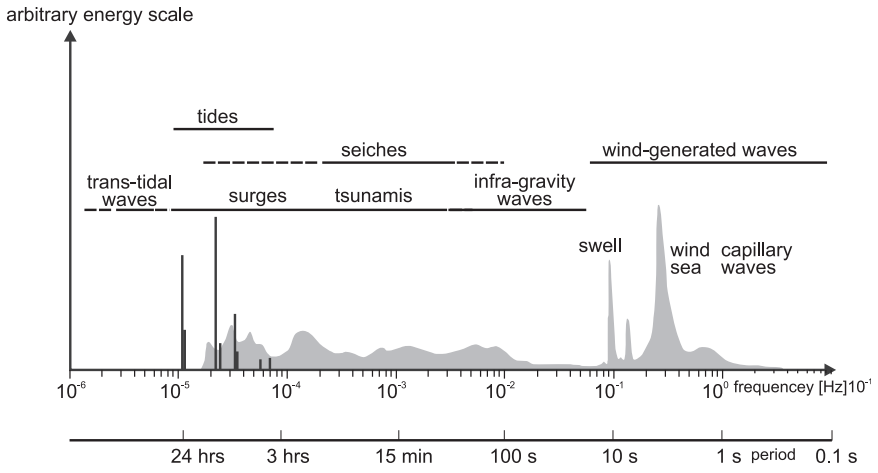

Figure 4.2 Types of wave motion in the oceans as a function of frequency and an indication of the relative ranking of energy associated with the each frequency grouping (Holthuijsen 2007 – after Munk, 1950).

Figure 4.3 Winds blowing across a pond (toward the camera) leading to the generation of capillary waves close to the edge of the vegetation and the growth of these in a downwind direction. Near the upwind boundary there is a zone of calm water where wind forces are insufficient to overcome surface tension.

much more quickly than the short-period ones and over distances of hundreds to thousands of kilometres they sort themselves into packets with very similar wave lengths. This process of wave dispersion results in the transformation of the highly irregular sea into a regular series of swell waves, and produces the well-known phenomenon that an approaching storm is signalled first by the appearance of the longest period waves and then by waves of decreasing period.

Infra-gravity waves have periods between 30 seconds and 5 minutes and most commonly are generated by groupiness in the wave record (surf beat) or by the interaction of gravity waves and the beach (see Chapter 5.5 for a description of these). In the Great Lakes and some of the smaller seas wind-generated waves have periods <10 s and so the infra-gravity energy may have periods of 20 seconds or less; thus there is some overlap in the range of periods associated with the two wave types.

As noted in Chapter 3, strong winds blowing onshore generate surges that can reach several metres in height on gently sloping coasts and may be >6 m where a hurricane makes landfall. In enclosed lakes and seas, a change in wind direction as a storm passes through can lead to a release of the surge and produce oscillations in the basin termed seiches. The period of a seiche is controlled to a large extent by the dimensions of the basin and for elongate lake basins there are different modes of oscillation along the lake and across the lake. Seiches can be amplified by harmonic resonance in harbours as the oscillation propagates through the entrance into the harbour basin. Tsunamis generated by earthquakes or undersea landslides generally have periods on the order of 100–200 seconds and wave lengths of tens to hundreds of kilometres (see Box 5.2). True tidal waves have periods ranging from a few hours to just over 24 hours. Finally, trans-tidal waves have periods longer than tides and are generated by low-frequency fluctuations in the earth's crust or by large-scale pressure fluctuations in the atmosphere which in turn affect the ocean surface elevation. We will be concerned here primarily with ordinary gravity waves generated by wind blowing over a water surface.

4.3 Measurement and description of waves

4.3.1 Wave measurement

Measurements of waves are a key input to models and studies of erosion and sediment transport as well as for the design of seawalls, harbours and other coastal facilities. While measurements of tides and sea level have been available for several centuries, routine measurements of waves have only become available in the last 30–40 years and the network of measuring stations is still much smaller than, for example, gauging stations on rivers. However, it is now possible to measure ocean waves from satellites so that the spatial coverage can be extensive.

Time scales of wave measurements

In common with all branches of geomorphology, coastal geomorphology examines the operation of processes and the evolution of landforms at a range of spatial and temporal scales. Thus, in measuring and describing waves in the coastal zone it is appropriate that we consider the spatial and temporal scales that are relevant to a particular application. Holthuijsen (2007) considers four spatial/temporal scales:

(1) Small scale, dealing with the description of a few wave periods or wave lengths within which it is possible to use theoretical models to describe in great detail the motion of the water surface, the velocity of water particles and the wave-induced pressures. This is termed the phase resolving approach since it has a resolution of a small fraction of a wave length or period. We will examine some of the wave theories used to describe waves at this scale in Chapter 5.2.

(2) Medium scale, dealing with something on the order of a hundred to several hundred wave periods or wave lengths – a few minutes to about 30 minutes and covering a distance on the order of 10 km. This period is short enough for conditions to be considered homogeneous or stationary and long enough to provide reliable statistics; thus data recorded from a wave staff or buoy is typically broken

up into packets of this length for analysis. At this scale we are not interested in resolving every aspect of water motion as we were at the small scale. Instead we want to be able to characterise statistical properties of the assemblage of waves during this time interval and thus to be able to compare these to similar recordings at other points – for example, during the course of a storm – or for other locations along the coast. This is termed the phase averaging approach. We can define statistical properties of the distribution of, for example, wave height or wave period for all waves measured during the interval, or we can examine the wave spectrum which depicts the amount of energy associated with each wave frequency during the interval considered.

(3) Large scale, dealing with time intervals on the order of the duration of individual storms and thus covering periods of tens of hours and distance scales on the order of hundreds to a few thousand km. This permits us to examine the spatial or temporal variability of the wave spectrum and for example to chart the passage of waves from their area of generation across large distances until they finally reach the coast.

(4) Finally, when we want to predict the effect of wave processes on coastal evolution at a particular location – for example the rate of evolution of a barrier spit or the potential impact of constructing a harbour breakwall – we need to consider average wave statistics over periods of tens of years. This requires the generation of a wave climate (Chapter 4.5).

Instrumentation

We can distinguish between instruments designed to measure some property or properties of waves at a single point and remote sensing instruments such as radar which provides a picture of wave conditions over a relatively large area of the sea surface. We can also distinguish instruments designed to measure the surface wave form directly from those which measure some property of the wave, such as pressure or orbital motion, as well as special applications such as swash run-up (Figure 4.4). Because real waves are variable in height and period, most instruments measure wave properties over some length of time or over some spatial area.

Instruments that measure the surface form can be divided into three groups: (1) marked staffs; (2) electrical/electronic staffs; and (3) accelerometer buoys (Figure 4.4). Perhaps the simplest form of gauge is a graduated staff fixed to the bed or attached to a pole or supporting structure such as a wharf. The rise and fall of the water surface associated with the wave can be estimated visually and recorded manually. This can be used in a simple study under low wave conditions to get an estimate of incident waves on a beach by recording (say) the passage of 25 waves. More practical is the combination of a fixed staff, or a board with a grid, with a movie or video camera which can provide a continuous record of the passage of a series of waves. Such an approach is often used in detailed studies of wave form, particularly when it is important to know whether the waves are breaking or not. However, this type of recording is more tedious to process and to extract useful data, so that its use tends to be restricted to highly specialised research studies rather than for routine data collection.

Wave staffs employing some form of electrical circuit have been used in numerous studies since 1945. These systems make use of the conduction of electricity by water, particularly sea water, and record either the change in electrical resistance or capacitance of the system as water rises and falls over a length of uninsulated cable which is part of an electrical circuit. The change in resistance or capacitance can be conditioned to produce a variation in an output signal, which may be a DC current or a frequency, and this signal is then recorded on a device such as a data logger or computer. Calibration of the instrument allows for conversion of the recorded data to a variation in water surface elevation with time. The sensor itself may be fixed to a support jetted into the sand in the nearshore or attached to some physical structure such as a jetty or platform (Figure 4.5). The advantage of the surface-piercing staff is that it provides a direct measure of the water surface form. The disadvantage is that it is subject to high wave forces when deployed in shallow water. These devices have traditionally

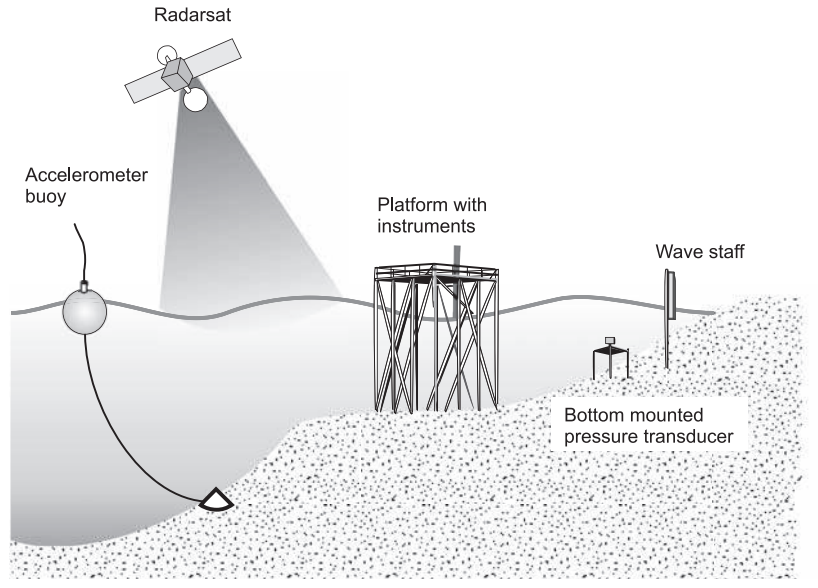

Figure 4.4 Schematic illustrating a variety of approaches to the measurement of waves.

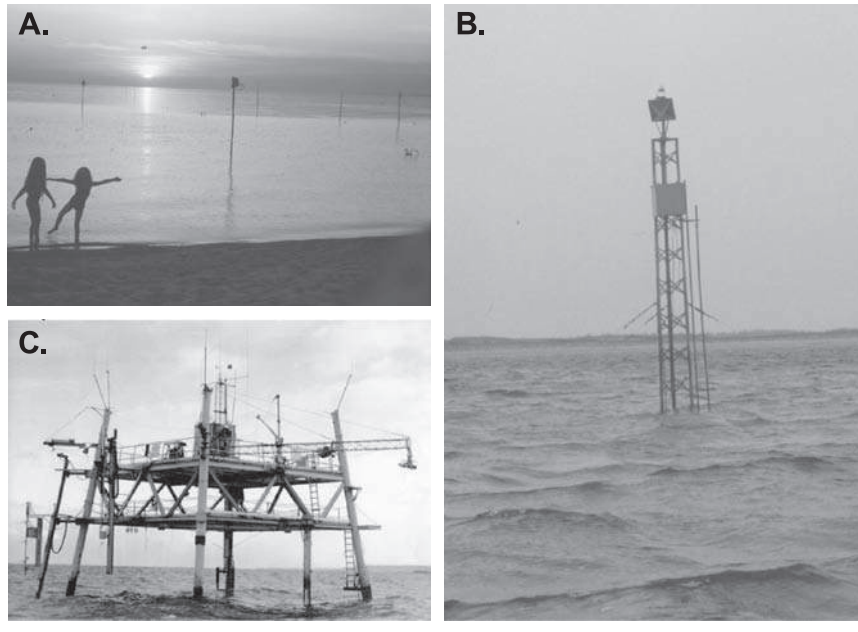

Figure 4.5 Photographs of instrumentation for measuring waves and wave generation: (A) resistance wave staffs deployed in Georgian Bay, Lake Huron as part of a study of wave transformation over nearshore bars (Davidson-Arnott and Randall, 1984); (B) mounted on a tower deployed in 6 m water depth (Greenwood and Davidson-Arnott, 1975; and (C) mounted on a platform as part of a study of wind wave generation and wave direction in Lake Ontario (Donelan *et al*., 1985, 1996; photo courtesy Mark Donelan).

been used in many studies of nearshore sediment transport, as well as for measurements of wave field growth, for example in the North Sea or in the Great Lakes.

In shallow water, waves are often measured indirectly through the use of a pressure transducer housed in a watertight case. This can be deployed some distance below the surface (in

shallow water it is often mounted to a frame fixed in the bed), and it senses the change in pressure associated with the passage of individual waves. The variation in pressure for an individual wave of known height and period can be predicted mathematically for a known depth using wave theory, so it is possible to develop a transform function that will relate the recorded variations in pressure to the surface wave form. The effect of the tides and other water level changes can be removed by extracting the mean pressure over some time period. Because of the decay in wave orbital motion with depth, short-period (small L) waves are filtered out of the record as water depth increases. As a result, in areas of restricted fetch the transducer needs to be deployed in quite shallow water. Since there is usually a spectrum of frequencies present in the pressure transducer record, the transform should be performed for all of the frequencies present. Again, this is not a trivial task, though it can be done routinely in a data analysis program. There is some loss of information on the true form of the surface wave as well as the loss of the higher frequencies with increasing depth of deployment, but the disadvantages of this are offset in studies in, and close to the breaker zone by the ease of deployment and reduced exposure to breaking wave forces.

Individual wave staffs or pressure transducers provide a one-dimensional picture of the variations in water surface elevation through time – i.e. they give information on wave height and period but not on the direction of travel. This requires either the deployment of several instruments in an array which permits determination of the wave direction through a comparison of travel time between various sensors, or simultaneous measurement of surface elevation and the orbital motion using an electromagnetic current meter or acoustic Doppler velocimeter (ADV).

Wave staffs and pressure transducers are only deployed in shallow water or on platforms so that measurement of waves in deep water usually involves an indirect measurement of the movement of the water surface using an accelerometer which measures the surface displacement over time and which is housed in a buoy (Figure 4.3). The output is a one-dimensional spectrum. Heave–pitch–roll buoys which incorporate an accelerometer mounted on gimbals and a compass which permits resolution of the changing gimbal angles, permit estimation of the two-dimensional frequency–direction spectrum. The buoy usually incorporates electronics for recording and storing the data, as well as some form of radio communication link either directly to shore or through a satellite. Changes in the surface slope over time can be used to define the height and period of the wave, and modern buoys can also determine wave direction. A free-floating buoy will provide a good description of the water surface but for practical reasons most buoys must be tethered to the bottom and thus the data from the buoy must be corrected for the effects of the mooring – not a trivial task. Buoys of this type are now being used to provide routine wave data in many parts of the world including the Great Lakes. There are extensive networks of buoys maintained by NOAA on all the mainland coasts of the USA and there is also a good network around the coast of western Europe. Descriptions of the networks and in many cases access to the data being recorded by individual buoys can be readily accessed on the World Wide Web.

A variety of indirect measures of wave processes are also employed. Electromagnetic current meters operate at frequencies that allow resolution of the horizontal and vertical water motion associated with the passage of waves. Similar readings can be obtained from an acoustic Doppler profiler (ADP) outside the breaker zone where bubbles are not a problem. Wave run-up on moderately steep shorelines can be measured using a form of inclined wave staff. Alternatively, the run-up spectrum can be determined from video records (Holman and Guza, 1984) and this has proved particularly useful in areas such as Oregon and California where surf conditions make deployment of instrumentation in the breaker zone very difficult.

Remote sensing of the sea surface is now increasingly being carried out using radar altimetry or synthetic aperture radar (SAR) from satellites, planes, ships or from stations on land (Figure 4.4). These describe the sea state over an

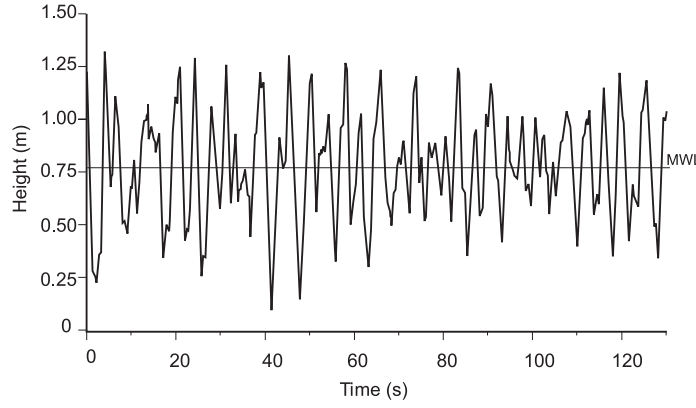

Figure 4.6 Two-minute wave record from the wave staff shown in Figure 4.5b. The data were recorded directly on a continuous strip chart recorder rather than reconstructed from a digital record. The approximate mean water level is indicated. Note the groups of larger and smaller waves in the record (see Section 5.5).

area of the ocean and therefore the output is different from those of individual instruments. These data may be particularly useful, for example, in providing real-time input into models predicting oil spill dispersion and they are a boon to surfers since they enable tracking of suitable large, long-period waves across oceans.

4.3.2 Analysis of wave records

Examination of a real wave record (Figure 4.6) shows a complex pattern with a range of wave heights and periods present. A thirty minute record from a wave staff or pressure transducer will typically have on the order of 1000–2000 waves in the record and characterisation of the record can be made through two approaches: (1) generation of the statistical properties of certain attributes based on measurements of all waves present in the record; and (2) determination of properties of the wave spectrum for the recording period.

In the first place it is possible to measure the height and period of each wave in the record and thus to obtain the frequency distribution of wave height and wave period. Before the advent of digital wave records this could be done manually from a trace of the wave record – for example the one shown in Figure 4.6. We can still print a continuous graphical output from a high-frequency digital record and this provides a useful visual impression of the sea surface. It is clear from Figure 4.6 that waves vary considerably in height and the record contains some small waves that appear to be carried upon larger waves. This begs the question – when is a wave not a wave? Alternatively, how big does an undulation on the water surface have to be for it to be considered a wave? It is also clear from an examination of the wave record that as we include smaller and smaller waves in the analysis, the distance between wave crests (and thus the time interval) becomes smaller and the mean value of T for the record will also become smaller.

Wave height and period for a wave record are defined with respect to zero-crossings – either upward or downward (Figure 4.7). The mean water level (mwl) derived from the measured record is defined as having an elevation of zero; hence zero-crossing. A wave is defined as having a crest that lies above the mwl and the trough below it. In zero-downcrossing (Figure 4.7a) a wave is the profile of the water surface between two successive downward crossings of the still-water line. Using this definition the wave is defined first by the trough ahead of the crest and then by the crest. This conforms to what an observer would see looking out to sea from a point in the surf zone and it also emphasises the steep front face of the wave close to the break point. The wave height H is defined as the difference between the lowest point in the trough and the highest point in the following crest, and wave period T as the time between the two downward crossing points. Alternatively waves may be defined by zero upcrossing points (Figure 4.7b) and the wave is identified first by the crest and then the succeeding trough. The height and length properties of individual waves will differ

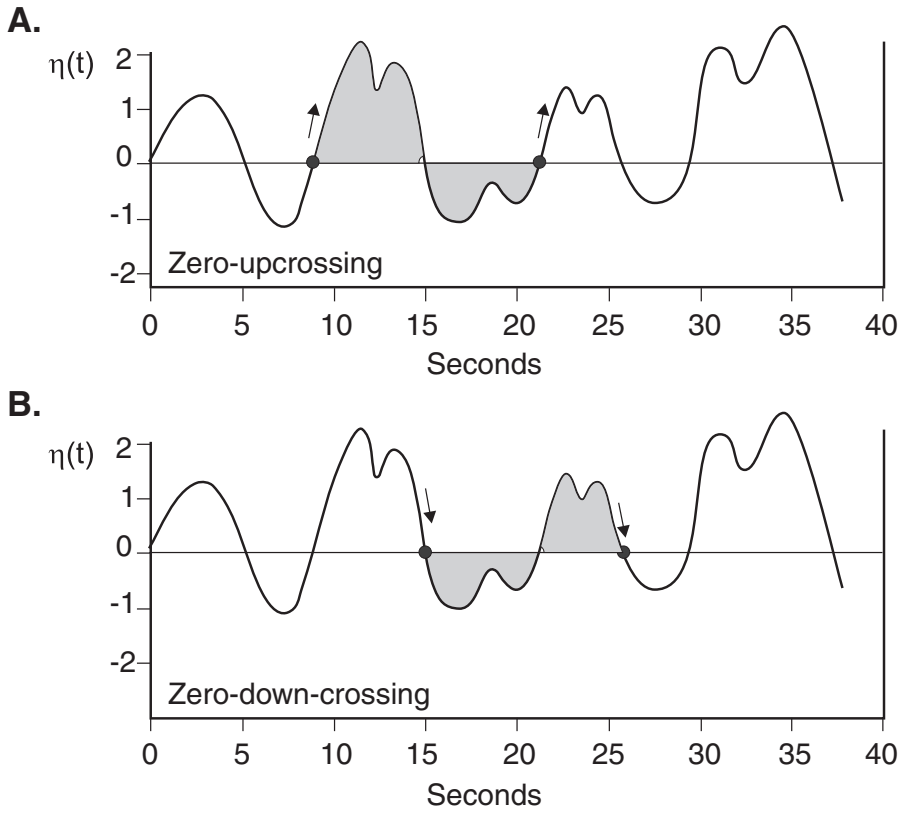

Figure 4.7 Analysis of waves using zero-crossing: (A) zero-downcrossing; (B) zero-upcrossing.

between the two definitions but the statistics for a typical record will be the same.

The analysis of a wave record in this manner will thus produce the height H and corresponding period T for every wave in the record and the distribution of these can readily be depicted (Figures 4.8a, b). We can then derive a number of statistics that are representative of the characteristics of H and T for that record. The most obvious are the mean wave height H and mean wave period T. Because we are often interested in wave energy and wave energy is proportional to H^2, the root mean square wave height H_{rms} can be calculated from

$$H_{\text{rms}} = \left(\frac{1}{N} \sum_{N}^{i=1} H_i^2 \right)^{0.5}. \tag{4.2}$$

Note that we can get this also directly from the complete set of measurements by taking the square root of the variance of the record.

Again, because wave energy is proportional to the square of wave height, the larger waves are often the ones that are of greatest significance; for example in modelling sediment transport or the impact of wave forces on a structure. Visual estimates of wave height tend to focus on the higher waves in a series and the height derived from this, termed the significant wave height, has been found to be roughly equal to the mean of the highest one-third waves. If we order the measured values of H and T we can separate out the highest one-third waves and directly obtain the mean height of those $H_{1/3}$ and the mean period associated with them $T_{1/3}$. Where the largest waves are of greatest interest (e.g. for wave overtopping of a breakwall) the value for $H_{1/10}$ and $T_{1/10}$ may be calculated.

4.3.3 Wave spectrum

The technique above describes the variation in the water surface in the time domain. While it

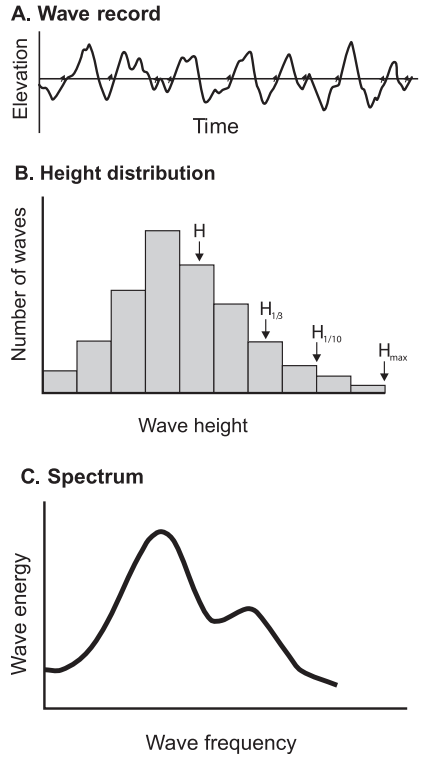

Figure 4.8 Description of a wave record: (A) graph of a portion of the record; (B) derivation of the statistical properties of the distribution of wave height H and period T; (C) the spectrum for a similar record relating wave energy (H^2) to wave frequency ($1/T$).

can provide useful data, and may be appropriate in some detailed studies of waves, it is tedious and provides only a portion of the information that we may be interested in. Routine analysis of wave records today is generally carried out using spectral analysis (Figure 4.8c) which transforms the history of the surface elevation into the frequency domain. Spectral analysis is a statistical technique which makes use of Fourier decomposition of the wave record into a series of sinusoidal waves of varying frequencies and corresponding amplitudes. It is a powerful technique that is used to examine a wide range of data that is periodic in time or space. Much of the development has come in the area of audio electronics (Cooley and Tukey, 1965), but it is now routinely applied to the analysis of wave and current records.

The energy in a progressive wave is made up of potential and kinetic energy and the total energy per unit width along the crest is given by

$$E = \frac{\rho g H^2 L}{8}. \tag{4.3}$$

The energy density $\overline{E}$ is the average energy per unit distance normal to the crest, = E/L. Thus wave energy is proportional to H^2. Likewise, the total energy in a wave record is proportional to the square of the deviations from the mean water surface – i.e. the variance of the record. It can be shown that a complex wave form can be produced by the addition of two or more simple sinusoids (Figure 4.9), and it is possible to reproduce any complex wave form by the appropriate combination of sinusoidal amplitudes, frequencies and phases. Spectral analysis of the wave record reverses this process and results in a decomposition of the record into frequency bands and provides an estimate of the amplitude of the sine wave associated with each band (Figure 4.10a). The amplitude squared can then be graphed against frequency to produce the variance spectrum (Figure 4.10b) which provides an estimate of the energy at each discrete frequency. Since all frequencies are present in the ocean, the variance associated with the amplitude at each frequency i is then distributed over the frequency interval at i to give the variance density spectrum (Figure 4.10c) and the continuous variance density spectrum can be obtained by smoothing this (Figure 4.10d). Note that if the energy density for all bands is summed it should equal the variance of the original wave record.

Because it is computationally much more efficient, the fast Fourier transform (FFT) is generally applied and this requires that the data length be a power of 2. As a result, most analysis is performed on records of 1024, 2048, 4096, etc. data points. Detailed treatment of the statistical technique can be found in a number of books, including Chatfield (2004), and applications to wave measurements in Hegge and Masselink (1996).

It should always be kept in mind that spectral analysis is a statistical technique, and in particular that the amplitude (energy) associated with each frequency is an estimate of the 'true' energy in that band. The raw spectrum provides estimates at frequencies of i/D but, because of uncertainties associated with each of these estimates,

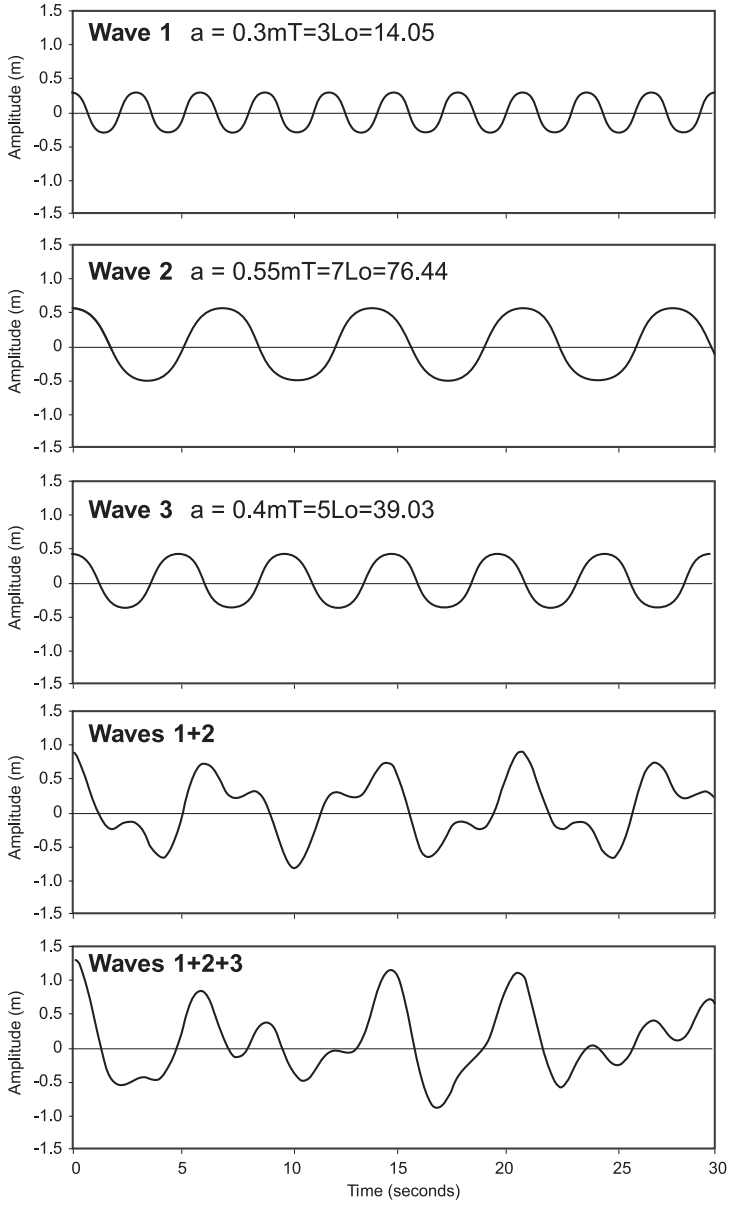

Figure 4.9 Complex wave forms resulting from the addition of two or more sinusoidal waves with differing frequency and amplitude.

the raw spectrum is highly variable and the confidence limits for each estimate are very wide. The raw spectrum is customarily smoothed to reduce the large, rapid fluctuations between bands and to improve the confidence interval by grouping bands and averaging over the new frequency interval. There is, however, a trade-off between increasing confidence in the estimate of spectral energy as more bands are grouped (for example in deciding whether the presence of a peak at a particular frequency is significant or not) and a reduction in the information provided because of the increased smoothing (the smaller peaks disappear with increased grouping).

The length of the record, and the sampling interval, place restrictions on the frequencies that can be resolved. Thus, if the water surface elevation is sampled twice a second (0.5 Hz) then the highest frequency that can be resolved is 1 Hz. This high-frequency cut-off is known as

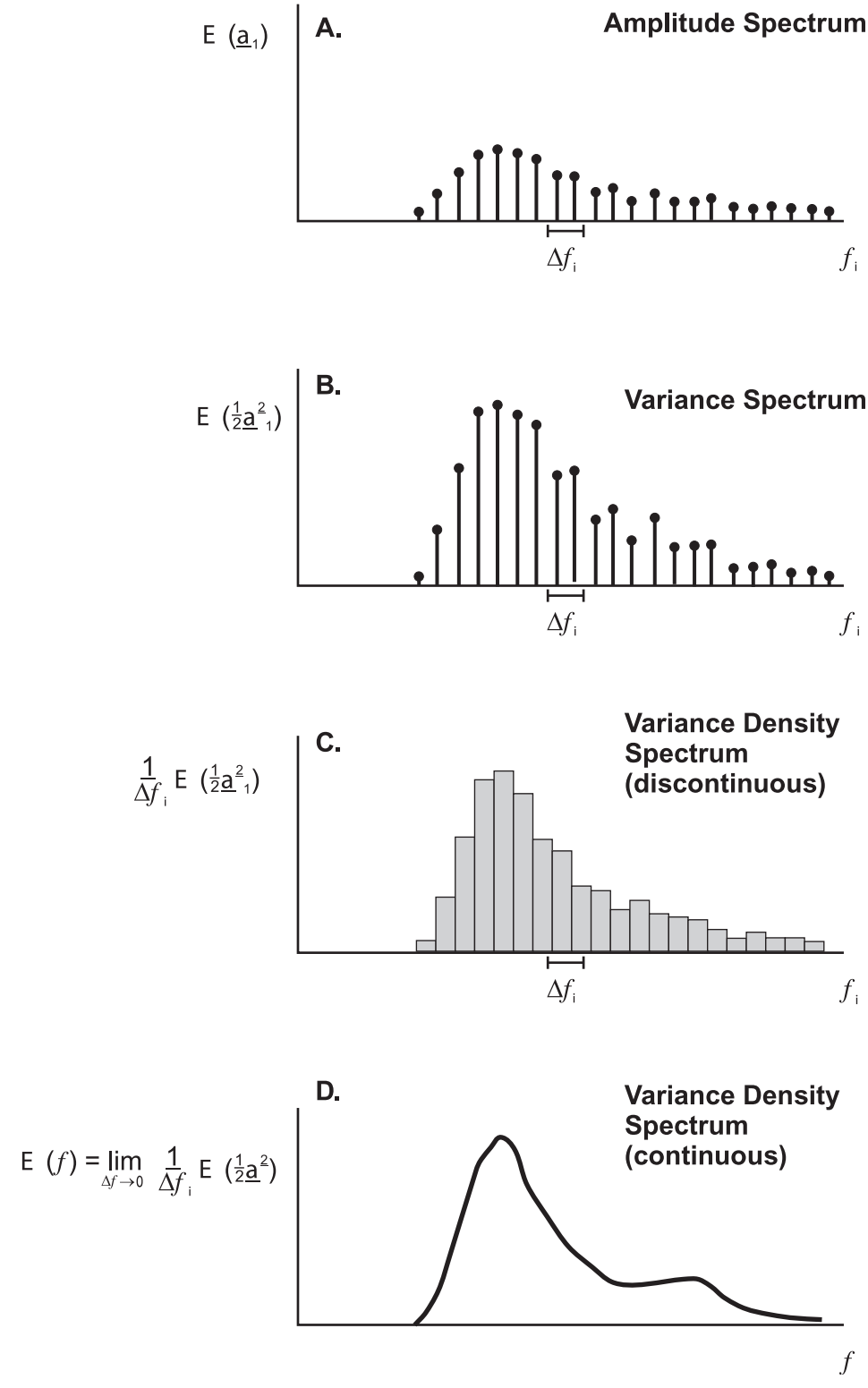

Figure 4.10 The transformation of the discrete amplitude spectrum of the random phase/amplitude model into the continuous variance density spectrum which provides a complete statistical description of sea surface elevation (Holthuijsen, 2007).

the Nyquist frequency. Likewise, the lowest frequency that can be resolved is equal to $1/N$, where N is the total length of the record. In practise, with smoothing of the record there is even greater restraint. A wave recording may consist of measurements made over some finite sampling period or it may be a sub-sample of a much longer record. In either case the sampling frequency (or digitising frequency for a continuous record), and the length of the record are important considerations. In general, a minimum of four data points should be used to define a wave so that a sampling frequency of 4 Hz can be used to resolve waves with a period of one second. Where low-frequency water motion with periods on the order of 30 seconds to several minutes may be present, a sampling time of 20–30 minutes is required.

Apart from its usefulness in identifying the energy associated with a particular frequency which may be important, for example, in designing harbours or breakwalls, peaks at various frequencies may provide evidence of the existence of particular physical phenomena. This is particularly true near the beach where the existence of standing gravity waves, edge waves, and secondary wave generation can be resolved from peaks in the spectrum, and particularly by comparing phase relationships between the water surface record and those of the two horizontal and the vertical water motions (Huntley, 1980).

It is also possible to obtain characteristic wave parameters from the spectrum. The standard deviation of the wave record σ_η (where η is the instantaneous water surface elevation) corresponds to $H_{\text{rms.}}$, and the equivalent significant wave height H_s is equal to $4 \times \sigma_\eta$, based on the assumption that wave heights follow a Rayleigh distribution. The significant wave height based on the spectrum is often designated H_{m0} where m_0 is the zeroth-order moment of the variance density spectrum (it is the variance of the surface water elevation). The frequency corresponding to the peak of the spectrum in the wind wave region is designated the peak frequency/period, equivalent to $T_{1/3}$.

The wave energy spectrum provides the best description of the wave field and modern wave prediction models all involve prediction of the evolution of the wave spectrum through time. Estimates of parameters such as significant wave height and period can then be drawn from these. The Fourier transform is based on the assumption that the series is stationary (hence records may be detrended to remove the tidal signal). Recent developments of wavelet analysis allow this assumption to be relaxed and thus permit full time-frequency representation of the time series (Donelan *et al.*, 1996; Massel, 2001).

4.4 Wave generation

The generation of waves by wind involves the transfer of energy from the wind to the water surface. The process is extremely complex physically and while over the past few decades there have been considerable advances in the development of models for predicting wave growth – see Komen *et al.* (1994) for a thorough review – the actual mechanism by which the energy is transferred to the water surface is relatively poorly understood. Nevertheless, the third generation of predictive models such as the WAM model described by Komen *et al.* (1994) are capable of providing highly accurate forecasts, based on the wind field, of both the generation of waves within a storm area and the dispersion of those waves outside the area of generation. A detailed understanding of the physics of the process is beyond our needs, but fortunately we can give a simple qualitative account of the controls on wave growth based both on empirical measurements and theoretical modelling. This then permits an understanding of the controls on the wave climate of any coastal location.

Simple visual observations on a small lake show that the water remains smooth and glassy in the absence of wind. If the wind increases in speed, higher gusts will produce small ripples on the surface ('cat's-paws') that are one or two cm in height and a few cm in wavelength (Figure 4.3). They travel in the direction that the wind is blowing (and a close look will show them moving outward in an arc centred on the wind direction). If the wind dies away after

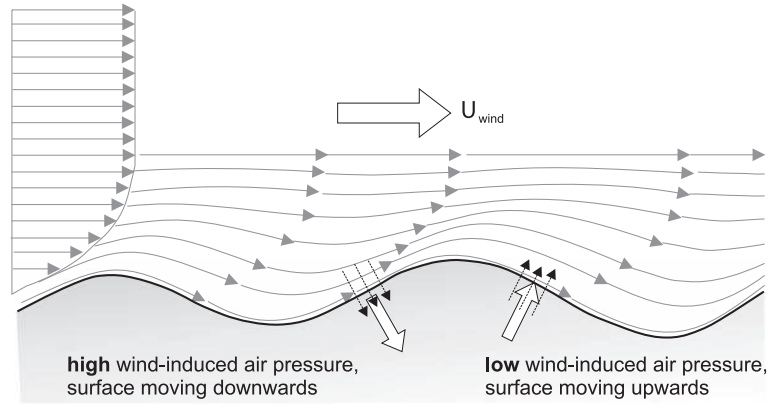

Figure 4.11 The wave-induced wind-pressure variation over a propagating harmonic wave (Holthuijsen, 2007).

a few tens of seconds then the ripples quickly dissipate and the water surface becomes calm again. This occurs because the energy in these small capillary waves is quickly dampened by surface tension of the water surface. Energy loss through surface tension is always a factor but its effects are most significant for the highest frequency waves and it has negligible effect on waves with frequencies lower than 0.25 Hz. If the wind continues to strengthen above the threshold dictated by surface tension, then the ripples do not die away but they continue to grow in both height and wave length as they move away from the upwind shoreline (Figure 4.3). This growth continues until they reach the opposite shoreline and break. If we were to measure the significant wave height and period ($H_{1/3}$ and $T_{1/3}$) at points across the lake then we would find that they increase with distance from the upwind shoreline – i.e. with the distance (and therefore time) over which the wind applies a force to the water surface. In addition $H_{1/3}$ and $T_{1/3}$ also increase with increasing wind speed. This is in accord with numerous observations and measurements, and it has long been recognised that the major controls on the size of waves generated are: (1) wind speed; (2) the fetch length (distance) over which the wind blows; and (3) the duration of the wind event. The fetch distance in effect can be thought of as imposing an upper limit on the duration that the wind can impart energy to waves on the water surface before they reach the opposite shoreline.

4.4.1 Wave generation process

The actual mechanism of wave generation by wind is highly complex and still poorly understood. It is generally agreed that the growth of waves is due primarily to pressure fluctuations rather than the simple frictional drag of the wind across the water surface (though this drag does produce a drift at the water surface in the direction of the wind). The problem is that wind is highly turbulent, with turbulence occurring at a range of frequencies and thus spatial scales. Moreover, as waves develop on the water surface the roughness of the surface changes and this in turn produces feedback between the evolving water surface topography and the behaviour of the lower boundary layer of the wind. Most models make use of the theory introduced by Miles (1957) which predicts that wave growth will be a function of resonant interaction between the growing waves and the pressure fluctuations associated with air movement across them, which then enhances the wave growth. Air pressure is at a maximum on the windward side of the crest and a minimum on the leeward slope which thus reinforces the upward movement as the crest approaches and the downward movement after it has passed. The result is a transfer of energy from the wind to the wave (Figure 4.11). As is the case with flow over sand dunes, the effect tends to be greater for larger forms and thus it becomes more effective as the waves grow in size. If the wave is high enough and steep enough it is possible to get flow separation over the crest.

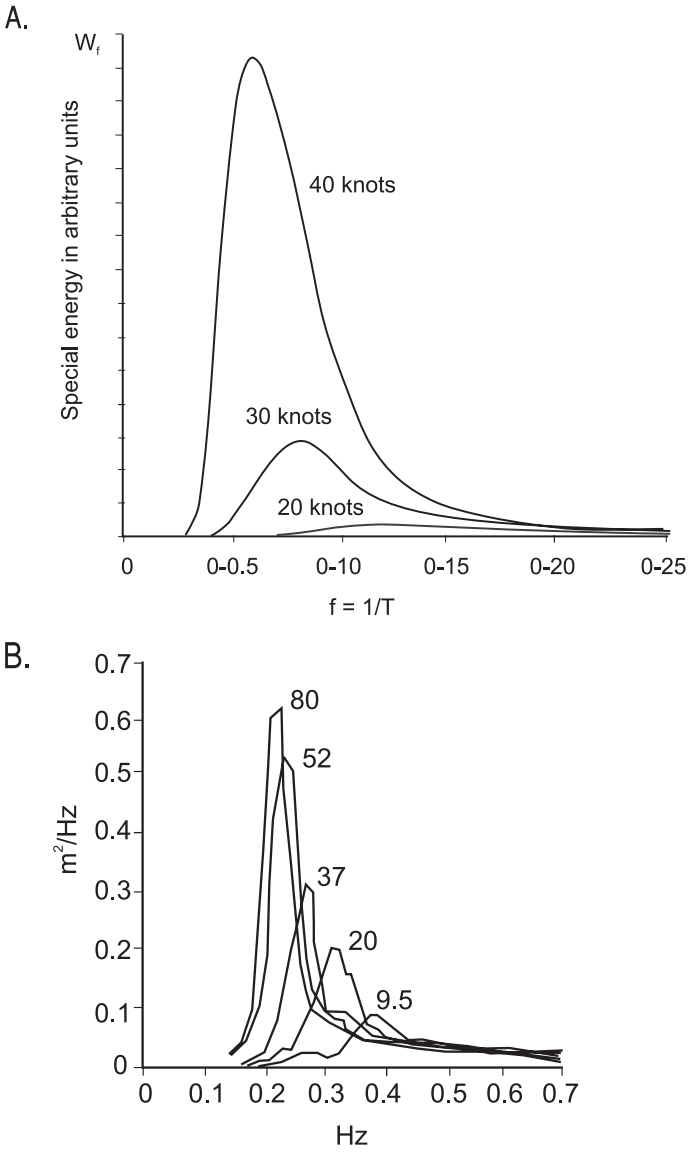

Figure 4.12 Spectral evolution: (A) wave spectra for a fully aroused sea for winds of 20, 30 and 40 knots; (B) evolution of wave spectra for constant wind speed with distance offshore (km) along a profile in the North Sea as part of the JONSWAP experiments (Hasselman *et al.*, 1973).

Since the wind is imparting energy to the water surface it is better to examine changes to the wave spectrum in relation to the three parameters controlling wave growth rather than simply looking at wave height and period. Early measurements showed that, for a given wind speed, the spectrum evolved to the point where it became essentially invariable but that the total energy in the spectrum increased with increasing wind speed and the peak frequency shifted toward the lower frequency, longer period waves (Figure 4.12a). Similarly, the energy in the spectrum increases and the peak frequency shifts towards lower frequencies as the distance over which a constant wind blows increases (Figure 4.12b). In the area where the wind is actively generating waves the spectrum is quite broad with a wide range of wave heights and periods as new waves are generated and older waves increase in height and period. These conditions in the area of active wave generation are termed sea. A young sea is characterised by continuing increase in the energy of the water surface but after some time the spectrum ceases to evolve and the energy level becomes nearly constant – a condition termed old sea or fully aroused sea

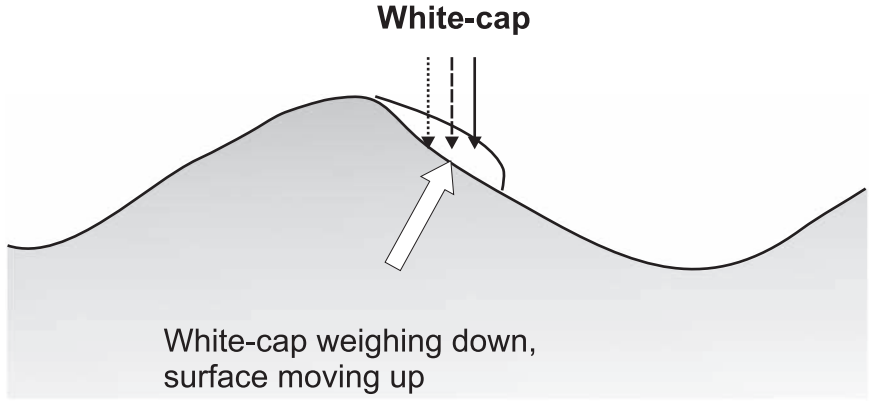

Figure 4.13 The presence of a white-cap on a wave forming a pressure pulse on the leeward side of the crest of a breaking wave (Holthuijsen, 2007).

(FAS). At this point the rate of energy transfer from the wind to the water surface must be balanced by the rate of energy dissipation. How does this wave energy dissipation take place?

There is a continual drain of energy from the waves due to viscosity, though this acts primarily on capillary waves and high-frequency gravity waves. There will also be some loss as waves travel outside the area of generation. However, the primary mechanism for energy dissipation as waves grow higher and longer is turbulence due to 'whitecapping' as a portion of a wave crest becomes oversteepened and breaks, dissipating energy due to turbulence as well as pressure effects on the front of the wave (Figure 4.13). This occurs frequently when waves with longer periods, and therefore greater celerity, overtake small waves causing local oversteepening of the small wave on the crest of the longer one. This phenomenon is readily observed whenever there is a stiff breeze blowing, even on relatively small water bodies. The process is usually highly localised because the waves are often travelling in slightly different directions and because the waves at this stage are very short-crested – individual wave crests can only be traced for a few tens of metres. As a result the oversteepening is restricted to a small area where the two wave crests reinforce each other.

Whitecapping thus preferentially affects the high-frequency waves in the spectrum. If the spectrum is plotted with energy on a logarithmic scale (Figure 4.10d) it slopes downward towards the right (higher frequencies) with a slope typically of f^{-4}. This slope reflects the achievement of saturation at those frequencies – i.e. energy at these frequencies is dissipated as fast as it is generated by the wind. The slope facing the lower frequencies is usually much steeper, reflecting a rapid drop-off in energy at periods longer than can be generated by the particular combination of wind speed and duration. The time it takes to reach the condition of FAS may be only a few hours for low wind speeds but is as long as several days for very high winds.

An area that is still poorly understood is the mechanism by which energy is transferred from higher frequencies generated by the wind towards lower frequencies – i.e. what causes the shift towards lower frequencies and longer wave lengths as the spectrum grows. It is now thought that this results from quadruplet wave–wave interaction which produces resonance among two pairs of wave components with identical wave lengths and wave numbers. The resonant interaction transfers energy between frequencies, though it does not affect the total energy. A large part of the energy is transferred to higher frequencies and is then dissipated through whitecapping, but some is transferred towards lower frequencies where it is absorbed without dissipation. The result

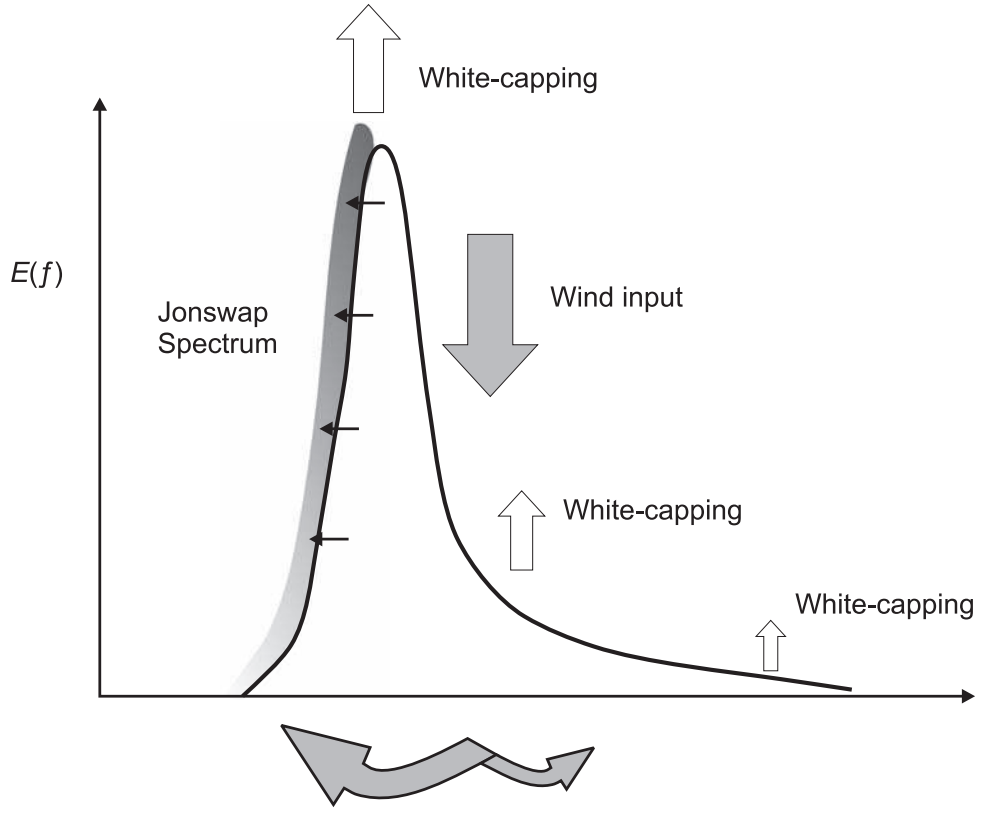

Figure 4.14 The flow of energy through an evolving JONSWAP spectrum in deep water (Holthuijsen, 2007).

is that growth in the energy spectrum takes place on the low-frequency side of the peak (Figure 4.14).

4.4.2 Limits to wave growth

So far we have assumed that wave generation takes place with no restrictions on the space and time scale and in water of infinite depth. However, the form of the spectrum and the final equilibrium condition will be affected by factors such as the initial sea surface condition, the fetch length over which the wind blows, the duration of the wind, water depth, and the effects of currents. Fetch length refers to the distance over which the wind is blowing and may be controlled by the size of the water body (e.g. in lakes and seas) or by the distance over which winds blow in the same direction, controlled by meteorological factors such as the dimensions of a mid-latitude depression or tropical hurricane. Because wind-generated waves are progressive, fetch length acts to restrict the length of time over which energy can be transferred to the wave group and it can be thought of as equivalent to a limit on duration, though the actual spectral shape may be somewhat different (Figure 4.12b).

The effect of shallow water is to increase the rate of energy losses through bottom friction and increased wave breaking, and hence to reduce the maximum wave dimensions. Shallow water also induces complications because wave celerity is reduced and this affects the resonance between the pressure fluctuations and waves. Both the growth of total energy and the migration of the peak frequency to lower values are reduced in comparison to results from deep water conditions (Young and Verhagen, 1996). However, prediction of the shallow water

spectrum is complicated by the effects of coastline irregularity and by varying depth contours.

The rate of energy transfer to the water surface has also been shown to vary with differences in air and water temperature and with the stability of the atmosphere. In general, the rate of transfer increases as the air temperature becomes cooler relative to the water surface. This has important effects in mid-latitude regions because lower waves can be expected in the spring when the air temperature tends to be warmer than the water and higher waves can be expected in the autumn when the sea temperatures are still relatively warm and air temperatures may be close to 0. The effect is diminished for very strong winds but may still be 5–10% greater for cold winds in the autumn compared to the same winds in the spring.

The complexity of waves in the area of wave generation is enhanced by the fact that wave generation takes place not just in the direction that the wind is blowing but in an arc up to 45° on either side of the mean wind direction. This increases the potential for whitecapping since waves are more likely to cross and produce local areas of oversteepening and it has implications for the way in which waves spread out across the ocean from the area of generation.

In areas of restricted fetch such as the semi-enclosed seas and the Great Lakes high wave conditions are almost always associated with storms and a broad spectrum. Swell waves are restricted generally to a few hours and occur as the winds die down. However, in the open ocean there is ample opportunity for waves to travel beyond the area of wave generation, and wave dispersion occurs as a function of the speed with which the waves (actually wave groups) travel. As noted earlier, the low-frequency, long wave length waves travel much faster and thus the waves sort themselves out by period. The wave spectrum becomes much narrower as the short-period waves are left behind and there is a transformation from the broad-banded sea, with short wave crests and much whitecapping, to a narrow-banded swell characterised by relatively low, long-crested waves without whitecaps. While dispersion can account for many of the observed changes, some other mechanisms, likely wave–wave interactions, must aid in the production of the longer crests and greater uniformity observed with swell waves.

4.5 Wave prediction

The term wave prediction can be used to include a variety of techniques used to forecast wave conditions at a particular location over some period of time. Wave forecasting refers to the prediction of wave conditions in an area for a period of hours or one or two days in the future, and is essentially similar to forecasting of meteorological data such as wind speed and direction, temperature, and precipitation. Indeed, forecasting of wave conditions utilises forecast wind speeds and directions and pressure gradients derived from meteorological charts. The ability to do so has now been greatly increased with the availability of satellite data which not only enhance the spatial coverage of meteorological data but also provide data on observed wave conditions which may aid the accuracy of wave growth predictions. Wave forecasting is used for a variety of purposes, mostly related to shipping, fishing and boating interests; indeed the first major efforts at wave forecasting arose out of the need by the American and British forces (and their allies) for accurate forecasts of wave conditions at landing sites in the Pacific and in Normandy during the Second World War.

Wave hindcasting is similar to wave forecasting and utilises the same predictive models. However, conditions are predicted for some time period in the past, and it frequently makes use of measured wind data rather than data derived from meteorological charts, particularly in areas of restricted fetch length where waves are primarily locally generated. Wave hindcasting is used to gather data for the design of installations such as harbour breakwalls, to correlate with events such as storm damage or with coastal erosion, or to produce a wave climate which can be used for the prediction of, for example, long-term rates of sediment transport or coastal erosion. For most geomorphological and engineering work hindcasting is used much more commonly than forecasting and this section will focus more on

that. However, it should be kept in mind that most of what will be covered with respect to hindcasting also applies to forecasting. Most models deal with wave generation in deep water since friction and shoaling will affect wave generation in shallow water and the shape of the resultant spectrum. In addition, the focal point for wave hindcasting is usually chosen to be in deep water so that most forecasting and hindcasting provides deep-water conditions.

4.5.1 Wave prediction models

We have seen earlier that waves are generated by a transfer of energy from winds to the water surface over which they are blowing, and that simple wave characteristics such as wave height and period are controlled by wind speed, duration, and fetch length. Because the theory of wave generation is still not fully developed, models for predicting wave characteristics rely heavily on some form of correlation of empirical data, matching measured wave characteristics with measurements of wind speed, direction and duration. The first operational model for wave prediction was put forward by Sverdrup and Munk (1947) based on work carried out during World War II. Their model essentially consisted of empirical equations which were used to

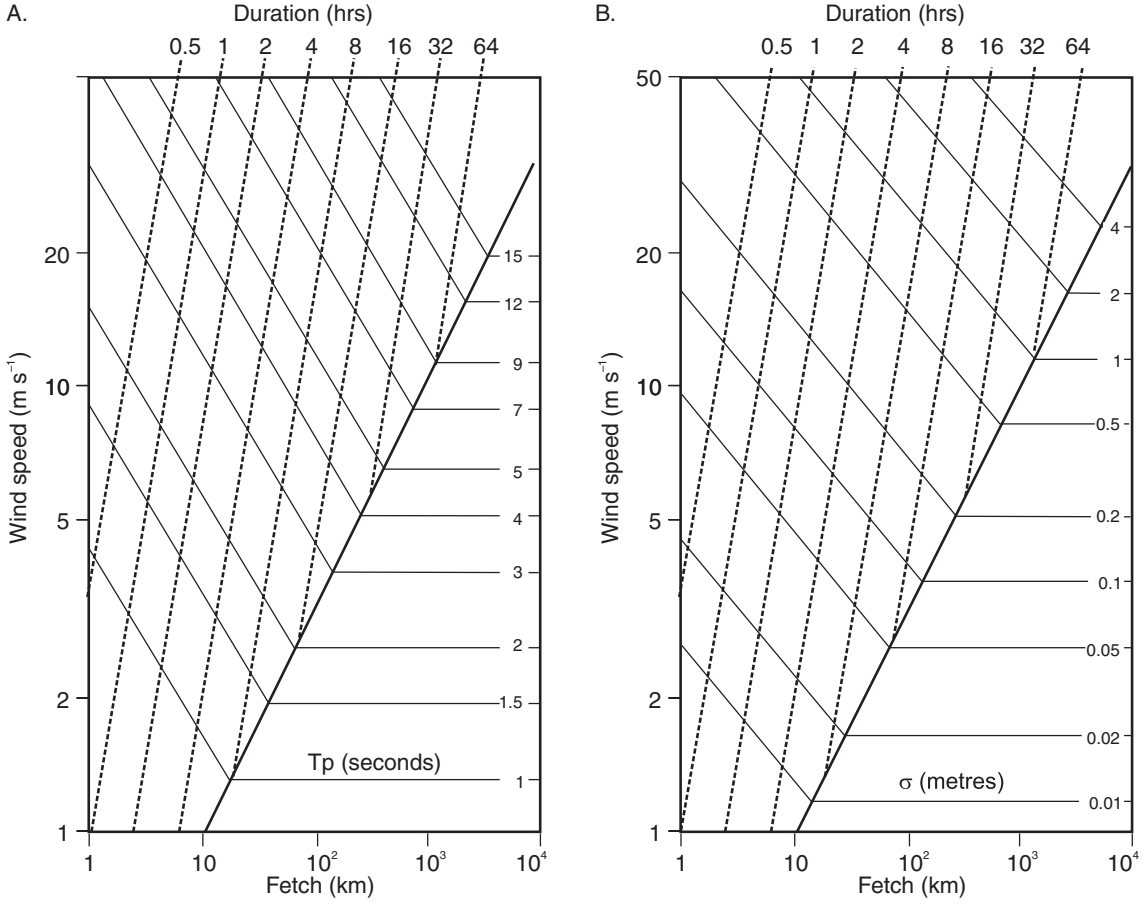

Figure 4.15 Nomograms for forecasting (A) peak wave period T_p and (B) root mean square wave height H_{rms} in areas of restricted fetch (Donelan, 1980). The graphs are entered horizontally from the left at the appropriate wind speed level. The point of intersection of that horizontal level and the appropriate fetch line (vertical) or duration (dashed line), whichever occurs first, defines T_p (A) or H_{rms} (B) – this is shown by the solid lines. The area to the right of the diagonal is the zone of full wave development for that combination of fetch length and wind speed where height and period can no longer increase. Note that $H_{1/3} \simeq 4H_{rms}$.

predict H_s and T_s for given wind speed, duration, and fetch length and the equations were revised on several occasions by Bretschneider (1952, 1958) and are referred to as the SMB method. The SMB equations were adopted by the US Army Corps of Engineers and widely propagated in their *Shore Protection Manual* (SPM, 1984), particularly in the form of nomograms (graphs) that permitted the interpolation of $H_{1/3}$ and $T_{1/3}$ from a given input wind speed and duration. The nomogram was particularly useful before the widespread use of computers and meant that engineers (and others) everywhere could predict wave conditions with relatively simple input data. The SMB method was widely used until the early 1980s because of its simplicity, and because it provided useful information for a variety of practical purposes. It has been dropped from the most recent version (2002) of the SPM, though the manual still retains a simple method for wave prediction under rather restricted conditions. Based on developments in wave theory and his work on wave measurements on Lake Ontario, Donelan (1980) produced simple nomograms for T_p and H_{rms} in areas of restricted fetch that can be used to explore wave generation in areas of restricted fetch (Figure 4.15).

The major strength of the SMB approach was that it gave direct prediction of the two most important wave characteristics – H_s and T_s – from which, together with wave direction, so much could be predicted. However, this is also its major weakness. As we have seen earlier, wave generation by winds produces not a single wave height and period, but a wave spectrum and, particularly as waves move out of the area of generation, it is necessary to know something about the whole spectrum because of the dependence of wave dispersion on period. Theoretically, it is more consistent to predict the spectrum and, since H_s and T_p can be predicted from the spectral shape, it is still possible to satisfy the simple requirements of engineers and coastal geomorphologists. As a result modern prediction models are based primarily on a prediction of the whole spectrum. The first spectral model was that of Pierson, Neumann and James, (1955 – the PNJ model) which examined changes in the spectrum beginning with a calm sea and was based almost entirely on empirical data. A number of numerical models predicting the spectra of wind-generated waves are now available. They may be divided into two types:

(1) (true) spectral models which utilise theoretical or empirical relationships to predict the evolution of the spectrum from consideration of energy inputs, losses and the redistribution of energy within the spectrum (e.g. Resio, 1981). These generally involve utilisation of the theory of wave generation resulting from the work of Miles (1957), Phillips (1957) and Hasselmann *et al.* (1973), extended and corrected by experimental data, which permit the formulation of a differential equation governing the growth of wave energy; and

(2) parametric models (e.g. Hasselmann *et. al.*, 1976) which solve the same energy or momentum transport equation but make assumptions about the shape of the spectrum so that the problem is reduced to prediction of a few non-dimensional parameters – i.e. it is computationally a lot simpler and easier to apply.

In particular, the work produced by the Joint North Sea Wave Project (JONSWAP) has provided a wealth of new field data and (we hope) improved prediction of the shape of the spectrum in an actively growing wind sea. There has also been considerable work carried out in the Great Lakes (e.g. Schwab *et al.*, 1984; Donelan *et al.*, 1985), which are an ideal place to study wave generation because of the restricted fetches in all directions and the relative abundance of meteorological station. A useful summary of early work on wave prediction models is found in Bishop and Donelan (1989).

Second-generation wave prediction models make use of a predefined spectral shape, such as the JONSWAP spectrum, and this reduces the computation required. Third-generation wave prediction models such as WAM (Komen *et al.*, 1994) and SWAN (Booij *et al.*, 1999; Holthuijsen, 2007) compute the quadruplet wave–wave interactions and do not impose any

a priori shape on the spectrum. Models such as SWAN and MIKE 21 incorporate refraction, diffraction and wave–current interactions and can model wave transformation into shallow water, thus providing extremely powerful tools for coastal design (Lin *et al.*, 2002).

4.5.2 Simple hindcasting for restricted fetches

Hindcast wave climates are now available for the Great Lakes, the coastlines of the USA and much of Canada as well as western Europe. Today wave hindcasting will be carried out using second- or third-generation wave models such as those noted in the previous section and a variety of meteorological inputs. However, there are many occasions when a simple prediction of wave conditions associated with a particular location and/or event is useful. This could be carried out for example, using the nomograms in Figure 4.15 or the ACES computer program put out by the US Army Corps of Engineers Coastal Research Centre. ACES is available free of charge but it is also incorporated in a commercial package that has more sophisticated input and output presentation. This kind of exercise is also useful because it highlights some of the requirements and operation of the more complex programs as well as the limitations. In doing this we can adopt a number of simplifications such as assuming a constant wind speed and direction and a limited duration of about 12–36 hours. It is most applicable to enclosed basins with fetches <200 km so that there is no significant wave input from outside the area of wave generation.

The first requirement is for input wind speed and direction. Ideally these should be over-water winds, but most meteorological stations are located on land and so it is necessary to choose a station that is likely to best represent over-water conditions. These data may need to be adjusted because speeds over water

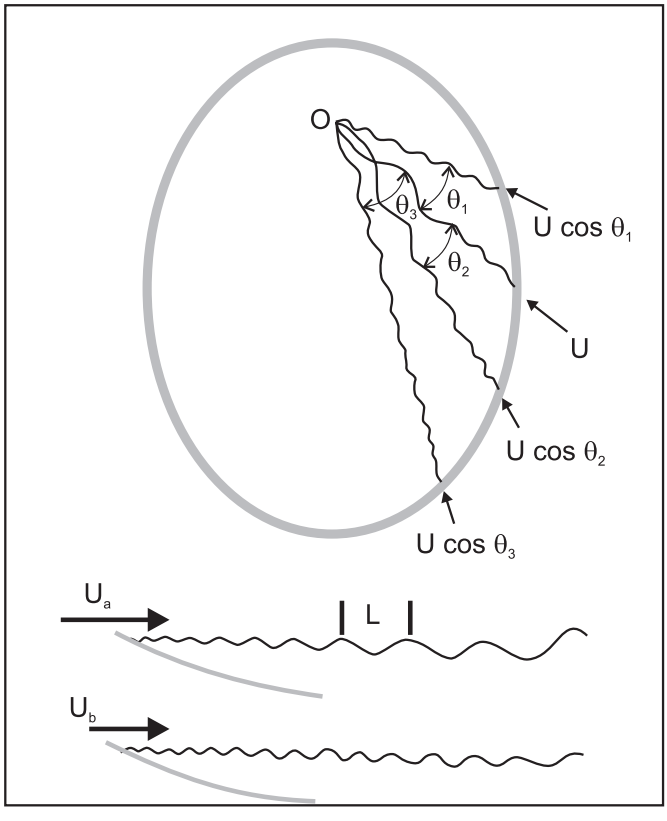

Figure 4.16 Schematic diagram showing the effect of fetch and wind speed on wave development: (a) increase in wave height and length along a fetch for wind speed U_a and for the effective wind U_b at some angle to the primary wind U_a. Wave height and length along the fetch U_b grow more slowly because the effective speed is less than that for the primary angle; (b) plan view showing the combined effect of the effective wind U cos θ and the corresponding fetch to the point of observation O. Note the rapid increase in fetch to the right of the wind (viewed from O) more than offsets the reduction of effective wind speed so that the largest waves approach from the θ_2 direction. (Donelan, 1980).

are usually higher than over the land where the surface is much rougher. If there are significant temperature differences between the air and water an adjustment will need to be made for this. If speed and or direction changes significantly through the event, it is possible to carry out the exercise in two or more stages. Use the average values for speed for the first stage to find the wave height and period at the end of this period. Next go to the mean wind speed for the second period and find the number of hours required at the new wind speed to achieve roughly the same height and period as the outcome from the first stage. Add these hours to the number of hours in the second stage and then determine the conditions at the end of the combined period.

The next step is to determine fetch lengths for the location of interest. The point from which fetch is measured will usually be located in deep water some distance offshore and in the middle of the reach. In enclosed bodies of water the fetch length in all directions is essentially determined by the location of the upwind shoreline and can be measured directly from a map or hydrographic chart. Because waves are generated over an arc around the wind direction and because the coastline may not be uniform, it is best to use an average of radials over a 30° interval (i.e. 15° either side of the direction) and a spacing of 3° (Donelan, 1980). In the ACES program fetches can be input for all relevant directions. Where there are small islands or shoals along the fetch line then some judgements will have to be exercised as to the likely magnitude of their effect.

4.6 Wave climate

A wave climate is the equivalent of the more familiar meteorological climate (temperature, precipitation, etc.) in that it is a summary of wave conditions (most commonly hourly values of H_s and T by direction averaged over one year). While there are some measured data

Box 4.1 Peak wave direction

A key element in any wave climate is the direction from which waves approach the coast. This is determined by the magnitude and frequency of winds from all directions in the area of wave generation, by the orientation of the coastline and by wave refraction and diffraction. Donelan *et al.* (1985) provide insights into many aspects of the controls on wave direction spectra. One outcome of this work that is directly applicable to large lakes and enclosed seas is the effect of basin shape on the peak wave direction. Donelan (1980) provides a simple explanation of this in relation to basin shape and wind direction (Figure 4.16). It is known that wave generation occurs not only in the direction in which the wind is blowing but also in an arc on either side of that direction. Wave generation in an off-wind direction can be related to what is termed the effective wind and is predicted by

$$U \cos \theta \tag{4.4}$$

where θ is the angle between the primary wind direction and the effective wind direction.

Thus, the effective wind decreases in speed as the angle from the primary direction increases. Since wave height, length and period increase with increasing wind speed we would expect the largest waves to be associated with the primary wind direction. However, we have seen that, for a given fetch, wave height, length and period also increase with increasing fetch up to the limit of a fully arisen sea. The dependence of wave characteristics on fetch and wind speed is illustrated in Figure 4.16a with the primary wind U_a being greater than the effective wind U_b at some angle to it. On an

enclosed body of water such as an estuary, large lake, or enclosed seas such as the Adriatic or Baltic, large changes in fetch length may occur with relatively small changes in direction (Figure 4.16b). In this case, the effect of increasing fetch length on wave size will more than compensate for the decrease in the effective wind speed up to some critical angle from the primary wind direction. Thus, waves from angle θ_1 will be much smaller than those associated with the primary wind direction because of the combined effect of decreasing fetch and decreasing effective wind speed (Figure 4.16b). However, towards the left, the effect of increasing fetch length initially more than compensates for the decreasing effective wind speed up to some angle θ_2. Beyond this, the effect of increasing fetch length is less than that produced by the decrease in effective wind speed, and consequently the waves associated with angle θ_3 are smaller.

The effect of this phenomenon will vary with the shape of the water body and the location of the point of interest on that water body. The variation in peak wave direction from wind direction for lakes of two different shapes is illustrated in Figure 4.17. It can be seen that for the most elongate lake, which is roughly the shape of Lake Ontario, the difference between the wind direction and peak wave direction can be as much as 50°.

The direction of peak wave approach can be determined for fetch-limited areas for winds from a particular direction using the following approach as outlined by Donelan (1980):

(1) Calculate the geometric fetch F_ψ for the incident wind angle ϕ by taking the equally weighted average of nine measurements, one along the angle ϕ and four each side at 3° intervals.
(2) Using the same procedure, determine F_ψ for angles at 3° intervals away from ϕ (only cases where the fetch length increases need be considered).
(3) The angle of approach for T_p (which roughly coincides with that for the highest waves) associated with the direction θ will be the condition for which

$$\cos\theta F_{\psi}^{0.426}$$

is a maximum, provided that fetch limited conditions apply over the direction ϕ.

The wave prediction routine in ACES includes the correction for effective wind angle.

for a few coastal locations, and these are gradually increasing, and compilations of ship observations, most coastal wave climates are determined by hindcasting either from meteorological charts or from measured wind data. Hindcast wave climates are usually based on a minimum of five years of recorded data, and more commonly ten to twenty years. In areas of restricted fetch hindcasting is relatively simple (Davidson-Arnott and Pollard, 1980), but on exposed oceanic coasts the wave climate will be influenced by events taking place a long distance away (Adams *et al.*, 2008). We can also distinguish between the deep-water wave climate and the transformation of this across the nearshore to produce the wave climate at the coast.

The wave climate data will frequently be broken down into seasonal or monthly averages as well, and some information on the wind climate, storm frequency and duration may also be included. Wave climate data can be used for a number of purposes, most commonly as input into modelling coastal erosion, sediment transport and the design of coastal structures (Resio *et al.*, 2002).

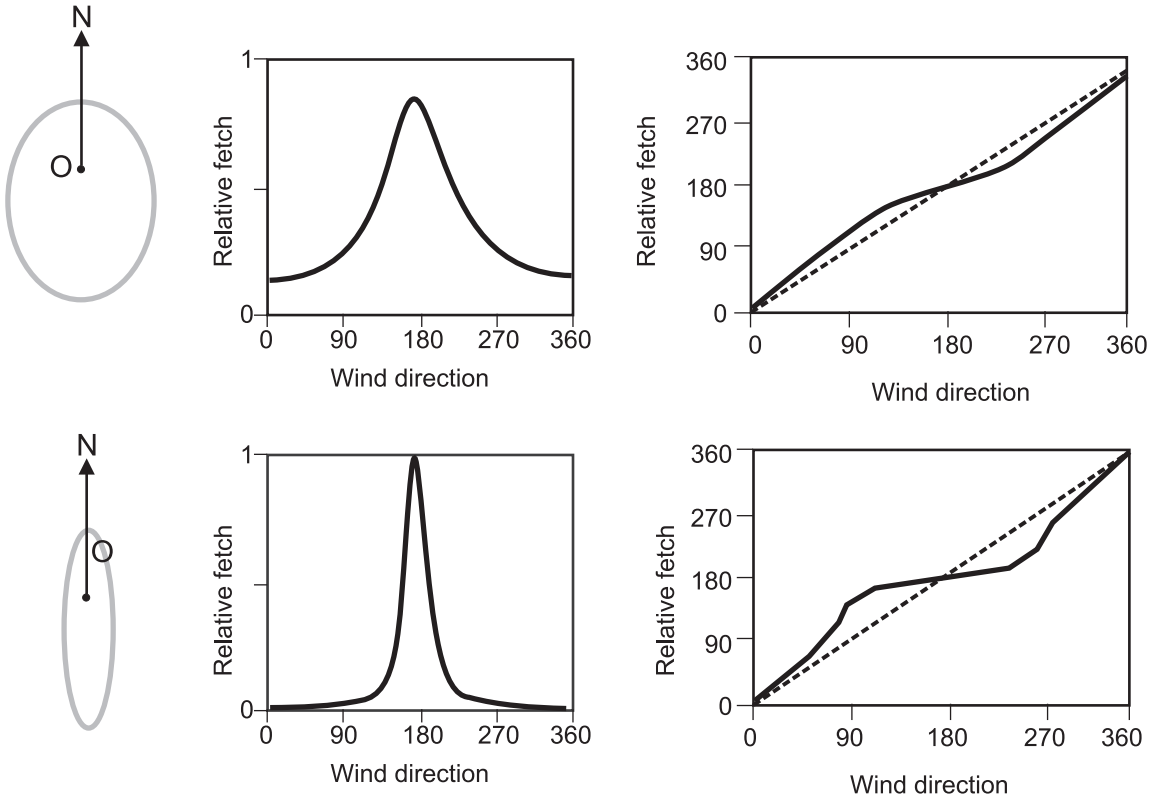

Figure 4.17 Peak wave direction at the focus of an elliptical water body versus wind direction for two basins with differing degrees of elliptical eccentricity: (a) elliptical eccentricity = 0.7; (b) elliptical eccentricity = 0.975 (this is similar to Lake Ontario). Each figure shows the variation in relative fetch with wind direction and the difference between the wind direction and the peak wave direction for a all directions. In the case of the mildly eccentric water body in (a) the maximum difference between wind direction and maximum wave direction is 20° while with greater eccentricity for the water body in (b) the differences are up to 50° (Donelan, 1980).

Further reading

Demirbilek, Z. and Vincent, C. L. 2002. *Water Wave Mechanics*. Chapter ll-1, EM 1110–2–1100 (Part ll), US Army Corps of Engineers, ll-1–1–121.

This is the most recent edition of the Shore Protection Manual produced by the US Army Corps of Engineers. It is available on the web as a PDF file and comes with a number of worked examples.

Holthuijsen, Leo H. 2007. *Waves in Oceanic and Coastal Waters*. Cambridge University Press, Cambridge, 387 pp.

This is a very readable description of wave generation, wave properties and wave modelling by one of the researchers involved in the development of the SWAN model.

References

Adams, P. N., Inman, D. L. and Graham, N. E. 2008. Southern California deep-water wave climate: Characterization and application to coastal processes. *Journal of Coastal Research*, **24**, 1022–1035.

Bishop, C. T. and Donelan, M. A. 1989.Wave prediction models. In Lakhan, V. C. and Trenhaile, A. S. (eds.), *Applications in Coastal Modeling*. Elsevier, Amsterdam, 75–105.

Booij, N., Ris, R. C. and Holthuijsen, I. H. 1999. A third-generation wave model for coastal regions, Part 1, model description and validation. *Journal of Geophysical Research*, **104**, 7649–7666.

Bretschneider, C. L. 1952. Revised wave forecasting relationships. *Proceedings of the 2nd Coastal Engineering Conference*, ASCE, pp. 1–5.

Bretschneider, C. L. 1958. Revisions in wave forecasting: deep and shallow water. *Proceedings of the 6th Coastal Engineering Conference*, ASCE, pp. 30–67.

Chatfield, C. 2004. *The Analysis of Time Series: an Introduction*. Chapman and Hall, London, 6th edn., 333 pp.

Cooley, R. J. W. and Tukey, J. W. 1965. An algorithm for the machine calculation of complex Fourier Series. *Mathematics and Computing*, **19**, 297–301.

Davidson-Arnott, R. G. D. and Pollard, W. H. 1980. Wave climate and potential longshore sediment transport patterns, Nottawasaga Bay, Ontario. *Journal of Great Lakes Research*, **6**, 54–67.

Davidson-Arnott, R. G. D. and Randall, D. C. 1984. Spatial and temporal variations in spectra of storm waves across a barred nearshore. *Marine Geology*, **60**, 15–30.

Donelan, M. A. 1980. Similarity theory applied to the forecasting of wave heights periods and directions. *Proceedings of the Canadian Coastal Conference*, National Research Council of Canada, pp. 47–60.

Donelan, M. A., Hamilton, J. and Hui, W. H. 1985. Directional spectra of wind-generated waves. *Philosophical Transactions Royal Society of London A*, **315**, 509–52.

Donelan, M. A., Drennan, W. M. and Magnusson, A. K. 1996. Nonstationary analysis of the directional properties of propagating waves. *Journal of Physical Oceanography*, **26**, 1901–1914.

Hasselman, K., Barnett, T. P., Bouws, E. and 13 others 1973. Measurement of wind-wave growth and swell decay during the Joint North Sea Wave Project (JONSWAP). Dt. hydrogr. A8 (Suppl.) no. 12, 95 p.

Hasselmann, K., Ross, D. B., Muller, P. and Sell, W. 1976. A parametrical wave prediction model. *Journal of Physical Oceanography*, **6**, 201–228.

Hegge, B. J. and Masselink, G. 1996. Spectral analysis of geomorphic time series: auto-spectrum. *Earth Surface Processes and Landforms*, **21**, 1021–1040.

Holman, R. A. and Guza, R. T. 1984. Measuring run-up on a natural beach. *Coastal Engineering*, **8**, 129–140.

Holthuijsen, Leo H. 2007. *Waves in Oceanic and Coastal Waters*. Cambridge University Press, Cambridge, 387 pp.

Huntley, D. A. 1980. Edge waves in a crescentic bar system. In McCann, S. B. (ed.), *The Coastline of Canada*, Geological Survey of Canada Paper 80–10, pp. 111–121.

Komen, G. J., Cavaleri, L., Donelan, M., Hasselmann, K. Hasselmann, S. and Janssen, P. A. E. 1994. *Dynamics and modelling of Ocean Waves*. Cambridge University Press, Cambridge, 532 pp.

Lin, W., Sanford, L. P. and Suttles, S. E. 2002. Wave measurement and modelling in Chesapeake Bay. *Continental Shelf Research*, **22**, 2673–2686.

Massel, S. R. 2001. Wavelet analysis for processing of ocean surface wave records. *Ocean Engineering*, **28**, 957–987.

Miles, J. W. 1957. On the generation of surface waves by shear flows. *Journal of Fluid Mechanics*, **3**, 185–204.

Munk, W. H. 1950. Origin and generation of waves. *Proceedings of the Coastal Engineering Conference*, ASCE, pp. 1–4.

Phillips, O. M. 1957. On the generation of waves by turbulent wind. *Journal of Fluid Mechanics*, **2**, 417–445.

Pierson, W. J., Neumann, G. and James, R. W. 1955. *Practical Methods for Observing and Forecasting Ocean Waves by Means of Wave Spectra and Statistics*. US Navy Hydrographic Office Publication 603, 284 pp.

Resio, D. T. 1981. The estimation wind-wave generation in a discrete spectral model. *Journal of Physical Oceanography*, **11**, 510–525.

Resio, D. T., Bratos, S. M. and Thompson, E. F. 2002. Meteorology and wave climate. Chapter 2 in EM 1110–2–1100 Part 2, *Coastal Engineering Manual*, US Army Corps of Engineers, 69 pp.

Schwab, D. J., Bennett, J. R., Liu, P. C. and Donelan, M. A. 1984. Application of a simple numerical wave prediction model to Lake Erie. *Journal of Geophysical Research*, **89**, 3586–3592.

Sverdrup, H. U. and Munk, W. H. 1947. *Wind, Sea and Swell: Theory of Relations for Forecasting*. US Navy Hydrographic Office Publication 601, 44 pp.

US Army Corps of Engineers, 1984. *Shore Protection Manual*, 2 volumes.

Young, I. R. and Verhagen, L. A. 1996. The growth of fetch limited waves in water of finite depth. Part 1: Total energy and peak frequency. *Coastal Engineering*, **29**, 47–78.

5

Waves – wave theory and wave dynamics

5.1 Synopsis

Wave theories provide a mathematical description of changes in the form of waves, and the orbital motion associated with them, from deep water to the breaker line and into the surf zone. Because of the limitations imposed by assumptions about the wave form and water depth, no one theory is valid over the full range of conditions. The theories can be used simply to predict wave height, celerity and length in any water depth as well as functions associated with the orbital motion, such as the maximum orbital motion near the bed and the orbital diameter. The formulae for the simplest theories can be programmed in a spread sheet, and there are computer programs available that will provide solutions for all of the basic theories. These theories also provide the basis for complex numerical simulation models that are used to predict waves, currents and sediment transport in the nearshore and breaker zones.

Wave shoaling describes changes to the wave form and orbital motion as it moves into shallow water. During the process of shoaling, interaction with the underwater topography results in a bending of the direction of travel of the wave crests so that they conform to the shape of the depth contours, a process termed wave refraction. Wave refraction leads to a concentration of wave energy in some location, especially headlands, and a divergence of energy in other areas.

Wave breaking occurs when that the front face of the wave becomes very steep and the forward motion becomes slower than the orbital motion in the wave crest. This leads to a jet of water from the top of the wave toppling forward onto the lower part of the wave as a spilling breaker, or plunging into the trough ahead of the wave. The turbulence produced during breaking results in a rapid decrease in wave energy and thus in the wave height. On steeply sloping shores wave breaking occurs on the beach, or cliff face for very steep coasts, but on gently sloping sandy beaches wave breaking may occur some distance offshore leading to the formation of a surf zone between the breaker line and the beach. The decrease in the forward momentum resulting from wave breaking and the injection of a mass of water into the surf zone leads to an increase in the water level against the beach, known as wave set-up. In turn this set-up drives the excess water offshore, either uniformly along the coast as an undertow or in a three dimensional circulation pattern with strong seaward-flowing currents spaced at intervals of several hundred metres alongshore.

5.2 Wave theories

Wave theories are applied to describe wave motion on the water surface and to predict such properties as the form of the surface wave, the motion of water particles (velocity and acceleration) within the wave from the surface to the

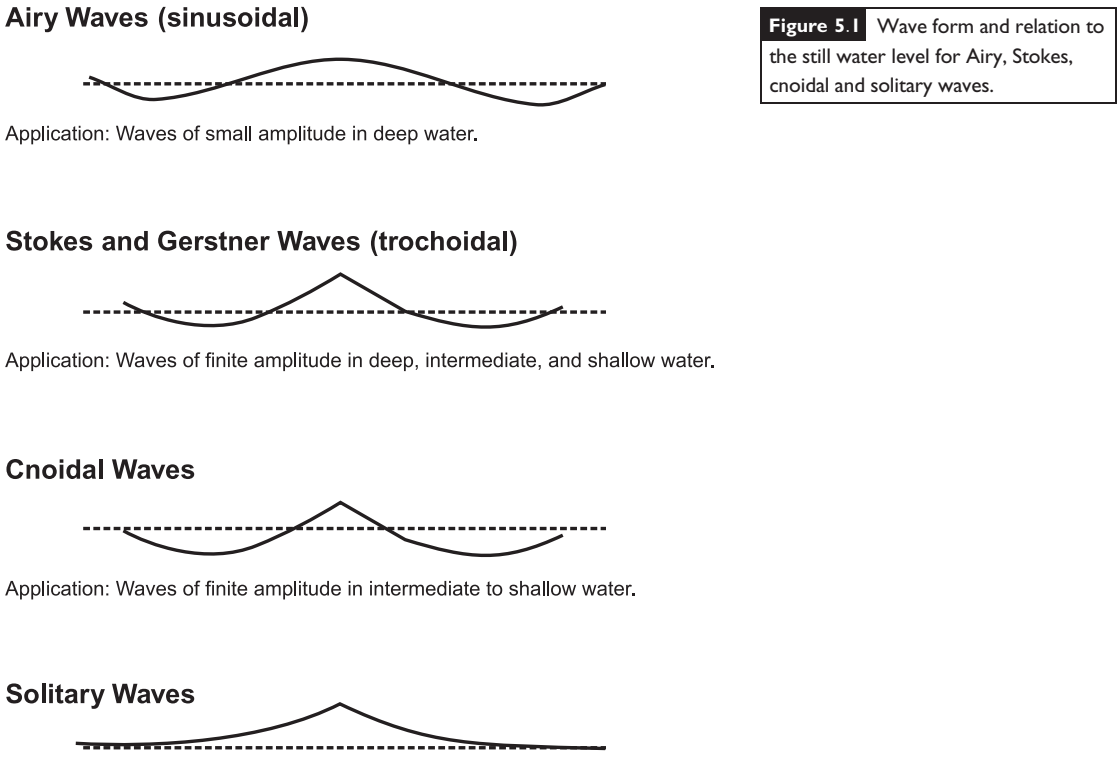

Figure 5.1 Wave form and relation to the still water level for Airy, Stokes, cnoidal and solitary waves.

limit of wave motion, and instantaneous pressure, and changes in these brought about by wave shoaling. The theories apply to regular waves and thus do not predict the complex motion found in irregular seas where short waves are superimposed on longer waves. Wave theories vary in their assumptions, notably about the shape of the wave surface profile and water depth, and this in turn affects the prediction of the shape of the orbital motion and thus the local fluid velocities and accelerations. In reality there is quite a range of wave form, and wave transformation during shoaling varies with the incident wave period and height, and the beach slope. As a result, no one theory can describe best the full range of conditions found in Nature. In addition, the more complex the wave form assumed, the more complex are the equations necessary to describe it. The wave form and assumption associated with the most widely used wave theories are outlined in Figure 5.1. Brief descriptions of each, and the numerical model of Dean (1965) can be found in Komar (1998) and Demerbilek and Vincent (2002).

We are particularly interested in being able to predict changes in wave length and height during shoaling, and the effects of this on orbital motion near the bed since this has a direct effect on sediment transport in the nearshore. The simplest of the wave theories, Airy wave theory, is generally adequate for these purposes and we will look at the key equations associated with it. In addition we will look briefly at Stokes's second-order theory, particularly for prediction of the net drift velocity.

5.2.1 Airy wave theory

Airy (1845) developed a theory for irrotational waves travelling over a horizontal bottom in any depth of water. The wave profile is assumed to be perfectly sinusoidal and only linear equations are necessary to describe the water surface and orbital motion – hence it is often termed

Table 5.1 | *Summary table of linear wave equations and the net drift velocity U_D from Stokes's second-order wave theory. Note that* $k = 2\pi/L$ *and* $\sigma = 2\pi/T$, $a = H/2$, h = *water depth.*

Parameter	General expression	Simplification
surface elevation η (x, t)	$\eta = a\cos(kx - \sigma t)$	
phase velocity C	$C = \frac{gT}{2\pi}\tanh\frac{2\pi h}{L}$	$C_0 = \frac{gT}{2\pi}$ $C_s = \sqrt{gh}$
wave length L	$L = \frac{gT^2}{2\pi}\tanh\frac{2\pi h}{L}$	$L_0 = \frac{gT^2}{2\pi}$ $L_s = T\sqrt{gh}$
horizontal orbital velocity u	$u = \frac{\pi h}{T}\frac{\cosh(k(z+h))}{\sinh(kh)}$	at the bed ($z = -h$) $U_{max} = \frac{\pi H}{T\sinh(kh)}$
horizontal orbital diameter A_s	$A = H\frac{\cosh(k(z+h))}{\sinh(kh)}$	at the bed ($z = -h$) $A_s = \frac{HT}{2\pi\sqrt{\frac{g}{h}}}$
net drift velocity (Stokes) U_D		at the bed ($z = -h$) $U_D = \left(\frac{\pi H}{L}\right)^2 \frac{C}{2\sinh^2\left(\frac{2\pi h}{L}\right)}$
wave height H	$H_i = H_0\left(\frac{\cosh^2 kh}{0.5(\sinh 2kh = kh)}\right)^{0.5}$	

linear wave theory in comparison to the other higher-order theories. It further assumes that the water surface slope is small, and that the water depth is much greater than the wave amplitude (hence it is also described as small-amplitude wave theory). Other key assumptions are that the fluid is homogeneous, incompressible and inviscid, that the water particles are irrotational, and that the bed is impermeable (there are no losses through the bed and the vertical velocity at the bed is zero). These assumptions generally hold in describing regular waves in deep water but, as water depth decreases, the assumptions about slope and the relationship between wave height and water depth are increasingly violated. As a result the accuracy of the predictions is reduced. The general expressions as well as simplifications for use in deep water and shallow water are summarised in Table 5.1. The expressions $2\pi/T$ and $2\pi/L$ occur frequently in the equations and are termed σ = wave radian (or angular) frequency and k = wave number respectively.

Wave profile

The water surface elevation for any combination of distance x (where x is positive in the direction of wave advance) and time (usually seconds) is given by the expression

$$\eta(x,t) = a\cos\left(\frac{2\pi x}{L} - \frac{2\pi t}{T}\right) \tag{5.1}$$

where x is distance in the direction of wave advance, t is time (seconds), a is wave amplitude, L is wave length and T is wave period.

If either x or t is held constant and the other varied the result is a sinusoidal profile of amplitude a and period T in space or time. Some form of this equation occurs in all the equations used to describe instantaneous water particle motion and serves to locate the point of interest on the wave profile.

Wave period, celerity and length

The general relationship between these three parameters is

$$C = \frac{L}{T}. \tag{5.2}$$

Wave period is assumed to be constant (a reasonable assumption even at the break point), and is generally known. The general expression for celerity is

$$C = \sqrt{\frac{gL}{2\pi}\tanh\left(\frac{2\pi h}{L}\right)} \tag{5.3}$$

(note that tanh is the hyperbolic tangent function and not tan (h) – the explanation for this is given in the next section). Equation 5.3 is the dispersion relation and shows that waves with longer wave lengths travel at higher speeds than those with shorter wave lengths. In deep water, because of the dependence of L on T, it also means that long-period waves travel faster than short-period ones. Combining (5.2) and (5.3) we get

$$C = \frac{gT}{2\pi}\tanh\left(\frac{2\pi h}{L}\right) \tag{5.4}$$

and combining (5.2) and (5.4) we get

$$L = \frac{gT^2}{2\pi}\tanh\left(\frac{2\pi h}{L}\right) \tag{5.5}$$

Equation 5.5 is difficult to evaluate since L appears on both sides (and we cannot find C in equation 5.4 until we know L). However L can be obtained by successive approximation. This is accomplished by using the value of L obtained in one iteration as the input value for the next iteration. If a reasonable initial value for L is used – e.g. the deep water value L_0 – a good estimate can be obtained after five or six iterations and much greater accuracy can be obtained in computer programs where a large number of iterations can easily be carried out. This expression can be applied in all water depths.

In deep and shallow water the equations for length and celerity can be greatly simplified. In deep water $\tanh(2\pi h/L) \gg 1$, and (5.4) and (5.5) reduce to

$$C_0 = \frac{gT}{2\pi} \tag{5.6}$$

and

$$L_0 = \frac{gT^2}{2\pi}. \tag{5.7}$$

In deep water the orbital diameter of water motion becomes negligible some distance above the bed and thus the characteristics of the surface form are essentially independent of the water depth. It can be seen from equations 5.6 and 5.7 that the wave length and celerity in deep water are dependent solely on the wave period T and that the length and celerity of waves increases with increasing wave period. As water depth decreases these parameters are increasingly affected by interaction of the orbital motion with the bed and the general expression should be used for $h/L_0 < 0.25$.

In shallow water $\tanh(2\pi h/L) \sim 2\pi h/L$ (at values of $x > 0.3$ $\tanh(x) = x$) and we get

$$C_s = \sqrt{gh} \tag{5.8}$$

and

$$L_s = T\sqrt{gh}. \tag{5.9}$$

Thus, in shallow water celerity is a function solely of depth, though length is still dependent on both depth and period. It can also be shown that

$$\frac{C}{C_0} = \frac{L}{L_0} = \tanh\left(\frac{2\pi h}{L}\right). \tag{5.10}$$

These equations are the same for Stokes's second-order wave theory.

Orbital motion

In addition to the movement of the surface form, water particles in a wave describe an orbit with the passage of each wave (see Figure 4.1). For sinusoidal waves in deep water this orbit is exactly circular and the diameter of the circle at the surface is equal to the wave height. The orbital diameter decreases with depth below the surface and is negligible at a depth equal to $L_o/2$. The orbital diameter decreases hyperbolically with depth below the surface and hence hyperbolic functions are used to predict these changes. In water depths $< L_o/2$ the wave orbits intercept the bed and the

water motion becomes increasingly elliptical. Wave theory can be used to predict water particle position, velocity and acceleration at any point along the wave (x or t) and at any depth z below the surface. These general expressions are quite complex, but a few of the more useful ones are given here. In addition, several simplifications can be made if they are evaluated at the bed ($z = -h$). Since this is where sediment erosion and transport occurs, this is of particular interest to us. The horizontal and vertical components of orbital velocity u and w are given by

$$u = \frac{\pi H}{T}\frac{\cosh(k(z+h))}{\sinh(kh)}\cos(kx - \sigma t) \tag{5.11}$$

$$w = \frac{\pi H}{T}\frac{\cosh(k(z+h))}{\sinh(kh)}\sin(kx - \sigma t). \tag{5.12}$$

Note. The first part of the expression provides the wave 'dimensions' of height and period, the second part uses the hyperbolic functions to evaluate the effect of depth below the surface on the orbital motion, and the third part of the expression locates the position on the wave form.

The horizontal and vertical diameters A and B can be predicted from

$$A = H\frac{\cosh(k(z+h))}{\sinh(kh)} \tag{5.13}$$

and

$$B = H\frac{\cosh(k(z+h))}{\sinh(kh)} \tag{5.14}$$

In deep water $A = B$ and the orbits are circular, and in shallow water $A > B$ and the orbits are elliptical.

In geomorphological studies, particularly in relation to bedforms, the horizontal orbital diameter at the bed is often an important parameter:

$$A_{(\text{bed})} = \frac{H}{\sinh(kh)}. \tag{5.15}$$

In shallow water this is predicted by

$$A_{s(\text{bed})} = \frac{HT}{2\pi}\sqrt{\frac{g}{h}}. \tag{5.16}$$

Another useful parameter related to bedforms and sediment transport is the maximum horizontal velocity at the bed. This occurs under the wave crest and trough – that is, for values of $\varphi = \pi, 2\pi, 3\pi$ etc. – and (5.11) reduces to

$$U_{\max(\text{bed})} = \frac{\pi H}{T\sinh(kh)}. \tag{5.17}$$

Wave energy

The energy in water waves is made up of two components:

(1) Kinetic energy associated with the orbital motion of the water particles;
(2) Potential energy resulting from displacement of the water surface away from the swl.

According to Airy wave theory, if potential energy is determined relative to the swl and all waves are propagated in the same direction, the two energies are equal, and the total energy per unit crest width is given by

$$E = E_k + E_p = \frac{\rho g H^2 L}{16} + \frac{\rho g H^2 L}{16} = \frac{\rho g H^2 L}{8}. \tag{5.18}$$

The energy per unit area, or energy density, $\overline{E}$ is given by

$$\overline{E} = \frac{E}{L} = \frac{\rho g H^2}{8}. \tag{5.19}$$

The rate at which energy is transmitted in the direction of wave propagation is the energy flux P (sometimes called wave power), and is given by

$$P = \frac{1}{8}\rho g H^2 C\frac{1}{2}\left(1 + \frac{2kh}{\sinh 2kh}\right). \tag{5.20}$$

Let

$$n = \frac{1}{2}\left(1 + \frac{2kh}{\sinh 2kh}\right) \text{ then } P = \overline{E}Cn \tag{5.21}$$

where $\overline{E}$ is the wave energy density E/L.

In deep water $2kh = 2\pi$, and $\sinh kh = \sinh 2\pi = \infty$. Equation 5.21 then reduces to: $n = 0.5(1+0) = ½$. Therefore in deep water energy is propagated at one half of the celerity of an individual wave. In shallow water $kh < 1$ and $\sinh 2kh = 2kh$. Equation 5.21 then reduces to: $n = 0.5\ (1+1) = 1$. Therefore in shallow water the rate of energy propagation is equal to the wave celerity.

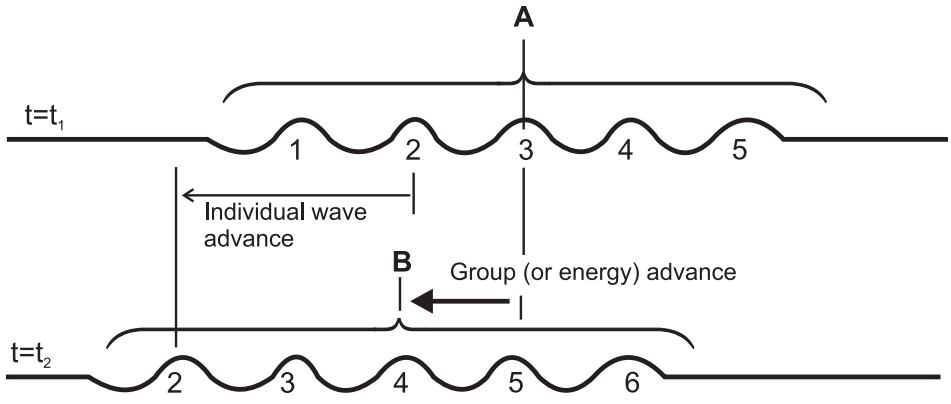

Figure 5.2 Schematic of the advance of a wave group over one wave period (Sunamura, 1992).

The expression *Cn* (sometimes written *Cg*) is known as the group celerity. If a group of say five or six waves is generated in a long wave tank, it can be easily demonstrated that as the waves travel down the tank, the first wave decreases in height until it disappears and the second wave now becomes the leading wave (Figure 5.2). At the same time, a new wave develops behind the last wave, thus maintaining the number of waves. The process keeps repeating, and the effect is that the group of waves travels down the tank at a speed equal to one-half the speed of the individual waves in the group (assuming they are in deep water). This phenomenon can sometimes be observed from a beach, particularly with low swell waves. The most important consequence of this phenomenon is in forecasting wave propagation and in particular the travel time of waves generated by a distant storm.

Wave height

If we assume that there are no energy losses through bed friction, wave breaking or wave refraction, then it is possible to predict wave height at any point as a wave moves into shallow water based on the energy equation and changes in celerity. In (5.17) it was shown that wave energy was proportional to H^2 and L, and in (5.19) that the rate of energy propagation is proportional to *Cn*. Thus, if E remains constant and we know C, then it is possible to predict H. It can be shown that

$$H = H_0 \sqrt{\frac{1}{2n}\frac{C_0}{C}}. \tag{5.22}$$

In practice H is derived from the equation

$$H_i = H_0 \left(\frac{\cosh^2 kh}{0.5(\sinh 2kh + kh)} \right)^{0.5}. \tag{5.23}$$

As we will see later, it is possible to modify the wave height predicted by Airy wave theory in a numerical model to allow for changes due to bottom friction and wave refraction. Energy loss due to friction during shoaling is really only of geomorphological significance on very gentle slopes, but the process of wave refraction is extremely important in changing the alongshore variability in wave energy.

5.2.2 Higher-order wave theories

Solution of the hydrodynamic equations for gravity waves can be improved over the linear model by making use of higher-order, non-linear expressions which can produce better agreement between theoretical and observed wave behaviour. In particular, linear wave theory which makes use of a symmetric wave form, cannot predict the mass transport phenomena which arise from asymmetry in the wave form. In this section we will examine the additional complexities introduced by the simplest of the higher-order theories – Stokes's second-order theory and the derivation of one more essential equation. We will also examine briefly other higher-order theories.

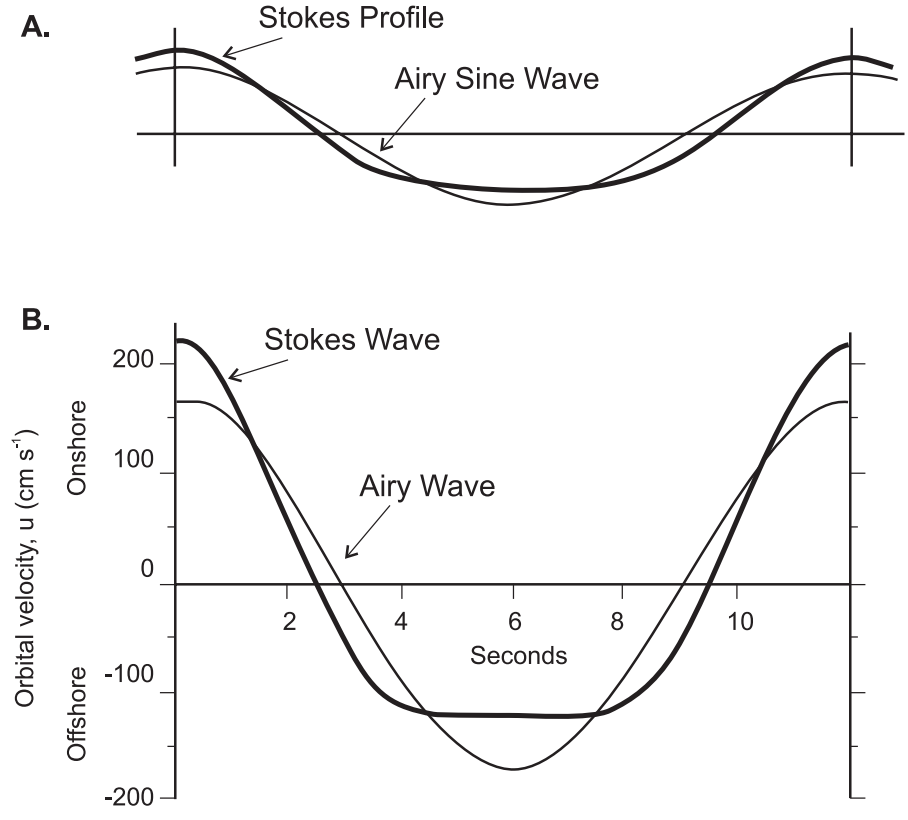

Figure 5.3 Comparison of properties of Airy and Stokes waves: (a) wave profile; (b) bottom orbital velocity (Komar, 1998).

Stokes's second-order wave theory

As waves move into water of decreasing depth the form of the wave becomes distorted so that it is no longer symmetrical and the wave crest becomes narrower and more peaked while the wave trough becomes flatter and wider (Figure 5.3a). This results in horizontal water velocity that is higher under the wave crest than the offshore velocity under the trough but of shorter duration (Figure 5.3b). Wave steepness H/L increases and the relative depth h/L decreases, and as this occurs the wave amplitude can no longer be considered small relative to water depth – instead we are dealing with finite-amplitude waves. Historically, the first finite-amplitude wave theory was that developed by Stokes (1847) which includes a perturbation solution that can be expanded to consider greater numbers of terms. Stokes's second order theory is the simplest of these, and can be programmed on a calculator or spread sheet, while routine access to high speed computers has led to Stokes's fifth-order theory being widely used in modelling (Demirbilek and Vincent, 2002).

The water surface elevation predicted by Stokes's second order theory is

$$\eta = \cos(kx - \sigma t) + \frac{\pi H^2}{8L}\frac{\cosh\left(\frac{2\pi h}{L}\right)}{\sinh^3\left(\frac{2\pi h}{L}\right)} \times \left(2 + \cosh\frac{4\pi h}{L}\right)\cos(2kx - 2\sigma t). \quad (5.24)$$

The first part of the equation is the same as (5.1) and represents the linear contribution to the surface form, while the second part is the second-order contribution. Third-order theory would involve an additional set of expressions including H^3.

An important difference in the orbital motion between linear wave theory and finite wave theories is that the orbital motion is no longer closed (Figure 5.4), so that as each wave

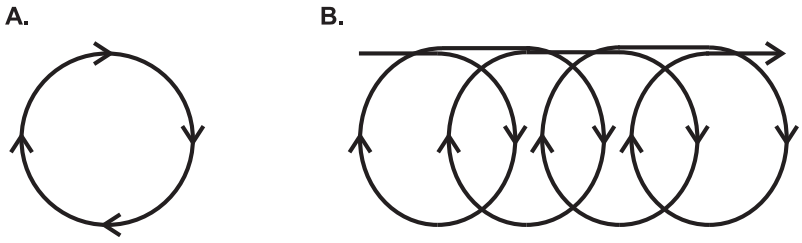

Figure 5.4 Net drift velocity in waves: (A) the closed orbit produced predicted by sinusoidal Airy wave theory; (B) the open orbit predicted by non-linear wave theory. At the end of each orbit the position of a water particle moves a short distance in the direction of wave advance. Division of this distance by the wave period give the net drift velocity.

passes a water particle moves a short distance in the direction of wave advance. The existence of this net motion, called Stokes drift, is well known and it can be predicted from Stokes's second order theory by

$$U_{(z)} = \left(\frac{\pi H}{L}\right)^2 \frac{C}{2} \frac{\cosh \frac{(4\pi z + h)}{L}}{\sinh^2\left(\frac{2\pi h}{L}\right)}. \quad (5.25)$$

From the viewpoint of sediment transport and beach equilibrium, it is extremely important because it provides one mechanism by which net sediment transport can occur once sediment has been set in motion by the much higher instantaneous velocities associated with the purely oscillatory portion of wave motion. At the bed $z = -h$ and $\cosh(4\pi(z+h)/L) = 1$, so (5.25) reduces to

$$U_{D(bed)} = \left(\frac{\pi H}{L}\right)^2 \frac{C}{2\sinh^2\left(\frac{2\pi h}{L}\right)}. \quad (5.26)$$

The net drift velocity at the bed is initially very small compared to the maximum orbital velocity, but it increases in magnitude as the wave shoals and near the breakpoint can be a substantial fraction of it.

Shallow-water theories

As waves move into shallow-water wave celerity becomes influenced more by wave amplitude than water depth. The water particle motion is now dominated by horizontal flows so that vertical accelerations become very small, and Stokes's theory becomes less and less valid (Figure 5.5). Cnoidal wave theory developed by Kortweg and de Vries (1895) is applicable in relative water depths $h/L<0.125$ and thus best used close to the break point. Mathematically it is difficult to apply and it is only recently that solutions have been developed for computer applications – e.g. in the ACES program. The properties of long waves close to the break point and particularly bores in the surf zone can be approximated by solitary wave theory.

Solitary waves consist essentially of a wave crest above the still water line (Figure 5.1) and they have infinite wave length and period. They are often described as waves of translation since the water particles are displaced quite a distance in the direction of the wave advance. This phenomenon can often be observed on sand bars at low tide when surf bores translate across the bar surface and into the trough landward of it (see Chapter 8).

Solitary waves are the most elementary solution of shallow-water Boussinesq equations which are written in terms of a depth-averaged velocity (Demirbilek and Vincent, 2002). Much of the recent modelling of waves in the surf and swash zones is now based on some form of Boussinesq model (e.g. Madsen *et al.*, 1997; Bayram and Larson, 2000; Karambas and Koutitas, 2002).

5.3 Wave shoaling and refraction

As waves in deep water propagate towards the land, they interact with the bed and can be affected by a whole suite of processes that lead

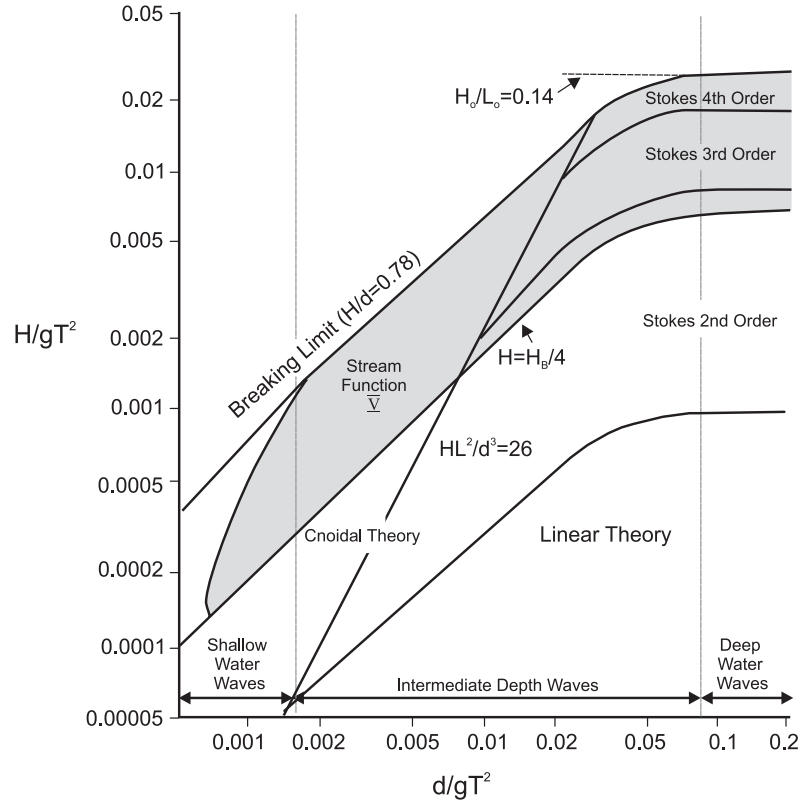

Figure 5.5 Range of suitability of various wave theories in relation to wave steepness and relative depth.

to transformation of the height, length, shape, speed and direction of the wave. As noted below, the peak period of the waves tends to remain constant, but there will be changes to the wave spectrum during the process of transformation. Processes that lead to transformation of waves as they propagate into shallow water include

(a) shoaling
(b) refraction
(c) diffraction
(d) dissipation due to bottom friction
(e) dissipation due to percolation (into the bed)
(f) breaking
(g) additional growth due to wind (and other wind effects)
(h) wave–current interaction
(i) wave–wave interaction
(j) run-up.

5.3.1 Wave shoaling

The term shoaling is used to describe the propagation of waves from deep water into decreasing water depth. This results in changes to wave height, celerity, the speed of propagation of wave energy C_n, and the wave length; and eventually leads to breaking of the wave in shallow water (Figure 5.6a). We have already seen that these are predicted by wave theories generally, and in particular by Airy wave theory using the equations shown in Table 5.1. Note that Airy wave theory does not account for energy losses due to friction or percolation, or for wave refraction or diffraction and thus predictions can be made for any arbitrary water depth based on H_0 and T.

As waves propagate into shallow water they begin to interact with the bed at h/L_0 <0.5. Changes in the ratios of C, L, H and C_n to their deep water values as well as the value for n are shown in Figure 5.6b. As water depth decreases the wave speed C and length L progressively decrease, and in general the height H increases. These changes are most readily apparent in long-period swell waves which interact with the bed earliest, and which are most nearly sinusoidal. Steep, short-period storm waves, characteristic of fetch-limited areas, do not feel the effects of

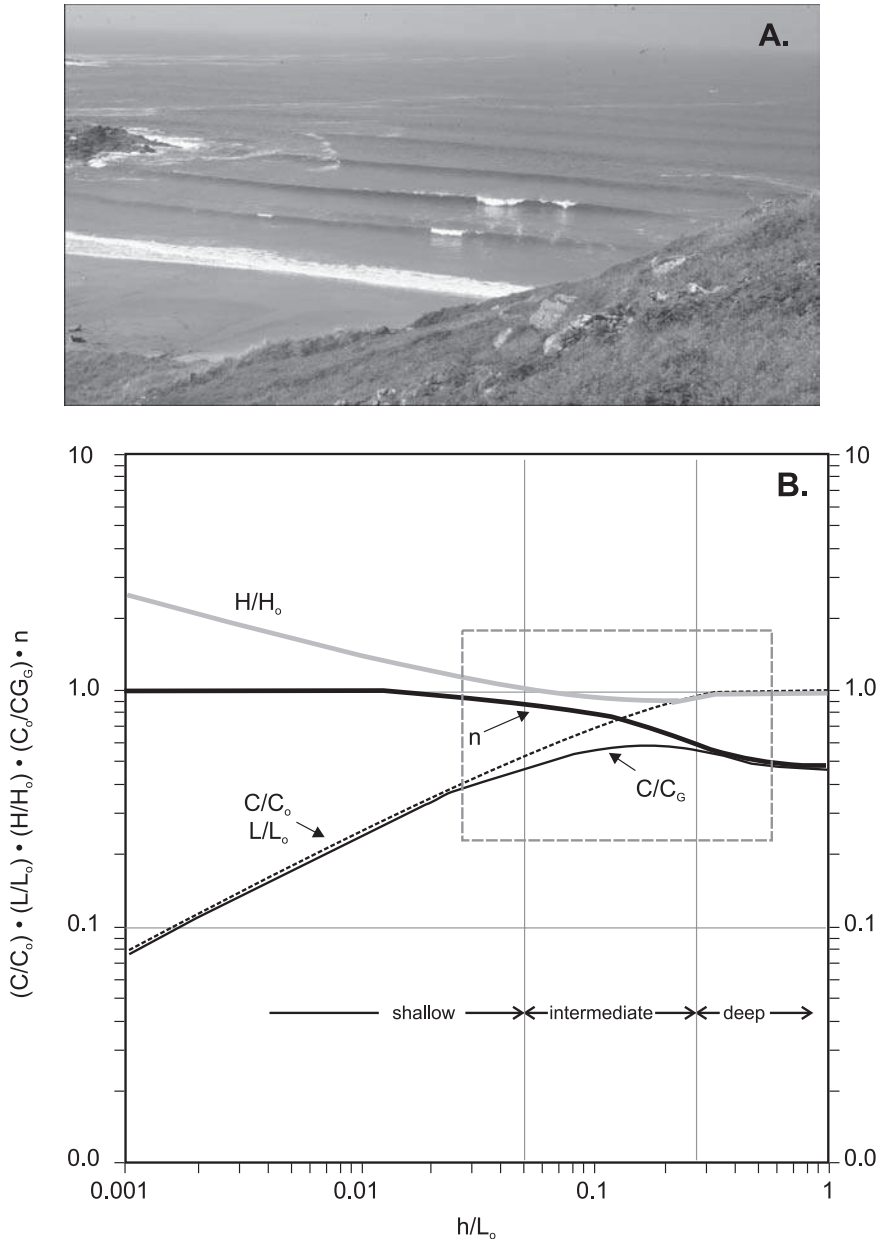

Figure 5.6 Wave shoaling: (A) photograph of low, swell waves shoaling and breaking on a gently sloping nearshore, west coast of Ireland showing the decrease in wave length and increase in wave height towards the break point; (B) the shoaling transformations for Airy waves (Komar, 1998).

the bed until they are in much shallower water and, because they are initially steeper, the transformation is not as apparent visually.

Changes in wave height during shoaling are a little more complex, and can be obtained from a consideration of wave energy flux and the ratio C_n/C_0. If we assume no energy losses due to bottom friction then the energy flux must remain constant outside the breaker zone and thus

$$P = ECn = ECn_0 = \text{constant}. \tag{5.27}$$

Initially, as the wave shoals, n increases faster than C decreases – this results in a temporary decrease in E which manifests itself as a decrease in H. Thus, there is initially a small decrease in wave height, followed by a rapid increase towards the break point (Figure 5.6b). This is easily measured in a wave tank and can be observed with waves approaching a natural beach, particularly with low swell wave (Figure 5.6a).

Using Airy wave theory the ratio of wave height H at an arbitrary depth to the deep-water wave height H_0 is given by

$$\frac{H}{H_0} = \frac{1}{2n} \times \frac{C_0}{C}. \tag{5.28}$$

The actual increase in wave height at breaking will be larger than that predicted by Airy wave theory, provided all the other assumptions are maintained, because of the failure of the small-amplitude assumptions of Airy wave theory close to the break point. The initial decrease in wave height means that wave steepness also decreases slightly, then increases rapidly in shallow water because of the combination of decreasing wave length and increasing wave height. Steepness increases rapidly until a point is reached where the wave becomes unstable and then breaks. However, before examining the processes involved in breaking waves, we will first look at wave refraction.

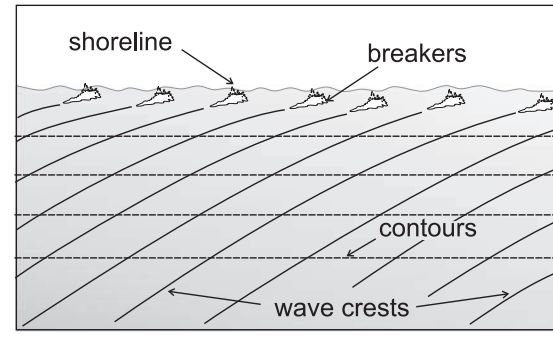

Figure 5.7 Refraction of wave crests along a straight beach with parallel contours.

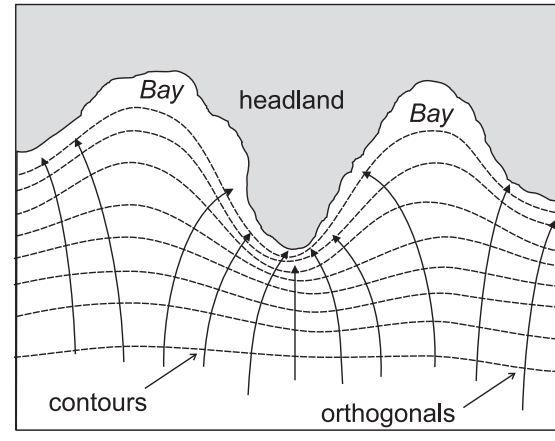

Figure 5.8 Refraction of waves shown by wave orthogonals over mildly complex topography associated with a series of headlands and bays.

5.3.2 Wave refraction

As waves move into intermediate and shallow water they tend to align themselves with the underwater contours through a process known as wave refraction. The basic process results from the fact that wave celerity decreases as the wave shoals and, if the waves are travelling at an angle to the bottom contours, the portion of the wave in deeper water will move faster than the portion in shallower water. This causes the wave crest to bend towards the alignment of the bottom contour. The refraction process is analogous to the refraction of light waves which is predicted by Snell's law, and simple refraction theory for water waves is based on this approach.

Wave refraction can be depicted by tracking the behaviour of wave crests (Figure 5.7), but in examining the effects of refraction on wave height and energy distribution along the shoreline it is often more useful to examine the behaviour of wave orthogonals – lines drawn perpendicular to the wave crest at all points during its travel. If we assume conservation of the wave energy between orthogonals from deep water towards the beach, then convergence of orthogonals reflects a compression of the wave at that location and results in an increase in energy (manifested by an increase in wave height). Conversely, divergence of orthogonals represents a stretching of the wave crest and produces a decrease in wave energy and height. Examples of the refraction of water waves over mildly complex topography are shown in Figure 5.8. Refraction thus has the effect of increasing or

Box 5.1 | Simple wave refraction modelling

The changes in the angle of an orthogonal as it passes over relatively simple topography can be approximated using Snell's law as follows:

$$\sin a_2 = \frac{C_2}{C_1} \sin a_1 \tag{5.29}$$

where a is the angle between the wave crest and the depth contours at two locations and C is the wave celerity at the same locations. In the more general case:

$$\sin a_i = \frac{C_2}{C_1} \sin a_0. \tag{5.30}$$

The geometry of this is illustrated in Figure 5.10. Assume a wave approaching the coast at an angle α_0 in deep water to straight parallel underwater contours. At point B the wave crest is at the contour line marking the transition from deep to intermediate water while at point A the crest is in deep water. Over one wave period the wave crest at A will travel a distance equal to the deep-water wave length L_0 reaching the contour at which $h/L_0 = 0.5$. However, the wave at point B will travel a slightly smaller distance $BD = L$ that reflects a reduction in the wave celerity as the wave shoals. For ΔABC $\sin \alpha_0 = L_0/BC$ and for ΔDBC $\sin \alpha = L/BC$. Then:

$$\frac{\sin a}{\sin a_0} = \frac{L}{L_0} = \frac{C}{C_0} = \tanh \frac{2\pi h}{L}. \tag{5.31}$$

decreasing the wave height reaching the shore and thus the longshore distribution of wave energy – a process that may be extremely important in determining the magnitude of wave erosion, impacts on harbour and shore protection structures and the direction and magnitude of longshore sediment transport. Wave refraction (together with diffraction) allows wave energy to reach parts of a complicated shoreline that face quite different directions from that of the incident waves (Figure 5.9).

5.3.3 Wave refraction modelling

As noted above, wave refraction theory assumes that wave energy is conserved between orthogonals. If s_0 is the spacing of orthogonals in deep water and s_i the spacing at some depth i, then:

$$P = EC_n s_i = EC_n s_0 = \text{constant}. \tag{5.32}$$

The wave height H at any location can be predicted from the spacing of orthogonals s at that location:

$$\frac{H}{H_0} = \left(0.5 \times \frac{1}{n} \times \frac{C_0}{C}\right)^{0.5} \left(\frac{s_0}{s}\right)^{0.5}. \tag{5.33}$$

The process of determining wave refraction and associated energy changes involves a number of simplifying assumptions, including: the absence of lateral spreading of energy along the crest (diffraction); that celerity is a function of depth; that changes in bathymetry are gradual, and that the waves are regular, long-crested and of small amplitude.

The first, simple wave refraction diagrams were constructed manually using graphical techniques (Munk and Traylor, 1947). These simple techniques using linear wave theory were adopted for computers in the mid-1960s (Wilson, 1966; Dobson, 1967) and operationalised by a number of people. The program WAVENRG by May (1974) is one of the latter and has been used in a number of studies in the Great Lakes (Greenwood and McGillivray, 1978; Davidson-Arnott and Amin, 1985; Lawrence and Davidson-Arnott, 1997). These programs generally require the input of bathymetric data in a grid format, and utilise these to calculate local slope. Each run requires the input of T, Ho, wave direction, and the location and spacing of the initial starting points for

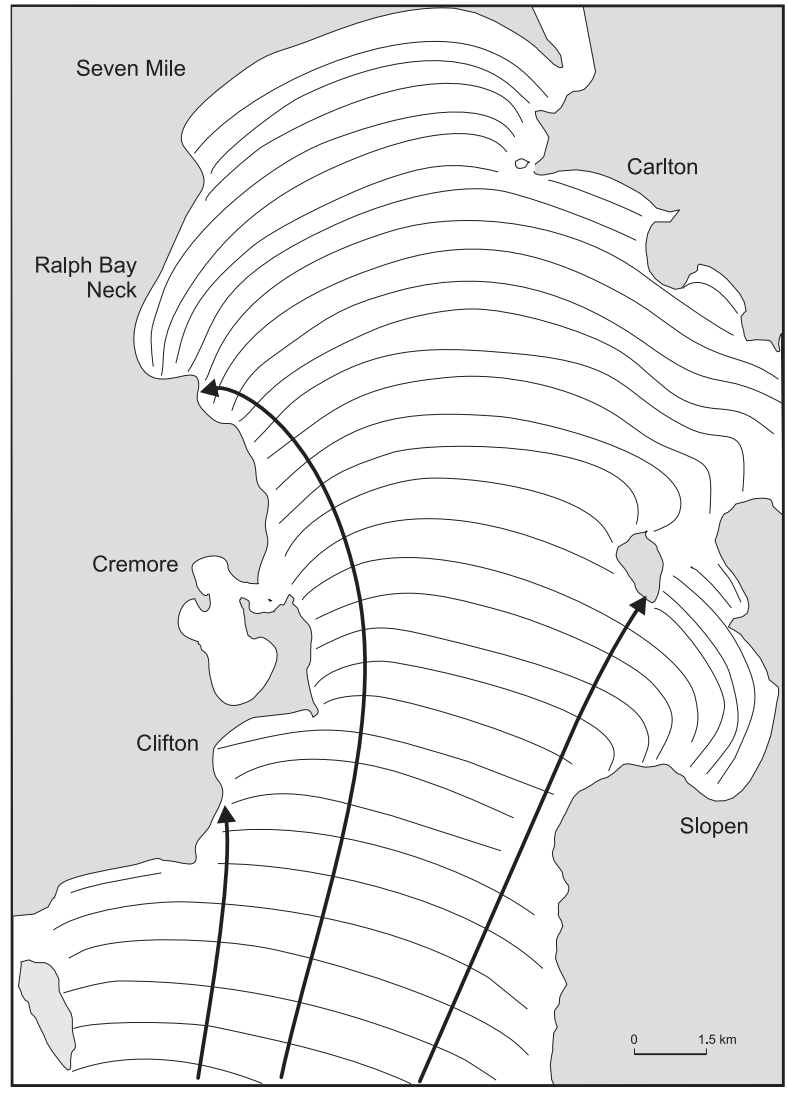

Figure 5.9 Wave refraction patterns for Frederick Henry Bay, Tasmania (Davies, 1958)

the orthogonals. Wave refraction diagrams using WAVENRG taken from Davidson-Arnott and Amin (1985) are shown in Figure 5.11. The computer programs can either be forward tracking, with rays sent shoreward from some deep-water location, or backtracking in which the waves are sent offshore from some preselected site(s). The former approach is more useful when considering the effects of a known wave climate with specified wave direction classes, whereas the latter may be more useful in evaluating conditions that may affect a particular site (e.g. location of a marina facility).

Wave diffraction is the process whereby wave energy is transferred laterally along the wave crest. This occurs in response to rapid changes in underwater topography, most notably around a headland (e.g. a spit, headland or harbour breakwall) and is responsible for the propagation of waves into areas behind the obstacle that might be in a shadow zone. Early computer models such as WAVENRG did not incorporate diffraction, with the result that in areas of rapid convergence wave height grew very large and produced wave breaking in quite deep water (see Figure 5.11).

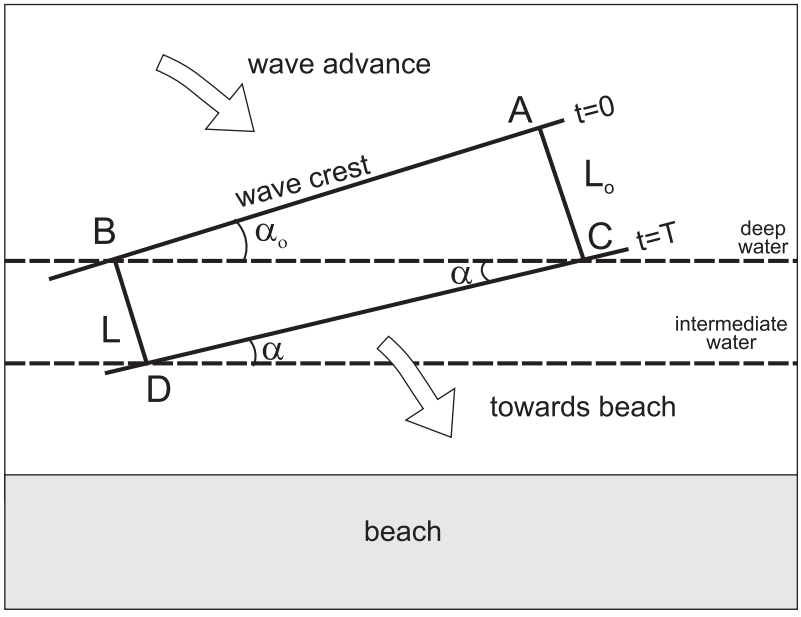

Figure 5.10 The refraction of a wave crest at the transition from deep to intermediate water with smooth, parallel underwater contours.

A. North-west [5.0 sec; 1.5 m]

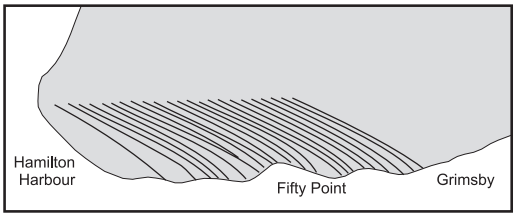

B. North [7.0 sec; 1.75 m]

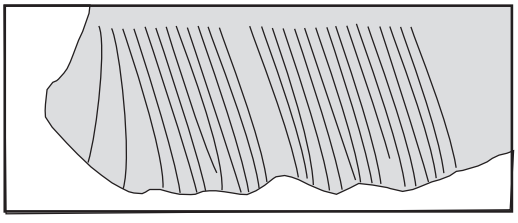

C. North-east [5.0 sec; 1.75 m]

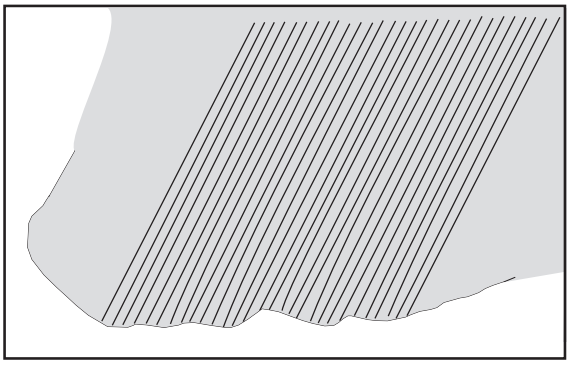

D. East [9.0 sec; 2.25 m]

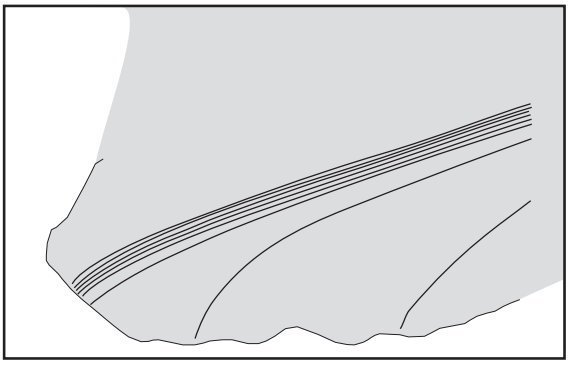

Figure 5.11 Wave refraction diagrams produced from the program WAVENRG (May 1974) for four directions for the south shore of Lake Ontario from Grimsby to Hamilton (after Davidson-Arnott and Amin, 1985). Note the spreading of energy for the East waves and the crossing of orthogonals for North-west waves. The period and height class used in the example are given for each direction.

First-generation programs using regular waves and linear wave theory have now been superseded by more complex numerical models such as MIKE 21 which can handle non-linear wave–wave interaction, wave–current interaction, bottom friction, more complex bathymetry as well as refraction and diffraction. Models such as STWAVE put out by the Coastal and Hydraulics laboratory of the US Army Corps of Engineers (Vincent *et al.*, 2002) are less complicated and can be run on a PC – they are therefore used in many engineering studies. All models have limitations that reflect the underlying assumptions of the models and the quality of the input data – therefore interpretation of the output from the programs should always take into account how closely the conditions to which they are applied meet the assumptions and requirements of the model.

5.4 Wave breaking

5.4.1 Breaker prediction

In deep water the maximum height that a wave form can remain stable is limited by a steepness value (H_0/L_0) beyond which breaking will be initiated. The limiting steepness in deep water is 0.142 and that this occurs when the (interior) crest angle is 120°. When the steepness exceeds this angle, the water particle motion in the crest exceeds the wave celerity and part of the crest spills down the front of the wave to form a spilling breaker. We have already seen that wave oversteepening occurs frequently in areas of active wave generation as local wave steepness exceeds this critical limit due to the movement of waves through each other. This results in breaking occurring at the wave crest for some distance (whitecapping).

Waves moving into shoaling water also break because of an increase in wave steepness, in this case brought about primarily by an increase in wave height and a decrease in wave length and celerity. In shallow water the limiting steepness is somewhat less than in deep water and is partially controlled by the relative depth (h/L) and the slope of the bed. A number of expressions have been derived to predict the depth of water in which breaking takes place h_b and the wave height at breaking H_b. Munk (1949), based on solitary wave theory predicts

$$\frac{h_b}{H_b} = 1.28 \tag{5.34}$$

and

$$\frac{H_b}{h_b} = 0.78. \tag{5.35}$$

Thus, waves begin breaking in water depths slightly greater than the wave height. It has been shown that the breaker depth also depends on initial wave steepness and local slope, but as a rough guide 0.78 is reasonable.

Breaker height was also predicted by Munk (1949) as

$$\frac{H_b}{H_0} = \frac{1}{3.3\left(\frac{H_0}{L_0}\right)^{0.33}}. \tag{5.36}$$

This assumes no losses of energy due to friction and no changes due to refraction. It can be seen from (5.36) that breaker height is dependent on the deep water wave height and steepness and that the ratio H_b/H_0 increases as the deep water wave steepness decreases. H_b/H_0 ranges from close to 1 for short-period, high waves in areas of wave generation to 1.4–1.6 for low, long-period swell waves. This accords well with our observations of the very large increases in breaking wave height observed on swell wave coasts such as California, Hawaii and the east coast of Australia.

5.4.2 Location of wave breaking

The location and consequences of wave breaking is controlled initially by the incident wave height and length, but it is also affected by the form and slope of the nearshore and beach foreshore. Three broad conditions can be recognised (Figure 5.12).

(1) *Very steep shorelines*.These shorelines are characterised by a steep nearshore profile with deep water close to shore, and are generally backed by a steep or vertical face (e.g. rocky shorelines, cliffs and bluffs, seawalls and other vertical structures). Waves may be

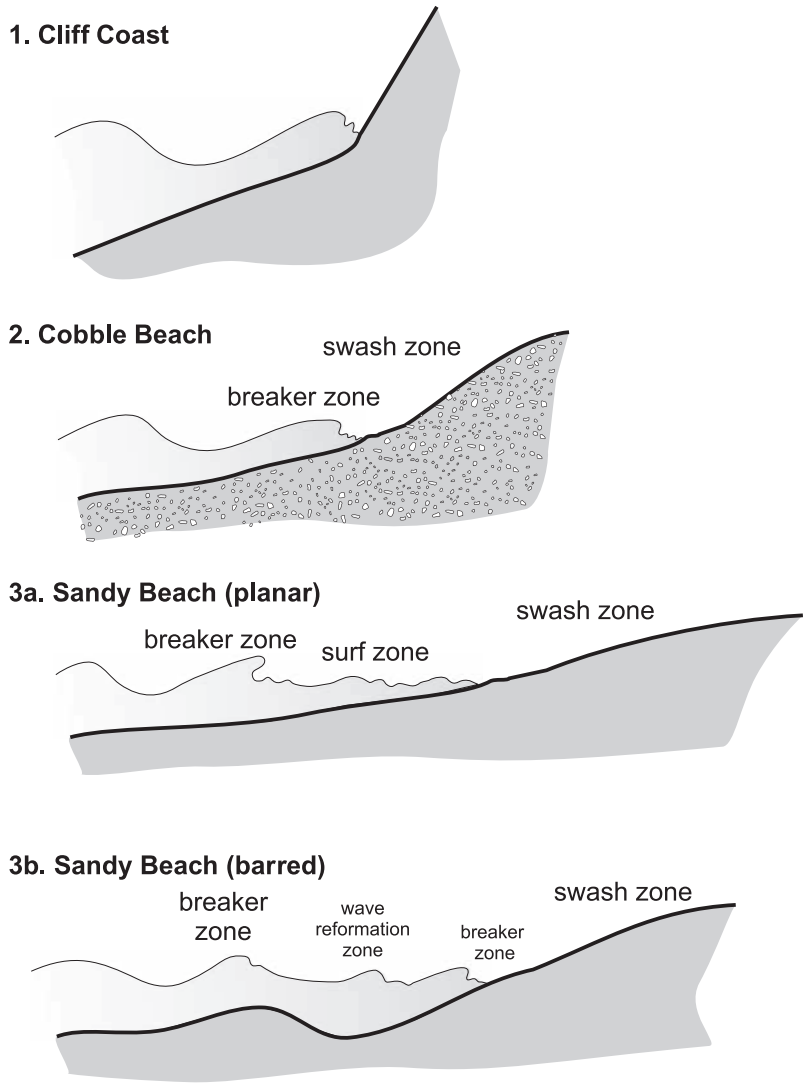

Figure 5.12 Scenarios for wave breaking and surf zone development on steep and gentle beaches.

completely reflected without breaking, or breaking may take place directly against the cliff or wall, resulting in some reflection and considerable energy dissipation. Wave breaking under these conditions often results in compression of air against the structure, with the resulting splash and spray reaching high into the air.

(2) *Moderately sloping beaches*. These shorelines are characterised by moderate beach and nearshore slopes. Frequently the beach is composed of gravel or cobbles, but similar conditions may occur with low to moderate waves breaking on the steep swash slope and berm of a typical swell profile. Wave breaking generally occurs at or near the toe of the beach, and wave energy is dissipated in turbulence associated with the breaking process as well as during swash run-up. Wave breaking can take a range of forms and some reflection usually occurs.

(3) *Gently sloping beaches*. These shorelines are characterised by a gentle nearshore slope (primarily fine-to-medium sand beaches) with wave breaking occurring some distance offshore and giving rise to a breaker zone (or zones) and a surf zone between the line of first breaking and the beach. Wave energy

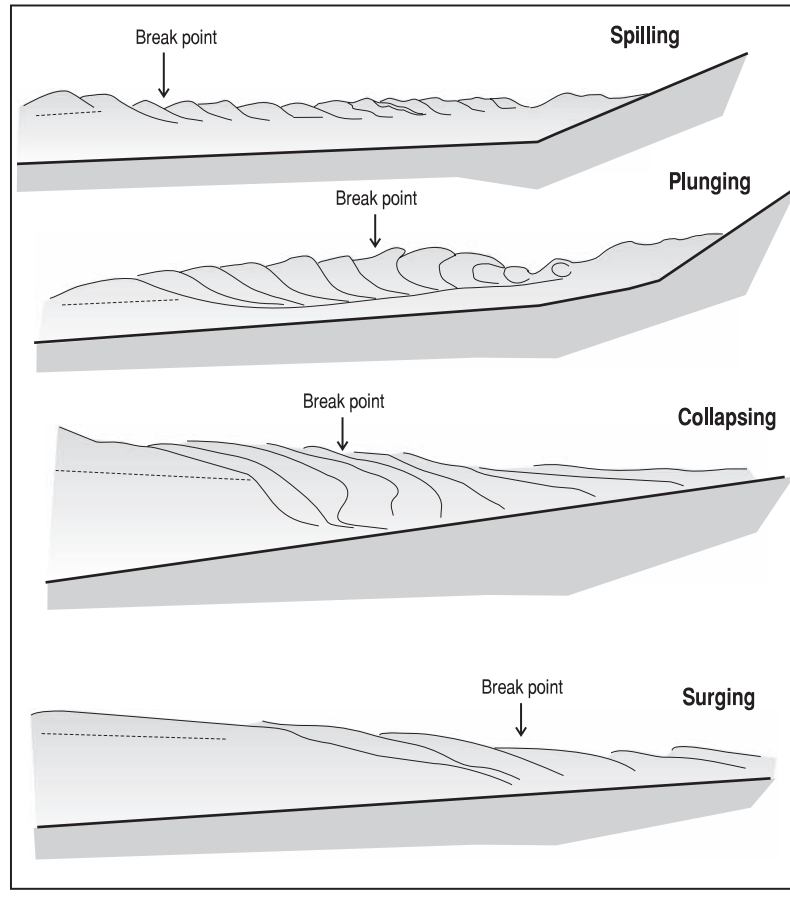

Figure 5.13 The four types of wave breaking on a beach (Galvin, 1968). Note that collapsing and surging breakers only occur at the beach face.

dissipation takes place during the initial breaking phase as well as by turbulence in the crest of surf bores progressing through the surf zone. Further dissipation takes place during run-up on the beach. Where the profile is planar the surf zone is characterised by surf bores crossing the entire surf zone from the break point (Figure 5.12 (3a)). However, where the profile is characterised by the presence of nearshore bars with deeper water in the troughs landward of the bars, wave breaking may cease in the troughs and each bar crest may be associated with a separate breaker and surf zone (Figure 5.12).

5.4.3 Breaker types

Simple field and laboratory observations indicate that waves do not all break in the same way, and that the manner of wave breaking may be important because of its effect on processes such as the rate of energy dissipation, sediment entrainment and surf zone dynamics. Three types of breaker are commonly recognised: spilling, plunging and surging. Galvin (1968) provides the definitive description of each type (Figure 5.13) and introduces a fourth type – collapsing. Spilling breakers are characterised by instability at the wave crest and the development of a plume of water and air bubbles that slides part way down the front face of the wave. The wave form remains intact as the wave continues landward and wave height decreases slowly (Figure 5.14a). As wave type shifts along the continuum towards plunging, the plume of water becomes larger and extends further down the front of the wave, accompanied by a more rapid decrease in wave height. Plunging breakers are characterised by the formation of a jet of water in the upper portion of the wave that

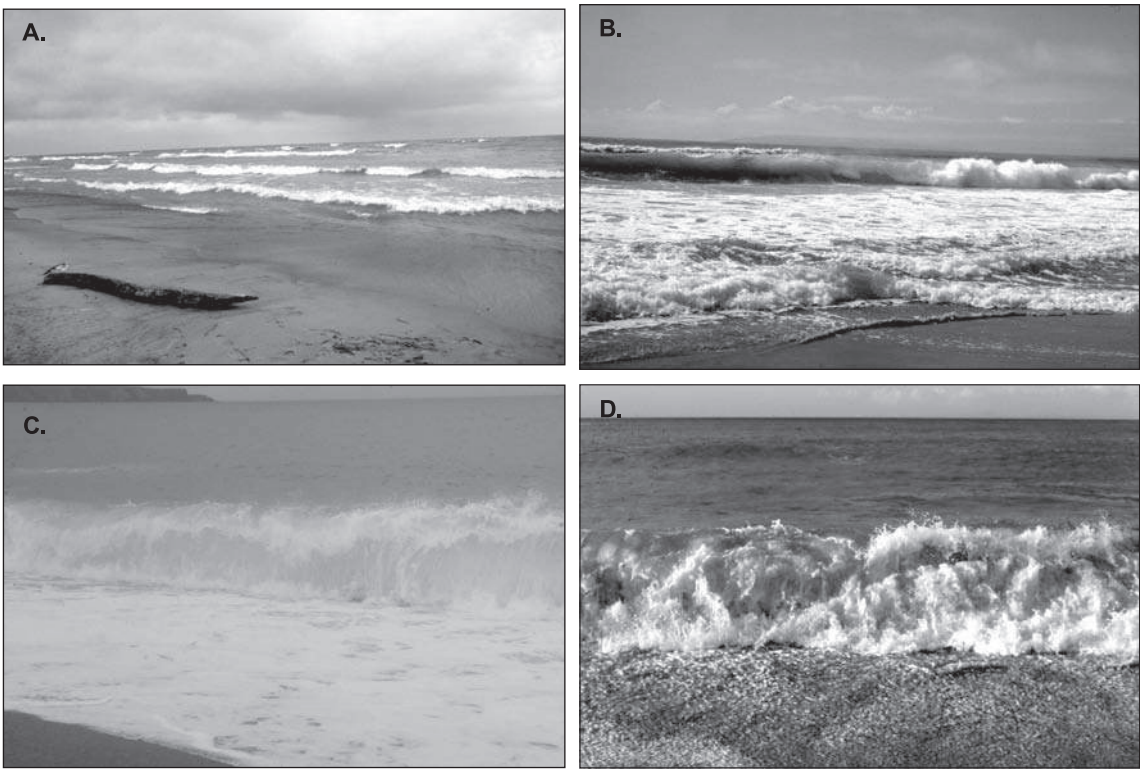

Figure 5.14 Examples of wave breaking types: (A) spilling breakers across a barred nearshore Point Pelee, Lake Erie, Canada. Breaking in the outer zone is confined to the wave crest but closer to shore on the inner bar wave breaking is transitional from spilling to plunging; (B) Plunging breaker, Pakiri, New Zealand. Note that the wave is approaching at a slight angle to the shoreline so that the process of breaking is nearly complete at the right. The hollow enclosed by the plunging jet is enhanced by the shadow it casts on the lower wave at the left of the photo; (C) plunging breaker on a steep cobble beach, St Mary's Bay, Newfoundland; (D) collapsing breaker, west coast Tobago.

curls forward enclosing an air pocket and then plunges into the water ahead of the wave generating considerable splash and the formation of very large vortices (Figure 5.14b). The process results in the very rapid transformation of the wave form.

Surging breakers occur when low, long waves reach a steep beach and result in the rapid movement of the base of the wave up the swash slope and the disappearance of the wave crest. At the extreme end of this continuum there is no evidence of instability and breaking but simply a back-and-forth movement of the water up and back across the foreshore slope with minimal generation of turbulence and foam on the surface. Collapsing breakers also occur where waves reach a steep foreshore and are intermediate between plunging and surging (Figure 5.14d). These waves form a peaked crest but as breaking takes place the wave base moves ahead up the swash slope and the crest collapses into it.

Galvin's work was based on high-speed filming of regular waves breaking on a plane laboratory slope so conditions are simplified compared to the irregular waves and topography commonly found on beaches. Nevertheless, this and other lab studies provide some useful insights into the process of wave breaking and the controls on breaker type. It is important to recognise that the breaker types represent a continuum with a range of transitional forms. It should be noted also that where waves break offshore and a surf zone is developed only the

continuum from spilling to plunging can occur, whereas all four forms can occur with wave breaking at the beach face.

Galvin observed that spilling and plunging breakers were formed with high steepness waves on gentle slopes, and surging and collapsing waves with relatively low steepness waves on moderate to steep slopes. He also noted that the sequence from spilling to surging is observed for a (given slope) if period is held constant and height decreased, or if height is held constant and period increased (in both instances this results in a decrease in wave steepness). If height and period are held constant, an increase in slope should produce the same sequence.

5.4.4 Breaker type indices and surf zone similarity

Galvin (1968) incorporated the variables of wave steepness and beach slope into two parameters designed to predict breaker type. The two parameters, an offshore parameter B_0 and an onshore parameter B_b, are

$$B_0 = \frac{H_0}{(L_0 \times m^2)} \tag{5.37}$$

$$B_b = \frac{H_b}{g \times m \times T^2} \tag{5.38}$$

where m is the beach slope.

Based on his laboratory data, Galvin determined the values for the two equations that define the transitions between breaker types as follows:

Parameter	Surge–plunge	Plunge–spill
B_0	0.09	4.8
B_b	0.003	0.068

A similar set of experiments carried out by Okazaki and Sunamura (1991) confirmed Galvin's results. Field measurements (e.g. Weishar and Byrne, 1978) show that on natural beaches, where slope changes continuously and waves are irregular, prediction of breaker type by a simple index is not highly accurate. Nevertheless, there have been a number of field and laboratory studies that show that the breaker index, or more generally some form of surf similarity parameter, can be applied to the prediction of beach states and can provide some explanation for phenomena observed in the beach and surf zone – there is a good review of these in Bauer and Greenwood (1988). The first use of a surf similarity parameter was that of Iribarren and Nogales (1949) who quantified the transition from non-breaking to breaking on a beach using

$$\xi = \frac{\tan\beta}{\left(\frac{H}{L_0}\right)^{0.5}} \tag{5.39}$$

where $\tan\beta$ is beach slope.

Battjes (1974) summarised the critical condition $\beta = 2.3$ that corresponds to a regime about halfway between complete reflection and complete breaking, and proposed that the expression be termed the Iribarren number. Guza and Inman (1975) adopted a similar scaling parameter based on earlier work by Carrier and Greenspan (1958) on non-linear, inviscid, shallow water wave. The surf scaling parameter ε is defined as

$$\varepsilon = \frac{a_b \theta^2}{g \tan^2\beta} \tag{5.40}$$

where α_b is the breaker amplitude, θ is the wave radian frequency, and β is the beach slope.

Wright and Short (1984) proposed that the surf-scaling parameter could be used to distinguish the two extremes of their model of beach states: (1) fully dissipative beaches with flat shallow profile and relatively large subaqueous sand storage; and (2) highly reflective steep beaches with relatively small subaqueous storage. According to the Wright and Short model, values of $\varepsilon \leq 2.5$ will produce strong reflection, surging breakers, and resonance at subharmonic frequencies. Beaches with values for $\varepsilon \geq 2.5$ will be characterised by plunging breakers and, when $\varepsilon \geq 20$ spilling breakers will occur, with increasing dissipation associated with higher values of ε. Their model is described in more detail in Chapter 8.

All of these parameters incorporate some measure of wave steepness and beach slope (Bauer and Greenwood, 1988). The slope is easily

defined on a planar laboratory beach but on any complex beach profile it is necessary to define the landward and seaward limits over which the slope is measured.

Wave breaking on natural beaches is also influenced by wind speed and direction. Where the wind is onshore, waves tend to break earlier than would otherwise be predicted and the form of breaking shifts towards the spilling end of the continuum (Galloway *et al.*, 1989; Douglas, 1990). On the other hand, offshore winds tend to delay wave breaking and result in a shift towards the plunging end of the continuum. This provides some explanation for the spilling breakers commonly observed for locally generated waves and for plunging breakers on beaches with light or offshore winds. Onshore winds also enhance the onshore flow of water in the wave crest and surf bores and reduce this for offshore winds.

5.4.5 Spilling and plunging breakers, and surf zone waves

As noted above, on gentle (usually sandy) beaches large waves break some distance offshore and a surf zone is generated between the point of breaking and the beach. On simple, planar beaches the surf zone can be divided into two regions (Svendsen *et al.*, 1978) followed by the run-up or swash zone (Figure 5.15). The outer surf zone is characterised by a relatively rapid transformation of the wave form, with the inner region characterised by the development of surf bores which undergo relatively little change in form and which are similar for both plunging and spilling breakers – i.e. on a planar profile the inner surf zone is similar for both breaker types. The processes involved in wave breaking are extremely complex (Figure 5.16), and much work remains to be done to model them. Apart from the papers of Galvin (1968; 1972) useful descriptions of, and insights into, wave breaking can be found in Miller (1976), Peregrine (1983), Basco (1985) and Duncan (2001). Basco suggests that a continuous spectrum of breaking wave forms occurs between strongly plunging and weakly spilling breakers with the major difference between the two extremes being the strengths of the vortex systems involved (Figure 5.17). In addition, the initial splash from the plunging jet itself becomes a plunging jet, creating a succession of vortices (Figure 5.16) – again this effect is much reduced with spilling breakers. Wave breaking results in

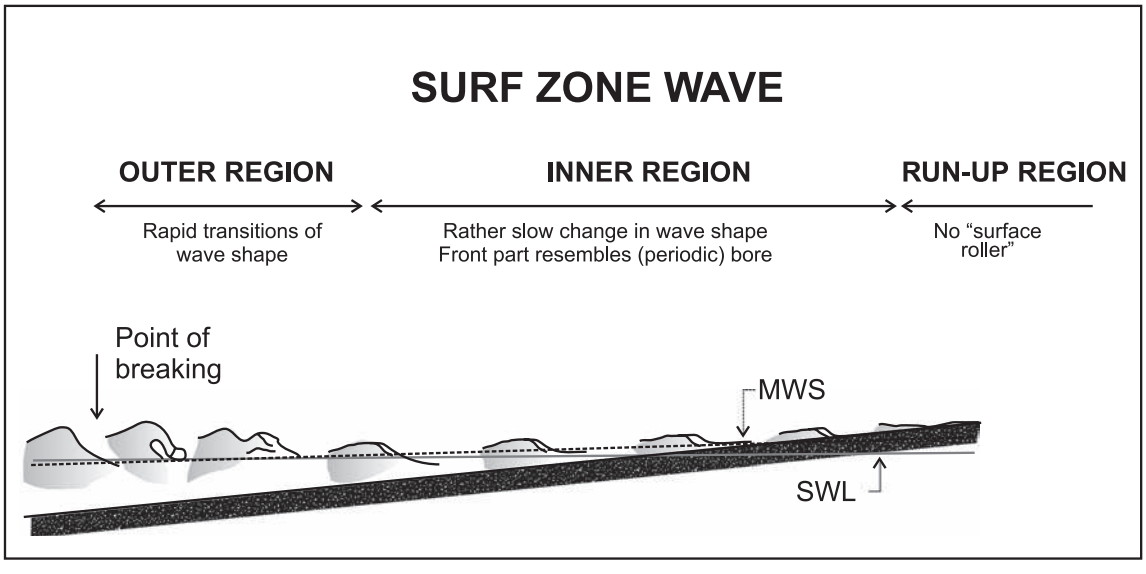

Figure 5.15 The inner and outer surf zone regions (Svendsen *et al.*, 1978).

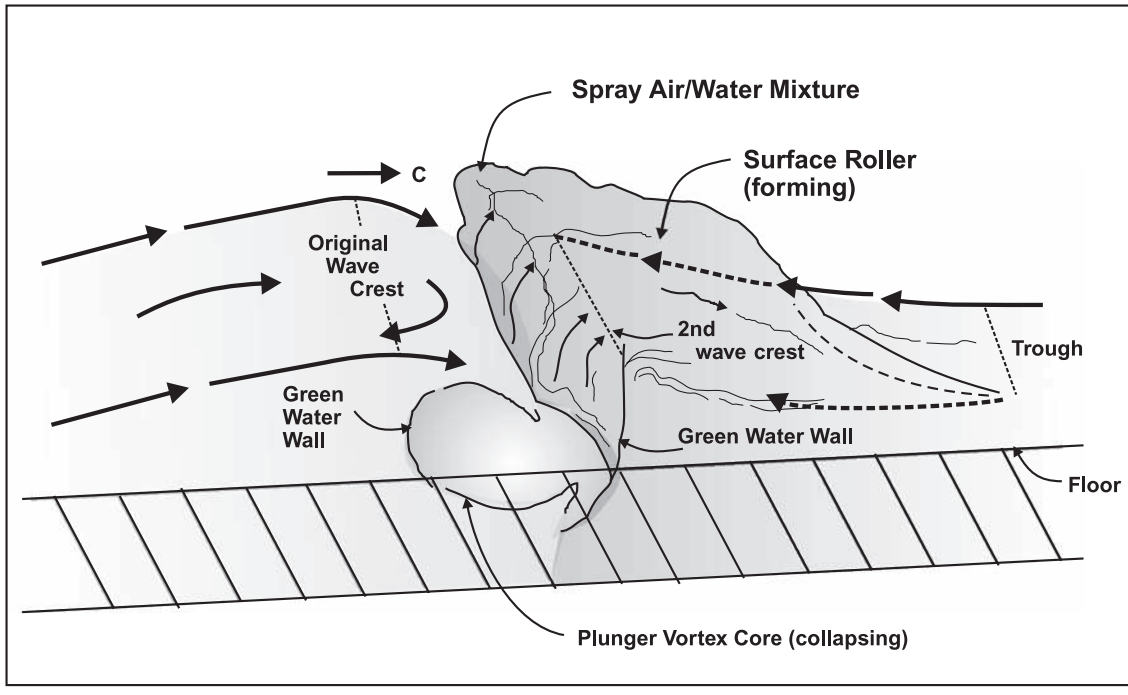

Figure 5.16 Schematic of the components of a strong plunging breaker (Basco, 1985).

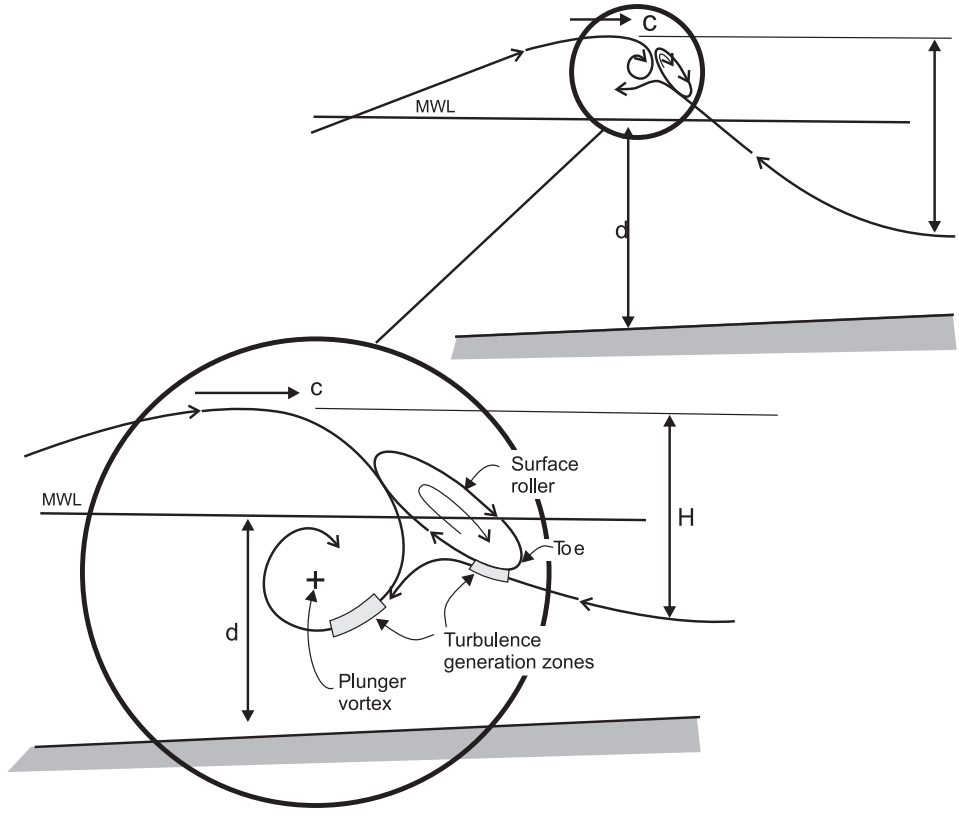

Figure 5.17 Similarity of fluid motion in spilling and plunging breakers (Basco, 1985).

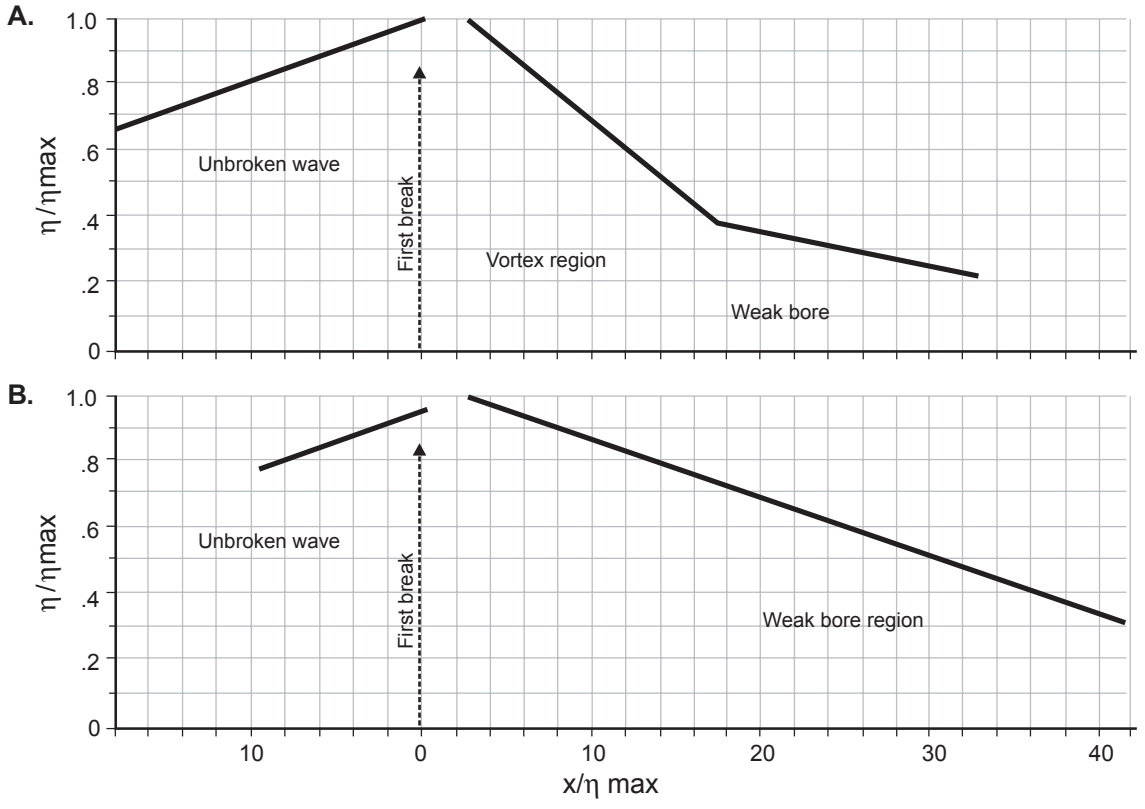

Figure 5.18 Changes to η, crest height above swl, during breaking for (A) plunging and (B) spilling breakers. The *X* axis is the dimensionless ratio X/ηmax and the *Y* axis is the dimensionless ratio η/ηmax (Miller, 1976).

the development of considerable turbulence and vorticity, with the main difference between the two classical breaker types being in the mechanisms producing the turbulence, the rate and scale of turbulence production, and advection. Spilling breakers are dominated by surface roller generated turbulence, with limited penetration of vortices. Classical plunging breakers have turbulence produced both by surface roller and by the plunger vortex, with vortices penetrating deep beneath the wave and eventually appearing in the trough of the succeeding wave (Basco, 1985; Ting and Kirby, 1995). The initial rate of height decay is much greater for the plunging breaker and thus the outer surf zone is wider for spilling breakers. Change in the wave height for spilling and plunging breakers is shown in Figure 5.18, and the degree of aeration (an indication of depth of vortex penetration) in Figure 5.19.

The way in which waves break in the nearshore undoubtedly has great influence on a number of processes and on the equilibrium beach form. For example, the greater depth of penetration of vortices produced by plunging breakers should lead to the suspension of larger quantities of sediment near the break point and may influence the rate of sediment transport in the surf zone. The vortices probably affect the eddy viscosity in the area of wave breaking and this in turn may affect unidirectional flow generation and movement. Differences in the rate of energy dissipation between spilling and plunging breakers should also influence the pattern of wave set up in the surf zone, and this will affect the manner in which offshore return flow develops.

Based on the ideas of Svendsen (1984) the surf bore can be modelled in two parts – the surface roller which consists of the breaking part at the

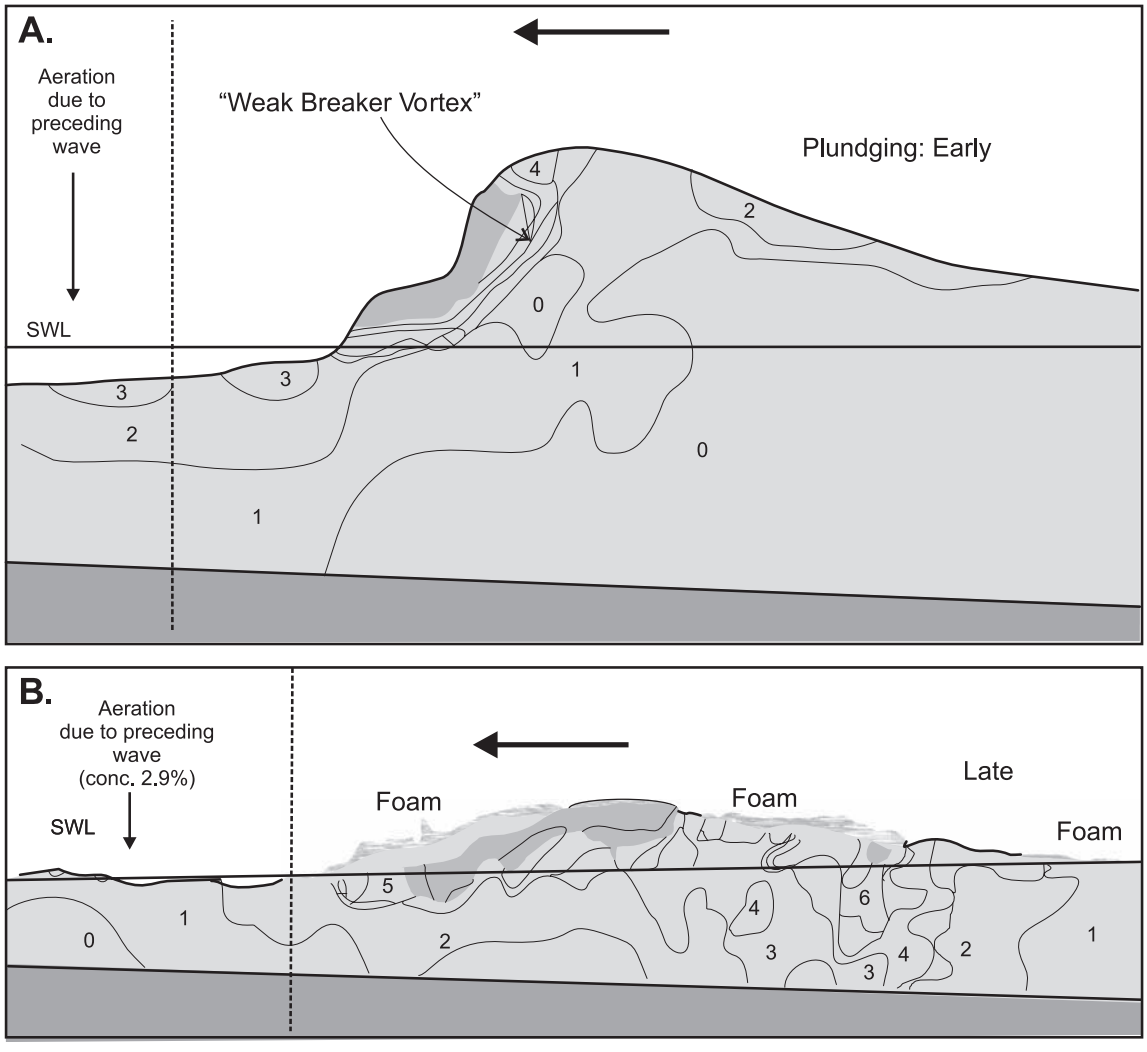

Figure 5.19 Contour maps of bubble concentrations in plunging breakers in (A) the early and (B) the late stages of breaking. Shaded areas indicate 100% bubble concentration (Miller, 1976).

top front of the wave and the main part of the wave which lies primarily below and behind this (Figure 5.20a). Flow in the roller is directed strongly landward while flows in the main part of the wave are nearly uniform throughout the depth and primarily horizontal, with onshore flows under the wave crest and offshore flows near the back of the bore (Figure 5.20b).

Wave height in the inner surf zone on a planar beach – i.e. the height of the surf bores has been found to be controlled primarily by water depth:

$$H_{rms} = \langle\gamma\rangle h. \tag{5.41}$$

The value of γ ranges from 0.3–0.6 (e.g. Thornton and Guza, 1982) with higher values being associated with steeper beach slope. Ideally, as the bore moves through the surf zone into decreasing water depth energy dissipation should result in a decrease in wave height, maintaining a constant relationship between wave height and water depth (Dally *et al.*, 1985). This energy dissipation comes primarily from losses due to turbulence in the roller but there are also some losses due to turbulence in the main body of the wave and to friction at the bed. Most modelling of energy dissipation and wave height decay

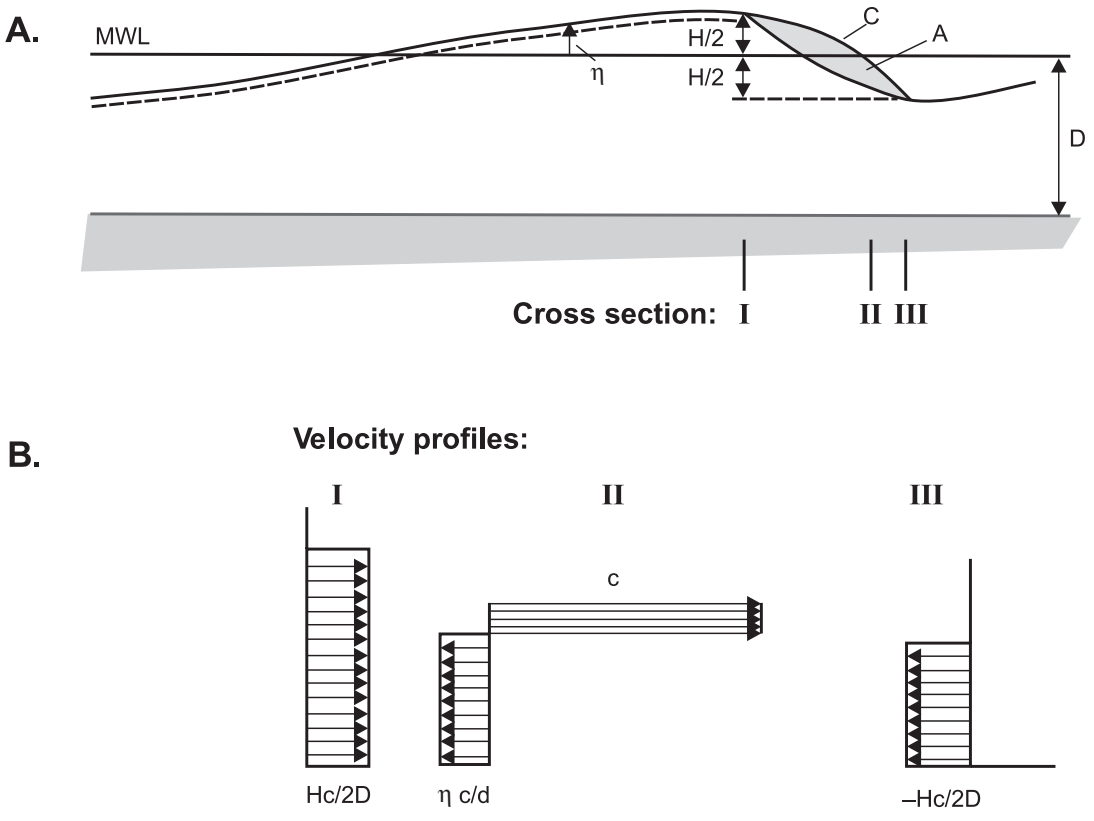

Figure 5.20 Characteristics of surf bores: (A) cross-sectional form showing the roller at the front face and the main body of the wave; and (B) the velocity profile at three locations (Fredsoe and Deigaard, 1992).

in the surf zone begins with consideration of the surface roller, based on initial work by Duncan (1981) and Svendsen (1984), and will make use of Boussinesq equations (Veeramony and Svendsen, 2000).

Regular waves in a wave tank break at the same location and all waves reach the same equilibrium. However, on a natural beach, especially with a fairly broad spectrum, waves will break at differing locations depending on their height and the surf zone will not be saturated (i.e. some portion of the wave spectrum remains unbroken and there will be some waves smaller than the depth limitation). As a result, models of wave transformation in the surf zone must be capable of dealing with random waves (e.g. Lippman *et al.*, 1996; Elgar *et al.*, 1997). One consequence of this is that the bore produced by a large wave breaking just after a smaller wave, will often travel faster and catch up with the wave ahead producing a temporary increase in wave height, water depth and turbulence.

On a barred nearshore, wave breaking results in a reduction in wave height over the bar crest. The situation is more complicated than for a planar slope because as the waves move across the bar into the deeper water of the trough breaking is reduced or may stop altogether, giving rise to a zone of regeneration and thus a larger proportion of unbroken waves. Waves then shoal again onto another bar or the beach (Figure 5.21) These complications can be accounted for in more recent models of the transformation of random waves (e.g. Ruessink *et al.*, 2003). A further complication associated particularly with waves shoaling and breaking across a nearshore bar is the generation of secondary waves and the growth of harmonic energy (energy at higher frequencies than that of the incident waves). These harmonic waves

Figure 5.21 Low, narrow-banded waves breaking on a two-bar profile, Pinery Park, Lake Huron. There are three breaker zones, one on each of the bars and one at the beach, and two zones of wave reformation in the deeper water of the trough landward of the bars where breaking ceases or is much reduced.

appear to be bound to the incident waves and travel at roughly the same speed. The result in the field is the appearance of many more wave crests in the wave record landward of the bar than seaward of it (Byrne, 1969; Davidson-Arnott and Randall, 1984; Masselink, 1998 – see Figure 5.22). The extent of wave breaking will depend on the spectrum of incident wave heights and on the depth of water over the bar crest. Where there is a significant tidal range, breaking will be more intense at low tide and may cease altogether at high tide (Figure 5.22).

5.4.6 Wave breaking at the beach face

Waves can break directly on the beach on medium-to-coarse sand beaches when a berm with a steep foreshore has developed, or on a gravel or cobble beach where the slope is usually quite steep, In this case there is no surf zone; instead, waves are transformed into swash run-up across the foreshore. This situation will occur for smaller waves when the nearshore is quite gentle and for larger waves where the slope is quite steep. Wave breaking will also take place against cliffs and artificial structures but we will leave consideration of this to Chapter 13. Wave breaking may still take place as spilling or plunging types with rapid transformation into a swash bore. In addition, collapsing and surging breakers are formed with decreasing wave steepness. The combination of steep beaches and low-steepness waves results in considerable reflection of wave energy. Such conditions often occur where wave refraction leads to the spreading of wave energy so that wave height is reduced while the period and length remain the same.

Wave run-up – swash and backwash

Wave energy dissipation is finally completed in the swash zone – the zone extending from the limit of wave uprush down to the low-tide line. On steep beaches it extends from the berm crest to just seaward of the step. On gently sloping beaches the limits are less well defined as the surf zone grades into the swash at the seaward margin and there is no distinct change in slope at the landward margin. Wave run-up or swash is driven primarily by the momentum of the wave itself and is moderated by the beach slope and infiltration into the sediments. The return flow of the backwash is driven primarily by gravitational forces and thus depends on the beach face

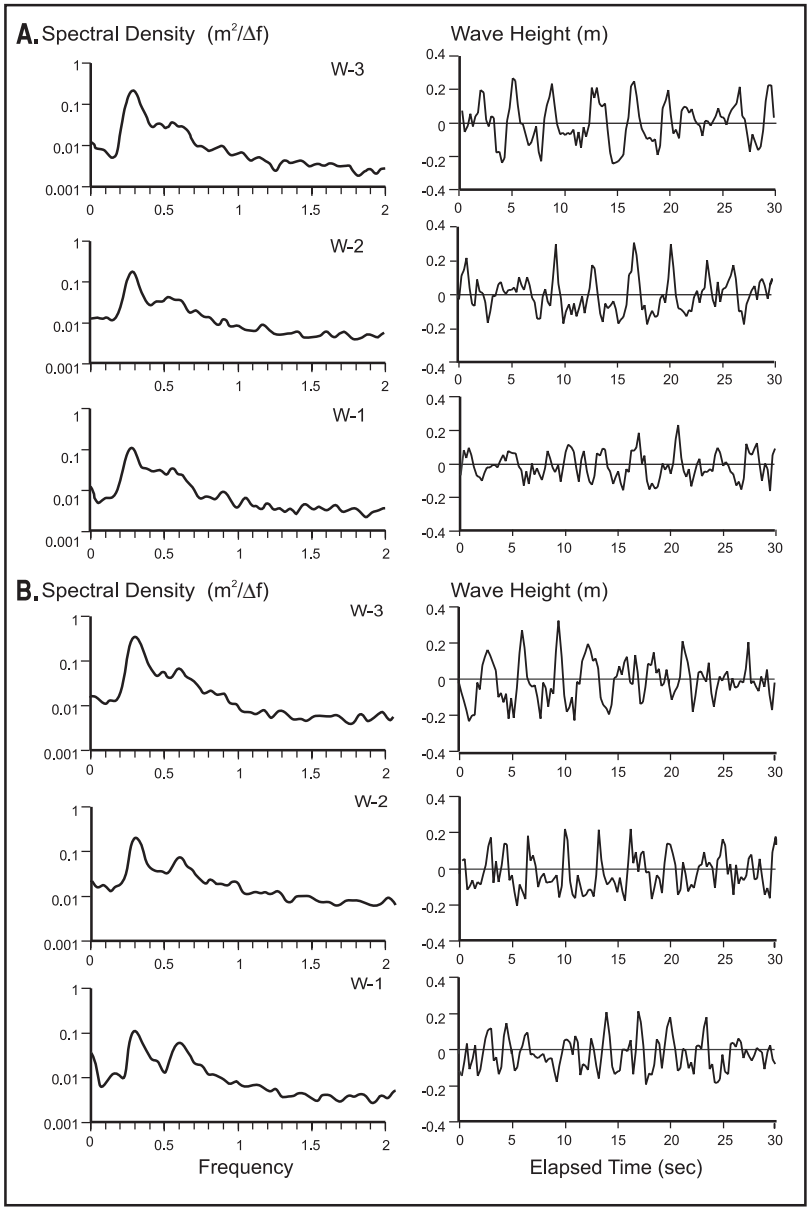

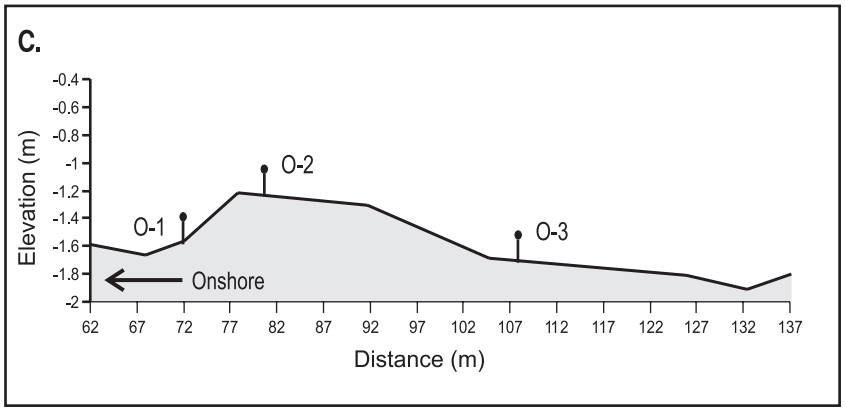

Figure 5.22 Spectral density and examples of the water surface record measured using three resistance wave staffs over the second intertidal bar of a ridge and runnel complex at Linden Beach, Nova Scotia during (A) the rising tide and (B) 95 minutes later at high tide. Location of the instruments on the profile is shown in (C). The examples of the water surface profile have been time shifted so that the records contain the same group of waves. Note the growth in harmonic energy in the spectrum across the bar into the trough and the large increase in the number of wave crests visible in the wave record, particularly in (B) (Dawson *et al.*, 2002).

slope and on the volume of water remaining. The dynamics of the swash zone are critical to the exchange of sediment between the beach and the nearshore and to the evolution of the beach form in response to changing wave and water level conditions.

Swash zone dynamics varies considerably along the continuum between steep and gently sloping beaches. On beaches with a gentle slope the subaerial portion of the profile may grade into the subaqueous portion without any marked change in slope. Waves arrive as surf bores and the transition from bore to swash is indistinct – it can be envisaged as the depth at which turbulence in the surface roller extends to the bed. The swash zone is comparatively wide and uprush velocities low, with the result that the duration of the swash–backwash cycle may be several multiples of the incident wave period and several bores may be present in the swash zone at one time. Because of the low gradient, the water table is usually close to the surface so infiltration is small. The run-up distance will vary over a time scale of tens to hundreds of seconds and is driven by low-frequency oscillations in the surf zone (described in the following section).

On steep beaches, in addition to bores arriving from the surf zone, breaking may occur directly on the swash slope or just seaward of it, thus bringing large amounts of turbulence onto the lower swash slope. The swash zone will be comparatively narrow and both the swash and backwash velocities are higher than for gently sloping beaches. Infiltration is significant, especially with increasing grain size. Run-up varies temporally at frequencies between that of the incident waves to several tens of seconds. However only one, or at most two, waves are present in the swash zone simultaneously. Variation in run-up distance is driven by differences in height of breaking waves and by the interaction of incoming waves with the backwash. When the backwash reaches the bottom of the swash slope as another wave is breaking, the interference results in a small swash excursion. However, if the backwash ends before the next wave breaks then maximum run-up will occur.

The swash uprush is characterised by the advection of turbulence from the surf zone bore or from breaking at the step or beach face, and sediment may be transported both in contact with the bed and in suspension above the bed (Masselink and Puleo, 2006). Flow velocity decreases with distance as does the depth of flow. There is a period where landward motion ceases before the backwash begins. However, the water may not be at rest because of lateral gradients due to oblique waves or the presence of lateral undulations of the swash slope associated with cusp formation which direct the top of the swash laterally and down slope without coming to rest. Flow in the backwash is initially slow and increases as a function of the gravitational force (slope angle) and the depth of flow. Most turbulence is generated from flow over the bed.

5.4.7 Mass flux and radiation stress

We saw earlier that there is a net forward movement of water associated with the net drift velocity under shoaling waves and that this can be roughly one-quarter of the wave celerity in shallow water. When waves break there is in addition a translation of water mass shoreward, primarily in the jet of plunging breakers and in the roller of spilling breakers and surf bores. The landward translation of this mass of water is eventually halted by the shoreline and thus, if room is to be made for the mass of water brought in by succeeding waves, the water must be transported back offshore. Offshore transport does in fact occur, and the mass flux of water into the surf zone is responsible for the generation of unidirectional alongshore and offshore currents in the surf zone (see Chapter 6). However, while nearshore circulation can be described as due to the mass flux of water, it has been shown that explanation and modelling of flows is best carried out by examination of the radiation stress, or excess flow of momentum, associated with shoaling and breaking waves.

Longuett-Higgins and Stewart (1964) demonstrated theoretically that, averaged over one wave period, waves exert a residual stress on the water column that is termed radiation stress. Radiation stress can be defined for a plane parallel to the wave advance (S_{xx})

parallel to the wave crest (S_{yy}) tangentially (S_{xy}). For waves approaching perpendicular to a gently sloping planar beach there will be a shoreward flux of momentum S_{xx} that is approximated by

$$S_{xx} = E\left(\frac{2kh}{\sinh(2kh)} = \frac{1}{2}\right) = E\left(2n - \frac{1}{2}\right). \quad (5.42)$$

In shallow water this becomes

$$S_{xx} = \frac{3}{2}E = \frac{3}{16}\rho g H^2. \quad (5.43)$$

As the wave shoals and wave height increases, the rate of landward momentum flux increases up to the break point. Following breaking, momentum flux decreases to zero at the top of the swash. Longuett-Higgins and Stewart (1964) showed theoretically and Bowen *et al.* (1968) showed experimentally that these variations in momentum flux lead to a (relatively) small decrease in mean water level outside the breaker zone (wave set-down) and a much larger set-up landward of the breaker line (Figure 5.24). On a planar beach the slope of the set-up is the same for waves of differing height but since wave breaking, and thus the initiation of set-up, begins further offshore in deeper water, the set-up is larger for larger waves. Set-down and set-up can be measured fairly easily on a planar profile in wave tanks (Bowen, 1969; Hsu *et al.*, 2006). Set-down and set-up have also been measured in the field (e.g. Holman and Sallenger, 1985) but here conditions are complicated by irregular waves and varying profile geometry (including nearshore bars) as well as by the difficulty in areas of wave generation of distinguishing between wave set-up and set-up

Box 5.2 | Tsunamis

A tsunami is a series of ocean waves of extremely long wave length and period that is generated by an impulsive disturbance that displaces the water, rather than by the wind. They are primarily associated with earthquakes and crustal movement along the ocean floor, but they can also be generated by subaerial and submarine landslides due to earthquakes and volcanic eruptions (Fine *et al.*, 2004; Maramai *et al.*, 2005). The term tsunami is Japanese meaning harbour wave – a reflection of the impact of these waves on protected harbours. It was adopted in the English scientific literature a few decades ago to avoid the common usage of tidal wave – a term that should be restricted to the waves associated with the diurnal tide-generating forces of the moon and sun.

Large tsunamis are produced by vertical motions associated with movement along faults on the ocean floor. The December 26, 2004 Indian Ocean tsunami was produced by a rupture along a fault line west of northern Sumatra, Indonesia which generated an earthquake measuring 9.1 on the Richter scale and produced a vertical displacement of the ocean floor of up to 15 m (Lay *et al.*, 2005). This kind of movement will generate a series of waves that travel in both directions away from the fault area (Figure 5.23). Thus waves from the Sumatran earthquake travelled westward across the Indian Ocean affecting the shoreline of India and Sri Lanka and places such as the Seychelles Archipelago off the coast of Africa (Jackson *et al.*, 2005). They also travelled eastward away from the earthquake site into the Andaman Sea affecting the coastline of Burma, Thailand and Malaysia. Depending on the relative vertical movement along the fault line the arrival of tsunami waves may be signalled first by the arrival of the wave trough, which manifests itself as a rapid withdrawal of water from the shoreline and the exposure of the nearshore bed. Eyewitness

accounts from Thailand note this as the first indication of the tsunami in that location.

Tsunamis have a wave length of tens of kilometres, a period of tens of minutes and travel at speeds of 500–800 km/h in the open ocean. Because of their long wave length their speed can be estimated using the shallow water expression for wave celerity (Equation (5.5)). Wave height in the open ocean may be <2 m and, because of their extreme wave length, would not be noticeable on a ship. However, the extreme wave length also mean that they interact with the bed even in the deepest parts of the ocean, and as they do so their speed and wave length are subject to shoaling processes and especially to refraction and diffraction. This can produce large variations in the height of the wave experienced along parts of the same coast. It also means that small coral atolls sitting on seamounts surrounded by very deep water may escape much of the potential impact because of the limited shoaling and refraction effects (Jackson *et al*., 2005). Where there is a wide continental shelf, shoaling results in a large increase in wave height and eventually to breaking at the coast. While tsunami waves can break as spilling or even plunging breakers, they have a low value for wave steepness and tend to come ashore as a surging breaker with a long period of onshore flow followed by an offshore directed return flow. This is evident in many of the photographs and videos that were posted on the web after the event, especially from resort areas in Thailand (Choowong *et al*., 2008).

While the tsunami associated with the 2004 Sumatran earthquake produced the largest loss of life on record, there are a number of other major tsunami events in recorded history including: the 1755 Lisbon earthquake (Chester, 2001); the 1964 Alaska earthquake which affected large parts of the Pacific Ocean, including Hawaii; and the 1998 Papua New Guinea earthquake (Morton *et al*., 2007). The 1929 earthquake off the Grand Banks triggered a large submarine slope failure that destroyed 12 transatlantic telegraph cables and the tsunami killed 28 people in Newfoundland (Fine *et al*. 2004). Even before the 2004 event there was growing recognition of the widespread occurrence of tsunamis and their potential effect on coastlines (Coleman, 1968; Young and Bryant, 1992; Clague *et al*., 2000). Recently there have been many reports studying the deposits associated with known tsunami events (e.g. Dawson and Stewart, 2007; Morton *et al*., 2008; Paris *et al*., 2007; Umitsu *et al*., 2007) and some controversy over distinguishing between tsunami deposits and those due to storm events (Bryant, 2001; Felton and Crook, 2003; Kortekas and Dawson, 2007).

The large number of tsunamis generated in the Pacific Ocean around the 'rim of fire' prompted the US Government, through NOAA, to deploy a tsunami warning system in the region known as DART. This uses a sea-floor-mounted pressure transducer system which can detect the motion associated with the long-period waves of the tsunami and is connected to a network of tsunami warning centres through a surface buoy linked to a satellite. Because of the high celerity of tsunami waves, the system can realistically only give warnings to coasts more than a few hundred km from the point of generation. No such warning system existed in the Indian Ocean area in 2004.

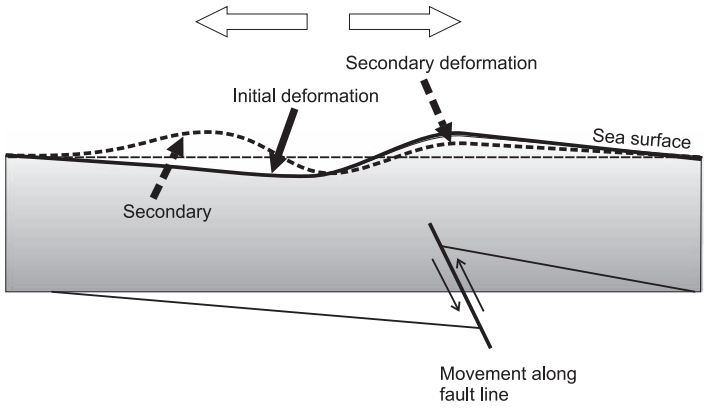

Figure 5.23 Generation of a tsunami by vertical movement along a fault line. The initial movement on the ocean floor results in a deformation of the sea surface downward and upward, and the generation of several waves as the sea surface is restored. Tsunami waves spread outward in both directions from the source.

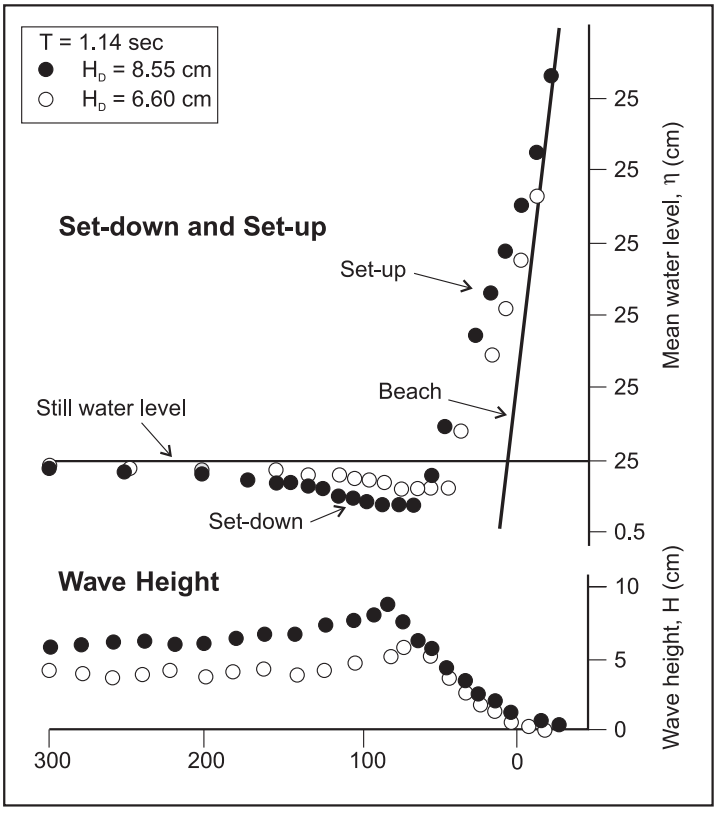

Figure 5.24 Wave set-down and set-up for waves of differing wave height in a laboratory wave tank (Bowen, 1969).

due to onshore winds. It is also difficult to measure the wave set-up when there is a wide surf zone or relatively flat beach and wide swash zone. Finally, in the field the angle of wave approach may vary considerably from shore perpendicular, especially for steep profiles where refraction effects are small and the amount of set-up will then depend also on the angle of wave approach at the shoreline (Hsu *et al.*, 2006).

5.5 Wave groups and low-frequency energy in the surf and swash zones

Observations and field measurements often show the presence of distinct groups of 4–8 larger, long-period waves which produce large breakers and lead to an increase in the water level in the surf zone and in the height of run-up. These may be followed by a period of much smaller waves during which time the water level in the surf zone decreases in elevation and run-up does not reach as far up the beach. This phenomenon is often most evident, especially to body surfers, when low-swell waves from a distant storm reach a beach in the absence of locally-generated waves which might obscure the record. Large swell from a distant storm can travel thousands of kilometres across the ocean and may produce a period of several hours of wave breaking that greatly exceeds the normal activity. Figure 5.25 shows the effect of such a group arriving at Maracas Beach on the north coast of Trinidad.

Measurements of water level, run-up and velocity in the surf zone and on the beach all show the presence of considerable energy at wave lengths (periods) that are much longer than the incident waves – these are known as long waves or as infragravity motion. The simplest manifestation is probably as long period (30–120 second) fluctuations in water level in the surf zone and run-up on the beach, and as pulses in the strength of rip currents. Energy at these periods is much longer than the incident wind wave energy, though the actual high frequency cutoff may be as low as 12–15 seconds in fetch-limited areas such as the Great Lakes (Bauer, 1990). It is convenient to divide surf zone infragravity wave motion into three types: (1) bound long waves; (2) leaky waves; and (3) edge waves (Figure 5.24).

Infragravity wave energy usually originates directly or indirectly from outside of the surf zone and was first described by Munk (1949) and Tucker (1950) as surf beat and much subsequent work has focused on the relationship between this

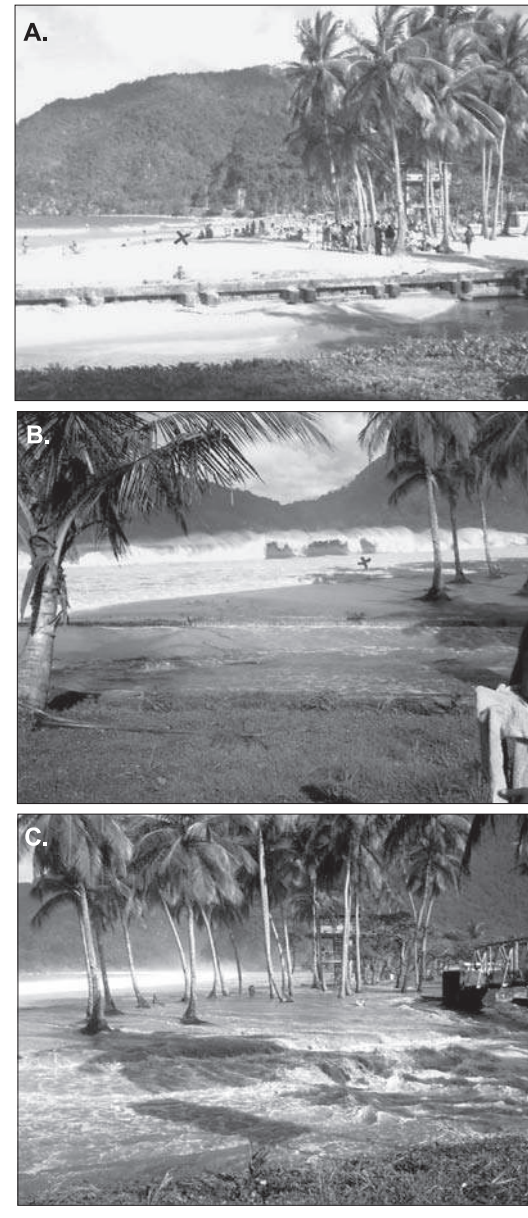

Figure 5.25 Sequence of photographs showing the arrival of a series of large swell waves at Maracas Bay on the north coast of Trinidad. The waves were generated by a storm in the North Atlantic and tracked across the ocean by satellite: (A) wave conditions in the early afternoon; (B) large swell wave breaking as a plunging breaker; (C) set-up and the large uprush from the wave inundate the backshore and flood the beach facilities.

and wave groups (Longuet-Higgins and Stewart, 1962; Huntley *et al.*, 1981; Symonds *et al.*, 1982; Haller *et al.*, 1999). The set-down under a group of higher waves is greater than that under a group of lower waves, thus producing a variation in the mean water level with a period equal to the wave group and 180° out of phase with it (Figure 5.25). The breaking of a group of large waves results in a temporary increase in the momentum flux in the surf zone and in the mass of water translated. This form of infragravity energy is termed a bound long wave because it is tied to the incoming wave groups and it will continue to propagate through the surf zone even after the incident waves associated with it have broken. Symonds *et al.* (1982) proposed a model relating low-frequency wave generation to the time-varying breakpoint of the incident waves in a group and much subsequent work has elaborated on the relationship between wave group breaking and the generation of low-frequency energy (Baldock *et al.*, 1997; Baldock *et al.*, 1999; Haller *et al.*, 1999; Svendsen and Veeramony, 2001; Karunarathna and Chadwick, 2007).

The group long wave may also be released when the wave group is destroyed through breaking and it will then propagate landward as a free wave. Reflection of this free long wave at the shoreline leads to the formation of a cross-shore standing wave in the surf zone as a result of interaction between the reflected wave and the incoming wave – this cross-shore standing wave is termed a leaky wave (not strictly speaking the best term since it does not actually leak energy offshore) and is two dimensional in nature since there is no alongshore variation in its structure. The conditions required for the formation of leaky waves can be predicted from

$$\frac{\omega^2}{gk_y} \tag{5.44}$$

where $\omega = 2\pi/T$ and k_y is the longshore wave number $2\pi/L$.

Where $\omega^2/gk_y > 1$ leaky waves will form and for values <1 edge waves will form. Because of the long periods associated with infragravity waves, the primary controlling variable is the

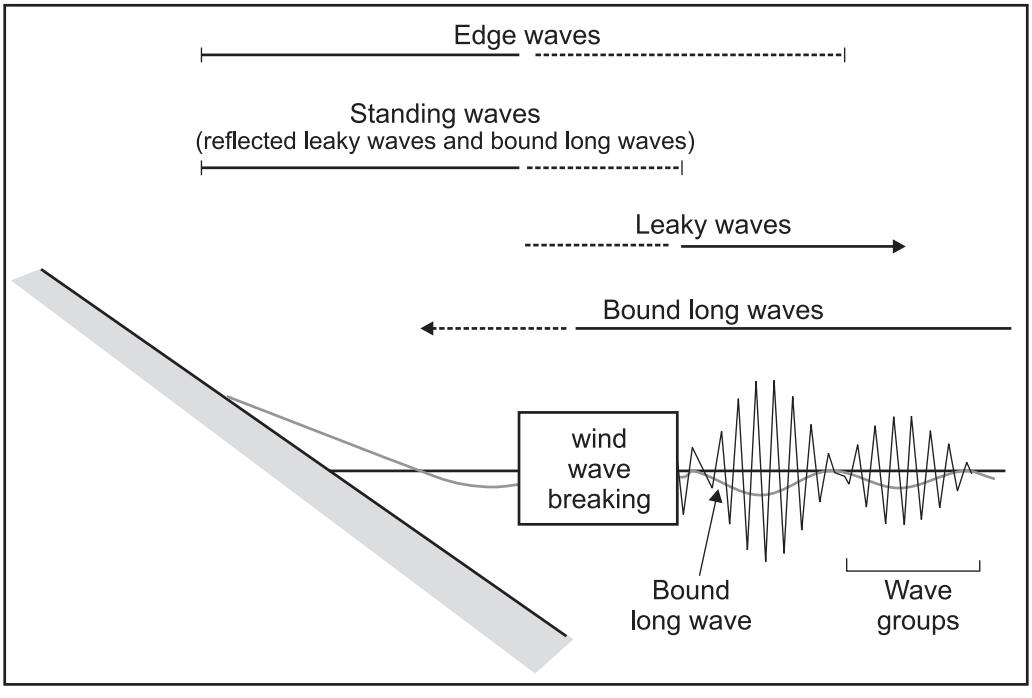

Figure 5.26 The three types of infragravity wave motion in the surf zone (Huntley and Kim, 1984).

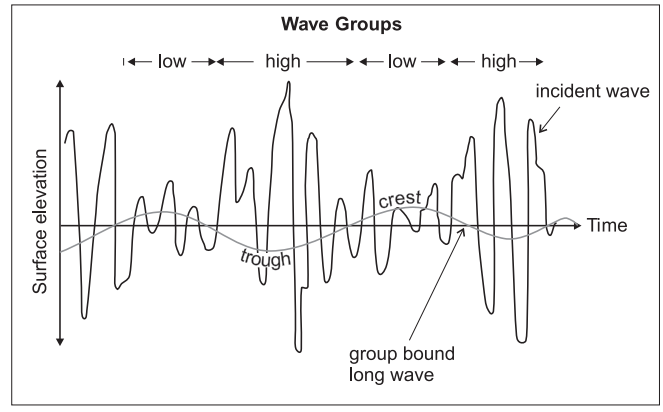

Figure 5.27 Schematic representation of a bound long wave associated with wave groups (Aagaard and Masselink, 1999).

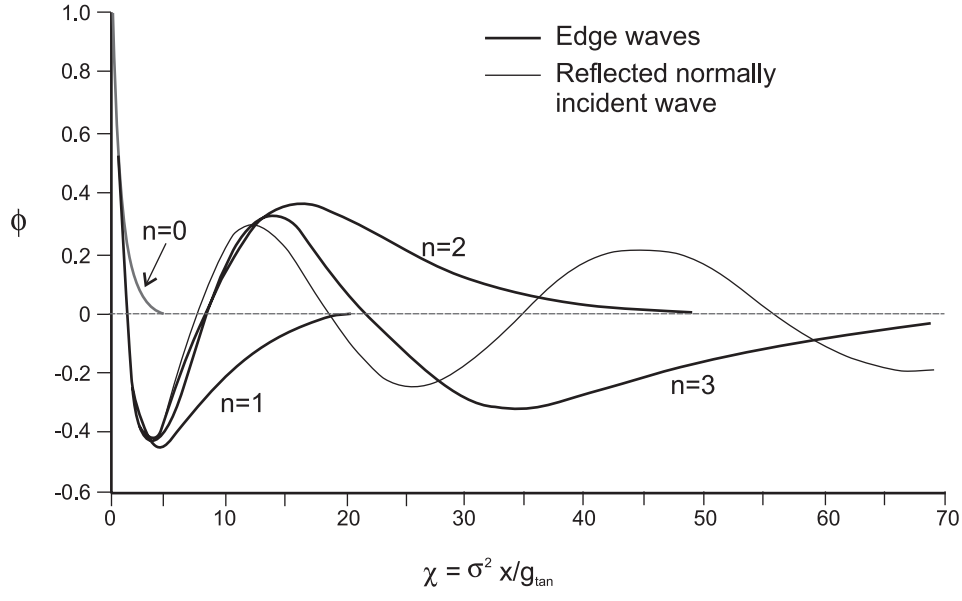

Figure 5.28 The cross-shore surface elevation structure of a leaky mode standing wave and modes $n = 0–3$ edge wave plotted in terms of non-dimensional offshore distance. The *y* axis represents the amplitude of the wave form normalised by the shoreline amplitude (Holman, 1983).

angle of wave incidence: L is very large for nearly normal wave approach and thus k_y is small. As the angle of wave approach increases, L decreases and the value of k_y becomes larger.

Edge waves can be defined as free waves that are standing in the cross-shore direction – i.e. there are vertical oscillations but the form does not move progressively offshore. The edge waves may travel along the beach as progressive edge waves, or they may form standing edge waves as a result of the interaction of progressive edge waves travelling in opposite directions – e.g. where a progressive edge wave is reflected by an alongshore structure such as a groyne or headland. The cross-shore structure of an edge wave is similar to a leaky wave, with an antinode at the shoreline and a series of zero crossings (oscillations about the swl). However, the amplitude of the leaky wave is relatively constant offshore while the edge wave decays exponentially and the number of zero crossings is given by the mode number n (Figure 5.28). A

mode 0 edge wave oscillates alongshore at the beach face and a mode 1 edge wave also has a sinusoidal oscillation alongshore and an antinode offshore (Figure 5.29). Mode 2 and higher edge waves will have more antinodes in the offshore direction. Because the energy in the edge wave decreases rapidly offshore it is unlikely that edge waves with a modal number greater than 1 will play a significant role influencing topographic development.

The longshore wave length of the edge wave can be predicted for planar beaches from

$$L_e = \frac{h}{2\pi} T_e^2 (2n = 1) \tan\beta. \tag{5.45}$$

Much energy in the past two decades has gone into modelling these motions theoretically and attempting to measure them in the field (Holman, 1983). While progress has been made, there is still considerable uncertainty as to the significance of their role in modulating sediment transport. Both standing and leaky mode waves, whether they are reflected or edge waves, have oscillatory motion and drift associated with them, though the overall motion with standing waves must be zero. Their potential significance lies in the fact that if sediment is set in motion by the incident waves, only small net flows are required to transport it. There is thus a great temptation to associate rhythmic features such as rip current spacing, crescentic bar dimensions, and the wave length of nearshore bars to the presence of these long waves. Equation (5.39) in particular was used indiscriminately at times in the 1980s and 1990s in a circular argument first to calculate the wave length of a controlling edge wave, and then to infer that the presence

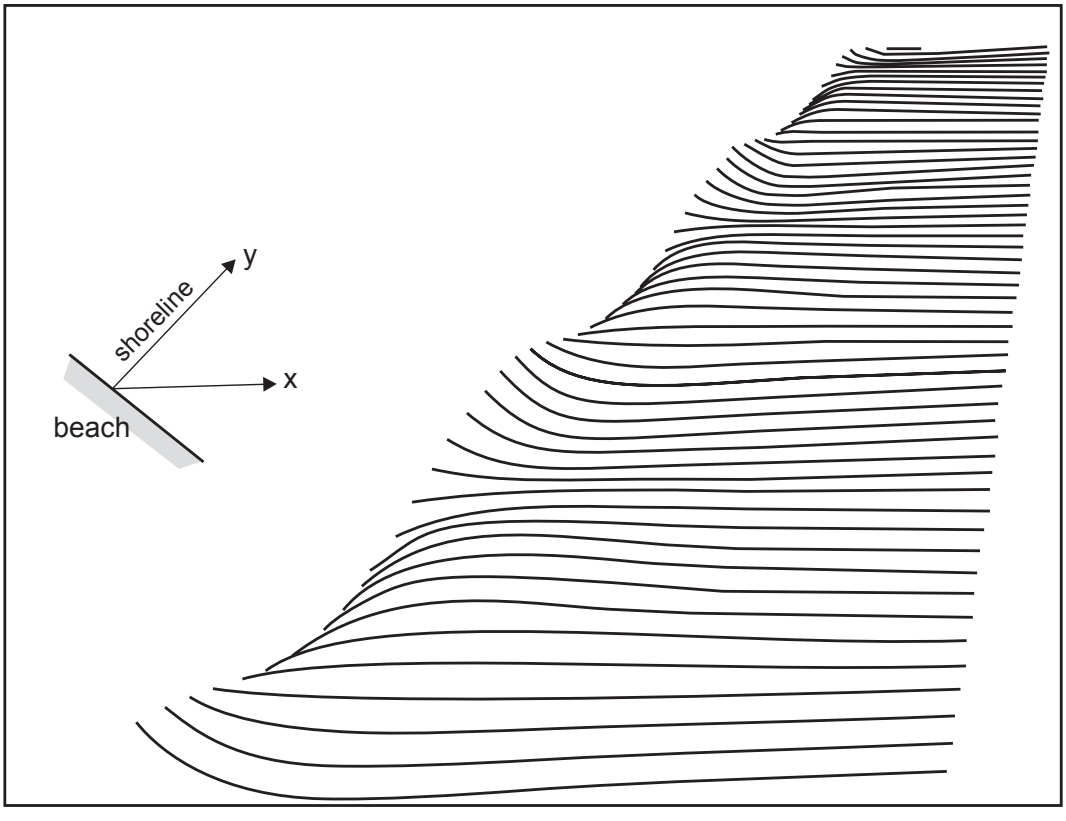

Figure 5.29 Perspective view of a mode 1 edge wave viewed obliquely from offshore. The wave is sinusoidal alongshore with nodal and antinodal points, as well as an offshore antinode (Holman, 1983).

of a potential edge wave length similar to that of a rhythmic feature was evidence of the role of edge waves in their formation – this without any actual field measurements to support the co-existence of an edge wave and the rhythmic topography in question. In practice, it requires a lot of instrumentation to determine the offshore and alongshore structure of low-frequency wave motion and to separate leaky waves from edge waves. Many field experiments have shown that infragravity energy in the surf zone is usually broad banded, without the selection or amplification of a particular cutoff frequency that would generate topography with a particular spatial pattern or form. Presently the pendulum seems to be swinging towards a recognition that when narrow-banded infragravity energy is detected related to the presence of edge waves, it is more likely that it is the topography that is driving the selected cut-off frequency and not vice versa.

Further reading

Basco, D. R., 1985. A qualitative description of wave breaking. *Journal of Waterway, Port, Coastal and Ocean Engineering*, **111**, 171–188.

This paper provides an excellent description of the wave breaking process along with useful sketches and photographs

References

Airy, G. B. 1845. *Tides and waves*. Encyclopaedia Metropolitan, pp. 241–396.

Baldock, T. E., Huntley, D. A, Bird, P. A. D., O'Hare, T. O. and Bullock, G. N. 1999. Breakpoint generated surf beat induced by bichromatic wave groups. *Coastal Engineering*, **39**, 213–242.

Baldock, T. E., Holmes, P. and Horn, D. P. 1997. Low frequency swash motion induced by wave grouping. *Coastal Engineering*, **32**, 197–222.

Basco, D. R., 1985. A qualitative description of wave breaking. *Journal of Waterway, Port, Coastal and Ocean Engineering*, **111**, 171–188.

Battjes, J. A. 1974. Surf similarity. *Proceedings of the 14th Coastal Engineering Conference*, ASCE, pp. 466–480.

Bauer, B. O. 1990. Assessing the relative energetics of infragravity motions in lakes and seas. *Journal of Coastal Research*, **6**, 853–865.

Bauer, B. O. and Greenwood, B, 1988. Surf zone similarity. *Geographical Review*, **78**, 137–147.

Bayram, A. and Larson, M. 2000. Wave transformation in the nearshore zone: comparison between a Boussinesq model and field data. *Coastal Engineering*, **39**, 149–171.

Bowen, A. J. 1969. Rip currents.1. Theoretical investigations. *Journal of Geophysical Research*, **74**, 5467–5478.

Bowen, A. J., Inman, D. L. and Simmons, V. P. 1968. Wave set down and set up. *Journal of Geophysical Research*, **73**, 2569–2577.

Bryant, E. A. 2001. *Tsunami–The Underrated Hazard*. Cambridge University Press, Melbourne, 350 pp.

Byrne, R. J. 1969. Field occurrences of induced multiple gravity waves. *Journal of Geophysical Research*, **74**, 2590–2596.

Carrier, G. F. and Greenspan, H. P. 1958. Water waves of finite amplitude on a sloping beach. *Journal of Fluid Mechanics*, **4**, 97–109.

Chester, D. K. 2001. The 1755 Lisbon Earthquake. *Progress in Physical Geography*, **25**, 363–383.

Clague, J. J., Bobrowsky, P. T. and Hutchinson, I. 2000. A review of geological records of large tsunamis at Vancouver Island, British Columbia, and implications for hazard. *Quaternary Science Reviews*, **19**, 849–863.

Choowong, M., Murakoshi, N., Hisada, K., and six others. 2008. 2004 Indian Ocean tsunami inflow and outflow at Phuket, Thailand. *Marine Geology*, **248**, 179–192.

Coleman, P. J. 1968. Tsunamis as geological agents. *Journal of the Geological Society of Australia*, **15**, 267–273.

Dally, W. R., Dean, R. G. and Dalrymple, R. A. 1985. Wave height variation across beaches of arbitrary profile. *Journal of Geophysical Research*, **90**, 11917–11927.

Davidson-Arnott, R. G. D. and Randall, D. C. 1984. Spatial and temporal variations in spectra of storm waves across a barred nearshore. *Marine Geology*, **60**, 15–30.

Davidson-Arnott, R. G. D. and Amin, S. M. N. 1985. An Approach to the problem of coastal erosion in Quaternary sediments. *Applied Geography*, **5**, 99–110.

Davies, J. L. 1958. Wave refraction and the evolution of shoreline curves. *Geographical Studies*, **5**, 1–14.

Dawson, J. C., Davidson-Arnott, R. G. D. and Ollerhead, J. 2002. Low-energy morphodynamics of a ridge and runnel system. *Journal of Coastal Research*, **SI** 36, 198–215.

Dawson, A. G. and Stewart, I. 2007. Tsunami deposits in the geological record. *Sedimentary Geology*, **200**, 166–183.

Dean, R. G. 1965. Stream function representation of non-linear ocean waves. *Journal of. Geophysical Research*, **70**, 4561–4572.

Demirbilek, Z. and Vincent, C. L. 2002. Water Wave Mechanics. Chapter 1 in EM 1110–2–1100 Part 2, Coastal Engineering Manual, US Army Corps of Engineers, 121 pp.

Dobson, R. S. 1967. *Some Applications of a Digital Computer to Hydraulic Engineering Problems*. Stanford University Department of Civil Engineering. Technical Report **80**, 7–35.

Douglas, S. L. 1990. Influence of wind on breaking waves. *Journal of Waterway, Port, Coastal and Ocean Engineering*, **116**, 651–663.

Duncan, J. H. 1981. An experimental investigation of breaking waves produced by a towed hydrofoil. *Proceedings of the Royal Society of London A*,**377**, 331–348.

Duncan, J. H. 2001. Spilling Breakers. *Annual Review of Fluid Mechanics*, **33**, 519–547.

Elgar, S., Raubenheimer, B., Herbers, T. H. C. and Gallagher, E. L. 1997. Spectral evolution of shoaling and breaking waves. *Journal of Geophysical Research*, **102**, 15797–15805.

Felton, E. A. and Crook, K. A. W. 2003. Evaluating the impacts of huge waves on rocky shorelines: an essay review of the book 'Tsunami – The Underated Hazard'. *Marine Geology*, **197**, 1–12.

Fine, I. V., Rabinovich, A. B., Bornhold, B. D., Thomson, R. E. and Kulikov, E. A. 2004. The Grand Banks landslide-generated tsunami of November 18, 1929: preliminary analysis and numerical modeling. *Marine Geology*, **215**, 45–57.

Fredsǿe, J. and Deigaard, R.1992. *Mechanics of Coastal Sediment Transport*. World Scientific, Singapore, 368 pp.

Galloway, J. S., Collins, M. B. and Moran, A. D. 1989. Onshore/offshore wind influence on breaking waves: An empirical study. *Coastal Engineering*, **13**, 305–325.

Galvin, C. J. Jr. 1968. Breaker type classification on three laboratory beaches. *Journal of. Geophysical Research*, **73**, 3651–3659.

Galvin, C. J. Jr., 1972. Wave breaking in shallow water. In Meyer, R. E. (ed.). *Waves on Beaches and Resulting Sediment Transport*. Academic, New York, pp. 413–455.

Greenwood, B. and McGillivray, D. G. 1978. Theoretical model of the littoral drift system in the Toronto waterfront, Lake Ontario. *Journal of Great Lakes Research*, **4**, 84–102.

Guza, R. T. and Inman, D. L. 1975. Edge waves and beach cusps. *Journal of Geophysical Research*, **80**, 2997–3012

Haller, M. E., Putrevu, U., Oltman-Shay, J. and Dalrymple, R. A. 1999. Wave group forcing of low frequency surf zone motion. *Coastal Engineering Journal*, **41**, 121–136.

Holman, R. A. 1983. Edge waves and the configuration of the shoreline. Chapter 2 in Komar, P. D. (ed.), *Handbook of Coastal Processes and Erosion*. CRC Press, Boca Raton, FL, pp. 21–33.

Holman, R. A. and Sallenger, A. H. 1985. Set-up and swash on a natural beach. *Journal of Geophysical Research*, **90**, 945–953.

Hsu, T. W., Hsu, J. R-C., Weng, W-K., Wang, S-K. and Ou, S-H. 2006. Wave setup and setdown generated by obliquely incident waves. *Coastal Engineering*, **53**, 865–877.

Huntley, D. A. and Kim, C. S. 1984. Is surf beat forced or free? *Proceedings of the 19th International Conference on Coastal Engineering*, ASCE, pp. 871–885.

Huntley, D. A., Guza, R. T. and Thornton, E. B. 1981. Field observations of surf beat. 1. Progressive edge waves. *Journal of Geophysical Research*, **86**, 6451–6466.

Iribarren, C. R. and Nogales, C., 1949. Protection des Ports., *XV11 International Navigation Congress*, **Section ii, Comm**. **4**, 31–80.

Jackson, L. E. Jr., Barrie, J. V., Forbes, D. L., Shaw, J., Manson, G. K. and Schmidt, M. 2005. *Effects of the 26 December 2004 Indian Ocean Tsunami in the Republic of Seychelles*. Geological Survey of Canada, Open File 4539, 73 pp.

Karambas, T. V. and Koutitas, C. 2002. Surf and swash zone morphology evolution induced by non-linear waves. *Journal of Waterway, Port, Coastal and Ocean Engineering*, **128**, 102–113.

Karunarathna, H. and Chadwick, A. J. 2007. On low frequency waves in the surf and swash. *Ocean Engineering*, **34**, 2115–2123.

Komar, P. D. 1998. *Beach Processes and Sedimentation*, 2nd edn., Prentice-Hall, NJ, 544 pp.

Kortweg, D. J. and de Vries, G. 1895. On the change of form of long waves advancing in a rectangular canal, and on a new type of stationary wave. *Philosphical Magazine*, **39**, 422–443.

Lawrence, P. L. and Davidson-Arnott, R. G. D. 1997. Alongshore wave energy and sediment transport on south-eastern Lake Huron, Ontario, Canada. *Journal of Coastal Research*, **13**, 1004–1015.

Lay, T., Kanamori, H., Ammon, C. J. and 11 others 2005. The great Sumatra Andaman earthquake of 26 December 2004. *Science*, **208**, 1127–1133.

Lippmann, T. C., Brookins, A. H. and Thornton, E. B. 1996. Wave energy transformation on natural profiles. *Coastal Engineering*, **27**, 1–20.

Longuett-Higgins, M. S. and Stewart, R. W. 1962. Radiation stresses and mass transport in gravity waves with applications to surf beat. *Journal of Fluid Mechanics*, **13**, 481–504.

Longuett-Higgins, M. S. and Stewart, R. W. 1964. Radiation stress in water waves; a physical discussion with applications. *Deep Sea Research*, **11**, 529–563.

Madsen, P. A., Sorensen, O. R. and Schaffer, H. A. 1997. Surf zone dynamics simulated by Boussinesq type model. Part 1. Model description and cross-shore motion of regular waves. *Coastal Engineering*, **32**, 255–287.

Maramai, A., Graziani, L. and Tinti, S. 2005. Tsunamis in the Aeolian Islands (southern Italy): a review. *Marine Geology*, **21**(5), 11–21.

Masselink, G. 1998. Field investigation of wave propagation over a bar and the consequent generation of secondary waves. *Coastal Engineering*, **33**, 1–9.

Masselink, G. and Puleo, J. A. 2006. Swash zone morphodynamics. *Continental Shelf Research*, **26**, 661–680.

May, J. P. 1974. WAVENRG: A computer program to determine the dissipation in shoaling water waves with examples from coastal Florida. In Tanner, W. F. (ed.) *Sediment Transport in the Nearshore Zone*. Coastal Research Notes, Department of Geology, University of Florida, 22–80.

Miller, R. L. 1976. Role of vortices in surf zone prediction: sedimentation and wave forces. In Davis, R. A. Jr. and Ethington, R. L. (eds.), *Beach and Nearshore Sedimentation*. S.E.P.M. Special Publication, **24**, 92–114.

Morton, R. A., Goff, J. R. and Nichol, S. L. 2008. Hydrodynamic implications of textural trends in sand deposits of the 2004 tsunami in Sri Lanka. *Sedimentary Geology*, **207**, 56–64.

Morton, R. A., Gelfenbaum, G. and Jaffe, B. E. 2007. Physical criteria for distinguishing sandy tsunami and storm deposits using modern examples. *Sedimentary Geology*, **200**, 184–207.

Munk, W. H., 1949. The solitary wave theory and its application to surf problems. *New York Academy of Science*, **51**, 376–424.

Munk, W. H. and Traylor, M. A. 1947. Refraction of ocean waves; a process linking underwater topography to beach erosion. *Journal of Geology*, **55**, 1–26.

Okazaki, S-I and Sunamura, T. 1991. Re-examination of breaker type classification on uniformly inclined laboratory beaches. *Journal of Coastal Research*, **7**, 559–564.

Paris, R., Lavigne, F., Wassmer, P. and Sartohadi, J. 2007. Coastal sedimentation associated with the December 26, 2004 tsunami in Lhok Nga, west Banda Aceh (Sumatra, Indonesia). *Marine Geology*, **238**, 93–106.

Peregrine, D. H. 1983. Breaking waves on beaches. *Annual Review of Fluid Mechanics*, **15**, 149–178.

Ruessink, B. G., Walstra, D. J. R. and Southgate, H. N. 2003. Calibration and verification of a parametric wave model on barred beaches. *Coastal Engineering*, **48**, 139–149.

Stokes, G. G. 1847. On the theory of oscillatory waves. *Transactions of the Cambridge Philosophical Society*, **8**, 441–445.

Sunamura, T. 1992. *Geomorphology* of Rocky Coasts. Wiley, Chichester, 302 pp.

Svendsen, I. A. 1984. Wave heights and set-up in a surf zone. *Coastal Engineering*, **8**, 303–329.

Svendsen, I. A., Madsen, P. A. and Buhr Hansen, J. 1978. Wave characteristics in the surf zone. *Proceedings of the 16th Coastal Engineering Conference*, ASCE, 520–539.

Svendsen, I. A. and Veeramony, J. 2001. Wave breaking in wave groups. *Journal of Waterway, Port, Coastal, and Ocean Engineering*, **127**, 200–212.

Symonds, G., Huntley, D. A. and Bowen, A. J. 1982. Long wave generation by a time-varying breakpoint. *Journal of Geophysical Research*, **87**, 492–498.

Thornton, E. B. and Guza, R. T. 1982. Energy saturation and phase speeds measured on a natural beach. *Journal of Geophysical Research*, **87**, 9499–9508.

Ting, F. C. K. and Kirby, J. T. 1995. Dynamics of surf-zone turbulence in a strong plunging breaker. *Coastal Engineering*, **24**, 177–204.

Tucker, M. J. 1950. Surfbeats: Sea waves of 1 to 5 minutes period. *Proceedings of the Royal Society of London A*, **202**, 565–573.

Umitsu, M., Tanavud, C. and Patanakanog, B. 2007. Effects of landforms on tsunami flow in the plains of Banda Aceh, Indonesia, and Nam Khem, Thailand. *Marine Geology*, **242**, 141–153.

Veeramony, J. and Svensen, I. A. 2000. The flow in surf-zone waves. *Coastal Engineering*, **39**, 93–122.

Vincent, C. L., Demirbilek, Z. and Weggel, J. R., 2002. Estimation of nearshore waves. Chapter 3 in EM 1110–2–1100 Part 2, Coastal Engineering Manual, US Army Corps of Engineers, 41pp.

Weishar, L. L. and Byrne, R. J. 1978. Field study of breaking wave characteristics. *Proceedings of the 16th Coastal Engineering Conference*, ASCE, pp. 487–506.

Wilson, W. S. 1966. A method for calculating and plotting surface wave rays. US Army Corps of Engineers. CERC Technical Memorandum 17.

Wright, L. D. and Short, A. D. 1984. Morphodynamic variability of surf zones and beaches: a synthesis. *Marine Geology*, **56**, 93–118.

Young, R. W. and Bryant, E. A. 1992. Catastrophic wave erosion on the southeastern coast of Australia: Impact of the Lanai tsunami ca. 105 ka? *Geology*, **20**, 199–202.

6

Surf zone circulation

6.1 Synopsis

Wave shoaling and breaking result in the transfer of momentum as well as a mass of water into the breaker and surf zones and leads to an increase in the water level against the shoreline, termed set-up. In turn, the set-up drives an offshore-directed flow that returns the water offshore beyond the breaker line. Mass transport of water onshore occurs relatively uniformly alongshore in the wave above the level of the wave trough. The return flow takes the form of either a two-dimensional undertow or a three-dimensional rip cell circulation. The resultant surf zone circulation is important for sediment transport and the development of nearshore and beach morphology and the flows are also important for marine organisms living in the bed and in the water column.

Undertow occurs as a seaward directed current in the zone between the bed and the wave troughs. The undertow occurs essentially uniformly alongshore and, because the cross-sectional area of discharge is large, the corresponding mean flows are relatively small – on the order of a few cm under low waves to a few tens of centimetres in intense storms. Because this flow takes place in the lower part of the water column where sediment concentrations are highest it is an important mechanism for the seaward transfer of sediment and for the development and migration of nearshore bars.

In rip cell circulation the seaward return flow is concentrated in narrow zones (rips) that periodically breach the breaker line alongshore. The offshore-directed flows in the rips are fed from two directions by alongshore currents in the surf zone (feeder currents) between the breaker line and the beach. Because the cross-sectional area of discharge is relatively small, the current speeds are much faster than in undertow, on the order of 0.5 ms^{-1} with flows exceeding 1 ms^{-1} in intense rips.

Where waves approach the shoreline at an angle to the shoreline a portion of the momentum flux is directed alongshore, generating a current that flows alongshore in the direction of wave approach. The speed of the longshore current increases with increasing wave height and increasing angle between the wave crest and the shoreline. Longshore currents coexist in the surf zone with undertow and rip cell circulation as well as with flows driven by the wind and by tidal currents.

6.2 Undertow

6.2.1 Definition and laboratory measurements

There is a small drift of water in the direction of wave advance in the open ocean (Stokes drift) which increases up to the break point and is still evident in the outer surf zone, especially with spilling breakers. However, with wave breaking there is actually a landward transfer of a substantial mass of water in the crest of the wave into the breaker and surf zone as part of the formation of turbulent flow structures associated with the

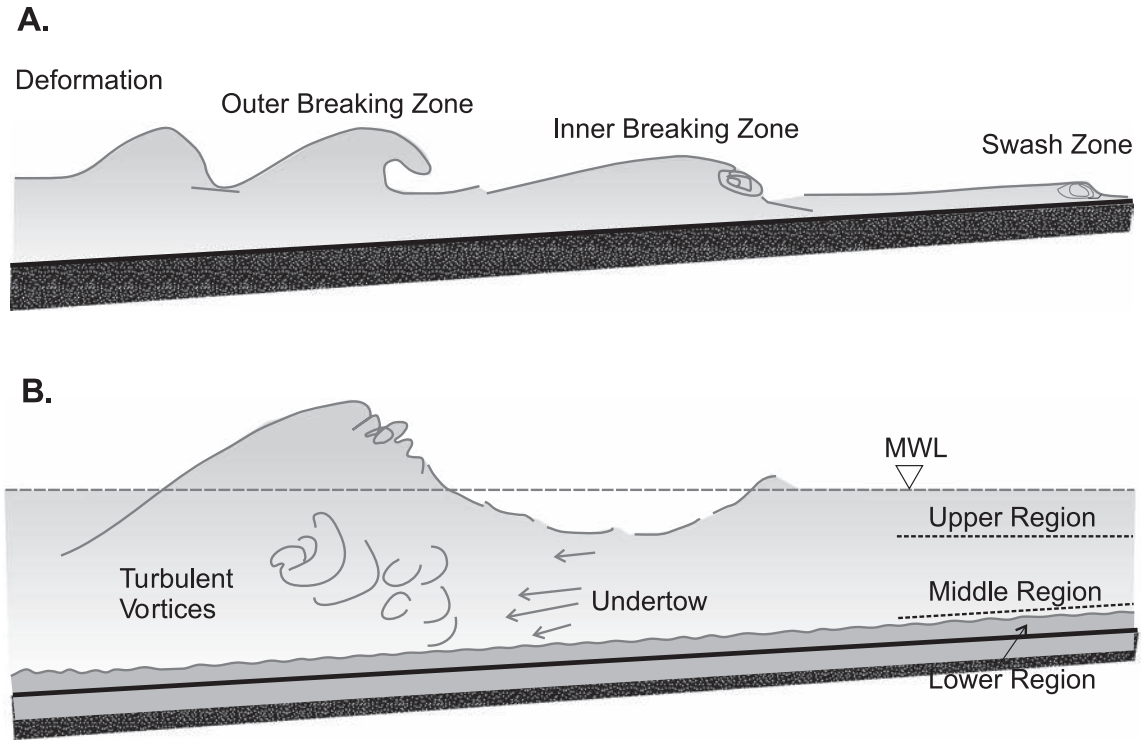

Figure 6.1 Zonation of the surf zone on a simple planar profile: (A) four regions can be identified across the surf zone beginning with the zone of strong wave deformation just before breaking, the area of breaking and rapid transformation in the outer surf zone, the inner surf zone characterised by slowly varying surf bores, and the swash zone where wave run-up occurs; (B) in the outer and inner surf zones the profile can be divided vertically into a region above the wave trough where breaking occurs, a middle zone dominated by turbulence generated by wave breaking and undertow, and a thin boundary layer between the middle zone and the bed.

breaking process. As we saw in Chapter 5, the initial breaking process can be quite mild, producing spilling breakers that result in a slow dissipation of energy and reduction in wave height, or violent in the form of plunging breakers where the overturning jet plunges into the trough ahead of the wave and there is a rapid dissipation of energy and reduction in wave height. On a simple planar profile (Figure 6.1a) the breaking wave is transformed into a bore with a surface roller that decays relatively uniformly across the inner surf zone to the swash zone. In the inner surf zone, bores associated with spilling breakers appear similar to those from plunging breakers. In the vertical (Figure 6.1b) the profile can be divided into three zones: (1) the upper zone located primarily above the trough of the waves where the rapid transformation takes place and where mass transport is primarily landward; (2) the middle zone located from the bottom of the wave trough to just above the bed where the turbulent flow structures generated in the upper layer break down and where the mean flow is directed offshore; and (3) the boundary layer close to the bed where there is interaction between the waves, currents, and the bed, with the mean flow generally being directed onshore (Christensen *et al.*, 2002).

Thus, each breaking wave adds to the water in the surf zone landward of the breaker line. This excess water in effect piles up against the beach and must eventually return offshore to balance the onshore flow. The force necessary to drive the water offshore comes from a set up of water against the shoreline which produces an offshore-directed pressure gradient. At any point in the vertical the difference between the momentum flux gradient and the pressure gradient is balanced

by turbulent shear stresses created by the undertow current (Ting and Kirby,1994). While it is possible to model the set-up in terms of the mass transfers of water, the more general case is modelled on the basis of the flux of momentum as described in Chapter 5 (Longuet-Higgins and Stewart, 1964; Bowen *et al.*, 1968). Note, however, that this momentum flux only accounts for the flow due to waves, not for any additional set-up due to storm surge.

The offshore return flow produced by wave advance and wave breaking can readily be demonstrated in a wave tank (flume) and observations of it (e.g. using dye dispersal) have been described for a long time (Bagnold, 1940; Longuet-Higgins, 1983). In the past three decades rapid advances in instrumentation beginning with small electromagnetic flow meters and more recently with acoustic Doppler velocimetry (ADV), laser Doppler velocimetry (LDV) and particle image velocimetry (PIV) have provided details of wave kinematics and permitted rapid advances in modelling of flows under waves and within the wave or wave/current boundary layer. The general form of the flows is shown in Figure 6.2a and a comparison of early wave tank experiments with theoretical predictions from Stive and Wind (1986) is shown in Figure 6.2b.

It is still difficult to measure the mass flux in the area above the wave trough because the instruments do not work well if they are exposed periodically and because of difficulties posed by bubbles generated by turbulence in the roller. It is possible using first order linear

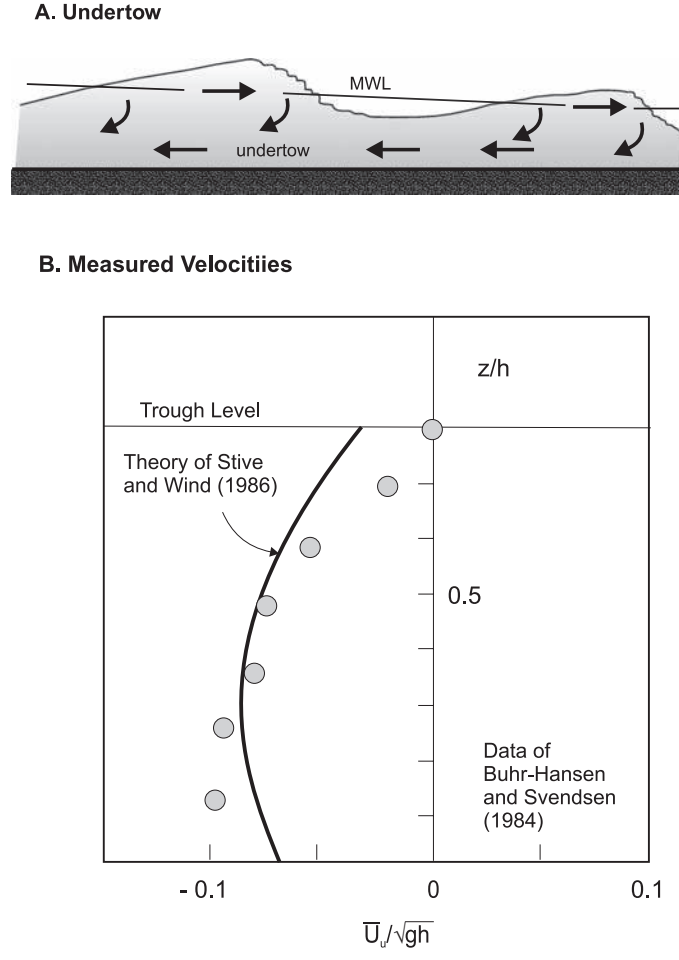

Figure 6.2 Flow velocity associated with undertow in a wave tank: (A) schematic of the pattern of net flow associated with undertow (after Svendsen, 1984a); (B) measurements of undertow in a wave tank (after Stive and Wind, 1986).

wave theory to estimate the mass transport above the level of the trough (Phillips, 1977; Dally and Dean, 1986; Masselink and Black, 1995) as

$$Q_s = \frac{1}{8}\sqrt{\frac{g}{h}H^2}. \quad (6.1)$$

Svendsen (1984a, b) used an alternative approach in which he modelled the onshore mass transport based on two mechanisms: (1) Stokes drift due to the non-linearity of unbroken waves; and (2) the mass transfer of water in the surface roller associated with breaking waves. This requires input of a larger number of parameters, and it becomes even more complex if allowance is made for winds and angle of wave incidence (Haines and Sallenger, 1994). Recent models have built on the approach of Dally and Dean (1984) and Svendsen (1984a, b) and have incorporated this into 3D models of flow in the surf zone. Improvements to the modelling have also come with the application of Boussinesq equations to provide a better representation of the non-linear properties of wave motion at breaking (e.g., Musumeci *et al.*, 2005).

6.2.2 Field measurements

In the 1950s and through to the 1970s much of the focus of attention in field studies was on rip cell circulation based particularly on work carried out on the US west coast and on the east coast of Australia. There was a tendency to suggest that in the field all circulation was three-dimensional and that 'undertow' was used by ignorant lay people who mistakenly labelled the offshore flow in a wave trough or in a rip current as undertow. However, the existence of persistent offshore flows at mid-depth was reported in a number of field studies in the 1980s (Wright *et al.*, 1982; Greenwood and Sherman, 1984; Davidson-Arnott and McDonald, 1989; Haines and Sallenger, 1994). Since then there have been considerable advances in describing the characteristics of undertow observed in the field both on barred (e.g., Greenwood and Osborne, 1990; Masselink and Black, 1995; Aagaard *et al.*, 1997; Masselink, 2004; Goodfellow and Stephenson, 2005; Houser *et al.*, 2006) and on non-barred profiles (e.g., Miles and Russell, 2004; Reniers *et al.*, 2004). Because undertow occurs (relatively) uniformly along the beach, velocities are much lower than those associated with rips and are characteristically on the order of 0.05–0.5 m s^{-1}. The undertow usually does not extend very far beyond the breaker line.

Measurements using wave staffs and bi-directional electromagnetic current meters at Wasaga Beach in Georgian Bay (Lake Huron) carried out over the period 1983–85 (Davidson-Arnott and McDonald, 1989) showed that circulation over the straight outer bars of the multiple bar system there was dominated by undertow and no evidence was found for the existence of rip currents. Mean offshore flows at mid-depth were characteristically <0.1 m s^{-1} under moderate storm conditions and seldom exceeded 0.2 m s^{-1} (Figures 6.4, 6.5 and 6.6). The set-up from wave breaking is complicated by the variable topography of the bars and by the effects of wind stress but some estimate of the magnitude can be obtained by comparing set-up at wave staff 5 just outside the main zone of breaking with that at wave staff 6 (Figure 6.4e). Mean flows are generally directed offshore and the magnitude of the flow reflects changes in significant wave height and the measured set-up through the storm. Measurements here and at Wymbolwood Beach 20 km to the east (Greenwood and Osborne, 1990; Osborne and Greenwood, 1992) show that the strength of the return flow is dependent on the height of the set-up, which in turn is controlled by the rate of energy dissipation over the bars, and particularly on the local seaward slope of individual bars. Thus, mean offshore flows during a moderate storm are greater over the second bar where breaking is more intense compared to the outer bar where most of the waves shoal, but do not break (Figure 6.5).

Measurements on the bar crest during one storm using a vertical array of current meters showed that the maximum offshore flow was located at mid-depth with flows decreasing towards the bed and towards the surface (Figure 6.6). This is in general agreement with wave tank measurements and predictions from theory but there is insufficient vertical control to

Box 6.1 Measurement of surf zone currents

Measurement of currents on the upper shoreface and especially in the surf zone is made difficult by the rapid reversal of direction associated with wave oscillatory motion (Davidson-Arnott, 2005). Oceanographers routinely deployed mechanical current meters in deep and intermediate water depth to measure tidal and wind-driven circulation even prior to World War II. These instruments used some form of Savonius rotor to measure speed and often a vane to measure the direction: they were therefore similar in design to instruments used in rivers and in air. When wave motion was present it was generally possible to assume that it was nearly uniform and to extract a mean value. However, in shallow water just outside the breaker zone, and in the surf zone, the oscillatory motion was too strong and too rapid to permit this type of instrument to be deployed. Most surf zone measurements in the 1950s and 1960s were average values obtained by tracking drogues or the movement of a cloud of dye.

While small, fast-response ducted impellor meters were used successfully in Australia in the late 1970s (Wright *et al.*, 1982) it was the introduction of the electromagnetic current meter in the late 1960s that permitted measurement of currents at 4 Hz or faster and facilitated the isolation of both high- and low-frequency motions (Huntley and Bowen, 1973). The current meters make use of Farraday's law of electromagnetic induction in which the movement of a conductor (water) through a magnetic field generates an electromotive force that is proportional to the relative motion of the fluid and magnetic field. The current meters typically have two orthogonal pairs of sensors to measure the u and v components of flow in a plane. While there are several manufacturers of electromagnetic current meters, the most popular models were made by Marsh McBirney and the 2 cm diameter model shown in Figure 6.3 became somewhat of a standard. It was commonly paired in surf zone studies with an optical backscatterance probe (OBS) which provided a rapid measure of suspended sediment concentration in a small sampling volume (Downing *et al.*, 1981). Together these made it possible to measure sediment flux at various heights in the water column and spatially alongshore and cross-shore. The instruments were often deployed on 'H' frames or 'Goalposts' and might also be co-located with a pressure transducer which would provide data on the waves and water level. Because of their widespread use, the electromagnetic flow meters were tested rigorously and a set of procedures established for calibration, and for data analysis (Aubrey and Trowbridge, 1985; Guza, 1988). While they are still in use, they are now being replaced by ADVs and ADCPs.

determine the form of the velocity profile (the vertical flow structure) explicitly. In part this is a function of taking measurements at only three heights, but it also reflects the difficulties of field instrumentation where the upper instrument needs to be positioned below the wave troughs of irregular waves and where the height of the lower instrument above the bed may change because of scour or accretion during the storm event. Recent studies such as those at the Field Research Facility at Duck, North Carolina (Garcez Faria *et al.*, 2000; Reniers *et al.*, 2004) using a vertical array of eight current meters on a towed sled have provided a much better description of vertical profile. An alternative approach is to deploy the sensors at a site with a large tidal range and thus to make measurements when the instruments become fully submersed (e.g., Miles and Russell, 2004).

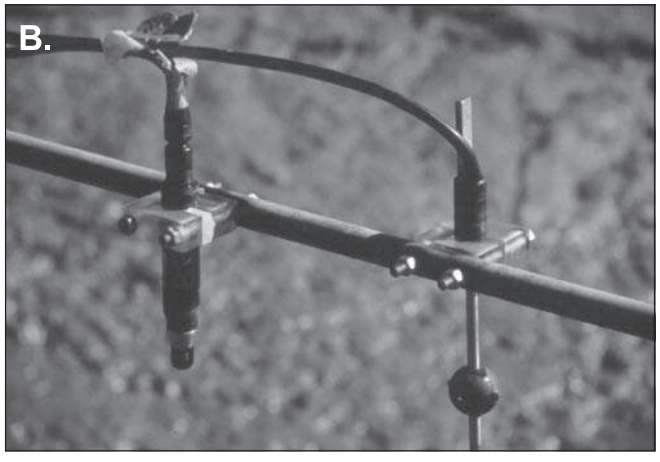

Figure 6.3 Photographs of deployment of electromagnetic current meters: (A) vertical array of electromagnetic current meters and OBS probes being set up in the intertidal zone, Skallingen, Denmark. The black cylinder mounted on the steel post at the left houses the electronics for the current meter and the posts along a line on the right are for measuring beach elevation change; (B) close-up of a 2 cm diameter Marsh McBirney current meter probe (right) and OBS probe (left) from a field experiment on a saltmarsh in the Bay of Fundy. The little nubs on the rubber sphere mark the location of the two pairs of orthogonal sensors. The cables connect the probes to the electronics and data logger.

6.3 Rip cells

6.3.1 Definition and dynamics

On some sandy beaches the offshore return flow occurs as part of a complex three-dimensional system termed a rip cell. They are also described as horizontal circulation patterns in contrast to the vertical pattern associated with undertow. These systems were first noted on the California coast by surfers and described by Shepard *et al.* (1941) and Shepard and Inman (1950). Under conditions of wave approach roughly perpendicular to the shoreline on a straight beach the rip cell takes on the form shown in Figure 6.7a. Longshore currents develop in the surf zone landward of the breaker line with flow speed increasing away from a 'divide'. These longshore currents travelling toward each other feed the rip current itself which flows offshore, crossing the breaker line in a narrow zone (on the order to 10–30 m) and then spreading out and dissipating seaward of the breakers (Figures 6.7a, b). On long sandy beaches subject to swell waves, rip currents develop at quasi-regular intervals alongshore and are often made visible by the 'quieter' water surface in the rips and by the foam, flotsam and suspended sediments associated with the rip head (Figure 6.7b). Where waves approach at an angle to the shoreline, net alongshore currents develop and the interaction of these with the general circulation in the rip cells results in increasing skewing of the rip channel orientation. This has the effect of reducing the feeder current in the direction opposite to that of the wave approach and enhancing the flow in the direction of wave approach. The rips offer a convenient passage through the breaker line for surfers and wind surfers. Because most of the offshore return flow is concentrated in a narrow zone, rip speeds are much higher than those associated with undertow, and typically range from $<0.3\ \mathrm{m\ s^{-1}}$ to $>1\ \mathrm{m\ s^{-1}}$ (Brander and Short, 2000).

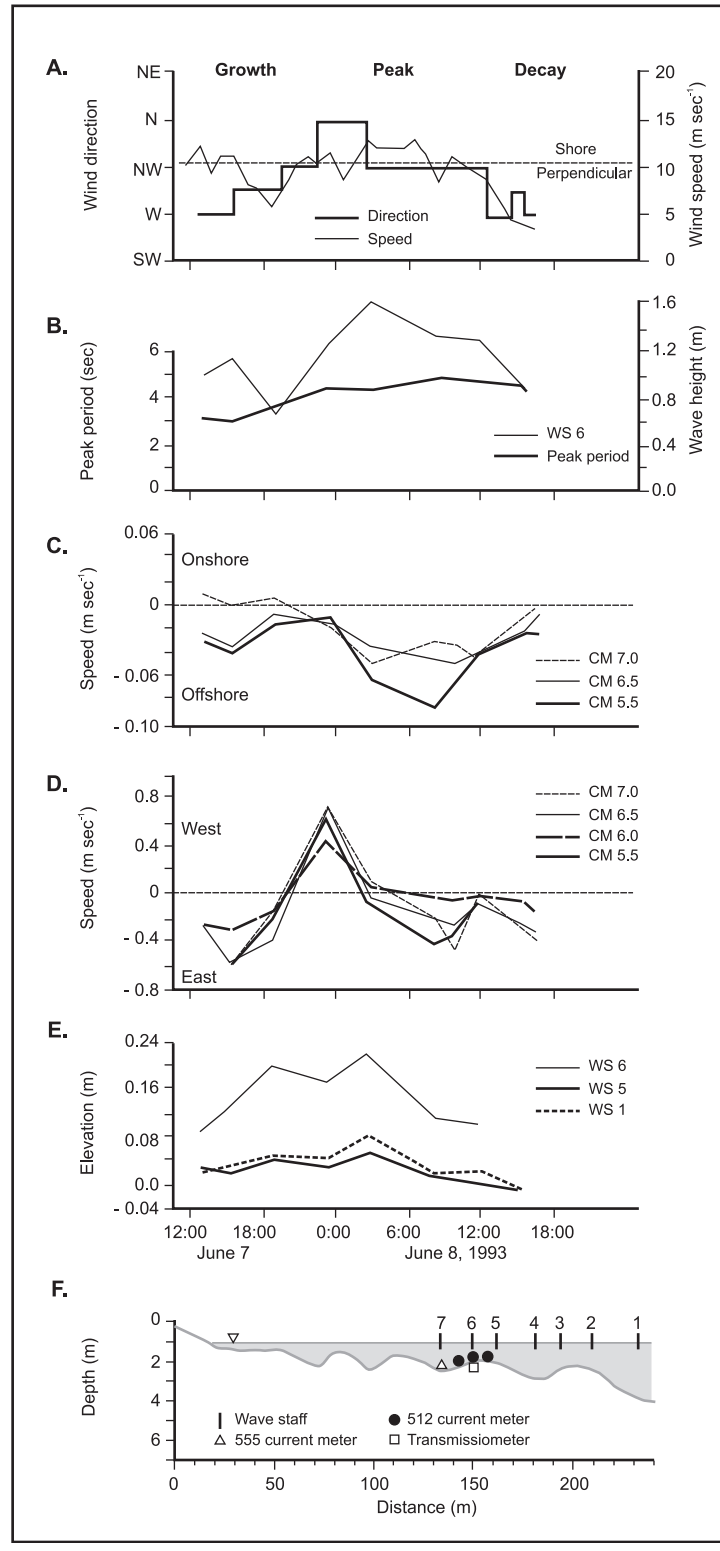

Figure 6.4 Mean flows over a straight nearshore bar at Wasaga Beach during a moderate storm: (A) wind speed and direction measured at the site; (B) variations in significant wave height and peak period at wave staff 6; (C) mean on–offshore and (D) mean alongshore speeds measured at three locations; (E) mean water level measured at three wave staffs; (F) profile of nearshore bar system and instrumentation location. The mean grain size is about 0.10–0.12 mm and tan $\beta = 0.005$ (Davidson-Arnott and MacDonald, 1989).

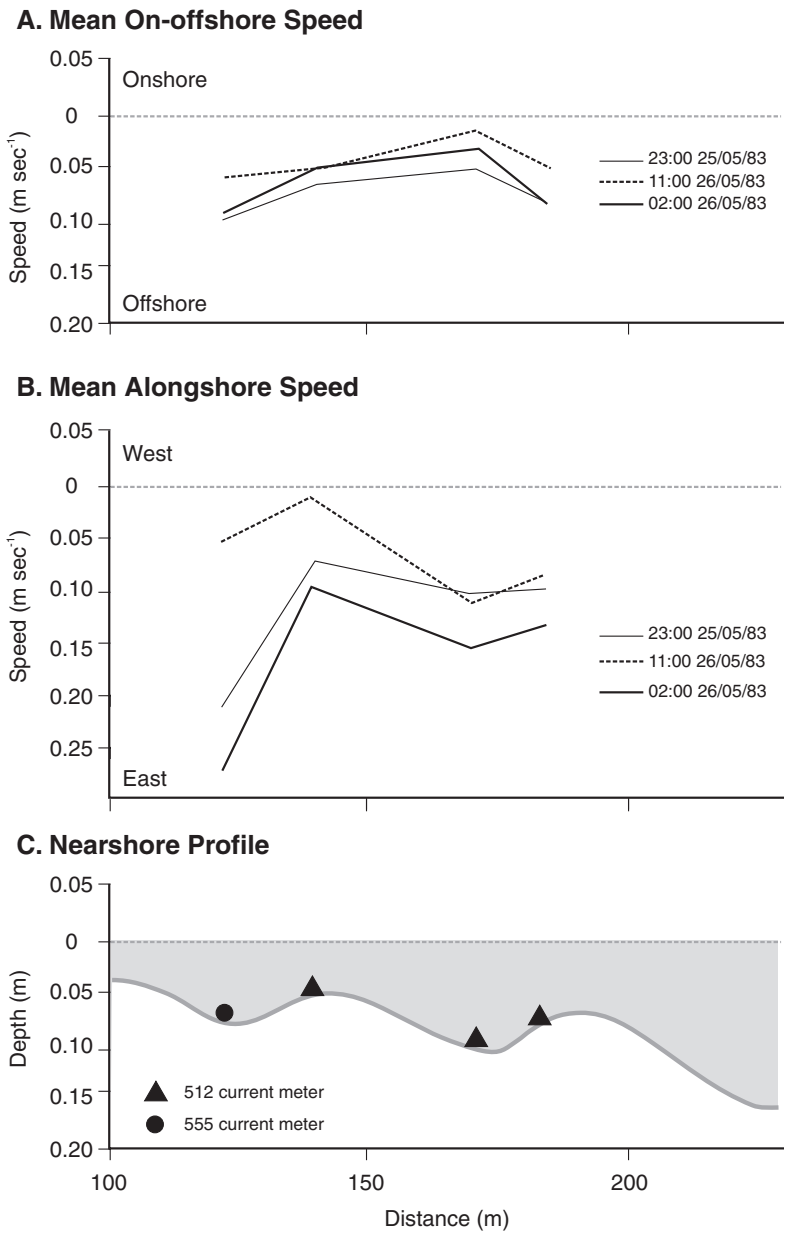

Figure 6.5 Variations in on-offshore and alongshore mean flows across two outer bars at Wasaga Beach during a moderate spring storm, May 25–26, 1983 (Davidson-Arnott and MacDonald, 1989).

On planar beaches the rip current may erode a channel below the general level of the sand in the breaker and outer surf zones (MacMahan *et al.*, 2005). The beach morphology takes on the form of giant cusps with the cusp horn located opposite the rip divide and the embayment located opposite the rip current (Figure 6.7a). The rip current cells may persist for a period of months in one location and thus over a period of a number of storm events and intervening lower energy conditions (MacMahan *et al.*, 2005).

Rip cell circulation is also associated with barred nearshore zones, and particularly with the three-dimensional or rhythmic topography that is characteristic of inner bar systems (Sonu, 1972; Greenwood and Davidson-Arnott, 1975; 1979; Short, 1979; Wright and Short, 1984; Bowman *et al.*, 1988; Gruszczynski *et al.*, 1993;

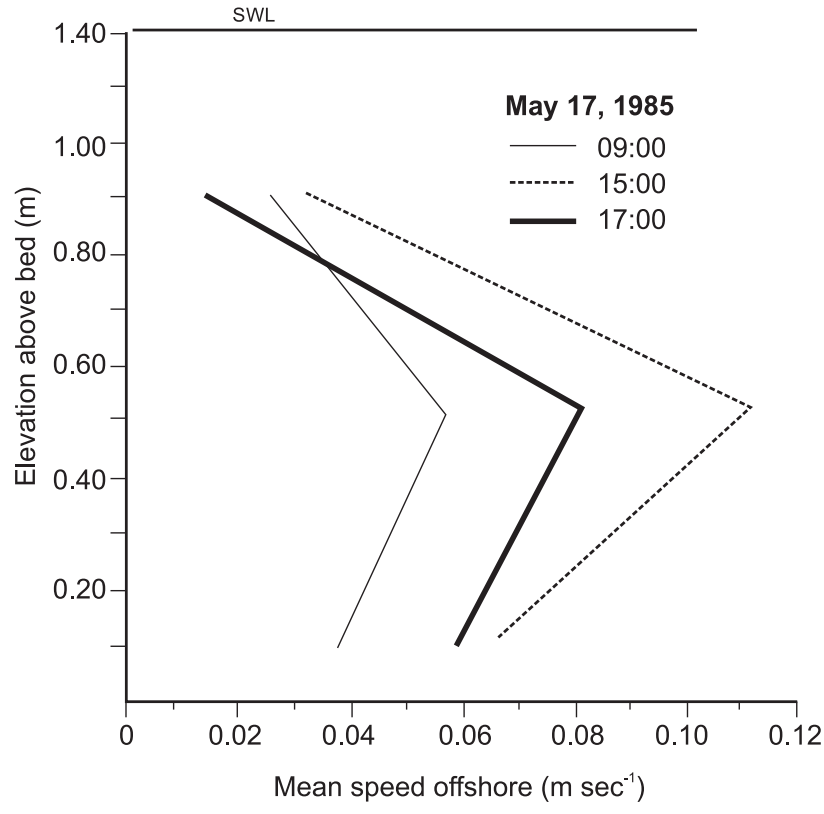

Figure 6.6 Vertical variations in mean flow over the crest of the second outer bar at Wasaga Beach during the growth, peak and decay of a moderate storm (Davidson-Arnott and McDonald, 1989).

Aagaard *et al.*, 1997; Brander, 1999a). Here the feeder currents occur in the trough landward of the bar and the rip current flows in a channel cut through the bar or between two transverse bars or shoals. Under wave approach perpendicular to the shoreline the rip systems may be nearly symmetric while under oblique wave approach the currents are oblique, with a meandering longshore current periodically breaking through the breaker line (Figures 6.8a, b). Because wave breaking is focused on the bar and there is little breaking in the trough and rip channel, it is possible to outline the general nearshore topography by averaging the light intensity from a video sequence or series of high frequency photographs (Holman *et al.*, 2006; Turner *et al.*, 2007). The bars and foreshore show up as light areas because of averaging of the white foam produced by wave breaking and the troughs and rip channels are dark because of the general absence of breaking there. An example of this application for a complex inner bar is shown in Figure 6.9.

Mean speeds measured over tens of minutes to hours in rip channels at a number of different sites tend to be quite low, ranging from 0.2–0.65 m s^{-1} (MacMahan *et al.*, 2006) but maximum velocities can be as high as 2 m s^{-1}. There have been suggestions that rip current speeds tend to pulsate, e.g., at infragravity frequencies driven by wave groupiness, and this has been observed in several field experiments (Brander and Short, 2001; MacMahan *et al.*, 2005). This may not have a significant effect on the overall rate of sediment transport in the channel but, because transport rates are often $\propto u^3$ or u^4 there is the potential for rates to be higher than under steady flows. It has generally been thought that mean flows increase with increasing wave energy (height) though the effect of this is limited by the fact that larger waves break in deeper water further offshore and so the maximum wave height on an inner bar is limited.

Several studies have demonstrated that rip current speeds increase with decreasing tidal

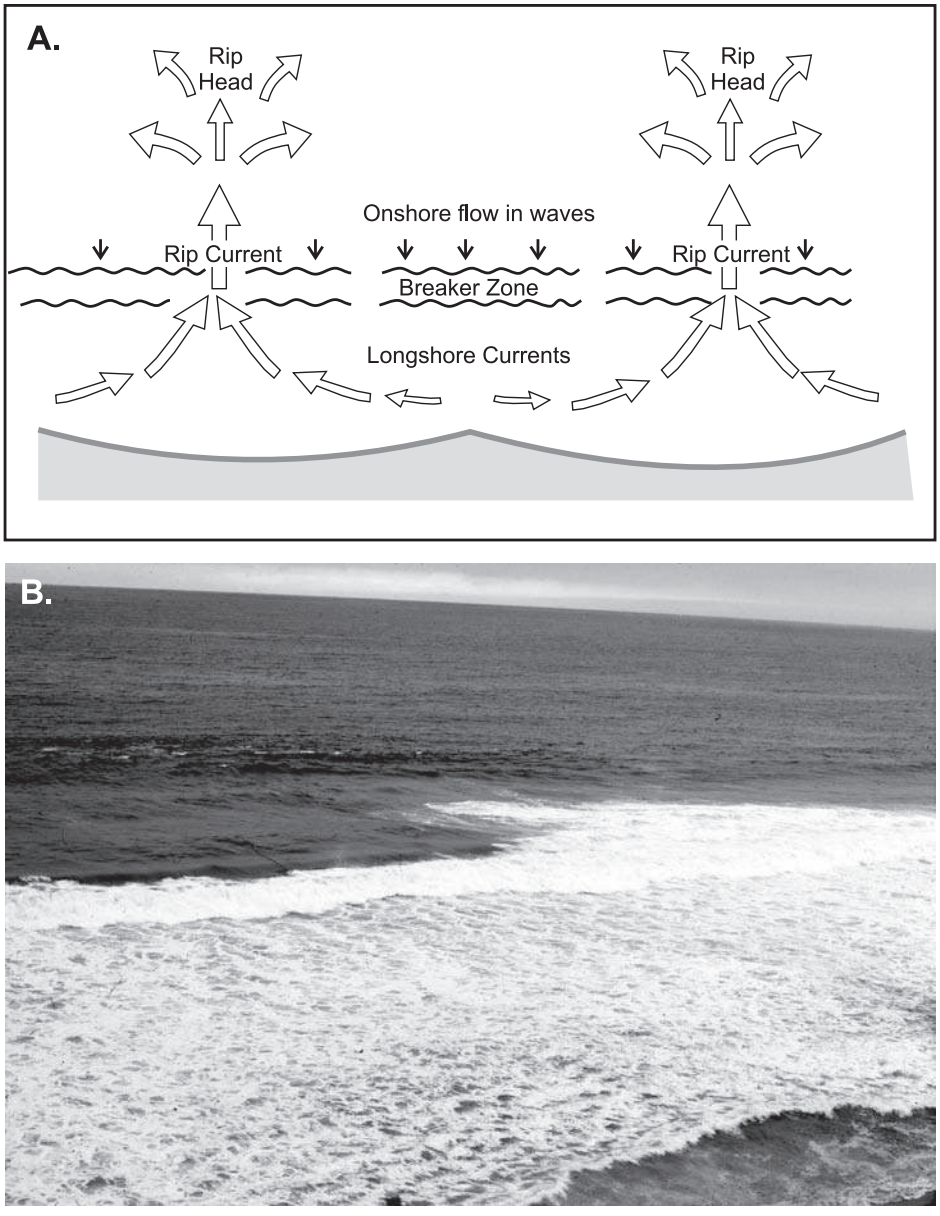

Figure 6.7 Rip cell circulation on a planar coast: (A) plan view of rip cell circulation on an open coast; (B) photograph of a rip current on the Monterey coast.

height so that flows are weak or even non-existent at high tide and much stronger at low tide (Aagaard *et al.*, 1997; MacMahan *et al.*, 2005). This reflects the fact that at high tide wave breaking on the bar is reduced and many smaller waves may not break at all. The cross-sectional area available for flow in the rip channel is also largest at this time. At low tide when water depth over a bar crest is relatively low there is nearly complete breaking of all waves and large amounts of water are injected into the trough landward of the bar (Aagaard *et al.*, 1997).

As is the case for the 2D undertow, the mass of water injected into the surf zone or landward

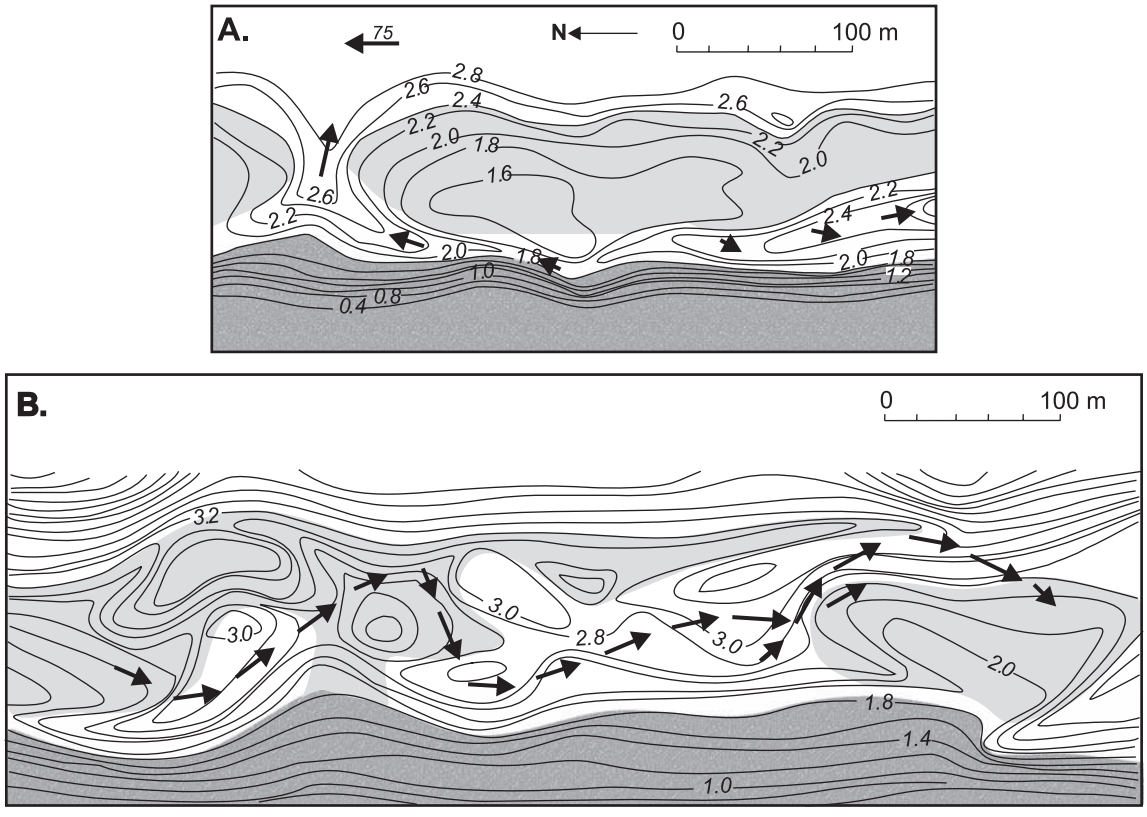

Figure 6.8 Rip cell circulation on a barred coast: (A) current speeds and direction measured with drogues for perpendicular wave approach in an inner bar system, Kouchibouguac Bay, New Brunswick. Note the transverse bar/cusp horn on the left and the drainage divide situated in the middle of the straight section of the bar. The current flow to the right feeds another rip channel just beyond the measured area; (B) current pattern traced by a drogue for complex topography under oblique wave approach producing a meandering pattern (e.g., Sonu, 1972).

trough must be returned seaward through the rip channel and thus it should be possible to compare measured discharge through the rip channel with onshore flows predicted using (6.1) (after Aagaard *et al.*, 1997):

$$V_{rip} = \frac{(Q_{drift} + Q_{roller})\lambda}{R_a} \qquad (6.2)$$

where V_{rip} is the mean velocity in the rip channel, Q_{drift} and Q_{roller} are the mean onshore discharge of water due to Stokes drift and the breaker roller, is the alongshore length between rip channels and R_a is the cross-sectional area of the rip channel.

Equation (6.2) shows that there are three main controls on rip current velocities – the input volume of water, the spacing of rip channels and the cross-sectional area of the channels. As the tide falls, the input volume of water increases (at least until the water depth over the bar crest becomes very small) and the cross-sectional area decreases because of decreasing water depth – hence we can expect quite large fluctuations in mean speed over time spans as short as individual tidal cycles. However, while over a time span of a few tidal cycles the channel dimensions and the spacing between rips can be assumed to be fixed, over a longer period or during major storms these two components can also vary. Thus the increased flow velocity in a rip due to increased wave input may lead to the scouring of a wider and/or deeper channel leading to negative feedback. Similarly

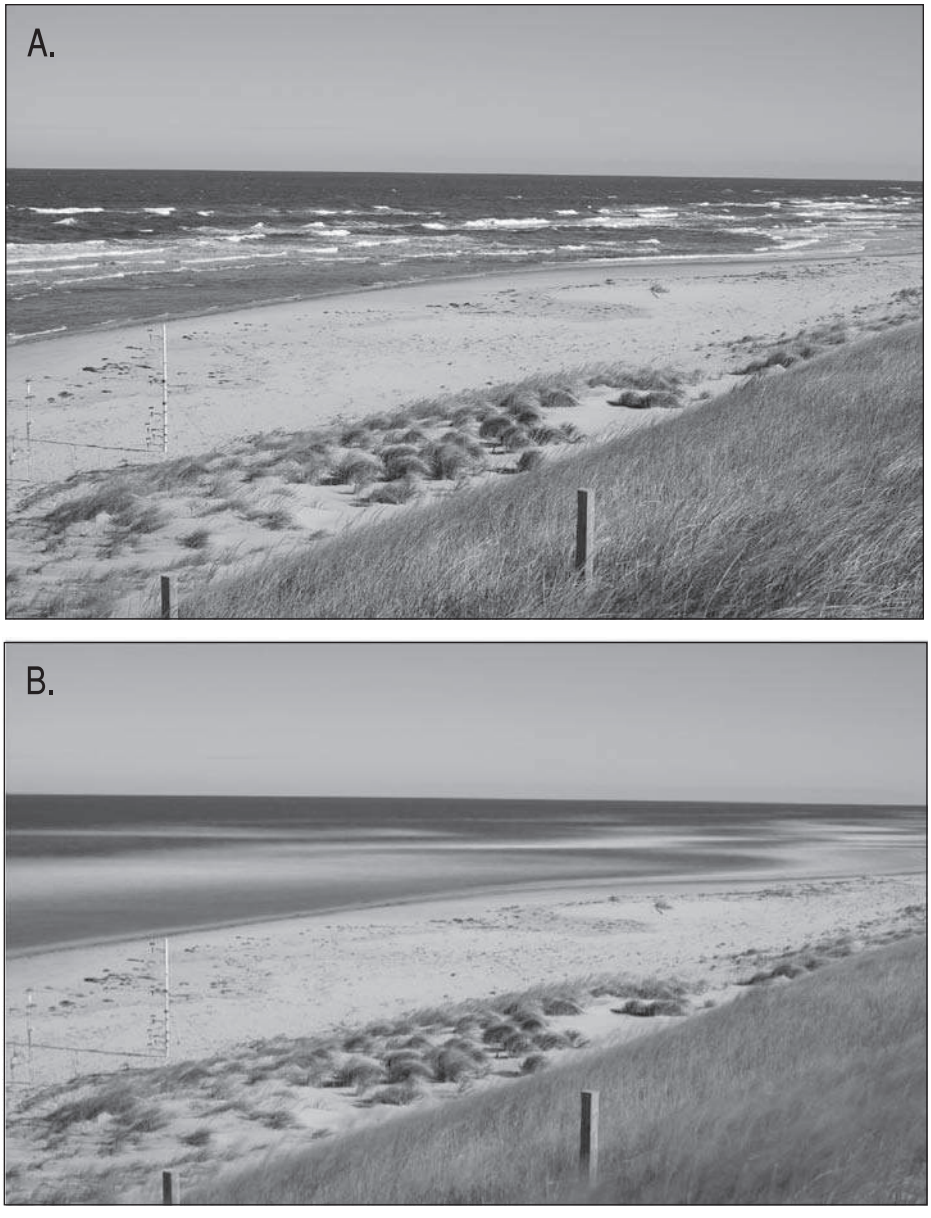

Figure 6.9 Wave breaking and rip cell circulation inferred from a 10 minute time-averaging of photographs taken at 2 second intervals in a complex inner bar system, Greenwich Dunes: (A) single photo showing waves breaking as spilling breakers on the inner bar; (B) time-averaged photograph. The zones of high light intensity mark wave breaking over the bar and the longshore trough and rip channels show up as the dark areas. Note the narrowing of the beach on the right of the photograph opposite the rip channel (photographs courtesy Hosahng Rhew).

the interaction between the seaward flowing rip and incident waves may produce negative or positive feedbacks for flow velocity and discharge. Deeper channels lead to larger unbroken waves entering the rip channel and this in turn produces a radiation stress gradient that tends to counter the pressure gradients that drive the flow. When flow is fast, the wave–current interaction encourages wave breaking and this produces a positive feedback on flows (Haller *et al.*, 2002).

6.3.2 Controls on rip spacing

The spacing between rip currents/rip current channels varies considerably from beach to beach and often over time at any particular beach (McKenzie, 1958; Short, 1985). Since spacing in effect characterises the collection area feeding the rip it might be expected that this would decrease as wave height increases, but observations by Short (1985) suggest the opposite and that during intense storm circulation may be dominated by a few mega rips with speeds up to 2 m s^{-1}. In general, there is poor correlation between rip spacing and parameters such as incident wave height and period and surf zone width (Huntley and Short 1992; Turner *et al.*, 2007). This may be due in part to the persistence of rip channels and rhythmic topography over a range of wave conditions and to the difficulties of observing the spacing during formative high-energy events.

Much effort was expended over two or three decades from 1970 trying to link rip current spacing, and the characteristic rhythmic topography associated with rip cells and crescentic nearshore bars, with some hydrodynamic mechanism that would produce periodic variations in incident waves or net drift velocities. Mechanisms of this type can be termed template models (Blondeaux, 2001) in that the hydrodynamic mechanism imposes a fixed form on the rip cell and/or bar pattern. This can be contrasted with self-organisational models in which there is positive feedback between the mechanism and the development of the modelled circulation or morphology. The mechanism that attracted most attention in terms of research devoted to testing it was proposed by Bowen (1969a), linking rip current spacing to edge waves. Bowen (1969a) argues that longshore variations in wave height will give rise to longshore variations in momentum flux and set-up and that this should lead to a flow of water from areas of high waves towards areas of low waves where the rip current would flow seaward. Bowen and Inman (1969) then go on to show that the interaction of an edge wave with incoming waves would lead to longshore variations in wave height, with the height being greatest where the edge wave and incident wave are in phase and lowest where they are 180 degrees out of phase. The rip currents would thus be located where the edge wave and incident waves are 180 degrees out of phase and the breakers are smallest (Figure 6.10). The result of this is that the alongshore spacing for the rip currents is equal to the alongshore wavelength of the edge wave. Similar reasoning was also applied to the formation of rhythmic or crescentic bars (Bowen and Inman, 1971).

There is evidence that rips form where wave heights are lowest as a result of wave refraction over complex topography, but it is yet to be demonstrated in the field that the model put forward by Bowen and Inman actually works in terms of wave height variation, let alone the link to edge waves. Despite much searching, no clear link has ever been established and it now seems that edge waves associated with rhythmic bars may be a product of the interaction between waves and existing topography rather than vice versa. Long-term studies, such as those using the Argus video system (Holman *et al.*, 2006; Turner *et al.*, 2007), show that rip cell spacing is quite variable. It now seems much more likely that the location of a rip channel is random and that the generation of the circulation may be better modelled as a form of self-organisation (e.g., Murray *et al.*, 2003) with spacing moderated by wave conditions and pre-existing topography (Aagaard and Vinther, 2008).

Rip currents erode and transport sediment, particularly in the rip channel itself (Cook, 1970; Davidson-Arnott and Greenwood, 1974; 1976; Gruszczynski *et al.*, 1993; Sherman *et al.*, 1993; Aagaard *et al.*, 1997; Brander, 1999b) and there is evidently a complex feedback between topographical evolution and the rip current itself. Rip channels tend to persist for periods of weeks or months and over several storm events. The channel spacing is of the same order as the rhythmic topography and ranges from about 150 m to more than 600 m. Rip cell circulation is expressly included in the beach stage model developed by Short and Wright from their work on beaches on the east coast of Australia (Short, 1979; Wright and Short, 1984) – see Chapter 8 for more on this.

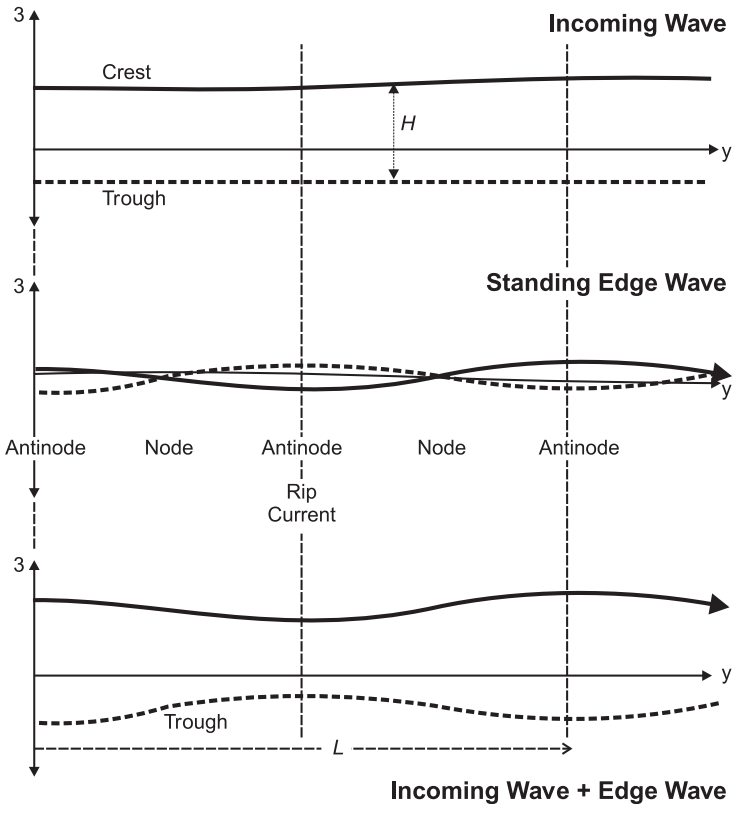

Figure 6.10 The addition of an incoming wave and a standing edge wave, producing an alongshore variation in breaking wave height (Bowen and Inman, 1969). Rip currents are located at the antinodes.

6.3.3 Rips and undertow

Why is the circulation on some beaches always dominated by undertow and others by rip cell circulation? Circulation over the straight multiple parallel bars at Wasaga Beach (Davidson-Arnott and MacDonald, 1989) is always two-dimensional whereas beaches in California (MacMahan *et al.*, 2005) and New South Wales, Australia (e.g., Short, 1985) are generally characterised by well-developed rip cell systems. The fine sand and very gentle slope at Wasaga Beach combined with short period wind waves results in wave breaking being dominantly spilling while swell waves and steeper nearshore slope in California and Australia tend to produce breakers in the plunging range. It is possible that the large vortices generated by plunging breakers may inhibit weak offshore flows associated with undertow, but undertow does occur under plunging breakers, particularly where there is no distinct trough and no preferential location for a breaker line. The existence of well-developed rip channels within barred systems is usually associated with the generation of rip cell circulation, but recent work by Aagaard and Vinther (2008) suggests that in some cases the system may be dominated by undertow even when distinct rip channels are present. They go on to suggest that morphodynamic adjustment may lag changing wave and water level conditions and that the type of circulation may be controlled both by the nature of wave breaking (supply of water to the trough) and the morphology of the bar–trough system (trough cross-sectional area).

6.4 Longshore currents

Where waves approach the shoreline at an angle, a portion of the momentum flux is directed alongshore and results in the generation of a longshore current that typically can have speeds of 0.2–1.0 m s^{-1}. Longshore currents occur

Box 6.2 | Rip currents and water safety

Waves and currents in the surf zone pose a hazard to all bathers, and particularly to non-swimmers or poor swimmers (Short, 1999). Every year thousands of people lose their lives through drowning. Where rip currents develop on popular sandy beaches, they generally account for more than half of all drownings (e.g. Klein *et al.*, 2003). In the United States 80% or more of lifeguard rescues involve people caught in rip current systems. Researchers working in the surf zone know that it is easy to drift alongshore and offshore in the rip cell and then to return to shore simply by moving laterally and then coming ashore with the waves in the zone between rip currents/rip channels. Indeed, rip current speeds can be measured by using a swimmer as a form of drogue and tracking their movement through the system (Brander and Short, 2000). The problem for non-swimmers and poor swimmers is twofold – it is very difficult to maintain a footing against waves and strong currents once the water depth is above the waist, and it is very difficult and tiring to swim against even weak currents. It is nearly impossible for strong swimmers to swim against typical rip current speeds of 0.3–1 m s^{-1}. Trained lifeguards combined with a good system of public education, both at the beach and away from it, can improve safety considerably (Short and Hogan, 1994). Klein *et al.*, (2003) report an 80% reduction in drowning fatalities along a 100 km stretch of sandy beaches in Brazil following the introduction of a safety and training programme.

Beaches in California and Australia get a lot of the attention, but drownings related to rip currents can occur wherever they are present, even under relatively small wave conditions. An example of this is a stretch of shoreline on the west side of Point Abino on the north shore of Lake Erie. The coast here is underlain by shallow limestone bedrock that forms small promontories separated by narrow sandy beaches backed by till bluffs (Figure 6.11a). The nearshore is characterised by the development of a rhythmic nearshore bar system with small rip channels at intervals. Water depth in these channels is generally a metre or less and they are generally active only during high wave conditions. However, a fixed rip channel is formed at the junction between the beach and the limestone bedrock of the point itself. Longshore currents generated by the wind and oblique wave approach under winds from the SW and W (from the left in Figure 6.11a) are forced seaward by the vertical face of the bedrock, scouring a channel that is nearly a metre deeper than the adjacent crest of the inner sand bar.

Drownings at this location in 1982 and 1991 both occurred with waves <1 m in height and winds from the SW < 10 m s^{-1}. In each case, children playing or swimming in the shallow water of the inner bar trough updrift of the point were carried alongshore and out into the rip channel. The adult who went to their rescue drowned because the depth in the channel was too great for them to stand and they quickly became exhausted trying to swim directly ashore against the current while trying to save lives. In both cases, had the adult known what was happening and been aware of the topography adjacent to Point Abino, it would have been simple to swim sideways a few metres onto the rock platform (Figure 6.11b) where they would have been able to stand. These two cases underscore the variety of factors that pose a hazard to swimmers (Short and Hogan, 1994) including: the speed of the current (which was enhanced here because of the physical barrier provided by the bedrock outcrop); water depth and varying topography; the physical difficulties posed by swimming in waves; the poor swimming ability and lack of training of the adults; and the absence of information on the nature of the potential hazards at the site.

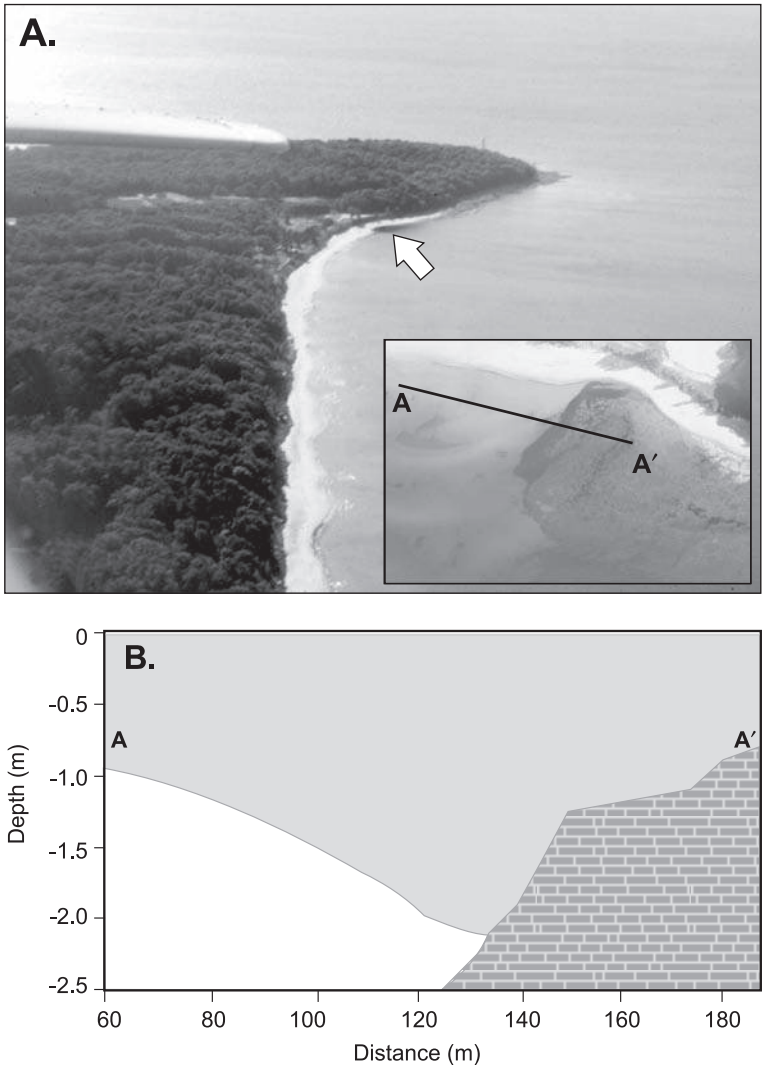

Figure 6.11 Rip channel at Point Abino on the north shore of Lake Erie: (A) oblique aerial photograph looking east along the shoreline with the sandy beach and nearshore rhythmic bars in the foreground and the limestone headland of Point Abino in the background. The arrow points to the dark line marking the location of the rip channel. The inset shows a view onshore of the rip channel with the end of the inner sand bar on the left; (B) profile parallel to the beach about 60 m offshore showing the drop-off from the nearshore sand bar into the rip channel trough and up onto the bedrock ledge of the point.

independently of rip cell circulation, but where rips are present the cellular circulation becomes skewed in the direction of the longshore current. Considerable effort has gone into attempts to measure the net longshore current (not always easy in the presence of strong oscillatory currents) and to develop theoretical and empirical models for predicting the mean flow. Longshore currents are a major control on longshore sediment transport so successful modelling of net longshore transport in numerical models often requires modelling of the longshore current first. Initial modelling of longshore currents was based on waves alone but recent models also account for the effects of winds. Longshore current velocity can be modelled theoretically but there are a number of empirical equations that produce acceptable results for simple situations. Longshore current speeds tend to be nearly uniform through the upper half of the water column and this may extend close to the bed in the zone of strong wave breaking.

6.4.1 Longshore currents on a planar beach

The work of Bowen (1969b) and Longuet-Higgins (1970a, b) showed that longshore currents generated by waves could be related to the

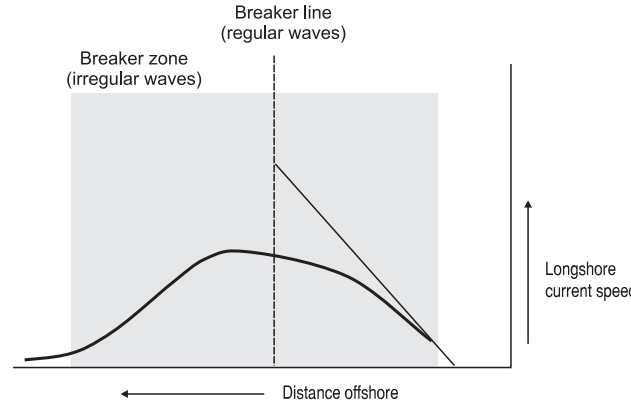

Figure 6.12 The general pattern of distribution of longshore current speeds across the surf zone on a planar profile for regular waves without lateral mixing (straight line and single breaker location) and for irregular waves (curved line and zone of wave breaking).

longshore-directed component of radiation stress. As we saw in Chapter 4, radiation stress measures the excess momentum associated with waves and the gradient of this in the surf zone leads to wave set-up. When waves break at an angle to the shoreline the longshore-directed radiation stress will generate a flow alongshore. The longshore component of radiation stress is given by

$$S_{xy} = E \sin\alpha \cos\alpha = \frac{1}{8}\rho g H^2 \sin\alpha \cos\alpha \qquad (6.3)$$

Thus, the alongshore-directed momentum flux is a function of the wave energy density and the angle of the breaking wave to the shoreline (the sin α term). The cos α term is used to correct for the fact that as wave angle to the shoreline increases a unit length along the wave crest is distributed over a proportionately greater length alongshore (we will see this again in predictions of longshore sediment transport rates in Chapter 7). It is then possible to predict the steady longshore current velocity by balancing the momentum force with frictional forces at the bed and with eddy viscosity. The solutions produced by Longuet-Higgins (1970a, b) assume monochromatic (regular) waves, linear wave theory, a planar slope and a saturated surf zone:

$$V = \frac{5\pi}{8}\frac{\tan\beta}{C_f} u_m \sin\alpha_b \cos\alpha_b \qquad (6.4)$$

where V is the longshore current velocity, C_f is a friction coefficient on the order of 0.01, tan β is the surf zone slope, u_m is the maximum orbital velocity and α_b is the wave angle to the shoreline at the breakpoint.

Equation (6.4) produces a triangular decay in longshore current velocity from a maximum at the breaker line to 0 at the beach (Figure 6.12) because the assumption of regular waves requires them to break at a single point. In reality the longshore current distribution does not have an abrupt cut-off at the breaker line but instead begins some distance offshore and produces a much smoother curve (Figure 6.12). Longuet-Higgins (1970a) modelled this by making allowance for lateral mixing which flattened the curve and extends it seaward of the breaker line with the shape of the distribution varying with the value assigned to the lateral mixing parameter P (Longuet-Higgins, 1970a). If irregular waves are considered, wave energy dissipation begins with breaking of the largest waves some distance offshore producing a smooth profile that approaches the form for regular waves in the inner surf zone, where almost all waves are broken and wave energy dissipation is controlled by water depth (Figure 6.12). Thornton and Guza (1986) introduced a formula for random waves on a planar beach that provides good comparison with measured data and numerical models now routinely include this (e.g., Larson and Kraus, 1991; Grasmeijer and Ruessink, 2003) as well as the effects of wind.

It may not always be necessary or practical to use the more complex theoretical expressions or to set up and run a numerical model such as MIKE 21 (e.g., Jones *et al.*, 2007). An empirical estimate of the mean longshore current based on significant wave height is given by Komar (1979):

$$V_l = 1.0\sqrt{gH_{bs}}\sin\alpha\cos\alpha. \quad (6.5)$$

In simple conditions, e.g., a planar nearshore, this can be used to provide an order of magnitude estimate of the mean longshore current.

6.4.2 Longshore currents on a barred beach

The presence of bars in the nearshore zone complicates the task of predicting longshore current velocity because of the variations in topography, wave breaking and set-up (Greenwood and Sherman, 1986; Larson and Kraus, 1991; Ruessink *et al.*, 2001). Maximum current speeds tend to occur on the landward edge of the bar crest or in the trough just landward of the bar. Measurements of longshore current speeds by Greenwood and Sherman (1984) across a profile with three bars at Wendake Beach, Georgian Bay, Canada showed that velocities were lower than would be predicted for a planar beach in the outer surf zone and higher than would be predicted in the inner surf zone. Measured current speeds at the height of the storm ranged from about 0.1 m s^{-1} to a maximum of about 0.4 m s^{-1} in the inner surf zone. The pattern of dimensionless mean current velocity is shown for the beginning and peak of a storm in Figure 6.13. These show that current speeds were lower just on the landward side of the bar crest and highest in the trough. There is no tidal modulation in the Great Lakes, though water depth over the bars does vary with wind and wave set up. Recent work on modelling longshore currents on barred beaches by Ruessink *et al.* (2001) found reasonably good agreement between predictions of a 1D model and measured data from Egmond aan Zee on the Dutch coast and the FRF of the US Army Corps of Engineers at Duck, North Carolina, USA. The model predictions were improved by including a term for the wave roller during breaking which had the effect of shifting the location of the maximum current shoreward into the trough. As we might expect from our earlier discussion of rip currents over barred topography (Aagaard *et al.*, 1997) the longshore current flow is tidally modulated and Ruessink *et al.* found that the improvement from including the wave roller was greatest at mid and high tide. Subsequent analysis of a number of data sets by Goda (2006) has supported the improvements produced in prediction of longshore current distribution and speed by including a roller term.

The presence of far infragravity oscillations (on the order of 200–400 seconds) in the spectra of longshore currents was first documented by Oltman-Shay *et al.* (1989), and these oscillations are now termed shear waves (Bowen and Holman, 1989). They result from instabilities in the horizontal shear of the longshore current and are likely to be better developed on barred shorelines where the longshore current flows in a well-defined trough. The effect is to produce a wave or meander in the longshore current that travels alongshore in the direction of the longshore current flow at a speed of about one third that of the mean longshore current. The alongshore propagation of the shear wave will produce pulses in flow and these will also show up in the seaward flow in rip currents. Shear waves likely have a significant impact on the suspension of sediment and net sediment transport in the surf zone (Aagaard and Greenwood, 1995; Miles *et al.*, 2002).

In addition to the effects of tidal stage, there is now increased recognition of the role of winds and tidal currents in determining the strength and distribution of longshore currents (Nummedal and Finley, 1978; Whitford and Thornton, 1993; Masselink and Pattiaratchi, 1998). Wind forces become significant on all beaches as the wind angle approaches shore parallel and as wind speed increases (Whitford and Thornton, 1993). Castelle *et al.* (2006) in a study on a multiple bar system on the west coast of France found a wide scatter between

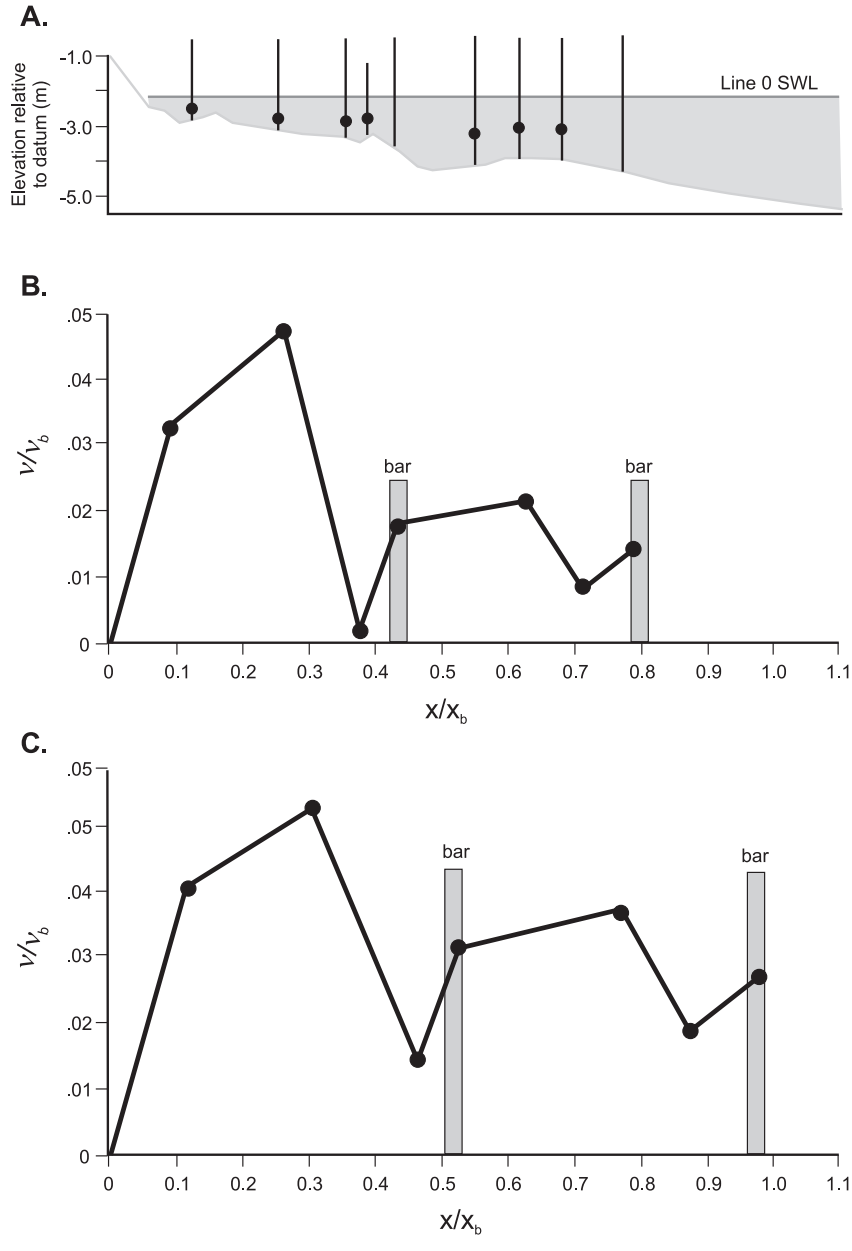

Figure 6.13 Measurements of longshore currents across a barred profile, Wendake Beach, Georgian Bay, Canada: (A) profile across the nearshore showing topography and location of electromagnetic current meters and resistance wave staffs used in the experiment; (B) dimensionless velocity profile near the beginning of the storm; (C) dimensionless velocity profile at the peak of the storm. *X* is distance offshore; X_b is width of the surf zone; *V* is the measured mean longshore current at a point and V_b is the mean depth-integrated longshore current at the breaker line without lateral mixing (Longuet-Higgins, 1972 – after Greenwood and Sherman, 1986).

measured and computed longshore currents for all conditions, but a very much stronger agreement when only conditions with weak winds were considered. On steep beaches with only a small wave angle the wind term may be negligible, but on gently sloping beaches the magnitude of the contribution from the wind may range from 0.1–1.0 of the contribution from waves (Whitford and Thornton, 1993). Some of this effect may result from the effect of wave refraction on gently sloping beaches which will reduce the wave angle at breaking. An example of this can be seen in the variations in measured longshore current speed and direction at Wasaga Beach over one storm (Figure 6.4d).

6.5 Wind and tidal currents

Swell waves reaching the coast of California or eastern Australia may have been generated by storms thousands of kilometres away and so are independent of local winds – in fact it is not uncommon on these coasts to have offshore winds with large waves. In this case the alongshore and offshore flows may be generated only by wave set-up. Where swell waves reach the coast and winds are offshore the effect of the winds is to reduce the onshore flow near the surface and thus reduce the strength of the undertow or rip circulation. Local sea breeze effects can produce rapid changes in wind and wave conditions and greatly influence current patterns and resulting morphological change (Sonu *et al.*, 1973; Masselink and Pattiaratchi, 1998). In fetch-limited areas and leeward coasts, large waves are almost always accompanied by strong onshore winds. The most significant effect of winds is to enhance set-up at the shoreline and thus to strengthen the nearshore circulation – in particular the offshore directed flows in undertow or rip currents. Storm surge thus occurs in addition to wave set-up, and together they may exceed 2 m in mid-latitude gales and over 3 m in hurricanes.

Tidal currents are unidirectional currents that are primarily directed alongshore and are most important seaward of the breaker line. In straits and areas with large tidal ranges, tidal currents themselves may be strong enough to transport sediment and they can operate in depths where wave orbital motion is quite weak. On micro-tidal coasts the currents are generally significant only in the vicinity of tidal inlets and estuaries.

Further reading

MacMahan, J. H., Thornton, E. B., and Reniers, A. J. H. M. 2006. Rip current review, *Coastal Engineering*, **53**, 191–208.

Svendsen, I. A. and Putrevu, U., 1996. *Surf zone hydrodynamics*. In Liu, P.L-F. (ed. *Advances in Coastal and Ocean Engineering*, Volume 2. World Scientific, Singapore, pp. 1–78.

References

Aagaard, T., Greenwood, B. 1995. Longshore and cross-shore suspended sediment transport at far infragravity frequencies in a barred environment. *Continental Shelf Research*, **15**, 1235–1249.

Aagaard, T., Greenwood, B. and Nielsen J. 1997. Mean currents and sediment transport in a rip channel. *Marine Geology*, **140**, 25–45.

Aagaard, T and Vinther, N. 2008 Cross-shore currents in the surf zone: rips or undertow? *Journal of Coastal Research*, **24**, 561–570.

Aubrey, D. G. and Trowbridge, J. H. 1985. *Kinematic and dynamic estimates from electromagnetic current meter data. Journal of Geophysical Research*, **90**, 9137–9146.

Bagnold, R. A. 1940. Beach formation by waves; some model experiments in a wave tank. *Journal Institute of Civil Engineers*, **15**, 27–52.

Blondeaux, P. 2001. Mechanics of coastal forms. *Annual Review of Fluid Mechanics*, **33**, 339–370.

Bowen, A. J. 1969a. Rip currents I: Theoretical investigation. *Journal of Geophysical Research*, **74**, 5469–5478.

Bowen, A. J. 1969b. The generation of longshore currents on a plane beach. *Journal of Marine Research*, **27**, 206–215.

Bowen, A. J. and Inman, D. L. 1969. Rip Currents II: Laboratory and field investigations. *Journal of Geophysical Research*, **74**, 5479–5490.

Bowen, A. J. and Inman, D. L. 1971. Edge waves and crescentic bars. *Journal of Geophysical Research*, **76**, 8862–8871.

Bowen, A. J. and Holman, R. A. 1989. Shear instabilities of the mean longshore current. 1 Theory. *Journal of Geophysical Research*, **94**, 18023–18030.

Bowen, A. J., Inman, D. L. and Simmons, V. P. 1968. Wave 'set down' and wave set-up. *Journal of Geophysical Research*, **73**, 2569–2577.

Bowman, D., Arad, D., Rosen, D. S., Kit, E., Goldbery, R. and Slavicz, A. 1988. Flow characteristics along the rip current system under low energy conditions. *Marine Geology*, **82**, 149–167.

Brander, R. W. 1999a. Field observations on the morphodynamic evolution of a low-energy rip current system. *Marine Geology*, **157**, 199–217.

Brander, R. W. 1999b. Sediment transport in low-energy rip current systems. *Journal of Coastal Research*, **15**, 839–849.

Brander, R. W. and Short, A. D. 2000. Morphodynamics of a large-scale rip current system at Muriwai Beach, New Zealand. *Marine Geology*, **165**, 27–39.

Brander, R. W., Short, A. D., 2001. Flow kinematics of low-energy rip current systems. *Journal of Coastal Research*, **17**, 468–481.

Castelle, B., Bonneton, P., Senechal, N., Dupuis, H., Butel, R. and Michel, D. 2006. Dynamics of wave-induced currents over an alongshore non-uniform multiple-barred sandy beach on the Aquitanian Coast, France. *Continental Shelf Research*, **26**, 113–131.

Christensen, E. D., Walstra, D. and Emerat, N. 2002. Vertical variation of the flow across the surf zone. *Coastal Engineering*, **45**, 169–198.

Cook, D. O. 1970. The occurrence and geological work of rip currents off Southern California. *Marine Geology*, **9**, 1973–1986.

Dally, W. R. and Dean, R. G. 1984. Suspended sediment transport and beach profile evolution. *Journal of Waterway, Port, Coastal and Ocean Division, American Society of Civil Engineers*, **110**, 15–33.

Dally, W. R. and Dean, R. G. 1986. Mass flux and undertow in a surf zone–discussion. *Coastal Engineering*, **10**, 289–307.

Davidson-Arnott, R. G. D. 2005. Beach and nearshore instrumentation. In M. L. Schwartz (ed.), *Encyclopedia of Coastal Science*, Springer, Dordrecht, pp. 130–138.

Davidson-Arnott, R. G. D. and Greenwood, B. 1974. Bedforms and structures associated with bar topography in the shallow-water environment, Kouchibouguac Bay, New Brunswick, Canada. *Journal of Sedimentary Petrology*, **44**, 698–704.

Davidson-Arnott, R. G. D. and Greenwood, B. 1976. Facies relationships on a barred coast, Kouchibouguac Bay, New Brunswick, Canada. In R. A. Davis Jr., and R. L. Ethington (eds.), *Beach and Nearshore Sedimentation*. Society of Economic Paleontologists and Mineralogists Special Publication No. 24, pp. 149–168.

Davidson-Arnott, R. G. D. and MacDonald, R. A. 1989. Nearshore water motion and mean flows in a multiple parallel bar system. *Marine Geology*, **86**, 321–338.

Downing, J. P., Sternberg, R. W. and Lister, C. R. B. 1981. New instrumentation for the investigation of sediment suspension processes in shallow marine environments. *Marine Geology*, **42**, 14–34.

Garcez-Faria, A. F., Tornton, E. B., Lippmann, T. C. and Stanton, T. P. 2000. Undertow over a barred beach. *Journal of Geophysical Research*, **105(C7)**, 16999–17010.

Goda, Y. 2006. Examination of the influence of several factors on longshore current computation with random waves. *Coastal Engineering*, **53**, 157–170.

Goodfellow, B. W. and Stephenson, W. J. 2005. Beach morphodynamics in a strong-wind bay: a low energy environment? *Marine Geology*, **214**, 101–116.

Grasmeijer, B. T. and Ruessink, B. G. 2003. Modeling of waves and currents in the nearshore: parametric vs. probabilistic approach. *Coastal Engineering*, **49**, 185–207.

Greenwood, B. and Davidson-Arnott, R. G. D. 1975. Marine bars and nearshore sedimentary processes, Kouchibouguac Bay, New Brunswick, Canada. In Hails, J. and Carr, A. (eds.), *Nearshore Sediment Dynamics and Sedimentation: An Interdisciplinary Review*. Wiley, Chichester, 123–150.

Greenwood, B. and Davidson-Arnott, R. G. D. 1979. Sedimentation and equilibrium in wave-formed bars: a review and case study. *Canadian Journal of Earth Sciences*, **16**, 312–332.

Greenwood, B. and Sherman, D. J. 1984. Waves, currents, sediment flux and morphologic response in a barred nearshore system. *Marine Geology*, **60**, 31–61.

Greenwood, B. and Sherman, D. J. 1986. Longshore current profiles and lateral mixing across the surf zone of a barred nearshore system. *Coastal Engineering*, **10**, 149–168.

Greenwood, B. and Osborne, P. D. 1990. Vertical and horizontal structure in cross-shore flows: an example of undertow and wave set-up on a barred beach. *Coastal Engineering*, **14**, 543–580.

Gruszczynski, M., Rudowski, S., Semil, J., Slominski, J. and Zrobek, J. 1993. Rip currents as a geological tool. *Sedimentology*, **40**, 217–236.

Guza, R. T. 1988. Comment on 'Kinematic and dynamic estimates from electromagnetic current meter data'

by D. G. Aubrey, and J. H. Trowbridge. *Journal of Geophysical Research*, 93, No. C2, 1337–1343.

Haines, J. W. and Sallenger, A. H. 1994. Vertical structure of mean cross-shore currents across a barred surf zone. *Journal of Geophysical Research*, **99**, 14223–14242.

Haller, M. C., Dalrymple, R. A. and Svendsen, I. A., 2002. Experimental study of nearshore dynamics on a barred beach with rip channels. *Journal of Geophysical Research*, **107 (C6)**, 3061.

Holman, R. A., Symonds, G., Thornton, E. B. and Ransinghe, R. 2006. Rip spacing on an embayed beach. *Journal of Geophysical Research*, **94 (C1)**, 995–1011.

Houser, C., Greenwood, B. and Aagaard, T. 2006. Divergent response of an intertidal swash bar, *Earth Surface Processes and Landforms*, **31**, 1775–1791.

Huntley, D. A. and Bowen, A. J. 1973. Field observations of edge waves. *Nature*, **243**, 160–161.

Huntley, D. A. and Short, A. D. 1992. On the spacing between observed rip currents. *Coastal Engineering*, **17**, 211–225.

Jones, O. P., Petersen, O. S. and Kofoed-Hansen, H. 2007. Modelling of complex coastal environments: Some considerations for best practise. *Coastal Engineering*, **54**, 717–733.

Klein, A. H. de F., Santana, G. G., Diehl, F. L. and de Menezes, J. T. 2003. Analysis of hazards associated with sea bathing: Results of five years work in oceanic beaches of Santa Catarina State, Southern Brazil. *Journal of Coastal Research*, **SI 35**, 107–116.

Komar, PD, 1979. Beach-slope dependence of longshore currents. *Journal of Waterway, Port, Coastal and Ocean Division, American Society of Civil Engineers*, **105**, 460–464.

Larson, M. and Kraus, MSc., 1991. Numerical model of longshore current for bar and trough beaches. *Journal of Waterway, Port, Coastal and Ocean Division, American Society of Civil Engineers*, **117**, 326–347.

Longuet-Higgins, M. S. 1970a. Longshore currents generated by obliquely incident sea waves 1. *Journal of Geophysical Research*, **75**, 6778–6789.

Longuet-Higgins, M. S. 1970b. Longshore currents generated by obliquely incident sea waves 2. *Journal of Geophysical Research*, **75**, 6790–6801.

Longuet-Higgins, M. S. 1972. Recent progress in the study of longshore currents. In Meyer, R. E. (ed.), *Waves on Beaches and Resulting Sediment Transport*. Academic, New York, pp. 203–248.

Longuet-Higgins, M. S. 1983. Wave set-up, percolation and undertow in the surf zone. *Proceedings of the Royal Society of London A*, **390**, 283–291.

Longuet-Higgins, M. S. and Stewart, R. W. 1964. Radiation stress in water waves; a physical discussion with applications. *Deep Sea Research.*, **11**, 529–563.

MacMahan, J. H., Thornton, E. B., Stanton, T. P. and Reniers, A. J. H. M. 2005. RIPEX: Observations of a rip current system. *Marine Geology*, **218**, 113–134.

MacMahan, J. H., Thornton, E. B., and Reniers, A. J. H. M. 2006. Rip current review. *Coastal Engineering*, **53**, 191–208.

Masselink, G. 2004. Formation and evolution of multiple intertidal bars on macrotidal beaches: application of a morphodynamic model. *Coastal Engineering*, **51**, 713–730.

Masselink, G. and Black, K. P. 1995. Magnitude and cross-shore distribution of bed return flow measured on natural beaches. *Coastal Engineering*, **25**, 165–190.

Masselink, G. and Pattiaratchi, C. B. 1998. The effect of sea breeze on beach morphology, surf zone hydrodynamics and sediment resuspension. *Marine Geology*, **146**, 115–135.

McKenzie, P. 1958. Rip current systems. *Journal of Geology*, **66**, 103–113.

Miles, J. R. and Russell, P. E. 2004. Dynamics of a reflective beach with a low tide terrace. *Continental Shelf Research*, **24**, 1219–1247.

Miles, J. R. Russell, P. E., Ruessink, B. G. and Huntley, D. A. 2002. Field observations of the effect of shear waves on sediment suspension and transport. *Continental Shelf Research*, **22**, 657–681.

Murray, A. B., LeBars, N. and Guillon, C. 2003. Tests of a new hypothesis for non-bathymetrically driven rip currents. *Journal of Coastal Research*, **19**, 269–277.

Musumeci, R. E., Svendsen, I. A. and Veeramony, J. 2005. The flow in the surf zone: a fully non-linear Boussinesq-type of approach. *Coastal Engineering*, **52**, 565–598.

Nummedal, D. and Finley, R. J., 1978. Wind-generated longshore currents. *Proceedings of the 16th Conference on Coastal Engineering*, **ASCE**, 1428–1438.

Oltman-Shay, J., Howd, P. A. and Birkmeier, W. A. 1989. Shear instabilities of the mean longshore current. 2: Field observations. *Journal of Geophysical Research*, **94**, 18031–18042.

Osborne, P. D. and Greenwood, B. 1992. Frequency dependent cross-shore sediment transport, 2. A barred shoreface. *Marine Geology*, **106**, 25–51.

Phillips, O. 1977. *The Dynamics of the Upper Ocean*. Cambridge University Press, Cambridge.

Reniers, A. J. H. M., Thornton, E. B., Stanton, T. P. and Roelvink, J. A. 2004. Vertical flow structure during

Sandy Duck: observations and modeling. *Coastal Engineering*, **51**, 237–260.

Ruessink, B., Miles, J., Feddersen, F., Guza, R. and Elgar, S. 2001. Modeling the alongshore current on barred beaches. *Journal of Geophysical Research*, **106**, 22451–22463.

Shepard, F. P. Emery, M. O. and Lafond, E. C. 1941. Rip currents: a process of geologic importance. *Journal of Geology*, **49**, 337–369.

Shepard, F. P. and Inman, D. L. 1950. Nearshore water circulation related to bottom topography and wave refraction. *Transactions of the American Geophysical Union*, **31**, 196–212.

Sherman, D. J., Short, A. D. and Takeda, I. 1993. Sediment mixing depth and bedform migration in rip channels. *Journal of Coastal Research*, **15**, 39–48.

Short, A. D. 1979. Three-dimensional beach-stage model. *Journal of Geology*, **87**, 553–571.

Short, A. D. 1999. Beach hazards and safety. In A. D. Short (editor), *Handbook of Beach and Shoreface Morphodynamics*, John Wiley & Sons, Chichester, 293–304.

Short, A. D. 1985. Rip-current type, spacing and persistence, Narrabeen Beach, Australia. *Marine Geology*, **65**, 47–71.

Short, A. D. and Hogan, C. L. 1994. Rip currents and beach hazards: their impact on public safety and implications for coastal management. *Journal of Coastal Research*, **SI 12**, 197–209.

Sonu, C. J. 1972. Field observations of nearshore current circulation and meandering currents. *Journal of Geophysical Research*, **7**, 3232–3247.

Sonu, C. J., Murray, S. P., Hsu, S. A., Suhayda, J. N. and Waddell, E. 1973. Sea-breeze and coastal processes. *EOS, Transactions of the American Geophysical Union*, **54**, 820–833.

Stive, M. J. F. and Wind, H. G. 1986. Cross-shore mean flow in the surf zone. *Coastal Engineering*, **10**, 325–340.

Svendsen, I. A. 1984a. Wave height and set-up in a surf zone. *Coastal Engineering*, **8**, 303–329.

Svendsen, I. A. 1984b. Mass flux and undertow in a surf zone. *Coastal Engineering*, **8**, 347–365.

Thornton, E. B. and Guza, R. T. 1986. Surf zone longshore currents and random waves, field data and models. *Journal of Physical Oceanography*, **16**, 1165–1178.

Ting, F. C. K. and Kirby, J. T. 1994. Observations of undertow and turbulence in a laboratory surfzone. *Coastal Engineering*, **24**, 51–80.

Turner, I. L., Whyte, D., Ruessink, B. G. and Ranasinghe, R. 2007. Observations of rip spacing, persistence and mobility at a long, straight coastline. *Marine Geology*, **236**, 209–221.

Whitford, D. J. and Thornton, E. B. 1993. Comparison of wind and wave forcing of longshore currents. *Continental Shelf Research*, **103**, 1205–1218.

Wright, L. D., Guza, R. T. and Short, A. D. 1982. Dynamics of a high-energy dissipative surf zone. *Marine Geology*, **45**, 41–62.

Wright, L. D. and Short, A. D. 1984. Morphodynamic variability of surf zones and beaches: a synthesis. *Marine Geology*, **56**, 93–118.

7

Coastal sediment transport

7.1 Synopsis

Modification of the coast takes place through the erosion, transport and deposition of material that is either eroded by waves and currents or brought to the coast, e.g., by rivers. Fine sediments in the silt and clay size range do not occur in appreciable amounts in the inner nearshore and surf zones on energetic coasts. They tend to be placed in suspension and diffuse uniformly through the water column. They are then removed offshore or alongshore where they settle out of suspension in deep water in the outer shoreface or further offshore. Fine sediments may also be brought into estuaries, bays and lagoons where they are deposited in quiet water, often promoted by the presence of vegetation such as seagrasses, salt marsh plants and mangroves. Coarser particles of sand and gravel are exchanged readily between the inner nearshore and surf zones and the beach, and may be transported alongshore in appreciable quantities. It is usual to distinguish between processes that lead to the net transport of sediment onshore or offshore (shore normal transport) and those tending to move sediment alongshore (longshore sediment transport), though both processes occur simultaneously.

Except in a few locations in the surf zone, such as rip channels and where longshore currents are fastest, unidirectional currents in the nearshore and surf zone are generally not strong enough to erode and transport coarse sediment directly. Instead, sediment is set in motion by the oscillatory currents associated with waves and by the turbulent vortices generated by wave breaking, particularly where waves break as plunging breakers. The direction of net transport of sediment then depends on the balance of all the forces acting on the sediment, including those due to incident and long waves, wave-generated on–offshore and alongshore flows, wind-driven currents and tidal flows.

7.2 Sediment transport mechanisms, boundary layers and bedforms

7.2.1 Transport mechanisms

Fine sediments in the silt and clay size range do not occur in appreciable amounts in the inner nearshore and surf zones on energetic coasts. They tend to be placed in suspension and diffuse uniformly through the water column, maintained by turbulence. They are then removed seaward or alongshore where they may settle out of suspension in deep water in the outer nearshore or offshore, or they may be brought into estuaries and lagoons where they are deposited in deeper basins, on mudflats or in marshes and mangroves. The cohesive property of these fine materials and the fact that they are often found in the presence of sheltering vegetation makes prediction of sediment entrainment quite complicated. We will therefore ignore them for now and consider them when we describe saltmarsh and mangrove coasts.

Particles in the sand and gravel size fraction (~0.1–64 mm) are cohesionless and readily set in

motion by waves. Particles in this size range are exchanged readily between the inner and outer shoreface and the beach and may be transported alongshore in appreciable quantities. They are thus characteristic of most beaches and surf zones and there is considerable body of empirical and theoretical studies of their dynamics. We will therefore focus attention on the processes of entrainment, transport and deposition of sand and the characteristics of the bedforms developed in it. Larger particles (cobbles and boulders) are also cohesionless but their large size also requires special treatment and transport requires very large waves (or possibly the presence of ice) so we will omit consideration of them for a while a well.

On all but the most sheltered sand beaches wave action during storms, or large-swell waves, results in instantaneous velocities near the bed that greatly exceed the threshold for initiation of movement over the whole of the nearshore and surf zones. It is usual to distinguish between processes that lead to the net transport of sediment onshore or offshore (cross-shore transport) and those tending to move sediment alongshore (longshore sediment transport), though both processes occur simultaneously. Except in a few locations in the surf zone, such as rip channels and where longshore currents are fastest, unidirectional currents in the nearshore and surf zone are generally not strong enough to erode and transport coarse sediment directly. Instead, sediment is set in motion by the oscillatory currents associated with waves and by the turbulent vortices generated by wave breaking, particularly where waves break as plunging breakers. Sediment is then transported in the direction of mean flow produced by processes such as Stokes drift, undertow and wind-driven currents, and these have the potential to transport large quantities of sediment. The direction of net transport of sediment then depends on the balance of all the forces acting on the sediment, including those due to incident and long waves, wave-generated on–offshore and alongshore flows, wind-driven currents and tidal flows.

As is the case for unidirectional flow in rivers, sediment may be transported continuously in contact with the bed through rolling and sliding, or in intermittent contact through saltation. Most sediment in the granule and gravel size fractions are transported this way and only placed in suspension for short periods in highly energetic breaker zones. Sediment may also be transported in suspension and this is characteristic of sand transport under energetic waves near and in the breaker and surf zones. Sand moving across bedforms such as ripples and dunes under oscillatory waves is thrown into suspension close to the bed during the period of maximum flows under the wave crest and trough. This sediment does not get very high in the water column – generally only a few cm to a few tens of centimetres above the bed – and there is continuous exchange between sediments in the bed and sediments in suspension above it. In areas of breaking waves, especially plunging breakers, large vortices impinging on the bed may throw sand into suspension throughout the water column. In practice, while reliable instrumentation now exists to measure suspended sediment concentrations some distance above the bed, it has proven difficult to measure sediment transport very close to the bed and the bedload transport itself. As a consequence, there is still considerable uncertainty as to the relative contribution of the two modes of transport (Komar, 1978).

7.2.2 Boundary layers, shear stress and initiation of motion

Friction and turbulence generated by fluid motion over a boundary such as the sea bed generates a boundary layer with flow velocity increasing away from the bed to a maximum at the top of the boundary layer beyond which flow is unaffected by conditions at the bed. The boundary layer under unidirectional flows consists of three principal layers – the bed layer, the logarithmic layer and the outer layer (Figure 7.1a). The outer layer may extend to the top of the flow in shallow rivers or there may be a free-stream layer above the top of the boundary layer. Bedforms have a greater effect on flow in the boundary layer than does sediment, particularly in the sand size range. Flows like these can be found in tidal currents,

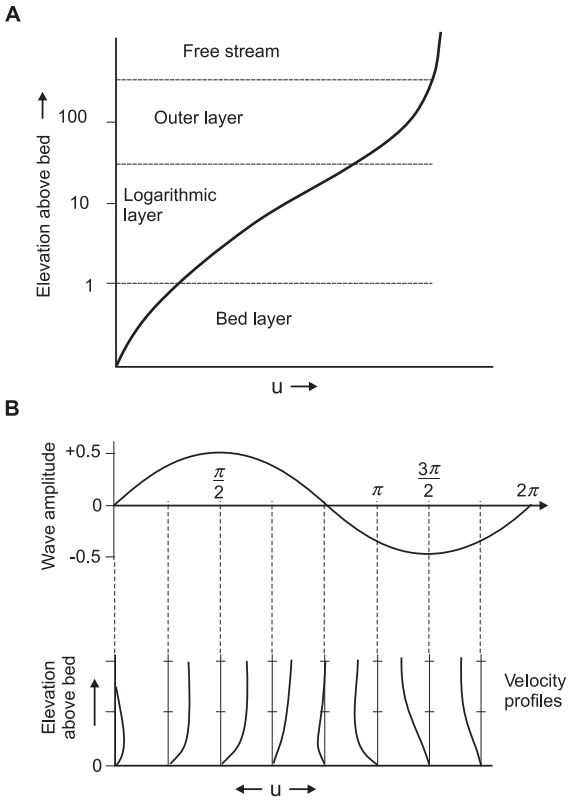

Figure 7.1 Boundary layers in coastal waters: (A) the boundary layer formed under unidirectional flows such as tidal currents, rip currents and winds; (B) the changing form of the oscillatory boundary layer for a single wave.

wind-driven currents on the shelf and in wind flows across the beach. The bed layer may also be divided into an inner layer close to the bed and an outer buffer layer that links this to the logarithmic portion of the profile. The inner layer is termed the viscous layer when the bed is smooth (Reynolds number (Re) <5) or the bed layer when the bed is rough and sediment on the bed projects into the turbulent flow (Re > 70). Bed roughness is produced initially by the material making up the bed (skin friction) and is generally considered to be proportional to the grain diameter D. The second contribution to bed roughness is that produced by bedforms such as ripples and dunes that are present much of the time and which have a much greater effect on the velocity profile.

Description and modelling of sediment transport under unidirectional flow in rivers and by wind action are usually carried out with reference to the bed shear stress τ. This can be measured directly or, more usually, is derived from the bed shear velocity U_*, which in turn is derived from the slope of the velocity profile in the logarithmic layer using the law of the wall. In unidirectional flows the logarithmic layer is comparatively thick (on the order of tens of centimetres to several metres) and it is feasible to take the average of readings over several minutes. However, under oscillatory flow the boundary layer essentially breaks down twice during each wave period and consequently a thick boundary layer does not develop. Instead the boundary layer grows and diminishes during each half of a wave period and the flow direction reverses between the crest and the trough of the wave (Figure 7.1b). The total wave boundary layer height is usually <0.1 m. Measurement of the velocity profile during a wave cycle thus requires the use of instruments, such as a hot film probe, to make high frequency measurements of the flow over very short distances close to the bed (e.g., Jonsson and Carlsen, 1976; Jensen *et al.*, 1989). Maximum values for bed shear stress thus occur under the wave crest and trough and there are two minima in each complete wave cycle. Assuming turbulent flow conditions the shear stress τ can be defined as:

$$\tau = (\mu + \xi)\frac{du}{dz} \tag{7.1}$$

where μ = molecular viscosity and ξ = eddy viscosity.

Molecular viscosity is a constant for given conditions and generally much smaller than the eddy viscosity. In rivers an average value for ξ can be used for a given set of flow conditions but in the case of oscillatory wave motion eddy viscosity changes as the flow speeds up and then slows down (Wiberg, 1995).

It is possible therefore to compute either the maximum bottom shear stress or an average value for the whole wave cycle. The maximum horizontal orbital velocity at the top of the wave boundary layer can be estimated from linear wave theory as

$$u_0 = \frac{\pi H}{T \sin kh}. \tag{7.2}$$

This is the same as (5.17) and the derivation is given there. The maximum bed shear stress τ_w can then be estimated from

$$\tau_w = 0.5 \rho f_w u_0^2 \tag{7.3}$$

where ρ is the fluid density; f_w is the wave friction factor.

The wave friction factor is one of those parameters that we can determine if we have measurements for all the other parameters. In predicting bed shear stress, f_w has to be estimated and a lot of work has gone into determining the best way to do this (e.g., Kamphuis, 1975; Nielsen, 1992). As would be expected from the discussion above, the friction factor should incorporate both the grain roughness and form roughness due to bedforms. Nielsen (1992) proposed the following empirical equation for obtaining f_w:

$$f_w = \exp\left[5.5 \left(\frac{K_s}{d_0}\right)^{0.2} x - 6.3\right] \tag{7.4}$$

where d_0 = orbital diameter at the bed; k_s = the Nikuradse roughness length.

The term k_s is made up of the grain roughness k' and the form roughness k''. According to Nielsen (1992), k' can be approximated by the diameter D of the grains making up the bed and k'' can be estimated from

$$k'' = 8 \frac{\eta^2}{\lambda} \tag{7.5}$$

where η = bedform height and λ = bedform spacing.

This probably works reasonably well for 2D ripple forms but there is likely considerable variation for complex 3D ripples and dunes. However, the ability to model the maximum bed shear stress is useful for predicting the threshold of sediment motion by waves since this is the start for modelling sediment transport in the nearshore.

Sand can be expected to start moving and rolling back and forth on the bed when τ_w exceeds the threshold for the sediments making up the bed. As is the case for unidirectional flow, we can use some form of the Shields diagram to predict this. In laboratory experiments the definition of incipient motion is fairly easily accomplished but in the field we can expect considerable variations in grain size and in bedforms over fairly small areas and temporal variations in bed shear stress a as a result of irregular waves (Davies, 1985). This means that we should think of the prediction of a threshold in terms of the probability (in space and time) of sediment motion. Simplified expressions are available for sediments in fine to coarse sand that provide a reasonable value, given this variability (e.g., Komar and Miller, 1973). However, during high wave events, sediment is in motion over the whole nearshore and thus in practice we need not worry too much about the initiation of motion – at least for sand.

7.2.3 Bedforms and facies

As is the case for unidirectional flow in rivers and air flow, transport of sediment in bedload or close to the bed by waves and by combined wave and current flow leads to the development of characteristic forms on the surface. Similarly, the bedforms are quasi-regular in morphology and spacing and their form seems to be controlled to a large extent by the diameter of the sediment, by the shear stress exerted on the bed, and by the velocity asymmetry in the waves or combined wave and current flow. Bedform generation and morphology have been studied in wave tanks and oscillatory tubes (Mogridge and Kamphuis, 1972; O'Donoghue and Clubb, 2001; van der Werf *et al.*, 2006) as well as in the field (Inman, 1957; Clifton *et al.*, 1971; Miller and Komar, 1980; Sherman and Greenwood, 1984; Osborne and Vincent, 1993; Swales *et al.*, 2006). We know quite a lot about ripples produced by pure oscillatory flow but it is still very difficult to predict bedform type and dimensions in the highly variable flows in the breaker and surf zones where wave motion is highly asymmetric and where the contribution of unidirectional flows varies rapidly both temporally and spatially. This in turn makes it difficult to predict form roughness in modelling sediment transport.

Under nearly symmetric oscillatory flow over a sand bed the sequence of bedforms observed as

bed shear stress is increased from the critical point for initiation of motion to very high values is: plain bed (lower flow regime); ripples; plane bed (upper flow regime). These conditions can be observed in laboratory oscillatory tubes, or in quite deep water some distance seaward of the breaker line (Carstens *et al.*, 1969; Clifton *et al.*, 1971; Mogridge and Kamphuis, 1972; Davidson-Arnott and Greenwood, 1976; Li and Amos, 1999; Doucette, 2000; O'Donoghue and Clubb, 2001). The ripples are symmetric in cross-sectional form and show little evidence of migration. This is in contrast to asymmetric ripples which develop under the highly asymmetric orbital motion associated with waves near the break, or under unidirectional flows.

Bagnold (1946) distinguished between rolling grain ripples and vortex ripples. Rolling grain ripples are formed under flow conditions just above the critical shear stress, where grains are transported close to the bed and no vortex is generated in the lee of the ripple. Ripple heights are comparatively subdued. At higher velocity ripples grow in height and a vortex develops on the lee side of the ripple crest during each half of the wave cycle. At higher flows still, ripple height begins to decrease as large amounts of sand are transported in suspension and the subdued ripples under these conditions are termed post-vortex. Eventually the ripples disappear entirely with sheet flow conditions over a planar bed.

Vortex ripples have well-defined crests, curved troughs and a regular spacing between the bedforms. In the field they tend to be 2D in form with ripple crests being continuous for distances many times longer than the spacing between ripples (Figure 7.2a). However, laboratory experiments in oscillatory wave tunnels suggest that, with fine sand, only 3D forms are observed (O'Donoghue and Clubb, 2001). As noted above, ripple height η varies with flow conditions and the maximum height also increases with an increase in sediment diameter. In fine-to-medium sand, ripples are typically 1–5 cm in height (Figure 7.2a) and may exceed 10 cm in coarse sand and granules (Figure 7.2b). The spacing between ripples λ also varies with flow conditions but the relationship is more complex than for ripple height. At low flows $\lambda \propto d_o$, where d_o is the orbital diameter at the bed, and it increases with increasing d_o up to a maximum point (Inman, 1957; Miller and Komar, 1980). Orbital ripples form under these conditions (Inman, 1957; Clifton, 1976). As the orbital diameter increases further the spacing remains at that limit, or decreases slightly, and $\lambda \propto 1/d_o$. Finally, anorbital ripples occur at very high flows and $\lambda \propto D$.

In the field where there are rapid variations in grain size, topography, wave orbital motion and the superimposition of longshore and rip currents there is a complex range of ripple and dune forms. In addition to 2D symmetric and asymmetric ripples, 3D ripples with short crest lengths and complex branching patterns can be observed. In troughs, where unidirectional flows associated with longshore and rip currents occur, 3D ripples characteristic of those in rivers can be observed. In the zone of shoaling waves cross ripples may be found. These appear as 2D vortex ripples oriented diagonally to the direction of wave advance with short ripples aligned perpendicular to these in the troughs between. The whole effect looks like the rungs of a ladder and so they are sometimes called ladderback ripples (Figure 7.2f).

As waves begin to shoal strongly, water motion at the bed becomes highly skewed so that the positive velocity under the crest is much larger than the negative velocity under the trough and, at the same time, net drift velocity (Stokes drift) increases. As a result, the ripple form becomes increasingly asymmetric and migration of the ripple form in the direction of wave advance occurs. In this asymmetric flow regime, ripples are replaced by lunate megaripples. These are a form of 3D dune, with an arcuate trough incised below the general bed surface and the horns of the trough pointing landward (Clifton *et al.*, 1971; Davidson-Arnott and Greenwood, 1976; Sherman *et al.*, 1993). Lunate megaripples are 1–4 m across and the base of the scour trough is typically 0.3–0.8 m below the flat top of the megaripple crest. In contrast to dunes in rivers where the crest appears as a triangular feature standing above the bed level, lunate megaripple crests occupy most of the form and the troughs appear to be incised below the general bed surface. The

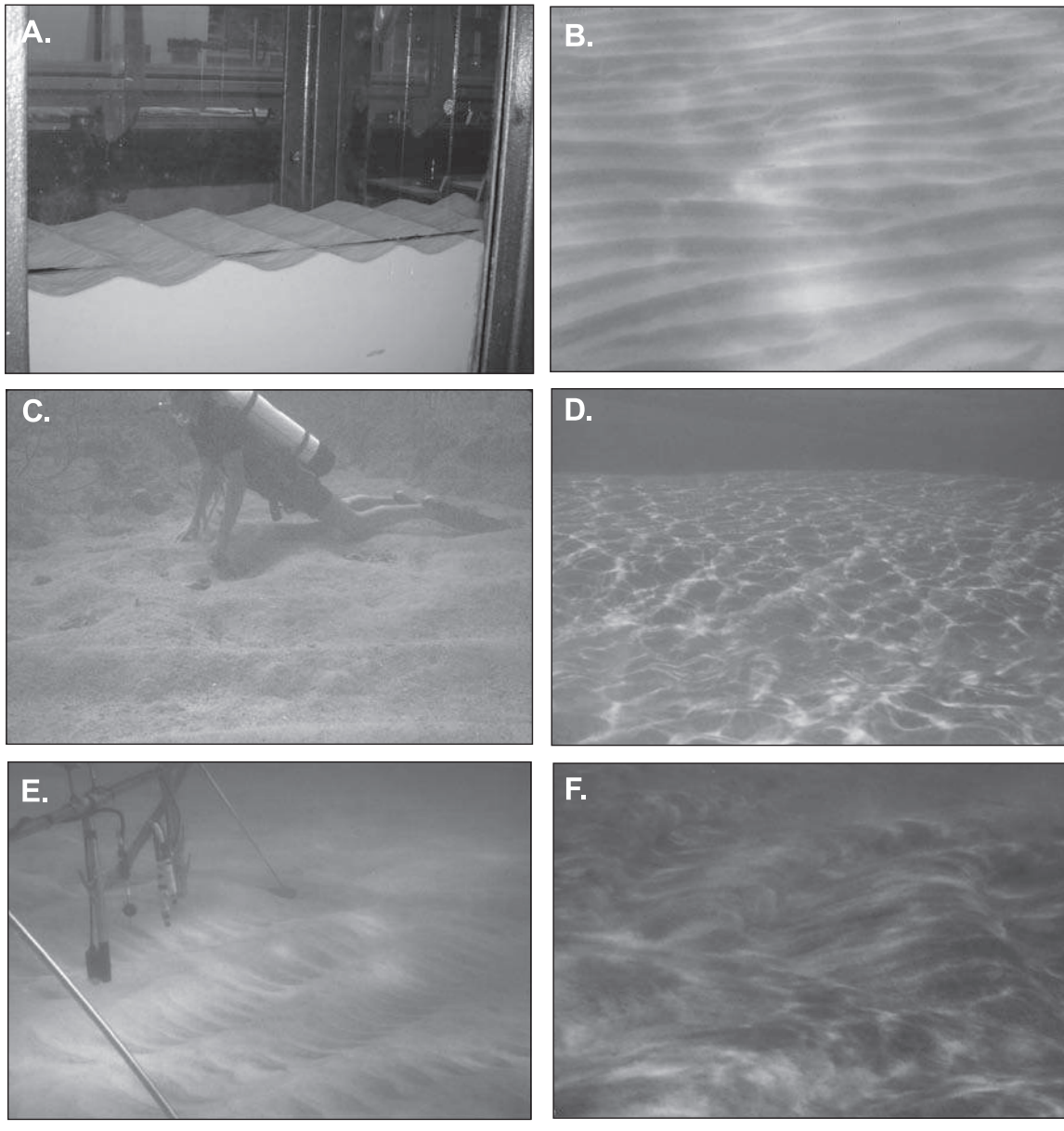

Figure 7.2 Photographs of bedforms on sandy coasts: (A) 2D vortex ripples generated in a laboratory oscillatory flume, University of Aberdeen (photo Jeff Doucette; (B) 2D vortex ripples characteristic of shoaling waves on a medium sand bed. Note the lateral extent of the ripple crests and the tuning fork junctions that are typical of these ripples in the field. The spacing between ripples is regular and it can be seen that this spacing adjusts to the junction (or splitting) of the crests; (C) large vortex ripples developed in coarse sand and granules, Veradero, Cuba at a depth of about 25 m; (D) 3D ripples on a bar crest; (E) cross-ripples or ladderback ripples (photo Jeff Doucette); (F) flow over quasi 2D dunes just seaward of the breakpoint. The photograph was taken just as the wave crest passed looking obliquely offshore. Plumes of sediment are visible seaward as vortices lift off during the offshore directed portion of the flow.

scour trough has a slip face on both sides, and under wave action sediment avalanches into the trough and up the other side under the passage of both the wave crest and the wave trough. However, because of the strong flow asymmetry, there is a net migration in the direction of wave advance and the resultant bedform is similar to that of a dune produced by unidirectional low on a river, though often with a rounded trough. The megaripple troughs are spaced en echelon with distances between them on the order of 2–4 m (Clifton *et al.*, 1971; Sherman *et al.*, 1993; Gallagher, 2003). Lunate megaripples develop also in combined wave and current flows and the direction of movement is then controlled by the resultant current. Thus lunate megaripples can migrate offshore in flows over the centre of crescentic bars or along rip current channels (Davidson-Arnott and Greenwood, 1976; Sherman *et al.*, 1993).

The transition to lunate megaripples is controlled initially by the intensity of the bed shear stress under waves. Several studies (Nielsen, 1992; Aagaard *et al.*, 2002) have found that the transition to lunate megaripples occurs when the non-dimensional shear stress θ_{max} is on the order of 0.8–1. However, it is evident from field measurements (Davidson-Arnott and Greenwood 1976; Aagaard *et al.*, 2002; Swales *et al.*, 2006) that the appearance of lunate megaripples is also dependent on the presence of either strong asymmetry in the wave orbital motion and/or relatively strong unidirectional flows superimposed on the oscillatory motion. Thus, Aagaard *et al.* (2002) found that lunate megaripples disappeared at values of θ_{max} well above 1 when longshore current velocity decreased rather than as a function of increasing bed shear stress. As might be expected from unidirectional flows, the occurrence of lunate megaripples may also depend on the grain size of sediments making up the bed. They do not appear to develop in very fine sands and the sequence appears to go directly from ripples to plane bed (Clifton *et al.*, 1971; Davidson-Arnott and Pember, 1980; Doucette, 2000).

The variation in maximum orbital velocity, orbital diameter, wave skewness and Stokes drift under shoaling waves and into the breaker and surf zones produces fairly consistent and recognisable sequences of bedforms. On a planar beach subject to large swell waves, Clifton *et al.* (1971) recognised a distinct suite of bedforms associated with a single breaker zone (Figure 7.3a). Here the large waves typically result in the formation of asymmetric ripples in quite deep water. These are succeeded by a zone of lunate megaripples just seaward of the breaker zone and these in turn wash out to form a planar bed in and around the breaker zone. The inner rough zone consists of irregular holes and humps in the inner surf zone close to the step. Flow conditions here are often complex and visibility low, so it is difficult to define the bedforms well. Finally, the swash slope is characterised by planar bedding, often in alternating laminae of light and dark minerals. Clifton *et al.* (1971) did not note the presence of cross ripples but a subsequent review by Clifton (1976) included them in a zone just seaward of the lunate megaripples and they have been observed in a number of areas (Ship, 1984; Osborne and Vincent, 1993).

On a barred nearshore several breaker zones may occur and the sequence is a bit more complex (Davidson-Arnott and Greenwood, 1974, 1976; Ship, 1984; Greenwood and Mittler, 1985; Swales *et al.*, 2006 – see Figure 7.3b). As is the case in other sedimentary environments, migration of the bedforms and/or burial below the active surface produces distinct suites of sedimentary structures which can be used to identify the hydrodynamics of the depositional environment (Figure 7.3b). The sequence of ripples, lunate megaripples and plane bed noted by Clifton *et al.* (1971) can occur on the seaward slope and crest of each bar (Figure 7.4a, b). On the outer bars where the water depth over the crest is relatively deep the pattern down the landward slope is the reverse of the seaward slope as wave orbital motion decreases into the deeper water of the trough. In the trough itself both 2-D asymmetric ripples aligned with waves and 3-D ripples produced by longshore currents flowing in the trough may be present (Figure 7.4c). This zone is often associated with the accumulation of coarse sand, shell and organic material that may give rise to larger ripples and produces a distinctive colouration and sorting of these sediments.

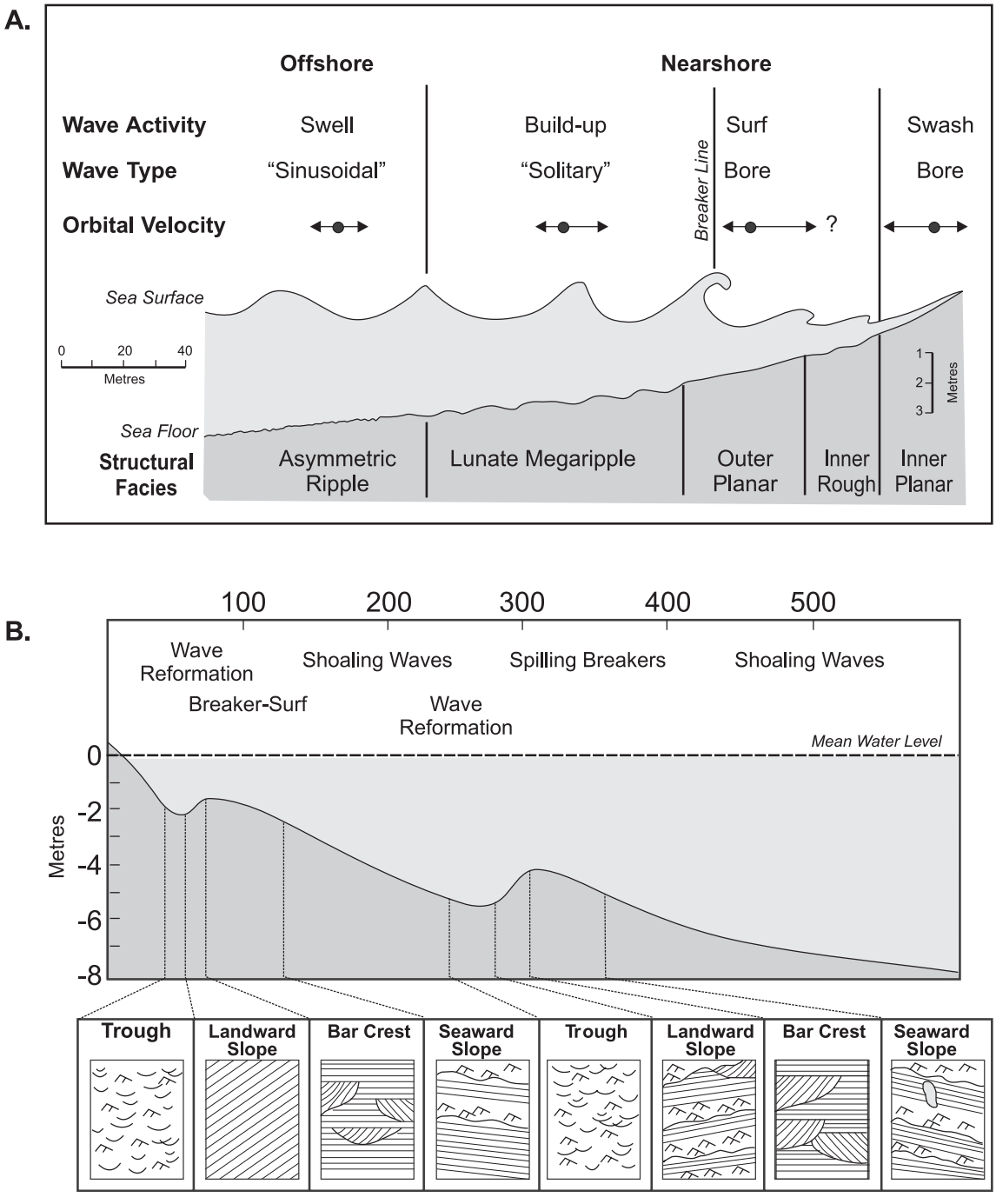

Figure 7.3 Hydrodynamics and bedform sequences in the nearshore: (A) sequence of bedforms under waves on a high energy, swell coast (Clifton *et al.*, 1971); (B) sequence of bedforms and sedimentary structures on a barred coastline (Davidson-Arnott and Greenwood, 1976).

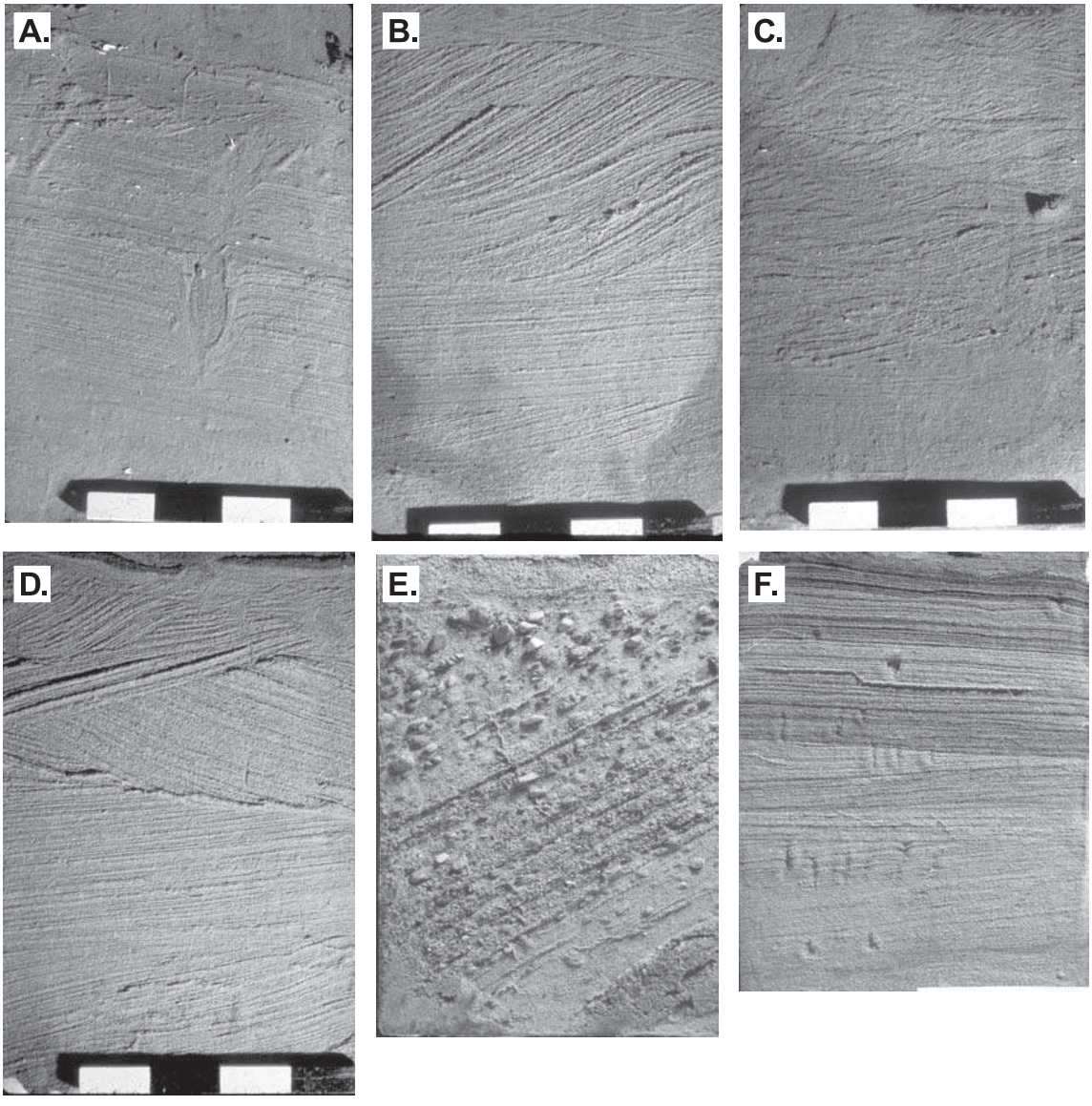

Figure 7.4 Photographs of resin peels taken from box cores showing the sedimentary structures formed by bedforms in the nearshore and foreshore. The cores were all oriented perpendicular to the shoreline with onshore to the left, and the bars on the scales are 5 cm: (A) alternating beds of ripple cross-lamination and planar bedding from the seaward slope of an outer bar in about 5 m water depth; (B) planar bedding and landward dipping cross-stratification produced by lunate megaripple migration on an outer bar crest in a water depth of 2.5 m. The black line is dyed sand placed on the surface prior to taking the core and the shape clearly marks a vortex ripple produced by low wave conditions; (C) ripple lamination in the trough landward of an outer bar. Sediments include shell hash washed over the bar crest and organic matter that accumulates in the trough under low wave conditions; (D) core taken on the crest near the centre of a crescentic outer bar showing offshore dipping cross-stratification produced by lunate megaripple migration in a zone of strong undertow or rip current activity; (E) landward-dipping cross stratification on the slip-face of an inner bar; (F) parallel lamination produced by swash and backwash on the beach foreshore.

Cores taken from the modern environment can also provide information on sediment transport modes and directions. Thus, early field evidence to support offshore flows across outer nearshore bars during storms came from identification of seaward-dipping cross-stratification produced by the offshore migration of lunate megaripples (Davidson-Arnott and Greenwood, 1976; Greenwood and Davidson-Arnott, 1979; Greenwood and Mittler, 1979; see Figure 7.4d). Where water depth over inner nearshore bars is very shallow (e.g., at low tide) wave bores produce nearly continuous sheet flow across the bar crest leading to the formation of an avalanche slope (Figure 7.4e) and landward migration of the bar (this process is described in detail in Chapter 8). Finally, shear sorting by the swash and backwash on the beach foreshore produces distinct planar lamination, often marked by alternating bands of dark and light minerals, parallel to the foreshore slope (Figure 7.4f).

7.2.4 Bed roughness and sediment suspension

In addition to the information they provide on flow conditions, especially in the interpretation of ancient sediments, the type of bedform present at any location in the zone of shoaling and breaking waves is an important determinant of the surface roughness and of the vertical and temporal variation in suspended sediment concentration. Thus the ability to predict the type of bedform present is crucial to the operation of models that are used to predict the flow field and resulting sediment transport under shoaling and breaking waves (Austin and Masselink, 2008).

Under nearly symmetric oscillatory flow where ripples are present (which they nearly always are), flow over the ripple crest produces two suspension events, one associated with the onshore flow and the other with the offshore flow (Inman and Bowen, 1963 – see Figure 7.5). As waves shoal and become more asymmetric, the offshore flow is suppressed and there tends to be a single peak in suspension. The height to which sand is suspended will vary with the intensity of the flows and wave period, and is much greater for flows over steep ripples with well-defined crests than for much lower, washed out ripples. In the latter case, the absence of a well-defined crest inhibits vortex formation and shedding (e.g., Osborne and Vincent, 1996; Doucette, 2000 – see Figure 7.6). Flows over the troughs of lunate megaripples can produce suspension clouds that extend much higher into the water column as a reflection of the greater turbulence across the trough. At higher flows, as the bed becomes planar, the bed roughness and bed shear stress decrease and the suspension events are much less pronounced. Under these conditions just outside the breaker zone the water column a few tens of centimetres above the bed may be quite clear but sediment concentration within a few cm of the bed becomes very large as sheet flow develops. Sand suspension in the water column then increases in the breaker and surf zones but this is largely due to turbulence advected downward from the breaking wave rather than flow across bedforms.

Ultimately simultaneous measurement of the velocity vector and suspended sediment concentration should enable determination of the net sediment transport rate. In a river an order of magnitude estimate can be done relatively simply by integrating the concentration over the stream depth and multiplying by the mean velocity. In the nearshore this is much more difficult because of the high frequency oscillatory motion, vertical variations in mean flow direction and because of the need to match rapidly varying concentrations with velocity asymmetries and with onshore/offshore velocity fluctuations over a range of frequencies from those of incident waves to low frequency motion generated by wave groups. We will examine this in more detail in the next section.

7.3 On–offshore sand transport

As we saw in the previous section, it is possible to determine the net shore normal movement of sediment in the inner nearshore and surf zones with instruments capable of measuring instantaneous water motion and suspended sediment concentration. The net transport at any elevation can be obtained from integrating the co-spectrum of velocity and sediment concentration which thus permits inclusion of all forms of water motion from the oscillatory component of waves,

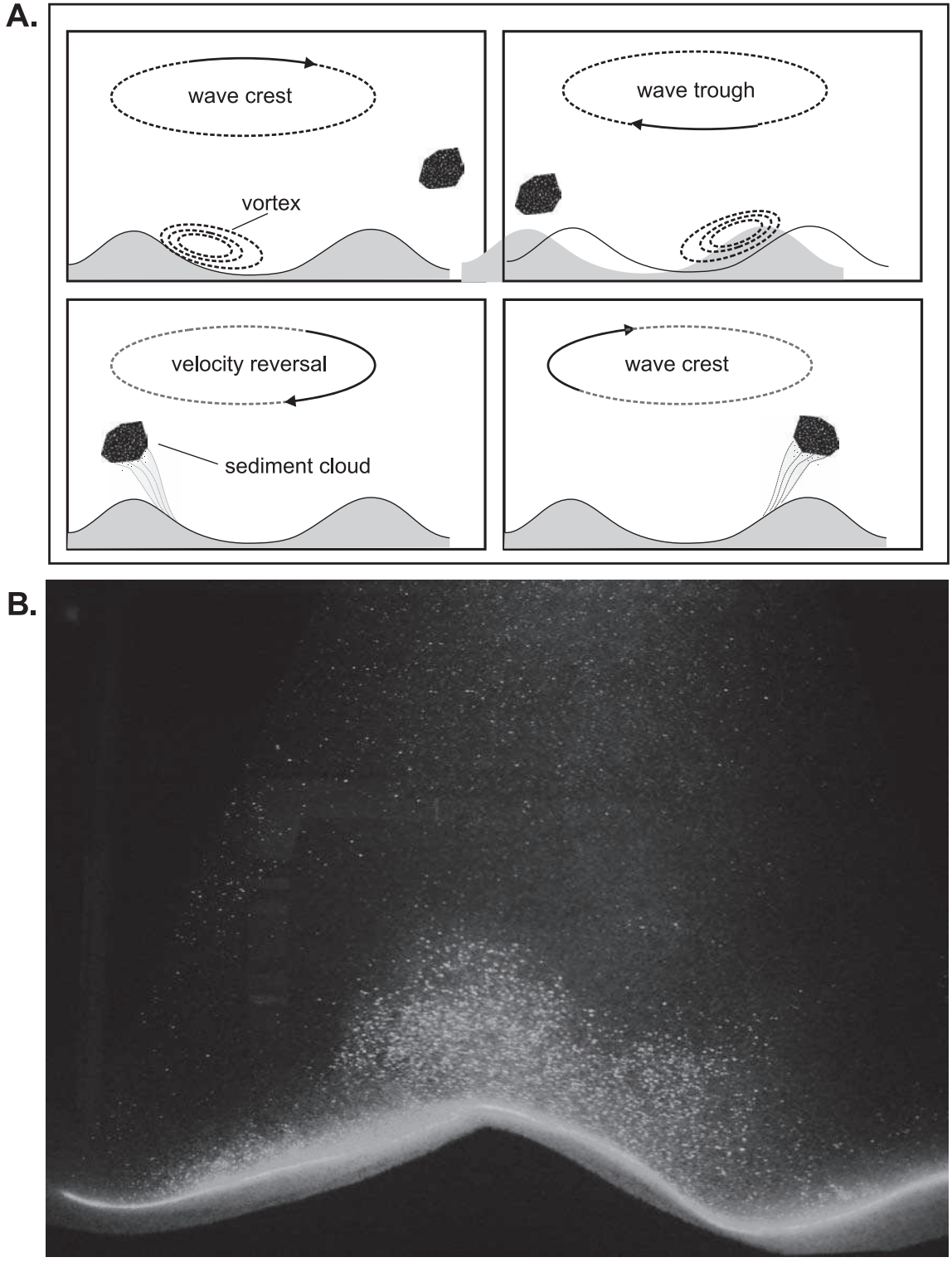

Figure 7.5 Flow over classic vortex ripples under symmetric oscillatory wave motion: (A) Schematic of vortices produced on either side of the ripple crest first due to shoreward motion under the crest and then to seaward flow under the trough. As the vortices are shed during the period of flow reversal they carry sand into suspension to a height two to three times the height of the ripple (after Inman and Bowen, 1963); (B) photograph of the plume lifting off the ripple crest in an oscillatory flume (photograph Jeff Doucette).

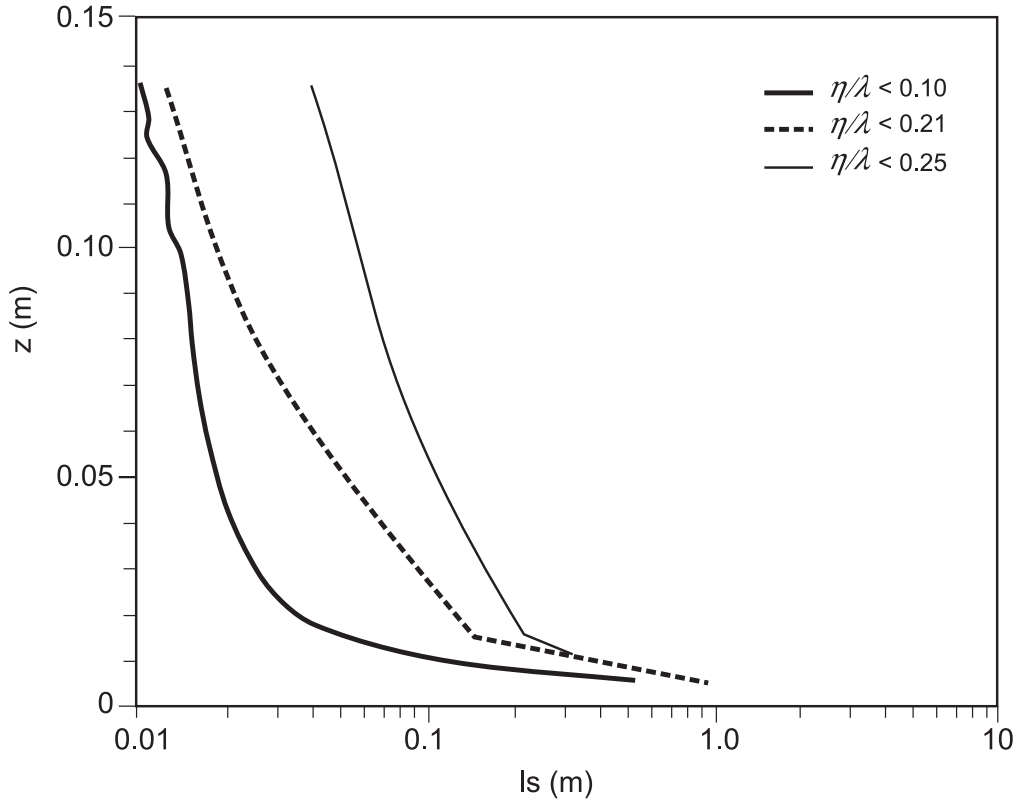

Figure 7.6 Spatially and temporally averaged sand concentration with elevation (z) above the bed over steep vortex ripples ($\tilde{\eta}\lambda = 0.25$), flat, transitional post-vortex ripples ($\tilde{\eta}\lambda < 0.1$) and steep, large-scale bedforms ($\tilde{\eta}\lambda = 0.21$) measured with an acoustic backscatter sensor (Osborne and Vincent, 1996).

to long waves, undertow and rip currents. Such an approach assumes that sediment moves at the same speed as the water. Because of the large number of instruments required to cover both vertical and horizontal variations, only a small number of such experiments have been carried out, and most of these only cover a portion of a profile normal to shore. On many beaches onshore and offshore transport tends towards an equilibrium or balance over a period of months or years, with offshore movement dominating during periods of intense storms, and onshore movement during non-storm conditions.

An important example of this is to consider the velocity profile for undertow produced by wave breaking and 2D return flow. Close to the bed the net flow is onshore but 10–20 cm above the bed the flow will be offshore and above the wave troughs it is likely to be onshore. Under low waves little sediment will reach high enough to be moved in the offshore direction and offshore flow speeds are low. Net transport is likely to be onshore because of the asymmetry or skewness in the strength of the oscillatory motion of shoaling waves and the small net drift velocity onshore (this may be complicated a bit by the presence of ripples but the effect is likely to enhance the onshore transport). This accords well with our general observation that, under low waves, sand tends to be moved onshore. As we increase wave action, sediment will reach higher into the water column and at the same time the strength of the undertow will increase. Initially only the total transport may increase, but eventually the higher concentration within the area influenced by the undertow will result in a change in the direction of net transport from onshore to offshore. This may be enhanced by

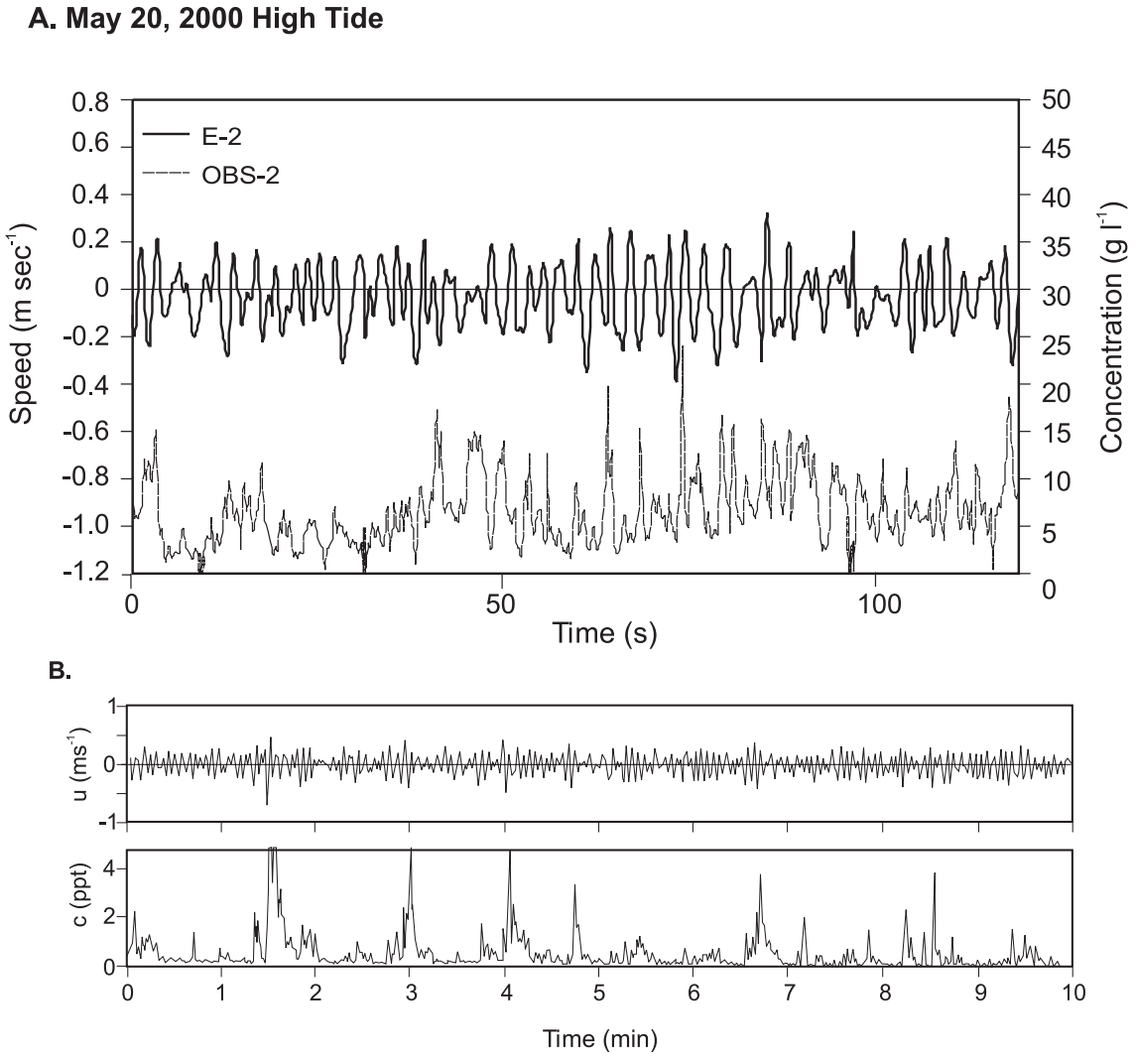

Figure 7.7 Time series of cross-shore velocity measured with an electromagnetic current meter and suspended sediment concentration measured with an OBS probe: (A) shoaling waves on the crest of an intertidal bar near high tide (Dawson *et al.*, 2002); (B) shoaling waves on a non-barred coast (Osborne and Greenwood, 1992). The instruments were located at an elevation of 0.1 m above the bed.

the effect of vortex generation by plunging breakers that will dramatically increase suspended sediment concentrations in the middle of the water column (Voulgaris and Collins, 2000). Again, this accords well with the general observation that, under high waves and onshore winds, net sand transport is offshore.

7.3.1 Suspended sediment concentration

In the field, much of the data on suspended sediment concentrations in the nearshore and surf zone has come from the deployment of electromagnetic current meters co-located with optical backscaterrance probes (OBS) (Downing *et al.*, 1981; Beach and Sternberg, 1988). Data from the on–offshore component of a current meter and OBS deployed at Linden Beach, Nova Scotia over an intertidal bar (Dawson *et al.*, 2002) provide an example of suspension under shoaling waves near the break point (Figure 7.7a). The small-scale fluctuations in concentration reflect the passage of individual waves over a rippled

bed. Major episodes of suspension are produced by groups of larger waves which 'pump' sediment up into the water column over several wave periods. Similar episodes (Figure 7.7b), can be seen for shoaling waves on a non-barred beach (Osborne and Greenwood, 1992). Larger suspension events also reflect the nature of the bed with higher concentration associated with flows over dunes or lunate megaripples (Hay and Bowen, 1994; Green and Black, 1999).

In practice, while mean flows are important in the nearshore and surf zone, the direction of net transport will also be influenced by oscillatory motion in both the wind wave frequency and infragravity frequencies as well as by mean flows. It is thus necessary to separate the flux at each elevation due to each of these components in the frequency spectrum. This is not a trivial task since it requires measurement of flow and concentration at a minimum of three heights above the bed and of course spatially across the profile. Results of a number of studies over nearshore bars have shown that transport at wind wave frequencies tend to be offshore during a storm while those at infragravity frequencies tend to be onshore (Figures 7.8a, b). The net transport then depends on the addition of these and that due to mean currents (Figure 7.9). There is some indication that mean flows may be more significant in the breaker and surf zones (e.g., Aagaard *et al.*, 1998) and less significant in the nearshore, seaward of the breaker zone (Ruessink *et al.*, 1998).

Clearly the ability to predict time-averaged suspended sediment concentration with height above the bed is important to developing predictions of cross-shore sediment transport. There are a number of approaches to predicting this that generally involve specifying a reference concentration close to the bed and then the distribution of sediment concentration with height above the bed. Where bedforms are present the concentration profile is exponential and can be predicted by (Nielsen, 1986)

$$C(z) = C_{ref} \exp\left(\frac{-z}{L}\right) \tag{7.6}$$

where $C(z)$ is the mean concentration at height z above the bed; C_{ref} is the reference concentration just above the bed; and L is a mixing length.

Field measurements confirm the general approach as well as the critical role of bedforms in determining the upward diffusion of sediment and the reference concentration (Green and Black, 1999; Webb and Vincent, 1999).

7.3.2 Sediment transport modelling

A major focus of research on nearshore processes is on the development and testing of models designed to predict cross-shore sediment transport rates under waves and currents. In turn, they can be used to predict morphological change in response to some modelled event or events (e.g., Schoonees and Theron (1995). Some, such as SBEACH (Larson and Kraus, 1989), are used routinely in coastal engineering modelling; while others, such as the model described by Baillard (1981) have been applied extensively to test results from field experiments (Ruessink *et al.*, 1998; Masselink *et al.*, 2008). The models can be tested at two time scales: (1) against measurements of incident waves, currents and sediment transport measured at a number of points along a profile. This tests the predicted gradients in sediment transport from which changes in the nearshore morphology can be predicted; (2) against measured morphological change between the beginning and end of an event. While the latter is fairly simple to carry out, in practice it is necessary to measure the former in order to determine whether the modelled mechanisms in fact agree with the measurements. None of this is easy or cheap. It requires the deployment of large numbers of instruments in a physically demanding environment. Measurements in the inner shoreface seaward of the breaker zone are a bit easier on instrumentation because of the less energetic conditions near the bed (Ruessink *et al.*, 1998) but require more effort to install and retrieve the instruments. It is logistically much easier to install instruments in the intertidal zone (Houser *et al.*, 2006; Masselink *et al.*, 2008) and to carry out intermediate surveys of profile changes but physical conditions are not favourable for the instrumentation. In the breaker and surf zones, especially under very energetic conditions where the surf zone may be several hundred metres wide satisfactory testing can only be

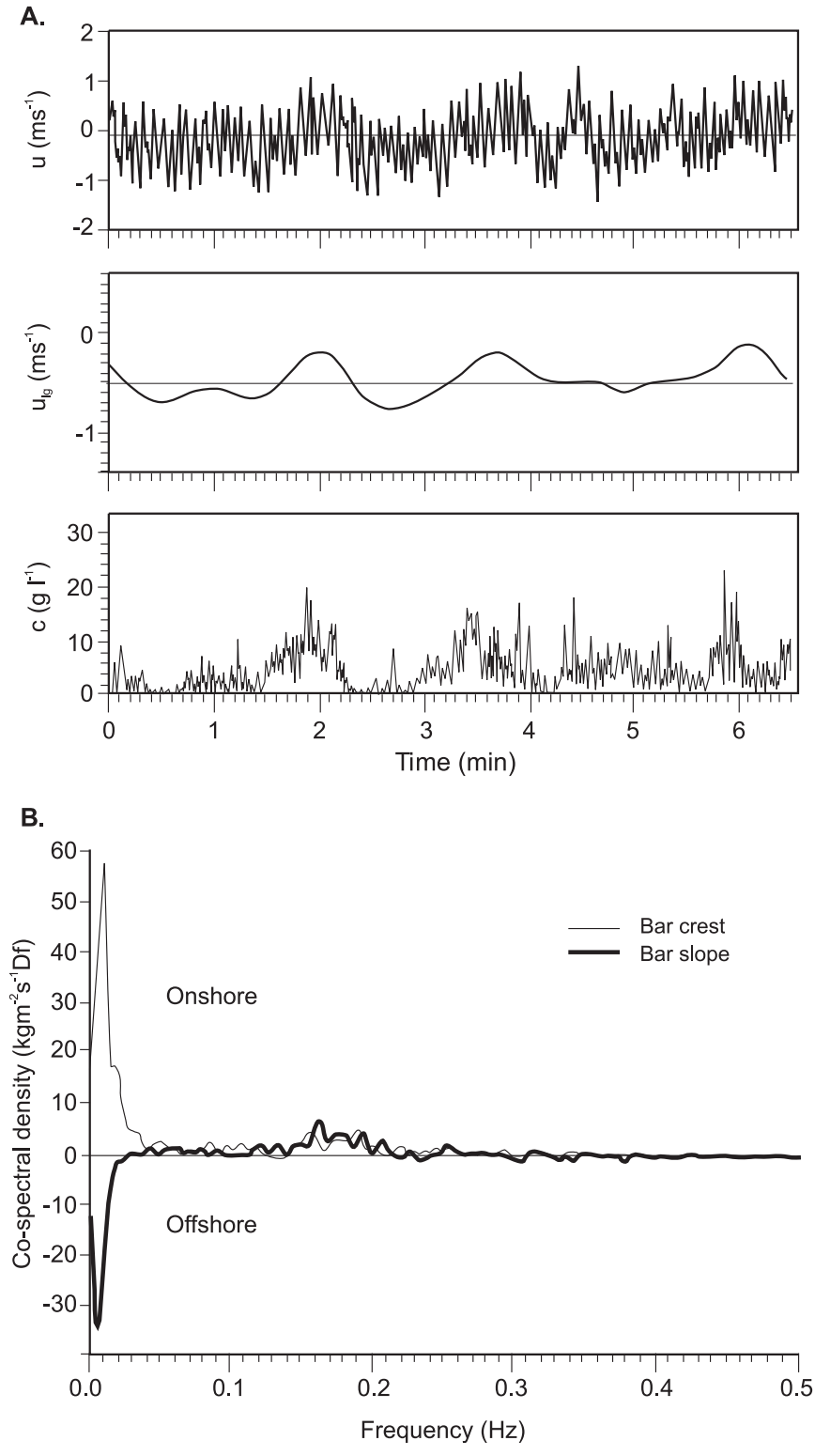

Figure 7.8 Frequency of water motion and cross-shore sediment transport. (A) Time series of cross-shore velocity *u*, low pass velocity u_{ig} and sediment concentration (at $z = 0.5$ m) on a dissipative beach. Concentration maxima are in phase with the onshore stroke of the infragravity waves (after Aagaard and Greenwood, 1995). (B) Reversals of sediment flux with infragravity waves on a dissipative beach – the flux is directed offshore over the lakeward bar slope and shoreward on the bar crest (Aagaard and Greenwood, 1995).

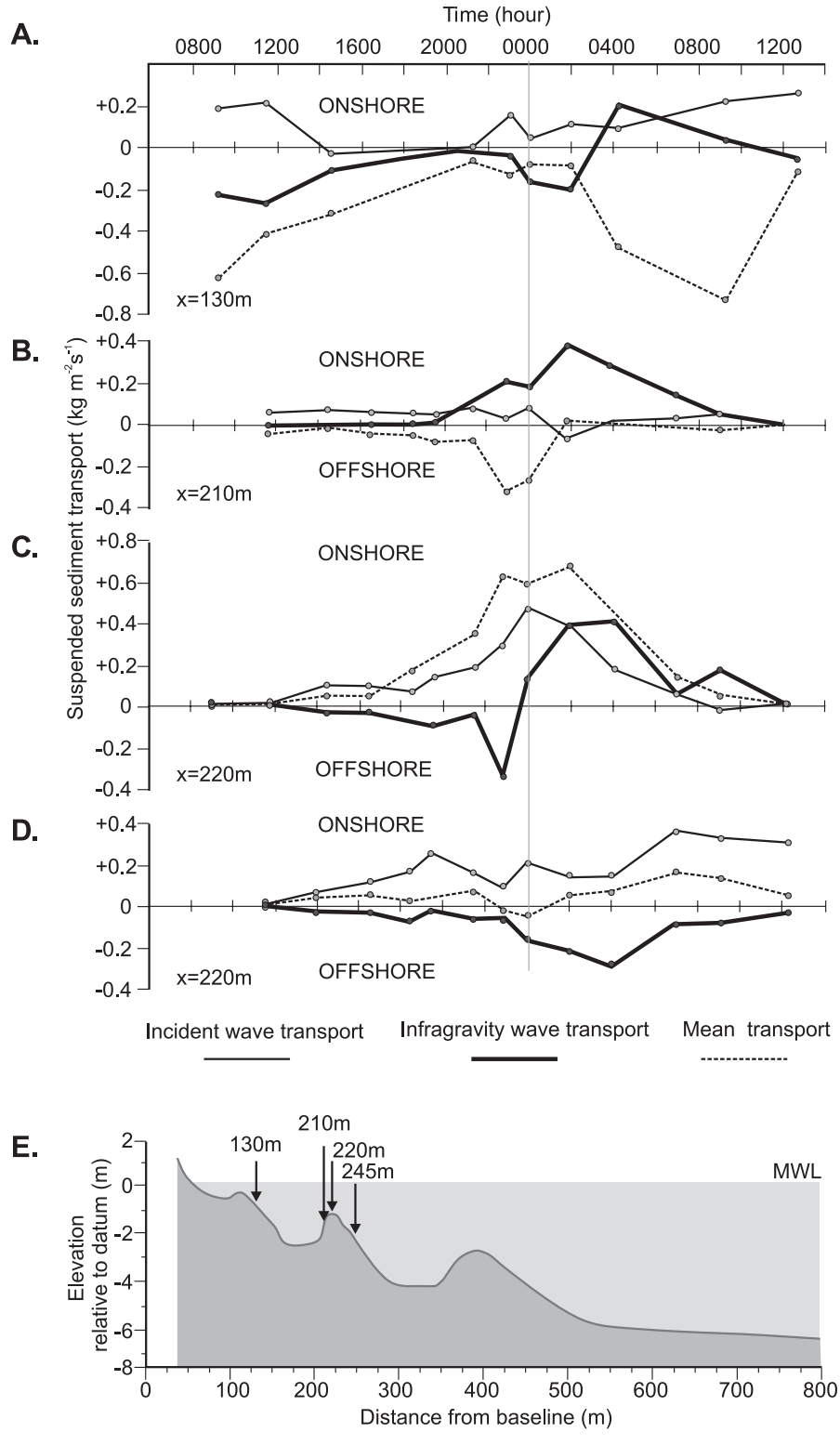

Figure 7.9 Cross-shore sediment flux measured at four locations on an intermediate beach during a moderate storm: (A) 130 m offshore; (B) 210 m offshore; (C) 220 m; (D) 240 m offshore. The profile form and location of the measurement stations is shown in (E). At each station the contribution to total sediment transport is shown separately for incident waves, infragravity waves and mean flows (Aagaard and Greenwood, 1994).

carried out where there are facilities such as the fixed pier at the Coastal Engineering Research Facility at Duck, North Carolina (Gallagher *et al.*, 1998).

The energetics approach proposed by Bagnold (1963, 1966) has provided a basis for much of the modelling of alongshore and on–offshore sand transport. In this approach sand movement is initiated by oscillatory wave motion, with the amount of sand moving being proportional to the local rate of energy dissipation. While this produces no net movement, any unidirectional current superimposed on the oscillatory motion would result in sand transport in the direction of the current. In applying this concept to on-offshore sediment transport Bowen (1980) examined in detail the factors controlling both bed load and suspended load transport and considered explicitly lags between fluid flows and sediment response as well initiation of sediment motion. Bowen's model suggests that the relative importance of bed load versus suspended load transport is a function of the orbital velocity magnitude divided by the sediment fall velocity – i.e., that suspended load is more important for energetic conditions and for finer sediments. Baillard (1981) adopted a similar approach to Bowen and the Baillard model has subsequently been tested in a number of field experiments (Gallagher *et al.*, 1998; Masselink *et al.*, 2008) and has been modified and applied to field and laboratory data or for use in numerical models (Nairn and Southgate, 1993).

There are now a number of numerical models readily available for use by scientists and engineers that run on desk top computers that can be used to predict nearshore sediment transport and profile evolution. Several are used routinely in engineering applications. How good are the models? It is difficult to say because it is not easy to test them adequately either in the laboratory or in the field. In the laboratory there are scaling issues and, even with very large and long tanks (100 m or more), the 2D nature of the processes is a restriction. In the field the number of data sets that provide sufficient data to test the models thoroughly is small and they have been obtained at only a few sites (e.g., the CERF facility) so the significance of local factors is difficult to judge. Application of the models to predict coastal change is somewhat of an art and it usually requires some sensible interpretation and verification as well as awareness of the limits and restrictions.

7.4 Longshore sand transport

Longshore sediment transport in the beach and nearshore zone results from the operation of three sets of processes: (a) beach drifting on the swash slope which is driven primarily by oblique wave action; (b) transport by wave-generated longshore currents in, and just seaward of the surf zone; and (c) transport seaward of the breaker zone by residual tidal currents and wind-driven currents. Within the breaker and surf zone wind-driven currents and tidal currents may also contribute to longshore transport but they are generally thought to be of lesser importance than those due to waves in this relatively shallow area.

Longshore sediment transport is extremely important on most coastlines. Locally it is important in the removal of sediment from the base of bluffs and cliffs, thus promoting further erosion and cliff retreat, and from river mouths and deltas. The sand and gravel component of this sediment is then transported alongshore to create beach and dune systems and large depositional features such as spits, baymouth barriers and barrier islands. The direction of net longshore sediment transport on a stretch of coastline may be manifested from natural features such as those noted above, and by the accumulation of sediment behind obstacles such as harbour breakwalls and groynes. Interference with the natural longshore sediment transport is the cause of many human-induced problems involving locally enhanced erosion and sedimentation and is critical to the evaluation of many coastal engineering works. Longshore sediment transport is also a key factor in determining local beach sediment budgets and in the definition of littoral cells – these will be described later in the chapter.

We will begin with a description of the actual processes that give rise to longshore sediment transport and the relation of these to beach and nearshore form on the one hand and to the

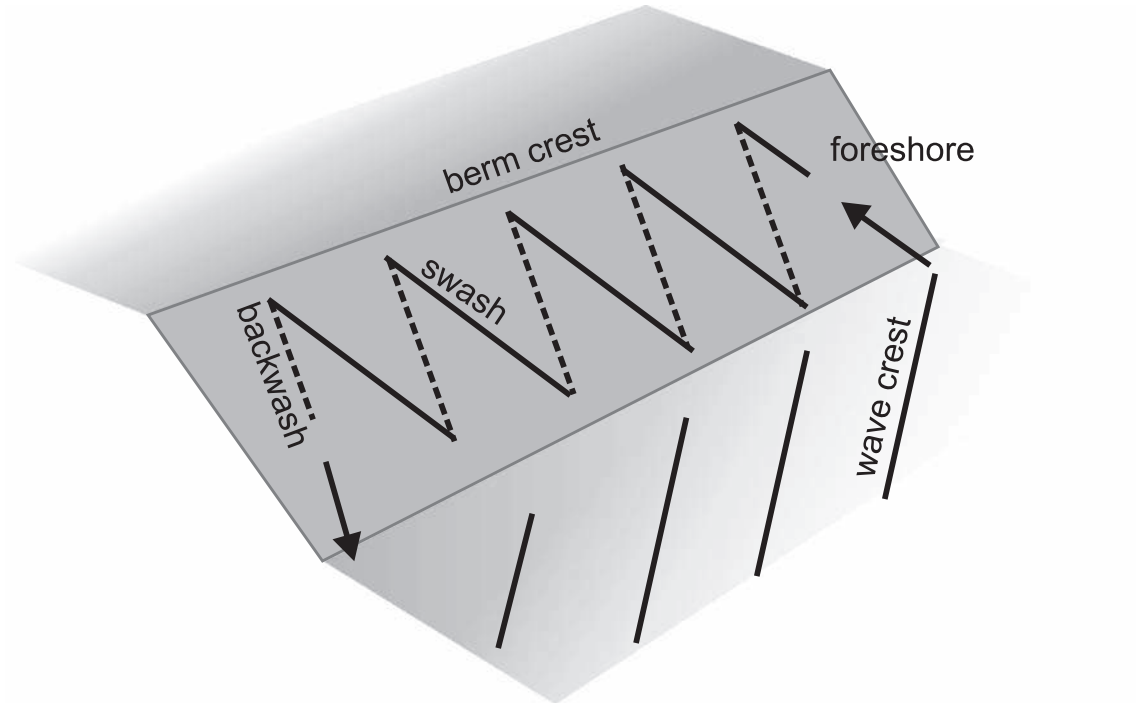

Figure 7.10 Beach drifting – schematic of the process of longshore transport on the swash slope. Swash run-up occurs perpendicular to the wave crest while return flow in the backwash occurs parallel to the beach slope producing a saw-tooth alongshore motion.

complexities of fluid motion in the nearshore and beach zones. This will be followed by a description of the techniques used to measure longshore sediment transport both instantaneously and net transport over periods of months to years and decades. Finally, modelling approaches to prediction of longshore transport on these two temporal scales will be examined as well as limitations of the data on which the models are based.

7.4.1 Processes of longshore sediment transport

Beach drifting

Beach drifting results from wave run-up on the beach foreshore (swash slope) where waves approach at an oblique angle to the local beach orientation. The swash (run-up) occurs at the angle of wave approach, but the return flow in the backwash is influenced primarily by gravity, and thus tends to return straight down the slope. Sediment entrained by waves is transported in the direction of wave advance in a series of saw tooth motions (Figure 7.10). Where the swash slope is steep and a substantial fraction of the swash does not infiltrate into the bed, some of the alongshore momentum in the wave uprush may carry over to the backwash so that some alongshore movement occurs during this phase as well, with the result that the transport rate is enhanced. The process is easily observed on sandy beaches with a steep foreshore slope under moderate wave conditions. The relative importance of beach drifting compared to transport in the surf zone in the total volume of sediment moved will vary considerably from beach to beach and also temporally at many beaches depending on wave conditions and beach form. Gravel and cobble beaches nearly always have a steep foreshore, with relatively deep water near the base so that wave breaking occurs on the foreshore and there is rarely an extensive surf zone. As a result, beach drifting makes up a substantial fraction of the total transport and often it is the dominant process. On medium-to-coarse

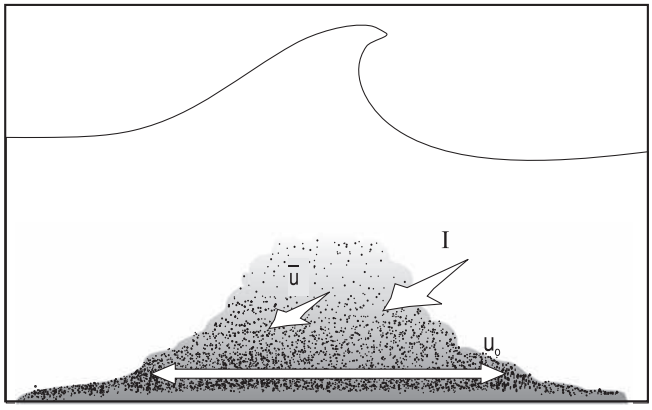

Figure 7.11 Surf zone transport – the process of longshore transport seaward of the swash slope. Sediment is set in motion by wave oscillatory motion (U_o) and by turbulent vortices generated by wave breaking and is then transported alongshore by longshore currents ($\overline{U_1}$) generated by waves, winds or tides (Komar, 1998).

sandy beaches the relative significance will vary with the form of the foreshore and wave conditions. Where a steep foreshore and berm are present, beach drifting will be significant under low-wave conditions where wave breaking takes place primarily at the beach and there is limited surf zone development. However, under high-wave conditions, waves break some distance offshore producing a wide, dissipative surf zone where most of the longshore sediment transport occurs. As we will see in Chapter 8, the swash slope is flattened by wave action under these conditions, thus reducing the effectiveness of gravity on the backwash, and the swash zone accounts for only a small portion of the profile over which longshore sediment transport takes place. On fine-sand beaches steepening of the profile through berm development is rare and thus beach drifting is of limited significance.

Surf zone transport

In the nearshore zone, in contrast to the swash slope, offshore motion under the wave trough is in a direction opposite to that of the wave advance and thus, ideally, there is no net longshore transport due to the wave oscillatory motion. However, as we saw in Chapter 6, longshore currents are generated in the surf zone by waves breaking at an angle to the shoreline. Sand will be set in motion close to the bed by oscillatory currents moving across ripples and dunes, and may be lifted well off the bed in areas of high turbulence and vorticity especially under plunging breakers. As a result sand will be carried alongshore with the current at a rate that will be some fraction of the mean speed of the current (Figure 7.11).

The longshore current may be continuous and relatively simple spatially on a planar beach but, as we saw in Chapter 6, where nearshore bars are present there will be more than one line of breakers in the offshore direction and alongshore the flow pattern may be disturbed by rip cells and by rip channels and nearshore bar topography so that sand moves obliquely offshore and onshore in a complex motion (Figure 7.12). Measurement and prediction of the transport rate are much more difficult under these conditions because of the need to determine the vertical suspended sediment concentration, the vertical variation in longshore current speed and the spatial pattern of currents. Nevertheless, conceptually, the same basic principles apply as for the simple case and we should be able to predict the total longshore transport as a product of the instantaneous velocity and sediment concentration through the breaker and surf zones.

Some longshore transport takes place in the zone of shoaling waves seaward of the breaker zone. There will be some small contribution from waves close to the breaker line, but further offshore it is likely to result from the effect of winds and tidal currents, with wave orbital motion still providing the driving force for initiation of motion.

Instantaneous versus annual rates

At any instant in time the direction and rate of longshore sediment transport (q_l) will depend on the incident wave and wind conditions,

Figure 7.12 Photograph of the surf zone at Greenwich Dunes during a strong northeaster. Wave breaking is taking place over three bars and troughs with a complex inner topography that includes rip channels and oblique bars. The surf zone is about 400 m wide and under these conditions beach drifting in the swash zone is of minor significance compared to transport in the surf zone.

particularly the direction of wave approach relative to the shoreline orientation. However, if we are interested in shoreline evolution due to erosion and sedimentation, it is the average annual total sediment transport and in particular the direction of the net or resultant transport that is probably the most crucial. The gross littoral sediment transport along a section of coast is a summation of the instantaneous volumes over the period of a year without regard to the actual direction of transport. In turn it can be subdivided into the sum of transports in one direction (to the right) and in the opposite direction (to the left). The gross littoral sediment transport Q_G is thus given by

$$Q_G = Q_L + Q_R \tag{7.7}$$

where Q_L and Q_R are the total longshore transport to the left and right respectively over a year.

Similarly, we can define the net sediment transport on an annual basis Q_N as the difference between the two transport volumes:

$$Q_N = Q_L - Q_R. \tag{7.8}$$

It is thus possible to have very high gross transport rates with very low net rates, if the frequency and magnitude of wave approach about shore normal are nearly equal. The net sediment transport is thus controlled by the magnitude and a frequency of waves from all directions, and is a function of the overall wave climate and the local orientation of the shoreline.

As we will see in the following sections, actual measurement of longshore sediment transport rates and directions is difficult and expensive, but there are a number of indicators that can be used to determine the direction of Q_N and these often give an order of magnitude indication of the quantity of this. These indicators can be associated with either natural or artificial features of the coastline (Figure 7.13a). The most obvious indicators reflect the effects of artificial structures such as groynes, jetties and harbours or natural features such as headlands which act to block alongshore transport and result in the impoundment of sediment on the updrift side of the structure or headland (Figure 7.13b). The

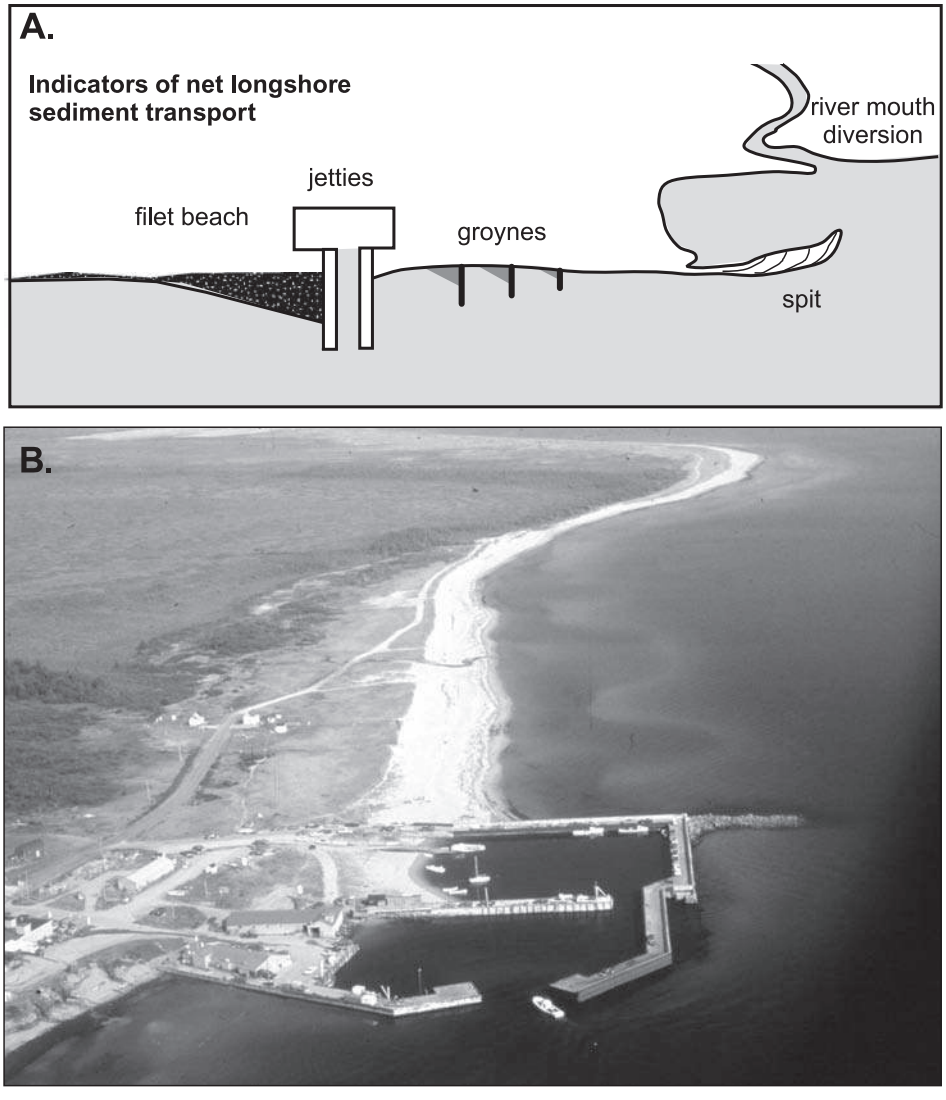

Figure 7.13 Indicators of net longshore sediment transport on the coast: (A) sketch of natural and artificial indicators; (B) photograph of accumulation of sediment on the updrift side of a harbour breakwall.

result is a large increase in beach width on the updrift side of the structure and a decrease in beach width and or enhanced erosion on the downdrift side leading to a pronounced offset of the coast. Similarly, net transport in one direction can lead to diversion of the mouths of small streams where they enter a lake or ocean (Figure 7.13a). On continuous sandy shorelines the beach width may increase in the direction of net sediment transport, accompanied by increasing height and width of the dune field landward of the beach. Barrier spits, and particularly flying spits (see Chapter 10 for definition) are depositional features resulting from longshore transport and thus the orientation of the feature itself is an indicator of the net drift. On barrier island coasts the ebb tidal delta on the seaward side of inlets separating the barrier islands tends to be skewed downdrift as wave action tends to move sediment into the inlet channel deflecting the current emerging from the inlet on the ebb tide in the direction of net drift.

7.4.2 Measurement of longshore sediment transport

Measurement of actual rates of sediment transport are usually carried out either to obtain values for a specific section of coastline, or to test or derive some form of equation that can be used to predict rates of sediment transport. Usually the experiments are designed to measure either the instantaneous transport rate, or to determine the net transport rate over a fairly lengthy period – months or years. In addition to the simultaneous measurement of suspended sediment concentration and current flow, described in Section 7.3 for on-offshore sediment transport, the techniques most commonly used include: (1) measurements in wave tanks; (2) the injection and recovery of some suitably tagged sediment – tracer studies; (3) measurement of the rate of accumulation behind a barrier such as an impermeable jetty or on a depositional feature such as a spit.

Wave tanks

Early attempts to predict sediment transport rates were based largely on data from small-scale three-dimensional wave tank studies (e.g., Saville, 1950). However, a number of researchers have pointed out the many scaling difficulties associated with these studies, and most of the early work has now been rejected (Komar and Inman, 1970). More recent work has included a number of experiments carried out by Kamphuis and some of his students at Queens University in Ontario (Kamphuis *et al.*, 1986; Kamphuis, 1991). The results of these tests did provide support for the inclusion of wave steepness or a breaker index in a predictive equation because of increased suspended sediment concentrations under plunging breakers. However, despite the valiant efforts at Queen's to obtain a scaling parameter between laboratory and field conditions, all small-scale wave tank data should be treated cautiously.

Tracers

Most attempts to measure instantaneous rates of sediment transport in the field have utilised some form of sediment tracer. Essentially this consists of monitoring the movement of suitably tagged particles of sediment. The two most common techniques used are: (1) to coat the grains with some form of fluorescent dye which is readily distinguishable under ultra violet light; and (2) to tag it with a radioactive isotope which has a short half-life. Useful reviews of the techniques are to be found in Madsen (1987) and Ciavola (2004). There are a number of logistical, practical and theoretical problems with all tracer studies.

Two types of experimental approach can be utilised. The Lagrangian approach involves measuring the advection rate of the tracer cloud (centroid velocity), by taking samples at suitable intervals from a large number of grid points, determining the tracer concentrations at each point for each sample set, and then measuring the distance travelled by the tracer cloud from one sample time to the next (Silva *et al.*, 2007). The Eulerian approach involves measuring the tracer concentration at a fixed point in the system at frequent intervals, integrating this over time, and dividing this integral into the mass of tracer injected (Duane and James, 1980). The tracer can either be injected once or a continuous injection can be undertaken with the measurements downdrift focusing on determining a constant rate at the sampling point or points.

Traps

Bedload sediment traps similar to those used in rivers do not work well in the surf zone because of the difficulty of separating net sediment transport from the oscillatory motion under waves and because of the effects of trap scour. Recently, attempts have been made to measure net longshore transport of suspended sediment using streamer traps (Kraus, 1987; Rosati *et al.*, 1991) and they have now been used in a number of studies under relatively low wave energies. The traps consist of series of polyester mesh bags a metre or more in length that are attached to a rigid rectangular frame that forms the opening to the trap (Figure 7.14). These are deployed in a vertical array on a tubular frame that is designed to be carried into the water. In the water they are oriented into the direction of

Box 7.1 | Measurements using tracers

Fluorescent tracer studies usually involve coating volumes of sediment taken from the experimental site with a fluorescent dye or ink which is mixed with an adhesive to make it bond to the particles. Care has to taken to avoid changing the dynamic behaviour of the particles (e.g., by having too thick a coating, or when particles are not properly disaggregated after the coating process) and so the sand is usually mixed and dried in a cement mixer in order to keep the particles separate (Silva *et al*., 2007). During the experiment, the dyed sand is injected (placed) in the surf zone and swash slope, and its movement is determined by sampling at pre-determined times and/or locations. The samples are later spread out on a surface and examined under ultraviolet light in a dark room. The tagged grains can then be readily identified and counted.

There are practical problems in collecting samples in the surf zone under breaking waves, and it is obviously impractical to carry this out over the whole surf zone under conditions such as those shown in Figure 7.12. It is also necessary to collect a core sample at each location in order to account for the depth of mixing resulting from the migration of bedforms and to sample only from this active layer (Ciavola *et al*., 1997). Thus, the usefulness of one of the pioneering studies of surf zone sediment transport (Ingle, 1966) which sampled only the surface sediments using Vaseline coated cards is extremely doubtful, though the general patterns he observed are still of some value. The problems and logistics involved in carrying out a successful tracer experiment are exemplified in the work of Duane and James (1980) and Inman *et al*. (1980).

The analysis of the samples is extremely tedious, and efforts to measure concentrations indirectly by dissolving the fluorescent coating and analysing this chemically have not proved successful. A better approach is likely to photograph the samples and to use an automated counting system to identify the fluorescing particles.

Tagging sediment with radio-isotopes is a more difficult operation and the use of radioactive tracers requires more careful handling. However, the detection of sediment concentrations is more easily accomplished, since there is no need to obtain actual samples. Instead, gamma radiation emitted by the tagged grains is recorded using a scintillometer which is traversed across the bed, with the count rate giving sediment concentration at that point. The technique can thus record the presence of buried grains, and can be used to define concentrations and the extent of the tracer cloud more precisely by carrying out a number of traverses. Although the technique has been used successfully in several studies (Heathershaw and Carr, 1977; Gillie, 1985), getting permission to carry out a study using radioactive materials is problematic now.

longshore current flow for a period of a few minutes. The mesh bags stream backward from the opening and permit water to flow through while retaining sand. The amount of sediment trapped decreases exponentially with distance above the bed as we would expect (Rosati *et al*., 1991; Tonk and Masselink, 2005) and the amount trapped is not widely out of line with measurements using co-located OBS probes and current meters. Streamer traps provide a comforting demonstration that sand is moving but, as Tonk and Masselink note, it is difficult to deploy them under energetic wave conditions, they require a lot of labour, and they sample for only a few minutes. Given this, it would seem better to focus on the deployment of

Figure 7.14 Photograph of a streamer trap. The fine mesh bag is attached to a rectangular frame which keeps it open. Several of these are fixed to a vertical post for deployment in the water.

instruments measuring suspended sediment concentration and currents simultaneously.

Rates of accumulation

Net sediment transport along a stretch of coast can frequently be estimated by measuring long-term accretion on spits, or behind barriers such as harbour breakwalls which act as a complete sediment trap (or nearly so). Similar short-term studies in conjunction with measurement of wave data have been used to verify predictive equations based on the longshore component of wave power (Watts, 1953; Bruno *et al.*, 1980; Dean *et al.*, 1982). In this case topographic surveys upstream of the obstruction are carried out frequently in order to permit comparison with measured wave data over a period of weeks to months. Data from dredging of channels, inlets and for sediment bypassing can also be utilised.

Measurement of longshore transport over a period of hours to days has also been carried out by short-term impoundment (Bodge and Dean, 1987; Wang *et al.*, 1998) This involves the construction of a temporary groyne extending across the beach into the inner nearshore using, for example, a flexible mesh tube that is filled with sand or constructing a groyne with materials such as vertical steel posts and plywood. The area updrift is surveyed repeatedly simultaneously with measurements of waves and longshore currents. The approach provides a good estimate of the total transport in the swash zone and close to shore under small wave conditions. Under large-wave conditions, especially on gently sloping beaches, increasing amounts are transported seaward of the temporary structure.

Quality of field data

In order to test the accuracy and reliability of formulae and numerical models used to predict longshore sediment transport it is necessary to have field data collected under a range of wind and wave conditions and beach and nearshore morphologies (Schoonees and Theron, 1995; Bayram *et al.*, 2007). These comparisons also allow for the calibration of model constants and an assessment of the conditions under which the model or formula is most applicable. It is evident from the description of the measurement techniques that this is not a trivial task. There are relatively few good data sets and they cover neither the full range of sandy beach morphologies nor the range of transport conditions. Tracer and short-term impoundment probably provide the best measure of transport rates but most studies have been carried out under low to moderate energy wave conditions and in close to the shoreline. Measurements using current meters and OBS probes can provide data on wide surf zones and under quite energetic conditions (e.g., Miller, 1999), but they often have limitations due to the small number of instruments deployed. These measurements may also be of limited usefulness because they do not provide a good measure of transport close to the bed, which may account for perhaps as much as two-thirds of the total transport (Tonk and Masselink, 2005). OBS data are quite sensitive to the presence of small amounts of suspended sediment in the water column and to variations in grain size. It is usually necessary to calibrate the OBS in the lab against sediment taken from the study site, though it may be possible to calibrate them in situ using a laser particle size analyser (Rogers and Ravens, 2008). Until recently there were very few studies that combined a good tracer experiment and adequate determination of actual rates, with suitable measurements of the process variables, and this is why

there is so little good field data to test theoretical and empirical predictions of instantaneous transport rates. Komar's data on Silver Strand and El Moreno beaches (Komar and Inman, 1970) set the standard for this type of tracer experiment, and these results have been used extensively, despite some limitations on their applicability, particularly to beaches with relatively gentle slopes and a wide surf zone.

7.4.3 Prediction of longshore sediment transport rates

Although progress is being made in the development of numerical models that attempt to simulate all the major controls on sediment transport, the most widely used approach to the prediction of longshore sediment transport rates is a semi-empirical black-box approach in which sediment transport rates are correlated with the longshore component of wave energy flux, P_L:

$$P_L = (ECn)_b \sin \alpha_b \cos \alpha_b \tag{7.9}$$

where $(ECn)_b$ is the total wave energy flux evaluated at the break point and α_b is the angle the breaking wave crests make with the shoreline.

Early versions of the predictive formula given in the Shore Protection Manual were used to predict volume transport rates, and thus had dimensional constants. Komar and Inman (1970) based on earlier work of Inman and Bagnold (1963) showed that a better approach was to predict the immersed weight transport rate I_L since this could be related to P_L by a simple dimensionless coefficient

$$I_L = KP_L \tag{7.10}$$

where K is an empirical constant.

The immersed weight of transport can be related to a volume transport Q_L by

$$I_L = (\rho_s - \rho) g a' Q_L \tag{7.11}$$

where ρ_s and ρ are the sediment and fluid densities respectively; g is the gravitational constant and a' is a correction factor for the pore space of sand (approximately 0.6 for medium sand).

Komar and Inman (1970) used the results of the tracer studies carried out by Komar together with several earlier field studies to derive the relationship $I_L = 0.77\ P_L$ (see Figure 7.15). Note that all the wave tank data plot below the regression line, which is based only on the field data. The computations of energy used here are based on H_{rms} – for energy calculations using H_s, K should be divided by 2. The value of 0.77 for K has been used widely for predicting volumes of longshore sediment transport, particularly on an annual basis though Komar (1998) has subsequently suggested a value of 0.7 based on evaluation of more recent field data. It should be treated with some caution because it is based on so little data. More recent measurements have suggested that it is probably at the low end of the scale for sand beaches, in part because values derived from accumulation behind jetties give higher values than tracer studies (Bruno *et al.*, 1980). Probably the best data on accretion behind a breakwater come from measurements at Santa Barbara, California, conducted during the National Sediment Transport Study (Dean *et al.*, 1982). They found an average value of 1.23 for K. Rosati *et al.*, in a new compilation of field data, suggest a value for K of 0.92.

Inman and Bagnold (1963) also relate I_L to the mean longshore current velocity and maximum wave orbital motion:

$$I_L = K' (ECn)_b \cos \alpha_b \frac{V_L}{u_m} \tag{7.12}$$

where $\overline{V}_L$ is the mean longshore current velocity, u_m is the maximum orbital velocity at the breaker line, and K' is a dimensionless coefficient.

Equation (7.12) provides a measure of the mean stress exerted by the waves which are assumed to act to keep the sediment in motion with the transport rate then being proportional to the mean longshore current. Komar (1998) assigns a value of 0.25 to K'.

There is obviously a need for further field studies to improve the data base on which these empirical relationship is based. However, simply deriving more estimates of K is not in itself particularly useful. In the first place, there is obviously not a single 'correct' value for K. Instead, K is probably a function of a complex set of variables that may include sediment size and sorting, beach slope, breaker type, and substrate. Indeed, it is interesting by

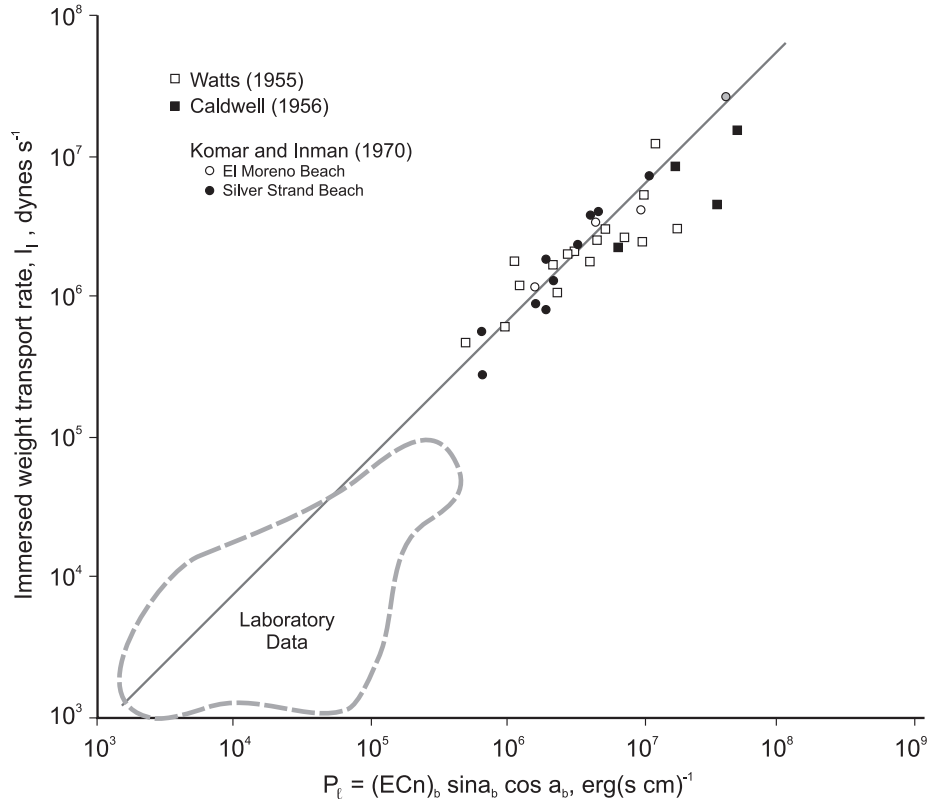

Figure 7.15 Derivation of the relationship between I_L and P_L based on available field data (Komar and Inman, 1970). Note that wave tank data plot below the line and were not used in deriving the regression.

comparison to fluvial or aeolian studies, that there is no explicit consideration of sediment size or threshold in (7.14) and (7.15). Results of Dean *et al.* (1982), and more recent work suggest that K does decrease with increasing grain size in the sand size range (Figure 7.16) but despite this K seems to be relatively insensitive to variations in sediment size in the sand size fraction, though it does become much more important for the transport of gravel and cobbles.

Another bulk transport expression was derived by Kamphuis (1991) based on his extensive wave tank studies:

$$Q_s = 2.27 H_{sb}^2 T_p^{1.5} m_b^{0.75} D^{-0.25} \sin^{0.6} \alpha_b \qquad (7.13)$$

where Q_s is the longshore transport rate in kg s^{-1}; m is the beach slope; and D is the particle diameter.

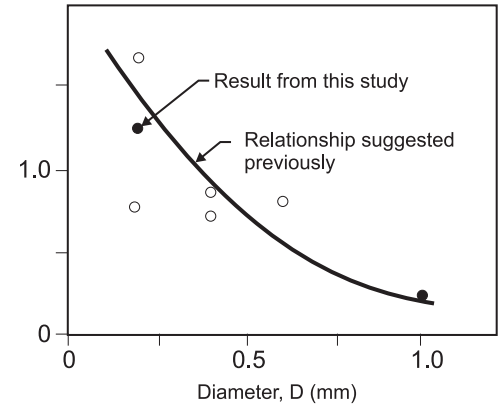

Figure 7.16 Plot of K versus sediment diameter for several field studies (Dean *et al.*, 1982).

The expression is interesting because it includes the effects of three parameters that intuitively should influence the transport rate – wave

steepness, beach slope and sediment size. Kamphuis's experiments found that transport rates were higher for plunging breakers rather than spilling breakers, hence the inclusion of wave period in the equation. The field experiments of Wang *et al.* (1998) showed better agreement with the Kamphuis equation than the CERC one and may reflect the relatively low wave energy conditions on the Gulf coast of Florida. However, the Kamphuis equation performed much worse in the study carried out by Tonk and Masselink (2005).

One of the limitations of both the CERC equation (7.11) and the Kamphuis equation (7.13) is that they only account for the contribution of waves to the longshore sediment transport. Therefore, they underestimate the transport rate when there is a substantial contribution from wind (Ciavola *et al.*, 1997; Tonk and Masselink, 2005). A new formula proposed by Bayram *et al.* (2007) builds on the approach of Inman and Bagnold (1963) in that it assumes that bed sediments are put in motion by wave action and that the sediment is then transported by any type of current. It also explicitly includes sediment size through the particle fall velocity w_s:

$$Q_{lst} = \frac{\varepsilon}{(\rho_s - \rho)(1-a)gw_s} F\overline{V} \tag{7.14}$$

where Q_{lst} is the longshore sediment transport rate ($m^3\ s^{-1}$); $\rho_s - \rho$ is the relative density of the sediment in water; a is the pore space of the sand; F is a measure of the suspended sediment concentration; $\overline{V}$ is the mean longshore current; and ε is a coefficient which expresses the efficiency of the waves in keeping the sand grains in suspension.

A value for ε can be estimated from

$$\varepsilon = \left(9.0 + 4.0\frac{H_{sb}}{W_s T_p}\right).10^{-5}. \tag{7.15}$$

A test of their formula against a chosen data set provided a better fit (Figure 7.17) than for equations (7.11), (7.12) and (7.13), with the next best prediction being the formula of Kamphuis (1991).

Whether the formula of Bayram *et al.* (2007) will prove to be an improvement over other less complex equations remains to be seen. What is clear is that improved prediction requires an increase in the amount and quality of the input data. This is particularly so because prediction of P_L and V_L are very sensitive to small changes in breaker angle and in the direction and speed of the incident winds. This can be done by running numerical models such as Mike21 or SWAN that can bring waves in from offshore across known bathymetry. The potential errors tend to accumulate when we attempt to predict an average annual longshore sediment transport rate for a stretch of coast based on the wave climate, local shoreline orientation, and bathymetry. Fortunately, at least some of the errors tend to cancel each other out.

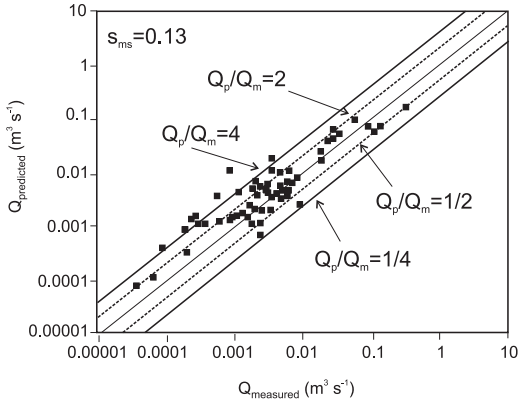

Figure 7.17 measured longshore sediment transport rates from a verification data set versus those predicted by (7.14) (from Bayram *et al.*, 2007).

In addition to the bulk formulae discussed in this section there are a number of formulae that predict bed load and suspended load transport at a point and which can be used to predict transport across the surf zone. Bayram *et al.* (2001) tested the predictive capability of six well known formulae against the measured cross-shore distribution of longshore sediment transport from three experiments carried out at the Coastal Research Facility at Duck, North Carolina. However, none of them provided very good estimates across the range of conditions sampled.

Box 7.2 Longshore sandwaves

Measurements of instantaneous longshore sediment transport and predictions using the formulae discussed in the previous section assume that sand transport takes place as individual grains and that it is uniform within a short stretch of shoreline. However, collective movement of sediment in the form of large bedforms can also occur in a manner similar to the movement of large dunes and sand bars in rivers, and the onshore/offshore movement of bars in the nearshore zone (described in Chapter 8). Bruun (1954) described migrating sandwaves or sand humps on the Dutch coast, and on the Californian coast dispersal of sediment from small deltas was described in terms of accretion and erosion waves (Inman and Bagnold, 1963; Inman, 1987; Hicks and Inman, 1987). Pringle (1985) described in detail the alongshore migration of features on the Holderness coast of Yorkshire termed ords which corresponded to the erosion portion of a sand wave. More recently the term longshore sandwave has been applied to features found at Long Point (Stewart and Davidson-Arnott, 1988; Davidson-Arnott and van Heyningen, 2003; see Figure 7.18) and at Southampton Beach, New York (Thevenot and Kraus, 1995).

Longshore sandwaves are best developed on sandy shorelines where there is a very strong net transport in one direction, with waves reaching the coast at a high angle. Their formation appears to be an example of self-organisation where an initial perturbation produces a positive feedback that enhances and maintains the feature and can lead to the development of a suite of similar features (Ashton *et al.*, 2001; Coco and Murray, 2007). Longshore sandwaves are 500–1500 m in length, 30–80 m in width at the downdrift end, and they migrate alongshore at 100–400 m a^{-1}. Because of their tapered form, alongshore migration produces a temporal alternation between a wide beach opposite the downdrift end, which protects the dune from wave erosion and supplies large amounts of sediment for dune accretion, and a narrow beach opposite the updrift end, which is characterised by erosion and cliffing of the foredune (Figures 7.18a–c). The accretion erosion cycle is easily recognised where there are prominent sandwaves (Hicks and Inman, 1987; Davidson-Arnott and Stewart, 1987; Thevenot and Kraus, 1995) but even where the sandwave form is more subtle the cycles can be distinguished in the behaviour of the toe of the foredune over a number of years (Verhagen, 1989; Ruessink and Jeuken, 2002).

7.5 Littoral sediment budget and littoral drift cells

Estimation of long-term sediment transport rates is often carried out as part of the determination of the littoral sediment budget for a section of coastline. The littoral sediment budget is often linked to the concept of a littoral drift cell and together they provide a coastal management framework for the assessment of the potential impact of human actions on clastic shorelines. Many jurisdictions now make use of littoral cells and littoral cell boundaries as the planning unit for structuring coastal zone management on clastic shorelines and collection of data on inputs and outputs of sediment within these boundaries is usually an important element of background studies carried out as part of the management exercise.

7.5.1 Littoral sediment budget

The littoral sediment budget is an accounting technique in which the volume (or mass) of all sediment inputs (termed sources) and outputs (sinks) to and from the beach and nearshore

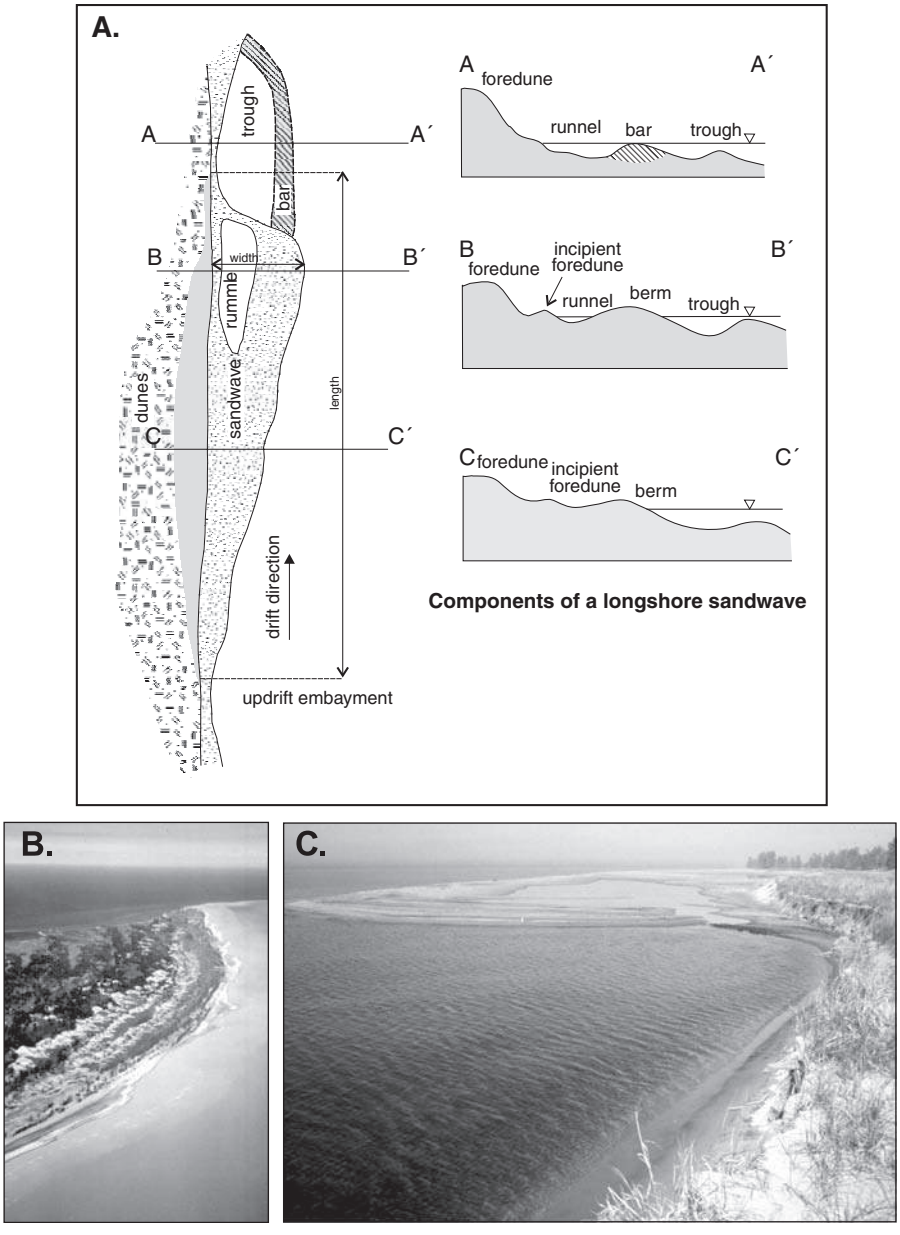

Figure 7.18 Longshore sandwaves: (A) schematic of the features of a longshore sandwave at Long Point; (B) oblique aerial photograph of the downdrift end of Long Point showing longshore sandwaves over a 10 km stretch of shoreline; (C) view looking updrift of the downdrift end of a longshore sandwave. The narrow beach in the foreground and evidence of dune erosion marks the erosional phase associated with passage of the sandwave immediately downdrift (Davidson-Arnott and van Heyningen, 2003).

zone are assessed for a section or reach of the shoreline (Rosati, 2005). The most common natural sources and sinks are shown schematically in Figure 7.19 and tabulated in Table 7.1. A source (and similarly a sink) can be defined either as a point source (e.g., a river mouth) where the input is confined to a local area, or a line source (such as cliff erosion) where the input takes place over a fairly long stretch of the shoreline. On a world-wide basis, inputs from rivers

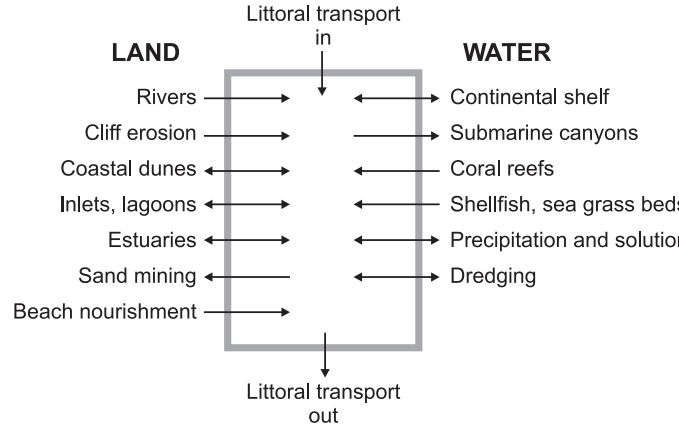

Figure 7.19 Schematic of the common natural sources and sinks for a littoral sediment budget.

are probably the most important source, followed by cliff erosion, and in the tropics biogenic inputs from coral reefs may dominate. In areas of recent glaciation erosion of cohesive bluffs can supply large quantities of sand and gravel. It is usually fairly easy to isolate from the list shown in Table 7.1 the sources and sinks that are likely to be important in a particular study area.

Since fine sediments are only found in very small quantities in energetic littoral zones, the littoral budget is generally quantified in terms of clastic sediments of sand size or greater (a cut-off of 0.1 mm is generally appropriate) though exceptions need to be made on coasts such as Guyana where there is a very large supply of mud. Ideally, if the budget along a stretch of coast is positive (inputs exceed outputs) then deposition should occur and the shoreline will prograde. If it is negative, then beach erosion will occur. The shore parallel boundaries of the area within which the budget is calculated are usually defined by the landward and offshore limits of sediment transport by wave action – i.e., from the landward edge of the backshore to the outer shoreface. The shore perpendicular boundaries may be an arbitrary stretch of shoreline where there is a point of interest, a geomorphic feature such as a beach or spit, or a littoral cell. On sandy coasts aeolian transport of sand inland represents a loss to the littoral sediment budget but it is also a gain to the complementary dune sediment budget and we will address this in Chapter 9. In addition to the natural sources, human actions can have also contribute through activities such as jetty and seawall construction, and through dredging, beach mining and beach nourishment (Table 7.1).

Quantification of a sediment budget for a stretch of coast is not easy and is often a matter of order of magnitude estimates, informed guesses, and the use of residuals where two of three components have been estimated and the remainder must constitute the third (Bowen and Inman, 1966; Rosati, 2005).

There are often good records of flows in rivers discharging at the coast and some measurements or estimates of sediment transport. Bedload transport is still difficult to measure in rivers, but there are at least a number of good predictive equations. Thus, an order-of-magnitude estimate of supply is readily obtainable. Rivers draining upland areas close to the coast provide large volumes of littoral sediment directly but much of the coarse material transported by rivers flowing across an alluvial plain tends to be deposited terrestrially. Thus a substantial portion of the littoral sediment supplied from rivers with large deltas may come from erosion of abandoned areas of the delta rather than directly through distributary channels. On coasts where Holocene sea level rise has drowned the lower portions of river basins, producing rias and shallow estuaries, much of the coarse sediment transported by the river may be trapped at the head of the estuary and not made available to the littoral system.

Littoral sediment supply from coastal erosion is perhaps the most easily quantified. Estimates

of the volume supplied annually is determined initially by multiplying the height and length of a suitable reach by the average annual recession rate determined from mapping or comparison of historical aerial photographs. Where there are fines present in the material supplied the proportion of these can be subtracted to give a corrected volume.

On most coasts it is difficult to quantify losses or gains across the offshore boundary and often a key determinant of the littoral budget is the difference between the supply of sediment by longshore transport from updrift and that lost to longshore transport downdrift. This is especially true for sediment budget calculations at a point on the coast such as those required for determining the design criteria for the entrance to a small harbour or for assessing the potential impact of such a structure. This requires accurate estimates of Q_N at a point, usually through the determination of a wave climate and numerical modelling of nearshore wave transformation with all the caveats noted in the previous section. We will come back to an example of this after an examination of littoral cells.

7.5.2 Littoral cells

An ideal littoral cell is a section of coast that contains a source, or sources of sediment, a well-defined and continuous zone of alongshore sediment transport and a downdrift sink or zone where sediment is either deposited or is lost offshore (Figure 7.20a). The concept seems to have been applied first to the California coast (Inman and Frautschy, 1966; Bowen and Inman, 1966) where a series of cells with longshore sediment transport to the south was identified. In each of these cells sediment input came primarily from rivers draining the coastal mountains, and to a lesser extent from cliff erosion. Sand transport generally increases southward until it is diverted offshore and lost down the heads of submarine canyons (Figure 7.20a). The heads of the canyons were often marked by rocky headlands because of the loss of the littoral sand supply. The existence of the heads of the submarine canyons within a few hundred metres of the beach is a consequence of the very narrow continental shelf in California, and in most littoral cells the sink is an area of net deposition marked by a feature such as a spit or dune field.

A related concept is that of the coastal sediment compartment (Davies, 1974) which is used on highly embayed coasts to delineate sections where there are major obstacles to longshore sediment transport. These are usually large headlands that serve to restrict the angle of wave approach to the shoreline, confining sediment movement to the area between the headlands and isolating the embayments from the rest of the coast. Beaches in these embayments tend to be very stable and to develop an equilibrium form both on–offshore and in plan view.

Littoral cells often have boundaries such as headlands that are easily demarcated and cells may be largely isolated from adjacent one. However, unlike coastal compartments, there can be exchange of sediment between adjacent littoral cells and the boundaries between them may be quite fuzzy. Littoral cell boundaries can be convergent, divergent or interruptive and it is possible to recognise sub-cells within major littoral cell units (Figure 7.20b). The identification of the cells and directions of net longshore sediment transport are the starting point for collecting information on sediment inputs and outputs and the determination of a littoral sediment budget (e.g., Sanderson and Eliot, 1999; Patsch and Griggs, 2008). This approach provides a systematic framework for research on coastal processes and coastal evolution, and for the establishment of coastal management plans. They have been adopted as the basis for coastal management in a number of jurisdictions, including Ontario and England (Cooper and Pontee, 2006).

7.5.3 Littoral transport gradients

Convergent sinks, such as those of headland/ bay beaches or the cuspate foreland of Point Pelee (Figure 7.21) are easily understood. However, as shown for the origin of Pointe-aux-Pins, deposition can also occur where there is no reversal in the dominant transport direction. Instead, deposition takes place because of a change in the gradient of longshore sediment transport – in this case because the shore alignment becomes more nearly perpendicular to the SW waves thus reducing the gross rate of eastward

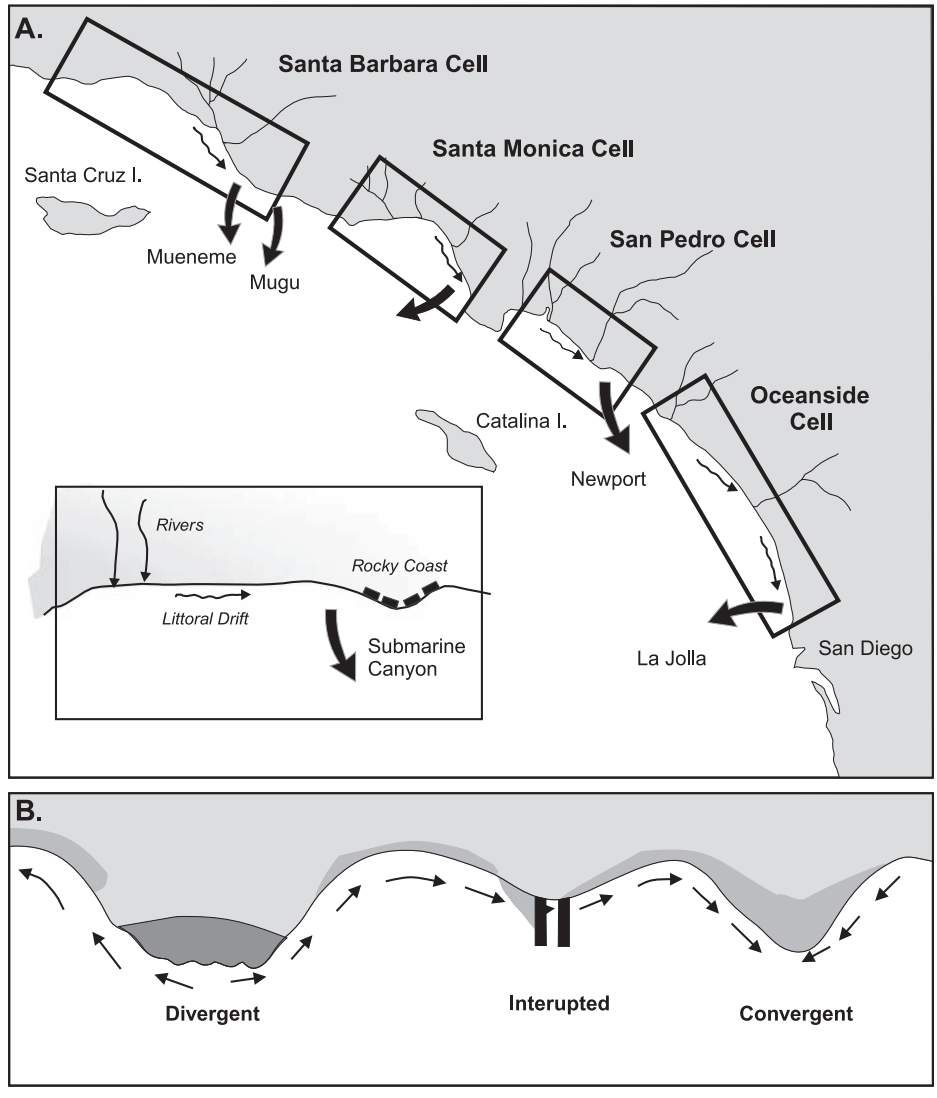

Figure 7.20 Littoral drift cells: (A) Littoral cells on the California Coast (after Bowen and Inman, 1966); (B) types of littoral cell boundaries.

transport. Thus, a decrease in the rate of net transport along a reach, assuming no shortage in the availability of sand, means that more sand enters the updrift boundary than leaves the downdrift boundary. The extra sand is deposited initially on the beach and nearshore, widening the beach in this area and possibly feeding more sand inland to the dune. The opposite occurs when there is an increase in the transport gradient and more sand leavers the downdrift boundary than enters updrift. The result here is to produce beach erosion, narrowing the beach and possibly eroding material from the foredune.

Gradients in longshore sediment transport formed the basis for the conceptual ABC model of May and Tanner (1973). This was developed to guide the application of WAVENERG which was one of the first computer wave refraction models made generally available to coastal geomorphologists and engineers (May, 1974). The ABC model shows one half of a headland/bay beach and illustrates changes in a variety of

Box 7.3 Littoral cells on the north shore of Lake Erie

Littoral cells on the north shore of Lake Erie in Ontario provide an illustration of some of the common features associated with littoral cell components (Figure 7.21a). Limestone bedrock outcrops along the very eastern portion of the shoreline forming small low headlands with a cover of till and lacustrine sediment. The rest of the shoreline of the north shore is developed in sedimentary materials, primarily till, glacio-lacustrine clay and deltaic sand and silt. Erosion of these materials and shoreline recession has led to the formation of bluffs that are 10–30 m high and which have very high recession rates – typically on the order of 0.3–2 m a^{-1} (Figure 7.21b). The accompanying nearshore erosion produces a steep nearshore profile with much of the coarse sediment transport taking place by beach drifting or in the narrow surf zone just lakeward of the step. Bluff and nearshore erosion accounts for almost all the littoral sediment supply, with only a very small amount coming from streams reaching the lake. The largest waves on Lake Erie are generated along the SW–NE axis of the lake which provides the longest fetch of about 300 km. Prevailing winds are from the SW and strong westerly, north-westerly and northeaster winds can be associated with the passage of mid-latitude cyclones with direction dependent on the track of the storm. Because of the greater frequency of winds from the West, net longshore transport is towards the East over a large portion of the north shore (a similar situation exists on the south shore).

Lake Erie reached its present level about 5 000 BP and shoreline recession since then exceeds 5 km in places. Although only about 40% of the eroded material contributes to the littoral sediment budget (the fines settle out in the central lake basin) the large volumes of sediment eroded and the lengthy period of stable lake level has led to the formation of three sedimentary sinks: the cuspate foreland of Point Pelee in the west, the barrier and lagoon system of Pointe-aux-Pins in the centre, and Long Point spit in the east (Figure 7.21a, c, d).

The cells are given informal names here to make it easy to distinguish them.

Point Pelee is a cuspate foreland formed by the convergence of two littoral drift cells (Figure 7.21a). The coast to the west of Point Pelee is sheltered from large NE waves by the presence of shoals and limestone outcrops around Pelee Island and thus net transport of sediments from bluff erosion is to the east, even though the fetch in this direction is quite short. Large waves generated by NE winds during storms produce a net westerly longshore transport of sediment eroded from the bluffs for a distance of tens of km to the east and this forms the eastern littoral cell supplying the foreland (Coakley, 1976). Eastward along the shoreline the fetch for westerly waves increases while that for NE waves diminishes. The combined effect of this leads to a reversal of the net transport (divergent boundary) and the initiation of a littoral cell with net transport to the east. The divide between the two cells is not sharp and there is likely a zone on the order of 10–20 km which contributes sediment to both cells, with actual transport direction varying seasonally and over several years as a function of changes in the frequency and magnitude of easterly versus westerly winds.

The second depositional complex is Pointe-aux-Pins (Figure 7.21d) which is a complex feature consisting of a short western barrier (Erieau) and an elongate eastern barrier (Rondeau) enclosing a bay that is about 10 km long and 4 km wide (Coakley, 1989). Early reports (Boyd, 1981) suggested that, similar to Pt. Pelee,

Pointe-aux-Pins was formed by the convergence of two cells. However, more recent work (Graham and Davidson-Arnott, 2005) has shown that net transport is towards the east at this location and that deposition occurs as a result of a decrease in the transport gradient resulting from the change in shoreline orientation. The south shore of Rondeau is thus the erosional updrift end of a complex spit feature — not the downdrift end as was originally proposed — and the whole feature is an example of a sink associated with an interruptive boundary.

The third major sink is Long Point, a flying spit that is fed by the Long Point west littoral cell which extends over 120 km eastward from Rondeau (Figures 7.18b, 7.21a). Almost all of this shoreline consists of eroding bluffs that supply over 300 000 m^3 of sand and gravel annually. Long Point was initiated about 5000 years BP, and during that time the shoreline and point of attachment of the spit has migrated about 5 km inland (Coakley, 1992). The initial trigger for the diversion of sediment towards the centre of the lake may have been a cross-lake glacial moraine but, once this occurred, the deep water at the terminus of the spit acted to trap all the littoral sediment that was not deposited in the barrier itself. Because the tip of the spit is in deep water, there is little refraction around the end of the spit (Davidson-Arnott and Conliffe Reid, 1994) and most of the littoral transport that reaches the distal end goes into building the spit platform and the subaerial beach and dune complex.

The Long Point east cell transports a small amount of sand westward towards Long Point, most of which is trapped in Turkey Point, a small spit that is building into Long Point Bay. The existence of this cell results from the growth of Long Point, which now shelters a substantial length of the coast to the east from SW waves, thus allowing easterly winds to dominate. Further east, the sheltering effect disappears, and westward longshore transport dominates the Port Colborne cell that transports sediment towards the entrance to the Niagara River.

parameters for wave approach perpendicular to the shoreline that would be expected as a result of wave refraction processes and the change in orientation of the shoreline (Figure 7.22). Wave energy E is greatest at the headland because of convergence and least in the bay because of divergence. The longshore component of wave energy flux P_L varies with the angle of wave approach to the shoreline and the total wave energy at the break point and is 0 at the headland and in the bay, where wave approach is perpendicular, and a maximum at C where the angle with respect to the shoreline is greatest. As we saw in Section 7.4.3, the immersed weight longshore sediment transport rate I_L and the volume of sediment transport rate q will be proportional to P_L and so all three of them plot on the same line (Figure 7.22). Points a and e mark the locations of maxima and minima for these parameters, and for their derivatives with distance alongshore. The rate of increase in q reaches a maximum at B and decreases to 0 at C, which is the location of maximum longshore transport. Between C and D the rate of sediment transport decreases rapidly, and then declines to 0 at E where all longshore transport ceases.

7.5.4 Modelling littoral sediment transport

The simple relationships between wave approach angle to the shoreline and transport gradients shown in Figure 7.22 can be applied to much more complex scenarios and form the basis for modelling of the littoral drift system using computer based wave refraction models and local wave climate statistics. These models can be used to predict the magnitude and net direction of transport along the coast, predict areas of likely erosion and deposition and can feed into determination of the littoral sediment budget.

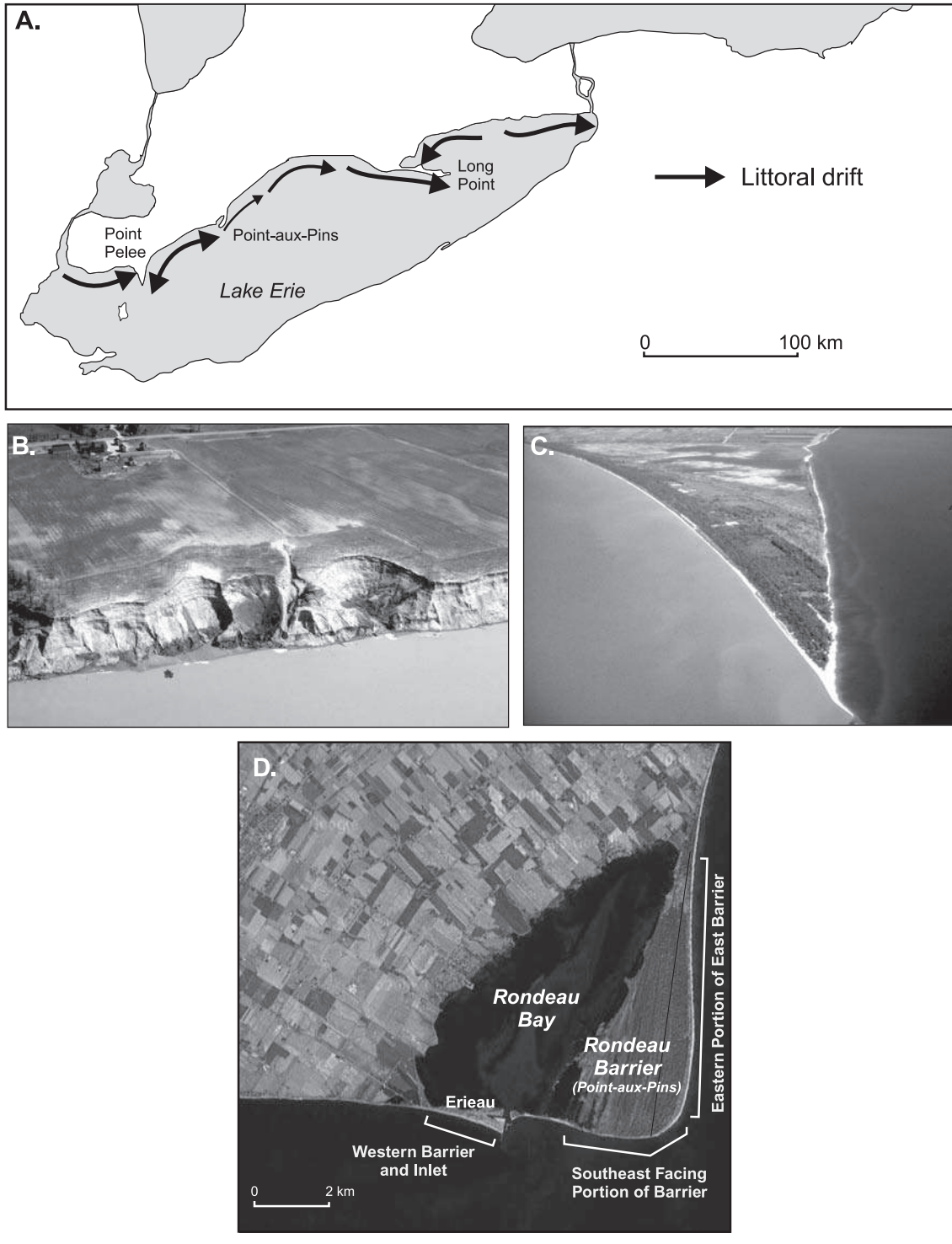

Figure 7.21 Littoral cells on the north shore of Lake Erie (after Boyd, 1981, Reinders, 1988 and Graham and Davidson-Arnott, 2005). (A) Map of the north shore of Lake Erie showing littoral cells, net longshore transport patterns and the major source and sink areas; (B) oblique aerial photograph of a typical source area showing bluff erosion near Port Burwell, about 30 km west of Long Point. The bluffs here are about 30 m high and the recession rate ranges from 1–2 m a^{-1}; (C) oblique aerial photograph looking north of Point Pelee. The cuspate foreland is about 8 km long and about 3 km wide at the landward margin; (D) vertical aerial photograph of the two barriers making up the central sink of the Pointe-aux-Pins system.

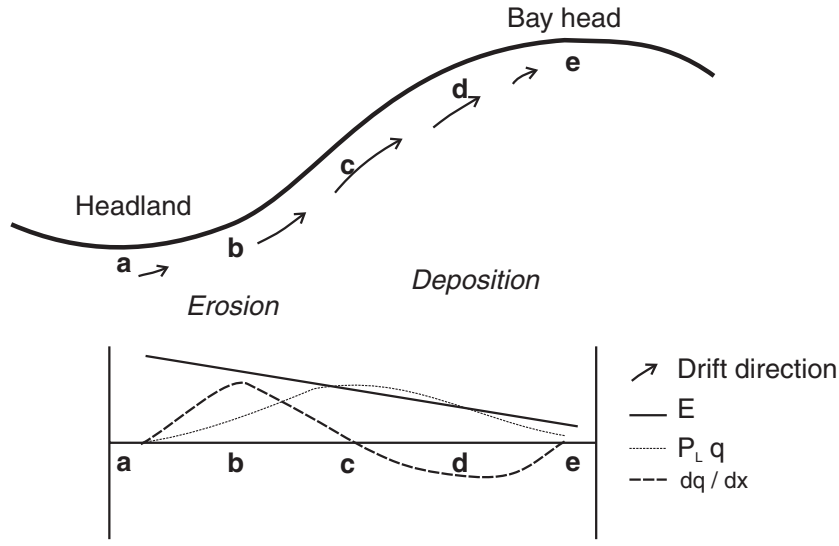

Figure 7.22 Schematic of one-half of a headland/bay beach showing the spatial pattern of a number of parameters resulting from shore normal wave approach and wave refraction. E = wave energy at the break point, P_L, q and I_L are the longshore component of wave energy flux, the volume of longshore sediment transport and the immersed weight longshore sediment transport and x is the alongshore distance from the headland. Points a–e mark locations of maxima and minima for key parameters. Wave energy is greatest at the headland because of convergence and least in the bay because of divergence. The rate of increase in q is a maximum at B and decreases to 0 at C which is the location of maximum longshore transport. Between C and D the rate of decreasing sediment transport reaches a maximum and transport ceases at E where waves are once again parallel to the shoreline.

Output from such numerical modelling should always be compared to qualitative geomorphic indicators in order to ensure that all key controls have indeed been incorporated in the modelling.

The WAVENRG program was used by Lawrence and Davidson-Arnott (1997) to model sediment transport and coastal erosion on the east coast of Lake Huron. They study area was a littoral cell stretching between a natural bedrock headland at Point Clark and the artificial barrier created by harbour breakwalls at Goderich. The coastline here consists of high bluffs developed in a cohesive till with about 20% sand and gravel component and recession rates vary from negligible to about 0.4 m a^{-1}. The average annual wave climate based on 35 years of hindcast data was used to select a set of wave classes based on H_s, T_p and wave direction (octants) for the ice-free year. Prevailing winds are from the west and southwest blowing over fetches of 100 and 150 km respectively, but dominant waves are produced by storm winds from the NW blowing over a fetch >300 km. The WAVENRG program was then run for each wave class and the value of P_B and P_L determined for points spaced equally along the shoreline by interpolating from the values determined for each orthogonal wave ray (see Figure 5.11 for an example of the program output). The average annual value of these two parameters was obtained from the hourly frequency associated with the class and value for total P_B and net P_L at each point then determined from the algebraic sum of all the wave classes.

It might be expected that bluff recession rates would be associated with areas of highest wave energy flux P_B, but a plot of P_B against bluff recession rates for the littoral cell shows no significant relationship (Figure 7.23a). A better explanation is obtained by examining the effect of protection provided by beach sediments. The alongshore variation in potential net longshore sediment transport S_L is plotted against the estimated cumulative supply of sediment available from bluff recession and transport from updrift (Figure 7.23b) and zones of erosion, transport

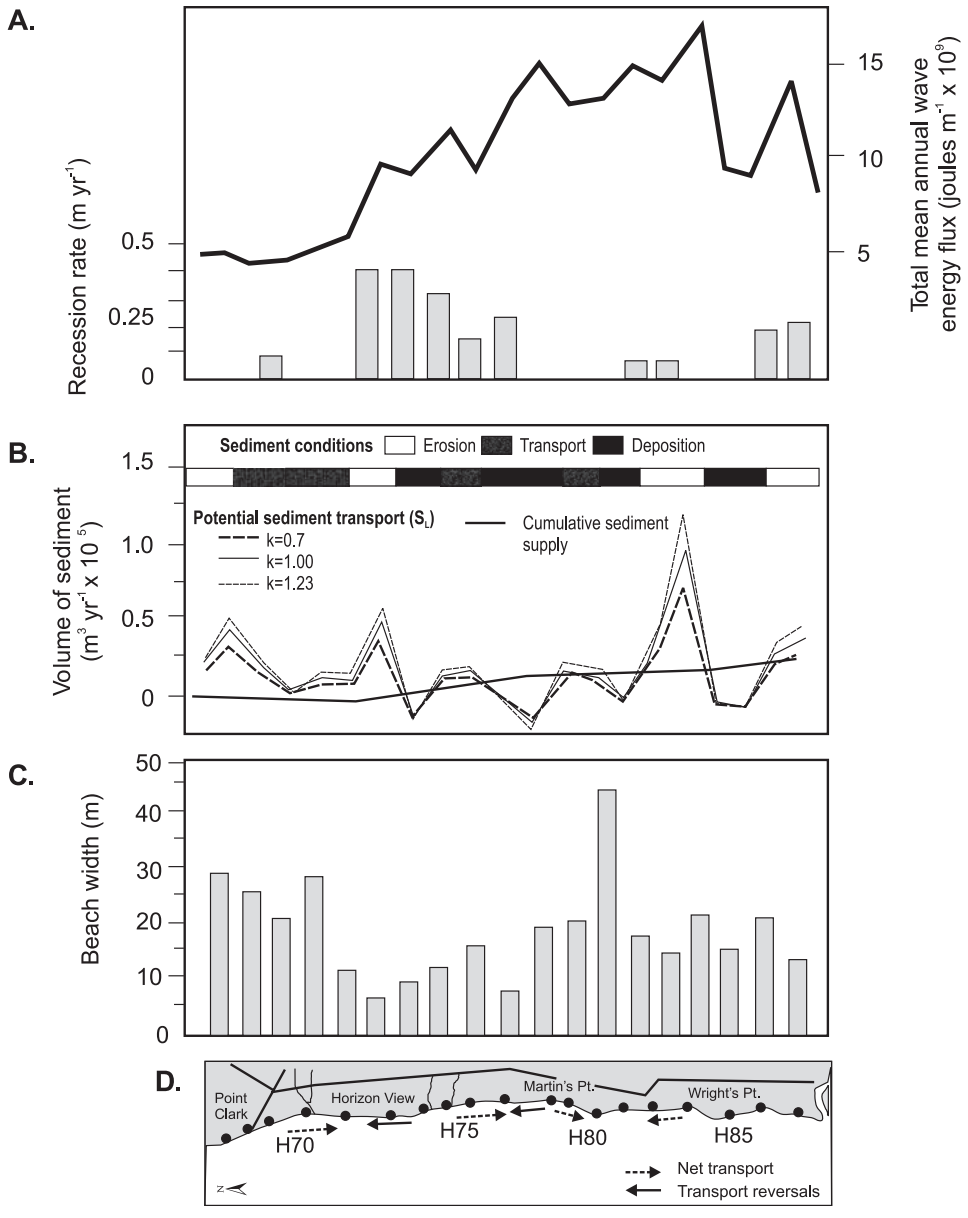

Figure 7.23 Comparison of modelling of littoral sediment transport with geomorphic indicators for a section of the Lake Huron shoreline: (A) plot of the spatial distribution of the mean annual bluff recession rate versus the mean annual total wave energy flux predicted from the model; (B) the alongshore distribution of potential sediment transport based on modelling and the available littoral sediment supply based on the bluff recession rate and bluff composition. Zones of potential erosion, transport and deposition are based on the alongshore transport gradient; (C) alongshore variations in beach width measured on one day; (D) map of the coastline between Point Clark and Goderich. The dots mark locations of calculations for model values and the numbered stations are sites of long-term bluff recession monitoring (Lawrence and Davidson-Arnott, 1997).

and deposition are indicated based on the transport gradients. Potential transport rates are plotted for three values for the coefficient K based on earlier studies on Lake Ontario (Davidson-Arnott and Amin, 1985) which suggested that a value of 1.25 for *K* was a better fit for the data than the standard 0.77. It can be seen that the areas with little erosion tend to correspond to zones where the cumulative supply is close to the potential transport, indicating the potential for greater protection from beach sediments while the highest erosion is associated with potential transport in excess of supply. The general pattern of beach width variation alongshore also fits with the predicted transport gradients (Figure 7.23c). The refraction model does not perform well in the shoal areas around Point Clark (Figure 7.23d) and large waves break several hundred metres offshore. Field evidence suggests that the sheltering effect from large waves from the NW is greater than estimated by the model, leading to some northerly transport in the lee and a small amount of accumulation.

First-generation models such as WAVENRG used regular wave inputs, had a relatively simple topographic extrapolation algorithm and did not allow for diffraction or wave-current interaction. Newer models such as MIKE21 (e.g., Johnson *et al.*, 2001) and SWAN (Booij *et al.*, 2001) combine wave prediction of random wave fields with more sophisticated modelling of nearshore bathymetry, refraction and diffraction. Thus, they offer the potential for better modelling of the natural system and assessment of the impacts of coastal structures. Nevertheless, there are still many uncertainties in the application of the models as a result of uncertainties in prediction of transport as well as the difficulty of establishing accurate wave climates. Thus all model outputs still require careful assessment against a range of coastal indicators.

Further reading

Fredsøe, J. and Deigaard, R. 1992. *Mechanics of Coastal Sediment Transport*. World Scientific, Singapore, 369 pp.

This book covers a lot of the basic processes related to coastal sediment transport.

References

Aagaard, T. and Greenwood, B. 1995. Suspended sediment transport and the role of infragravity waves in a barred surf zone. *Marine Geology*, **118**, 23–48.

Aagaard, T., Nielsen, J. and Greenwood, B. 1998. Suspended sediment transport and nearshore bar formation on a shallow intermediate state beach. *Marine Geology*, **148**, 203–225.

Aagaard, T., Greenwood, B. and Nielsen, J. 2002. Bed level changes and megaripple migration on a barred beach. *Journal of Coastal Research*, **SI 34**, 110–116.

Ashton, A., Murray, A. B. and Arnault, O. 2001. Formation of coastal features by large-scale instabilities induced by high angle waves. *Nature*, **414**, 296–300.

Austin, M. J. and Masselink, G. 2008. The effect of bedform dynamics on computing suspended sediment fluxes using optical backscatter sensors and current meters. *Coastal Engineering*, **55**, 251–260.

Bagnold, R. A., 1946. Motion of waves in shallow water. Interaction between waves and sand bottoms. *Proceedings of the Royal Society of London A*, **187**, 1–15.

Bagnold, R. A. 1963. Mechanics of marine sedimentation. In Hill, M. N. (ed.), *The Sea*, Wiley–Interscience, New York, pp. 507–528.

Bagnold, R. A. 1966. An approach to the sediment transport problem from general physics. *US Geological Survey*, Professional Paper 422-I, 37 pp.

Baillard, J. A. 1981. An energetics total load sediment transport model for a plane sloping beach. *Journal of Geophysical Research*, **86**, 10,938–10,954.

Bayram, A., Larson, M., Miller, H. C. and Kraus, N. C. 2001. Cross-shore distribution of longshore sediment transport: Comparison between predictive formulas and field measurements. *Coastal Engineering*, **44**, 79–99.

Bayram, A., Larson, M. and Hanson, H. 2007. A new formula for the total longshore sediment transport rate. *Coastal Engineering*, **54**, 700–710.

Beach, R. A. and Sternberg, R. W. 1988. Suspended sediment transport in the surf zone: response to cross-shore infragravity motion. *Marine Geology*, **80**, 61–79.

Bodge, K. R. and Dean, R. G. 1987. Short-term impoundment of longshore transport. *Coastal Sediments, '87*, ASCE 469–483.

Booij, N., Holthuijsen, L. H. and Battjes, J. A. 2001. Ocean to near-shore wave modelling with SWAN. *Proceedings Coastal Dynamics '01*, ASCE 335–344.

Bowen, A. J. 1980. Simple models of nearshore sedimentation; beach profiles and longshore bars. In McCann, S. B. (ed.), *The Coastline of Canada*. Geological Survey of Canada, **Paper 80–10**, 1–11.

Bowen, A. J. and Inman, D. L. 1966. Budget of Littoral Sands in the Vicinity of Point Arguello, California. *Coastal Engineering Research Centre, Technical Memorandum* **19**, 41 pp.

Boyd, G. L., 1981. *Great Lakes Erosion Monitoring Program – Final Report*. Ocean Science and Surveys. Bayfield Lab for Marine Science and Surveys, Burlington, Ontario.

Bruno, R. O., Dean, R. G. and Gable, C. G. 1980. Longshore transport evaluations at a detached breakwater. *Proceedings of the 17th Conference on Coastal Engineering*, ASCE, pp. 1453–1475.

Bruun, P. 1954. *Coast Erosion and the Development of Beach Profiles*. Beach Erosion Board, Technical Memorandum, **44**, 66 pp.

Carstens, M. R., Neilson F. M. and Altinbilek, H. D. 1969. Bedforms Generated in the Laboratory Under an Oscillatory Flow: Analytical and Experimental Study. *Coastal Engineering Research Centre, Technical Memorandum*, **28**, 39 pp.

Ciavola, O. 2004. Tracers. In Schwartz, M. (ed.), *Encyclopedia of Coastal Sciences*. Kluwer, Dordrecht, 1253–1258.

Ciavola, O., Taborda, R., Ferreira, O. and Dias, J. A. 1997. Field measurements of longshore sand transport and control processes on a steep meso-tidal beach in Portugal. *Journal of Coastal Research*, **13**, 1119–1129.

Clifton, H. E. 1976. Wave-formed sedimentary structures – conceptual model. In: Davis, R. A., Ethington, R. L. (editors), *Beach and Nearshore Sedimentation*, Society for Economic Paleontology and Mineralogy, Special Publication 24, pp. 126–148.

Clifton, H. E., Hunter, R. E., Phillips, R. L. 1971. Depositional structures and processes in the non-barred high-energy nearshore. *Journal of Sedimentary Petrology*, **41**, 651–670.

Coakley, J. P. 1976. The formation and evolution of Point Pelee, western Lake Erie. *Canadian Journal of Earth Sciences*, **13**, 136–144.

Coakley, J. P. 1989. The origin and evolution of a complex cuspate foreland: Pointe-aux-Pins, Lake Erie, Ontario. *Géographie Physique et Quarternaire*, **43**, 65–76.

Coakley, J. P. 1992. Holocene transgression and coastal-landform evolution in northeastern Lake Erie, Canada. In Fletcher, C. H. and Wehmiller, J. F. (eds.), *Quaternary Coasts of the United States: Marine and Lacustrine Systems*. Society for Sedimentary Geology, Special Publication 48, pp. 415–426.

Coco, G. and Murray, A. B. 2007. Patterns in the sand: From forcing templates to self-organisation. *Geomorphology*, **91**, 271–290.

Cooper, N. J. and Pontee, N. I. 2006. Appraisal and evolution of the littoral 'sediment cell' concept in applied coastal management: Experiences from England and Wales. *Ocean and Coastal Management*, **49**, 498–510.

Davidson-Arnott, R. G. D. and Greenwood, B. 1974. Bedforms and structures associated with bar topography in the shallow-water wave environment, Kouchibouguac Bay, New Brunswick, Canada. *Journal of Sedimentary Petrology*, **44**, 698–704.

Davidson-Arnott, R. G. D. and Greenwood, B. 1976. Facies relationships on a barred coast, Kouchibouguac Bay, New Brunswick. In Davis, R. A. Jr. and Ethington, R. L. (eds.), *Beach and nearshore Sedimentation*. SEPM, Special Publication No. 24, pp. 149–168.

Davidson-Arnott, R. G. D. and Pember, G. F. 1980. Morphology and sedimentology of multiple parallel bar systems, Southern Georgian Bay, Ontario. In McCann, S. B. (ed.), *The Coastline of Canada*, Geological Survey of Canada Paper 80–10, pp. 417–428.

Davidson-Arnott, R. G. D. and Amin, S. M. N. 1985. An approach to the problem of coastal erosion in Quaternary sediments. *Applied Geography*, **5**, 99–116.

Davidson-Arnott, R. G. D. and Stewart, C. J. 1987. The effect of longshore sandwaves on dune erosion and accretion, Long Point, Ontario. *Proceedings of the Canadian Coastal Conference*, National Research Council of Canada, pp. 131–144.

Davidson-Arnott, R. G. D. and Conliffe Reid, H. E. 1994. Sedimentary processes and the evolution of the distal bayside of Long Point, Lake Erie. *Canadian Journal of Earth Sciences*, **31**, 1461–1473.

Davidson-Arnott, R. G. D. and van Heyningen, A. 2003. Migration and sedimentology of longshore sandwaves, Long Point, Lake Erie, Canada. *Sedimentology*, **50**, 1123–1137.

Davies, A. G. 1985. Field observations of the threshold of sediment motion by wave action. *Sedimentology*, **32**, 685–704.

Davies, J. L. 1974. Coastal sediment compartment. *Australian Geographical Studies*, **12**, 139–151.

Dawson, J. C., Davidson-Arnott, R. G. D. and Ollerhead, J. 2002. Low-energy morphodynamics of a ridge and runnel system. *Journal of Coastal Research*, **SI 36**, 198–215.

Dean, R. G., Berek, E. P., Gable, C. G. and Seymour, R. J. 1982. Longshore transport determined by an efficient trap. *Proceedings 18th Coastal Engineering Conference*, ASCE, 954–968.

Downing, J. P., Sternberg, R. W. and Lister, C. R. B. 1981. New instrumentation for the investigation of sediment suspension processes in the shallow marine environment. *Marine Geology*, **42**, 19–34.

Doucette, J. S. 2000. The distribution of nearshore bedforms and effects on sand suspension on low-energy, micro-tidal beaches in Southwestern Australia. *Marine Geology*, **165**, 41–61.

Duane, D. B. and James, W. R. 1980. Littoral transport in the surf zone elucidated by an Eulerian sediment tracer experiment. *Journal of Sedimentary Petrology*, **50**, 929–952.

Gallagher, E. L., 2003. A note on megaripples in the surf zone: evidence for their relation to steady flow dunes. *Marine Geology*, **193**, 171–176.

Gallagher, E. L., Elgar, S. and Thornton, E. B. 1998. Megaripple migration in a natural surf zone. *Nature*, **394**, 165–168.

Gillie, R. D. 1985. Evaluation of field techniques for measurements of longshore transport. *Proceedings Canadian Coastal Conference*, National Research Council of Canada, 89–103.

Graham, M. and Davidson-Arnott, R. G. D. 2005. Shoreline change and sediment transport patterns in the vicinity of Pointe-aux-Pins, Lake Erie: implications for past and future evolution. *Proceedings Canadian Coastal Conference*, CCSEA, 10pp.

Green, M. O. and Black, K. P. 1999. Suspended-sediment reference concentration under waves: field observations and critical analysis of two predictive models. *Coastal Engineering*, **38**, 115–141.

Greenwood, B. and Davidson-Arnott, R. G. D. 1979. Sedimentation and equilibrium in wave-formed bars: a review and case study. *Canadian Journal of Earth Sciences*, **16**, 312–332.

Greenwood, B. and Mittler, P. R. 1979. Structural indices of sediment transport in a straight, wave-formed bar. *Marine Geology*, **32**, 191–203.

Greenwood, B. and Mittler, P. R. 1985. Vertical sequence and lateral transitions in the facies of a barred nearshore environment. *Journal of Sedimentary Petrology*, **55**, 366–375.

Hay, A. E. and Bowen, A. J. 1994. Coherence scales of wave-induced suspended sand concentration fluctuations. *Journal of Geophysical Research*, **99**, 12,749–12,765.

Heathershaw, A. D. and Carr, A. P., 1977. Measurements of sediment transport rates using radioactive tracers. *Proceedings Coastal Sediments '77*, ASCE, 399–416.

Hicks, D. M. and Inman, D. L. 1987. Sand dispersion from an ephemeral river delta on the Central California coast. *Marine GeoIogy*, **77**, 305–318.

Houser, C., Greenwood, B. and Aagaard, T. 2006. Divergent response of an intertidal swash bar. *Earth Surface Processes and Landforms*, **31**, 1775–1791.

Ingle, J. C. 1966. *The Movement of Beach Sand*. Elsevier, New York, 221 pp.

Inman, D. L. 1957. *Wave-generated ripples in nearshore sands*. Beach Erosion Board, Technical Memorandum 100.

Inman, D. L. 1987. Accretion and erosion waves on beaches. *Shore and Beach*, **55**, 61–66.

Inman, D. L. and Bagnold, R. A. 1963. Littoral processes. In Hill, M. N. (ed.), *The Sea*, Wiley–Interscience, New York, pp. 529–553.

Inman D. L. and Bowen, A. J. 1963. Flume experiments on sand transport by waves and currents. *Proceedings of the 8th Conference on Coastal Engineering*, ASCE, pp. 137–150.

Inman, D. L. and Frautschy J. D. 1966. Littoral processes and the development of shorelines. *Proceedings Coastal Engineering Conference*, ASCE, pp. 511–536.

Inman, D. L., Zampol, J. A., White, T. E., Hanes, D. M., Waldorf, B. W. and Kastens, K. A. 1980. Field measurements of sand motion in the surf zone. *Proceedings Coastal Engineering Conference*, ASCE, pp. 1215–1234.

Jensen, B. L., Summer, B. M. and Fredsøe, J. 1989. Turbulent oscillatory boundary layers at high Reynolds numbers. *Journal of Fluid Mechnics*, **206**, 265–297.

Johnson, H. K., Appendini, C. M., Soldati, M., Elfrink, B. and Sørenson, P. 2001. Numerical modelling of morphological changes due to shoreface nourishment, *Proceedings Coastal Dynamics '01*, ASCE, pp. 878–887.

Jonnson, I. G. and Carlsen, N. A. 1976. Experimental and theoretical investigations in an oscillatory turbulent boundary layer. *Journal of Hydraulic Research*, **14**, 45–60.

Kamphuis, J. W. 1975. Friction factor under oscillatory waves. *Journal of Waterway, Harbors and Coastal Engineering*, ASCE, **101**, 135–144.

Kamphuis, J. W. 1991. Alongshore sediment transport rate. *Journal of the Waterway, Port, Coastal and Ocean Division*, ASCE, **117**, 624–640.

Kamphuis, J. W., Davies, M. H., Nairn, R. B. and Sayao, O. J. 1986. Calculation of littoral sand transport rate. *Coastal Engineering*, **10**, 1–21.

Komar, P. D. 1978. The relative significance of suspension versus bed-load on beaches. *Journal of Sedimentary Petrology*, **48**, 921–932.

Komar, P. D. 1998. *Beach processes and Sedimentation*. Prentice-Hall, NJ, 2nd edn., 544 pp.

Komar, P. D. and Inman, D. C. 1970. Longshore sand transport on beaches. *Journal of Geophysical Research*, **75**, 5914–5927.

Komar, P. D. and Miller, C. M. 1973. The threshold of sediment movement under oscillatory water waves. *Journal of Sedimentary Petrology*, **43**, 1101–1110.

Kraus, N. C. 1987. Application of portable traps for obtaining point measurement of sediment transport rates in the surf zone. *Journal of Coastal Research*, **2**, 139–152.

Larson, M. and Kraus, N. C. 1989. *SBEACH: Numerical Model for Simulating Storm-Induced Beach Change*. CERC Technical Report 89–9.

Lawrence, P. L. and Davidson-Arnott, R. G. D. 1997. Alongshore wave energy and sediment transport on south-eastern Lake Huron, Ontario, Canada. *Journal of Coastal Research*, **13**, 1004–1015.

Li, M. Z. and Amos, C. L. 1999. Field observations of bedforms and sediment transport thresholds of fine sand under combined waves and currents. *Marine Geology*, **158**, 147–160.

Madsen, O. S. 1987. Use of tracers in sediment transport studies. *Proceedings Coastal Sediments 01*, **ASCE**, pp. 424–435.

Masselink, G., Austin, M., Tinker, J., O'Hare, T. and Russell, P. 2008. Cross-shore sediment transport and morphological response on a macrotidal beach with intertidal bar morphology, Truc Vert, France. *Marine Geology*, **251**, 141–155.

May, J. P. 1974. WAVENRG: A computer program to determine dissipation in shoaling water waves with examples from coastal Florida. In Tanner, W. F. (ed.), *Sediment Transport in the Nearshore Zone*. Coastal Research Notes, Department of Geology, Florida State University, 22–80.

May, J. P. and Tanner, W. F. 1973. The littoral power gradient and shoreline changes. In Coates, D. R. (ed.), *Coastal Geomorphology*, SUNY, New York, 43–60.

Miller, H. C. 1999. Field measurements of longshore sediment transport during storm. *Coastal Engineering*, **36**, 301–321.

Miller M. C. and Komar, P. D. 1980. A field investigation of the relationship between oscillation ripple spacing and the near-bottom water orbital motion. *Journal of Sedimentary Petrology*, **50**, 183–191.

Mogridge, G. R. and Kamphuis, J. W. 1972. Experiments on bedform generation by wave action. *Proceedings 13th Conference on Coastal Engineering*, ASCE, 1123–1142.

Nairn, R. B. and Southgate, H. N. 1993. Deterministic profile modelling of nearshore processes. Part 2. Sediment transport and beach profile development. *Coastal Engineering*, **19**, 57–96.

Nielsen, P. 1986. Suspended sediment concentrations under waves. *Coastal Engineering*, **8**, 51–72.

Nielsen, P. 1992. *Coastal Bottom Boundary Layer and Sediment Transport*. Advanced Series on Ocean Engineering, 4, World Scientific, Singapore, 324 pp.

O'Donoghue, T. and Clubb, G. S. 2001. Sand ripples generated by regular oscillatory flow. *Coastal Engineering*, **44**, 101–115.

Osborne, P. D. and Greenwood, B. 1992. Frequency dependent cross-shore suspended sediment transport. 1: A non-barred shoreface. *Marine Geology*, **106**, 1–24.

Osborne, P. D. and Vincent, C. E. 1993. Dynamics of large and small scale bedforms on a macrotidal shoreface under shoaling and breaking waves. *Marine Geology*, **115**, 207–226.

Osborne, P. D. and Vincent, C. E. 1996. Vertical and horizontal structure in suspended sand concentrations and wave-induced fluxes over bedforms. *Marine Geology*, **131**, 195–208.

Patsch, K. and Griggs, G. 2008. A sand budget for the Santa Barbara littoral cell, California. *Marine Geology*, **252**, 50–61.

Pringle, A. W. 1985. Holderness coast erosion and the significance of ords. *Earth Surface Processes and Landforms*, **10**, 107–124.

Reinders, F. J. and Associates Canada Limited 1988. Littoral Cell Definition and Sediment Budget for Ontario's Great Lakes, Final Report 1988. Ontario Ministry of Natural Resources, Conservation Authorities and Water Management Branch.

Rogers, A. L. and Ravens, T. M. 2008. Measurement of longshore sediment transport rates in the surf zone on Galveston Island, Texas. *Journal of Coastal Research*, **24**, 62–73.

Rosati, J. D. 2005. Concepts in sediment budgets. *Journal of Coastal Research*, **21**, 307–322.

Rosati, J., Gingerich, K. J., Kraus, N. C., Smith, J. M. and Beach, R. A. 1991. Longshore sand transport rate distributions measured in Lake Michigan. *Coastal Sediments '91*, ASCE, 156–183.

Ruessink, B. G., Houwman, K. T. and Hoekstra, P. 1998. The systematic contribution of transporting mechanisms to the cross-shore sediment transport in water depths of 3 to 9 m. *Marine Geology*, **152**, 295–324.

Ruessink, B. G. and Jeuken, M. C. J. L. 2002. Dunefoot dynamics along the Dutch coast. *Earth Surface Processes and Landforms*, **27**, 1043–1056.

Sanderson, P. G. and Eliot, I. 1999. Compartmentalisation of beachface sediments along the southwestern coast of Australia. *Marine Geology*, **162**, 145–164.

Saville, T. Jr. 1950. Model study of sand transport along an infinitely long, straight beach. *Transactions of the American Geophysical Union*, **31**, 555–565.

Schoonees, J. S. and Theron, A. K. 1995. Evaluation of 10 cross-shore sediment transport/morphological models. *Coastal Engineering*, **25**, 1–41.

Sherman, D. J. and Greenwood B. 1984. Boundary roughness and bedforms in the surf zone. In Greenwood B. and Davis, R. A. Jr. (eds.), *Hydrodynamics and Sedimentation in Wave-dominated Coastal Environments*. Developments in Sedimentology 39, Elsevier, Amsterdam, pp. 199–218.

Sherman, D. J., Short, A. D. and Takeda, I. 1993. Sediment mixing-depth and bedform migration in rip channels. *Journal of Coastal Research*, **15**, 39–48.

Ship, R. C. 1984. Bedforms and depositional sedimentary structures of a barred nearshore system, eastern Long Island, New York. *Marine Geology*, **60**, 235–259.

Silva, A., Taborda, R., Rodrigues, A., Duarte, J. and Cascalho, J. 2007. Longshore drift estimation using fluorescent tracers: New insights from an experiment at Comporta Beach, Portugal. *Marine Geology*, **240**, 137–150.

Stewart, C. J. and Davidson-Arnott, R. G. D. 1988. Morphology, formation and migration of longshore sandwaves; Long Point, Lake Erie, Canada. *Marine Geology*, **81**, 63–77.

Swales, A., Oldman, J. W., and Smith, K. 2006. Bedform geometry on a barred sandy shore, *Marine Geology*, **226**, 243–259.

Thevenot, M. M. and Kraus, N. C. 1995. Longshore sand waves at Southhampton Beach, New York: observation and numerical simulation of their movement. *Marine Geology*, **126**, 249–269.

Tonk, A. and Masselink, G. 2005. Evaluation of longshore transport equations with OBS sensors, streamer traps, and fluorescent tracer. *Journal of Coastal Research*, **21**, 915–931.

van der Werf, J., Ebbe J., Ribberink, J. S., O'Donoghue, T. and Doucette, J. S. 2006. Modelling and measurement of sand transport processes over full-scale ripples in oscillatory flow. *Coastal Engineering*, **53**, 657–673.

Verhagen, H. J. 1989. Sand waves along the Dutch coast. *Coastal Engineering*, **13**, 129–147.

Voulgaris, G. and Collins, M. B. 2000. Sediment resuspension on beaches: response to breaking waves. *Marine Geology*, **167**, 167–187.

Wang, P., Kraus, N. C. and Davis, R. A.Jr. 1998. Total longshore sediment transport in the surf zone: field measurement and empirical prediction. *Journal of Coastal Research*, **14**, 269–282.

Watts, G. M. 1953. *A study of Sand Movement at South Lake Worth Inlet*, Florida. Beach Erosion Board, Technical Memorandum 42.

Webb, M. P. and Vincent, C. E. 1999. Comparison of time-averaged acoustic backscatter concentration profile measurements with existing predictive models. *Marine Geology*, **162**, 71–90.

Wiberg, P. L. 1995. A theoretical investigation of boundary layer flow and bottom shear stress for smooth, transitional and rough flow under waves. *Journal of Geophysical Research*, **100**, 22667–22679.

Part III

Coastal Systems

8

Beach and nearshore systems

8.1 Synopsis

Sandy beach and nearshore zones extend from the limits of wave action on the beach backshore offshore to the limit of the movement of sand on the bed by waves. These are the most dynamic of coastal systems and there is a continuous exchange of sediment between the two, driven by alternations between storm and fairweather conditions. Because even quite small waves are capable of moving sand, the continued presence of beaches reflects a dynamic equilibrium between processes that act to move sediments offshore and those that tend to move them onshore. On sandy coasts the profile normal to the coast tends towards an equilibrium form with slope decreasing exponentially offshore. The actual steepness of the profile is controlled primarily by grain size, with the slope decreasing with decreasing grain size. Repeated measurements over a period of years shows that the elevation of the bed can fluctuate over one or two metres or more close to shore, but that the amount of fluctuation or reworking by waves decreases into deeper water. This is a response to decreasing wave orbital motion with water depth and the decreasing frequency of storm events with waves large enough to move sediment in deeper water.

The beach and nearshore profile may be smooth, or more often it is characterised by the presence of sand bars and associated troughs landward of them. The number of bars, bar morphology and the dynamic movement of the bars are controlled by factors such as the wave climate, nearshore slope and sediment size. Bars may be linear and parallel to the shore, but they also assume a variety of crescentic or rhythmic forms, with the latter usually associated with rip cell development. Bars can develop in the intertidal zone on gently sloping coasts, especially in mesotidal or macrotidal areas. They continuously change their form and position in response to changing wave conditions. On coasts with a limited fetch which are subject primarily to storm waves, bars may be present throughout the year, but on coasts subject to long-period swell waves, prolonged periods of non-storm conditions can lead to onshore migration of the bars and their incorporation in the beach face.

The subaerial beach may be straight over distances of many kilometres, but where there are bedrock headlands present, the beach usually takes on a curved form that reflects the refraction pattern of incident waves. Beach form may also be rhythmic in form on a scale of hundreds of metres, reflecting the pattern of rhythmic inner bars and the development of rip cell circulation. On a smaller scale, beach cusps, with a wavelength of metres to tens of metres, form under low wave conditions where the foreshore is quite steep.

8.2 Beach and nearshore sediments and morphology

Beaches consist of an accumulation of unconsolidated sediments ranging from fine sand to large cobbles which have been transported and

deposited by waves and currents. Sandy beach systems are found along about 20% of the world's coasts and gravel or cobble beaches account for another 10 % or so, particularly in high latitude areas. In this context we will exclude muddy coasts from the definition of beaches because the cohesion of muddy sediments gives rise to completely different dynamics and forms. This is convenient also because muddy coasts do not really fit the public perception of beaches. While the strict definition of a beach covers the zone extending from the landward limit of wave action during storms to the low tide limit (Figure 8.1) it is recognised that sediments continue offshore and that there is a significant exchange of sediments between those that are exposed on the beach and those underwater. We can characterise the whole zone over which sediment transport by waves occurs as the littoral zone. The littoral zone incorporates the nearshore zone between the low tide line and the offshore limit of wave action on the bed and the beach which lies landward of this. On sandy coasts the beach is usually backed by a dune system and both sandy and gravel/cobble beaches can be backed by a barrier and lagoon system or by cliffs.

The primary beach and nearshore system can be subdivided into three sub-systems along a profile normal to the shoreline (Figure 8.1):

(1) The outer shoreface extending offshore to the wave base. This zone is dominated by oscillatory motion generated by shoaling waves, by tidal currents and by wind-driven circulation. Large rip cell circulation extends into this zone from the breaker zone during intense storms. The slope is generally planar

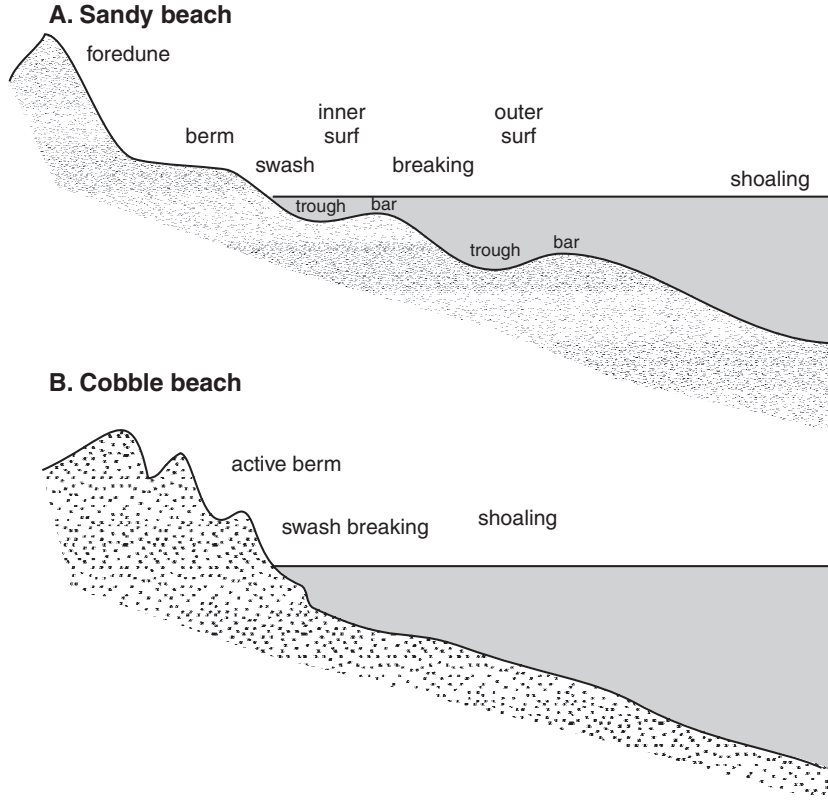

Figure 8.1 Profile of the littoral zone for (A) a gently sloping sandy beach and (B) a steep cobble beach showing the dynamic zones and characteristic features.

to curvilinear in profile, though some 3D topography may be present.

(2) The inner shoreface extending roughly from mlw to seaward of the (outer) breaker zone. On sandy beaches the transition is often marked by a sharp break in slope. This zone may be absent on very steep shorelines, e.g. cobble beaches, or on highly reflective sandy beaches. The main processes are associated with: wave breaking and the generation of surf bores; mean flows associated with wave set up, including longshore, rip and undertow; infragravity edge and reflected waves; tidal currents; and wind-generated currents. The topography may be simple and planar or curvilinear in profile, or complex with one or more nearshore bar and trough systems present. Three-dimensional topography is common, particularly on barred shorelines.

(3) The beach system extending from mean low water to the landward limit of wave action. The main processes are associated with swash and backwash action. Water motion and sediment transport is influenced by infiltration into the subaerial part of the beach and by offshore flows driven by gravitational effects on the swash slope. On steep beaches and/or under low-wave conditions primary wave breaking may occur here; Wave/wave interaction and wave/bed interaction may produce reflection and lead to transfers of energy to low frequencies. On low-gradient beaches backwash is less effective and the beach becomes an extension of the surf zone and run-up is dominated by surf beat. In the intertidal zone ephemeral swash bars may be present, and on wide intertidal zones several permanent bars and troughs may occur.

Except in very sheltered embayments storm waves are capable of moving sediments up to 10 cm or more in diameter and transporting them onshore, offshore and alongshore. Simple observations show that beaches, and especially sandy beaches, are highly dynamic in form, changing in response to varying wave and tidal conditions both temporally at one location and spatially in response to differing sediment size, exposure and tidal range. As is the case in other environments involving sediment transport by fluids (rivers, aeolian), there is considerable feedback between the processes controlling sediment transport and the characteristic forms at both the micro-scale (ripples, dunes) and particularly the meso-scale (bars and troughs; swash slope forms). The interaction between coastal process and morphology is termed beach and nearshore morphodynamics. We will assume for the purpose of simplicity that the profile is entirely developed in sediment – i.e. that bedrock or mud does not outcrop along the profile. The form of the profile is thus assumed to be in equilibrium with the factors that control sediment movement, including sediment size, shape and density, and wind, wave and tidal processes.

8.2.1 Measurement of morphological change

The processes associated with waves, currents and sediment transport and the instruments used to measure them have already been described in Chapters 4–7. Morphodynamics also requires measurement of form and form change (accretion and erosion). This section provides an overview of approaches and instrumentation for carrying this out.

Profile form

The form of the beach and nearshore profile on sandy beaches, and especially the spatial and temporal variability of that form, has probably received more attention than any other aspect of coastal morphology. In part this is because of the belief that the beach form is in dynamic equilibrium with waves and other controlling processes. Thus spatial variability in form can be linked to changes in beach orientation and wave climate, while temporal changes at a site reflect changes in the intensity and character of the incident waves – e.g. transitions from high-energy conditions during storms to low-energy swell waves during fair-weather periods.

Over many decades the standard technique for measuring the beach and shallow profile was through the use of a level and stadia rod along profiles set up normal to the shore and

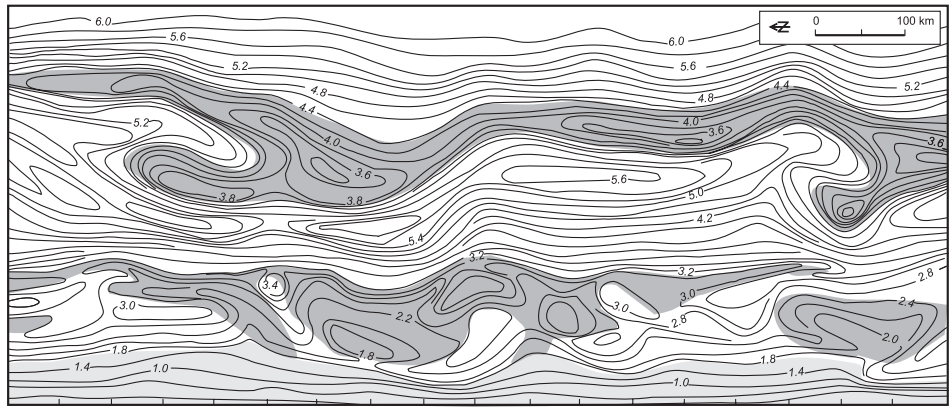

Figure 8.2 Contour map of the beach and nearshore zone associated with a crescentic two bar system in Kouchibouguac Bay, New Brunswick produced by surveying along lines at 30 m intervals and echo sounding along every.

surveyed out to the limit of wading (Evans, 1940; King and Williams, 1949; Davis *et al.*, 1972). Extending the profile seaward was initially carried out by sounding with a lead line but in the 1960s this could be carried out with echo sounders in a boat small enough to be able to permit an overlap of the surveys. Complete mapping into quite shallow water can be carried out with multibeam echo sounding (Gorman *et al.*, 1998). Morphological change along a profile can be determined by repeated surveys and by surveying a number of closely spaced profiles the data could be aggregated to produce a contour map (Davis and Fox, 1972; Greenwood and Davidson-Arnott, 1975 – see Figure 8.2). Surveys are now routinely done with a total station and the advent of differential GPS with a vertical accuracy of ±2–3 cm permits much more rapid acquisition of detailed surveys. Similarly, data from an echo sounder can now be recorded simultaneously with positional data from a DGPS. The output from all of these is readily incorporated into a wide range of contouring and Geographic Information System (GIS) software packages which can produce digital elevation models and permit easy extraction of volume change through repetitive surveys.

A non-trivial task is that of obtaining surveys of profile changes during high energy conditions. While measurements of the process dynamics – waves, currents and suspended sediment concentration – have been made during storms for several decades, most morphological change has been determined from surveys carried out before and after the event. Profiles may be surveyed under moderate wave conditions using some form of buggy (e.g. the CRAB used at the field research facility at Duck, North Carolina – Plant *et al.*, 1999). A towed sled equipped with instrumentation for measuring waves currents and suspended sediment concentration can also be used to track position and depth along the profile using a total station or GPS (Sallenger *et al.*, 1983; van Maanen *et al.*, 2008 – see Figure 8.3). However, the sleds and buggies are really only operational up to moderate wave conditions. During high wave conditions measurements can be obtained after a fashion from piers such as the Field Research Facility at Duck or from temporary structures, but these are major logistical undertakings at a few restricted sites.

Some insights into nearshore bar dynamics have come from the analysis of wave breaking intensity recorded by time exposures of the beach and nearshore. This has been done at a number of locations world-wide using the Argus video monitoring system (Holman and Lippman, 1986) where ten minute video records are averaged to produce a single image with the location of bars and the beach face outlined by a bright band associated with the location of wave

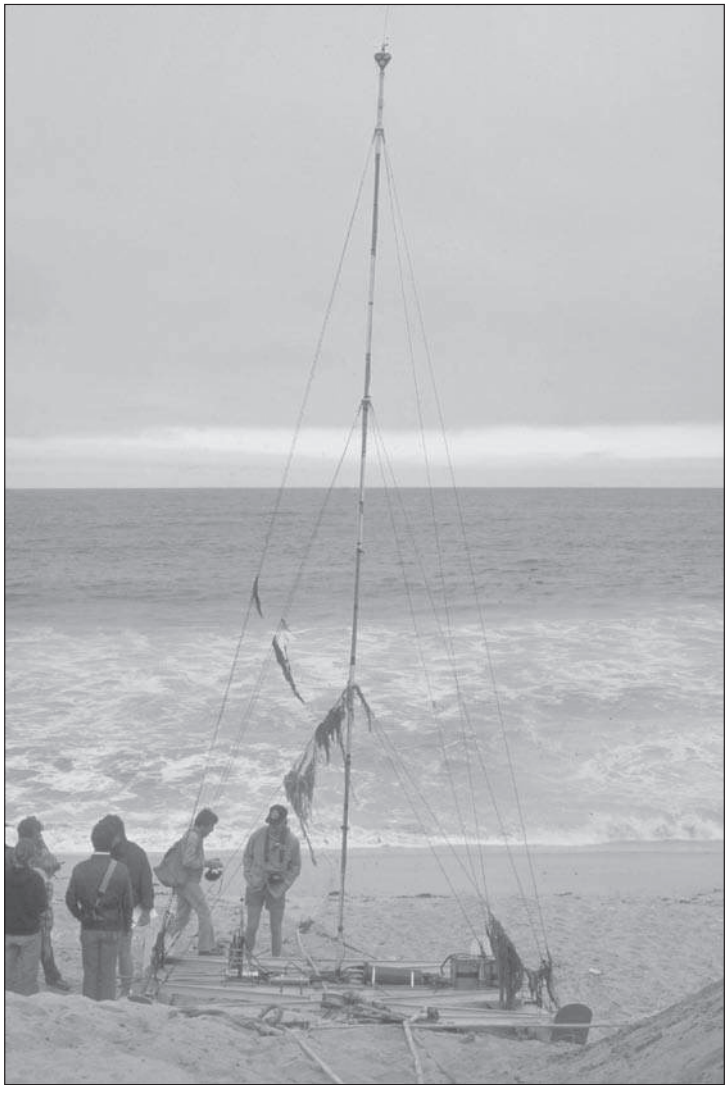

Figure 8.3 Photograph of the sled used by Sallenger *et al.* (1983) to measure wave and current dynamics and topography on the California coast. The sled was winched offshore as well as onshore, necessitating a complicated offshore mooring and providing a number of logistical difficulties. Other systems use a boat to carry the sled offshore and only winch it onshore.

breaking and the troughs and rip channels being relatively dark. This can also be done using a SLR camera and taking a series of images and processing them in the same way that the Argus video scenes are processed (see Figure 6.9). Alternatively the shutter can be opened for tens of seconds thus producing a single averaged image (Shand *et al.*, 2001 – see Figure 8.4). Continuous monitoring over months and years provides a data set of 2D bar form and position which has greatly enhanced our knowledge of bar dynamics on this time scale. However, the images do not provide actual elevation data and some caution has to be exercised because of the errors associated with rectification to horizontal coo-ordinates and because breaking intensity will vary with incident wave height and period, and with tidal stage (Morris *et al.*, 2001).

The use of digital images from still and video cameras to produce Digital Elevation Models (DEMs) through a variety of computer software packages is of especial interest in mapping shoreline changes and changes in the morphology of the beach and foredune area (Chandler, 1999). The technique makes use of overlapping pairs of photographs produced either in the

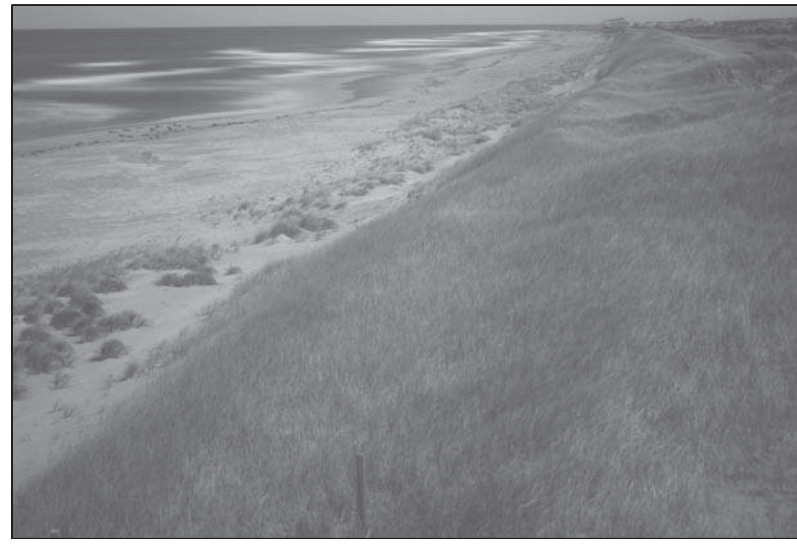

Figure 8.4 Photograph of the nearshore bar and trough system at Greenwich Dunes obtained using a 30 second exposure from a digital SLR camera mounted on a tower 12 m above the beach. The exposure was taken at night and the brightness has been enhanced in post processing.

traditional way through the movement of the camera installed in a plane, helicopter, or a land-based vehicle, or through the use of images taken from two fixed positions. In the case of aerial photography or moving vehicles the position of each digital image can be linked to real time positional data provided by DGPS. Where fixed cameras are used on the beach control points whose position and elevation have been surveyed precisely are used to aid in rectification Hancock and Willgoose, 2001). The advantage of these automated photogrammetric systems is that they can provide a very large number of data points for construction of the DEMs and much of the processing can be automated, thus allowing the evolution of topography over days, weeks or months to be captured.

In the past decade the use of airborne LiDAR to map extensive sections of beach and dune systems has increased dramatically (e.g. Zhang *et al.*, 2005; Robertson *et al.*, 2007). Use of a system which simultaneously uses a near-infrared laser to measure ground topography and a green laser to measure underwater topography can permit mapping both of beach and dune change as well as the nearshore zone (Robertson *et al.*, 2007). This coverage still essentially provides before and after measurements, but the level of accuracy and the spatial coverage are a long way from the rod and level surveys of thirty years ago.

Bed elevation measurements

Simple measurements of change in bed elevation at a point and the total depth of activation can be made with rods emplaced along a profile or on a grid and which are measured before and after a storm (Greenwood *et al.*, 1979). The maximum scour depth can be resolved by placing a washer on the sand surface and then measuring the depth of burial following the storm. Results from a grid of these can be used to measure volume change in the nearshore (Greenwood and Mittler, 1984). It is possible to measure these with SCUBA during periods of moderate wave activity and tall rods placed along a line in the intertidal and shallow subtidal have been monitored through a storm (Aagaard *et al.*, 1998), Recently automated devices which act in a similar fashion have been developed using a vertical array of photo cells spaced at a small increment (Lawler, 1992) or the difference in conductivity between sediments and sea water to distinguish the bed level (Ridd, 1992). These devices both have some problems in distinguishing the bed during periods of high sediment transport and suspension because the sand/water interface becomes quite blurred. The value of these instruments is that they are relatively low cost and therefore provide the potential for deployment of sufficient sensors to give reasonable spatial coverage across the surf zone, and to provide

Box 8.1 The Argus video system

The use of GPS which integrates signals from three or more satellites to determine location and elevation for a variety of surveying tasks is now becoming standard in measuring beach form and change as it is in so many other fields (Plant *et al.*, 1999). Video technology has been applied for more than a decade to measure waves and swash run-up (see below) but it has also been applied to measurement of the position of nearshore bars through time exposure of wave breaking (Holman and Lippman, 1986; Konicki and Holman, 2000; Ruessink *et al.*, 2000; Holman and Stanley, 2007). The intensity of wave breaking is captured by creating time exposure images over a period on the order of 10 minutes and the resultant smooth white bands outlining the zones of wave breaking on shallow bar crests and at the beach. Video cameras can also be used to monitor changes in dynamic features such as tidal inlets and associated ebb and flood tidal deltas (Morris *et al.*, 2001). Following his early work on swash dynamics using a video camera, Rob Holman developed a commercial video monitoring system called Argus which could be set up on a high building or bluff overlooking a beach and programmed to take video and still photographs over periods of years. Argus cameras have been deployed to monitor beaches in many countries and their capability has been enhanced over the years (Holman and Stanley, 2007). Their success has spurred the recent development of a number of digital video and still camera monitoring systems and their application to a wide variety of monitoring programmes.

measurements throughout a storm. Attempts have been made to use bottom mounted sonars, either fixed or mounted on a frame to permit survey of a traverse thus permitting determination of two-dimensional bedform properties and migration rates (Greenwood *et al.*, 1993).

8.2.2 Beach sediments

We can recognise three types of beaches based on sediment size: (1) sand beaches (mean sediment size ranging from about 0.1–4 mm); (2) gravel beaches composed of pebbles and/or cobbles (mean grain size about 0.5–25 cm; and (3) mixed sediment beaches – sand and pebble, or sand and cobble (Figure 8.5). Two forms of mixed sediment beach can be identified (Jennings and Shulmeister, 2002), one where sediment is uniformly mixed over the profile and one where there is a distinct sorting with coarse material forming a steep upper beach and sand forming a gently sloping lower beach (Figure 8.5d). The composition and size of the beach sediments reflects primarily the source material and secondarily the processes of sorting, abrasion by wave action and chemical weathering. Since quartz crystals are highly resistant to weathering and abrasion, a large proportion of sediment transported to the beach from rivers or cliff erosion consist of quartz with secondary amounts of feldspars and perhaps some minor heavy minerals such as magnetite and garnet. In volcanic areas black sand beaches are common made up of fragments of andesite or basalt, or crystals of augite or hornblende. In tropical regions carbonate sediments are supplied from the abrasion of corals, coralline algae and shells (Figure 8.5a). Shells and shell hash is a component of many beach sediments and occasionally on low energy beaches shells can be the dominant material (Figure 8.5e).

The dynamics of sediment erosion, transport and deposition by waves, especially on the swash slope is greatly influenced by the density and shape of the particles making up the beach. Fine grains of heavy minerals such as magnetite are hard to erode because of their high density and they also tend to get buried below the lighter, coarser quartz grains. Irregular fragments of shell tend to have a much lower settling velocity than equivalent size spherical quartz grains while fragments of coral and oolites have

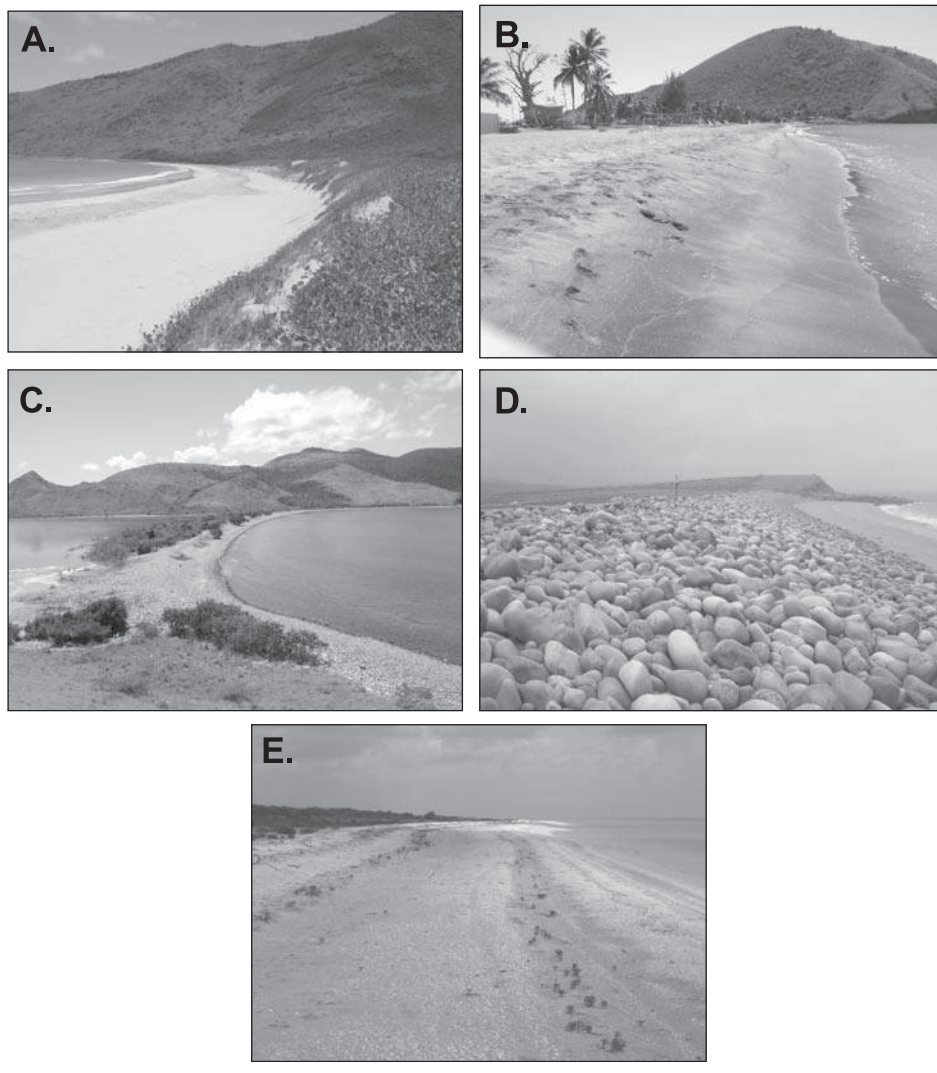

Figure 8.5 Photographs of beach types: (A) gently sloping beach in fine carbonate sands, Sandbanks Beach, St Kitts; (B) medium to coarse sandy quartz and feldspar beach with berm and steep swash slope, South Frigate Beach, St Kitts; (C) cobble beach in andesite with steep swash slope, Great Salt Pond, St Kitts; (D) mixed igneous and metamorphic cobbles and quartz sand beach, west coast Ireland; (E) small storm beach ridges in shells at Sabancuy on the Yucatan coast of Mexico (photo courtesy Patrick Hesp).

a much lower density than the equivalent quartz spheres and are thus easier to transport by both water and wind.

It has long been recognised that particle size is an important control on the slope of the subaerial beach (Bascom, 1951; McLean and Kirk, 1969) due to the effect of infiltration in reducing the volume of water in the backwash (Figure 8.6). The amount of infiltration generally increases with increasing grain size and the volume loss due to infiltration means that not all of the sediment brought up the foreshore slope by a swash event is returned by the succeeding backwash. Sediment build-up on the upper foreshore leads to a steepening of the slope until the enhanced effect of gravity on the backwash velocity compensates for the loss of volume due to infiltration, producing an equilibrium slope. On very fine sand beaches (0.1–0.2 mm) the slope is always gentle (tan β, 0.03–0.005) because

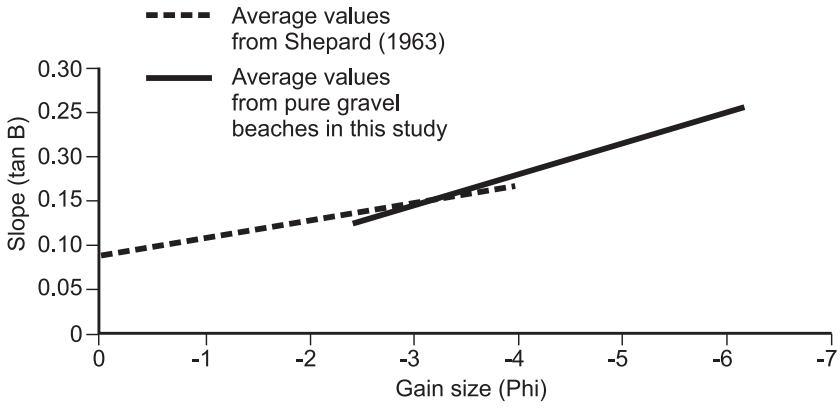

Figure 8.6 The relationship of beach foreshore slope to particle size for pure gravel beaches in New Zealand (Jennings and Shulmeister, 2002). The dashed line is the average value for sand and fine-gravel beaches based on Shepard (1963).

infiltration is low and berm development is consequently limited. At the other end of the size scale, cobble beaches always have high rates of infiltration and a steep slope (tan β, 0.1–0.25). Again, the slope does not vary much with changing wave conditions. The slope for mixed sand and gravel beaches is quite variable, both spatially and temporally at one beach because the finer sediments may infill the pore spaces of the larger particles, thus reducing infiltration and consequently the gradient (McLean and Kirk, 1969). The slope of medium to coarse sand beaches does increase with increasing size, but is also highly variable temporally as a result of changing wave conditions. Consequently, modelling must take into account not only grain size but wave conditions and tidal range over a period of hours or days (Madsen and Plant, 2001).

On sandy beaches the nearshore slope is comparatively gentle and there is considerable exchange of sediment between the beach and the nearshore. Wave asymmetry and the sorting process associated with ripples tends to move coarse sediments landward towards the step while finer sediments are preferentially transported offshore above the bed in the undertow or rip currents (Horn, 1992). Thus, seaward of the breaker zone grain size tends to decrease (Figure 8.7) and there is consequently a gradual decrease in the bed slope. Towards the seaward end of the profile sorting becomes poorer as fine sediments that settle out of suspension after a storm are incorporated and in some cases mean sediment size increases as a result of winnowing of fines to leave a coarse lag (Liu and Zarillo, 1989).. In the breaker and surf zones grain size variations reflect topographical controls (Greenwood and Davidson-Arnott, 1972 ; Wang and Davis, 1998). Sediments on the crest and seaward slope of bars are generally well-sorted while sediments at the base of the trough are more poorly sorted as a result of both the accumulation of coarse material washed over the bar and fine sediments settling out of suspension during low-wave conditions (Figure 8.7). Relatively coarse sediments are also found in rip channels where there is considerable bed load transport. Where the foreshore is quite steep there is a usually a distinct step present at the base characterised by the accumulation of coarse, poorly sorted sediment. Landward of the step mean grain size decreases and the sorting improves. Finally, on the backshore, surficial sediments are often aeolian in origin and tend to be finer and better sorted than those on the foreshore (Figure 8.4).

On most cobble beaches the profile remains steep beyond the step and wave breaking is largely confined to the foreshore or to a point just seaward of the step. This, and the practical difficulty of sampling cobbles in the nearshore mean that most information on particle size variation comes from the foreshore. The shape and size of the cobbles is greatly influences transport and deposition and the result is that quite distinct

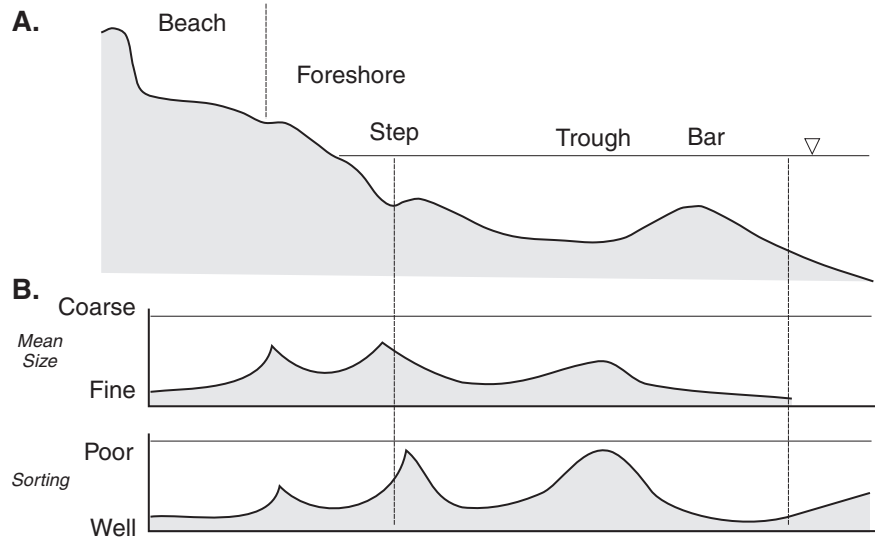

Figure 8.7 Schematic variations in sediment size and sorting on a sandy beach with one nearshore bar: (A) shore-normal profile and zones; (B) variations in mean grain size and sorting. The patterns are highly generalised and the *y* axis scales are arbitrary.

zones are often present (Figure 8.8). Round and rod- shaped cobbles roll easily and thus they tend to move up slope with the swash and roll back towards the step with the backwash. They therefore tend to be over represented near the lower part of the profile. Discs can be flipped up into the wave and present a large surface area so are often carried right to the top of the swash and thus up to and over the berm crest. Once they come to rest they present a large surface area and thus friction tends to hold them in place. Large discs are therefore often concentrated at the top of the profile (Bluck, 1967; Orford, 1975; Sherman *et al.*, 1993). However, it is evident that much of the time the distribution of cobble shape and size is more complex than the original model of Bluck (1967) because of rapid reworking through the neap/spring tidal cycle, varying wave energy levels and alongshore variations associated with the development of rhythmic beach cusps (Sherman *et al.*, 1993).

8.2.3 Sandy beach profile

Sweep zone

Repeated surveys along a profile line over months and years on sandy beaches shows that there is considerable variability in shallow water and on the beach foreshore, and that the extent of the vertical change decreases into deep water to the point of closure where changes become imperceptible (Hallermeier, 1981). The zone between the maximum bed elevation and the minimum bed elevation is termed the sweep zone and it represents the extent of reworking by wave action and migration of topographic forms, though it does not account for a small amount of additional reworking due to bedform migration (Figure 8.9). The depth of closure conceptually marks the offshore limit of the zone of sediment circulation between the nearshore and the beach systems though sand movement and bedform generation will occur to greater depths. The greatest vertical change is found on barred beaches where onshore and offshore migration of the bar and trough system lead to large vertical changes at any location. The step and base of the foreshore is also an area of extensive reworking.

The depth of closure clearly reflects in some way the largest storm waves and it is possible to predict the depth of closure using a simple empirical equation such as that provided by Hallermeier (1981):

$$h_c \approx 2H_{sig} + 11\sigma \tag{8.1}$$

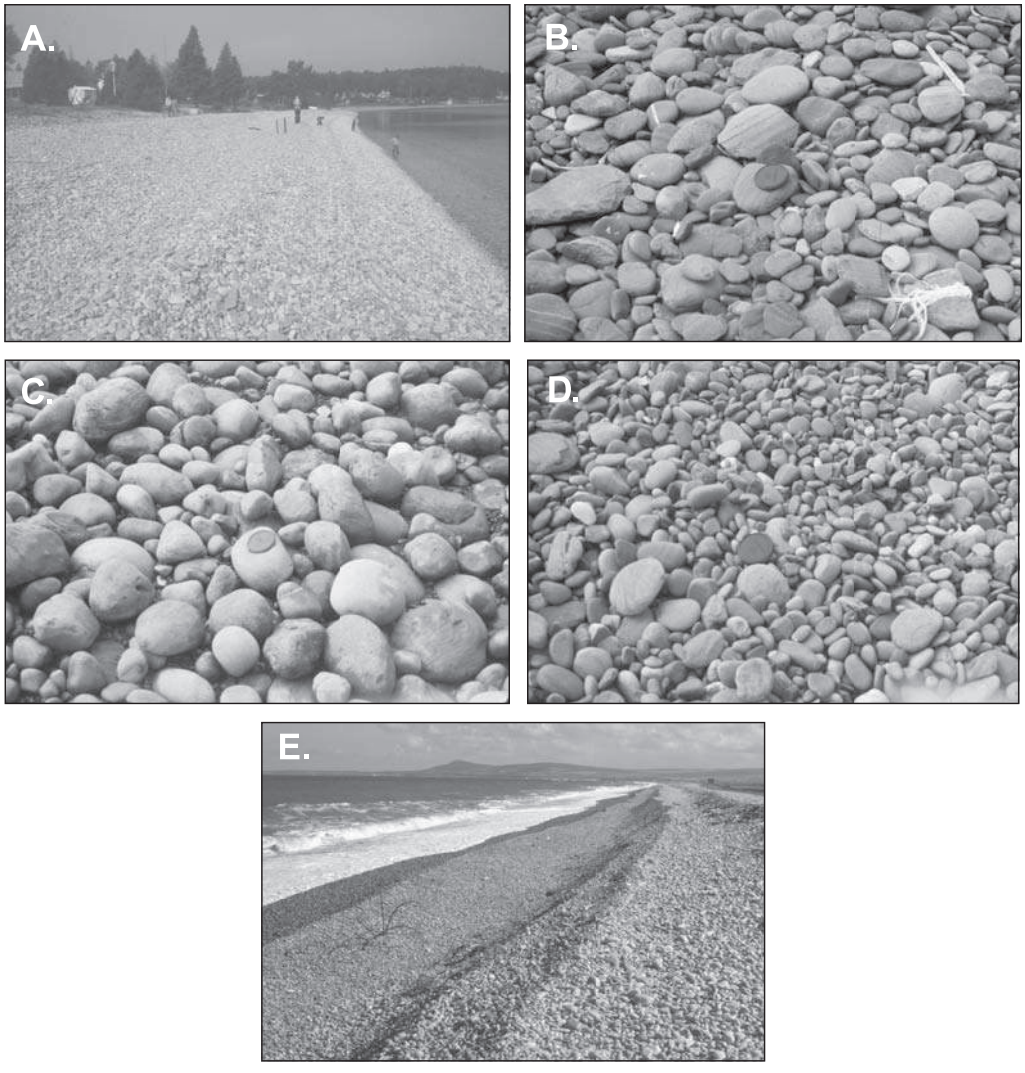

Figure 8.8 Gravel beach sediments: (A) gravel beach in dolomitic cobbles, Barrow Bay, west coast Georgian Bay, Ontario; (B) disc-shaped cobbles on the crest of the berm ridge; (C) rounded pebbles in the infill zone near the bottom of the swash slope; (D) imbricate pebbles and cobbles below the berm crest; (E) gravel beach in rounded pebbles and small cobbles east coast Scotland. The largest cobbles are found on the crest of the highest berm ridge but particle size variation over the profile is complicated by the presence of smaller berms formed under varying wave and tidal conditions.

where h_c is the depth of closure, H_{sig} is the mean annual significant wave height and σ is the standard deviation of H_{sig}.

Equation (8.1) is a simplified version of one that included both height and period of waves that was exceeded for only 12 hours in any one year. Since these may not be readily available and since there is likely considerable uncertainty in the actual definition of closure depth, (8.1) probably provides a reasonable estimate. Interestingly it does not account for sediment size, though on most equilibrium profiles this is likely quite similar and in the fine sand range. Evaluation of 10 years of profile data from Duck, North Carolina gives support to the basic relationship proposed by Hallermeier (Nicholls *et al.*, 1998).

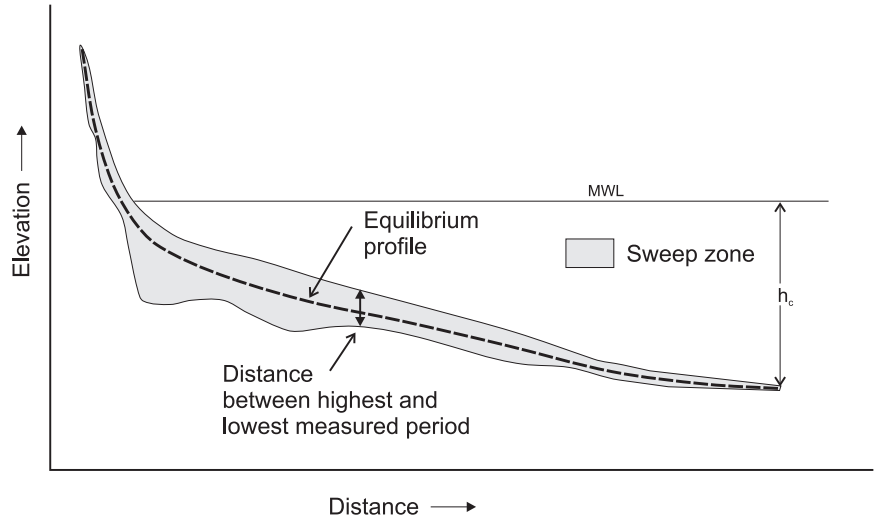

Figure 8.9 Schematic representation of the sweep zone and depth of closure for a typical barred profile in medium sand.

Equilibrium profile form

Sand has a small mass compared to the forces exerted by wave motion, especially by large waves during storms. Observations and measurements indicate that sand is transported continuously in suspension, as bed load and collectively through migration of sand bars. The continued existence of sand on the beach and in the nearshore, and the existence of characteristic profile types, suggests that there is a dynamic equilibrium between the forces controlling sand movement and that it should be possible to predict profile form and changes from some relatively simple combination of parameters. Much effort has gone into elucidating the nature of the controls on profile equilibrium and on developing and justifying predictive relationships. It is useful to identify what are likely some of the important controls but given the complexity and variability of coasts world-wide, it seems overly optimistic that their behaviour can be predicted by some simple combination of wave steepness and sediment size!

Sand size decreases offshore from the surf zone. If we ignore for the moment the small form variation due to the presence of bars and troughs in the inner nearshore on some sandy beaches, it can be seen that the general profile form of a sandy beach and nearshore tends to be exponential (Figure 8.9). It is likely that this is related to the increase in bed shear velocity and wave asymmetry as waves shoal across the nearshore, as well as to the general decrease in sand size with depth and distance offshore. There have been a number of approaches to deriving a theoretical profile shape related to the dynamics of waves and sediment transport (e.g. Bowen, 1980) or to energy dissipation (Bruun, 1954). Dean, in various publications over a number of years (e.g., Dean, 1991; Dean *et al.*, 1993) has promoted an equilibrium profile of the form

$$h = Ax^m \tag{8.2}$$

where h is the depth at an offshore distance x, A is an empirical coefficient and the exponent m is usually assigned a value of 2/3.

The coefficient A is a function of grain size and Dean (1997) derived a simple empirical relationship based on plotting A against grain size for a number of profiles:

$$A = 0.067 w_s^{0.44} \tag{8.3}$$

where w_s is the settling velocity equivalent to the mean grain size of the sediment.

An alternative approach uses an exponential model of the form (Komar and McDougal, 1994)

$$h = \frac{S_0}{k}(1 - e^{-kx}) \tag{8.4}$$

where S_0 is the slope at the shoreline, and k is an empirical constant that can be defined by

evaluating the equation at a known depth and distance offshore.

The Dean equilibrium profile is used extensively in the engineering literature, particularly as input to predicting the form of nourished beach profiles. There has been much discussion and criticism of the concept (e.g., Pilkey *et al.*, 1993; Cowell *et al.*, 1999; Are and Reimnitz, 2008). It seems simplistic to use a single value for grain size when many profiles show changes in grain size with depth offshore: and how do you obtain this mean? The equilibrium profile does not directly account for the presence of nearshore bars and troughs, or the general flattening of the profile in the surf zone before the steep section of the foreshore that is characteristic of non-barred profiles. This is obviously a weakness for its application on many coasts, particularly since beach nourishment is generally focused on the shallow part of the profile. Inman *et al.* (1993) suggested a compound profile and Stive and de Vriend (1995) modelled shoreface profile evolution based on three simple hinged panels that recognised that the response and evolution of the upper, middle and lower shoreface occurs at different time scales, and therefore need not be part of the same equilibrium at any point in time. Finally, it should be recognised that while many shorelines have profiles that are entirely covered in sand, the underlying bedrock or erosional surface may still influence the overall profile shape.

8.2.4 Barred and non-barred profiles

The form of the equilibrium profiles described above is generally smoothly curving and profiles in nature may approximate this form, or may be planar but with a flatter slope in the surf zone. An examination of profiles world-wide suggests four basic profile types: (1) a smooth planar to curvilinear profile without any bars in the intertidal or nearshore; (2) a profile with one or more bars in the nearshore that exist year round; (3) a profile where bars are present some or most of the time but where the bar may disappear, usually through landward migration and 'welding' to the beach; and (4) profiles with one or more permanent bars in the intertidal zone and usually one or more in the subtidal zone as well (Figure 8.10). Where bars are present they tend to be areas of preferred wave breaking, with breaking being reduced or ceasing altogether in the deeper water of the intervening troughs. Where bars are absent the surf zone may vary in width with no preferential location of breaking except as a function of incident wave height.

Bars will be absent on sandy beaches when waves break only at the shoreline because of some combination of steep slope (bedrock controlled) and/or small wave height (e.g. limited fetch areas within island archipelagos or in estuaries). However, if the profile is fully developed in sand and waves are on occasion large enough to break some distance offshore, then the presence or absence of bars in the nearshore appears to be controlled by wave climatology and sediment size – i.e. it is a response to the dynamic controls on sediment transport. Bars are absent from low latitude coasts dominated by swell waves only, particularly where wave refraction leads to divergence, producing low steepness waves that break at or close to the beach. Sediment transport on these coasts tends to be directed landward, building a relatively steep, reflective profile that exhibits relatively little dynamic change. They are also absent where relatively light winds blow over long distances, e.g. the trade wind coasts of the Caribbean (Figure 8.10a).

In mid-latitude fetch-limited areas, such as the Great Lakes, Gulf of St Lawrence and Mediterranean and Baltic seas, bars are present on almost all sandy coasts and are a constant feature of the profile (Figures 8.10b–d). Here most periods of high waves and strong sediment transport are associated with the passage of mid-latitude cyclones which produce short, steep waves and are accompanied by strong onshore winds and storm surge. On the east coast of the US bars are usually present because prevailing winds are offshore and much of the time wave action is associated with storms generating local waves. However, on the west coast of North America (e.g. California and Oregon) and the New South Wales coast of Australia bar generation takes place during storms but onshore migration occurs during non-storm periods driven by Pacific swell waves and if there is a sufficiently long interval between storms the

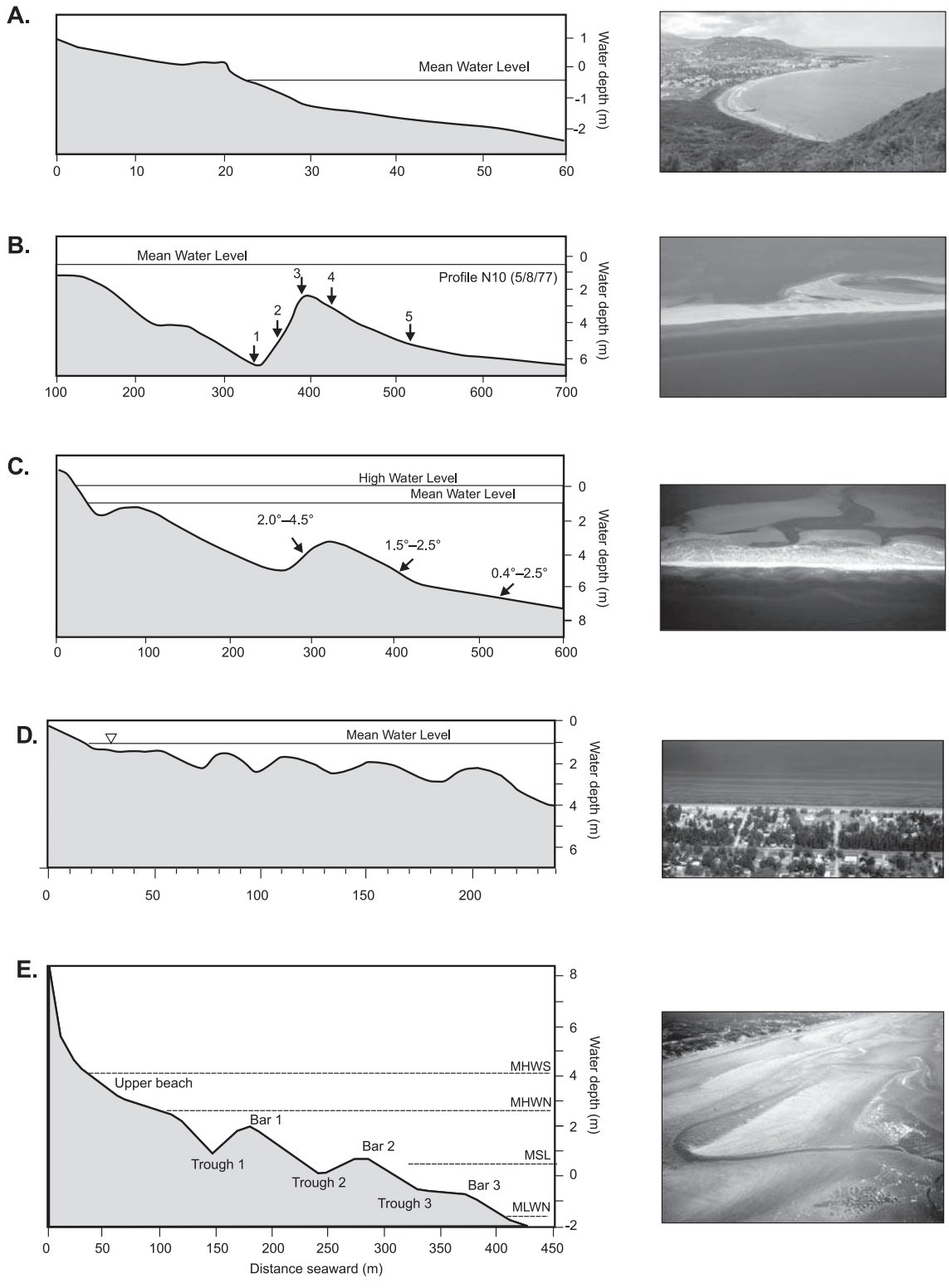

Figure 8.10 Photographs and typical profiles for beaches with differing profile form: (A) non-barred beach, North Frigate Bay, windward coast St Kitts, West Indies; (B) straight outer bar, Miramachi Bay, New Brunswick (Greenwood and Mittler, 1984); (C) crescentic two-bar system at Kouchibouguac Bay, New Brunswick, Canada (Greenwood and Davidson-Arnott, 1975); (D) multiple bars in the sub-tidal zone, Wasaga Beach, Georgian Bay (Davidson-Arnott and Pember, 1980); (E) multiple bars in the intertidal and sub-tidal zone a macrotidal coast, Wisant Bay, NW France (Sedrati and Anthony, 2007) (photograph courtesy of Edward Anthony).

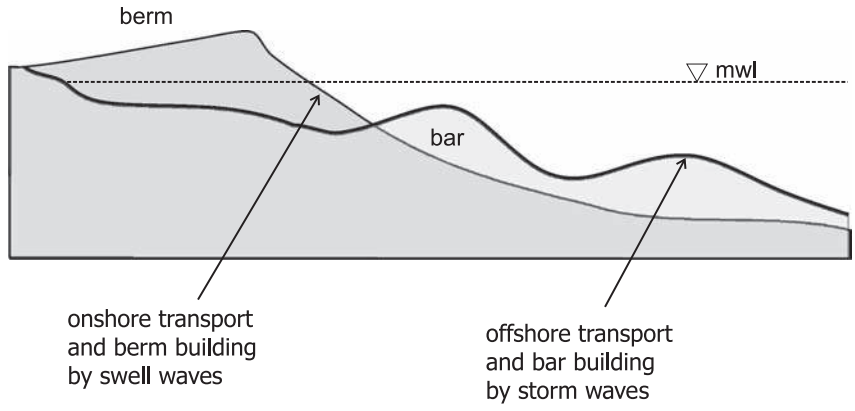

Figure 8.11 Idealised barred and non-barred profiles related to seasonal wave climate.

bars will weld to the beach producing a planar profile (Figure 8.11). Recognition of this on the California coast led to the distinction between winter (barred) and summer (non-barred) profiles (Shepard, 1950b – Figure 8.11) and the complex process of bar migration and shape changes are incorporated in the schematic Beach Stage model of Short (1979) and Wright and Short (1983) which will be described in Section 8.3.3.

Landward migration of bars from the nearshore sometimes results in one or more appearing temporarily in the intertidal zone of micro tidal coasts during the process of migration. However, on mid-latitude mesotidal and low macrotidal beaches relatively stable bars are formed within the intertidal zone where some combination of low gradient and high tidal range exposes a wide intertidal zone at low tide (Figure 8.10e). Usually one or more bars also exist in the subtidal zone and wave conditions operating on the bars appear to be similar for both the intertidal and subtidal bars.

Several simple parameters have been used in an attempt to discriminate between barred and non-barred states. Gourlay (1968) introduced the dimensionless fall velocity parameter Ω which has been used to distinguish between barred beaches (Ω < 1) and non-barred beaches (Ω > 1):

$$\Omega = \frac{H_b}{w_s T} \tag{8.5}$$

where w_s is the settling velocity of the sediment.

This was used extensively by Wright and Short (1984) in Australia to distinguish different profile states. Note that, because of the dependence of nearshore slope on sediment size, this is essentially a form of surf similarity parameter. Other parameters have been developed from wave tank studies including one by Dalrymple (1992):

$$P = \frac{gH_0^2}{w_s^3 T} \tag{8.6}$$

where bars develop for $P > 9000$ and non barred profiles occur when $P < 9000$. Short and Aagaard (1993) reviewed the literature on multibarred beaches and introduced a bar parameter B_*:

$$B_* = \frac{x_s}{gT^2 \tan\beta} \tag{8.7}$$

where X_s is an offshore distance corresponding to a particular depth at which the gradient becomes very small. No bars occur when $B_* < 20$ and an increasing number of bars occur for values $B_* > 20$.

Essentially the first two parameters relate profile form to the wave steepness and profile slope (based on the known relationship between sediment size and beach slope). The parameter of Short and Aagaard (1993) is based on the premise that standing infragravity waves are responsible for the formation of bars (which seems less and less likely) and works as long as waves are large enough to break offshore. Short and Aagaard's data set shows good correlation with slope so the additional explanation may be fortuitous.

Profiles from beaches with restricted fetch where bars are present all year round offer the best opportunity to examine relationships between bar properties and controls. Some of the earliest papers on bars (Evans, 1940; King and Williams, 1949) established that the height and spacing of bars tend to increase offshore as does the depth of water over the bar crest. On occasion the outermost bar is lower than the next one landward and this is likely because it is no longer active. Profiles from 12 sites in the Great Lakes and Gulf of St Lawrence (Davidson-Arnott, 1987) show the general trend related to bar height and spacing (Figure 8.12a). This study also found that the number of bars was highly correlated with the nearshore slope and that there was a much weaker tendency for bar number to increase with increasing fetch length for the same nearshore slope (Figure 8.12b). This is at least in part related to the distance offshore at which initial wave breaking occurs and thus the width of the zone available for wave reformation before breaking is initiated on the succeeding bar. The height of the bars and depth of water over the crest also increases seaward and is roughly proportional to the height of the breaking waves associated with them (Pruszak *et al.*, 1997). Observations suggest

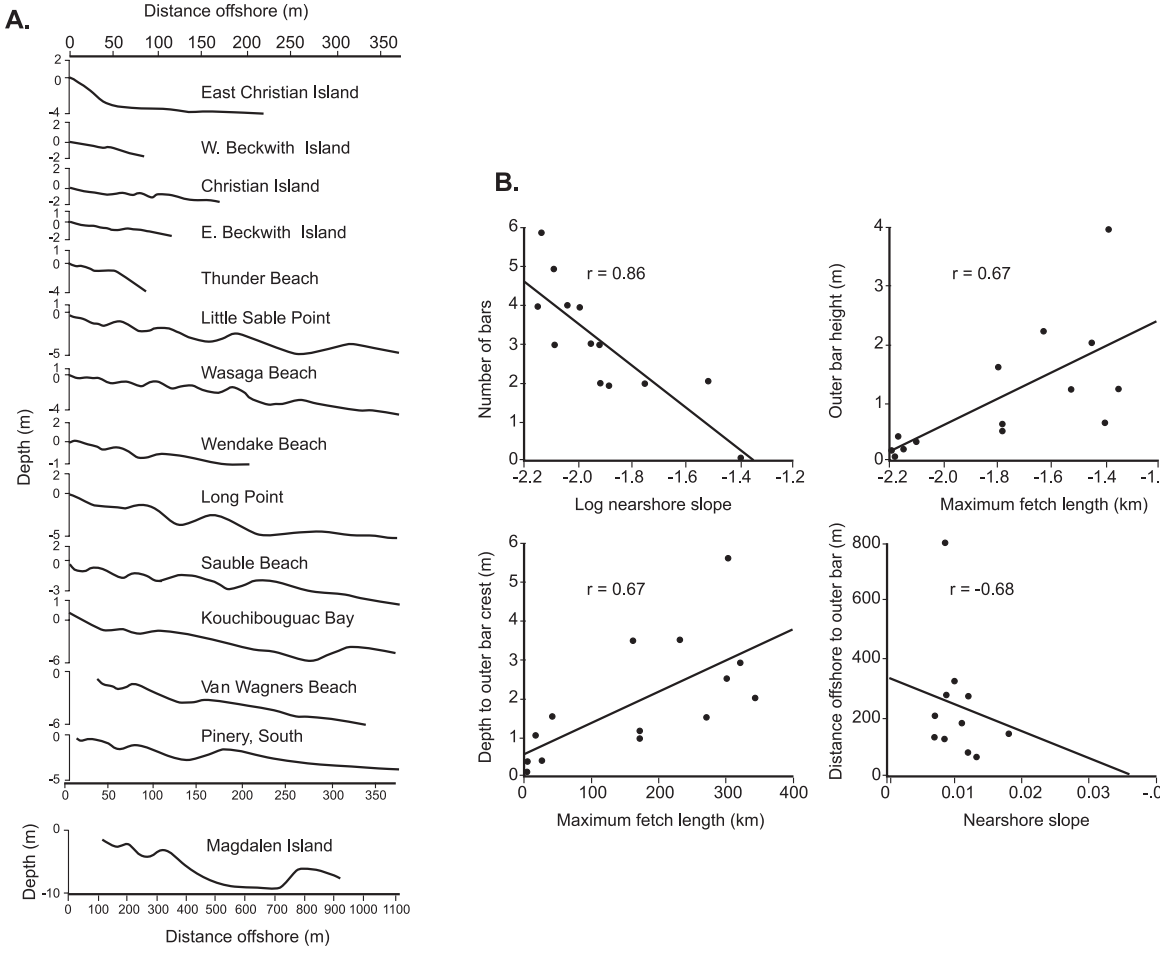

Figure 8.12 Morphological variations in nearshore bar profiles from fetch-limited areas of the Great Lakes and Gulf of St Lawrence: (A) profile form; (B) plots of regressions between morphological properties of the bars shown in (A) and various controlling parameters (from Davidson-Arnott, 1988).

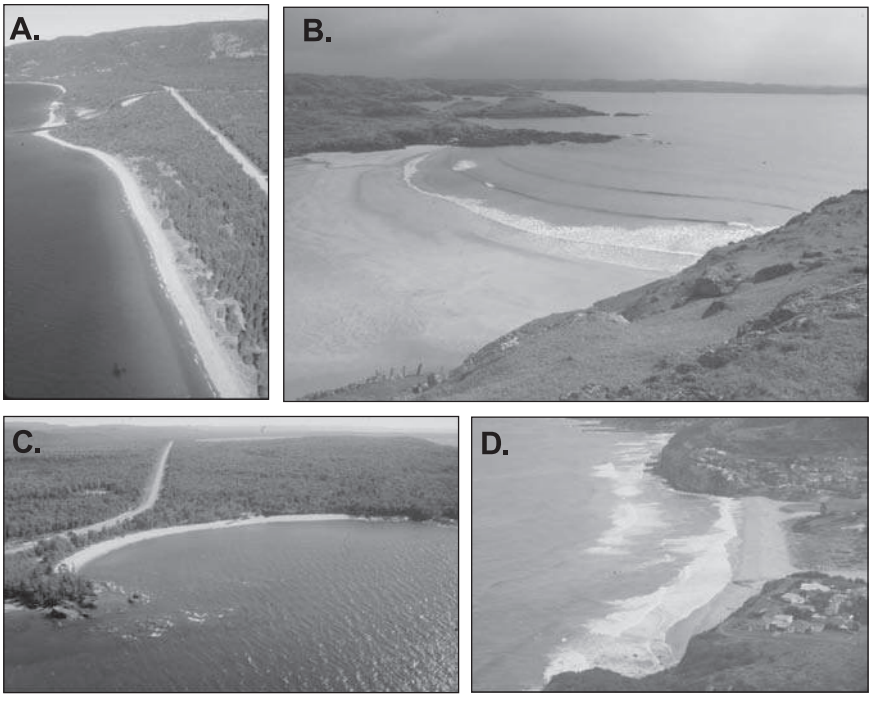

Figure 8.13 Beach planform: (A) convex shoreline in the vicinity of a small river mouth, east coast, Lake Superior; (B) photograph of a headland-bay beach, Oldshore Beg, NW Scotland; (C) curvilinear form of a headland-bay beach, north shore, Lake Superior; (D) a straight beach, Stanwell Park beach, NSW, Australia.

that during large storms bars migrate offshore until they are in an equilibrium depth associated with the height of the breaking waves (King and Williams, 1949; Greenwood and Davidson-Arnott, 1979; Sallenger *et al.*, 1985).

8.2.5 Beach plan view

In plan view sand and gravel beaches can be convex, straight or concave. Convex beaches occur infrequently, mostly around the distal end of sand spits and on deltas (Figure 8.13a). Much of the time beaches develop on a high relief coast where many of them are located in some form of embayment between headlands or anchored downdrift of a promontory and here they assume a concave form (Figure 8.13b). On coastal plains the underlying bedrock ceases to influence the large-scale beach planform development, and the form becomes very much controlled by alongshore and on-offshore sediment transport. Straight beaches are common under these conditions.

A useful concept in relation to evolution and dynamics of beach planform is the distinction between swash aligned and drift aligned beaches (or segments of beaches). Ideally swash aligned beaches are oriented perpendicular to the direction of waves (parallel to the wave crest) along a section of beach. Since the longshore sediment transport gradient (Section 7.5.3) will be 0 everywhere, an equilibrium exists whereby sand moves onshore and offshore but not alongshore. Drift aligned beaches are oriented at an angle to the dominant waves and so there is a net sediment transport in one direction with the beach equilibrium depending on a balance between the transport of sediment downdrift and the input of sediment from updrift.

The concave form of headland-bay beaches can therefore be explained in terms of wave refraction processes and the operation of the A-B-C model outlined in Section 7.5.3 (Figure 8.14). Along the sides of the headland waves arrive at an angle to the shoreline and

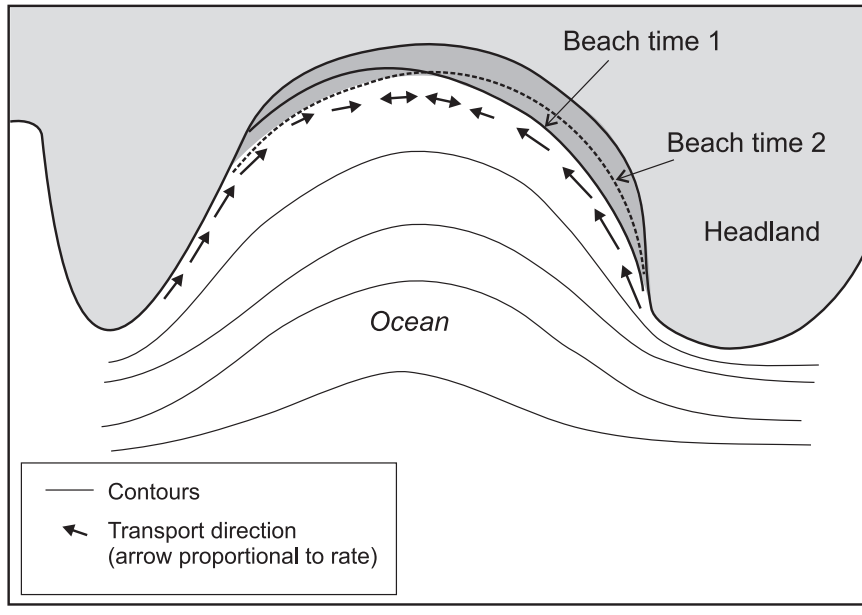

Figure 8.14 Patterns of sand movement and beach alignment on an ideal headland-bay beach and rotation of the beach under differing wave direction.

any sediment supplied from cliff erosion are transported towards the head of the bay forming a thin, drift aligned beach. Towards the head of the bay refracted wave crests become more and more aligned parallel to the shoreline, thus reducing the transport gradient and leading to more deposition and a deeper, wider beach. In the centre of the bay refraction is minimal and the beach is aligned parallel to the wave crests – i.e. swash aligned. The wave refraction pattern for Frederick Henry Bay, Tasmania (Figure 5.9) provides a good example of a series of small bays all with beaches aligned to the refracted wave crests. Sand in such embayments tends to shift from one end to the other in response to small changes in the angle of arriving waves, thus maintaining the form which is described as swash aligned.

As the spacing between the headlands increases, the central section of the beach becomes straight with curving sections at either end. Because of the reduced sheltering with more widely spaced headlands, waves can arrive at the shoreline from an increased range of angles and the orientation of the beach tends to shift from one side to the other in response to this (Figure 8.14). The beach may then rotate from one side to the other depending on individual storm events or changes in wave climate over several years (e.g. Ranasinghe *et al.*, 2004b).

On sections of exposed coast with abundant sediment and a marked longshore drift direction, the presence of widely spaced promontories or small headlands which provides some shelter from waves from the dominant direction give rise to log-spiral or zeta form beaches (Figure 8.15). Here waves from the dominant, updrift direction refract, and diffract around the headland producing a beach that is swash aligned in the lee of the headland with local sand transport in the direction opposite to the dominant drift direction along the coast some of the time. This produces a tight spiral form that can be described by a log spiral function (Yasso, 1965) or by a parabolic function. The rapid evolution of a log spiral form in unconsolidated sediments following construction of a marina on Lake Michigan (Terpstra and Chrzastowski, 1992) provides a nice example of this (Figure 8.15a). The concept of producing a static

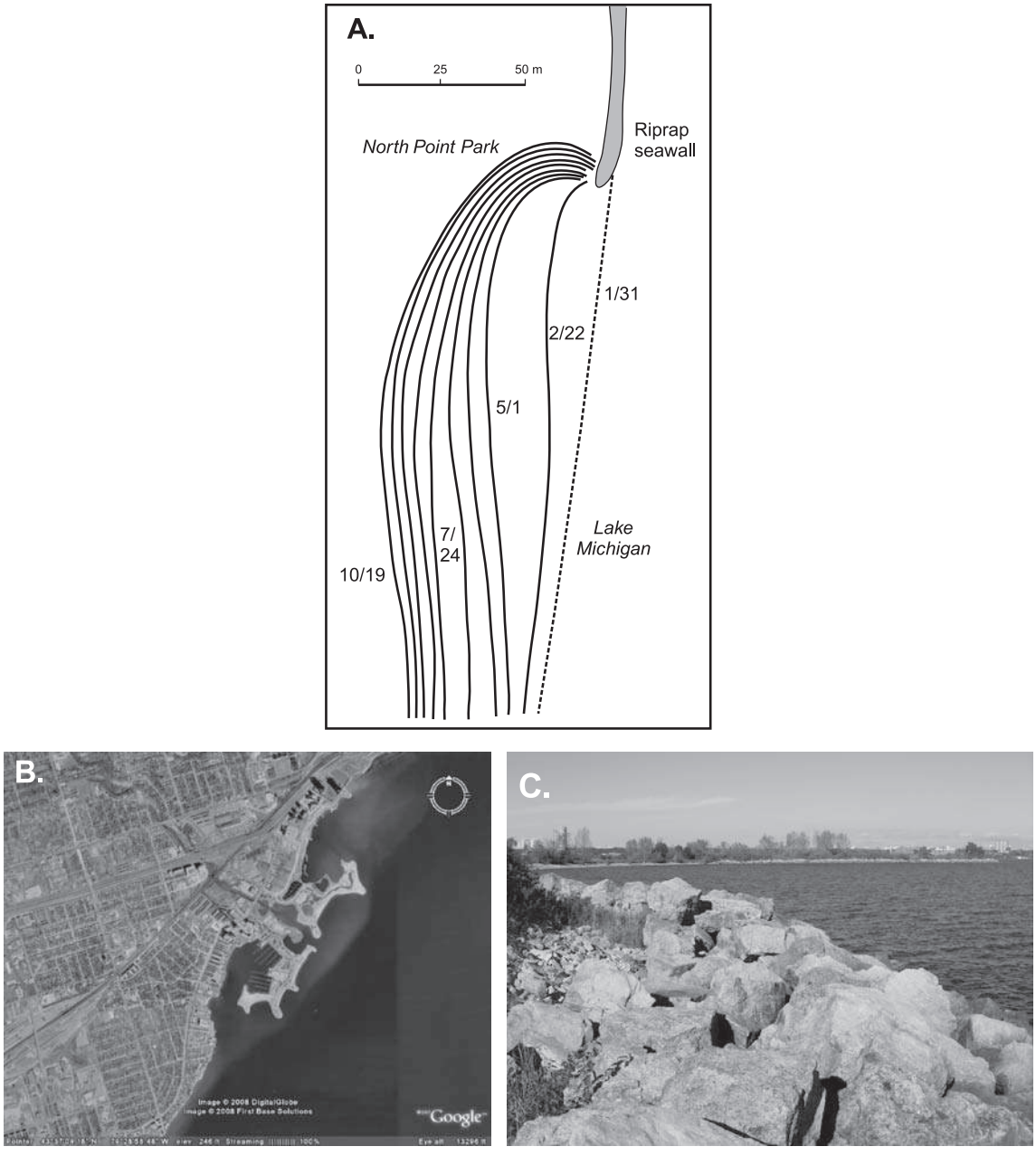

Figure 8.15 (A) Evolution of a log spiral beach downdrift from a seawall on the Illinois shoreline of Lake Michigan (after Terpstra and Chrzatowski, 1992; (B) artificial headlands and crenulate bays on a complex landfill feature, Toronto waterfront, Ontario, Canada; (C) ground view of the armourstone structures forming one of the headland structures in (B) with the Toronto skyline in the background.

equilibrium beach form has been applied to shoreline stabilisation through the use of artificial headlands (e.g. Silvester, 1974; Bishop, 1983; Hsu *et al.*, 1989; Short and Masselink, 1999; Ojeda and Guillén, 2008). The object here is to use armourstone or similar non-erodible material to produce artificial headlands or large groynes and then to fill the area between with beach sediments. The sediments are then moved by wave action until a crenulate form is attained

with the beach aligned to the waves along its length. If the beach nourishment material is quite coarse, then losses offshore and alongshore during storms are small and the beaches ideally become stable over long periods (Bishop, 1983). The concept has been used extensively in the design of artificial complexes built out into lakes and oceans that serve the purpose of stabilising the shoreline and at the same time providing for a number of recreational activities (Figures 8.15b, c).

Wave refraction and transport gradients are not the only controls on beach planform. In many cases forms evolve from headlands that reflect the underlying bedrock control or beaches are partially anchored to features as diverse as stable lag gravel and boulder deposits, drowned drumlins, eroding bluffs and the entrance to tidal inlets. On rocky coasts beach form reflects the process of erosion as much as it does sediment deposition. On pure sandy coasts planform may be a complex response to sediment transport and the angle of wave approach (e.g. Ashton *et al.*, 2001) which may influence the shape of the coastline at a range of scales from a few tens of metres to tens of kilometres.

8.3 Nearshore morphodynamics

Beach and nearshore morphodynamics are generally considered at four different temporal scales and these usually involve increasing spatial scales:

(1) *Instantaneous* (seconds to minutes): measurements of fluid processes and sediment transport processes. Morphology, incident wave field and water level are essentially constant. Local fluid and sediment transport conditions can be measured and are controlled directly by the incident wave field, winds and tides;

(2) *Short-term* (hours to days): measurements over a storm, or storm and succeeding fair weather period. Incident wave field, water levels and morphology all change.

(3) *Annual* (monthly to yearly changes): seasonal changes in morphology reflecting seasonal patterns of storm frequency and intensity and the characteristics of the incident waves and winds

(4) *Decadal*: measurements of topographic change over a period of 10–50 years. Seasonal patterns can still be recognised but changes reflect variations in storm intensities and in patterns of longshore migration of sand waves as well as changes in beach and dune sediment budget.

8.3.1 Morphological classification of bars

Bars occur in both the subtidal and intertidal zones. They are usually oriented parallel to the shoreline but oblique and transverse forms can occur close to the beach. The profile may have a single bar but 2–4 bars are common and some profiles with a very low gradient may have 10 or more bars. In plan form, bars may be linear (straight), sinuous or crescentic (three-dimensional topography). While classifications in themselves do not provide an explanation for this variability, it helps to bring some order to the complexity of the systems observed in nature and to the very large literature on bars that has developed over the past two decades.

Wijnberg and Kroon (2002) in their review of nearshore bar systems modified and updated a review and classification produced by Greenwood and Davidson-Arnott (1979) and this is shown in Table 8.1 along with the equivalent groups proposed by Greenwood and Davidson-Arnott and reference to a classic paper describing the bar type. Examples of these forms are shown in Figure 8.10. The Greenwood and Davidson-Arnott (1979) classification identified group-V bars – relatively low-amplitude bars formed by plunging breakers – not included in the updated version. The original identification of Group 5 bars reflected the large amount of work carried out in small wave tanks, and the volume of publications throughout the 1960s resulting from this, where wave breaking excavated a trough and the material was moved seaward to form a bar. It was assumed that bars observed in nature must be formed this way, particularly those monitored on the California coast. We can now recognise this as a phenomenon of scaling in small wave tanks and, while

Table 8.1 *Classification and characteristics of nearshore and intertidal bars (after Greenwood and Davidson-Arnott, 1979; Wijnberg and Kroon, 2002).*

Bar type	Location	Slope	Wave Energy	Tidal Range	Bar group	Notes
Low-amplitude ridges (King and Williams, 1949)	intertidal	0.01—0.005	low	meso- macro	I	Probably modified form of Goup VI bars
Slip-face ridges (Davis *et al*., 1972)	intertidal	0.03—0.01	low to moderate	micro- meso-	II	Migrate into intertidal zone from sub-tidal Group VI bars
Shore-attached bars (Sonu, 1968)	sub-tidal (to intertidal)	0.03—0.005	moderate	micro-macro	II	May be relatively stable on fetch limited coast
Three-dimensional longshore bars (Homma and Sonu, 1962)	sub-tidal	0.03—0.005	moderate to high	micro-macro	VI	3D form is probably secondary — rip cell circulation
Two-dimensional longshore bars (Evans, 1940)	sub-tidal	0.03—0.005	high	micro-macro	VI	2D form probably reflects dominant undertow
Highly protective settings						
Transverse finger bars (Niederoda and Tanner, 1970	sub-tidal	0.01—0.0005	very low	micro-	IV	usually shore connected
Multiple-parallel Zenkovitch (1967)	sub-tidal (and intertidal)	0.01—0.0005	very low	micro (and macro?)	III	likely group VI bars formed on very gentle slope — energy level to moderate

plunging breakers may produce irregular surf zone topography on natural beaches, this is no longer recognised as a form of nearshore bar.

Bar morphology and dynamics have been described from a growing range of locations and as we understand more about bar processes we can further refine the classification system to reflect similarities in bar generation and to incorporate understanding of the morphological changes that accompany bar migration on coasts with a broad range of wave conditions. It may be time now to consolidate the number of bar classes and to recognise that features such as number of bars and straight versus crescentic plan forms as variations that reflect the extent of the influence of factors such as wave climate, tidal range, beach slope and proximity to the beach. The result of this consolidation is to distinguish two broad 'wave-formed' bar systems: outer bar systems found (and formed) some distance seaward of the shoreline and distinctly separated from processes operating on the foreshore and low tide terrace; and inner bar systems found close to the shoreline, often attached to it through transverse bars, and greatly influenced by the development of rip cells and giant cusps.

A good starting point for the consolidation is with the 2D and 3D bars of Wijnberg and Kroon (Table 8.1 – Group VI of Greenwood and Davidson-Arnott). These are formed some distance offshore and appear to function independently from the beach. They are generated or maintained in place by steep, short-period waves during storms and dominated by shoaling waves and spilling breakers. They probably form as a result of sediment transport convergence with onshore transport under shoaling and breaking waves and offshore transport due to undertow (see Section 8.3.2). Straight forms reflect the dominance of 2D undertow circulation while wavy or crescentic forms probably result from increasing influence of rip cells, either during formation, or subsequently during non-storm conditions when bars may migrate landward under swell wave conditions (Figures 8.10b, c).

There no longer seems to be a good reason to have a separate class for multiple parallel bars (Group III). These bars are not confined to very sheltered environments, as proposed by Wijnberg and Kroon, but can occur in quite energetic locations (Davidson-Arnott and Pember, 1980; Davidson-Arnott and McDonald, 1989 – see Figure 8.10d). The number of bars reflects primarily the existence of a very gentle slope with limited energy loss through breaking at each bar location. The gentle slope may result from the presence of very fine sand or it may be the result of a sub-horizontal underlying rock platform (Davidson-Arnott and Pember, 1980). However, processes on the outer bars are dominated by shoaling waves, spilling breakers and undertow (Davidson-Arnott and McDonald, 1989) and appear to be essentially the same as for the larger but smaller number of bars found in other locations. The outer bars are dominantly straight and continuous over long distances but the inner bars close to shore become much more complex in plan form and the longshore continuity decreases – as is case for inner bar systems in other locations.

Similarly, recent work on low-amplitude intertidal bars (ridge and runnel) indicates that the dominant processes on the bars, particularly the outer bars, are associated with wave breaking and surf zone processes (Kroon and Masselink, 2002; Dawson *et al.*, 2002; Masselink, 2004; Masselink *et al.*, 2006; van Houwelingen *et al.*, 2006). The number of bars in the intertidal zone tends to increase with increasing tidal range but, as was noted above for multiple parallel bars, bar number appears to be more closely controlled by slope of the intertidal zone and to a lesser extent by wave steepness and absolute wave height (e.g., Reichmüth and Anthony, 2007). On intertidal ridge and runnel bars swash processes are subordinate, especially during high-wave conditions, and consequently on–offshore movement of the bars reflects variations in wave height during storms and the influence of wave shoaling during non-storm conditions.

At several locations where ridge and runnel bars have been described one or more similar bars exists in the subtidal (e.g., Dawson *et al.*, 2002; Sedrati and Anthony, 2007; Price and Ruessink, 2008 – see Figure 8.10e). There does not appear to be a good data set on the subtidal

bars in locations where dynamics of the intertidal bars have been measured, but qualitative observations suggest that there is little difference between the subtidal bars and the outer intertidal ones that are exposed for short periods during spring low tides. Towards the shore, bars are increasingly modified by channels that cut through them, draining the runnels as the tide falls and their form may be modified as well by swash processes around low tide. At some sites the intertidal bars are found 2–3 wavelengths seaward of the spring high tide line and thus the influence of the shoreline is limited. However, where bars are present in the zone between MHWN and MHWS they tend to be dominated by swash rather than surf, and exhibit steep slip faces on the landward side and much greater mobility (Reichmüth and Anthony, 2007) – thus distinguishing them from the more stable bars of the outer system.

The inner bar system develops in quite shallow water and usually has some connections to the foreshore and low tide terrace. Bar morphology is highly varied and variable, with straight, crescentic and transverse bars all commonly formed (Figure 8.2). On beaches with medium-to-coarse sand, where a steep foreshore and berm develops under low-wave conditions, the inner system is usually associated with well-developed rip cells with a quasi-regular alongshore spacing producing what is termed rhythmic topography (Sonu, 1968; Dolan, 1971; Davis *et al.*, 1972; Greenwood and Davidson-Arnott, 1975; Falquéz *et al.*, 2008). The beach face develops embayments separated by horns which together form giant cusps (Komar, 1971; 1983) with a spacing of a hundred to several hundred metres. Bars in the inner nearshore are then linked to the beach either directly to the horns or at broad pads on the low-tide terrace adjacent to the horns (Figure 8.16). Water depth over the bars is shallow, especially at low tide and portions of the bars may be exposed at spring low tide. As a result, these bars are subject to shoaling and breaking waves at high tide but at low tide swash processes dominate bringing surges of water across the bar into the landward trough and often leading to the formation of a slip face. Longshore currents develop in the trough landward of the bar and then flow seaward through distinct rip channels or across the low point of crescentic bars. Where wave approach is at a high angle to the beach the whole topography, bars and rip channels, may be oriented obliquely in the direction opposite to that of wave advance. Waves commonly propagate through the deeper water of the rip channels and refract around the ends of transverse bars to travel up the longshore trough resulting in highly variable sediment transport directions in the trough and on the beach face (Figure 8.16).

8.3.2 Nearshore bar formation

The regularity of bars and their presence on so many shorelines has long stimulated interest in how they are formed and what controls the regularities in offshore and alongshore features. They clearly represent the net result of sediment transport in the surf zone and their stability over periods of days and weeks suggests that their position represents some form of equilibrium – likely a dynamic one with continued circulation of sediment through the system. There are many mechanisms that might potentially contribute to or control bar formation through their influence on water motion and sediment transport, including those associated with incident wave shoaling and breaking, infragravity waves and unidirectional rip cell circulation and undertow. One major problem has been to observe and measure the formation of a bar in the field. On coasts where bars are present all the time, onshore and offshore migration of the form has been observed but it is only recently that there have been a couple of (rather fortuitous) measurements of bar formation close to the shore (Aagaard *et al.*, 1998; Aagaard *et al.*, 2008). On coasts such as California and New South Wales, Australia, where bar migration and welding to the shoreline can produce complete disappearance of bars, the generation of new bars takes place some distance offshore under very energetic conditions and there does not yet appear to be a good data set documenting bar formation under these conditions.

One obvious solution to the problem is to carry out experiments in a wave tank and, as

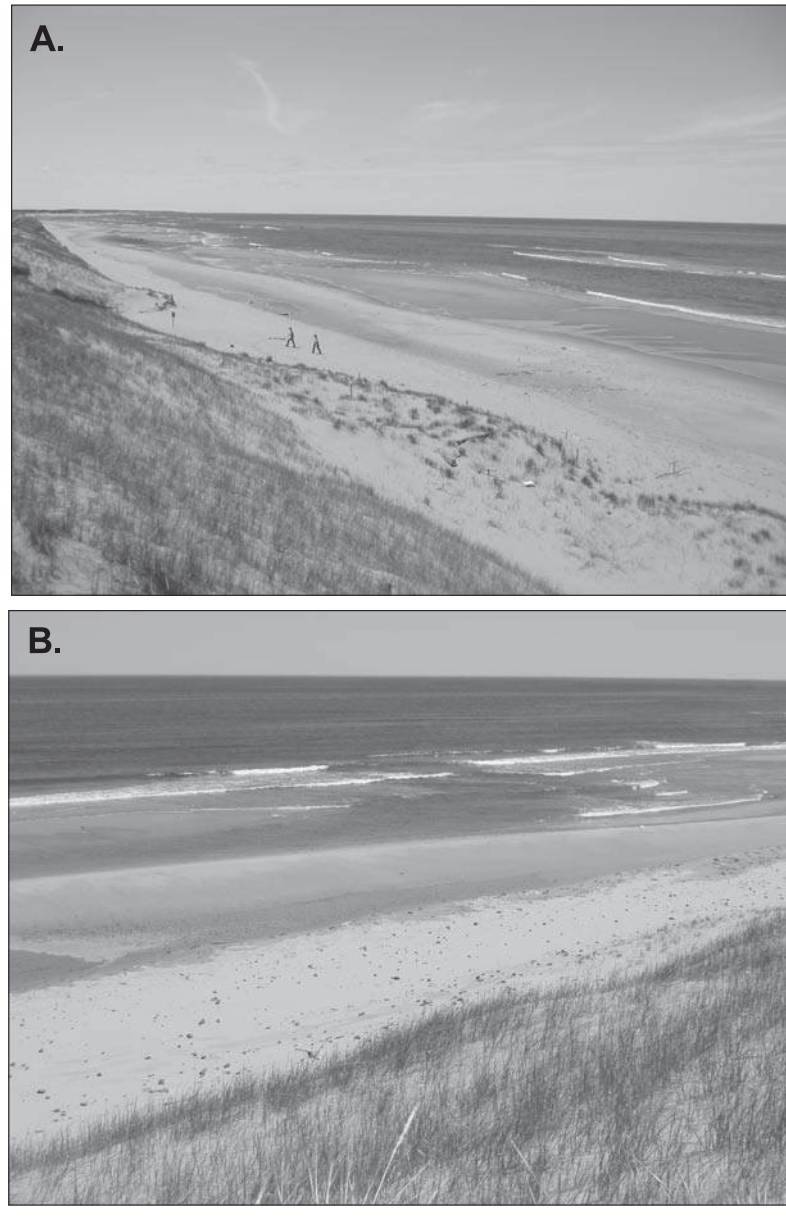

Figure 8.16 Complex inner bar and trough system exposed at spring low tide, Greenwich Dunes Prince Edward Island: (a) View west along the beach showing the berm crest and landward runnel with some water from the previous high tide. On the right side of the picture the low tide terrace is exposed as a flat pad with a straight inner bar and trough just seaward of it. Low waves are breaking on the bar with translatory swash bores moving across it into the trough. In the middle distance above the two figures a rip channel can be seen breaking seaward obliquely through a bar. Note, this photograph is taken with a polarising lens to enhance the contrast between sand and water; (b) Photograph looking offshore at one of the rip cell systems near the top left of the previous photograph. On the left the inner bar is nearly exposed with only a few of the swash bores able to cross the bar into the trough landward of it. The trough leads into a rip channel which cuts through the bar separating it from the one on the right. Low waves are able to propagate through the channel and are eroding the embayment that is developing on the foreshore opposite it.

noted earlier, there is a long history of this (Keulegan, 1948; King and Williams, 1949; Shepard, 1950a; Watts, 1954) and many others since then. 'Bars' were formed by sand moving seaward from a trough excavated by plunging breakers. However the limited wave height (a few cm) in these relatively short wave tanks and the use of monochromatic waves meant that key controls in nature were missing. While the newer and larger facilities can generate full-spectrum waves and the greater size permits larger waves, the significant wave heights are still quite small – e.g. the study of Wang *et al.* (2003) carried out in the Large-scale Sediment Transport Facility of the Army Corps of Engineers at Vicksburg, Mississippi had a H_b of 0.27 m. Finally, the laboratory experiments rarely include the effect of wind in addition to waves.

Present research seems to focus on two broad groups of models for bar formation (Thornton

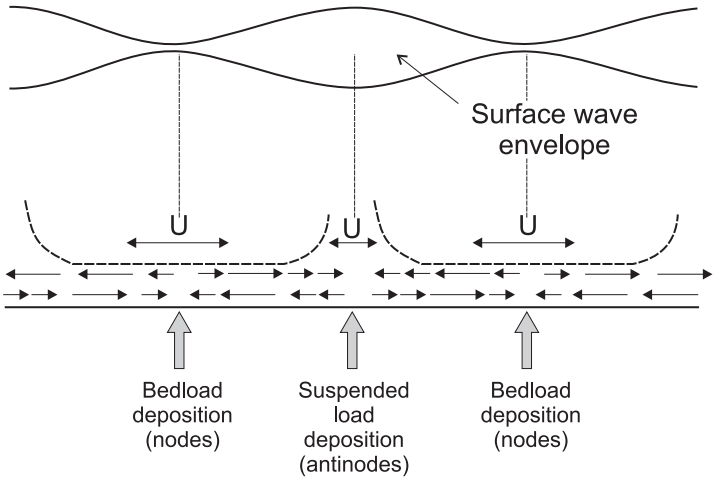

Figure 8.17 Drift velocity field and directions of sediment transport on a flat bed under the influence of a standing wave (Carter *et al.*, 1973).

et al., 1996; Aagaard and Masselink, 1999: (1) bar formation by infragravity standing waves or edge waves; and (2) bar formation by cross-shore flows and the break point mechanism. Other mechanisms falling outside these two principal groups may be identified as self-organisational (Wijnberg and Kroon, 2002) involving non-linear interactions in the surf zone (e.g. Damgaard Christiansen *et al.*, 1994; Boczar-Karakiewicz and Davidson-Arnott, 1987; Vittori *et al.*, 1999). However, there is some degree of self-organisation in all of the models.

Formation due to standing waves

The models of bar formation by infragravity waves, both leaky waves and edge waves rely on the incident waves to generate sand movement in the breaker and surf zones with the drift velocities associated with the standing waves leading to movement of sediment towards points of convergence. Both forms of infragravity standing wave have a cross-shore structure that produces nodal points at distances that increase exponentially offshore (see Figure 5.26) and this accords well with the increased spacing offshore found in nature. The spacing is too small for standing waves produced by reflection of incident wave frequencies, but spacing for infragravity frequencies can be made to fit observed spacing in the field (e.g. Short, 1975; Bauer and Greenwood, 1990; Aagaard, 1990; Aagaard and Greenwood, 1995). The drift velocity field under standing waves produces convergence at the nodes for bed load, and at the antinodes for suspended sediment (Carter *et al.*, 1973; Bowen, 1980 – Figure 8.17). This provides some difficulties because bars are likely to develop at only one or other of the nodes and it is not obvious which one it should be. O'Hare and Huntley (1994) provide a refinement of the model based on the variation in short wave height and long waves for wave groups in which sediment transport is independent of height.

Leaky waves have a uniform structure alongshore and thus can be associated with the generation of long, linear bars. Edge waves have a three-dimensional form and thus the zones of convergence produce crescentic forms (Bowen and Inman, 1971 – see Figure 8.18). The generation of edge waves of the required frequency is complex and it is not certain what particular mechanism, e.g. non-linear interaction or the isolation of particular cut-off frequencies, would provide the necessary stability over a period of many hours for the bar to generate. There is always the suspicion that where edge waves are observed they are the product of the existing bathymetry rather than the control (Huntley, 1980).

At present the balance of opinion seems to be shifting away from models based on standing waves as the primary generator of nearshore bars, though it is still likely that they have some influence on patterns of water motion and thus on the second order form of bars.

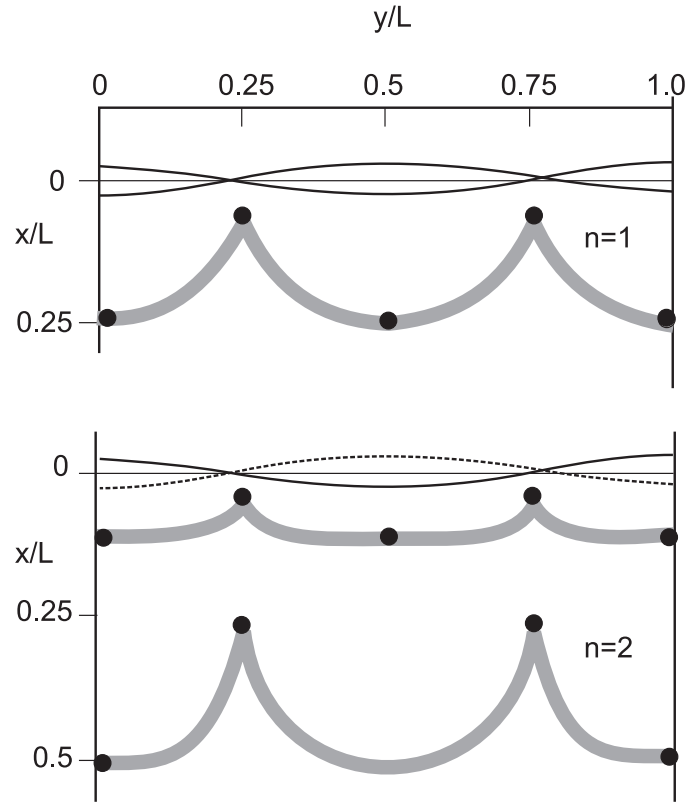

Figure 8.18 The theoretical form of crescentic bars generated by mode 1 and mode 2 edge waves (Bowen and Inman , 1971). A mode 0 edge waves has no offshore crossing point and therefore generates rhythmic topography (cusps) on the beach but not bars. Note that the wavelength of the crescent is the same for both bars produced by the mode 2 edge wave. This is a weakness of the model because most crescentic bar systems show that the wavelength of an outer bar is much greater than that for an inner bar.

Formation by cross-shore flows and the break point mechanism

The second bar forming mechanism involves convergence of sediment due to wave breaking and sediment transport by offshore-flowing currents. Seaward of the breaker zone sediment transport is generally landward under shoaling waves due to velocity skewness or asymmetry and this increases towards the breaker zone. Wave set-up in the surf zone generates an offshore flow and if this is dominantly in the form of undertow then it can transport sediment seaward close to the bed, with flow decreasing in the breaker zone. The result could be erosion of sediment from the landward margin to produce a trough and deposition in the zone of convergence in the breaker zone (Dyhr-Nielsen and Sorensen, 1970; Dally and Dean, 1984; Dally, 1987). As the bar forms there is likely some positive feedback because the steepening of the seaward slope and shallower water depth as the bar develops will lead to increased wave breaking (both the proportion of waves breaking and the intensity of breaking will increase) thus enhancing the undertow and focussing the zone of sediment transport convergence (Holman and Sallenger, 1993; Garcez Faria *et al.*, 2000). This kind of mechanism has been conjectured as far back as 1863 by Hagan writing on bar formation in the Baltic (quoted in Evans, 1940) and similar ideas are found in King and Williams (1949). The formation of multiple bars requires the generation of distinct zones of breaking waves, with wave breaking ceasing and wave reformation in the deeper water landward of the trough. The steepening of the nearshore profile on the seaward slope of the bar encourages a focus of wave breaking in this zone and an increase in the rate of energy dissipation. This is what is observed for spilling breakers on bars and it is brought out especially by the time-averaged photography that is used to define bar morphology in the Argus system.

Greenwood and Davidson-Arnott (1979) put forward a conceptual model for convergence of landward transport under waves and seaward flows due to rip currents over the outer bar based on sedimentary structures in box cores (see Section 7.2.3) and this provided the basis for an early computer simulation model (Davidson-Arnott, 1981) which then explored the effects of varying wave characteristics, beach slope and tidal range on the bar morphology generated on a two-dimensional profile. The increased recognition of the role of undertow, as opposed to rip cell circulation made it feasible to consider this form of bar generation because it did not limit the seaward transport to distinct and confined zones. The model of Dally and Dean (1984) using regular waves and subsequent modelling using random waves (Stive and Battjes, 1984) and Thornton *et al.* (1996) using the energetics models of Bowen (1980) and Baillard (1981) provides a practical basis for applying this. Recent field experiments (Aagaard *et al.*, 1998; Greenwood *et al.*, 2006; Aagaard *et al.*, 2008) have provided evidence to support this model.

Key elements of the cross-shore flow and break point mechanism are the role of morphodynamic feedback between the bar form and the wave and current hydrodynamics and the tendency for the bar form to migrate to an equilibrium position where there is a balance between the strength of the undertow and the intensity of wave breaking on the bar. One outcome of this is that the position of the bar should move with changing incident wave conditions – landward into shallower water if the bar is in water that is too deep to generate the required undertow, and offshore if wave breaking is too intense leading to transport by the undertow onto the seaward side of the bar. Field studies in North America in the 1950s and 1960s were carried out mostly in California where only onshore bar migration was observed. However Greenwood and Davidson-Arnott (1975) working on the East coast measured offshore movement in response to storms with greater intensity, and onshore movement with less intense storms. This oscillation in response to changing wave conditions has now been documented in many areas (e.g., Lippman *et al.*, 1993; Lee *et al.*, 1998; Plant *et al.*, 2001; Houser and Greenwood, 2005) and offshore migration over a period of months to years has been documented for coasts with a strong alongshore component of sediment transport (Ruessink *et al.*, 2000; Shand *et al.*, 2001).

The processes that control bar location and migration are therefore quite complex. Offshore migration of the outer bar crest takes place until it reaches a position where only a fraction of the incident waves are breaking and the mean offshore flow in the undertow will just balance the onshore transport under waves. This is estimated to be when the local relative wave height H_{rms}/h is ~ 0.3. In some cases, the storm event will not be of sufficient duration for this to be achieved and thus the response time, based on the rate of onshore or offshore migration of the bar, may be insufficient to reach the equilibrium position. The result is that we can envisage the bar position as being controlled by wave height and the location of wave breaking, and thus the offshore position of a bar over a year should tend toward a position determined by the highest waves (Plant *et al.*, 1999). As Houser and Greenwood (2005) note, the outer bar is subject to a wide range of wave conditions and therefore it should have a much wider range of movement as well as a greater chance, for example, of moving onshore under low waves to a position where it will be highly unstable under high waves from a rapidly developing storm. On a multiple bar profile the inner bars are subject to a much narrower range of wave conditions because of the filtering effect of wave breaking on the bars seaward of them. They should therefore exhibit much greater stability, unless the outer bar migrates offshore to a depth where it ceases to act as much of a filter.

In the inner bar system, and similarly for intertidal bars, the relative water depth over the crest varies considerably within an individual tidal cycle and between neap and spring tides. This has an important determinant on the temporal and spatial pattern of the morphodynamic regime on the bar (Masselink, 1993, 2004; Kroon and Masselink, 2002; Price and Ruessink, 2008) and thus the proportion of time that conditions over the bar are dominated by shoaling, surf or swash conditions. When the water depth

Table 8.2 *Dynamic range of beach and nearshore morphology as a function of wave climate, sediment size and tidal range.*

Wind and wave climate offshore — shallow after shoaling and refraction			Sediment size beach and nearshore slope			Tidal range		
swell	sea	mixed	fine	medium	coarse	micro	meso-low macro	high macro
low	medium	high	low	high	low	medium	medium	low

is small sediment transport is dominantly onshore under swash bores and these conditions can produce rapid onshore movement and development of a slip face.

8.3.3 Nearshore and beach morphodynamic controls and models

Over periods of weeks, months and years the configuration of the nearshore and beach will change in response to changing wave conditions. On some coasts the range of change is quite small and it is possible to describe a characteristic morphology that may vary somewhat in space and time but which maintains the basic form unchanged. On other coasts there is a marked change in form with seasons driven by seasonal variations in the characteristics of incident waves. The winter/summer profile described for California (Figure 8.11) is a classic example of this. Beach and nearshore form may also be driven by changes associated with longer term cycles such as ENSO which alter the dominant wind direction , wave direction, severity of storms and water level. Based on the material covered earlier in the chapter we can identify the likely controls on the stability or dynamic range of morphological variation as being: (1) the wind and wave climate; (2) sediment size, and beach and nearshore slope; and (3) the tidal range (Table 8.2).

While some examples of morphodynamic response had been described in work prior to 1980 (King and Williams, 1949; Shepard, 1950a; Davis and Fox, 1972; Davis *et al.*, 1972; Sonu, 1973; Greenwood and Davidson-Arnott, 1975; Owens and Froebel, 1977) it was Short and Wright working on the coast of New South Wales, Australia who put together a systematic description of beach morphodynamic stages for a high-energy microtidal coast. They attempted to define conditions that would predict the form of the beach and nearshore profile and the range of forms that could be expected on it based on the dimensionless fall velocity parameter Ω (Wright and Thom, 1977; Short, 1979; Wright *et al.*, 1982; Wright and Short, 1983; 1984; Wright *et al.*, 1985). As we have seen earlier (equation (8.5)), Ω is a form of surf similarity parameter, incorporating wave steepness and beach slope (through the dynamic relationship between sediment size and beach slope). Use of the w_s parameter overcomes a tricky problem (Nielsen and Hanslow, 1991) of how exactly to define beach slope on the curvilinear profile of prototype beaches. Other difficulties arise because small waves may break on the steep, reflective portion of the foreshore while under more energetic conditions larger waves will break on the gently sloping dissipative portion of the inner nearshore.

Wright and Short (1983, 1984) distinguished between two end member beach types – dissipative and reflective – and a series of intermediate beach types. Reflective beaches tend to occur for $\Omega < 1$ and dissipative beaches for $\Omega > 6$ while values of 2–5 are associated with intermediate beaches. Beaches that are intermediate may move between different modal stages producing a distinct suite of topographies. The original scheme of Wright and Short (1984) has been extended and modified somewhat by studies carried out by Sunamura (1988) and Lippmann and Holman, 1990 and is depicted schematically in Figure 8.19. The sensitivity or relative contribution among the three variables to determining the beach state is shown in Figure 8.20).

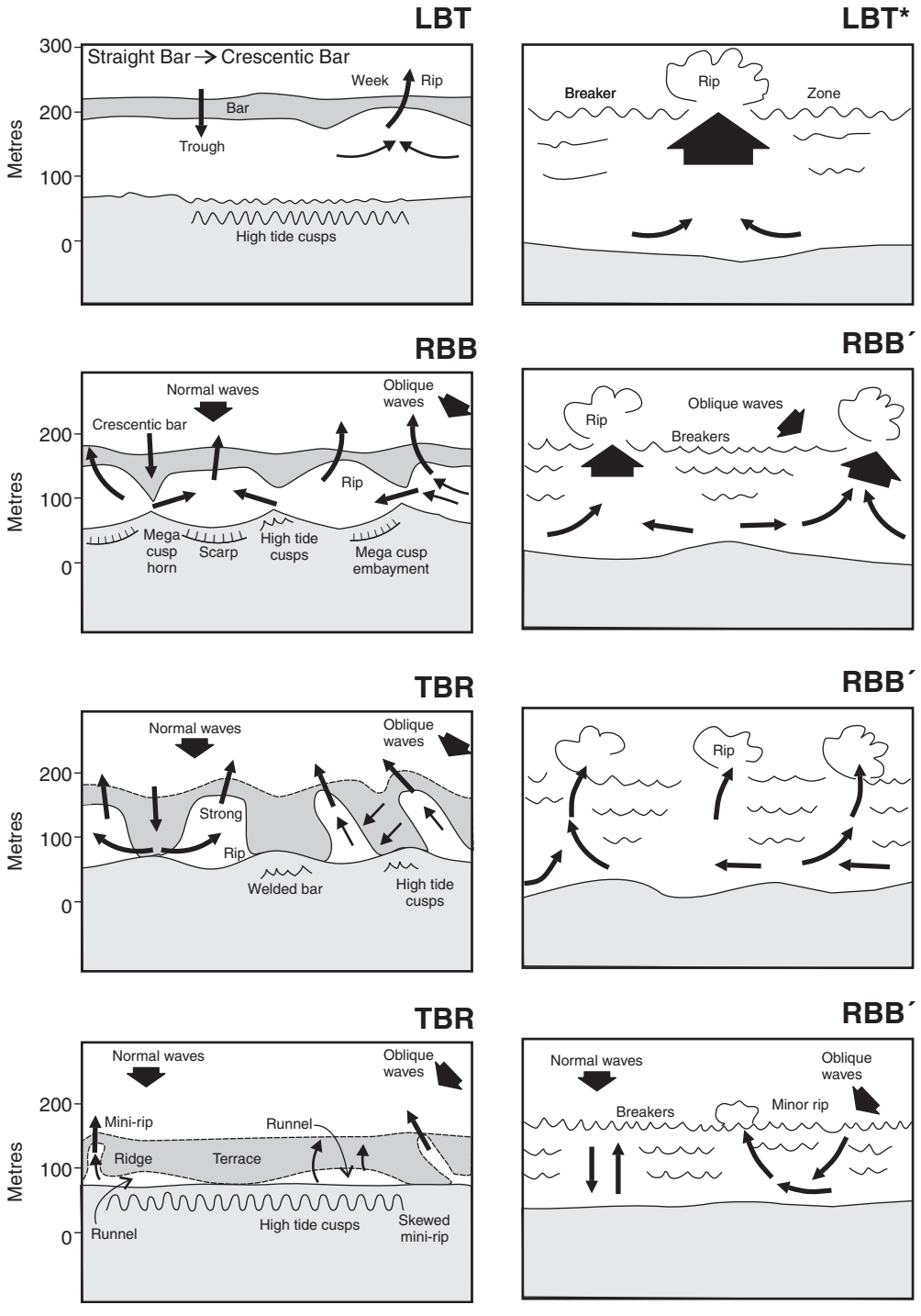

Figure 8.19 Plan views of the sequence of beach and nearshore morphology for a wave-dominated beach for accretionary (left) and erosional (right) wave conditions (Short, 1999; based on Short, 1979; Wright and Short, 1984; Sunamura, 1988 and Lippmann and Holman, 1990). LBT = Longshore bar trough; RBB = Rhythmic Bar and Beach TBR = Transverse Bar Rip.

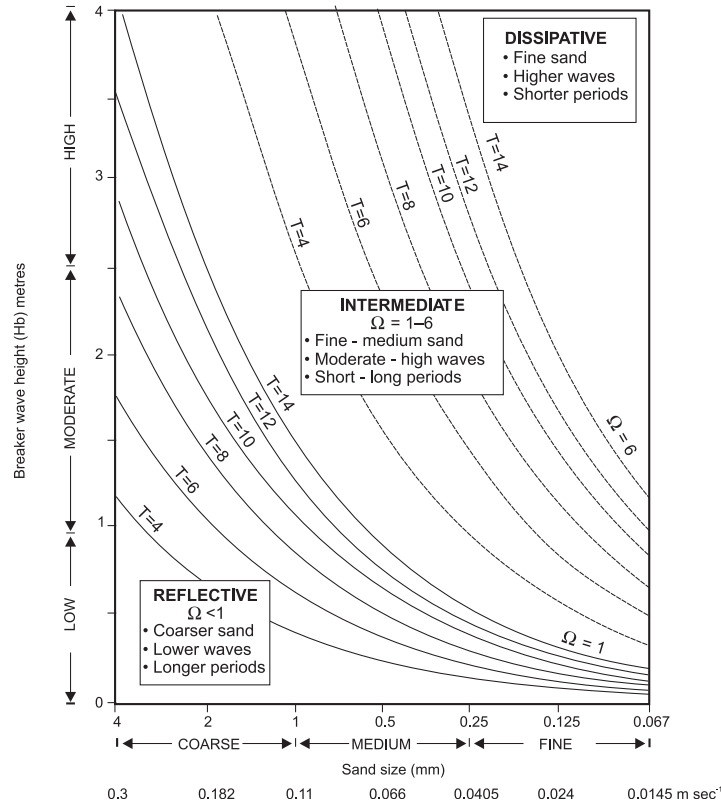

Figure 8.20 Nomogram showing the contribution of wave height, sediment size and wave period to *W* and beach type. The intersection of grain size and wave height is determined first and then the wave period is used to determine boundaries between the three domains (Short, 1999).

An accretionary sequence on a beach exposed to the full range of wave conditions could begin with the formation of a longshore bar and trough during an extended period (several days) of storm conditions and high, steep waves. If this is followed by an extended period (weeks) of lower, long-period swell waves the bar could migrate shoreward through the rhythmic bar and beach stage where the bar becomes rhythmic or crescentic, through the attachment of the bar to the beach forming transverse bars with rip channels separating them and ultimately the complete welding of the bars to form a steep, high berm (left side of Figure 8.19). Onshore movement occurs because swell waves shoaling across the bar are able to move sediment landward due to the asymmetry of oscillatory motion and there is no counterbalancing offshore transport by undertow. The bar becomes crescentic as rip cell circulation is established and this is reinforced when the bars become shore attached and there is translation of large amounts of water across the shallow transverse bars which drives strong rip currents in the channels separating them. A study by Brander (1999) demonstrated the strong feedback between the evolution of the transverse bar and rip channel morphology with reduced rip channel width being accompanied by increased flow speed and deepening of the channel.

The full accretionary sequence requires the right combination of wave conditions and sufficient time. In many cases the accretionary phase is interrupted by a storm and an erosional phase occurs with sediment and the bar(s) moving offshore – again this requires an intense storm to reset the system completely. An analysis of four years of data using the Argus system (Ranasinghe *et al.*, 2004a) at Palm Beach New South Wales provides evidence for the robustness of the stages and their sequence and numerical modelling supports the role of high energy wave conditions in producing the longshore bar trough (LBT) morphology and of lower wave conditions in

producing the progression through the other three states. The sequence shown in Figure 8.19 is for a coast with a single bar but the basic beach state model can be modified to accommodate the situation where there are two bars or even three bars (Short and Aagaard, 1993).

The beach stage model applies best to microtidal coasts with a broad wave climate – i.e. one exposed to both periodic storms which act to move sediment offshore and generate a bar, and swell waves which are large enough to move sediment on the bar onshore thus initiating the process of bar migration. Elements of the model can be seen in field studies carried out in other locations (Lippmann and Holman, 1990), but it clearly does not encompass the full range of nearshore and beach morphodynamics (e.g., Masselink and Pattiaratchi, 1998). As noted earlier, sand beaches in the tradewind zone such as those from St Kitts shown in Figures 8.5a, b have a planar profile all year, but they do experience periods of beach erosion and offshore transport under high wave conditions. Sandbank beach (Figure 8.5a) represents the fine sand end of the spectrum so that only a very subdued berm develops and the beach simply gets wider with onshore movement. The grain size at North Friar's beach (Figure 8.5b) is medium sand which develops a high berm under lower wave energy conditions. Both beaches fall into the intermediate class based on values of Ω which should give rise to some forms of nearshore bar. Lippmann and Holman (1990) note a rapid transition to a linear bar under storm waves and an equally rapid (1–2 days) transformation of the linear bar into a rhythmic one. However, other locations do not show this. Thus, the straight nearshore bar shown in Figure 8.10b appears to be straight at all times in contrast to the crescentic system in Figure 8.10c which never becomes straight. This distinction is maintained despite the fact that the two beaches have a similar grain size and wave climate.

In fetch-limited areas (maximum fetch <300 km) the range of wave conditions is quite narrow and high energy wave events are always associated with the passage of storms and strong onshore winds (Goodfellow and Stephenson, 2005). In the mid-latitudes these coasts are almost always characterised by the development of two or more bars in the nearshore. Generally swell conditions are absent (though waves with relatively low steepness may occur for a few hours after a high wind event and in locations where wave refraction results in a large reduction in wave height). In this area the outer bar(s) become largely inactive or relict during periods between storms because waves are not large enough to move sediment on them. The bars are therefore a permanent feature of the profile. Where the prevailing winds are offshore (e.g. north and east facing beaches in the Great Lakes and Gulf of St Lawrence) the inner bars may also be relatively stable during non-storm conditions because periods with waves large enough to move sediment on these bars are relatively rare or last only a few hours at a time (e.g., Greenwood and Davidson-Arnott, 1975). However, on south and west facing beaches where there is sufficient fetch, wave action may occur on many days leading to onshore migration of the inner bars and welding to the beach (e.g. Davis and Fox, 1972; Owens and Froebel, 1977; Stewart and Davidson-Arnott, 1988 – see Figure 18.21). A slip face develops on the migrating bar even before it emerges at low tide, as a result of wave translation across the bar crest at low tide. The crest is flattened and often the bar becomes much wider. On relatively fine grained beaches a slip face bar may persist for weeks in the intertidal zone (Houser *et al.*, 2006) and its position may shift offshore under higher wave conditions and onshore when wave energy and storm surge decline or it may merge with the beach and be reset by another period of high wave activity (Quartel *et al.*, 2007).

In a number of locations measurements of nearshore bar dynamics have been carried out for periods of years using standard surveying and echo sounding or using time exposures to monitor the position of the bar crests. These studies have shown that the long-term response of the profile can be quite different, despite similar average profile morphology. Bars on the Dutch coast may migrate offshore continuously and eventually disappear, while new ones are generated close to shore. These in turn migrate

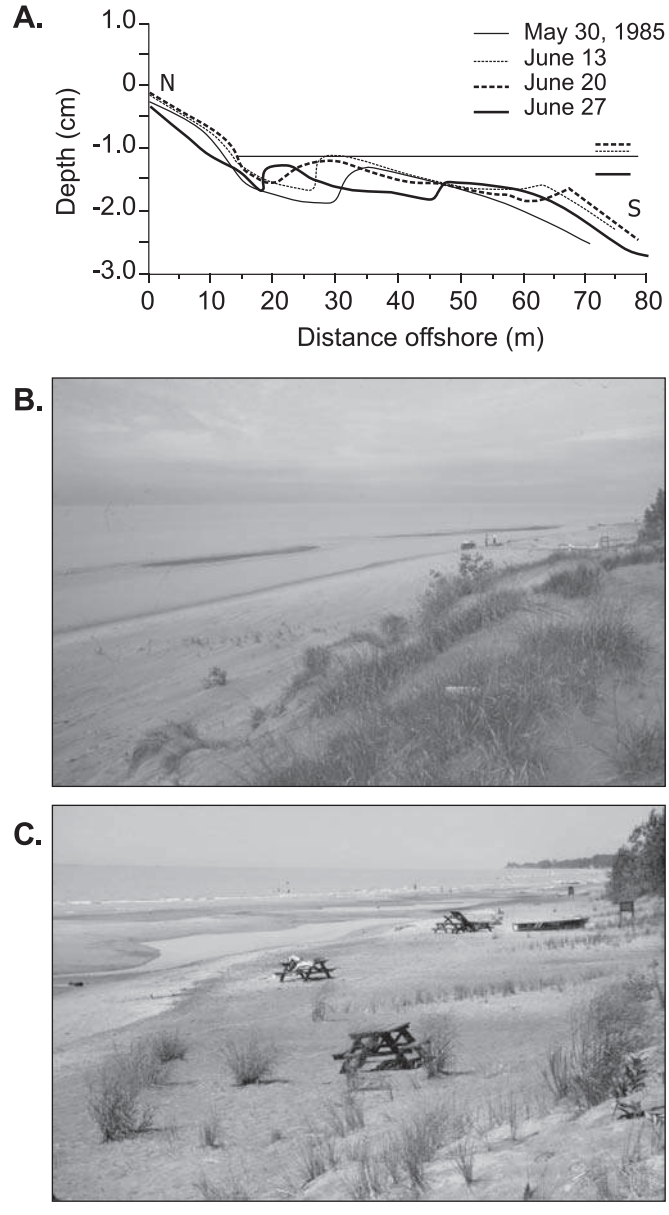

Figure 8.21 Onshore migration of inner sandbars as slip face ridges and welding to the beach at Long Point, Lake Erie during the summer low wave conditions, 1985: (A) profile change; (B) photograph of the beach on May 30, showing low waves breaking across the inner bar and generating a slip face; (C) the beach at the end of the summer after welding of two slip face bars.

offshore, maintaining an equilibrium spacing between bars (Wijnberg and Terwindt, 1995; van Enckevort and Ruessink, 2003a). Episodes of bar switching (Wijnberg and Wolf, 1994; Shand *et al.*, 2001) involve the realignment of outer bars following the junction of two bars in a transition zone. Some of the variability in the seasonal positions of the bars may reflect alongshore bar movement (van Enckevort and Ruessink, 2003b).

The Beach Stage model of Wright and Short was developed for microtidal beach settings and additional complexities are introduced as the tidal range increases to meso- and macrotidal (Masselink and Hegge, 1995). As we saw in Section 8.3.1, bar generation and first-order dynamics still appears to be controlled by the shoaling waves and surf zone processes but increasingly these become modulated by the changes in water depth over tidal cycles, by

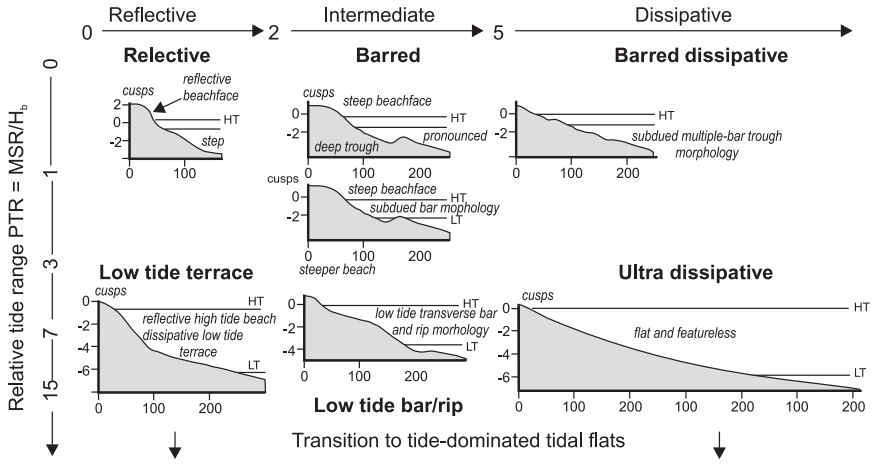

Figure 8.22 Beach states as a function of the dimensionless fall velocity and the relative tidal range (after Masselink and Short, 1993).

drainage at low tide which has the effect of creating channels through the bars, and probably also by the increased role of strong tidal currents flowing alongshore in the trough (Sedrati and Anthony, 2007). Masselink and Short (1993) make use of the relative tide range (RTR) to permit comparison between beaches on the basis of tidal range:

$$RTR = \frac{TR}{H} \tag{8.8}$$

where TR is the tidal range and H is the modal wave height.

Based on the combination of the two parameters Masselink and Short (1993) identify characteristic profile forms that is expanded to include mesotidal and macrotidal bars (Figure 8.22).

There has been considerable work on intertidal bars on both sides of the English Channel where mesotidal and low macrotidal beaches are common (Michel and Howa, 1999; Kroon and Masselink, 2002; Masselink *et al.*, 2008; Reichmüth and Anthony, 2007). In general these studies have found that the intertidal bars are a permanent feature of the intertidal zone and that they respond in a similar way as subtidal bars to changes in wave energy (Masselink *et al.*, 2006). On quite steep slopes 2–4 bars may be present and as the slope becomes less steep a larger number of bars are formed (Hale and McCann, 1982; Dawson *et al.*, 2002; Masselink *et al.*, 2006) in the same way that gentle slopes on microtidal coast promote a greater number of subtidal bars. Masselink *et al.* (2006) distinguish between low-amplitude ridges (the classic ridge and runnel of King and Williams, 1949) and sand waves (Hale and McCann, 1982) but in view of the consolidation of subtidal classes in Section 8.3.1, it may be best to view them as part of a continuum where the wave and hydrodynamic processes are similar and the prime difference is a response to decreasing intertidal gradient. When the tidal range gets very large (high macrotidal) the profile form tends to become rectilinear with a steep upper slope and flat, featureless low tide zone (Levoy *et al.*, 2000 – see Figure 8.23).

8.4 Beach morphodynamics

As we would expect from the discussion in Section 8.2.2, the extent to which the beach form responds to changes in these forcing functions is also influenced by beach sediment size. Change in beach profile form tends to be muted for beaches in fine sand, which maintain a gently sloping planar profile. However, beaches developed in medium and coarse sand experience quite large changes in form that reflect a tendency towards a

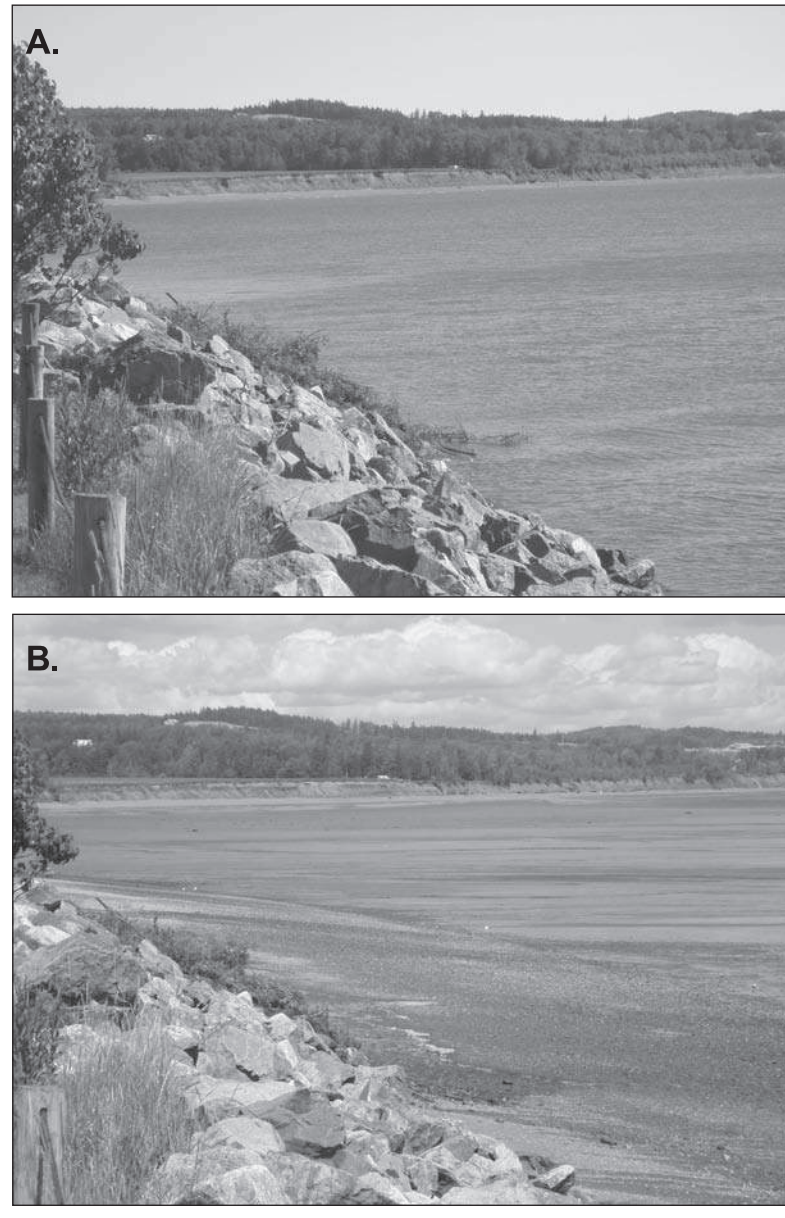

Figure 8.23 Photographs of a low tide terrace beach, Minas Basin, Bay of Fundy: (A) at high tide; (B) at low tide showing the steep upper foreshore and the low tide terrace which drains completely at spring low tide. Spring tidal range here is about 13 m. Note the riprap in the foreground protecting a small cottage community from flooding during very high tides and the eroding bluffs in the background.

dynamic equilibrium driven by the interaction of swash and the beach water table. On gentle slopes the swash zone merges into the nearshore zone without any notable break, but with steeper slopes, and especially on beaches with coarse sand and gravel, the transition to the nearshore is marked by a distinct step at the base of the foreshore (Austin and Buscombe, 2008).

8.4.1 Sandy beach morphodynamics

Beach form changes readily in response to changes in wave conditions between storm events and periods of swell waves or fair weather conditions (Ortega-Sánchez *et al.*, 2008; Quartel *et al.*, 2008). This response is modulated by changes in water level due to wave and wind set-up which affects the landward limit of wave

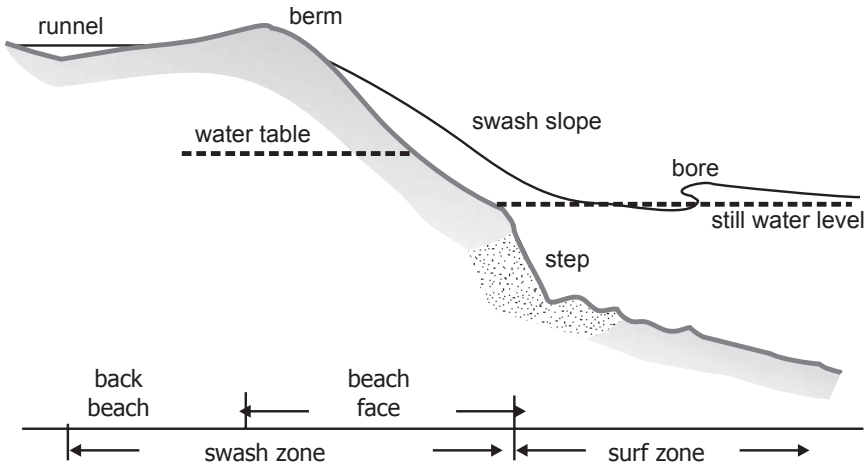

Figure 8.24 Schematic profile through the lower beach and foreshore showing the main topographic features and the location of the ground water table. The profile is shown here for a beach in medium sand with a well-developed berm.

action and to diurnal and neap/spring tidal cycles. The general tendency for equilibrium beach slope to increase with increasing grain size was noted in Section 8.2.2. Grain size also influences the dynamic response of beaches to variations in wave characteristics, overall wave energy, and to water level variations, especially through interaction of the swash with the beach water table (Buscombe and Masselink, 2006). In general, periods with high waves, especially steep, short period waves during a storm, leads to erosion of the beach and flattening of the beach profile producing the storm profile of Figure 8.11. High water levels associated with storm surge and high tide may permit waves to reach the backshore and lead to erosion of aeolian sediments at the back of the beach and perhaps to erosion of the foredune. Extended periods of relatively low waves lead to onshore transport of sediment from the inner nearshore and the build-up of the beach to form a berm – the fair-weather profile of Figure 8.11. The beach water table plays an important role in modulating both the erosion of the berm during periods of high waves and the build-up of the beach during periods of low waves.

Beach water table

The beach water table represents the upper level of groundwater that underlies the beach (Figure 8.24). At the landward margin of the beach the groundwater continues under features such as sand dunes or bluffs and there is often a hydraulic gradient towards the beach that may, for example, lead to a zone of seepage near the dune toe. The groundwater table outcrops at the seaward margin of the beach, usually on the middle to lower portion of the foreshore. The beach groundwater system interacts with the atmosphere, receiving inputs of precipitation through infiltration and losing mass through capillary rise and evaporation (Horn, 2002). On occasion the ground water table may be at the surface over a portion of the beach profile, for example where the berm crest is built up above the beach surface, leading to the formation of a runnel which may be filled with water for part of the tidal cycle (Figures 8.24, 8.16a). On a fine-sand beach the surface slope may not be much greater than the slope of the groundwater table with the result that the groundwater table is close to the surface over most of the profile. Under these circumstances, capillary rise maintains a damp beach surface and evaporation leads to deposition of salts.

At the seaward margin there is considerable interaction between the groundwater and the ocean, due to movement of the mean water level with tide and wind effects, and to the effects of swash and backwash action. On the

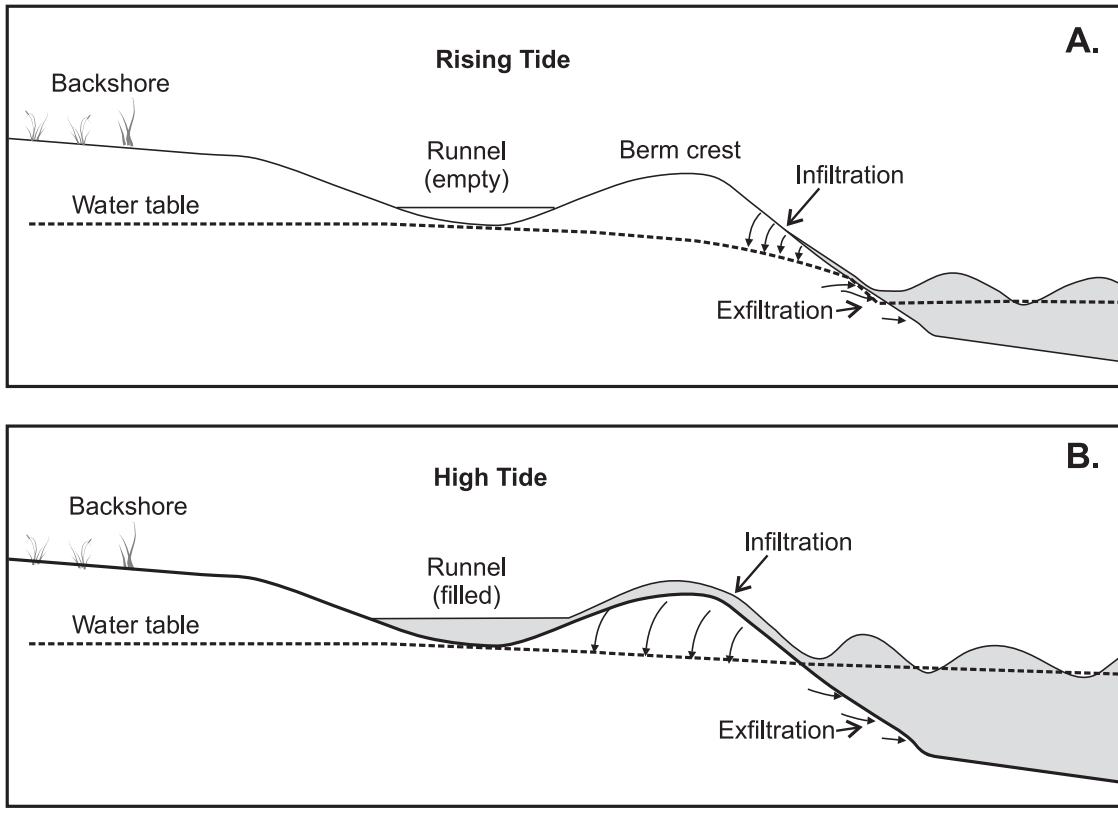

Figure 8.25 Dynamics of the groundwater table under: (A) rising tide; and (B) falling tide. During the rising tide increasing swash excursion leads to infiltration of water to the groundwater and a local increase in the level of the groundwater table. During the falling tide swash does not reach as far up the swash slope and there is net exfiltration of water from the groundwater which is evident as seepage. This produces a net draw-down of the beach groundwater table near the berm.

rising tide, the increase in the mean water level results in swash reaching further up the foreshore and the dry portion of the foreshore slope is inundated more and more frequently. This produces a net infiltration of water into the beach surface which infiltrates to the groundwater and leads to a rise in the groundwater table at that location (Figure 8.25a). Conversely, on the falling tide the swash zone migrates offshore and downward and there is exfiltration from a seepage zone which results in a fall in the groundwater table close to the foreshore slope (8.25b). The mean water level can drop more quickly than water can be discharged through exfiltration, with the result that the groundwater table can become decoupled from sea level (Horn, 2002). This happens particularly during spring tides when the low tide terrace seaward of the bottom of the foreshore may be exposed and seepage occurs over quite a wide zone (Figure 8.16a).

Berm building

The migration of the swash zone up and down the foreshore with the diurnal tidal cycle produces a distinctive cycle of 'cut and fill' on the swash slope that was described in a classic paper by Duncan (1964). As the tide rises, a wedge of sediment is moved up the swash slope by the waves, with a zone of erosion occurring on the lower portion where entrainment is made easier by the positive pore water pressure generated in the exfiltration zone. At the top of the swash water infiltrates into the unsaturated zone above

the outcrop of the water table, thus reducing the volume of the backwash and allowing sediment to be deposited there. On the falling tide sediment is stranded near the top of the swash but erosion occurs on the lower portion as the effluent zone migrates downward. During low wave conditions this process results in a steepening of the foreshore slope and the building of a berm crest over a period of days, while the foreshore may prograde due to the landward movement of sediment from the inner nearshore (Hine, 1979).

Berm building under low-wave conditions due to the interaction between waves and the beach groundwater table is further enhanced by the spring/neap tidal cycle. As the tidal range increases during the transition from neap to ebb tides, the high-tide limit of the swash migrates further up the foreshore and leads to overtopping of the berm for a period of tens of minutes to an hour or more. Sediment tends to be deposited at the berm crest and down the landward slope as water infiltrates into the beach. At spring tides water may inundate the whole zone, flooding the runnel and extending right up the beach (Figure 8.16a). The result of this is to build up the height of the berm. On the return to neap tides, waves no longer overtop the berm at high tide and changes take place only on the swash slope, often leading to the seaward building of the berm (Weir *et al.*, 2006). During this period, the berm crest area dries out and there is the potential for considerable aeolian transport of sediment which may complete the infilling of the runnel and transfer sediments to the backshore and embryo dune area.

Early studies (Bagnold, 1940; Bascom, 1953) have suggested that berm height increases with increasing wave height though this may be more evident in wave tank studies than in the field where tidal fluctuations and varying wave conditions make it more difficult to extricate this influence from among a number of others. Some work has also suggested that berm height increases with increasing grain size and certainly the height of gravel and cobble berms appears to be higher for given wave conditions (Bascom, 1953). Field studies are also complicated by the fact that an increase in wave height is often accompanied by increased wave and wind set-up, which leads to erosion and flattening of the berm.

Bar welding

The emergence and onshore migration of swash bars (which may be the final phase of onshore migration of bars from the nearshore zone) is the second major mechanism of beach restoration and berm building during the interval between storms. The emergence and transformation to a berm occurs in a process termed bar welding and, as shown in Figure 8.21 may include the welding of more than one bar as new bars are formed in the inner surf zone and migrate onshore. Bar welding and berm formation are the final phase of the accretional cycle of the Beach Stage Model but, as we have seen, swash bar formation and bar welding can also occur where bars continue to exist in the nearshore (Aagaard *et al.*, 2005).

Beach cusps

As we saw in Section 8.3.1, the development of rip current cells and associated rhythmic inner bars leads to the development of cusps opposite the rip channels and horns opposite the feeder current divides. These giant cusps (Komar, 1971, 1983) are best developed when a steep, reflective foreshore slope and berm have developed. They have an alongshore wave length that is controlled by the dimensions of the rip cells and the rhythmic inner bars, usually 100–300 m, and they may persist for weeks or even a few months.

In contrast, beach cusps are much smaller features with length scales on the order of a few metres to a few tens of metres (Figures 8.26, 8.27). They consist of an embayment between two horns which point seaward. They form best when there is some a combination of a steep foreshore and relatively low waves that permits the backwash cycle from one wave to be completed or nearly completed before the next wave breaks. Cusps also appear to develop more often in medium to coarse sand or gravel which permits some infiltration of the swash during uprush, particularly on the cusp horns. Cusps have attracted a lot of attention – probably much more than is deserved given their limited significance for beach dynamics, but we all have a fascination for trying to understand any natural phenomenon that gives rise to a regular pattern. In reality, while cusps do have a regular pattern, and a characteristic spacing, actual field

Figure 8.26 Beach cusps: (A) cusps developed on Tairua Beach, North Island, New Zealand (photo courtesy Giovanni Coco, NIWA and Environment Waikato). Still photograph taken from video recordings from a camera mounted on Paku Hill about 70 m above the beach (see Almar *et al.*, 2008 for description of the site and the video recording system); (B) large cusps developed in gravel and cobbles, St Mary's Bay, Newfoundland. The cusps on the upper beach have a wavelength of about 90 m (Brian Greenwood for scale)

measurements can show quite a large coefficient of variation for their wavelength (Nolan *et al.*, 1999). There are useful reviews in Seymour and Aubrey (1985), Masselink *et al.* (1997), Komar (1998) and Almar *et al.* (2008).

Observations show that near the top of the swash run-up flow in the vicinity of the horns tends to be divided and directed towards the middle of the embayment (Figure 8.28a). There is some infiltration of water near the top of the cusp horns

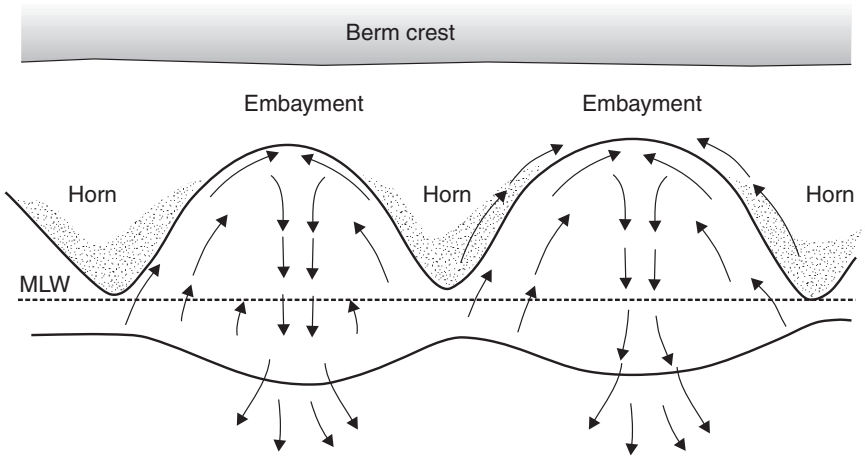

Figure 8.27 Sketch of swash and backwash flows in developing cusps. The swash uprush tends to be diverted away from the high points of the cusp horns towards the centre of the embayment, especially near the end of the swash and beginning of the backwash.

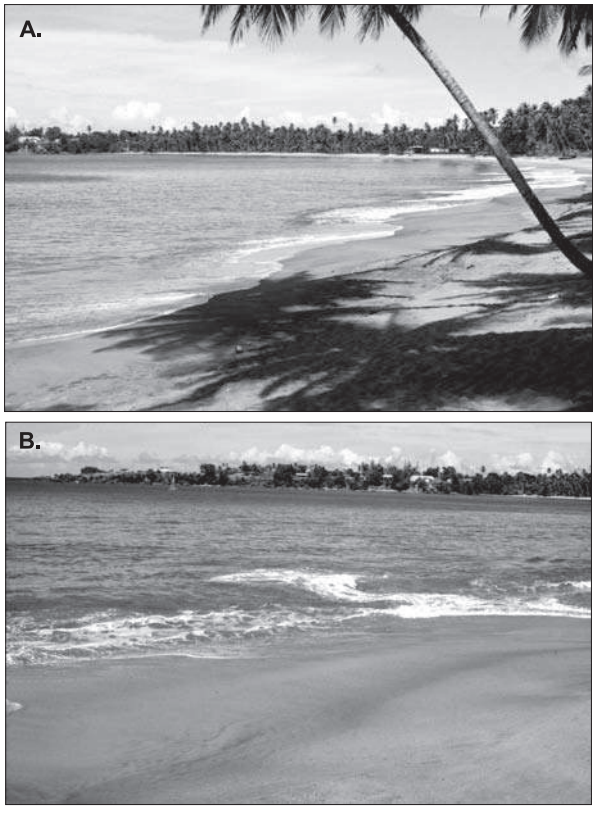

Figure 8.28 Photographs of swash and backwash associated with developing cusps on a medium sand beach, Courland Bay, Tobago; (A) limit of swash run-up showing alongshore variations produced by the small alongshore undulations; (B) concentrated flow at the base of the embayment near the end of the backwash portion of the cycle showing the offshore transport of sediment eroded from the embayment.

and this, together with the diversion towards the centre of the embayment, results in most of the backwash being concentrated in the embayment. The concentration of backwash in the embayment produces a deep flow that tends to scour the embayment, thus enhancing the alongshore relief and at the end of the backwash this jet can flow seaward beyond the beach in a form of miniature

rip (Figure 8.28b). Once initiated, cusps can develop through erosion of the embayment, deposition on the ridges that form the cusp horns or some combination of the two. There are conflicting reports of whether cusps are erosional or depositional features, i.e. whether their formation is accompanied by net accretion or erosion of the foreshore slope. It seems likely that either can be true, but the conditions under which they develop usually favour stability or slight accretion of the foreshore as a whole. In addition, a change to steep, higher-frequency waves usually results in erosion of the foreshore and destruction of any cusps present.

The low waves and steep foreshore slope are favourable to the generation of edge wave and so it is not surprising that one of the proposed mechanisms for cusp formation is the presence of a mode 0 edge wave (Guza and Inman, 1975, Huntley and Bowen, 1978). The edge wave that leads to cusp formation may be either synchronous (period equal to the incident waves) or more often sub-harmonic (period equal to one-half the incident wave frequency). The beach cusp spacing based on the edge wave mechanism can be predicted from

$$\lambda_c = m\frac{g}{\pi}T_j^2 \sin\beta \qquad (8.9)$$

where λ_c is the cusp spacing, T_i is the incident wave frequency and m is 1 for synchronous edge waves and 0.5 for subharmonic edge waves.

While a number of studies have suggested that edge waves are responsible for the initiation of cusps (Huntley and Bowen, 1978; Sallenger, 1979) many recent studies have failed to establish this link (Holland and Holman, 1996; Masselink *et al.*, 1997; Almar *et al.*, 2008). A limitation of the edge wave model is that once the cusps develop they tend to suppress edge wave motion.

An alternate model that seems to be gaining favour is that cusps simply represent a form of self organisation (Werner and Fink, 1993). Cusps arise because of non-linear interactions between flow, sediment transport and morphology, provided that suitable conditions exist to reinforce the original perturbation that initiates the interaction. The results of field studies by Holland and Holman (1996) and Masselink *et al.* (1997) appear to favour this mechanism as do the three years of beach video monitoring by Almar *et al.* (2008). Under this model of formation the key control on cusp spacing is simply the horizontal distance of the swash excursion (Werner and Fink, 1993; Coco *et al.*, 1999).

References

Aagaard, T. 1990. Infragravity waves and nearshore bars in protected, storm-dominated coastal environments. *Marine Geology*, **94**, 181–203.

Aagaard, T. and Greenwood, B. 1995. Longshore and cross-shore suspended sediment transport at far infragravity frequencies in a barred environment. *Continental Shelf Research*, **15**, 1235–1249.

Aagaard, T. and Masselink, G. 1999. The surf zone. In Short, A. D. (ed.), *Handbook of Beach and Shoreface Morphodynamics*. Wiley, Chichester, pp. 72–113.

Aagaard, T., Nielsen J. and Greenwood, B. 1998. Suspended sediment transport and nearshore bar formation on a shallow intermediate state beach. *Marine Geology*, **148**, 203–225.

Aagaard, T., Kroon, A., Andersen, S., Möller Sørensen, R., Quartel, S. and Vinther, N. 2005. Intertidal beach change during storm conditions; Egmond, The Netherlands. *Marine Geology*, **218**, 65–80.

Aagaard, T., Kroon, A., Hughes, M. G. and Greenwood, B. 2008. Field observations of nearshore bar formation. *Earth Surface Processes and Landforms*, **33**, 1021–1032.

Almar, R., Coco, G., Bryan, K. R., Huntley, D. A., Short, A. D. and Senechal, N. 2008. Video observations of beach cusp morphodynamics. *Marine Geology*, **254**, 215–223.

Are, F. and Reimnitz, E. 2008. The A and m coefficients in the Bruun/Dean equilibrium profile equation seen from the Arctic. *Journal of Coastal Research*, **24 SP**2, 243–249.

Ashton, A., Murray, A. B. and Arnault, O. 2001. Formation of coastal features by large-scale instabilities induced by high angle waves. *Nature*, **414**, 296–300.

Austin, M. J. and Buscombe, D. 2008. Morphological change and sediment dynamics of the beach step on a macrotidal gravel beach. *Marine Geology*, **249**, 167–183.

Bagnold, R. A. 1940. Beach formation by waves: some model experiments in a wave tank. *Journal of the Institute of Civil Engineers*, **15**, 27–52.

Baillard J. A. 1981. An energetics total load sediment transport model for a plane sloping beach. *Journal of Geophysical Research*, **86**, 10938–10954.

Bascom, W. N. 1951. The relationship between sand size and beach face slope. *Transactions of the American Geophysical Union*, **52**, 866–874.

Bascom, W. N. 1953. Characteristics of natural beaches. *Proceedings of the Coastal Engineering Conference*, ASCE, pp. 163–180.

Bauer, B. O., and Greenwood, B. 1990. Modification of a linear bar-trough system by a standing edge wave. *Marine Geology*, **92**, 177–204.

Bishop, C. T. 1983. A shore protection alternative: artificial headlands. *Proceedings of the Canadian Coastal Conference*, National Research Council of Canada, pp. 305–319.

Bluck, B. J. 1967. Sedimentation of beach gravels: Examples from south Wales. *Journal of Sedimentary Petrology*, **37**, 128–156.

Boczar-Karakiewicz, B. and Davidson-Arnott, R. G. D. 1987. Nearshore bar formation by non-linear wave processes: A comparison of model results and field data. *Marine Geology*, **77**, 287–304.

Bowen, A. J. 1980. Simple models of nearshore sedimentation; beach profiles and longshore bars. In McCann, S. B. (ed.), *The Coastline of Canada*. Geological Survey of Canada Paper 80–10, pp. 1–11.

Bowen, A. J. and Inman, D. L. 1971. Edge waves and crescentic bars. *Journal of Geophysical Research*, **76**, 8862–8871.

Brander, R. W. 1999. Field observations on the morphodynamic evolution of a low-energy rip current system. *Marine Geology*, **157**, 199–217.

Bruun, P. 1954. *Coast Erosion and the Development of Beach Profiles*. Beach Erosion Board, Technical Memorandum 44, 66 pp.

Buscombe, D. and Masselink, G. 2006. Concepts in gravel beach dynamics. *Earth-Science Reviews*, **79**, 33–52.

Carter, T. G., Liu, P. L. and Mei, C. C. 1973. Mass transport by waves and offshore sand bedforms. Journal of Waterway, Harbors and Coastal Engineering. *ASCE*, **WW2**, 165–184.

Chandler, J. 1999. Effective application of automated digital photogrammetry for geomorphological research. *Earth Surface Processes and Landforms*, **24**, 51–63.

Coco, G., O'Hare, T. J. and Huntley, D. A. 1999. Beach cusps: a comparison of data and theories for their formation. *Journal of Coastal Research*, **15**, 741–749.

Cowell, P. J., Hanslow, D. J. and Meleo, J. F. 1999. The shoreface. In Short, A. D. (ed.), *Handbook of Beach and Shoreface Morphodynamics*. Wiley, Chichester, pp. 39–71.

Dally, W. R. 1987. Longshore bar formation – surf beat or undertow? *Proceedings Coastal Sediments '87*, ASCE, pp. 71–86.

Dally, W. R. and Dean, R. G. 1984. Suspended sediment transport and beach profile evolution. *Journal of Waterway, Port, Coastal and Ocean Engineering*, **110**, 15–33.

Dalrymple, R. A. 1992. Prediction of storm/normal beach profiles. *Journal of Waterway, Port, Coastal and Ocean Engineering*, **118**, 193–200.

Damgaard Christensen, E., Deigaard, R. and Fredsøe, J. 1994. Sea bed stability on a long straight coast. *Proceedings ICCE '94*. ASCE, New York, pp. 1865–1879.

Davidson-Arnott, R. G. D., 1981. Computer simulation of nearshore bar formation. *Earth Surface Processes and Landforms*, **6**, 23–34.

Davidson-Arnott, R. G. D., 1988. Controls on the formation and form of barred nearshore profiles, *Geographical Review*, **78**, 185–193.

Davidson-Arnott, R. G. D. and Pember, G. F. 1980. Morphology and sedimentology of multiple parallel bar systems, Southern Georgian Bay, Ontario. In McCann, S. B. (ed.), *The Coastline of Canada*, Geological Survey of Canada Paper 80–10, pp. 417–428.

Davidson-Arnott, R. G. D. and McDonald, R. A. 1989. Nearshore water motion and mean flows in a multiple parallel bar system. *Marine Geology*, **86**, 321–338.

Davis, R. A. Jr., and Fox, W. T. 1972. Coastal Processes and nearshore sand bars. *Journal of Sedimentary Petrology*, **42** 401–412.

Davis, R. A. Jr., Fox, W. T., Hayes, M. O. and Boothroyd, J. C. 1972. Comparison of ridge and runnel systems in tidal and non-tidal environments. *Journal of Sedimentary Petrology*, **42**, 413–421.

Dawson, J. C., Davidson-Arnott, R. G. D. and Ollerhead, J. 2002. Low-energy morphodynamics of a ridge and runnel system. *Journal of Coastal Research*, **SI 36**, 198–215.

Dean, R. G. 1991. Equilibrium beach profiles: characteristics and applications. *Journal of Coastal Research*, **7**, 53–84.

Dean, R. G. 1997. Models for barrier island restoration. *Journal of Coastal Research*, **13**, 694–703.

Dean, R. G., Healy, T. R. and Dommerholt, A. P. 1993. A 'blind-folded' test of equilibrium beach profile concepts with New Zealand data. *Marine Geology*, **109**, 253–266.

Dolan, R. 1971. Coastal landforms, crescentic and rhythmic. *Geological Society of America Bulletin*, **82**, 177–180.

Duncan, R. 1964. The effects of water table and tidal cycle on swash-backwash sediment distribution and beach profile development. *Marine Geology*, **2**, 186–197.

Dyhr-Nielsen, M. and Sørensen, T. 1970. Some sand transport phenomena on coasts with bars. *Proceedings Coastal Engineering Conference*, ASCE, 855–866.

Evans, O. F. 1940. The low and ball of the east-shore of Lake Michigan. *Journal of Geology*, **48** 467–511.

Falqués, A., Dodd, N., Garnier, R., Ribas, F., MacHardy, L. C., Larroudé, P., Calvete, D. and Sancho, F. 2008. Rhythmic surf zone bars and morphodynamic self-organization. *Coastal Engineering*, **55**, 622–641.

Garcez-Faria, A. F., Tornton, E. B., Lippmann, T. C. and Stanton, T. P. 2000. Undertow over a barred beach. *Journal of Geophysical Research*, **105 (C7)**, 16999–17010.

Gorman, L., Morang, A. and Larson, R. 1998. Monitoring the coastal environment; Part IV: mapping, shoreline change and bathymetric analysis. *Journal of Coastal Research*, **14**, 61–92.

Goodfellow, B. W. and Stephenson, W. J. 2005. Beach morphodynamics in a strong-wind bay: a low energy environment? *Marine Geology*, **214**, 101–116.

Gourlay, M. R. 1968. *Beach and Dune Erosion Tests*. Delft Hydraulics Laboratory Report No. M935/M936.

Greenwood, B. and Davidson-Arnott, R. G. D., 1972. Textural variation in the sub-environments of the shallow-water wave zone, Kouchibouguac Bay, New Brunswick. *Canadian Journal of Earth Sciences*, **9**, 679–688.

Greenwood, B. and Davidson-Arnott, R. G. D. 1975. Marine bars and nearshore sedimentary processes, Kouchibouguac Bay, New Brunswick, Canada. In Hails, J. and Carr, A. (eds.), *Nearshore Sediment Dynamics and Sedimentation: An Interdisciplinary Review*. Wiley, Chichester, pp. 123–150.

Greenwood, B. and Davidson-Arnott, R. G. D. 1979. Sedimentation and equilibrium in wave-formed bars: a review and case study. *Canadian Journal of Earth Sciences*, **16**, 312–332.

Greenwood, B. and Mittler P. R. 1984. Sediment flux and equilibrium slopes in a barred nearshore. *Marine Geology*, **60**, 79–98.

Greenwood, B., Hale, P. B. and Mittler, P. R. 1979. Sediment flux determination in the nearshore zone. *Proceedings Workshop on Instrumentation for Currents and Sediments in the Nearshore Zone*. National Research Council of Canada, pp. 99–115.

Greenwood, B., Richards, R. G. and Brander, R. W. 1993. Acoustic imaging of sea-bed geometry: a high resolution remote tracking sonar (HERTSII). *Marine Geology*, **112**, 207–218.

Greenwood, B., Permanand-Schwartz, A. and Houser, C. A. 2006. Emergence and migration of a nearshore bar: sediment flux and morphological change on a multi-barred beach in the Great Lakes. *Géographie Physique et Quaternaire*, **60**, 31–47.

Guza, R. T. and Inman, D. L. 1975. Edge waves and beach cusps. *Journal of Geophysical Research*, **80**, 2997–3012.

Hale, P. B., and McCann, S. B. 1982. Rhythmic topography in a mesotidal, low-wave energy environment. *Journal of Sedimentary Petrology*, **52**, 415–429.

Hallermeier, R. J. 1981. A profile zonation for seasonal sand beaches from wave climate. *Coastal Engineering*, **4**, 253–277.

Hancock, G. and Willgoose, G. 2001. The production of digital elevation models for experimental model landscapes. *Earth Surface Processes and Landforms*, **26**, 475–490.

Hine, A. C. 1979. Mechanisms of berm development and resulting beach growth along a barrier spit complex. *Sedimentology*, **26**, 333–351.

Holland, K. T. and Holman, R. A. 1996. Field observations of beach cusps and swash motions. *Marine Geology*, **134**, 77–93.

Holman, R. A. and Lippman, T. C. 1986. Remote sensing of nearshore bar systems – making morphology visible. *Proceedings Coastal Engineering Conference*, ASCE, 929–944.

Holman, R. A. and Sallenger, A. H. 1993. Sand bar generation: a discussion of the Duck experiment series. *Journal of Coastal Research*, **SI 15**, 76–92.

Holman, R. A. and Stanley, J. 2007. The history and technical capabilities of Argus. *Coastal Engineering*, **54**, 477–491.

Hom-ma, M. and Sonu, C. J. 1962. Rhythmic pattern of longshore bars related to sediment characteristics. *Proceedings Coastal Engineering Conference*, ASCE, pp. 248–278.

Horn, D. P., 1992. A numerical model for shore-normal sediment size variation on a macro-tidal beach. *Earth Surface Processes and Landforms*, **17**, 755–773.

Horn, D. P., 2002. Beach groundwater dynamics. *Geomorphology*, **48**, 121–146.

Houser, C. and Greenwood, B. 2005. Profile response of a lacustrine multiple barred nearshore to a sequence of storm events. *Geomorphology*, **69**, 118–137.

Houser, C. and Greenwood, B., and Aagaard, T. 2006. Divergent response of an intertidal swash bar, *Earth Surface Processes and Landforms*, **31**, 1775–1791.

Hsu, J. R. C., Silvester, R. and Xia, Y. M. 1989. Generalities on static equilibrium bays. *Coastal Engineering*, **12**, 353–369.

Huntley, D. A. 1980. Edge waves in a crescentic bar system. In McCann, S. B. (ed.), *The Coastline of Canada*. Geological Survey of Canada Paper 80–10, pp. 111–121.

Huntley, D. A. and Bowen, A. J. 1978. Beach cusps and edge waves. *Proceedings 16th Conference on Coastal Engineering*, ASCE, 1378–1393.

Inman, D.L., Elwany, M.H. and Jenkins, S.A. 1993. Shore rise and bar berm on ocean beaches. *Journal of Geophysical Research*, **98**, 18181–18199.

Jennings, R. and Shulmeister, J. 2002. A field based classification scheme for gravel beaches. *Marine Geology*, **182**, 211–228.

Keulegan, G.H. 1948. *An Experimental Study of Submarine Sandbars*. Beach Eroson Board, Technical Report 3, 40 pp.

King, C.A.M. and Williams, W.W. 1949. The formation and movement of sand bars by wave action. *Geographical Journal*, **112**, 70–85.

Komar, P.D., 1971. Nearshore cell circulation and the formation of giant cusps. *Geological Society of America Bulletin*, **82**, 2643–50.

Komar, P.D., 1983. Rhythmic shoreline features and their origin, In Gardner, R. and Scoging, H. (editors), *Mega-Geomorphology*, Clarendon, Oxford, pp. 92–112.

Komar, P.D. 1998. *Beach Processes and Sedimentation*, Prentice-Hall, 2nd edn., 544 pp.

Komar, P.D. and McDougal, W.G. 1994. The analysis of beach profiles and nearshore processes using the exponential beach profile form. *Journal of Coastal Research*, **10**, 59–69.

Konicki, K.M. and Holman, R.A. 2000. The statistics and kinematics of transverse sand bars on an open coast. *Marine Geology*, **169**, 69–101.

Kroon A. and Masselink, G. 2002. Morphodynamics of intertidal bar morphology on a macrotidal beach under low-energy wave conditions. North Lincolnshire, England. *Marine Geology*, **190**, 591–608.

Lawler, D.M. 1992. Design and installation of a novel automatic erosion monitoring system. *Earth Surface Processes and Landforms*, **17**, 455–463.

Lee, G., Nicholls, R.J. and Birkemeier, W.A. 1998. Storm-driven variability of the beach-nearshore profile at Duck, North Carolina, 1981–1991. *Marine Geology*, **148**, 163–177.

Levoy, F., Anthony, E.J., Monfort, O. and Larsonneur, C. 2000. The morphodynamics of megatidal beaches in Normandy, France. *Marine Geology*, **171**, 39–59.

Lippman, T.C., Holman, R.A. 1990. The spatial and temporal variability of sand bar morphology. *Journal of Geophysical Research*, **106**, 973–989.

Lippman, T.C., Holman, R.A. and Hathaway, K.K. 1993. Episodic, non-stationary behaviour of a double bar system at Duck, NC, USA, 1986–1991. *Journal of Coastal Research*, **SI 15**, 49–75.

Liu, J.T. and Zarillo, G.A. 1989. Distribution of grain size across a transgressive shoreface. *Marine Geology*, **87**, 121–136.

Masden, A.J. and Plant, N.G. 2001. Intertidal beach slope prediction compared to field data. *Marine Geology*, **173**, 121–139.

Masselink G. 1993. Simulating the effects of tides on beach morphodynamics. *Journal of Coastal Research*, **SI 15**, 180–197.

Masselink G. 2004. Formation and evolution of multiple intertidal bars on macrotidal beaches: application of a morphodynamic model. *Coastal Engineering*, **51**, 713–730.

Masselink, G. and Short, A.D. 1993. The effect of tide range on beach morphodynamics, a conceptual model. *Journal of Coastal Research*, **9**, 785–800.

Masselink, G. and Hegge, B. 1995. Morphodynamics of meso- and macrotidal beaches: examples from central Queensland, Australia. *Marine Geology*, **129**, 1–23.

Masselink, G. and Pattiaratchi, C.B. 1998. The effects of sea breeze on beach morphology, surf zone hydrodynamics and sediment resuspension. *Marine Geology*, **146**, 115–135.

Masselink G. Hegge, B and Pattiaratchi, C.B. 1997. Beach cusp morphodynamics. *Earth Surface Processes and landforms*, **22**, 1139–1155.

Masselink, G., Kroon, A. and Davidson-Arnott, R.G.D. 2006. Intertidal bar morphodynamics – a review. *Geomorphology*, **73**, 33–49.

Masselink, G., Austin, M., Tinker, J., O'Hare, T., and Russell, P. 2008. Cross-shore sediment transport and morphological response on a macrotidal beach with intertidal bar morphology, Truc Vert, France. *Marine Geology*, **251**, 141–155.

McLean, R.F. and Kirk, R.M. 1969. Relationship between grain size, size-sorting, and foreshore slope on mixed sand-shingle beaches. *New Zealand Journal of Geology and Geophysics*, **12**, 138–155.

Michel, D. and Howa, H.L. 1999. Short-term morphodynamic response on a ridge and runnel system on a mesotidal sandy beach. *Journal of Coastal Research*, **15**, 428–437.

Morris, B.A., Davidson, M.A. and Huntley, D.A, 2001. Measurements of the response of a coastal inlet using video monitoring techniques. *Marine Geology*, **175**, 251–272.

Nicholls, R.J., Birkemeier, W.A. and Lee, G.-H. 1998. Evaluation of depth of closure using data from Duck, NC, USA. *Marine Geology*, **148**, 179–201.

Niederoda, A.W. and Tanner, W.F. 1970. Preliminary study of transverse bars. *Marine Geology*, **9**, 41–62.

Nielsen, P. and Hanslow, D.J. 1991. Wave runup distributions on natural beaches. *Journal of Coastal Research*, **7**, 1139–1152.

Nolan, T. J., Kirk, R. M. and Shulmeister, J. 1999. Beach cusp morphology on sand and mixed sand and gravel beaches, South Island, New Zealand. *Marine Geology*, **157**, 185–198.

O'Hare, T. J. and Huntley, D. A. 1994. Bar formation due to wave groups and associated long waves. *Marine Geology*, **116**, 313–325.

Ojeda, E. and Guillén, J. 2008. Shoreline dynamics and beach rotation of artificial embayed beaches, *Marine Geology*, **253**, 51–62.

Orford, J. D. 1975. Discrimination of particle zonation on a pebble beach. *Sedimentology*, **22**, 441–463.

Ortega-Sánchez, M., Fachin, S., Sancho, F., and Losada, M. A. 2008. Relation between beachface morphology and wave climate at Trafalgar beach (Cadiz, Spain). *Geomorphology*, **99**, 171–185.

Owens, E. H. and Frobel, D. H. 1977. Ridge and runnel systems in the Magdalen Islands, Quebec. *Journal of Sedimentary Petrology*, **47**, 191–198.

Plant, N. G., Holman, R. A., Freilich, M. H. and Birkemeir, W. A. 1999. A simple model for interannual bar behaviour. *Journal of Geophysical Research*, **104**, C7, 15, 755–15,776.

Plant, N. G., Freilich, M. H. and Holman, R. A. 2001. Role of morphologic feedback in surf zone sand bar response. *Journal of Geophysical Research*, **106**, 973–989.

Pilkey, O. H., Young, R. S., Riggs, S. R., Smith, A. W. S., Wu, H. and Pilkey, W. D. 1993. The concept of shoreface profile of equilibrium: a critical review. *Journal of Coastal Research*, **9**, 255–278.

Price, T. D. and Ruessink, B. G. 2008. Morphodynamic zone variability on a microtidal barred beach. *Marine Geology*, **251**, 98–109.

Pruszak, Z., Rozynski, G. and Zeidler, R. B. 1997. Statistical properties of multiple bars. *Coastal Engineering*, **31**, 263–280.

Quartel, S., Ruessink, B. G. and Kroon, A. 2007. Daily to seasonal cross-shore behaviour of quasi-persistent intertidal beach morphology. *Earth Surface Processes and Landforms*, **32**, 1293–1307.

Quartel, S., Kroon, A. and Ruessink, B. G. 2008. Seasonal accretion and erosion patterns of a microtidal sandy beach. *Marine Geology*, **250**, 19–33.

Ranasinghe, R., Symonds, G., Black, K. and Holman, R. 2004a. Morphodynamics of intermediate beaches: A video imaging and numerical modelling study. *Coastal Engineering*, **51**, 629–655.

Ranasinghe, R., McLoughlin, R., Short, A. and Symonds, G. 2004b. The Southern oscillation Index, wave climate and beach rotation. *Marine Geology*, **204**, 273–287.

Reichmüth, B. and Anthony, E. J. 2007. Tidal influence on the intertidal bar morphology of two contrasting macrotidal beaches. *Geomorphology*, **90**, 101–114.

Ridd, P. V. 1992. A sediment level sensor for erosion and siltation detection. *Estuarine, Coastal and Shelf Science*, **35**, 355–362

Robertson, W., Zhang, K. and Whitman, D. 2007. Hurricane-induced beach change derived from airborne laser measurements near Panama City, Florida. *Marine Geology*, **237**, 191–205

Ruessink, B. G., van Enckvort, I. M. J., Kingston, K. S. and Davidson, M. A. 2000. Analysis of two- and three-dimensional nearshore bar behaviour. *Marine Geology*, **169**, 161–183.

Sallenger, A. H. 1979. Beach cusp formation. *Marine Geology*, **29**, 23–37.

Sallenger, A. H. Jr., Howard, P. C., Fletcher, C. H. and Howd, P. A. 1983. A system for measuring bottom profile, waves and currents in the high-energy nearshore environment. *Marine Geology*, **51**, 63–76.

Sallenger, A. H. Jr., Holman, R. A. and Birkemeier, W. A. 1985. Storm-induced response of a nearshore bar system. *Marine Geology*, **64**, 237–258.

Sedrati, M. and Anthony, E. 2007. Storm-generated morphological change and longshore sand transport in the intertidal zone of a multi-barred macrotidal beach. *Marine Geology*, **244**, 209–229.

Seymour, R. J. and Aubrey, D. G. 1985. Rhythmic beach cusp formation: a conceptual synthesis. *Marine Geology*, **65**, 23–37.

Shand, R. D., Bailey, D. G. and Shepherd, M. J. 2001. Longshore realignment of shore-parallel sand-bars at Wanganui, New Zealand. *Marine Geology*, **179**, 147–161.

Shepard, F. P. 1950a. Longshore bars longshore troughs. *Beach Erosion Board, Technical Memorandum* **20**, 38 pp.

Shepard, F. P. 1950b. Beach cycles in southern California. *Beach Erosion Board, Technical Memorandum* **15**, 32 pp.

Shepard, F. P. 1963. *Submarine Geology.* 2nd edn., Harper and Row, New York, 557 pp.

Sherman, D. J., Orford, J. D. and Carter, R. W. G. 1993. Development of cusp-related, gravel size and shape facies at Malin Head, Ireland. *Sedimentology*, **40**, 1139–1152.

Short, A. D. 1975. Offshore bars along the Alaskan Arctic coast. *Journal of Geology*, **83**, 209–221.

Short, A. D. 1979. Three dimensional beach stage model. *Journal of Geology*, **87**, 553–571.

Short, A. D. and Aagaard, T. 1993. Single and multi-bar beach change models. *Journal of Coastal Research*, **SI 15**, 141–157.

Short, A. D., and Masselink, G. 1999. Embayed and structurally controlled beaches. In Short, A. D. (ed.), *Handbook of Beach and Shoreface Morphodynamics*. Wiley, Chichester, pp. 230–250.

Silvester, 1974. *Coastal Engineering*. Elsevier, Amsterdam, 2 volumes.

Sonu, C. J. 1968. Collective movement of sediments in nearshore environments. *Proceedings Coastal Engineering Conference*, ASCE, pp. 373–400.

Sonu, C. J., 1973. Three-dimensional beach changes. *Journal of Geology*, **81**, 42–64.

Stewart, C. J. and Davidson-Arnott, R. G. D. 1988. Morphology, formation and migration of longshore sandwaves; Long Point, Lake Erie, Canada, *Marine Geology*, **81**, 63–77.

Stive, M. J. F. and Battjes, J. A. 1984. A model for offshore sediment transport. *Proceedings Coastal Engineering Conference*, ASCE, pp. 1420–1436.

Stive, M. J. F. and de Vriend, H. J. 1995. Modelling shoreface profile evolution. *Marine Geology*, **126**, 235–248.

Sunamura, T. 1988. Beach morphologies and their change. In Horikawa, K. (ed.), *Nearshore Dynamics and Coastal Processes*. University of Tokyo Press, Tokyo, pp. 136–166.

Terpstra, P. D. and Chrzastowski, M. J. 1992. Geometric trends in the evolution of a small log-spiral embayment on the Illinois shore of Lake Michigan. *Journal of Coastal Research*, **8**, 603–617.

Thornton, E. B., Hurmiston, R. T. and Birkmeir, W. 1996. Bar/trough generation on a natural beach. *Journal of Geophysical Research*, **101 C5**, 12097–12110.

van Enckevort, I. M. J. and Ruessink B. G. 2003a. Video observations of nearshore bar behaviour. Part 1: alongshore uniform variability. *Continental Shelf Research*, **23**, 501–512.

van Enckevort, I. M. J. and Ruessink B. G. 2003b. Video observations of nearshore bar behaviour. Part 2: alongshore non-uniform variability. *Continental Shelf Research*, **23**, 513–532.

van Houwelingen, S., Masselink, G. and Bullard, J. 2006. Characteristics and dynamics of multiple intertidal bars, north Lincolnshire, England. *Earth Surface Processes and Landforms*, **31**, 428–443.

van Maanen, B., de Ruiter, P. J., Coco, G., Bryan K. R. and Ruessink, B. G. 2008. Onshore sandbar migration at Tairua Beach (New Zealand): Numerical simulations and field measurements. *Marine Geology*, **253**, 99–105.

Vittori, G., De Swart, H. E. and Blondeaux, P. 1999. Crescentic bedforms in the nearshore region. *Journal of Fluid Mechanics*, **381**, 271–303.

Wang, P. and Davis, R. A. Jr. 1998. A beach profile model for a barred coast – case study from Sand Keys, West-Central Florida. *Journal of Coastal Research*, **14**, 981–991.

Wang, P., Ebersole, B. A. and Smith, E. R. 2003. Beach-profile evolution under spilling and plunging breakers. Journal of Waterway, Port, *Coastal and Ocean Engineering*, **129**, 41–46.

Watts, G. M. 1954. Laboratory study of the effects of varying wave period on beach profiles. *Beach Erosion Board*, Technical Memorandum, **53**, 19 pp.

Weir, F. M., Hughes, M. G. and Baldock, T. E. 2006. Beach face and berm morphodynamics fronting a coastal lagoon, *Geomorphology*, **82**, 331–346.

Werner, B. T. and Fink, T. M. 1993. Beach cusps as self-organised patterns. *Science*, **260**, 968–971.

Wijnberg, K. M. and Wolf, F. C. J. 1994. Three-dimensional behaviour of a multiple bar system. *Proceedings of Coastal Dynamics '94*, ASCE, pp. 59–73.

Wijnberg, K. M. and Terwindt, J. H. J. 1995. Quantification of decadal morphological behaviour of the central Dutch coast. *Marine Geology*, **126**, 301–330.

Wijnberg, K. M. and Kroon, A. 2002. Barred beaches. *Geomorphology*, **48**, 103–120.

Wright, L. D. and Thom, B. G. 1977. Coastal depositional landforms, a morphodynamic approach. *Progress in Physical Geography*, **1**, 412–459.

Wright, L. D. and Short, A. D. 1983. Morphodynamic of beaches and surf zones in Australia. In Komar, P. D. (ed.), *Handbook of Coastal Processes and Erosion*. CRC Press, Boca Raton, FL, pp. 35–64.

Wright, L. D. and Short, A. D. 1984. Morphodynamic variability of surf zones and beaches: a synthesis. *Marine Geology*, **56**, 93–118.

Wright, L. D., Guza, R. T. and Short, A. D. 1982. Dynamics of a high energy surf zone. *Marine Geology*, **45**, 41–62.

Wright, L. D., Short, A. D. and Green, M. O. 1985. Short-term changes in the morphodynamic states of beaches and surf zones: an empirical predictive model. *Marine Geology*, **62**, 339–364.

Yasso, W. E. 1965. Plan geometry of headland bay beaches. *Journal of Geology*, **73**, 702–714.

Zhang, K., Whitman, D., Leatherman, S. and Robertson, W. 2005. Quantification of beach changes caused by Hurricane Floyd along Florida's Atlantic coast using airborne laser surveys. *Journal of Coastal Research*, **21**, 123–134.

9

Coastal sand dunes

9.1 Synopsis

Sandy beaches offer an exposed source of sediment and so almost all sandy beaches are fringed by some form of sand dune formed by sand transported by wind action and deposited in the vegetation landward of the beach. Dunes range from small forms less than a metre in height and a few metres in width and alongshore extent on small rocky embayments, to features that may be 100 m or more in height, extending for tens of km alongshore on sandy barrier systems or low coastal plains. Generally most of the sediment transported landward from the backshore is trapped initially by vegetation colonising the area just landward from the limit of storm wave action, leading to the development of a foredune ridge complex parallel to the shoreline. On some beaches, because of limited sediment availability or low frequency of strong onshore winds, only a single foredune complex will develop. However, in other areas where there is an abundant supply of sediment and sufficiently strong onshore winds, extensive dune fields may develop, either through inland migration of parabolic or long-walled transverse dunes, or through shoreline progradation and the formation of a succession of foredune ridges.

The area close to the beach is a zone of high stress for plants as a result of high temperatures near the bed, moisture deficit, exposure to salt spray, low nutrient supply and especially because of disturbance due to burial by sand transported by the wind and to the effects of wave action during storms. As a result, plants found in the pioneer zone of the backshore and within the foredune system are limited to a few species, especially grasses, that are adapted to these stresses. There is usually a gradient of decreasing stress inland away from the beach and this gradient is reflected in increasing plant diversity and a shift to species that are less tolerant of stress – usually this is manifested as increased coverage by bushes and trees.

Sand accumulates within and behind plants because of the reduction in wind speed close to the bed by the plant foliage and this sheltering effect provides protection against remobilisation by winds. Continued deposition in the dune occurs because the plants continue to grow as more sand is trapped, unlike fixed obstacles such as sand fencing. During periods between major storms vegetation may grow seaward trapping sand in newly developing embryo dunes and during storms with elevated water levels and high waves the embryo dune and foredune are eroded and sand is returned to the littoral system. This beach/dune interaction is a significant process controlling the evolution of the foredune system.

In addition to their natural beauty and the unique ecological habitat that they provide, dunes are a significant resource for human activities including their contribution to a host of recreational activities, their role in preventing saltwater intrusion into coastal aquifers, and the protection they offer to the area

behind the foredune from storm surge and high wave action.

9.2 Morphological components of coastal dunes and dune fields

Coastal sand dunes are sedimentary deposits formed by the transport of sediment inland from the beach by wind action. In sediment budget terms, the beach is the source and the dunes represent the sink. Because fine sediments are generally scarce in active sandy beaches, coastal dune deposits have very small amounts of sediment <0.15 mm in size. Likewise, because of the small air density compared to water, particles >1 mm are selectively left on the beach during deflation and are also generally scarce. Where gravel and pebbles are present they tend to be part of underlying beach deposits or have been emplaced in the dune by swash action during storms.

9.2.1 Types of dune

A distinction can be made between impeded dunes that are largely fixed in place by vegetation and transgressive dunes (Pye, 1983) where vegetation is limited or absent. In the latter case sand is readily mobilised from the bare surface by wind action and the dune form reflects primarily patterns of wind flow (Table 9.1). In practice there is a continuum of coastal dune forms from those that are continuously covered by vegetation both temporally and spatially, through forms with varying degrees of vegetation cover and stabilisation, to completely unstabilised forms where there is too little moisture to support vegetation or where the sediment supply and transport is so large that vegetation cannot colonise the unstable sand surface. Mobility of free dunes in humid areas is often also limited by the presence of the water table and interdune ponding.

9.2.2 Primary dunes – foredunes and embryo dunes

The foredune system, including embryo dunes and the foredune ridge, is often termed the primary dune system with sand supplied directly from the beach and the form and orientation reflecting the beach as a source of sediment and the effects of wave action. In very dry coastal areas where beaches are backed by deserts there is insufficient vegetation to form impeded dunes and the beach is simply a source for sand which migrates inland in the form of free dunes (Figure 9.1a). However, where there is sufficient vegetation to trap sediment blowing inland off the beach we can distinguish between the foredune system adjacent to the beach and any dune field that may be present inland of this (Figures 9.1b, 9.2a). The foredune system consists of a generally continuous established foredune which runs parallel to the shoreline and any associated embryo dune (also termed an incipient foredune – Hesp, 1983) which may form at the toe of the seaward slope of the foredune ridge or on the backshore separate from the foredune ridge. Where the seaward face of the foredune has been eroded by wave action to produce a distinct scarp or cliff, the foredune system may also include an unvegetated dune ramp built against the scarp and again an embryo dune may develop on the backshore (Figure 9.2b). As we will see later in the section on foredune dynamics, most foredunes are compound features whose internal structures likely contain a record not only of accretion from aeolian transport but several, and sometimes many, episodes of erosion by wave action associated with storms and storm surge. A key characteristic of foredune ridges is that they form parallel to the beach irrespective of the prevailing or dominant wind direction. This is because of the role of plants in trapping the sediment and in turn the role of wave action in trimming the seaward edge of the vegetation so that it follows the shoreline trend.

Embryo dune are initiated seaward of the stoss slope of the foredune, where sand accumulates within and behind individual plants on the beach (Figure 9.2). Vegetation growth onto the beach may result from vegetative propagation of plants from the base of the dune in the form of surface runners or subsurface rhizomes; or from the establishment of new plants from seed or vegetation fragments

Table 1 *Coastal dune form and stability in relation to vegetation cover.*

	Vegetation cover	Dune form	Notes
Free dunes	vegetation absent or scarce	barchans, barchanoid ridges; transverse and oblique ridges	wide range of dune forms similar to desert dunes; found on beaches and dune fields
	vegetation bordering dunes	precipitation ridges	found at downwind border of transgressive dune fields
		blowouts, parabolic dunes	eroded in foredunes and stabilised dune fields
	vegetation covering dunes	stabilised ridges; dune fields	wide range of formerly active dune forms on transgressive dune fields
	vegetated dunes	embryo dunes; nebkhas	small, often laterally discontinuous forms developed in and around vegetation mostly stable,
		foredune ridges	large stable, laterally continuous features formed parallel to the beach
	vegetated dunes	relic foredune ridges, transverse ridges	formed on prograding or regressive shorelines; cut off from beach by development of new foredune(s)
Impeded dunes			

on the beach itself. In simple models of dune systems where there is beach progradation the embryo dunes coalesce and grow in height over time, eventually forming a continuous dune ridge that develops into a new foredune. The growth of the new vegetated foredune results in the trapping of all or most of the sand supply form the beach, and this cuts off the supply of sediment to the older dune landward. On stable and eroding shorelines the embryo dunes are ephemeral features that develop over a period of months to several years and are then removed by wave action during large storms. Embryo dunes are typically a few centimetres to one or two metres in height and 10–20 m in width. Established foredune ridges may be only a metre or so on short, narrow beaches, but are usually 5–20 m in height and 30–50 m wide, and they may grow to over 100 m in areas of strong onshore winds and large sand supply (Figures 9.3a, b).

9.2.3 Secondary dunes – parabolics and dune fields

Dune forms that are found in dune fields landward of the foredune system make up the secondary dune system. Where the littoral sediment budget is positive and beach progradation takes place the former foredune ridges may be preserved intact in terms of form and position under a dense vegetation cover and they thus mark the position of former shorelines. However, in most areas disturbance of the vegetation occurs from time to time due to both natural and human-induced causes resulting in the destabilisation of the foredune system or of older dunes landward of the foredune system. The result is the development of a variety of secondary forms from small bowl-shaped blowouts only a few tens of metres across, to large elongated parabolic dunes hundreds of metres across and more than 1 km in length, to migrating free forms which may be shaped as barchanoid

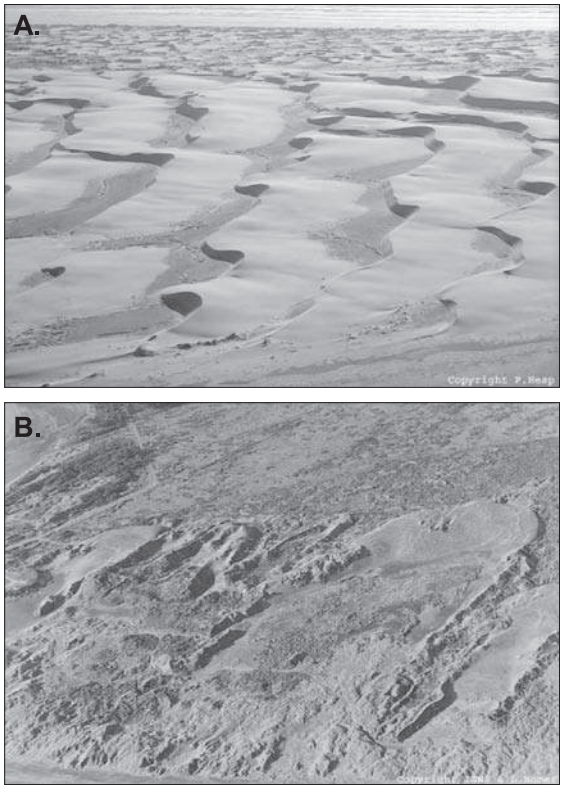

Figure 9.1 Photographs of coastal dunes and dune fields. (A) Sinuous, barchanoidal transverse duneson a transgressive dunefield in an arid environment at Guerrero Negro, Baja California, Mexico (photograph Patrick Hesp). (B) Active parabolic dunes on the Manawatu coast, North Island, New Zealand. A highly erosional foredune/blowout complex is present on the seaward margin (photograph Patrick Hesp).

ridges, transverse ridges or large sand sheets which may occupy hundreds to thousands of square kilometres. The orientation of these secondary features is no longer controlled by proximity to ocean waves and thus tends to be much more reflective of the wind climate and dominant wind direction as well as vegetation cover, the water table and the underlying topography.

9.3 Plant communities of coastal dunes

Coastal foredunes develop in response to the presence of vegetation which serves both to promote deposition of sand through the reduction in wind flow near the bed and to stabilise the resulting dune deposit by sheltering the bed from subsequent entrainment. The form and evolution of the dune, and especially of the embryo dunes, on a scale of years to decades is greatly influenced by the form and growth habits of the colonising vegetation, by its ability to adapt to a number of types of disturbance (e.g. burial by sand, sand blasting, wave erosion) and to factors which inhibit growth such as salt spray, high surface temperatures, moisture availability and lack of nutrients (Ranwell, 1972; Packham and Willis, 1997). In most dunes there is a distinct gradient in both the exposure to disturbance and to limiting factors away from the beach, and this often leads to the development of a well-defined sequence of vegetation associations along this gradient (Doing, 1985; Hesp, 1991; Hesp and Martínez, 2007; Dech and Maun, 2007). The influence of these limiting factors is so common to foredunes around the world that the vegetation in this zone often looks very similar because of the nature of adaptation even though the plant species themselves may be different. At the same time, some species form the dominant colonising vegetation over extensive areas – e.g. marram grass (*Amophila sp*.) in western Europe and north-eastern North America (including the shoreline of the Great Lakes) and *Ipomoea sp*. in tropical areas.

9.3.1 Environmental gradients and plant zonation on dunes

The classic model of plant succession on dunes (Cowles, 1899) emphasised the role of a succession of plant species in increasing stabilisation of the surface through time and the improved moisture retention and nutrient availability associated with the replacement of grasses by bushes and then forest. The model has some validity for progradational dune systems but it is now recognised that temporal evolution at any one location is likely more a reflection of spatial (morphological) evolution of the dune system leading to a reduction in disturbance and limiting factors such as exposure to salt spray and moisture stress (Hesp and Martinez, 2007; Miyanishi and Johnson, 2007; Miot da Silva

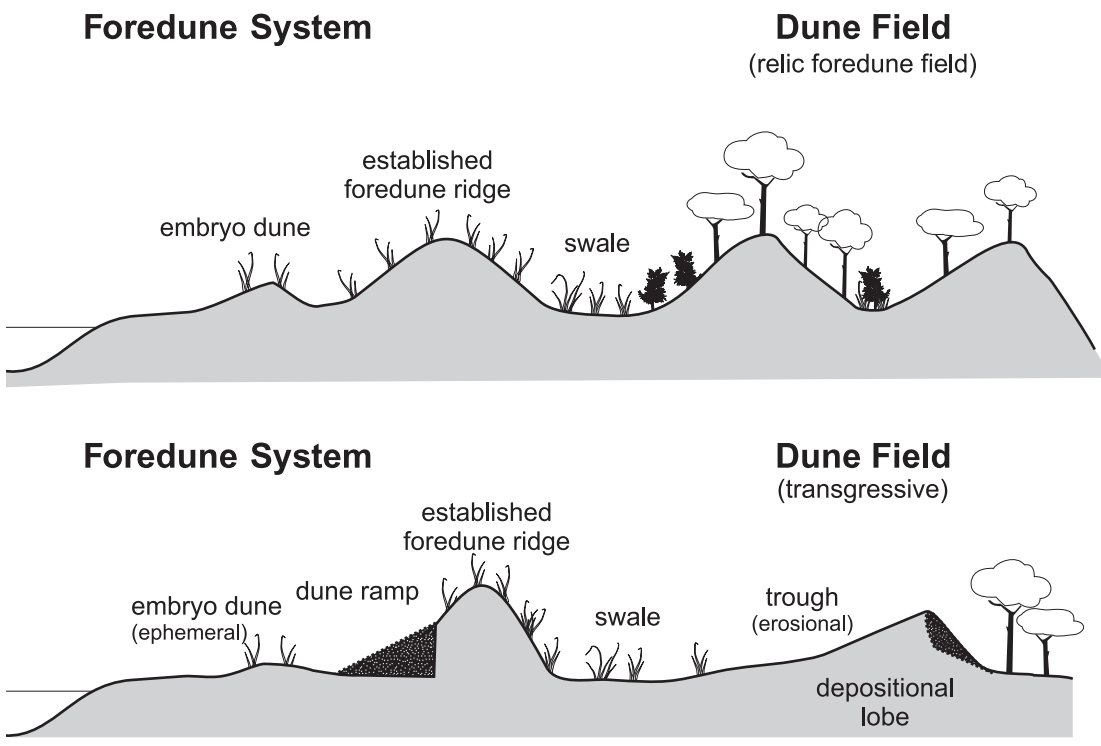

Figure 9.2 Sketch of profiles across: (a) a prograding beach showing the characteristics of the foredune system and relic foredune ridges; and (b) across a scarped foredune with dune ramp and active lee slope with a transgressive dune field landward characterised by parabolic dune development.

et al., 2008; Lane *et al.*, 2008). Thus, in the absence of salt spray, cottonwood trees (*Populus deltoides*) are a common coloniser on Great Lakes coastal dunes even in areas with a high sediment supply. Trees that are adapted to salt spray (such as coconut and manchineel) are common close to the shoreline on low energy tropical beaches where dune accretion rates are small. Where the beach sediment budget is near-neutral and the dune budget is positive there may be little change in the gradient of salt spray and sand burial over decades, and consequently little change in the plant communities. On the other hand, disturbances due to erosion by waves, blowout and parabolic dune development can quickly lead to a change in the dominant vegetation assembly locally, or over large parts of the dune field depending on the severity of the disturbance (Saunders and Davidson-Arnott, 1990; Maun, 2004). Thus, primary dune colonisers such as marram or ipomea can be found in inland locations where there has been local disturbance and reactivation of sand movement and plants typical of the stabilised portion of the lee slope may be found near the beach where wave erosion during a storm has removed much of the foredune. Alternatively foredune growth may lead to an increase in the water table in the dune slack landward of the bottom of the lee slope and thus to replacement of plants associated with dry conditions by plants such as rushes and sedges.

Doing (1985) divided the foredune system into six zones and summarised the zonation of plant communities within these for a range of locations world-wide. The basis for the zonation is the degree of sheltering from burial by sand and to a lesser extent the effect of disturbance by wave action and salt spray. The zones tend to be compressed in areas where sand supply is limited (narrow beaches on rocky coasts; wind

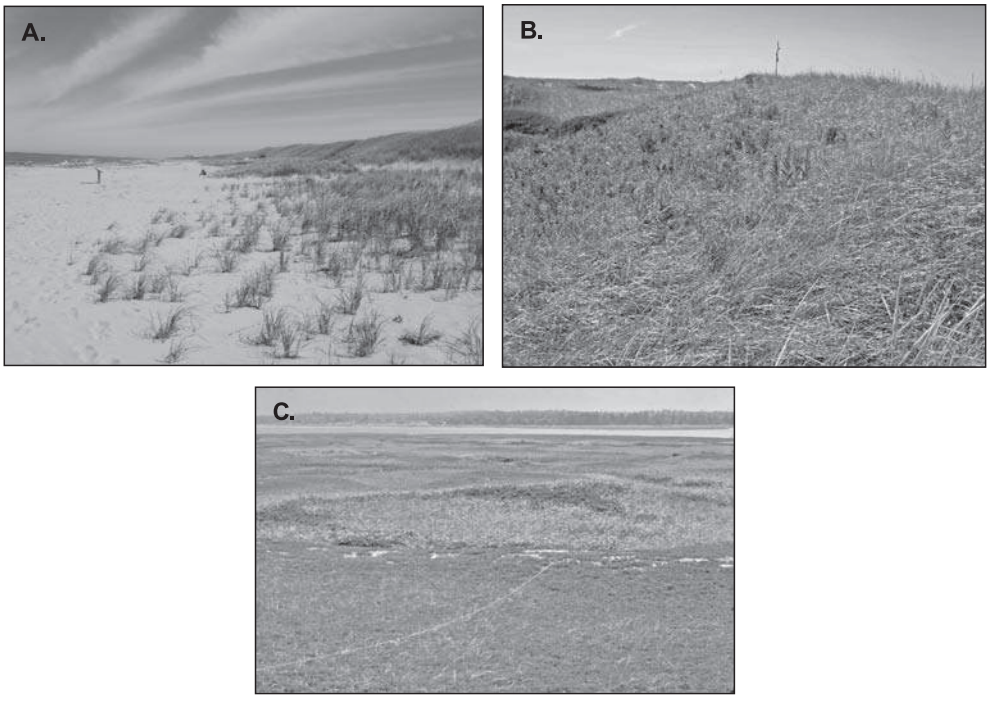

Figure 9.3 Foredune form and vegetation communities at Greenwich Dunes, NE Prince Edward Island, Canada: (A) Clumps of marram on the backshore and embryo dune and a dense covering on the stoss slope of the foredune. Note the panicles on many of the plants in the embryo dune – a sign of vigorous growth; (B) lee slope of the foredune with a transition from vigorous marram interspersed with Beach Pea (an annual) near the crest to seaside goldenrod and bayberry on the lower slopes; (C) a carpet of Hudsonia in the foreground with some senescent marram, gives way to clumps of bayberry, grasses and rushes in swales.

climate with a relatively small proportion of winds capable of onshore sand transport) or where the trapping ability of the pioneer species is high. In areas with high sand supply and/or plant communities with relatively poor ability to withstand burial or salt spray the zones may be quite wide and diffuse as disturbance extends inland for some distance (Miot da Silva *et al.*, 2008). The morphology and evolution of the embryo dune and foredune are influenced by the growth form of the particular plant species that are characteristic of a zone in a particular climatic region. Thus, for example, in tropical and subtropical areas the dominant vegetation of the embryo dune zones (2 and 3) is *Ipomoea pes-caprae* and *Spinifex*, both of which have surface runners which cover the sand surface and tend to produce a broad, relatively flat embryo dune. In contrast the dominant coloniser of these zones in eastern Canada and the NE United States is marram grass *(Amophila breviligulata)* which grows in high, dense clumps and extends seaward through the growth of subsurface rhizomes. Foredune development associated with marram tends to produce much narrower, sharp crested and hummocky ridges compared to those associated with *Ipomoea* and *Spinifex* (Hesp, 1989; 2004).

Foredune development and dune stability also depend on the ability of the dune plant communities to trap sand, and in areas of high sand supply to withstand burial to depths up to > 0.5 m (Moreno-Casasola, 1986). *Amophila breviligulata* which is the primary dune coloniser in eastern Canada, the Great Lakes and the NE United States is able to survive burial of 1 m or more (Maun and Lapierre, 1984; Maun, 2004) and propagates rapidly. As a result, foredunes in these areas tend to be relatively stable and major episodes of instability and parabolic dune formation often result

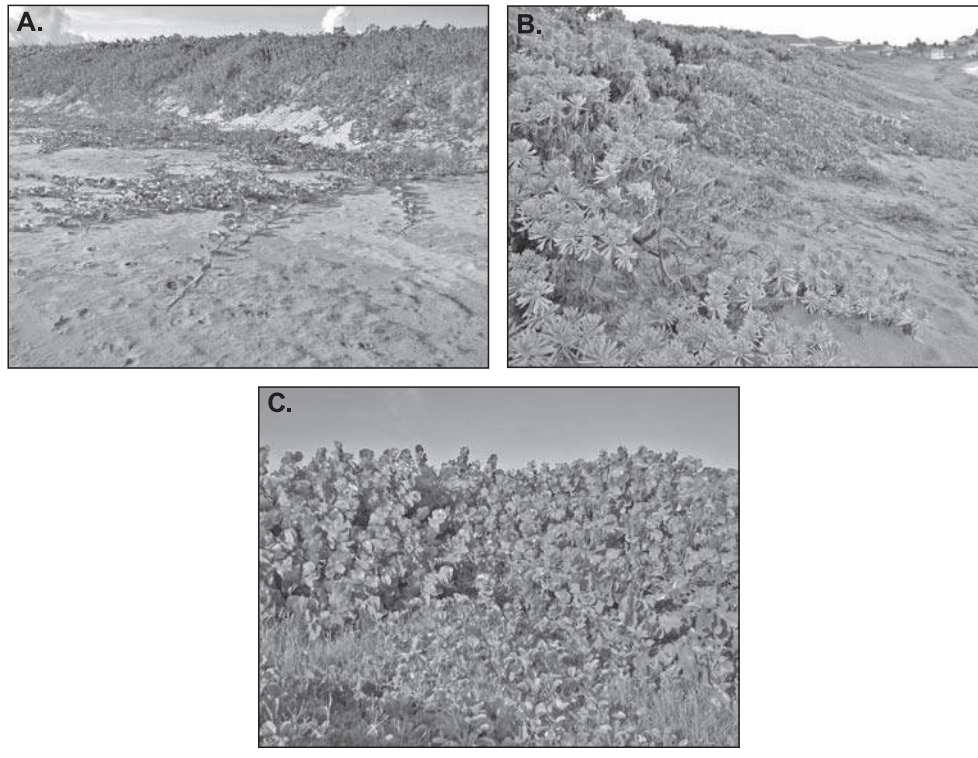

Figure 9.4 Foredune form and vegetation communities, Sandbank Beach, St Kitts, West Indies. (A) View of backshore with Ipomoea runners on the sand surface, Black Torch at the base of the dune and sea grape near the crest of the dune; (B) West Indian Sea Lavender (foreground) and Black Torch (background) on the lower foredune slope; (C) Sea Grape on the foredune crest, with a mixture of Seashore Saltgrass, Black Torch and Beach Morning Glory in the foreground.

from the impact of human activities, including agriculture and recreation, rather than natural phenomena. Where the pioneering species are less tolerant of burial, transgressive dune fields may be more common. The classic Coos Bay transgressive dunefield described by Cooper (1958) developed because of the inability of native species to withstand burial and thus foredunes were nearly absent. The introduction of *Amophila arenaria* from Europe has led to much greater stabilisation and the subsequent formation of a foredune system. Similarly, in New Zealand the native pingao grass (*Desmoschoenus spiralis*) is relatively slow growing and unable to withstand high rates of burial leading to generally higher degree of foredune instability and development of transgressive dune fields. Introduction of *Amophila arenaria* has changed the characteristic morphology of the foredune system and led to greater stabilisation.

9.3.2 Examples of foredune form and plant communities

Examples of a temperate and a tropical foredune and the plant communities associated with them are shown in Figures 9.3 and 9.4. The temperate example is taken from Greenwich Dunes, Prince Edward Island on the east coast of Canada at about 46° N latitude and the tropical example from the windward coast of St Kitts, an island in the Caribbean at about 15° N latitude. The two foredunes are roughly similar in height and are formed primarily in medium quartz sand.

Prince Edward Island

In Prince Edward Island and throughout the Gulf of St Lawrence the dominant vegetation of the stoss side of the foredune is marram (*Ammophila breviligulata*) and it also tends to be the most common plant on the upper backshore and any incipient dunes (Grandtner, 1993). In some areas

another grass, *Elymus mollis*, may occur together with marram and in colder, more northerly latitudes Elymus becomes the primary coloniser. Isolated clumps of the annual Sea Rocket (*Cakile edentula*) are found in places though they tend to be more common in areas not subject to human traffic. This is another species that is widespread throughout eastern Canada, the NE United States and is also found on the shores of the lower Great Lakes. In other parts of the Gulf of St Lawrence, Sandwort (*Honckenya peploides*) and Saltwort (*Salsola* sp.) may also be found on the backshore and embryo dune zones.

Ammophila is the dominant vegetation on the stoss slope and crest of the foredune where salt spray and deposition rates are still high Figure 9.3a). In these zones it grows vigorously in dense clumps, reaching heights of 50–100 cm. with broad, dark green leaves and many individual plants will flower and produce seeds. On the lee slope where deposition rates and salt spray are much reduced marram vigour becomes greatly reduced as is evident by much lower height and density, smaller leaf size and the absence of plants which produce panicles (Figures 9.3b, c). This senescence is well-known and also occurs in *Ammophila arenaria* and *Uniola paniculata*, both of which are also tolerant of high rates of burial by sand. The exact cause is not known but the plants respond quickly to inputs of fresh sand (e.g. around a blowout) so it would seem to be related to the absence of annual deposits of fresh sand (Maun and Baye, 1989). On the lee slope Beach Pea (*Lathyrus japonicus*) and Seaside Goldenrod (*Solidago sempivirens*) become common within the marram (Figure 9.3b). Where the foredune is quite wide there is more protection from spray and sand deposition, allowing clusters of shrubs to establish, chiefly Bayberry (*Myrica pensylvanica*) and Wild Rose (*Rosa virginiana*). Further inland on stable dunes False Heather (*Hudsonia tomentosa*) can be found the areas between shrubs, often occurring in association with senescent marram and an assemblage of lichens and mosses (Figure 9.3c). In places where the water table is close to the surface a variety of rushes and sedges are found together with low shrubs of bog cranberry.

St Kitts

North Friars Beach in St Kitts is exposed to the NE trade winds as well as to periods of large swell during the winter from storms in the North Atlantic and occasionally to the passage of hurricanes with large waves and high storm surge. There is a broad, flat backshore and embryo dune zone (Figure 9.4a) which is colonised primarily by surface runners (stolons) of Beach Morning Glory (*Ipomoea pes-caprae*), by Seashore Salt Grass (*Sporobulus virginicus*) and succulents such as Sea Purslane (*Sesuvium portulacastrum*). A variety of other plants may be present in small numbers (Stoffers, 1993).

At the toe of the foredune shrubs such as Black Torch (*Erithalis fruticosa*) and West Indian Sea lavender (*Tournefortia gnaphalodes*) become established (Figure 9.4b). These can withstand some disturbance and burial and are salt tolerant. About a third of the way up the foredune Sea Grape (*Coccoloba uvifera*) becomes dominant. This is a large bush or small tree that forms a dense, nearly impenetrable thicket up to 2–3 m in height (Figure 9.4c). It has large, leathery leaves that are nearly circular and have a distinctive red central vein. It bears grape-like clusters of fruit – hence its name. A cover of Sea Grape provides almost total protection to the dune. There is little possibility of remobilisation of sand below it, though sand blown off the beach can travel some distance inland simply by rebounding several times off the leaves and stems. On leeward coasts where dunes are rare, it grows on the backshore and can trap sediment washed inland as a result of storm surge and high waves during the passage of hurricanes. Dunes stabilised by Sea Grape provide excellent shelter from storm surge, wave action and strong winds during hurricanes, though they are often destroyed in the interest of a clear view of the ocean during construction of resort hotels.

9.4 Aeolian processes in coastal dunes

Coastal sand dunes are initiated and modified by aeolian sediment transport and a general understanding of the nature of fluid processes

associated with wind, and the movement of sediment in air is necessary to understand their development over time. The definitive work is still that of Bagnold (1941), but there are useful summaries related to coastal dunes in Pye (1983), Horikawa *et al.* (1986), Sarre (1987), and Nickling and Davidson-Arnott (1990). We will look first at the classic approach to wind flow and sediment transport which relates sediment transport to the bed shear velocity u_* and then review the complexities on natural beaches resulting from the spatial and temporal variability of wind flow, the effects of rapid changes in topography which affect the wind speed and direction, and factors such as beach surface moisture, pebble lags and vegetation which affect the supply of sediment to the air stream.

9.4.1 Winds and boundary layer processes

Air and water

Both air and water are Newtonian fluids but they differ significantly in their properties with respect to sediment entrainment and transport – i.e., their density and viscosity (see Table 9.2). Water is about a thousand times more dense than air and so the relative density (or buoyancy) of sand particles in air is very much less than in water. One result of this is that while even small waves can move sand in the water, sand transport by wind only occurs with relatively high wind speeds – in most cases over 6 m s^{-1} – and wind speeds measured one or two metres above the bed are often 5–10 times as fast as flows in rip currents during aeolian transport events.

Aeolian boundary layer

As with all fluid flow, wind blowing across a surface is affected by friction with the bed which leads to the generation of a boundary layer in which flow speed is retarded by contact with the land surface, and obstacles on it, and the pattern of wind flow is affected by the topography of the bed over which it passes. In Section 7.2.2 we saw that the boundary layer for wind flow over the surface consists of an inner bed layer a few centimetres thick, a logarithmic section which may be several metres in thickness, and an outer layer that may stretch for several hundreds of metres or more over very rough terrain (Figure 7.1). Above this lies the free stream where flows are essentially unaffected by retardation at the bed. In contrast to the wave boundary layer, which is built and destroyed with every wave, the aeolian boundary layer is continuous in time.

As long as there is no sediment transport, the velocity profile for air blowing over a smooth sand surface is logarithmic near the ground and can be adequately described by the equation

$$U = \frac{2.3}{K} U_* \log_{10} \frac{Z}{Z_0} \tag{9.1}$$

where

U = wind speed at some height above the surface; K is the von Karman constant (= 0.4)
u_* = bed shear velocity; Z = height above the sand surface at which U is measured and
Zo= roughness factor.

The bed shear velocity (U_*) is proportional to the slope of the wind velocity profile when plotted with a logarithmic height scale (Figure 9.5a, b) and is related to the shear stress (τ) at the bed and the air density (ρ) by

$$U_* = \sqrt{\frac{\tau}{\rho}}. \tag{9.2}$$

Bagnold (1941) used a value of $d/30$ for Zo, where d is the grain diameter, and while other values can be used, it does indicate that surface roughness over sand is initially a function of the grain diameter. Once the wind speed is high enough to entrain sand particles the velocity profile is altered by the sand movement, which drains momentum from the wind close to the bed and a new roughness factor Z_o' develops – estimated by Bagnold (1941) to be 0.3 cm. This appears to be related both to the actual effect of sand in transport in the lower layers and to the effects of bed roughness produced by ripple development. It is standard practice in both wind tunnel and field experiments to estimate u_* from measurements of wind speed at several heights within the logarithmic boundary layer through the use of a regression of wind speed (the dependent variable) against the log of height (Bauer *et al.*, 1992).

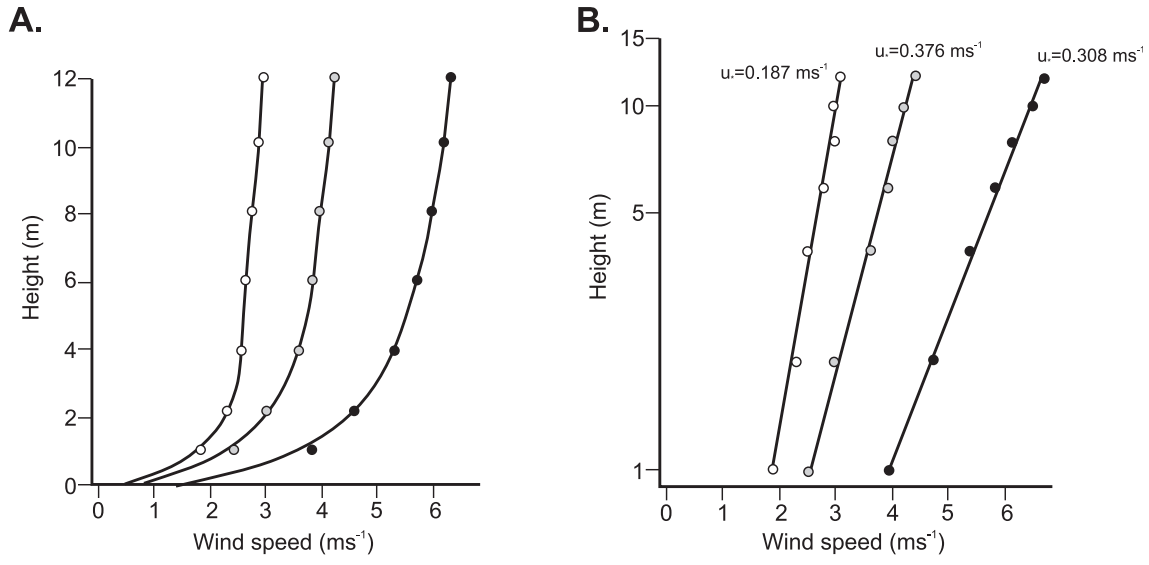

Figure 9.5 Wind velocity profiles plotted on (A) an arithmetic scale; (B) a logarithmic scale (Nickling and Davidson-Arnott, 1990).

The presence of ripples and dunes as well as obstacles such as driftwood on a beach also produces roughness which alters flow close to the bed and thus the shape of the velocity profile. Where the surface is covered by tall grasses or shrubs the wind velocity profile is displaced upwards from the surface (Olson, 1958a) to a new reference plane which is a function of the height, density, porosity and flexibility of the roughness elements. The upward displacement is termed the zero plane displacement height D. For these situations the wind profile equation becomes

$$\frac{U}{U_*} = \frac{1}{K}\frac{(Z-D)}{Z_0}. \tag{9.3}$$

The displacement height D can be thought of as the point at which the mean velocity tends to zero. However, this is of limited value for estimating wind transport on vegetated dunes where most erosion takes place in bare patches between vegetation elements and where gusts and variations in wind direction change the relative exposure of sand to transport over very short time periods and distances.

In wind tunnel experiments the wind speed is usually held constant or changed very slowly but in the field the flow is highly turbulent and so the wind speed is characterised by gusts with speeds well above the average and periods of time when the flow is much below the mean (Figure 9.6). Flow speed measured close to the bed is generally much less than at 2.5 m above the bed (Figure 9.6b). Both anemometers respond to rapid changes in flow speed and, while the pattern of medium-scale turbulence (on the order of tens of seconds) is similar for both instruments, there is considerable difference in the high-frequency fluctuation. Under these conditions it is only feasible to define the velocity profile (Figure 9.6c), and to estimate u_* from it, for averages taken over a period of several minutes. Typically a record of 10 or 15 minutes is used – long enough to get a robust mean but short enough to assume stationarity in the record. A shorter record time can be used though the error bars for estimating u_* increase rapidly for a duration <3 minutes (Namikas *et al.*, 2003). Note that in a wind tunnel where velocity measurements are typically made with a rake of pitot tubes, the lowermost measuring point is on the order of 10 grain diameters above the bed. In the field anemometers are usually deployed above 25 cm to place them outside the height of most sand saltation and the estimate of

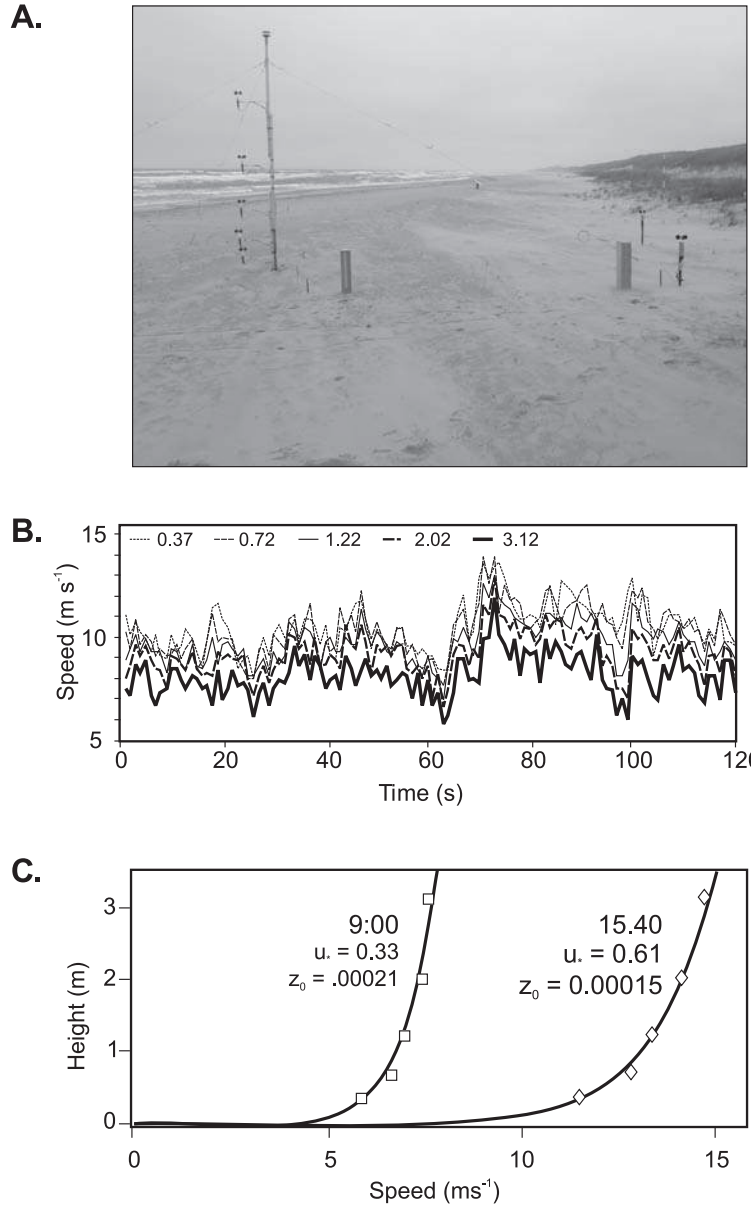

Figure 9.6 Measurement of the velocity profile on the beach at Greenwich Dunes during a transport event: (A) photograph of the tower on the mid-beach with five cup anemometers spaced lograthmically above the bed; (B) wind speed for all five anemometers over a two minute period showing the similarity of wind flow at all heights. Note that the range of even the lowermost anemometer is 6 m s^{-1}; (C) example of two velocity profiles (plotted conventionally with height on the *y* axis) taken on the same day with different mean wind speeds. The beach is planar and nearly flat and the wind angle is highly oblique so there is limited internal boundary layer development. As a result the fit of the regression line used to estimate U_* and Z_0 from these velocity profiles is very good.

roughness length is likely to be very different to one that would be made from measurements taken much closer to the bed.

Where the roughness of the surface changes the wind profile responds to the new frictional drag and a new boundary layer develops downwind close to the bed and evolves through turbulent mixing until a new equilibrium logarithmic profile is established. On beaches and dunes rapid changes in the surface form (e.g. from waves to foreshore, backshore, and foredune) and vegetation height and density (grasses, shrubs, trees) means that new internal boundary layers are frequently being generated (Figure 9.7). As a result, the logarithmic portion of the boundary layer from which u_* can be estimated may only be a few tens of centimetres thick, thus making it difficult to place a minimum of three anemometers within this layer, and to determine how thick it is in the first place.

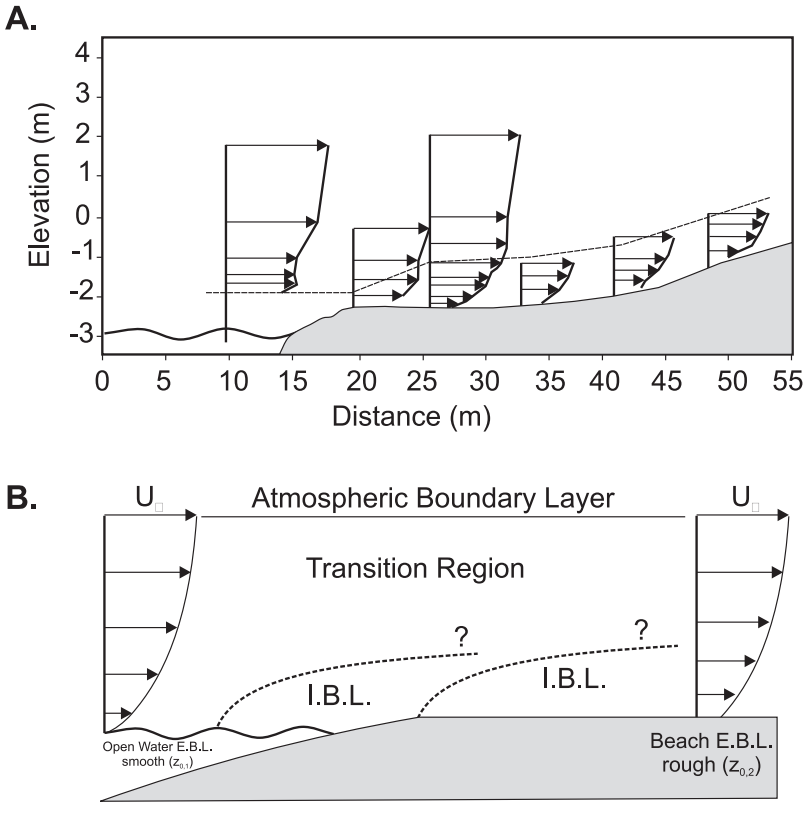

Figure 9.7 Effects of form and roughness change on wind blowing from the water across the beach: (A) measurement of the velocity profile at several points along a transect from the water to the backshore; (B) development of internal boundary layers (Bauer *et al.*, 1996).

Wind flow and topographic effects

In addition to the effects of surface roughness, wind flow direction and speed are also affected by the beach and dune topography. Where the wind blows onshore there is little effect over plane, gently sloping dissipative beaches, but on beaches where there is a steep foreshore and berm crest flow is accelerated over the top of the foreshore and crest, often promoting erosion there, and a zone of flow separation develops landward of the berm crest (Figure 9.7). Flow over the foredune is affected by the form in the same way that desert dunes are and this has implications for sand transport over the dune (Rasmussen, 1989; Arens *et al.*, 1995; McKenna Neuman *et al.*, 1997; Nickling and McKenna Neuman, 1999). There is compression of flow off the beach as the wind encounters the stoss slope of the foredune leading to an increase in speed (speed-up) up the slope and sometimes generating a stagnation zone with lower wind speeds (speed-down) near the toe (Hesp *et al.*, 2005; Walker *et al.*, 2009). The difference in wind speed can be expressed as a percentage relative to the speed measured at the same height in the flow seaward of the limit of influence of the foredune. Speedup is then defined as values greater than 100% and speed-down as values less than that. Where the stoss slope is steep, speed-up at the dune crest may reach 200% of the flow near the bottom for direct onshore winds, but the effect is reduced as the angle of wind approach becomes more oblique and the apparent slope decreases (Figure 9.8a). The topographic speed-up effect can be counterbalanced by the drag effect of vegetation on the dune slope and where this consists of shrubs, the effect of the vegetation may outweigh that of the topography, resulting a speed-down (Figure 9.8b).

At the foredune crest the direction of wind flow and the topography will determine whether flow remains attached or whether a zone of flow separation develops (Walker, 1999). On cliffed dunes with a very sharp angle at the crest flow separation may result in the

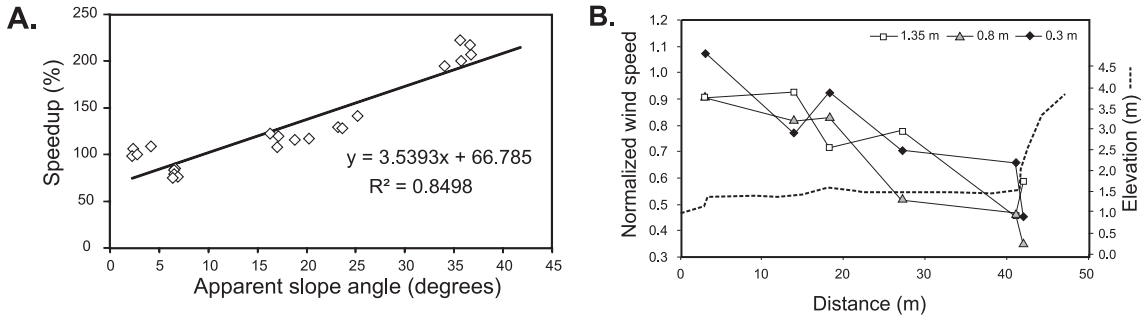

Figure 9.8 The effect of dune form and vegetation on flow over the foredune: (A) speed-up as a function of wind angle relative to the foredune, measured at Greenwich Dunes (Johnston, 2004); (B) decrease in flow speed measured at a height of 0.8 m up the foredune slope at North Friar's Beach, St Kitts. The profile and vegetation are similar to that shown in Figure 9.4a.

development of a turbulent shear layer that can entrain sediment and carry it in a form of short-term suspension or jettation for several tens of metres. The presence of the foredune ridge topography also induces some degree of topographic steering of alongshore or obliquely offshore winds (Svasek and Terwindt, 1974; Walker *et al.*, 2006) so that winds are steered into the foredune. This results in the situation where winds that are alongshore or slightly offshore can produce transport off the beach backshore into the embryo dune and base of the stoss slope. Where winds blow offshore the topographic effects are reversed and flow separation and reattachment can result in onshore transport from the top of the backshore (Lynch *et al.*, 2008; Walker *et al.*, 2009).

As is the case for unvegetated desert dunes, there is a feedback effect between foredune growth and wind flow which also influences the patterns of sand transport across the dune and it must be accounted for in modelling foredune evolution (van Boxel *et al.*, 1999; van Dijk *et al.*, 1999). However, modelling of coastal dune evolution must also account for the presence of vegetation and for the scarping of the stoss slope of the foredune by storm waves. The combination of stabilisation by vegetation and scarping by waves can produce a much steeper slope than can occur in desert dunes.

9.4.2 Modes of sand transport

As is the case with sediment transport in water, aeolian sediment transport can occur as suspension, saltation and by rolling or sliding along the bed (Figure 9.9). Silt and clay size particles, though harder to erode, are generally carried high into the air and transported long distances, maintained in suspension by turbulence. However, aeolian entrainment and transport of these sediment sizes is generally unimportant in the context of coastal dunes. Fine-to-medium sand can be launched into suspension (sometimes termed jettation) off sand ramps built against obstacles, and especially over the crest of dune ridges where there is extensive bare sand. Sand is generally too large to be maintained for very long in suspension.

Most sand transport occurs in saltation with grains being launched to heights of a few centimetres to 0.5 m or more and travelling downwind distances ranging from a few cm to several metres. This is termed high-energy saltation to distinguish it from low-energy saltation (reptation) of fine-to-coarse sand ejected a few cm into the air stream and travelling only a few cm, not always downwind. Reptation results primarily from the impact or splash of high-energy saltating grains with the bed. This impact can eject one or more high-energy grains and often several low-energy reptating grains.

Bagnold (1941) estimated that about 75% of sand transport takes place by saltation and the remaining 25% takes place as creep – fine sand to granule-sized particles which move through rolling or sliding along the bed. Some creep may result from fluid stresses alone but most occurs as the result of the impact of saltating grains

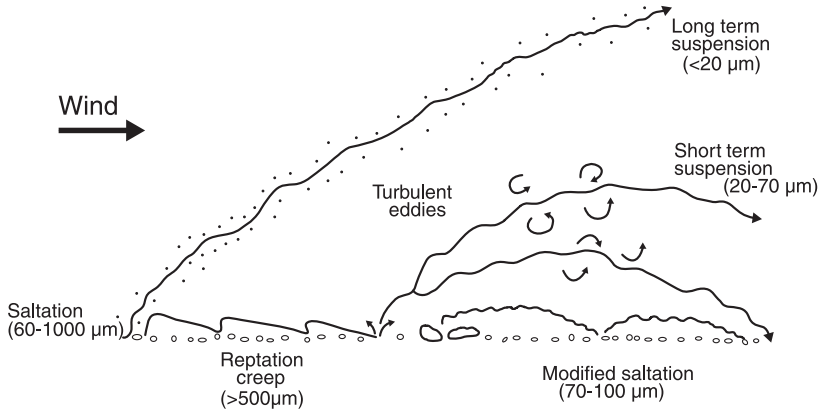

Figure 9.9 Modes of aeolian sediment transport (after Nickling and Davidson-Arnott, 1990).

with the bed. Actual amounts in creep decrease with decreasing particle size and may be as low as 10–15% for fine sand.

Wind tunnel studies show that when saltation is fully developed the concentration of grains in the air is highest within 1–2 m cm of the bed and it drops off rapidly above 10–15 cm so that there are very few grains travelling above about 30 cm. Field measurements (Namikas, 2003) based on trapping of sand in transport across the backshore of a beach in California show typical hop lengths on the order of 10–50 cm (Figure 9.10). Because of the rapid increase in wind speed with distance above the bed, grains that are ejected higher into the air stream are accelerated more and have much longer hop lengths than ones that only reach a few centimetres. On natural beaches there is a much greater range of saltation behaviour than is commonly observed in wind tunnel studies. Where a thick layer of dry sand exists on the backshore and the beach is relatively smooth transport most closely resembles that observed in the wind tunnel. However, if sand is transported across a damp, much harder surface (e.g. where dry sand has been stripped to expose damp sand below) or across an armouring of pebbles, the loss of energy on impact is reduced and rebounds are much more elastic so particles are transported faster and higher (McKenna Neuman and Muljaars Scott, 1998). Most wind tunnel studies make use of flat beds but on the beach topographic irregularities exist at a range of scales from sand ripples and dunes, to berm crests and beach scarps, to foredunes and blowouts. Flow is accelerated around and over these protuberances producing increased turbulence.

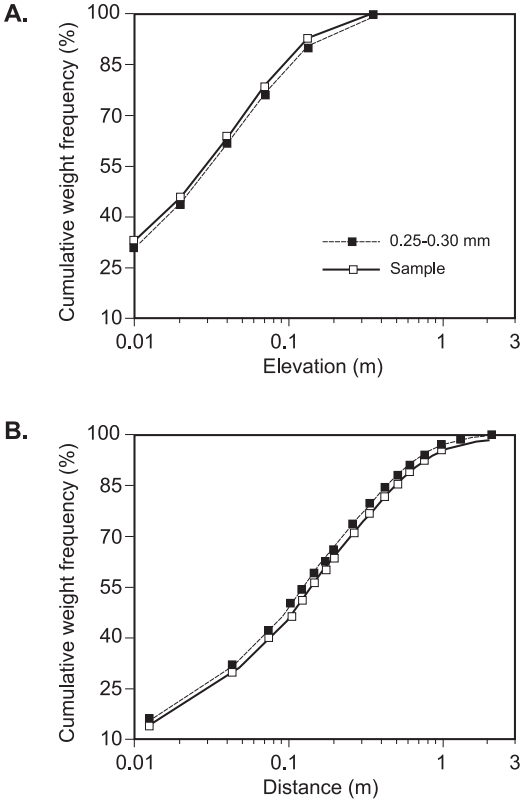

Figure 9.10 Cumulative frequency distribution of the weight of trapped sediment as a function of (A) elevation and (B) distance. Sand in (a) was captured in a vertical array of traps while that in (b) was captured in compartments within a horizontal trap (after Namikas , 2003)

9.4.3 Thresholds and initiation of sand transport for dry sand

Wind blowing over a sand surface will initiate sediment transport when the forces acting on an individual grain overcome the gravitational and frictional forces holding the grain in place. The forces acting on a grain can be resolved into a drag force that acts parallel to the bed and a lift force that acts vertically (Figure 9.11). Because the two are both a function of the shear velocity at the bed, initiation of sediment motion is generally related to some critical shear stress (τ). In practise it is difficult to measure the shear stress directly, even in a wind tunnel, so that initiation of sediment movement is generally related instead to the bed shear velocity U_* using the relationship in (9.2). As we saw in the preceding section u_* can be determined from the velocity profile as long as the anemometers are all in the logarithmic layer. If the wind velocity is measured at a single height either at the site or from a nearby weather station then U_* can be estimated from (9.1) with appropriate values for roughness and K. This is subject to some error on most beaches unless data on the range of roughness values has been obtained previously. However, because of the large spatial variability in wind flow over the beach, this is not likely that significant.

Bagnold (1941) in wind tunnel experiments found that the shear velocity at which sediment movement is initiated, the threshold shear velocity U_{*t}, is dependent on particle size and relative density (Figure 9.12). The threshold shear velocity can be predicted from

$$U_{*t} = A\left(\frac{\rho s - \rho}{\rho} gd\right)^{0.5} \quad (9.4)$$

where A is an empirical coefficient = 0.1 for particles with a particle Reynold's number Re_p>3.5; ρ_s is the sediment density and d is the particle diameter.

Bagnold also noted the existence of both a fluid threshold related to the initiation of sediment movement by the fluid alone, and an impact threshold where sand transport in the wind tunnel continued at a slightly lower speed than the initial speed necessary to start grains moving because of the role of the impact of saltating grains in causing sediment entrainment (Figure 9.12). Note that quartz particles around 0.1 mm in diameter are the easiest to entrain, and that this shear velocity corresponds to a wind speed (at 10 metres) of about 15 kph (just over 4 ms^{-1}). The threshold increases rapidly with increasing grain size and density, and the upper limit for sediment transport under natural conditions is about 2.5 mm. The mean grain size of most dune sands is <0.5 mm. The threshold shear velocity also increases into the silt and clay range because of cohesive bonding with fine particles. On natural beaches the threshold is complicated by the presence of a range of grain size, shape and mineralogy, all of which will affect the precise threshold limit.

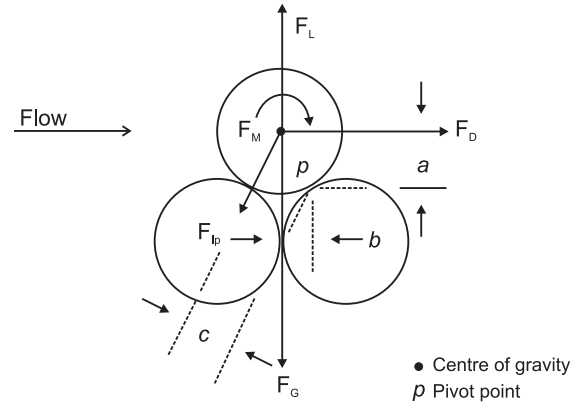

Figure 9.11 Forces acting on a particle on the bed. The drag force results from the pressure exerted on (the portion of) the face of the particle facing the wind while the lift force results from the compression and acceleration of flow over the particle.

Much of the work on threshold of motion has been carried out in laboratory wind tunnels where the wind speed is highly regulated. On natural beaches wind speed is usually highly variable over seconds and minutes even if the mean speed over tens of minutes is quite stable (Figure 9.6c). This gustiness in the wind produces three scenarios for the initiation and continuation of sediment transport (Figure 9.13): (1) wind speed fluctuates about the mean but never exceeds the threshold so no transport is recorded; (2) mean wind speed is below the threshold but speeds in some gusts exceed the threshold and transport is recorded for brief periods of time; and

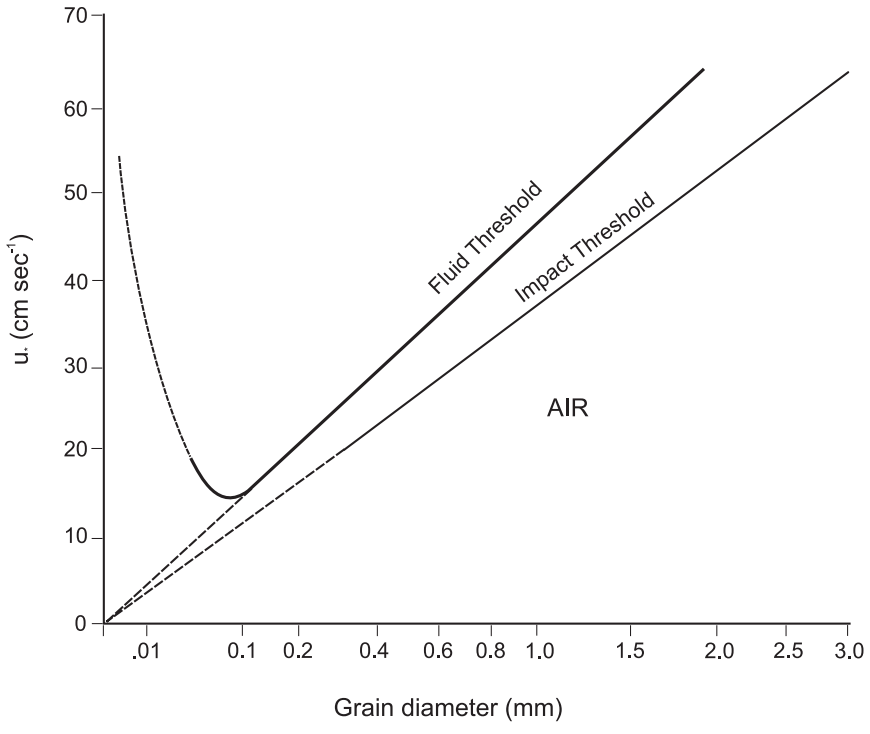

Figure 9.12 The relationship of threshold shear velocity u_{*t} to grain size (after Bagnold, 1941).

(3) mean wind speed is considerably greater than the threshold so transport rates are high but occasionally during a lull the speed falls below the threshold resulting in a short period with low or no transport. The data presented in Figure 9.13 were recorded simultaneously at different locations on the beach, with the threshold varying as a function of the beach surface moisture. A similar set of scenarios can be applied to a single location over time where the threshold remains the same but mean wind speed varies.

The impact threshold in Figure 9.12 is largely irrelevant in field conditions because of the rapid fluctuations in wind speed shown in Figure 9.13. However, it does point to the importance of the saltation cascade and the role of grain impacts in the process of sediment entrainment. Wind tunnel studies (e.g. Nickling, 1988) show that once grain movement is initiated, there is a rapid and exponential increase in sediment transport downwind as a result of grain impacts and once this is initiated, the role of fluid entrainment becomes secondary. This distinguishes aeolian saltation from saltation in water, where most entrainment is due to fluid forces, and results from the differences in relative density between the two fluids and because of the comparatively high speed at which particle impacts take place in aeolian transport. It also means that larger particles whose threshold is much higher than the incident wind speed can still be ejected into the flow and take part in the saltation process.

Stout and Zobeck (1997) utilised the intermittent nature of sand transport as measured by a saltation probe to define a measure of threshold wind speed based on the Time Fraction Equivalence Method. Essentially this equates the threshold with the wind speed percentile corresponding to the proportion of time that no sediment transport occurs. Conceptually this is attractive but it has been shown that there are many instances in a simultaneous wind speed and saltation transport record where sand transport occurs with the wind substantially below the threshold and where no transport occurs for situations with wind speed substantially above

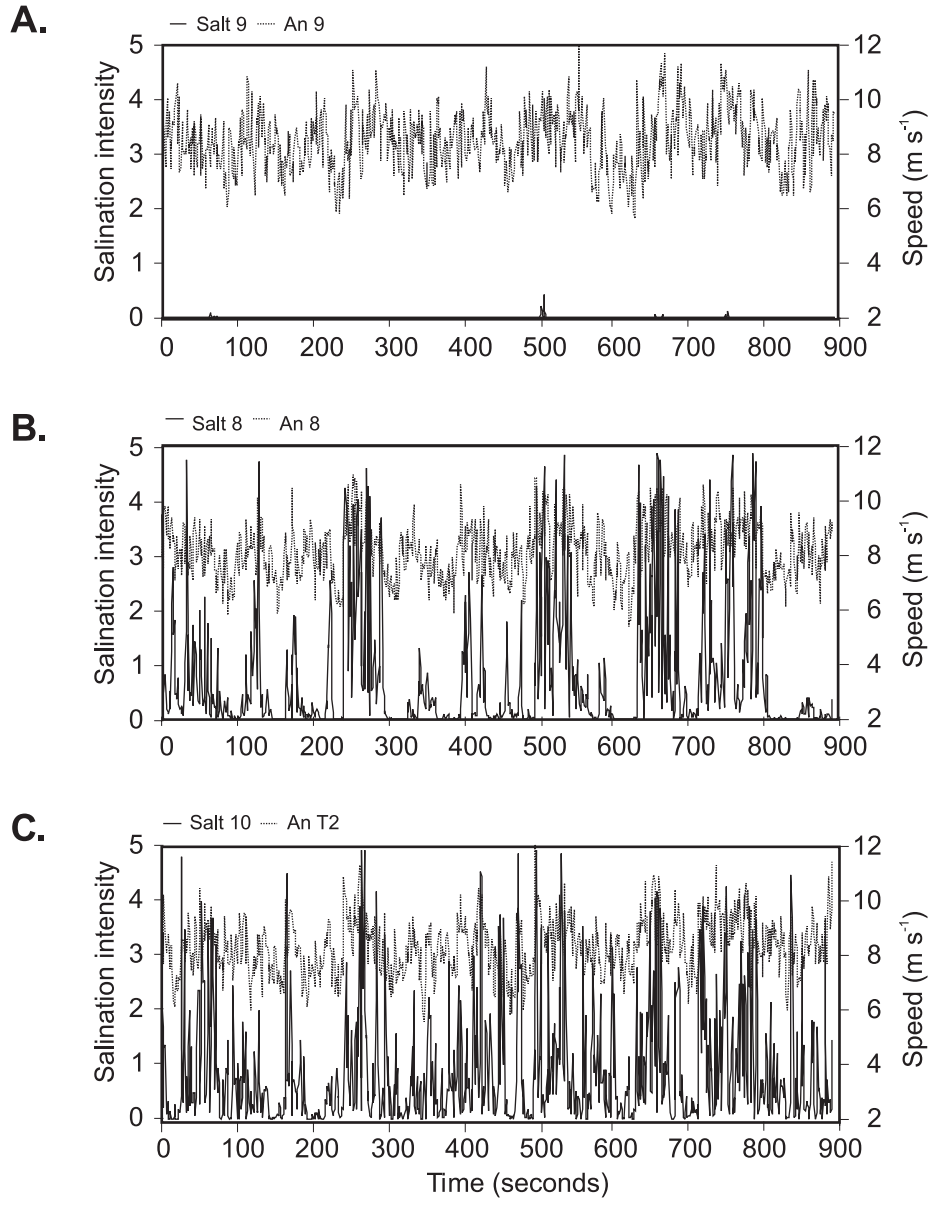

Figure 9.13 Relationship between wind gusts, sand transport rate and threshold illustrated by measurements of wind speed using a cup anemometer and sediment transport measured with a co-located saltation probe at three different locations on a beach. The saltation probe counts the number of grain impacts per second on a 2 cm high metal band using a piezoelectric crystal: (A) on the beach foreshore the wind record shows large and rapid fluctuations in speed but the sand is damp and the speed only exceeds the threshold on two or three occasions, producing small bursts of transport; (B) on the mid-beach, the sand is drier and consequently the threshold is lower. The speed exceeds the on many occasions producing bursts of transport intensity separated by short intervals when the speed falls below the threshold and no transport occurs; (C) on the backbeach the sand is drier and threshold is slightly lower than on the midbeach. Sand transport is nearly continuous and only occasionally does the speed fall below the threshold and sand movement cease momentarily.

the threshold (Wiggs *et al.*, 2004a; Davidson-Arnott *et al.*, 2005; 2008; Davidson-Arnott and Bauer, 2009). In the field, the concept of a precisely defined threshold of motion based on mean grain size and mean wind speed should be replaced with a probabilistic one based on the distribution of grain size, wind speed fluctuations and moisture content variability.

9.4.4 Effects of beach surface moisture on the threshold of motion

In addition to the effects of grain size, several variable factors can act to increase the threshold for movement of sediment by wind by binding grains together: (1) the presence of a coating of fine sediment and organic material, e.g. deposited in a runnel; (2) the effects of binding salts; and (3) the apparent cohesion produced by the presence of moisture in the sand. In most areas algae and fine sediments have very limited effect on beach sediments. Salt crusting is quite a common occurrence on beaches (Figure 9.14) but in most cases the crusts are very thin and easily broken. As a result it likely has a negligible impact on the delivery of sand from the beach to the dune. However, beach surface moisture is usually an important control on aeolian sand transport on beaches and on some coasts it is the most important modifier of predicted transport based on wind speed.

It has long been known that moisture acts to bond particles as a result of adhesion of water to particles and because of the tension forces produced by water at the points of contact of the sand particles. These produce an apparent cohesion that increases the force required to dislodge particles from the bed. There have been a number of models of these forces and attempts to predict the effect of moisture on the threshold (McKenna Neuman and Nickling, 1989; Cornelis *et al.*, 2004) and two useful reviews by Namikas and Sherman (1995) and Cornelis *et al.* (2003). The theoretical models generally require too much input data to be applicable in field studies.

Sources of beach moisture include: precipitation; condensation (dew); spray from breaking waves; wave run-up (which in turn is controlled by wave characteristics, tidal stage, storm surge and the beach topography); capillary rise from water table or moist subsurface; and seepage from the base of the foredune. These, together with grain size and packing, determine the gradient in moisture with depth from the surface. Moisture will also vary within the beach sediments as a function of packing, small-scale bedding features and beach topography. The spring/neap tidal cycle is particularly important on many beaches in determining the extent of dry sand available for transport because the berm is built up during spring tides and then the upper part dries out over several days if low waves coincide with neap tides.

Wind tunnel studies (e.g. Belly, 1964) and theoretical models (McKenna Neuman and Nickling, 1989; Cornelis *et al.*, 2004) show that surface moisture content of 2–3% is sufficient to shut down the aeolian sand transport system. However field studies show transport occurring with surface moisture content >5% and in some cases >10% (Sarre, 1989; Gares *et al.*, 1996 Davidson-Arnott and Dawson, 2001; Wiggs *et al.*, 2004b; Davidson-Arnott *et al.*, 2008; Bauer *et al.*, 2009). As McKenna Neuman and Langston (2006) point out, the high degree of control of the system required for wind tunnel experiments has resulted in the use of a flat, uniformly moist surface, small test area and short run lengths all of which tend to reduce complexity. As a result, while they provide some insights into the physics of the entrainment process with moisture present, the empirical and theoretical models based on them produce predictions that do not accord with field measurements. There are three major factors accounting for this discrepancy: (1) instantaneous wind speeds may exceed the threshold for motion even though the mean wind speed lies below the threshold (Figure 9.13b); (2) the moisture content of a natural beach varies spatially (both across the surface and vertically within the beach) as well as temporally so that the threshold may be exceeded in some areas even though the majority of the area lies below the threshold; and (3) once small amounts of sand begin to move the impact of saltating grains results in the ejection of grains from the downwind surface even though the bonding forces are too large for entrainment by fluid forces alone.

What is increasingly recognised is the highly dynamic nature of beach surface moisture

Figure 9.14 Salt crusting on the beach at Greenwich Dunes. Note the thin crust which has been broken in many places (photo Irene Delgado-Fernandez).

(Jackson and Nordstrom, 1997; 1998; Wiggs *et al.*, 2004b; Yang and Davidson-Arnott, 2005; McKenna Neuman and Langston, 2006; Bauer *et al.*, 2009). Spatially at a scale of metres to tens of metres there is a general trend for moisture to increase towards the beach and to vary both normal to shore and alongshore with surface topography such as berms, cusps and intertidal sandbars (Figure 9.15a). With onshore winds the point at which entrainment is initiated is thus a complex function of wind speed and surface moisture content and the distance that the wind travels across relatively dry sand depends also on the angle of wind approach (Oblinger and Anthony, 2008). The moisture content tends to be quite uniform over small areas when the sand is very dry (<1%) and when it is quite damp (>10%) but at intermediate moisture contents it is quite variable (Yang and Davidson-Arnott, 2005). Surface moisture content will also vary temporally with high temperatures and sunshine leading to rapid drying (Figure 9.15b) while cool temperatures during the night can lead to condensation and a rise in moisture content. The rate of drying also increases with increasing wind speed so that a layer one or two grains in thickness can dry out leading to entrainment and stripping of that layer, exposing the damp sand below and shutting the system down again. The result is that where the sand is quite moist erosion takes place intermittently with sand transport initiated during gusts and evaporation preparing the surface during periods of low winds. Finally, once a sand grain is entrained any moisture film on the surface is quickly evaporated and thus there is a build-up of dry sand which can be transported readily, particularly when winds blow nearly parallel to the shoreline (Figure 9.15c).

9.4.5 Instantaneous sediment transport rate

Once sand movement is initiated by fluid forces the impact of saltating grains drives the development of the saltation cloud and ultimately controls the rate of sand transport by saltation. Theoretically we can model this transport rate if we know the probability distribution of horizontal and vertical lift-off velocities and the lift-off angle together with wind flow close to the bed (Anderson and Haff, 1988; Kang *et al.*, 2008). Studies of the impact of grains with the surface and measurements of the velocities of individual particles have been made using high speed photography, and more recently using a phase Doppler particle analyser (Dong *et al.*, 2004a; Kang *et al.*, 2008) while field measurements have examined the height and hop length of saltation transport (Namikas, 2003). Results of these studies produce different probability functions but there seems general agreement that horizontal speeds follow a Gaussian distribution and this is also true for particles within the saltation cloud (Dong *et al.*, 2004a). The distribution of vertical lift-off velocities is exponential (Kang *et al.*, 2008). The distribution is controlled by the nature of the collision, including the size of the impacting grain, the angle of the impact with the bed, and the size and packing of particles on the bed. Within the saltating cloud the particle velocities depend on the amount of acceleration by the horizontal component of wind flow and the effects of grain-grain collisions in the saltation cloud. While these models are not yet suitable for practical application in the field they do provide some insights into the effects of varying grain size and especially the hardness and packing of the bed on sand transport rates.

A number of relatively simple semi-empirical formulae are available to predict the mean sand transport rate under aeolian action and almost all show the transport rate to be some function of U_*^3 or U^3. The coefficients in these equations are largely derived from wind tunnel studies and must therefore be treated with some caution. One of the first

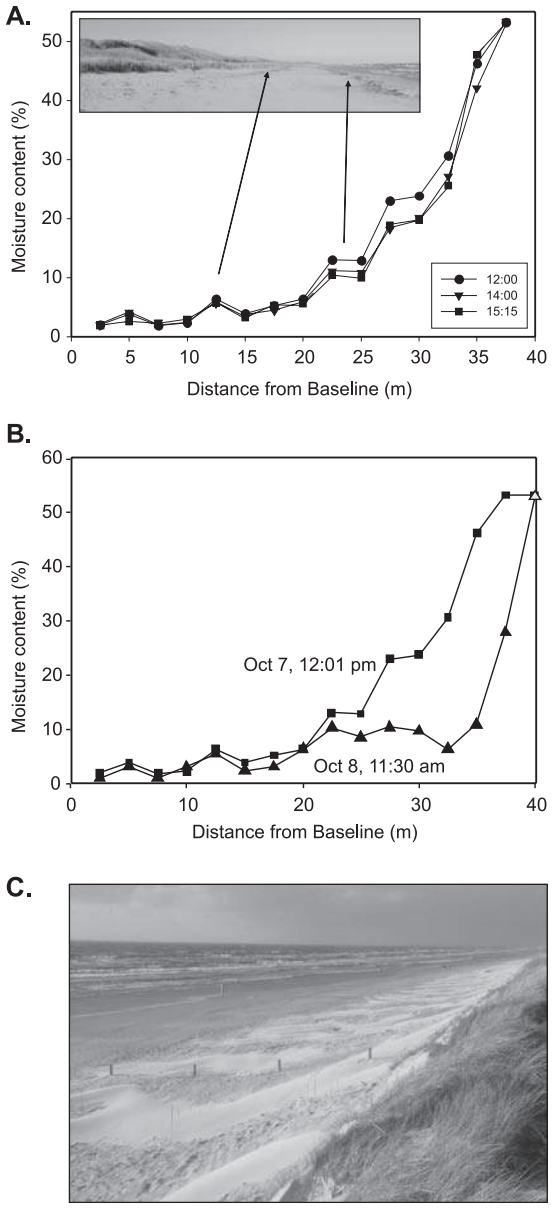

Figure 9.15 Spatial and temporal variations in beach surface moisture measured at Greenwich dunes: (A) Typical pattern of near surface moisture measured with a Delta-T probe showing a dry surface on the berm with increasing moisture content towards the area wetted by swash action and a moist zone of seepage near the base of the foredune; (B) surface drying over a 2 day period along one profile; (C) formation of low dunes composed of dry sand as a result of alongshore winds, Skallingen, Denmark.

Box 9.1 Measurement of beach surface moisture

Apart from wind speed, the presence of moisture on the sand surface is probably the most important control on whether sand movement is initiated and if so how much sand is transported. Measurements of wind speed have been routine for over 50 years but measurement of surface moisture has proved to be tedious and difficult to accomplish. Ideally we would like to measure the moisture content in a layer just two or three grains thick.

Until recently, near-surface moisture was measured by obtaining a sample of a surface layer either by scraping the surface with a spatula or by coring and removing the upper 0.5–1.0 cm. Greater precision and control of the thickness can be achieved by using a machined scraper (McKenna Neuman and Nickling, 1989; Wiggs *et al*., 2004b). The sediment is then bagged, weighed in the lab, oven dried and weighed again and moisture content expressed as a percentage by weight determined from

$$w = \frac{(w_s - w_d)}{w_d} \times 100 \quad (9.5)$$

where w = weight % moisture content; w_s = weight of the sample; and w_d = weight of the sample after drying.

Moisture content can also be expressed as a weight by volume but this requires either taking a sample of known volume which is difficult to do when scraping the surface, or measuring the porosity of the beach sediments. Sampling for gravimetric moisture is tedious and time consuming, and also has the disadvantage that it cannot be used to monitor moisture continuously and remotely. Atherton *et al*. (2001) were the first to use a moisture probe made by Delta-T Instruments of Cambridge, UK which measures the impedance in a sampled volume of sediment. They demonstrated that the probe provided consistent results and could be calibrated for the sediment properties at a site. Yang and Davidson-Arnott (2005) used dielectric foam to reduce the exposed length of the probe from 6 cm to 2 cm in order to sample as close to the surface as possible while still maintaining a high degree of precision. This approach has been used in other studies. Probe calibrations are highly linear in beach sands and replicability is good (Figure 9.16). They thus offer a means of measuring near surface moisture rapidly along a transect, or over a large area of beach, during field experiments (Davidson-Arnott *et al*., 2008; Bauer *et al*., 2009). Some care has to be taken because the calibration is sensitive to the presence of salt in the moisture (Atherton *et al*., 2001; Yang and Davidson-Arnott, 2005). Measurement of the moisture content in the top 2 cm using the moisture probe often correlates well with surface moisture, but when there are strong vertical gradients in moisture errors may arise. Where the moisture content increases rapidly with depth the surface moisture is overpredicted and when the surface is dampened by a brief shower it is underpredicted.

Recent tests using surface brightness suggests that this offers the potential for remote monitoring of large areas of the beach and for providing a more consistent measure of the moisture content at the actual surface (McKenna Neuman and Langston, 2006; Darke and McKenna Neuman, 2008; Darke *et al*., 2009). Simple observations show that a sand surface appears darker as the moisture content increases and Mckenna Neuman and Langston (2006) showed that the average brightness on a 256 shade grey scale of a small area (0.4 × 0.6 m) of sand in wind

tunnel tests correlated well with gravimetric moisture content measured by surface scraping. This was extended to a natural beach by Darke and McKenna Neuman (2008). The small area captured by the vertical camera essentially replicated instrument measurements at a point on the beach. Darke *et al.* (2009) showed that surface moisture over an extensive area could be captured using an oblique photograph from a camera mounted on a tower overlooking the beach. The correlation of surface brightness with moisture content in an individual image is very good, but varies with sun angle and cloud cover (Figure 9.17a). This variation can be accounted for by normalising the brightness against a white board placed in the field of view of the camera with its surface parallel to the beach. Rectification of the photograph (Figure 9.17b) using a large number of control points surveyed by DGPS permits moisture maps to be extracted routinely from images (Figure 9.17c). The technique can be utilised for mapping moisture during short-term field experiments and for longer term seasonal and annual monitoring.

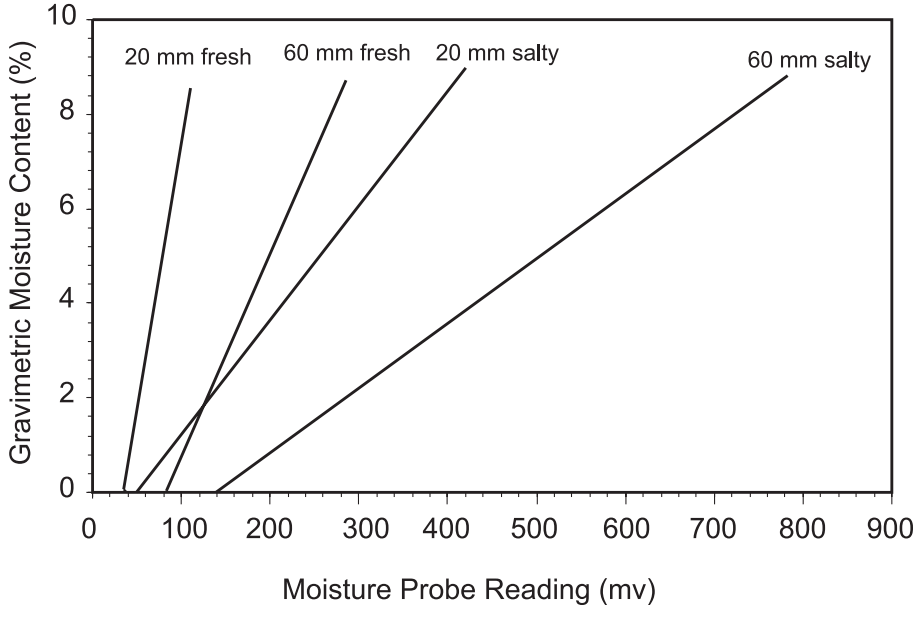

Figure 9.16 Calibration curves for the Delta-T probe generated for the standard probe length of 6 cm and for the shortened length of 2 cm used to sample close to the surface. Measurements are shown for samples taken on the backshore where salt content was minimal and for the lower foreshore where the sediment is wetted by sea water (Yang and Davidson-Arnott, 2005).

expressions for predicting the sand transport rate was that of Bagnold (1941) and it is still used extensively:

$$q = C\sqrt{\frac{d}{D}}\frac{\rho}{g}U_*^3 \tag{9.6}$$

where d = grain diameter; D = standard grain diameter of 0.025 cm; and C = coefficient which depends on the sorting of the sediment = 1.5 nearly uniform sand, 1.8 naturally graded sand and 2.8 for a wide range of sizes.

Bagnold's equation does not include a threshold term. A similar model with an explicit threshold term is that of Kawamura (1951):

$$q = C\frac{\rho}{g}(U_* - U_{*t})(U_* + U_{*t*}) \tag{9.7}$$

where $C = 2.78$ and U_{*t} is estimated from (9.4).

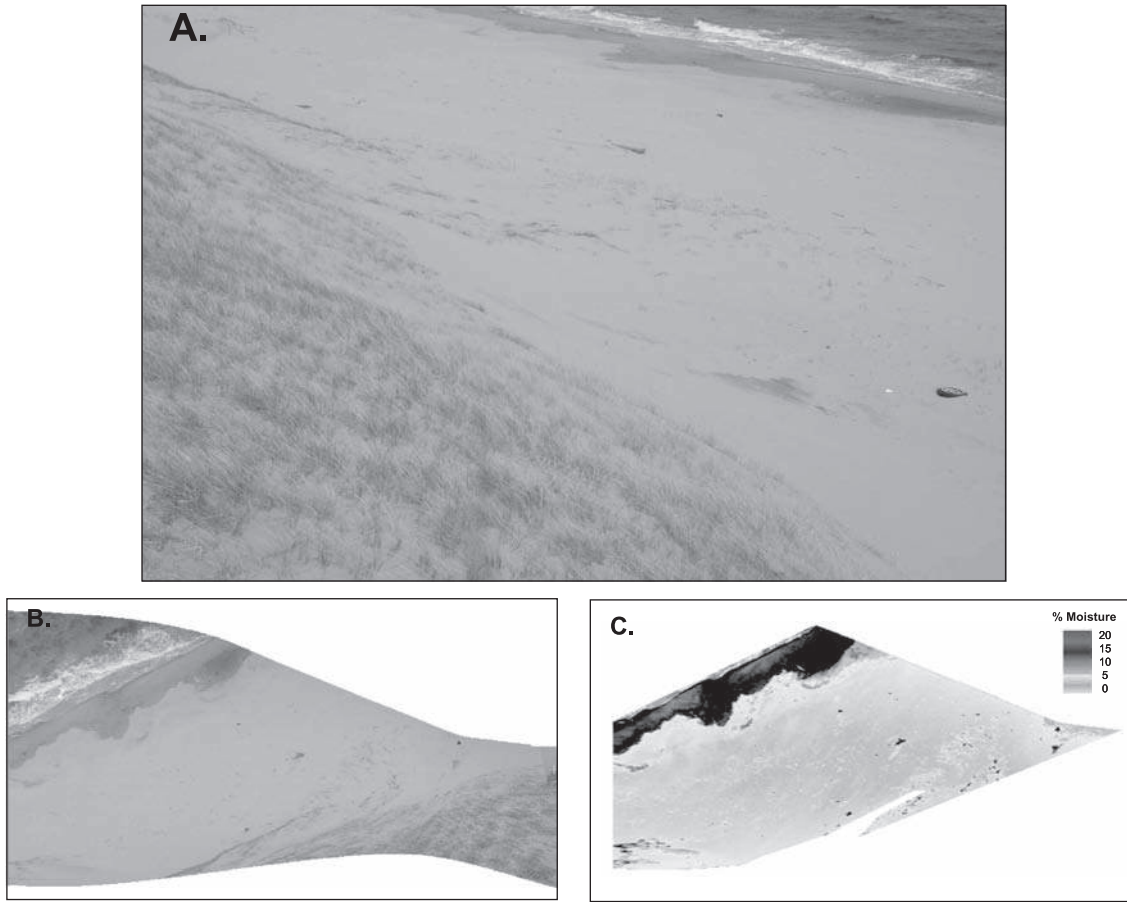

Figure 9.17 Use of surface brightness to measure beach surface moisture: (A) grey scale image of the beach derived from an original colour photograph taken with an 8 Mp digital SLR camera; (B) rectified photograph; (C) moisture map produced from the rectified image in (b). The process involves normalising the brightness based on the brightness of a white board in the field of view and then using a calibration equation derived from simultaneous measurements of surface moisture and brightness. In this map the water and vegetation have been extracted and only the bare sand portion of the beach is displayed.

There are several other variations on this basic approach (Zingg, 1953; Lettau and Lettau, 1977) and a rather different model by Kadib (1964) which incorporates a transport intensity function based on Einsteins's bed load transport model. The small differences in the formulation actually result in quite large absolute differences in the predicted transport rate (Nickling and Davidson-Arnott, 1990; Sherman *et al.*, 1998) though these are often somewhat hidden by plotting the transport rate on a logarithmic scale. Because wind data are generally available as wind speed at one height, U_* must be estimated by rearranging (9.1) and estimating Z_0 from the grain size. This results in a minimum estimate for U_* and thus in a minimum estimate for the transport rate.

In practice, since predictions of sediment transport into the dune over periods of weeks, months or years are made using wind speed measured at a standard elevation at meteorological stations, which may be kilometres or tens of kilometres from the site, it would seem more practical to make use of a model based on wind speed – i.e. on U^3 rather than U_*^3. There is some physical justification for this because of the dominant role played by the impact of saltating grains in generating the saltation cascade and particle speeds at impact are controlled more

by the wind speed than the shear velocity. An alternate approach makes use of Reynolds stress which takes into account turbulent fluctuations and in particular the burst-sweep cycle which has been used extensively in laboratory and field studies of fluvial transport and transport by unidirectional currents on the sea bed (e.g. Heathershaw and Thorne, 1985). The recent availability of 3D sonic anemometers now makes it feasible to make these measurements in the field (van Boxel *et al.*, 2004; Walker, 2005; Walker *et al.*, 2009). However, Sterk *et al.* (1998) concluded from field experiments that horizontal drag and not shear stress was primarily responsible for saltation transport and this is related to the horizontal wind speed and wind speed fluctuations. This is in accord with the experience of a number of experiments measuring sand transport by wind on beaches.

9.4.6 Prediction of annual transport rates

Assuming an unlimited supply of dry sand on the beach, we could use the average annual wind climate and one of the transport equations in section 9.4.5 to predict the potential supply from the beach to the foredune. Fryberger and Dean (1979) outline a method for analysing the sand drift potential in desert regions based on standard meteorological wind data in speed and direction classes. They use an equation modified from Lettau and Lettau (1977), with wind speeds measured at a height of 10 m:

$$Q \propto U^2(U - U_t)t \tag{9.8}$$

where Q is the proportionate amount of sand drift (expressed in vector units), U is wind speed at 10 m, U_t is the threshold wind speed and t is the frequency of occurrence of the class expressed as a percentage of the total period.

The approach has been applied to coastal dunes and dunefields (e.g. Wal and McManus, 1993; Olivier and Garland, 2003; Hesp *et al.*, 2007b; Lynch *et al.*, 2006). The calculations can readily be programmed on a computer (Saqqa and Saqqa, 2007) though some caution has to be exercised in using wind direction and speed classes rather than continuous data (Pearce and Walker, 2005). This approach is useful for comparing relative magnitudes of potential transport but the output is in vector units and all transport directions are considered which may not be suitable for vegetated foredunes.

Alternatively, where foredunes are well vegetated, offshore aeolian transport can be neglected and the actual mass transport can be predicted directly from the hourly wind climate data.

9.4.7 Equilibrium transport and supply limiting factors

Equilibrium transport

The equations described in the previous section apply to conditions where there is an unlimited supply of loose, dry sand. Once transport is initiated, wind tunnel experiments show that the system quickly (within a few metres) achieves an equilibrium in which the number of grains being ejected from the bed is equal to the number of grains falling back to it. In part this equilibrium reflects the reduction in momentum in the boundary layer close to the bed as ejected grains are accelerated in the flow. Entrainment of more grains would result in a further reduction in speed close to the bed, thus leading to deposition. Momentum is replaced by turbulence from higher in the flow and since most transport occurs in a layer <0.3 m thick this occurs quite rapidly in the natural system. A second limit to transport may simply be increasing numbers of grain–grain collisions, particularly the collision of ascending grains which have just been ejected from the bed with descending ones which affects both the trajectory of the ascending grain and likely reduces the impact force of the descending grain. Thus, ideally there is a maximum transport capacity associated with a particular wind speed and this represents the equilibrium or transport-limited condition to which (9.6) and (9.7) apply.

Supply limiting factors

On natural beaches and coastal dune systems measured deposition over periods of months to years is generally much less than values predicted using the standard equilibrium equations because of the effects of factors limiting

entrainment and supply (Sarre, 1989; Kroon and Hoekstra, 1990; Davidson-Arnott and Law, 1990, 1996; Meur-Férec and Ruz, 2002). A number of factors may act to limit the entrainment of sand from a unit area of the beach surface and thus the actual mass of sediment being transported may fall below the predicted transport based on U_* or U. These supply-limiting factors (Nickling and Davidson-Arnott, 1990) include: (1) those that tend to bind the surface grains together, such as moisture, algal mats and cementation by salt and freezing of pore water; and (2) those that act to cover a portion of the surface, such as pebble and cobble accumulation on the beach, the presence of a surface covering of wrack (accumulation of seaweed, sea grasses) logs and by snow, and vegetation growth.

The first group of factors act chiefly to raise the threshold wind velocity necessary to entrain sediment or, in the case of binding by algal mats and salt, the combination of speed and time necessary to break up the crust and thus expose the loose sediment below to transport. This is not generally possible where the surface layer is frozen – that requires warmer temperatures and/or solar radiation leading to sublimation or melting of the ice. If information on these factors is not available then transport may be predicted based on wind speed data under conditions where no transport actually occurs. Where transport does occur with moist beach conditions the rate of transport is initially lower than would be predicted based on wind speed alone because of the lower rate of entrainment from the moist surface. However, sand grains dry rapidly during the saltation process and so a supply of dry sand may build up over time and ultimately provide a sufficient volume of dry sand for equilibrium sediment transport to be reached. At the moment it is still uncertain as to whether transport over a considerable length of damp surface can result in transport equal to the transport-limited condition (Davidson-Arnott *et al.*, 2008).

Accumulation of seaweed and other plant material on the beach acts both to protect the surface underneath from wind action and may also trap sand that is being transported from bare areas. The organic material may come from seaweed or kelp, or from sea grass beds (Figure 9.18b). Branches and logs perform a similar function and on beaches such as those on the coast of Oregon, Washington and British Columbia they may be the dominant control on sand supply to the foredune and foredune development (Anderson and Walker, 2006).

Pebbles and cobbles deposited on the beach act to protect the area below them and often simultaneously to generate sheltered areas in their lee in a similar fashion to the development of pebble lag surfaces in arid and semi-arid regions. Laboratory and field experiments show that the effects of pebble lag development are complex (Nickling and McKenna Neuman, 1995; Davidson-Arnott *et al.*, 1997). Sand transport rates are initially enhanced over those from a bare surface as the pebble lag coverage increases as a result of increased scour by turbulence generated in accelerated flow around and over the individual pebbles (Figure 9.19a, b) and then decreases rapidly until transport is almost completely shut down at a surface coverage of about 20–30%. A part of the initial increase in transport rate may also reflect the increased rebound of sand particles from the pebbles which may increase the effective height of saltation and hence the path length and transport rate.

The slope of the bed may also affect the threshold of movement and the rate of transport (Iversen and Rasmussen, 1994) and it is possible to adjust predicted sand transport rates to account for this (Sherman *et al.*, 1998). However, the effects are likely small for slopes <10–15°. Moreover, the effect of the slope on the transport rate acts in the opposite direction to slope effect on wind speed; flow compression as the wind blows up a slope enhances speed, and the opposite happens with flow expansion downslope.

Fetch effects

The fetch effect is defined as the progressive increase in the sand transport rate downwind from the boundary of a no transport zone such as the upwind end of the sand bed in a wind tunnel, the edge of an agricultural field, or the swash zone on a beach (Gillette *et al.*, 1996; Bauer and Davidson-Arnott, 2002). The significance of this is that if the fetch distance is shorter than

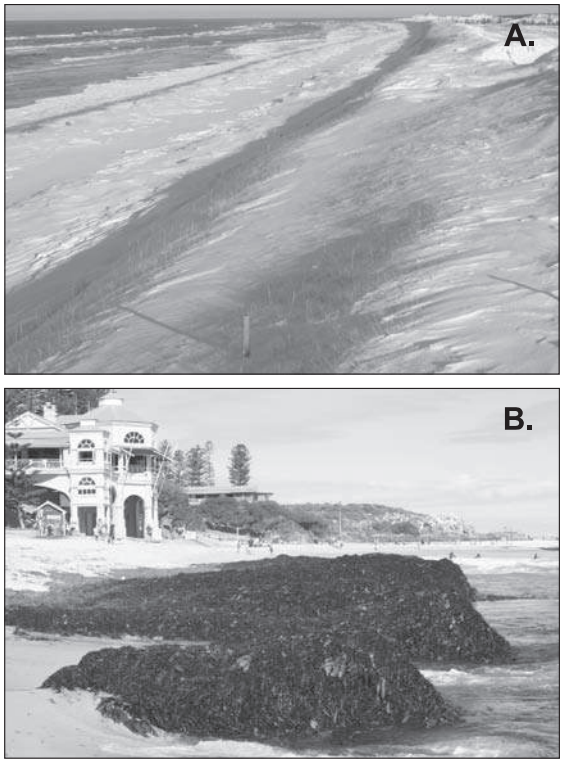

Figure 9.18 Protection of the beach from aeolian transport: (A) snow and ice cover Greenwich Dunes,January 1, 2008; (B) seaweed on the beach, Cottersloe Beach, Perth (photograph Jeff Doucette).

the distance required to achieve equilibrium transport, then the actual transport rate will be less than that predicted by any of the equilibrium transport equations. As we noted at the beginning of this section, wind tunnel measurements have tended to assume that sediment transport quickly comes into equilibrium with the incident wind and that the boundary layer adjusts within a few metres to the apparent roughness effect of saltating grains (Owen, 1964; Shao and Raupach, 1992). Field studies of wind erosion of agricultural fields have shown that the fetch effect can extend for distances of tens to hundreds of metres and the effect here has been attributed to the gradual abrasion of clods by saltating sand (Gillette *et al.*, 1996). In general, even with fine, dry sand, it takes a finite distance for equilibrium transport to be achieved. Any factor which acts to reduce grain emission from the surface compared to the ideal case will lead to a fetch effect, including those described above.

The fetch effect was noted on beaches by Svasek and Terwindt (1974) and direct measurements made by Davidson-Arnott and Law (1990). Since then there have been a number of field studies that have reported critical fetch distances of tens of metres (Nordstrom and Jackson 1992, 1993; van der Wal, 1998; Davidson-Arnott and Dawson, 2001; Davidson-Arnott *et al.*, 2008; Bauer *et al.*, 2009) – see Figure 9.20. Several of the studies on beaches have taken place with sand transport over a moist beach surface and thus the distance to reach a transport limited situation can be attributed to a reduction in the rate of grain ejection due to the apparent cohesion and probably also to increased intermittency close to the swash limit (Davidson-Arnott *et al.*, 2005, 2008; Bauer *et al.*, 2009). However, the fetch effect has also been observed for a relatively dry beach (Davidson-Arnott and Law, 1990; van der Wal, 1998; Davidson-Arnott *et al.*, 2008 – see Figure 9.20b) and so this cannot be invoked for these conditions. Recently, Dong *et al.* (2004b have reported on fetch effects observed with dry sand in a long (16 m) wind tunnel. They measured sediment transport at 1 m intervals down the tunnel and except at the lowest speeds transport continued to increase up to the end of the working section. As we would expect from other work, the increase over the first few metres is exponential but the increase with distance beyond this is much slower and is more evident in an arithmetic plot (Figure 9.20c) than the traditional logarithmic plots such as those used in the original paper by Dong *et al.* (2004b). The continuing increase in transport rate with dry sand may reflect a slow increase in the number of grains travelling at higher elevations and hence at greater speeds (Dong *et al.*, 2004b; Wang *et al.*, 2008).

The cosine effect

The sand transport rate is usually expressed in terms of a mass per unit time per unit width along the direction of transport – e.g., kg m^{-1} s^{-1}. In Figure 9.20a it can be seen that sand transport across a unit width *b*

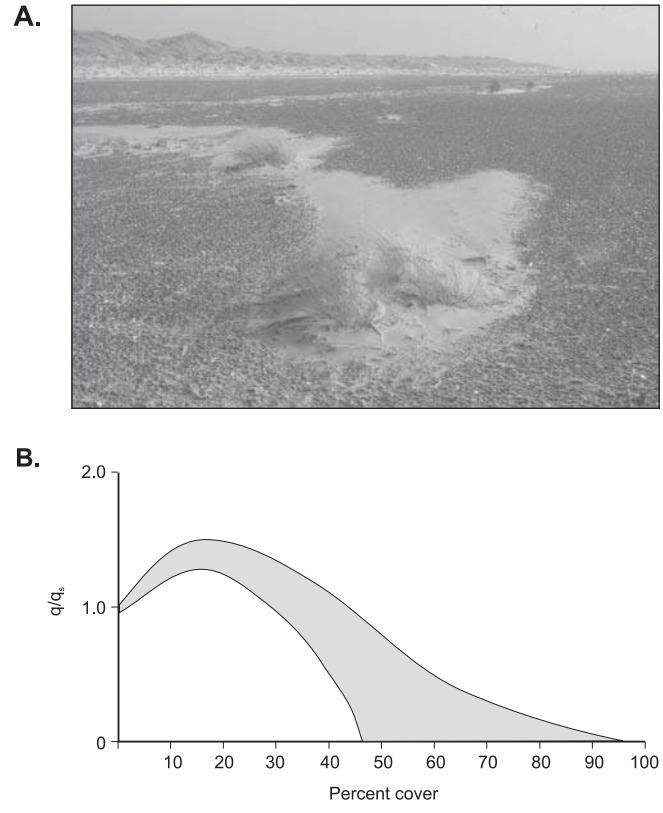

Figure 9.19 Effects of pebble lag on sand transport by wind: (A) pebble lag on the beach at Skallingen, Denmark; (B) Generalised curve showing normalised sediment transport versus % cover based on the findings of Logie (1982), Nickling and McKenna Neuman (1995) and Davidson-Arnott *et al*., 1997.

along the wind streamline is deposited across a length of dune front l. As the wind angle varies from shore perpendicular this length l increases as a function of the cosine of the angle to shore perpendicular. The result of this change in angle is that a unit mass of sand is deposited over an increasing length of dune front and the mass of deposition over a fixed length of dune front decreases to 0 with a shore parallel wind. Since sand deposition in the dune is usually measured in terms of a mass or volume per metre length of beach, the predicted mass transport must be adjusted to account for this cosine effect.

A framework for modelling sand supply to coastal dunes

When the beach width $w > F_c$ the fetch effect does not have any impact on sand transport across the dune line and the actual transport rate q per unit width is equal to the maximum transport rate q_m (Figure 9.20a). However, when $w << F_c$, q will be $<< q_m$ for shore-normal winds and this brings into play a complex interaction between wind angle, fetch length and the cosine effect (Davidson-Arnott and Dawson, 2001; Bauer and Davidson-Arnott, 2002). As the wind angle relative to shore normal becomes more oblique, F_m increases and there is an associated increase in q as long as F_m remains less than F_c. This sets up a trade-off between increasing transport rates on the beach with increasing obliquity, and decreasing amounts of deposition in the dune per unit distance alongshore (Davidson-Arnott and Dawson, 2001, Bauer and Davidson-Arnott, 2002). As a result, for very narrow beaches the wind angle at which maximum transport into the dune occurs may be as much as 60°–70° from shore perpendicular, though absolute values will be considerably less than q_m. Because strong onshore winds are accompanied by large waves and storm surge, beach width is often reduced under these conditions,

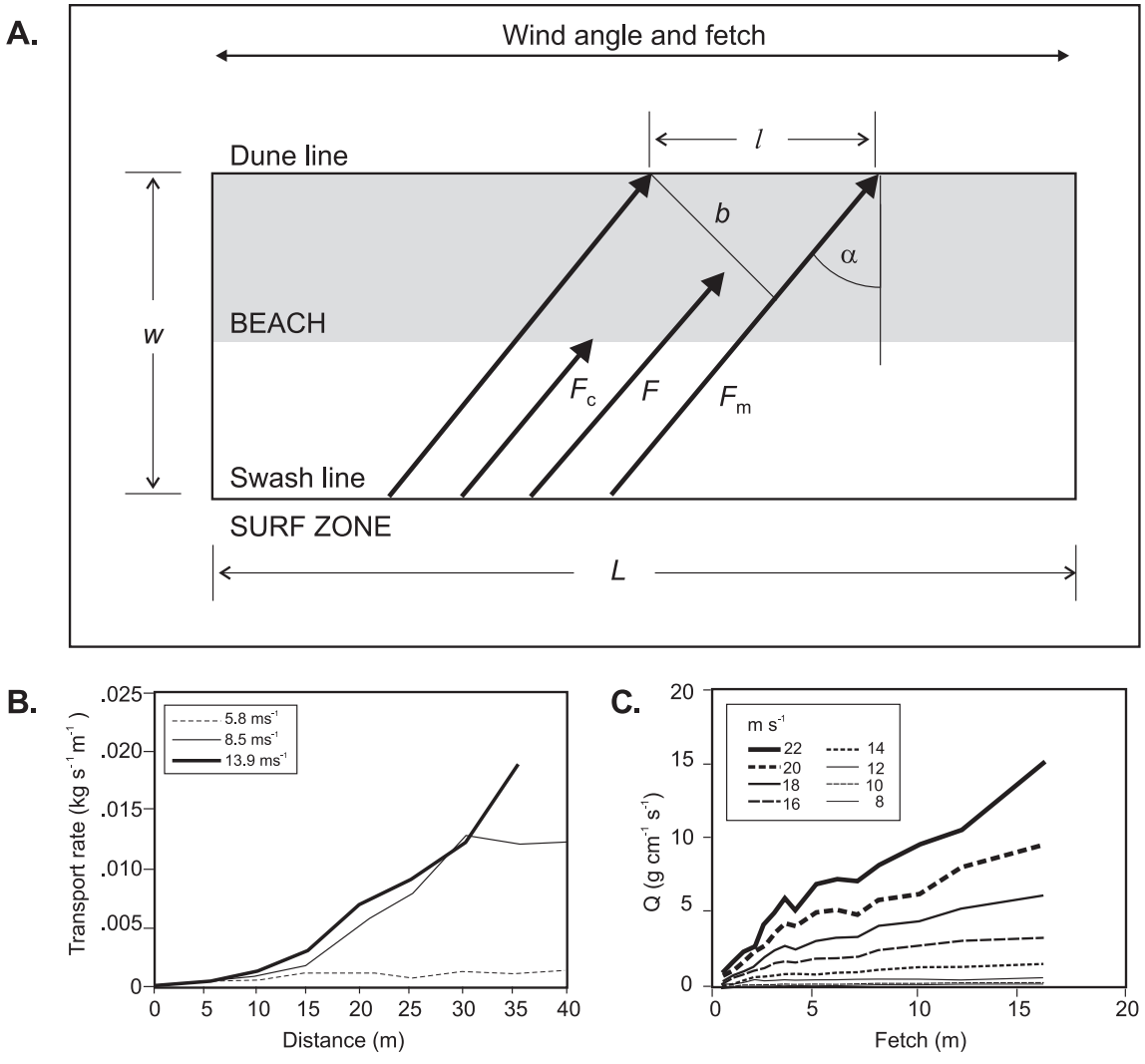

Figure 9.20 The fetch effect. (A) Basic terminology defining the fetch effect on a rectangular beach of length *l* and width *w*. The beach is defined here as the zone between the limit of wave uprush on the beach and the dune line (limit of dune vegetation or break in slope), F_c is the critical fetch length required to achieve equilibrium transport under the existing conditions (wind speed, grain size, moisture content, etc.) and the shaded area is the region landward of F_c where sediment transport is at the maximum; F_m is the maximum fetch which is determined by the beach width and wind angle α relative to shore perpendicular. Distance *l* represents a unit alongshore length at the dune line mapped out by two parallel streamlines of the wind field separated by the perpendicular distance *b* such that $b = l(\cos \alpha)$ (after Bauer and Davidson-Arnott (2002). (B) increase in sand transport rate, measured with vertical sand traps, with distance from the top of the swash at Long Point, Lake Erie for three different wind speeds and relatively dry sand (after Davidson-Arnott and Law, 1990). The traps were set up along a line parallel to the wind direction and distances are measured with respect to the swash limit. Note that equilibrium transport is achieved for winds of 5.8 m s^{-1} (F_c = 15 m) and 8.5 m s^{-1} (F_c =30 m) but not for winds of 13.8 m s^{-1}. (C) Increase in sand transport rate measured at 1 m intervals along a wind tunnel for a range of wind speeds (after Dong *et al.*, 2004b – original data kindly supplied by Dr Z. Dong).

to the point where waves may reach the dune toe. The effect of this is to enhance the importance of oblique winds in delivering sediment to foredunes, especially where beach width *w* is <40–60 m under non-storm conditions (Cloutier and Héquette, 1998). The model of Bauer and Davidson-Arnott thus provides a framework for predicting long-term sand

supply to the foredune, but successful implementation requires considerable data on beach conditions that are not easily obtained over long periods of time (Lynch *et al.*, 2006).

9.5 Sand deposition

Sand transported by the wind is deposited as a result of a decrease in wind speed either because of changes within the wind flow itself or because of interaction of the wind with the beach and dune topography, obstacles on the bed or the presence of vegetation. On bare surfaces the sand is readily mobilised again but in the lee of objects and especially within vegetation the sand may be sheltered and accretion occurs. Deposition in the lee of objects such as litter or sand fences on the beach and foredune is limited by the height of the object, but vegetation growth can often keep up with deposition and it is this factor that leads to the continued growth of embryo dunes and foredunes.

9.5.1 Deposition in the absence of vegetation

As we would expect from Figure 9.13, during a transport event sand will continually be deposited during periods of lower wind speed and entrained during gusts. Sand may also be deposited on, and in the lee of, bedforms such as ripples and dunes (Figure 9.15c). Deposition can also occur as a result of modification of the wind flow over the surface. Thus, the band of dry sand visible in front of the vegetated dune in Figure 9.6a reflects a decrease in wind speed across the foreshore leading to deposition of some of the material in transport with the rest being transported into the embryo dune.

Solid objects on the beach such as litter, pebbles and logs cause flow separation as the wind blows across them, and a sheltered zone develops in the lee into which sand is deposited. The result is a triangular wedge of sediment that grows upward until it reaches the zone of turbulence associated with the wake where speeds are sufficient to keep sediment moving (Figure 9.21a). These sand shadows provide small amounts of temporary storage but are largely irrelevant in the long-term beach and dune sediment storage.

Sand fencing is often used as part of a dune rehabilitation project or simply to retard sand transport from the beach into buildings and parking lots located too close to the beach (Nordstrom *et al.*, 2007). Sand (snow) fences are rigid but also permeable. The wind flow is greatly retarded between the upright slats of the fence and the reduction in wind speed leads to sand deposition in the lee. Most of this sand comes through the gaps in the fence but some may be transported over the fence and be deposited in the sheltered zone behind (Figure 9.21b). As sand builds up behind the fence the lower portion becomes impermeable and this may lead to deposition in front of the fence. Where large volumes of sand are transported, several generations of fences may have to be deployed if further deposition is required. Where fencing is deployed in aid of dune restoration, care has to be taken to avoid placing the fences too close to newly planted vegetation because large accumulations may result in burial depth being too great for the plants to successfully emerge. Sand fences can become quite hazardous as some of the slats get broken and the wires holding them together break, so that a better solution is to use a brushwood fence (Anthony *et al.*, 2007) which appears to be as efficient in trapping sand and can be safely left to be buried.

9.5.2 Deposition within vegetation

Deposition of sand within vegetation is the key to the development of embryo dunes and ultimately the whole foredune complex. There has been much research on the effect of plants on wind flow and turbulence, and to modelling their effect on the erosion potential from semi-arid areas and agricultural fields (Wolfe and Nickling, 1993; Lancaster and Baas, 1998; Finnegan, 2000; Leenders *et al.*, 2007) as well as the effect of wind on plants (de Langre, 2008). The effect of plants on the wind flow over the backshore, embryo dune and foredune depends first on the plant form as well as on the height and density of cover and on the flexibility of the plant (Olson, 1958b). Thus the impact on the velocity profile of the relatively flat leaves and

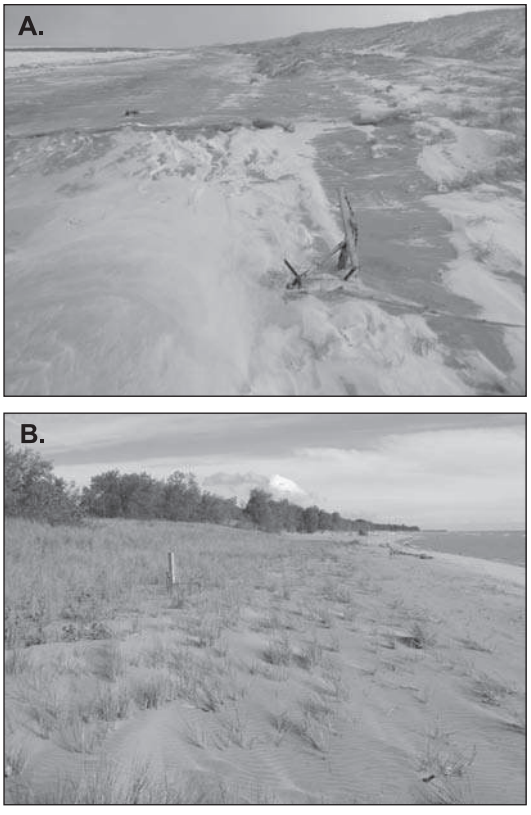

Figure 9.21 Deposition of wind-blown sand. (A) Deposition in the lee of a solid object – sand and snow accumulating in the lee of a log on the beach. The movement of the log during a storm had unfortunate consequences for the saltation probe at right used for monitoring sand transport by wind. (B) Sand shadows produced by deposition within, and in the lee of, clumps of marram grass.

creeping stolons of Ipomoea is different to flow over stands of grasses such as Amophila or shrubs such as sea grape (see Figure 9.3). Plants also allow the wind to flow through the canopy as well as around it.

Plants trap sand transported from the beach in two ways. The reduction in flow speed within and in the lee of individual plants leads to sand deposition in these areas and to the formation of sand shadows (Hesp, 1981) which extend downwind from the plants (Figure 9.21b). These may coalesce as the spacing between plants is reduced (Arens *et al.*, 2001). With low, spreading forms such as *Honkenya peploides* there is a much more limited protected area in the lee of the plant and a greater proportion of deposition occurs within the plant itself. A substantial amount of deposition occurs simply because the leaves and stems of plants provide a physical obstacle to saltating grains. Some grains colliding with a leaf or stem bounce off into the airstream again but others fall to the bed among the stems of grasses or below the canopy of creeping plants or bushes and are trapped there because of the shelter provided by the canopy above.

The effectiveness of vegetation in reducing transport is primarily controlled by the % cover but it is also a complex function of plant height, form and flexibility, and of the spatial pattern of bare surfaces (Hesp, 1989). Field studies show that the sand transport rate is reduced to negligible amounts compared to a bare surface for a vegetation cover of 20–25% (Lancaster and Baas, 1998; Kuriyama *et al.*, 2005). Vegetation is typically sparse at the seaward edge of the foredune and onto the backshore, and it tends to increase towards the foredune itself. Sand can initially be transported through the bare patches between individual plants and clumps of plants but as the vegetation cover increases more sand is deposited and there are fewer areas where the wind speed exceeds the threshold for initiating further transport. Where the cover is quite sparse near the beach sand is deposited over quite a broad area forming a relatively flat surface, but if the vegetation is quite dense near the edge of the beach, deposition occurs in a relatively narrow band generating a ridge (Hesp, 1989; Arens *et al.* 2001).

As deposition within the plants occurs, it is necessary to consider the accommodation space provided by the plant cover – i.e., the volume of sediment that can be trapped by the plants and the area sheltered by them. With grasses such as Amophila and Uniola as deposition takes place the height and surface area is reduced, thus reducing its effect on wind flow and the size of the sheltered area. In mid- and high latitudes the grasses reach their maximum height in the early autumn at a time when the delivery of sand from the beach is likely to be at its greatest. As the grasses die back there is some loss of foliage and at the same time there is increasing burial of the vegetated area closest to the beach in the embryo

dune zone and at the base of the foredune (Figure 9.22) so that sediment can pass through up the stoss slope of the foredune towards the dune crest. The maximum depth of sediment that can be trapped and retained over the winter period depends on the vegetation height and is generally on the order of 0.2–0.5 m.

Where sediment is trapped by annuals such as *Cakile edentula* on the foreshore a mound of sand may be preserved over the winter but new plants will have to germinate and establish quickly in the spring in order to preserve the deposit. In low latitudes the plants are active all year round and pioneer vegetation such as ipomoea and spinnifex, which have a smaller accommodation space than the taller grasses, can respond continuously to burial. Shrubs and trees obviously have a much greater accommodation space than grasses and stoloniferous plants, but at the same time they grow much more slowly and are less able to tolerate substantial amounts of burial – for example due to the migration of a parabolic dune.

In the mid- and high latitudes there are marked seasonal patterns in wind regime, plant growth and sand transport potential, particularly where winters are cold enough for the ground to freeze and for snow to cover the beach and foredune. This affects both the timing of sand supply to the foredune and the locations where transport and deposition are most active. Figure 9.23 is based on measurements made at Long Point, Lake Erie (Law and Davidson-Arnott, 1990 and is applicable to much of eastern Canada and the north-east United States. In the summer, transport rates are generally low and plants are growing vigorously so deposition is small and confined to the embryo dune zone. In the early autumn, transport increases considerably but sand is still trapped primarily near the base of the stoss slope. In late autumn and into the early winter, sand transport is at a maximum and a combination of burial and plant die back permits sand to move up the stoss slope and onto the foredune crest. In the winter, supply from the beach is reduced because of freezing of interstitial water and because of the snow cover. However, towards the end of the winter and into the spring sublimation and melting permit some supply from the beach. There is also considerable reworking of sediment near the dune crest because of the reduced vegetation cover. Where the beach seldom freezes, such as in Western Europe and the west coast of the US and Canada, winter months tend to have the greatest transport activity.

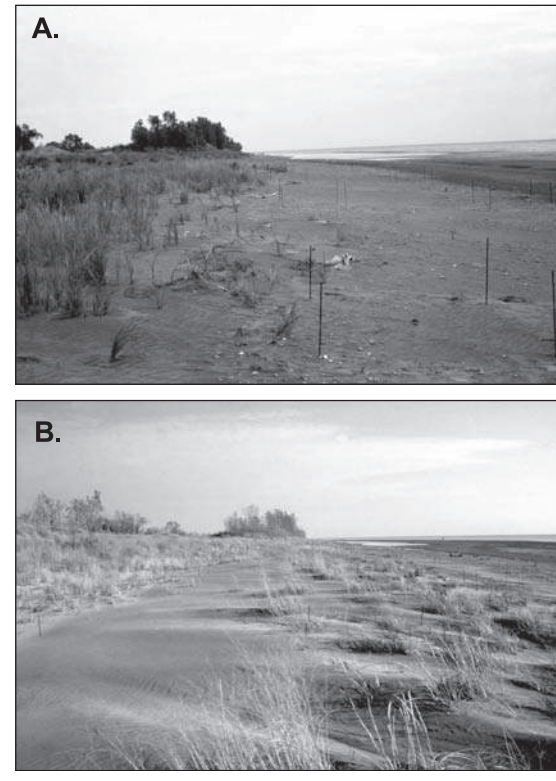

Figure 9.22 Accretion of sand in marram grass in the embryo dune and foredune zones at Long Point, Lake Erie: (A) photograph looking alongshore at the beginning of September when the vegetation is at it highest; (B) photograph taken at the end of November showing formation of a small ridge in the embryo dune zone, burial of vegetation and accumulation towards the base of the foredune.

9.6 Beach/dune interaction and foredune evolution

The previous sections have examined the basic form of the foredune system and the factors controlling sediment transport and deposition. This

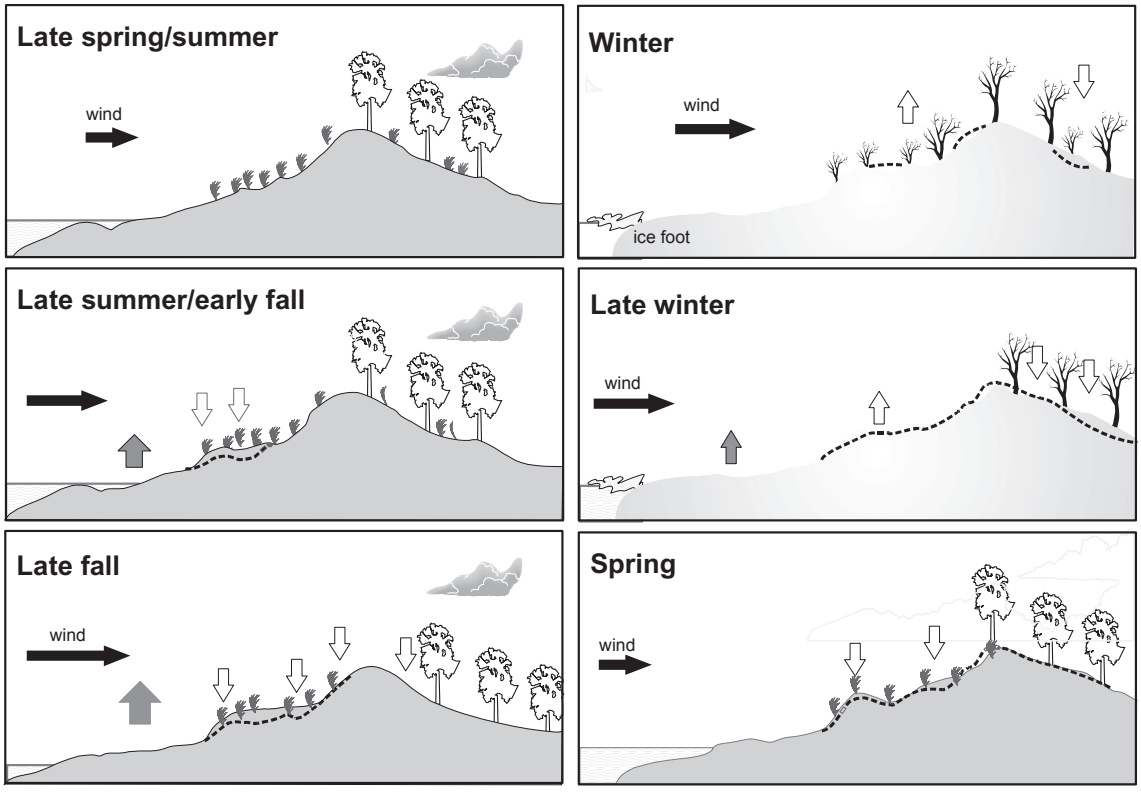

Figure 9.23 Cartoon summarising the seasonal pattern of erosion and deposition of sand on the beach and foredune on a mid-latitude coast with winter ice (modified after Law and Davidson-Arnott, 1990).

section examines the dynamics and evolution of the foredune system and the factors controlling them (Bauer and Sherman, 1999). These controls and interactions can be summarised in a simple schematic that identifies the main components and interactions that affect the development of the foredune system and associated plant communities, and separates the internal working of this from external controls such as climate and sea level change (Figure 9.24). Examination of this may be helpful in explaining observed variations between foredune systems on a regional and global scale, and in suggesting what the potential direct and indirect effects of climate change might be on coastal dunes and their vegetation associations. The term dune/beach interaction (Psuty, 1988) is useful because it emphasises the role played by littoral processes (waves, currents sediment transport) in influencing the development of the foredune system, directly through wave erosion and overwash and indirectly through the littoral sediment budget and the availability of sand for aeolian sediment transport.

9.6.1 Models of foredune evolution

There have been several attempts, using some or all of the controls identified in Figure 9.24, to develop conceptual models to describe beach/dune interaction and foredune development. Most are highly schematic, though there have been attempts to quantify a few of them in a very general way. Differences between the schemes reflect differences of scale and the factor(s) thought to be critical to foredune growth and modification. On a timescale of years to decades, two somewhat contrasting conceptual models of controls on foredune development have been proposed – the sediment budget model of Psuty (1988), and the beach stage model of Short and Hesp (1982).

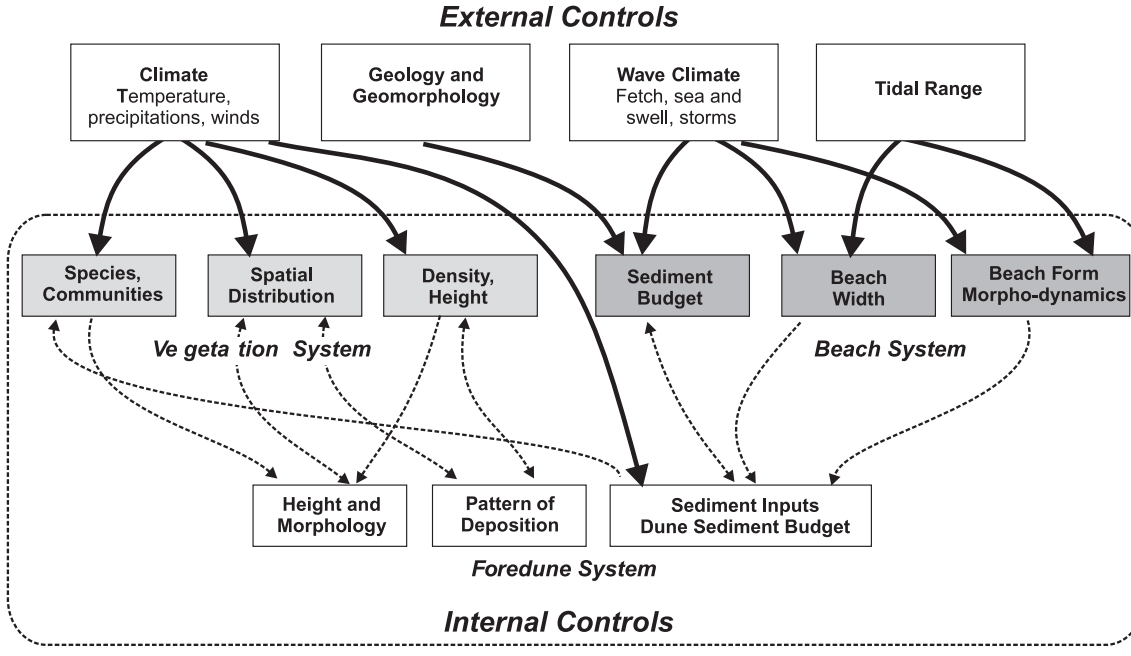

Figure 9.24 Schematic model of the major controls on the development of coastal dunes and dune fields (Reed *et al.*, 2009).

Beach stage model

Short and Hesp (1982) suggests that sand supply to the foredune and dune field evolution is determined by the form of the beach which influences both the width of dry beach which provides a source of sediment for aeolian transport into the dune, as well as influencing the distribution of surface shear stress across the beach. At one end of the morphodynamic continuum, dissipative beaches are characterised by high potential for aeolian sediment transport and a high frequency of foredune destabilisation by storm waves which initiates episodes of transgression (Short and Hesp, 1982). At the other end of the continuum reflective beaches are characterised by low potential sediment transport and few episodes of destabilisation leading to stable foredune development and limited inland transport of sand. Intermediate beach types have higher probabilities of foredune destruction and the development of large scale parabolic dunes. Underlying assumptions of the model include stable sea level, a positive littoral sediment budget and a relatively high energy, microtidal coast and thus it does not have universal applicability. Some aspects of the model were incorporated in a computer simulation model by Sherman and Lyons (1994).

This approach is also incorporated in a more recent conceptual model by Patrick Hesp (Hesp, 2002) which includes the effects of large storm events as well as controls on longer term evolution of both accreting and eroding coasts (Figure 9.25). The range of scenarios reflects the large number of factors that influence foredune development and gives a comprehensive overview of the complexity of the temporal and spatial patterns that can be observed world-wide.

Sediment budgets

In contrast to the beach stage model is the scheme originally put forward by Psuty (1988) and elaborated in several publications over a number of years (e.g. Psuty, 2004). The Psuty model relates evolution of the foredune system to the relationship between the beach sediment budget and the dune sediment budget (Figure 9.26). The quadrant diagram of Psuty (1988) illustrates that the littoral sediment budget determines whether the shoreline is transgressive, stable or progrades, as well as controlling the amount of time that a

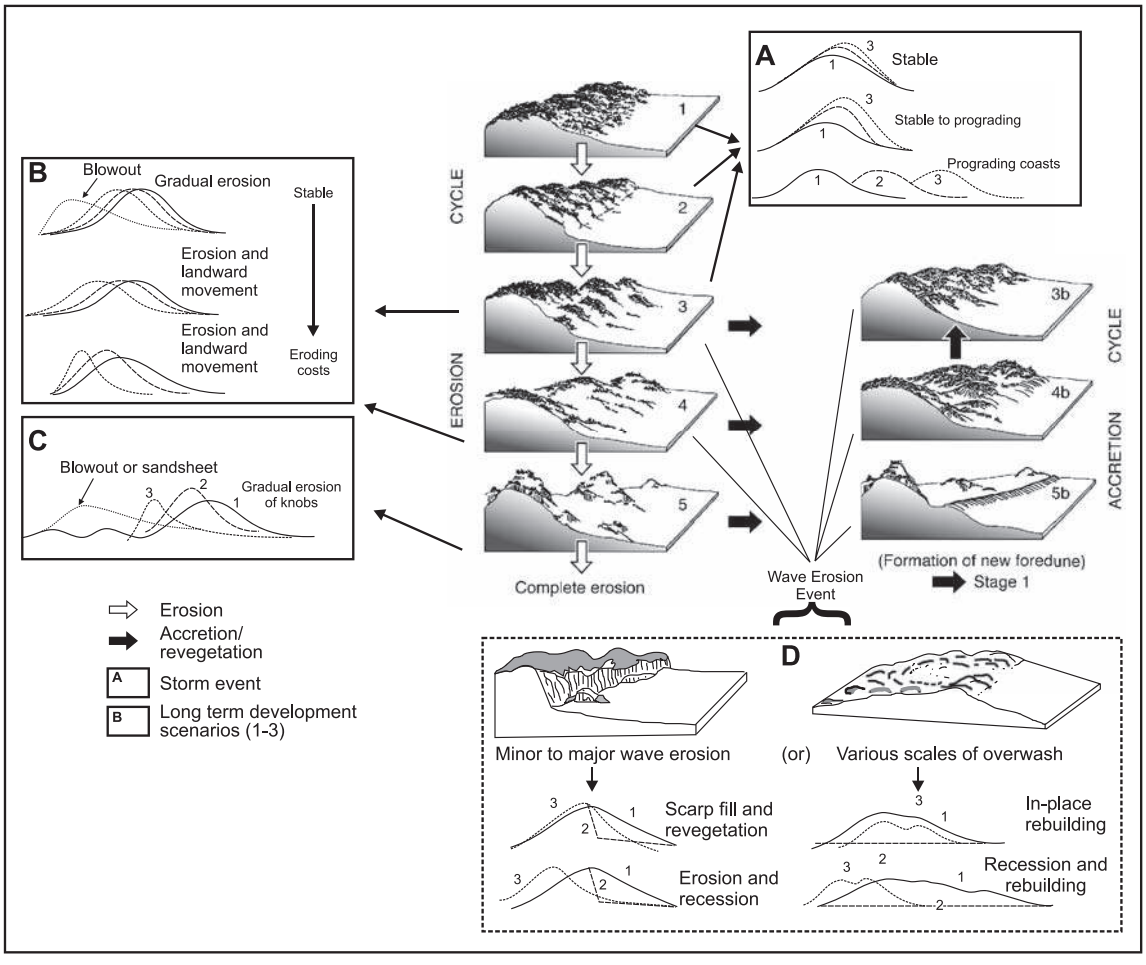

Figure 9.25 A model for established foredune morphology, dynamics and evolutionary trends on stable, accreting and erosional coasts (Hesp, 2002). A foredune may develop towards and remain in a particular morpho-ecological stage (Types 1–5) or it may evolve to another stage over time. Wave erosion events may occur at any time leading to adjustments ranging from minor scarping to major scarping or overwash. Foredunes may recover, build landward or disappear altogether. In the long-term foredunes may be relatively stable (Box A) or erosional (Box B and C).

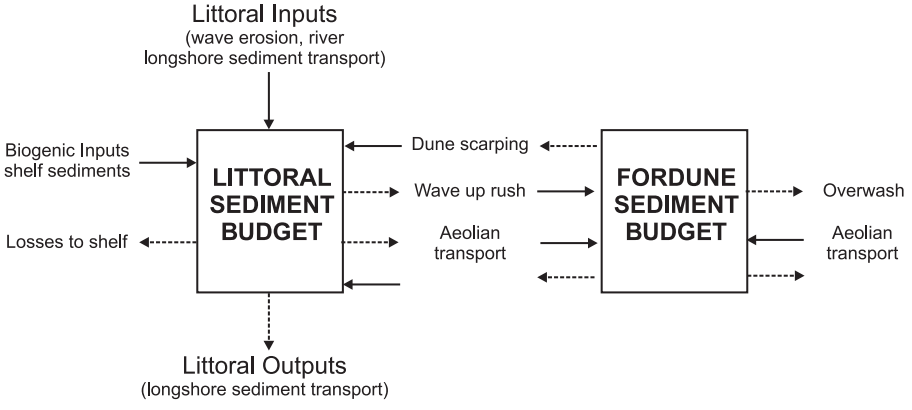

Figure 9.26 Beach and foredune sediment budgets and the interaction between them.

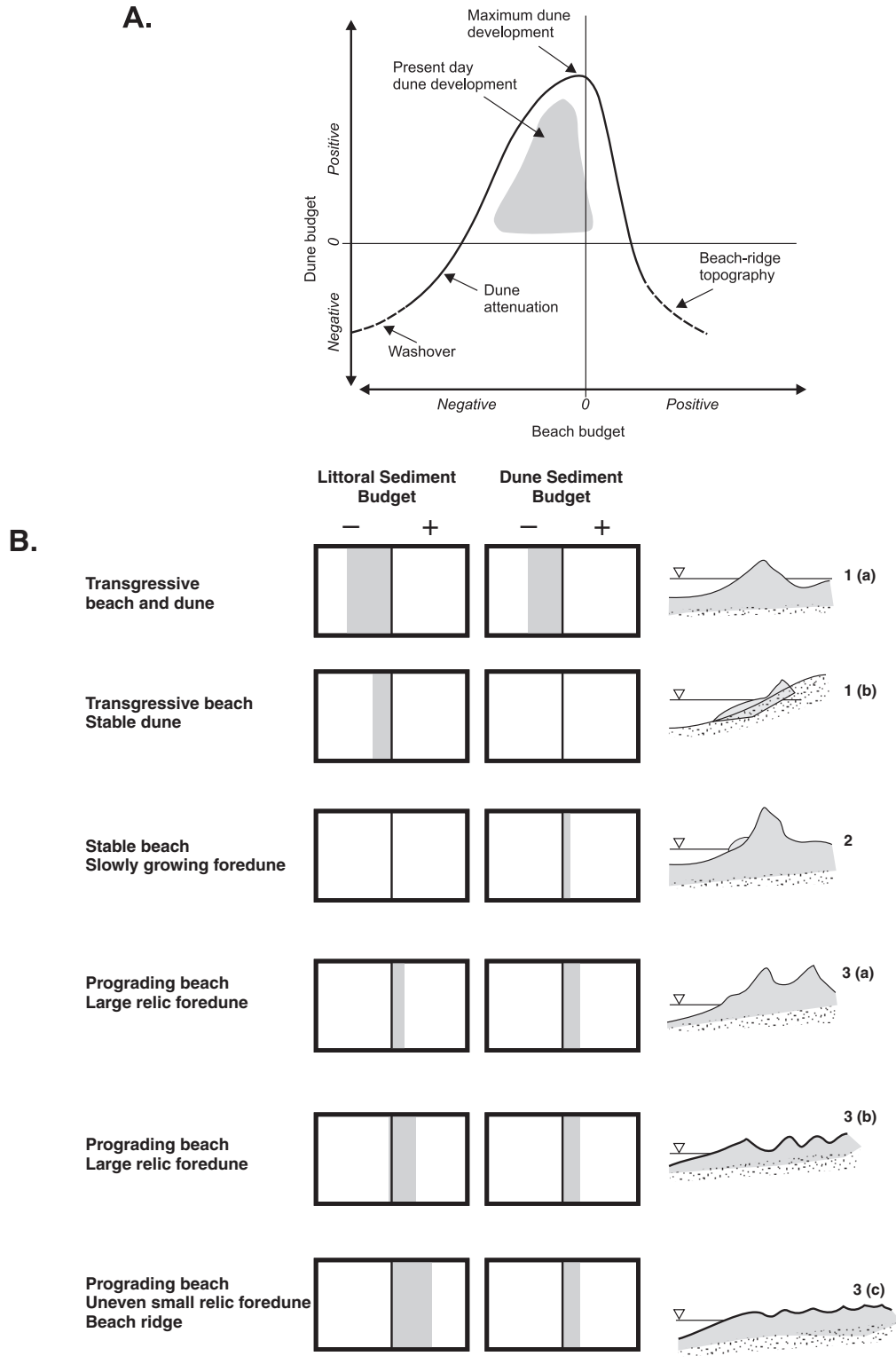

Figure 9.27 Scenarios for foredune development based on the relationship between the littoral and foredune sediment budgets: (A) quadrant diagram of Psuty (1988) showing the effects of the interaction between beach and dune sediment budgets on foredune development; (B) schematic of foredune development related to beach and dune sediment budgets based on Psuty (1988) and Nickling and Davidson-Arnott (1990).

particular foredune ridge receives sediment directly from the beach (Figure 9.27a). The (fore) dune sediment budget determines how much sand is available for foredune building. In nature it is difficult to conceive of a situation with a large positive littoral sediment budget and negative dune budget so the curve on the right side of the diagram should more realistically flatten off around the neutral line. Based on the scheme of Psuty (1988) and Nickling and Davidson-Arnott (1990), the response of the beach and dune system to these combinations is shown schematically in Figure 9.27b. Scenario 1 illustrates a negative littoral sediment budget leading to transgression of the shoreline. If the beach and dune sediment budget are both highly negative (Panel 1a), the foredune system may eventually be destroyed by breaching and overwash. If the deficit of the littoral sediment budget is moderate, then transgression still occurs but the dune sediment budget may be maintained. Under these conditions the foredune form migrates inland at the same rate as shoreline transgression (Panel 1b). Psuty notes that this is common to many of dune systems world-wide and this is to be expected under conditions of ongoing sea level rise (Davidson-Arnott, 2005). Such conditions result in the formation of a single, high foredune ridge which has steep stoss and lee slopes. Where the littoral budget is near neutral (Panel 2) the shoreline position remains fixed and the foredune is maintained or grows slowly. Finally, where both the littoral and foredune budgets have a surplus, progradation takes place (Panel 3a, b, c) with the rate of progradation depending on the relative size of the littoral and dune sediment budget surpluses. As the rate of progradation increases, the time available for building each foredune ridge decreases, resulting in the construction of more, but lower dunes.

Psuty (2004) notes the existence of a number of continuum scenarios, for example a gradient of decreasing sediment supply away from a river mouth, and this is reflected in a similar gradient in the dune sediment budget and foredune form. The reverse of this is common to barrier spits where the sediment budget increases towards the distal end.

9.6.2 Accretion and erosion of the foredune system

Beach–dune interaction involves both the transport of sand by aeolian processes from the beach to the dune, and sometimes from the dune back onto the beach, and removal of sand from the dune by wave action during storms. Aeolian transport into the dunes represents a loss of sand from the littoral sediment budget and ultimately leads to narrowing of the beach and greater susceptibility to wave action, unless there is sufficient replenishment from updrift or offshore. During storms, elevated water levels and high waves lead to erosion of the embryo dunes, scarping of the foredune and, in extreme events, to destruction of the foredune itself. Wave erosion returns sand to the littoral system and acts to widen the beach and reduce the level of wave action at the dune toe. Initially unvegetated sand ramps can be built against the scarped foredune and vegetation establishment traps sand and rebuilds the base of the dune. Foredunes therefore are almost always compound features, incorporating varying degrees of cut and fill, and the disturbance caused by wave erosion or burial of vegetation by sand can trigger blowouts and parabolic dune development in the foredune.

Deposition on the foredune

In areas of restricted fetch such as lagoon and estuary shores, beaches are very narrow and there is a limited range of both erosion and accretion ((Nordstrom and Jackson, 1994; Nordstrom, 2000). However, on exposed beaches, the combination of waves, tidal range and storm surge act to promote a wide beach from which sand is supplied to the foredune system. Measurements of deposition in the dunes over individual storms, months and years have been made on a number of locations world-wide (e.g. Hesp, 1983; Sarre, 1989; Davidson-Arnott and Law, 1996; Bretel *et al.*, 1999; Aagaard *et al.*, 2004; Anthony *et al.*, 2006) by repeated surveys of individual transect lines or making use of deposition pins or some form of bedframe device (Davidson-Arnott and Law, 1990). Measurements at Skallingen on the Danish North Sea coast (Aagaard *et al.*, 2004;

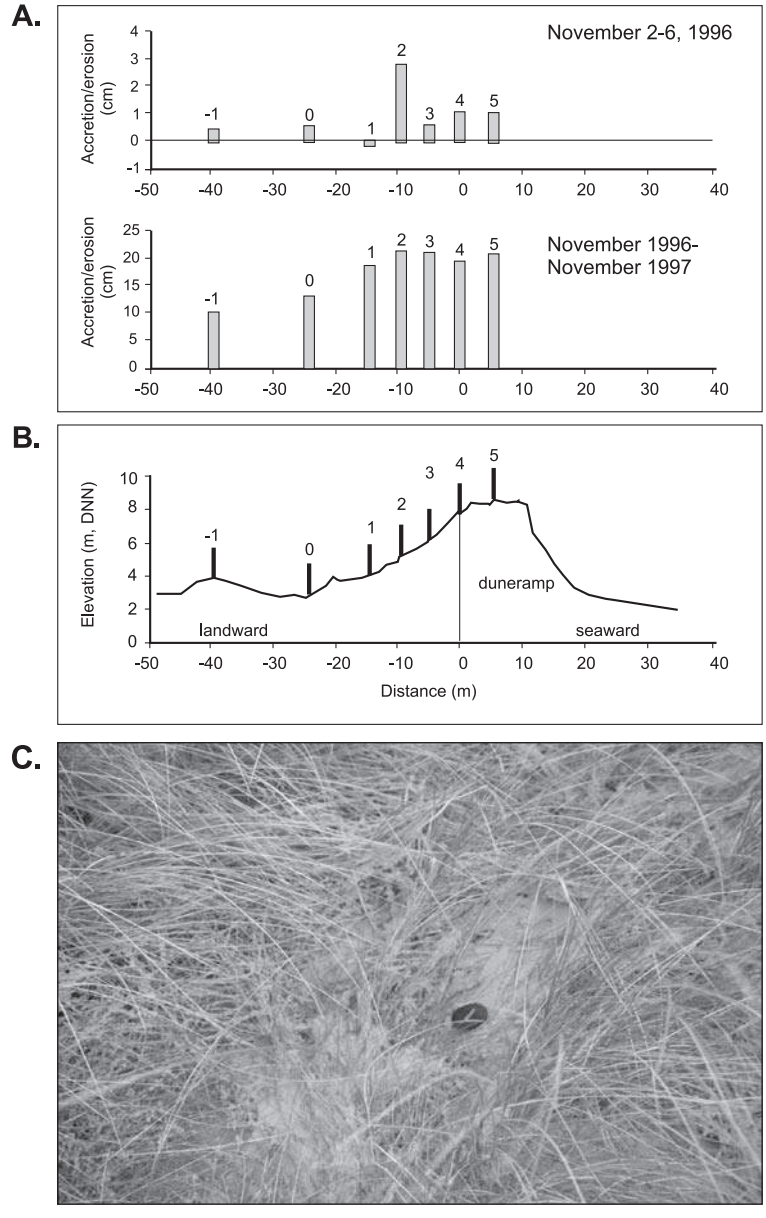

Figure 9.28 Erosion of the foredune ramp and accretion on the lee slope of the foredune measured bybedframes along one transect at Skallingen over one storm November 2–6, 1996 and over the period November 1996–November 1997 (after Aagaard *et al.*, 2004): (A) measured deposition over the storm and over the year; (B) profile surveyed across the beach and foredune prior to the survey; (C) sand deposited on dune grasses on the lee slope of the dune following the November 2 storm.

Christiansen and Davidson-Arnott, 2004) illustrate large amounts of deposition on the lee slope of the foredune during an intense autumn storm (Figure 9.28) derived largely from erosion of the dune ramp on the stoss slope of the dune and the bare cliffed face of the dune above it (Figures 9.28a, b). Sand was blown up and over the dune crest and deposited up to 40 m inland coating the leaves of the vegetation (Figure 9.28c). Deposition from this one storm averaged about 0.5 m^3 per metre width of beach based on three profiles monitored. Over the period of 1 year, about 0.15–0.20 cm of sand accumulated over the profile landward of the crest and total deposition averaged about 8.5 m^3 m^{-1}. Similar rates of accumulation were measured wherever dune ramps were well developed, but much lower rates where the dune ramp was low (Christiansen and Davidson-Arnott, 2004). The average deposition over a period of several years is of the order of

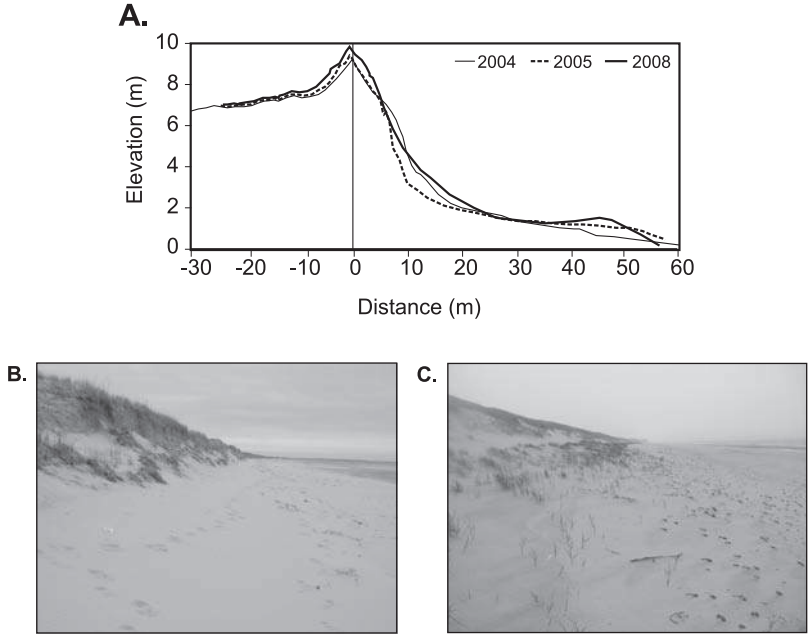

Figure 9.29 Moderate erosion of the dune at profile 6, Greenwich Dunes (see Figure 9.26 for line location) by a storm in late December, 2004: (A) profiles surveyed in May 2004, May, 2005 and June, 2006 using a DGPS; (B) photograph taken in May, 2005 looking alongshore to the west showing removal of all vegetation from the backshore, scarping of the lower slope and slumped blocks of sand and Amophila from the upper slope; (C) photograph taken in June, 2008 showing growth of the dune ramp to infill the cliffed lower portion of the slope and development of a new embryo dune in front of it.

4–5 m^3 m^{-1}. These can be compared to measured rates of deposition of 2.6–10.3 $m^3 m^{-1}$ at Long Point, Lake Erie (Davidson-Arnott and Law, 1996); 1–3 m^3 m^{-1} at Greenwich Dunes; 1.96–5.91 m^3 m^{-1}on the coast of the Danube delta (Vespremeanu-Stroe and Preoteas, 2007), and 5–6 m^3 m^{-1} on the coast of Normandy, France (Bretel *et al.* 1999). Much higher rates are reported for areas with a drier climate such as the east coast of Australia and South Africa.

Foredune erosion

During storms higher waves and storm surge lead to erosion of the beach and as waves reach higher up the beach with greater storm intensity they begin to erode the embryo dune and then the foredune itself (Kriebel and Dean, 1985). Depending on the extent to which dune erosion occurs, we can identify four levels of disturbance to the dune vegetation and the foredune itself (e.g. Hesp and Martínez, 2007):

(1) Minor – waves reach the embryo dune or base of the foredune, there may be minor erosion and trimming of vegetation at the seaward edge. Deposition in the vegetation by swash may produce small amounts of accretion. Recovery occurs within a few months to a year;

(2) Moderate – waves erode the embryo dune and/or dune ramp (if present) and scarp the base of the foredune (Figure 9.29). The upper part of the stoss slope remains intact and pioneer vegetation is preserved in places on the lower slopes. Recovery occurs in 2–5 years;

(3) Severe – waves erode the dune severely producing a vertical cliff that may extend right to the dune crest (Figure 9.30). Little or no pioneer vegetation is preserved. Unvegetated dune ramps may form over one or more years but recovery may take 5–10 years depending on the time it takes for vegetation to become re-established;

(4) Catastrophic – waves breach the dune completely with sediment being deposited as an overwash fan across the back dune area. Recovery may take more than 10 years depending on the lateral extent of destruction – see Section 10.3.1.

9.6.3 Blowouts, parabolics and dune fields

Blowouts

Destabilisation of vegetated foredunes (and dune fields) can occur locally, leading to erosion by

Figure 9.30 Examples of severe erosion of the foredune as a result of storm surge and large waves: (A) Skallingen, Denmark, October, 2000; (B) Long Point, Lake Erie, May 1985.

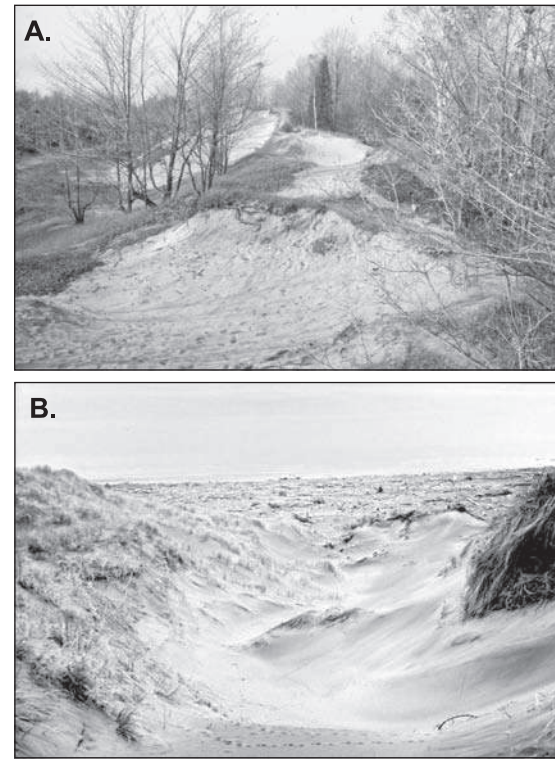

Figure 9.31 Blowouts in coastal dunes: (A) small saucer blowouts in the crest of a Holocene dune ridge, Red Bay, Ontario; (B) view looking seaward to the beach through a trough blowout, Manawatu dunes, New Zealand (see Hesp, 2002).

wind action which hollows out the sand surface to produce a variety of saucer-, cup- or trough-shaped depressions (Hesp, 2002) with depth and elongation of the form increasing from the initial relatively shallow, round saucer shape (Figure 9.31a). Vegetation disturbance leading to blowout development may be initiated by physical processes such as storm wave erosion of the front face of the foredune, topographic acceleration of airflow over the dune crest or around topographic irregularities or as a result of local burial of plants by excessive sand deposition. It may also result from drought and fire, or from the effects of trampling and overgrazing by animals; and often by a wide range of human activities (Hesp, 2002). Once formed, the morphology of the blowout affects air flow in the vicinity, leading to topographic steering and local flow accelerations which often enhance the deepening and elongation of the blowout (Gares and Nordstrom, 1995; Hesp and Hyde, 1996; Hesp and Pringle, 2000; Hansen *et al.*, 2008). As the depression deepens slumping of the sides occurs and this sand is then blown out over the rim of the blowout (Figure 9.31b). Where trough blowouts extend to the backshore, topographic steering results in wind being funnelled through the upwind entrance. This results in erosion of the blowout and the transport of additional sand through the blowout and over the lee slope (Hesp and Pringle, 2000).

Blowouts in vegetated dunes may stabilise over time depending on the particular combination of wind and weather conditions, sand supply and vegetation propagation. Stabilisation is promoted when vegetation becomes established on the bottom of the depression and then spreads upwards to colonise the sides. This can occur where the bottom of the blowout

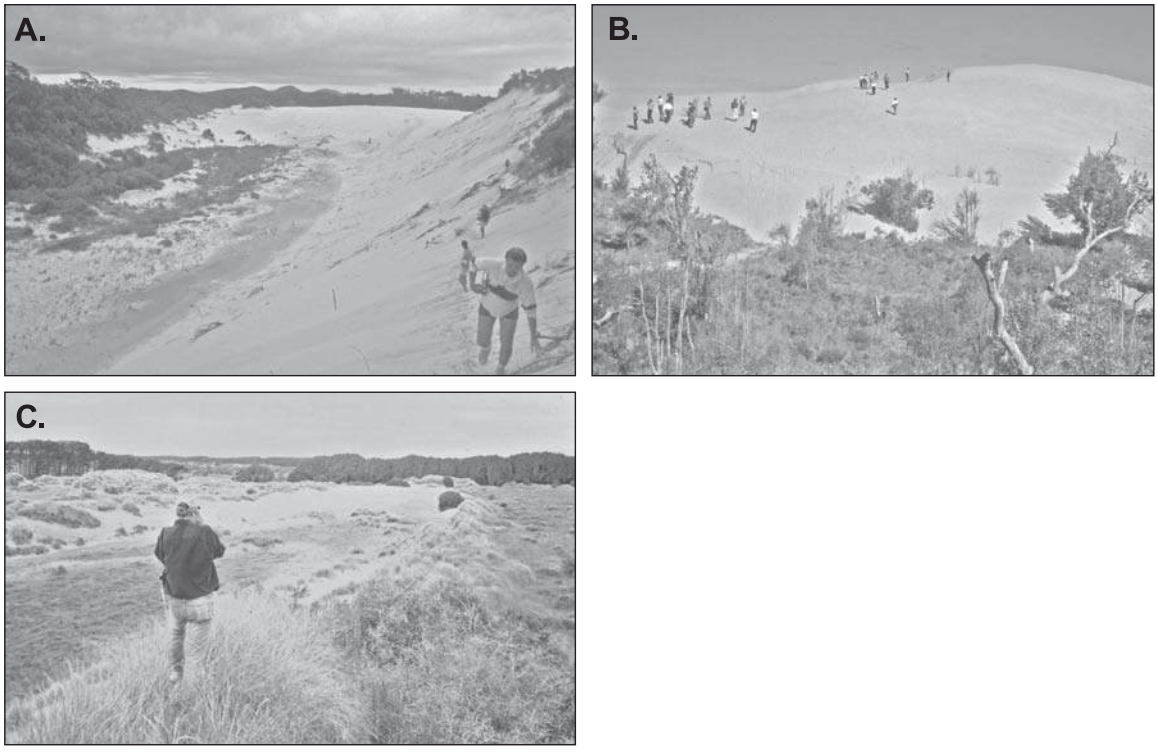

Figure 9.32 Parabolic dunes: (A) view inland along the trough of a large parabolic dune extending through older Holocene dunes, NSW, Australia. Erosion on the upwind side has reached the water table but the sidewall crests are still stabilised by trees; (B) slip face of an advancing parabolic dune, Newcastle Bight, NSW, Australia; (C) view inland from the right trailing arm of a hairpin parabolic, Manawatu dunefield, New Zealand (Patrick Hesp for scale). The dune is moving across pasture land so the form is relatively low and the slip face moves rapidly at rates up top several tens of metres per year. See Figure 9.1b for an aerial view of this dunefield.

intersects the groundwater table, but often there is sufficient moisture near the surface to retard sand movement and permit plant establishment. Plant colonisation may also be aided by the slumping of intact blocks carrying plants. Thus many blowouts stabilise over time and are preserved as vegetation becomes established, or they may be infilled gradually as sand blows in from the beach. The result is that the simple two-dimensional topography of many foredune ridges becomes more complex over time.

Blowout development is a normal feature of many dune systems under natural conditions. Blowouts may be initiated or enhanced by human activities such as trampling, use of all terrain vehicles and grazing of livestock and large-scale destabilisation of dunes can occur as a result of these activities.

Parabolic dunes

Parabolic dunes consist of high, U-shaped migrating dunes with an active slip face at the landward margin. They have an elongate erosional basin on the upwind side (Figure 9.32a) which supplies sand to the active depositional lobe (Figure 9.32b), and trailing ridges which are U-shaped or hairpin-shaped and form the sides of the basin (Hesp, 2002). Over time the upwind end of the trough tends to become stabilised as sand movement is reduced by erosion to the water table Figure 9.32a). Eventually sand supply to the slip face and forward migration of the dune ceases as a result of the spread of vegetation. The height of the migrating dune is a function of the volume of sediment supply/availability which reflects the thickness of sand deposits over the regional water table.

Parabolic dunes may be initiated in the foredune system and migrate landward into older aeolian deposits in a dune field or they may be initiated in the dunefield itself. Where the vegetation cover consists of grasses and low bushes the slip face is also low and the rate of forward migration can be several tens of metres per year (Figure 9.32c) but if the dune is advancing through forest cover then the reduction in wind speed at the forest edge results in the building of the front wall to form a precipitation ridge that results in burial and death of the trees (Figure 9.32b). The rate of landward migration is then much slower but can take place over many decades and reach several km inland (Clemmensen *et al.*, 2001; Hesp and Martínez, 2007).

Dunefields

In many cases periodic disturbance on a time scale of several decades to centuries produces a succession of overlapping dune forms with sediments from the older episodes being buried beneath younger deposits (Hesp and Thom, 1990; Clemmensen *et al.*, 2001). In New South Wales, Australia, transgressive dune fields show multiple phases of development with periods of stability and foredune growth followed by disturbance and inland migration of sand leading to burial of older transgressions (Lees, 2006). The episodic transgressive dune field development may result from disturbance caused by large storm(s), drought, fluctuating lake levels (Olson, 1958c; Loope and Arbogast, 2000) or human activities Clemmensen *et al.*, 2007) and may be moderated by the need to develop a critical mass of sand in the foredune so that the migrating dune front is able to bury vegetation landward of it.

Where large volumes of sand are supplied to the dune (large positive littoral sediment budget and consequently positive dune sediment budget) foredune development may be either discontinuous in space or time depending on the relative ability of the plant communities to withstand burial. Transgressive dune fields develop, characterised by sand sheets and large-scale sand seas or dunefields with the downwind borders consisting of precipitation ridges and the development of deflation basins and plains upwind (Cooper, 1958; Hesp and Martínez, 2007). Some of the largest transgressive dune fields have been described from the coast of Brazil (Hesp *et al.*, 2007a; Giannini *et al.*, 2007; Martinho *et al.*, 2008) and others from the east coast of Australia (Hesp and Thom, 1990); Denmark (Clemmensen et al, 2007; Aagaard *et al.*, 2007) Argentina (Tripaldi and Forman, 2007) and South Africa (Illenberger and Rust, 1988). In many cases these dune fields were established during the Holocene transgression when large volumes of sediment were brought onshore across the continental shelf. Similar processes were involved in transgressive dune fields formed in the lower Great lakes of the USA and Canada (Martini, 1981; Davidson-Arnott and Pyskir, 1988; Arbogast and Loope, 1999).

9.7 Management of coastal dunes

There is a huge literature on management of sandy beach and dune systems, many of them case studies, and reviews of coastal management policies. Approaches to management can be crudely defined as ranging between two extremes:

(1) the ecological approach – coastal sand dunes are fragile ecosystems which may be destabilised as a result of any human activities and thus management focuses on keeping human activities in dunes to a minimum and allowing the foredune system to evolve naturally. Where systems have been destabilised due to human actions, aggressive intervention may occur to stabilise the system, ranging from sand fencing and planting of pioneer dune species; and

(2) the engineered approach – dunes are simply heaps of sand that have been blown by wind. Very similar forms can be constructed readily with earth moving equipment and stabilised by planting with suitable species, aided by the addition of some fertiliser. If the dunes are eroded, new dunes can quickly be created and additional sediment pumped in or trucked in if necessary.

Box 9.2 Potential impacts of climate change on coastal foredune systems

The impacts of global warming and climate change on coastal foredunes are most likely to reflect changes in temperature and precipitation, intensity and frequency of storm events and increasing rates of relative sea level rise (Nicholls *et al*., 2007). The increase in global temperatures and changes in precipitation can potentially have an impact on the growth and density of plants, both in the foredune system where disturbance is relatively high, and in areas where there is an extensive dune field landward of this system. Increased temperature, especially if accompanied by reduced precipitation, has the potential to reduce the density of plant cover and thus to destabilise the foredune system. The impact may be relatively modest for foredune systems where the vegetation is already adapted to high temperatures and moisture deficiencies but it may increase the frequency of disturbance due to fire and drought years, especially in places such as the east coast of Australia and Mediterranean systems such as those in southern Europe and California. Such sensitivity to climate variation has been documented for several coastal dunefields as well as for inland dunefields such as those in the Great Plains of Canada (Hugenholtz and Wolfe, 2005) and western Argentina (Tripaldi and Forman, 2007)

Increasing temperatures will likely lead to poleward migration of plant species which in turn will affect the nature of plant communities, most significantly those in the embryo dune and foredune zones where stresses are greatest. The most significant effect is likely to be at high latitudes and especially in the Arctic (Kaplan and New, 2006) and on the East and West Coasts of Canada and Alaska. The most significant impacts are likely an increase in plant density in some areas and thus greater trapping efficiency near the beach, and the possibility that species with a high trapping ability and resistance to burial such as *Amophila* and *Elymus* will extend their distribution towards higher latitudes. However, because of the great latitudinal range of many pioneer species and the similarity in the function of different species, the actual impact on foredune dynamics may well be quite small.

Shorter and milder winters will reduce snow cover, leading to enhanced sand transport into the dune. Warming in the Arctic is already leading to reduced ice cover and increasing both the duration of open water and the open water fetch (Shimada *et al*., 2006). This will have the effect of increasing wave action leading to greater coastal erosion (especially in the western Arctic) and this in turn may provide a greater supply of coarse sediments for beaches and increased beach width, thus enhancing the potential for sand supply to coastal dunes. Presently in the western Arctic dune development is rare, in part because of the extensive ice cover and in part because of the relatively sparse vegetation cover near the beach – the exception being small dunes developed around the margin of thermokarst lakes which may be exposed at the shoreline (Ruz, 1993). This is in contrast to the east side of Hudson Bay where foredune development occurs in areas where rivers bring fresh sediment supply to the coast and foredune stabilisation is associated with the presence of *Elymus arenaria* (Ruz and Allard, 1994). With increasing temperature conditions may be more favourable for the spread of *Elymus* northward along the shoreline of Hudson Bay and westward thus potentially promoting greater dune development in areas where sand is abundant.

Increased storm frequency as a result of global warming might decrease the recovery time between storms, especially the ability of pioneering vegetation to colonise the base of the stoss slope of the foredune and for the development of new embryo dunes on the backshore. The result would be an increase in the proportion of the foredune that is scarped (both spatially and temporally) and this in turn may increase the potential for sand transport over the foredune crest and onto the lee slope. Increased intensity of tropical storms, an increased frequency of intense storms (e.g. category 4 and 5 hurricanes) and increased intensity of mid-latitude cyclones also potentially impact dune systems. On stable sandy mainland coasts it is likely that the beach profile would adjust to such changes and the impact on dunes may be negligible. However, combined with sea level rise, increased storm intensity, and particularly increased storm surge will likely result in increased barrier overwash and thus an increase in the pace of onshore migration and the proportion of space and time that the barriers are occupied by washover fans and regenerating dunes.

Probably the greatest potential impact of climate change is due to enhanced global sea level rise. The impact of this is global in scale though its significance varies locally – for example it may be countered by ongoing isostatic rebound or large littoral inputs leading to progradation. On low-lying coasts characterised by sandy beach and dune systems, simple inundation due to sea level rise will produce a large displacement of the shoreline and wave erosion will result in further landward displacement. A key component of coastal response to sea level rise is the fate of the sediments in the dune systems on mainland and barrier coasts. The Bruun model (Bruun, 1962) predicts offshore movement and storage on the outer nearshore profile – the sediment is thus lost from the dune system. The model is only of limited applicability to coastal systems due to the important role of nearshore and coastal morphology in sediment movement, and in the case of dunes recent work shows that much of the sediment eroded during sea level transgression will likely move landward through inlets, overwash and landward migration of the foredune (Dean and Maurmeyer, 1983; Davidson-Arnott, 2005). In effect, the foredune system and dune field acts as a sink in the same way that tidal inlets, lagoons and estuaries do (Davidson-Arnott (2005).

In some areas (e.g., parts of Miami, the Mexican Riviera and the south coast of Belgium, dunes may not be managed at all – they are simply built over, and the focus is on maintaining a recreational beach.

9.7.1 Managing the dune – the ecological approach

A key element of the ecological approach to dune management is to keep the human impact on dunes, and especially the vegetation that stabilises the dune, to a minimum. It is well recognised that the most critical area is in the embryo dune and foredune zones where sand supply for the beach is at a maximum and vegetation cover tends to be lowest. In dune fields landward of the foredune, once a stable vegetation, and especially forest cover, is established it is possible to build houses and roads without leading to major disturbance, as long as the remainder of the dune area is kept vegetated. However, on transgressive dune fields where sediment supply is very high and there are episodic occurrences of instability and parabolic dune migration, almost all human activities may have to be curtailed. It is important that any dune management plan recognise the inherent dynamics of the system, and particularly that

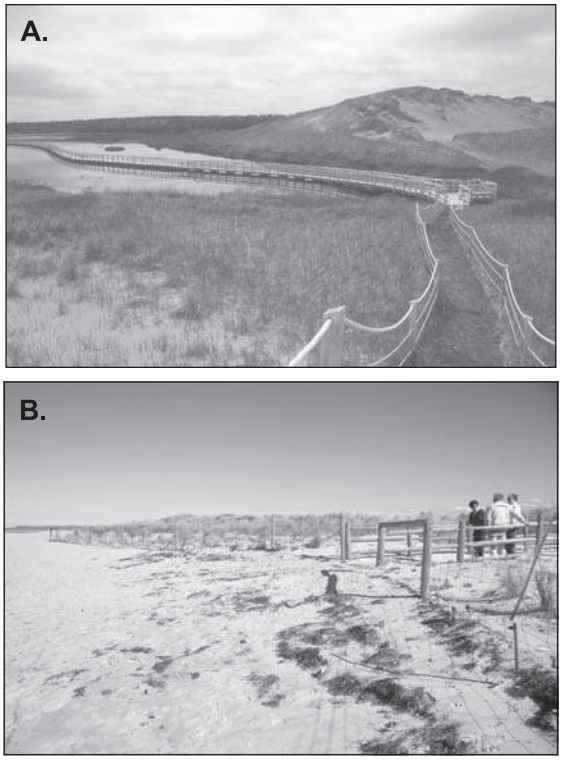

Figure 9.33 Managing people in natural dune areas: (A) nature trail and beach access, Greenwich Dunes, Prince Edward Island National Park. The trail uses a boardwalk to cross stabilised transgressive dunes (background) and the pond in the middle area. The passage across the foredune (foreground) uses a simple set of wooden posts with ropes which act both to keep people to the path and as a handhold up the steep lee slope. A simple plastic mesh on the ground allows some vegetation growth and can be raised to allow sand to fall through; (B) protection of the vegetated embryo dune zone at the back of a beach in NSW, Australia. The fencing is designed as an indication of the protected area, not as a true deterrent to entry, and the open mesh allows natural throughflow of aeolian sand transport.

blowouts and even parabolic dune development is part of the natural condition (van der Meulen and Salman, 1996).

In coastal parks where a relatively natural dune system is preserved, visitor management involves establishing facilities such as parking lots, visitor centres and other facilities some distance back from the foredune zone. Access to the beach, which is generally the prime draw, is restricted to a few pathways that are designed to minimise human impact on the vegetation through the use of wood chips or other material, and may involve the construction of boardwalks that are elevated above the dune (Figure 9.33a). Fencing is generally used to keep people from wandering off the pathway and often consists of simple posts and ropes which act more as a guide than a deterrent. Similar fencing can be used at the back of the beach to keep people from trampling on the vegetation of the embryo dunes (Figure 9.33b).

On sandy beach/dune systems away from parks the ecological management approach for all forms of housing (cottages to large hotel complexes) involves similar principles though greater impact on the natural system has to be accepted. Coastal planning generally involves the establishment of some form of setback line which keeps housing, road access and other activities which are destructive of dunes away from the foredune area. Setbacks are designed both to minimise human impact on the active dune system and at the same time to protect the inhabitants from the threats of flooding and wave impacts from severe storms (Ferreira *et al.*, 2005).

In Ontario, setbacks for sandy beach and dune systems come under the Dynamic Beach section of the Management Policy (Sullivan and Davidson-Arnott, 1995). The term is used to give explicit recognition to the functioning of the foredune as a reservoir of sand that is activated through erosion during severe storms, and as a natural protective barrier against the hazards posed by storm surge and high waves. The setback limit is determined by three components (Figure 9.34): (1) the flood standard, which is the 100 year flood elevation (based on the combined probability of fluctuating lake level and storm surge events) plus an allowance of 15 m for wave uprush and other related hazards; (2) the dynamic beach allowance which is designed to accommodate the effects of wave erosion of the embryo dune and foredune during a storm. This could have been determined locally through modelling, as was done for the determination of the 100 year flood elevation. However, it was recognised that there was much greater uncertainty

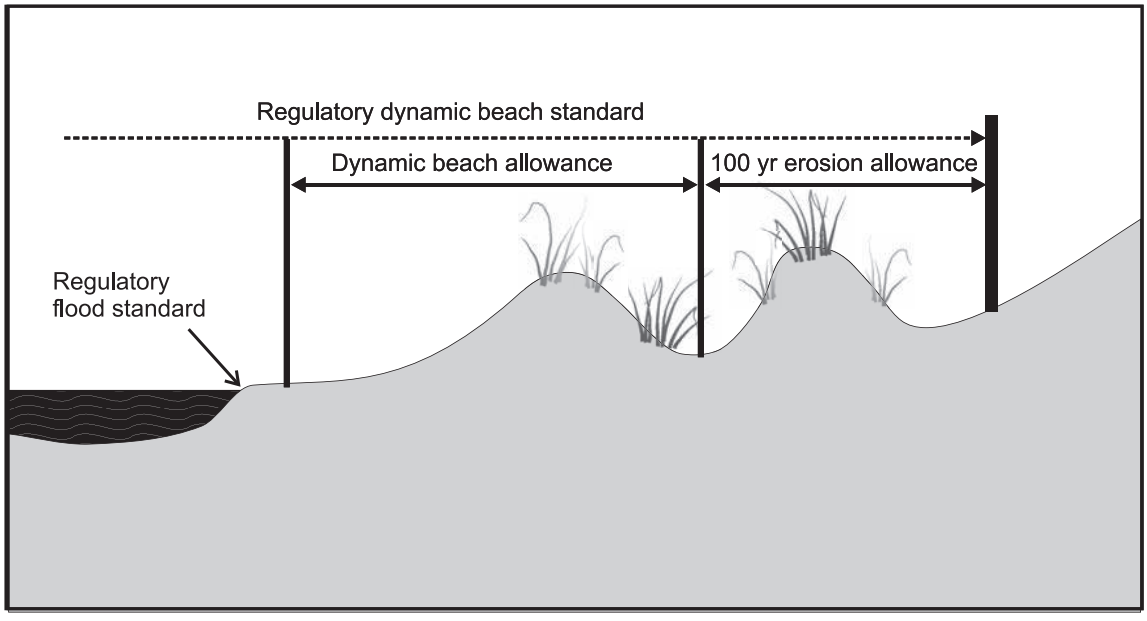

Figure 9.34 Determination of setback limits for Dynamic Beaches in Ontario.

in terms of the spatial and temporal variability of this erosion and that the available models were not very good. Instead, a standard allowance of 30 m was made based on a number of test sites where maximum erosion during one or more high water phases was known; (3) the 100 year erosion allowance, which is used on shorelines where there is a negative sediment budget and shoreline recession.

These setbacks are the minimum required by the policy. Conservation authorities who implement a management plan may introduce even stricter measures, for example, requiring that dwellings not encroach lakeward of the lee slope of the foredune. The setbacks are likely larger than necessary in many areas, but the philosophy adopted was one of erring on the side of caution, given the large uncertainties involved, and allowing local property developers to apply for a reduction in the setback if they could demonstrate through an approved study that this was the case. The basic principles of this policy are similar to those established in many parts of the world and clearly are much easier to implement along sections of the shoreline where there is not already considerable encroachment of this zone.

Managing the dune – the engineered approach

In contrast to the approach outlined in the previous section, where the focus is on preserving the natural processes and ecological integrity of the dune as much as possible, the focus in the engineering approach is on maintaining and maximising the amenity contribution of the dune system, with the ecological integrity being secondary. In the Netherlands dunes are an integral part of a policy of dynamic preservation of the coastline (van Koningsveld and Mulder, 2004). A primary objective of this is to maintain the Dutch coastline as far as possible in its present position and to protect the area landward, much of which is below sea level, from a repeat of the widespread breaching of dykes and flooding that occurred in 1953. A key part of this is the commitment to extensive beach nourishment wherever the volumes of sediment in the beach and nearshore are insufficient to maintain the beach dune system. This is done on an impressive scale, with an estimated nourishment of 6×10^6 m^3 annually (Hanson *et al.*, 2002). Where existing dunes are too low, new dunes are created by mechanical means and then stabilised by seeding and/or

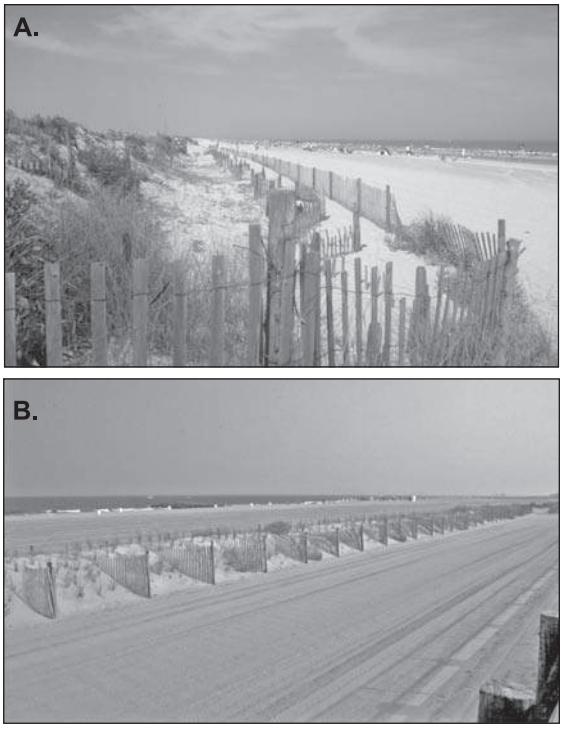

Figure 9.35 Managing the beach and dune system in New Jersey: (A) nourished beach with managed dune. The beach here is likely much wider than would be the case for a natural beach; (B) nourished beach with narrow 'dune' zone and access path at rear. Note the use of sand fences to trap sand as well as to manage people.

planting with appropriate vegetation. Natural processes are then allowed to function as long as the critical beach width and dune height are maintained. The dunes also play a significant role in maintaining a freshwater lens and in helping to reduce salt water intrusion (van den Acker, 2007).

An extensive programme of beach nourishment and dune building has also taken place in New Jersey. The state had developed a reputation for excessive use of hard structures but a disastrous storm in 1962 has led to the gradual implementation of a policy designed to work more closely with Nature (Nordstrom *et al.*, 1999, 2002). An important element of the management scheme is the use of dredged material where necessary to produce a wide beach and to supply sand for dune development on the backshore. Dunes may be allowed to develop naturally, but in many areas they are encouraged by use of sand fences and planting of vegetation (Figure 9.35a). The width of the dune field may also be constrained in order to provide a wide beach for recreational purposes and to permit the establishment of facilities such as boardwalks and access routes on the landward boundary (Figure 9.35b). In these instances the dunes may not function adequately as natural systems and do not develop the same species richness as do natural dunes (Nordstrom *et al.*, 2002). However, where the dunes are much wider, their functioning more closely resembles that of the original natural system.

References

Aagaard, T., Davidson-Arnott, R., Greenwood B. and Nielsen, J. 2004. Sediment supply from shoreface to dunes: linking sediment transport measurements and long term morphological evolution. *Geomorphology*, **60**, 205–224.

Aagaard, T., Orford, J. and Murray, A.S. 2007. Environmental controls on coastal dune formation; Skallingen Spit, Denmark. *Geomorphology*, **83**, 29–47.

Anderson, R.S. and Haff, P.K. 1988. Simulation of eolian saltation. *Science*, **241**, 820–823.

Anderson, J.L. and Walker, I.J. 2006. Airflow and sand transport variations within a backshore-parabolic dune plain complex: NE Graham Island, British Columbia, Canada. *Geomorphology*, **77**, 17–34.

Anthony, E.J., Vanhee, S. and Ruz, M., 2006. Short-term beach-dune sand budgets on the North Sea coast of France: Sand supply from shoreface to dunes, and the role of wind and fetch. *Geomorphology*, **81**, 316–329.

Anthony, E.J., Vanhée, S. and Ruz, M-H. 2007. An assessment of the impact of experimental brushwood fences on foredune sand accumulation based on digital elevation models. *Ecological Engineering*, **31**, 41–46.

Arbogast, A.F. and Loope, W.L. 1999. Maximum-limiting ages of Lake-Michigan coastal dunes: their correlation with Holocene lake level history. *Journal of Great Lakes Research*, **29**, 72–382.

Arens, S.M., Baas, A.C.W., van Boxel, J.H. and Kalkman, C. 2001. Influence of reed stem density on foredune development. *Earth Surface Processes and Landforms*, **26**, 1161–1176.

Arens, S.M., van Kaam, P. and van Boxel, I.H. 1995. Airflow over foredunes and implications for sand

transport. *Earth Surface Processes and Landforms*, **20**, 315–325.

Atherton, R.J., Baird, A.J. and Wiggs, G.F.S. 2001. Inter-tidal dynamics of surface moisture content on a meso-tidal beach. *Journal of Coastal Research*, **17**, 482–489.

Bagnold, R.A. 1941. *The Physics of Blown Sand and Desert Dunes*. London: Marrow.

Bauer, B.O. and Sherman, D.J. 1999. Coastal dune dynamics: Problems and prospects. In A.S. Goudie, I. Livingstone and S. Stokes (editors) *Aeolian Environments, Sediments and Landforms*. John Wiley and Sons, Chichester, 71–104.

Bauer, B.O. and Davidson-Arnott, R.G.D. 2002. A general framework for modelling sediment supply to coastal dunes including wind angle, beach geometry and fetch effects. *Geomorphology*, **49**, 89–108.

Bauer, B.O., Sherman, D.I. and Wolcott, I.F. 1992. Sources of uncertainty in shear stress and roughness length estimates derived from velocity profiles. *Professional Geographer*, **44**, 453–464.

Bauer, B.O., Davidson-Arnott, R.G.D., Sherman, D.J., Nordstrom, K.F., Ollerhead, J. and Jackson, N.L., 1996. Indeterminacy in eolian sediment transport across beaches. *Journal of Coastal Research*,**12**, 641–653.

Bauer B.O., Davidson-Arnott R.G.D., Hesp P.A., Namikas S.L., Ollerhead J. and Walker I.J. 2009. Aeolian sediment transport conditions on a beach: Surface moisture, wind fetch, and mean transport rate. *Geomorphology*, **105**, 106–116.

Belly, P.-Y. 1964. *Sand movement by wind*. US Army Corps of Engineers CERC, Technical Memorandum1, 38 pp.

Bretel, P., Levoy, F., Rousset, H. and Larsonneur, C. 1999. Critical approach of eolian deposits quantification. *Coastal Sediments '99*, ASCE, 1207–1219.

Bruun, P. 1962. Sea-level rise as a cause of shore erosion. *Journal of Waterways Harbors Division, American Society of Civil Engineers*, **88**, 117–130.

Christiansen, M. and Davidson-Arnott, R.G.D., 2004. The effects of dune ramps on sediment supply to coastal foredunes, Skallingen Denmark. *Geografisk Tidsskrift (Danish Journal of Geography)*, **104**, 29–41.

Clemmensen, L.B., Pye, K., Murray, A. and Heinemeier, J. 2001. Sedimentology, stratigraphy and landscape evolution of a Holocene coastal dune system, Lodbjerg, NW Jutland, Denmark. *Sedimentology*, **48**, 3–27.

Clemmensen, L.B., Bjørnsen, M.,Murray, A. and Pedersen, K. 2007. Formation of aeolian dunes on Anholt, Denmark since AD 1560: A record of deforestation and increased storminess. *Sedimentary Geology*, **199**, 171–187.

Cloutier, M. and Héquette, A. 1998. Aeolian and overwash sediment transport across a low barrier spit, southeastern Canadian Beaufort Sea. *Zeitschrift fur Geomorphologie*, **42**, 349–365.

Cooper, W.S. 1958, Coastal sand dunes of Oregon and Washington. *Geological Society of America Memoir* **72**, 169 pp.

Cowles, H.C. (1899). The *Ecological Relations of the Vegetation of the Sand Dunes of Lake Michigan*. University of Chicago Press, Chicago 119 pp.

Cornelis, W.M. and Gabriels, D. 2003, The effect of surface moisture on the entrainment of dune sand by wind: An evaluation of selected models. *Sedimentology*, **50**, 771–790.

Cornelis, W.M., Gabriels, D. and Hartmann R. 2004. A parameterisation for the threshold shear velocity to initiate deflation of dry and wet sediment. *Geomorphology*, **59**, 43–51.

Darke, I and McKenna Neuman, C. 2008. Field study of beach water content as a guide to wind erosion potential. *Journal of Coastal Research*, **24**, 1200–1208.

Darke, I., Davidson-Arnott, R.G.D. and Ollerhead, J.2009. Measurement of beach surface moisture using surface brightness. *Journal of Coastal Research*, **21**, 248–256.

Davidson-Arnott, R.G.D. 2005. A conceptual model of the effects of sea-level rise on sandy coasts. *Journal of Coastal Research*, **21**, 1166–1172.

Davidson-Arnott, R.G.D. and Pyskir, N.M., 1988. Morphology and formation of an Holocene coastal dune field, Bruce Peninsula, Ontario. *Géographie Physique et Quaternaire*, **42**, 163–170.

Davidson-Arnott, R.G.D. and Law, M.N. 1990. Seasonal patterns and controls on sediment supply to coastal foredunes, Long Point, Lake Erie. In Nordstrom, K.F., Psuty, N.P. and Carter R.W.G. (editors), *Coastal Dunes: Form and Process*, Wiley a, pp. 177–220.

Davidson-Arnott, R.G.D. and Law, M.N. 1996. Measurement and prediction of long-term sediment supply to coastal foredunes. *Journal of Coastal Research*, **12**, 654–663.

Davidson-Arnott, R.G.D. and Dawson, J.D. 2001, Moisture and fetch effects on rates of aeolian sediment transport, Skallingen, Denmark. *Proceedings of the Canadian Coastal Conference*, CCSEA, pp. 309–321.

Davidson-Arnott, R.G.D. and Bauer, B.O. 2009. Aeolian sediment transport on a beach: Thresholds, intermittency and high frequency variability. *Geomorphology*, **105**, 117–126.

Davidson-Arnott, R. G. D., White, D. C. and Ollerhead, J. 1997. The effect of pebble lag concentration on aeolian sediment transport on a beach. *Canadian Journal of Earth Sciences*, **34**, 1499–1508.

Davidson-Arnott, R. G. D., MacQuarrie, K. and Aagaard, T. 2005. The effect of wind gusts, moisture content and fetch length on sand transport on a beach. *Geomorphology*, **68**, 115–129.

Davidson-Arnott, R. G. D., Yang, Y, Ollerhead, J., Hesp, P. A. and Walker, I. J. 2008. The effects of surface moisture on aeolian sediment transport threshold and mass flux on a beach. *Earth Surface Processes and Landforms*, **33**, 55–74.

Dean, R. G. and Maurmeyer, E. M. 1983. Models of beach profile response. In Komar, P. D. (ed.), *Handbook of Coastal Processes and Erosion*.CRC Press, Boca Raton, FL, pp. 151–165.

Dech, J. P. and Maun, M. A. 2007. Zonation of vegetation along a burial gradient on lee slopes of Lake Huron sand dunes. *Canadian Journal of Botany*, **83**, 227–236.

de Langre, E. 2008. Effects of wind on plants. *Annual Review of Fluid Mechanics*, **40**, 141–168.

Doing, H. 1985. Coastal fore-dune zonation and succession in various parts of the world. *Vegetatio*, **61**, 65–75.

Dong, Z., Wang, H., Liu, X., Li, F. and Zhao, A. 2004a. Experimental investigation of the velocity of a sand cloud blowing over a sandy surface. *Earth Surface Processes and Landforms*, **29**, 343–358.

Dong, Z., Wang, H., Liu, X. and Wang, X. 2004b. The blown sand flux over a sandy surface: A wind tunnel investigation on the fetch effect. *Geomorphology*, **57**, 117–127.

Ferreira, O., Garcia, T., Matias, A., Tabordac, R. and Dias, J. A. 2005. An integrated method for the determination of set-back for coastal erosion hazards on sandy shores. *Continental Shelf Research*, **26**, 1030–1044.

Finnegan, J. 2000. Turbulence in plant canopies. *Annual Review of Fluid Mechanics*, **32**, 519–571.

Fryberger, S. G. and Dean, G. 1979. *Dune forms and wind regime*. In McKee, E. D. (ed.) Global Sand Seas, US Geological Survey, Professional Paper 1052, pp. 137–169.

Gares, P. A. and Nordstrom, K. F. 1995. A cyclic model of foredune blowout evolution for a leeward coast: Island Beach, NJ. *Annals of the Association of American Geographers*, **85**, 1–20.

Gares, P. A., Davidson-Arnott, R. G. D., Bauer, B. O., Sherman, D. J., Carter, R. W. G., Jackson, D. W. T. *et al.* 1996. Alongshore variations in aeolian sediment transport, Carrick Finn Strand, Ireland. *Journal of Coastal Research*, **12**, 673–682.

Giannini, P. C. F., Sawakuchi, A. O., Martinho, C. T. and Tatumi, S. H. 2007. Eolian depositional episodes controlled by late Quaternary relative sea level changes on the Imbituba–Laguna coast (southern Brazil). *Marine Geology*, **237**, 143–168.

Gillette, D. A., Herbert, G., Stockton, P. H. and Owen, P. R. 1996. Causes of the fetch effect in wind erosion. *Earth Surface Processes and Landforms*, **21**, 641–659.

Grandtner, M. M. 1993. Dry coastal ecosystems of Eastern Canada. In Van der Maarel, E. (ed.) *Ecosystems of the World. Dry Coastal Ecosystems*, Vol. 2B. Elsevier, Amsterdam, pp. 289–297.

Hansen, E., De Vries-Zimmerman, S., van Dijk, D and Yurk, B. 2009. Patterns of wind flow and aeolian deposition on a parabolic dune on the southeastern shore of Lake Michigan. *Geomorphology*,**105**, 147–157.

Hanson, H., Brampton, B., Capobianco, M. and five others. 2002. Beach nourishment projects, practices, and objectives–a European overview. *Coastal Engineering*, **47**, 81–111.

Heathershaw, A. D. and Thorne, P. D. 1985. Sea-bed noises reveal role of turbulent bursting phenomenon in sediment transport by tidal currents. *Nature*, **316**, 339–342.

Hesp, P. A. 1981, The formation of shadow dunes. *Journal of Sedimentary Petrology*, **51** 101–112.

Hesp, P. A. 1983. Morphodynamics of incipient foredunes New South Wales, Australia. In Brookfield, M. E.and Ahlbrandt, T. S. (editors) *Eolian Sediments and Processes*. Amsterdam, Elsevier, pp. 325–342.

Hesp, P. A. 1989. A review of the biological and geomorphological processes involved in the initiation and development of incipient foredunes. *Proceedings of the Royal Society of Edinburgh*, **96B**, 181–201.

Hesp, P. A. 1991. Ecological processes and plant adaptations on coastal dunes. *Journal of Arid Environments*, **21**, 165–191.

Hesp, P. A. 2004. Coastal dunes in the tropics and temperate regions: location, formation, morphology and vegetation processes. In Martínez, M. L. and Psuty, N. P. (eds.) *Coastal Dunes: Ecology and Conservation*. Ecological Studies, Vol. 171.Springer-, Berlin, pp. 29–49.

Hesp, P. A. 2002. Foredunes and blowouts: initiation, geomorphology and dynamics. *Geomorphology*, **48**, 245–268.

Hesp, P. A. and Thom, B. G. 1990. Geomorphology and evolution of active transgressive dunefields. In

Coastal Dunes: Form and Process, ed. K. F. Nordstrom, N. P. Psuty and R. W. G. Carter Wiley, pp. 253–288.

Hesp, P. A. and Hyde, R. 1996. Geomorphology and dynamics of a trough blowout. *Sedimentology*, **43**, 505–525.

Hesp, P. A. and Pringle, A. 2000. Wind flow and topographic steering within a trough blowout. *Journal of Coastal Research, Special Issue* **34**, 597–601.

Hesp, P. A. and Martínez, M. L. 2007. Disturbance processes and dynamics in coastal dunes. In Johnson, E. A. and Miyanishi, K. (eds.), *Plant Disturbance Ecology*. Academic, San Diego, pp. 215–247.

Hesp, P. A., Davidson-Arnott, R. G. D., Walker, I. J. and Ollerhead, J. 2005. Flow dynamics over a foredune at Prince Edward Island, Canada. *Geomorphology*, **65**, 71–84.

Hesp, P. A., Dillenburg, S. R., Barboza, E. G., Clerot, L. C. P., Tomazelli, L. J. and Norberto Ayup Zouain, R. 2007a. Morphology of the Itapeva to Tramandai transgressive dunefield barrier system and mid- to late-Holocene sea level change. *Earth Surface Processes and Landforms*, **32**, 407–414.

Hesp, P., Abreu de Castilhos, J., Miot da Silva, G., Dillenburg, S., Martinho, C. T., Aguiar, D. *et al.* 2007b. Regional wind fields and dunefield migration, *southern brazil. Earth Surface Processes and Landforms*, **32**, 561–573.

Horikawa, K., Holta, S. and Kraus, N. C. 1986, Literature review of sand transport by wind on a dry sand surface. *Coastal Engineering*, **9**, 503–526.

Hugenholtz, C. H. and Wolfe, S. A. 2005. Biogeomorphic model of dunefield activation and stabilization on the northern Great Plains. *Geomorphology*, **70**, 53–70.

Illenberger, W. K. and Rust, I. C. 1988. A sand budget for the Alexandria coastal dune field, South Africa. *Sedimentology*, **35**, 513–522.

Iversen, J. D. and Rasmussen, K. R. 1994. The effect of surface slope on saltation threshold. *Sedimentology*, **41**, 721–728.

Jackson, N. L. and Nordstrom, K. L. 1997. Effects of time-dependent moisture content of surface sediments on aeolian transport rates across a beach, Wildwood, New Jersey, USA. *Earth Surface Processes and Landforms*, **22**, 611–621.

Jackson, N. L. and Nordstrom, K. L. 1998, Aeolian transport of sediment on a beach during and after rainfall, *Wildwood, NJ, USA.Geomorphology*, **22**, 151–157.

Johnston, P. 2004. *Wind Flow and Sediment Transport on a Vegetated Foredune*. M.Sc. Thesis, University of Guelph, 114 pp.

Kadib, A. L. 1964. Calculation procedure for sand transport by wind on natural beaches. *US Army Corps of Engineers*, CERC Miscellaneous paper 2–64.

Kang, L., Guo, L., Gu, Z. and Liu, D. 2008. Wind tunnel experimental investigation of sand velocity in aeolian sand transport. *Geomorphology*, **97**, 438–450.

Kaplan, J. O. and New, M. 2006. Arctic climate change with a 2°C global warming: Timing, climate patterns and vegetation change. *Climatic Change*, **79**, 213–241.

Kawamura, R. 1951. Study of sand movement by wind. University of Tokyo, Report of the Institute or Technology 5, #314.

Kriebel, D. L. and Dean, R. G., 1985, Numerical simulation of time-dependent beach and dune erosion. *Coastal Engineering*, **9**, 221–245.

Kroon, A. and Hoekstra, P. 1990. Eolian sediment transport on a natural beach. *Journal of Coastal Research*, **6**, 367–380.

Kuriyama, Y., Mochizuki, N. and Nakashima, T. 2005. Influence of vegetation on aeolian sand transport rate from a backshore to a foredune at Hasaki, Japan. *Sedimentology*, **52**, 1123–1132.

Lancaster, N. and Baas A. 1998. Influence of vegetation cover on sand transport by wind: Field studies at Owens Lake, California. *Earth Surface Processes and Landforms*, **23**, 69–82.

Lane, C., Wright, S. J., Roncal, J. and Mashinski, J. 2008. Characterizing environmental gradients and their influence on vegetation zonation in a sub-tropical coastal sand dune system. *Journal of Coastal Research*, **24**, 213–224.

Law, M. N. and Davidson-Arnott, R. G. D. 1990. Seasonal controls on aeolian processes on the beach and foredune. In Davidson-Arnott, R. G. D. (ed.), *Proceedings of the Symposium on Coastal Sand Dunes*. National Research Council of Canada, pp. 49–68.

Leenders, J. K., van Boxel, J. H. and Sterk, G. 2007. The effect of single vegetation elements on wind speed and sediment transport in the Sahelian zone of Burkina Faso. *Earth Surface Processes and Landforms*, **32**, 1454–1474.

Lees, B. 2006. Timing and formation of coastal dunes in northern and eastern Australia. *Journal of Coastal Research*, **22**, 78–89.

Lettau, K. and Lettau, H. 1977. Experimental and micrometeorological field studies of dune migration. In Lettau, K. and Lettau, H. (eds.), *Exploring the World's Driest Climate IES Report 101*, University of Wisconsin Press, Madison, pp. 110–147.

Logie, M. 1982. Influence of roughness elements and soil moisture on the resistance of sand to wind erosion. In

Yaalon, D. H. (ed.), *Aridic Soils and Geomorphic Processes*. Catena Supplement 1, Braunschweig, 161–173.

Loope, W. L. and Arbogast, A. F. 2000. Dominance of an ~150-year cycle of sand supply in late Holocene dune-building along the eastern shore of Lake Michigan. *Quaternary Research*, **54**, 414–422.

Lynch K, Jackson D. W. T. and Cooper A. 2006. A remote-sensing technique for the identification of aeolian fetch distance. *Sedimentology*, **53**, 1381–1390.

Lynch K, Jackson D. W. T. and Cooper A. 2008. Aeolian fetch distance and secondary airflow effects: the influence of micro-scale variables on meso-scale foredune development. *Earth Surface Processes and Landforms*, **33**, 991–1005.

Martinho, C. T., Dillenburg, S. R. and Hesp, P. A. 2008. Mid to late Holocene evolution of transgressive dunefields from Rio Grande do Sul coast, southern Brazil. *Marine Geology*, **256**, 49–64.

Martini, I. P. 1981, Coastal dunes of Ontario: Distribution and geomorphology. *Géographie Physique et Quaternaire*, **35**, 219–229.

Maun, M. A. 2004. Burial of plants as a selective force in sand dunes. In In Martínez, M. L. and Psuty, N. P. (eds.) *Coastal Dunes: Ecology and Conservation. Ecological Studies Vol. 171*. Springer, Berlin, pp. 119–135.

Maun, M. A. and Lapierre, J. 1984. The effects of burial by sand on Ammophila breviligulata. *The Journal of Ecology*, **72**, 827–839.

Maun, M. A. and Baye, P. R., 1989. The ecology of Ammophila breviligulata Fern. on coastal dune systems. *Critical Reviews in Aquatic Sciences*, **1**, 661–681.

McKenna Neuman, C. and Nickling, W. G. 1989. A theoretical and wind tunnel investigation of the effects of capillary water on the entrainment of sediment by wind. *Canadian Journal of Soil Science*, **69**, 79–96.

McKenna Neuman C. and Langston G. 2006. Measurement of water content as a control of particle entrainment by wind. *Earth Surface Processes and Landforms*, **31**, 303–317.

McKenna Neuman, C. and Muljaars Scott, M. 1998. A wind tunnel study of the influence of pore water on aeolian sediment transport. *Journal of Arid Environments*, **39**, 403–419.

McKenna Neuman, C., Lancaster, N. and Nickling, W. G. 1997. Relations between dune morphology, air flow, and sediment flux on reversing dunes, Silver Peak, Nevada. *Sedimentology*, **44**, 1103–1113.

Meur-Férec, C. and Ruz, M.-H. 2002. Transports éoliens réels et théoreiques en haut de plage et sommet de dune (Wisant, pas de Calais, France. *Géomorphologie: Relief, Processus, Environnement*,**4**, 321–334.

Miot da Silva, G., Hesp, P. A., Peixoto, J. and Dillenbeurg, S. R. 2008. Foredune vegetation patterns and alongshore environmental gradients: Moçambique Beach, Santa Caterina Island, Brazil. *Earth Surface Processes and Landforms*, DOI: 10.1002/esp1633.

Miyanishi, K. and Johnson E. A. 2007. Coastal dune succession and the reality of dune processes. In *Plant Disturbance Ecology* ed. E. A. Johnson and K. Miyanishi. Academic, San Diego, pp. 215–247.

Moreno-Casasola, P. 1986. Sand movement as a factor in the distribution of plant communities in a coastal dune system. *Vegetatio*, **65**, 67–76.

Namikas, S. L. 2003. Field measurement and numerical modelling of aeolian mass flux distribution on a sandy beach. *Sedimentology*, **50**, 303–326.

Namikas, S. L. and Sherman, D. J. 1995. A review of the effects of surface moisture content on aeolian sand transport. In: Tchakerian, V. P. (editor.), *Desert Aeolian Process*, Chapman and Hall, London, pp. 269–293.

Namikas, S. L., Bauer, B. O. and Sherman D. J. 2003. Influence of averaging interval on shear velocity estimates for aeolian transport modeling. *Geomorphology*, **53**, 235–246.

Nicholls, R. J., Wong, P. P., Burkett, V. R., Codignotto, J. O., Hay, J. E., McLean, R. F., Ragoonaden, S. and Woodroffe, C. D. (2007). Coastal systems and low-lying areas. *Climate Change 2007: Impacts, Adaptation and Vulnerability. Contribution of Working Group II to the Fourth Assessment Report of the Intergovernmental Panel on Climate Change*, ed. M. L. Parry, O. F. Canziani, J. P. Palutikof, P. J. *van der Linden* and C. E. Hanson, Cambridge University Press, Cambridge, pp. 315–356.

Nickling, W. G. 1988. The initiation of particle movement by wind. *Sedimentology*, **35**, 499–511.

Nickling, W. G. and Davidson-Arnott, R. G. D. 1990. Aeolian sediment transport on beaches and coastal sand dunes. In Davidson-Arnott, R. G. D. (ed.), *Proceedings of the Symposium on Coastal Sand Dunes*. National Research Council of Canada, pp. 1–35.

Nickling, W. G. and McKenna Neuman, C. 1995. Development of deflation lag surfaces. *Sedimentology*, **42**, 403–414.

Nickling, W. G. and McKenna Neuman, C. 1999. Recent investigations of air flow and sediment transport over desert dunes. In Goudie, A. S. and Livingstone, I. and

Stokes, S. (editors), *Aeolian Environments: Sediments and Landforms*. Wiley, Chichester, pp. 15–47.

Nordstrom, K. F. 2000. *Beaches and Dunes of Developed Coasts*. Cambridge University Press, Cambridge, 338 pp.

Nordstrom, K. F. and Jackson, N. L. 1992. Effect of source width and tidal elevation changes on aeolian transport on an estuarine beach. *Sedimentology*, **39**, 769–778.

Nordstrom, K. F. and Jackson, N. L. 1993. The role of wind direction in eolian transport on a narrow sand beach. *Earth Surface Processes and Landforms*, **18**, 675–685.

Nordstrom, K. F. and Jackson, N. L. 1994. Aeolian processes and dune fields in estuaries. *Physical Geography*, **15**, 358–371.

Nordstrom, K. F., Lampe, R. and Vandermark, L. M. 1999. Reestablishing naturally functioning dunes on developed coasts. *Environmental Management*, **25**, 37–51.

Nordstrom, K. F., Jackson, N. L., Bruno, M. S. and Butts, H. A. 2002. Municipal initiatives for managing dunes in coastal residential areas: a case study of Avalon, New Jersey, USA. *Geomorphology*, **47**, 137–152.

Nordstrom, K. F., Jackson, N. L., Hartman, J. M. and Wong, M. 2007. Aeolian sediment transport on a human-altered foredune. *Earth Surface Processes and Landforms*, **32**, 102–115.

Oblinger, A. and Anthony, E. 2008. Surface moisture variations on a multibarred macrotidal beach: Implications foe aeolian sand transport. *Journal of Coastal Research*, **24**, 1194–1199.

Olivier, M. J. and Garland, G. G. 2003. Short-term monitoring of foredune formation on the east coast of South Africa. *Earth Surface Processes and Landforms*, **28**, 1143–1155.

Olson, J. S. 1958a, Lake Michigan dune development 1. Wind velocity profiles. *Journal of Geology*, **66**, 254–263.

Olson, J. S. 1958b, Lake Michigan dune development 2. Plants as agents and tools in geomorphology. *Journal of Geology*, **66**, 345–351.

Olson, J. S. 1958c, Lake Michigan dune development 3. Lake level, beach and dune oscillations. *Journal of Geology*, **66**, 473–483.

Owen, P. R., 1964. Saltation of uniform grains in air. *Journal of Fluid Mechanics*, **20**, 225–242.

Packham, J. R. and Willis, A. J., 1997. Ecology of Dunes, *Salt Marsh and Shingle*.Chapman and Hall, London, 334 pp.

Pearce, K. I. and Walker, I. J. 2005. Frequency and magnitude biases in the Fryberger model, with implications for characterizing geomorphically effective winds. *Geomorphology*, **68**, 39–55.

Psuty, N. P. 1988, Sediment budget and dune/beach interaction. *Journal of Coastal Research, Special Issue*, **3**, 1–4.

Psuty, N. P. 2004. The coastal foredune: a morphological basis for regional coastal dune development. In Martínez, M. L. and Psuty, N. P. (editors) *Coastal Dunes: Ecology and Conservation. Ecological Studies Vol. 171*. Springer, Berlin, pp. 11–28.

Pye, K. 1983. Coastal dunes. *Progress in Physical Geography*, **7**, 531–597.

Ranwell, D. S., 1972. *Ecology of Salt Marshes and Sand Dunes*. Chapman and Hall, London, 258 pp.

Rasmussen, K. R. 1989. Some aspects of flow over coastal dunes. *Proceedings of the Royal Society of Edinburgh*, **96B**, 129–147.

Reed, D. J., Davidson-Arnott, R. G. D. and Perillo, G. M. E. 2009. Estuaries, Coastal Marshes, Tidal Flats and Coastal Dunes. Chapter 5 in Slaymaker, O. (ed.), *Landscape Changes in the 21st Century*. Cambridge University Press, Cambridge, pp. 130–167.

Ruz, M.-H. 1993. Coastal dune development in a thermokarst environment: some implications for environmental reconstruction, Tuktoyaktuk Peninsula. *Permafrost and Periglacial Processes*, **4**, 255–264.

Ruz, M.-H. and Allard, H. 1994. Foredune development along a subarctic emerging coastline, eastern Hudson Bay, Canada. *Marine Geology*, **117**, 57–74.

Sarre, R. D. 1987. Aeolian sand transport. *Progress in Physical Geography*, **11** 157–182.

Sarre, R. D. 1989. Aeolian sand drift from the intertidal zone on a temperate beach: Potential and actual rates. *Earth Surface Processes and Landforms*, **14**, 247–258.

Saunders, K. E. and Davidson-Arnott, R. G. D. 1990. Coastal dune response to natural disturbances. In Davidson-Arnott, R. G. D. (ed.), *Proceedings of the Symposium on Coastal Sand Dunes*. National Research Council of Canada, pp. 321–346.

Shao, Y. and Raupach, M. R. 1992. The overshoot and equilibrium of saltation. *Journal of Geophysical Research*, **97**, 559–564.

Sherman, D. J. and Lyons, W. 1994, Beach state controls on aeolian sand delivery to coastal dunes. *Physical Geography*, **15**, 381–395.

Sherman, D. J., Namikas, S. L., Jackson, D. W. T. and Wang, S. L. 1998. Wind blown sand on beaches: An evaluation of models. *Geomorphology*, **22**,113–133.

Shimada, K., Kamoshida, T., Itoh, M., Nishino, S., Carmack, E., McLaughlin, F., Zimmermann, S. and Proshutinsky, A.2006. Pacific Ocean inflow:

influence on catastrophic reduction of sea ice cover in the Arctic Ocean, *Geophysical Research Letters*, **33**, L08605

Short, A. D. and Hesp, P. A. 1982, Wave, beach and dune interactions in southeastern Australia. *Marine Geology*, **48**, 259–284.

Saqqa, W. A. and Saqqa, A. W. 2007. A computer program (WDTSRP) designed for computation of sand drift potential (DP) and plotting sand roses. *Earth Surface Processes and Landforms*, **32**, 832–840.

Sterk, G., Jacobs, A. F. G. and van Boxel, J. H. 1998. The effect of turbulent flow structures on saltation sand transport in the atmospheric boundary layer. *Earth Surface Processes and Landforms*, **28**, 877–887.

Stoffers, A. L. 1993. Dry coastal ecosystems of the West Indies. In Van der Maarel, E. (ed.) *Ecosystems of the World. Dry Coastal Ecosystems*, Vol. 2B. Elsevier, Amsterdam, pp. 407–421.

Stout, J. E. and Zobeck, T. M. 1997. Intermittent saltation. *Sedimentology*, **44**, 959–970.

Sullivan, J. and Davidson-Arnott, R. G. D. 1995. Hazards and regulatory standards: Great Lakes–St Lawrence River System shorelines. *Proceedings Canadian Coastal Conference*, **CCSEA**, 799–814.

Svasek, J. N. and Terwindt, J. H. J. 1974. Measurement of sand transport by wind on a natural beach. *Sedimentology*, **21**, 311–322.

Tripaldi, A. and Forman, S. L. 2007. Geomorphology and chronology of Late Quaternary dune fields of western Argentina. *Palaeogeography, Palaeoclimatology, Palaeoecology*, **251**, 300–320.

van Boxel, J. H., Arens, S. M. and van Dijk, P. N. 1999. Aeolian processes across transverse dunes. 1: Modelling the air flow. *Earth Surface Processes and Landforms*, **24**, 255–270.

van Boxel, J. H., Sterk, G. and Arens, S. M. 2004, Sonic anemometers in aeolian transport research. *Geomorphology*, **59**, 131–147.

van den Akker, C. 2007. On the spreading mechanism of shallow groundwater in the hinterland of the Dutch dune hill area. *Engineering Geology*, **91**, 72–77.

van der Meulen, F. and Salman, H. P. M. 1996. Management of Mediterranean coastal dunes. *Ocean and Coastal Management*, **30**, 177–195.

van der Wal, D. 1998. Effects of fetch and surface texture on aeolian sand transport on two nourished beaches. *Journal of Arid Environments*, **39**, 533–547.

van Dijk, P. M., Arens, S. M. and van Boxel, J. H. 1999. Aeolian processes across transverse dunes: Modelling the sediment transport and profile development. *Earth Surface Processes and Landforms*, **24**, 319–333.

van Koningsveld. M. and Mulder, J. P. M. 2004. Sustainable coastal policy developments in The Netherlands. A systematic approach revealed. *Journal of Coastal Research*, **20**, 375–385.

Vespremeanu-Stroe, A. and Preoteasa, L. 2007. Beach–dune interactions on the dry-temperate Danube Delta coast. *Geomorphology*, **86**, 267–282.

Wal, A. and McManus, J. 1993. Wind regime and sand transport on a coastal beach-dune complex, Tentsmuir, eastern Scotland. In K. Pye (ed.), *The Dynamics and Environmental Context of Aeolian Sedimentary Systems* (pp. 159–172). Geological Society Special Publication 72, London, pp. 159–172.

Walker, I. J. 1999. Secondary airflow and sediment transport in the lee of reversing dues. *Earth Surface Processes and Landforms*, **24**, 437–448.

Walker, I. J. 2005. Physical and logistical considerations of using ultrasonic anemometers in aeolian sediment transport research. *Geomorphology*, **68**, 57–76.

Walker, I. J., Hesp. P. A., Davidson-Arnott, R. G. D. and Ollerhead, J. 2006. Topographic steering of alongshore airflow over a vegetated foredune: Greenwich Dunes, Prince Edward Island, Canada. *Journal of Coastal Research*, **22**, 1278–1291.

Walker, I. J., Hesp. P. A., Davidson-Arnott, R. G. D. Bauer, B. O. and Ollerhead, J. 2009. Response of three-dimensional flow to variations in the angle of incident flow and profile form of dunes: Greenwich Dunes, Prince Edward Island, Canada. *Geomorphology*, **105**, 127–138.

Wang, D., Wang, Y., Yang, B. and Zhang, W. 2008. Statistical analysis of sand grain/bed collision process recorded by high-speed digital camera. *Sedimentology*, **55**, 461–470.

Wiggs, G. f. S., Atherton, R. J. and Baird, A. J. 2004a. Thresholds of aeolian sand transport: Establishing suitable values. *Sedimentology*, **51**, 95–108.

Wiggs, G. F. S., Baird, A. J. and Atherton, R. J. 2004b. The dynamic effect of moisture on the entrainment and transport of sand by wind. *Geomorphology*,**59**, 15–30.

Wolfe, S. A. and Nickling, W. G. 1993. The protective role of sparse vegetation in wind erosion. *Progress in Physicl Geography*, **17**, 50–68.

Yang, Y. and Davidson-Arnott, R. G. D. 2005. Rapid measurement of surface moisture content on a beach. *Journal of Coastal Research*, **21**, 447–452.

Zingg, A. W. 1953. Wind tunnel studies of the movement of sedimentary material. *Proceedings of the 5th Hydraulic Conference*, Bulletin 34, Institute of Hydraulics, pp. 111–135.

10

Barrier systems

10.1 Synopsis

The term barrier is used to describe a range of emergent depositional landforms which are separated from the mainland coast by a lagoon, bay or marsh. The barrier may be composed entirely of cobbles or gravels or, more commonly, they are dominantly composed of sands with minor amounts of gravel, silt and clay. They may be associated with coasts with a strong longshore sediment transport component and often form the sink or downdrift end of a littoral cell or coastal compartment. The lagoon or bay, intertidal flats and marshes that are protected by the barrier are usually highly productive ecologically with marshes and sea grass beds providing the base for a food web that includes a wide range of shellfish, crustaceans and invertebrates, nurseries for fish and habitats for a wide range of birds and mammals.

The barrier itself forms the emergent depositional component of a larger barrier system that includes the nearshore and beach, back barrier sediments and the protected lagoon, bay or marsh landward of it. Barriers have a subaqueous platform or base on which they are built and an overlying subaerial component. The platform is built alongshore and offshore by littoral processes and by sediments washed over the barrier by storm waves. The subaerial component of the barrier consists of the beach and backshore, dunes (in sandy systems) and a variety of back-barrier sediments that are washed over during storms or transported by wind both from the seaward side and from the lagoon or bay.

Barriers are the most dynamic of depositional coastal landforms and they respond rapidly to changes in littoral sediment supply and sea level, as well as to the dynamic processes associated with severe storms. During storms, high waves and storm surge may lead to breaching of the high point of gravel barriers or the dunes of sandy barriers forming overwash fans on the landward side and occasionally to the formation of an inlet connecting the lagoon or bay to the ocean. Permanent inlets may form a connection between the lagoon, or bay, and the open ocean with tides driving water into and out of the bay through the inlet. Erosion and sedimentation in and around the inlets lead to inlet migration, infilling and sometimes closure.

10.2 Barrier types and morphology

10.2.1 Definition and morphological classification of barriers

Coastal barriers are linear depositional landforms that are separated from the mainland by a bay, lagoon or marsh and therefore act as a barrier between the mainland and processes operating on the open coast. Barriers are composed of sand or gravel, or a mixture of both, and substantial quantities of fine sediments may accumulate in the marshes and lagoon behind the barrier. Barriers can range in size from a few tens of metres in length for small barriers across a stream mouth, to spits that may be tens of kilometres

long and hold many millions of cubic metres of sediment, and to barrier island and spit chains that extend hundreds of kilometres. There are sufficient differences in dynamics to warrant a distinction between sandy barriers and gravel or cobble barriers. Sandy barriers can be built well above the limit of wave action through the transport of sand inland by wind and the development of dune systems. However, gravel and cobble barriers can only be built to the limit of wave action during storms and are always subject to overtopping unless there has been a fall in sea level.

Barriers make up more than 10% of the world's coastline and are particularly well developed on microtidal trailing edge coasts such as the east coast of North America, South America, the east coast of Australia, Southern Africa and Western Europe from Holland to Denmark and parts of the Baltic. Barriers are also formed in large lakes such as the North American Great Lakes, and one of the earliest descriptions of barrier spits was written by G. K. Gilbert (1890) on barriers preserved along the shoreline of Lake Bonneville. Most modern barrier systems are only a few thousand years old as a result of rapid shoreline change during the Holocene transgression. In areas with large volumes of available sediment and coastal progradation such as the east coast of Australia south of the Great Barrier Reef there may be one or more older barriers preserved inland of the modern coast. However, on the east coast of North America many early barriers were drowned and reworked during the transgression.

There have been a number of attempts to produce a classification of barrier types including extensive descriptions in Zenkovitch (1967). A simple one based on barrier geometry and number of free ends is shown in Figure 10.1 (Ollerhead, 1993). The grouping of features at this level is quite useful and it is relatively simple

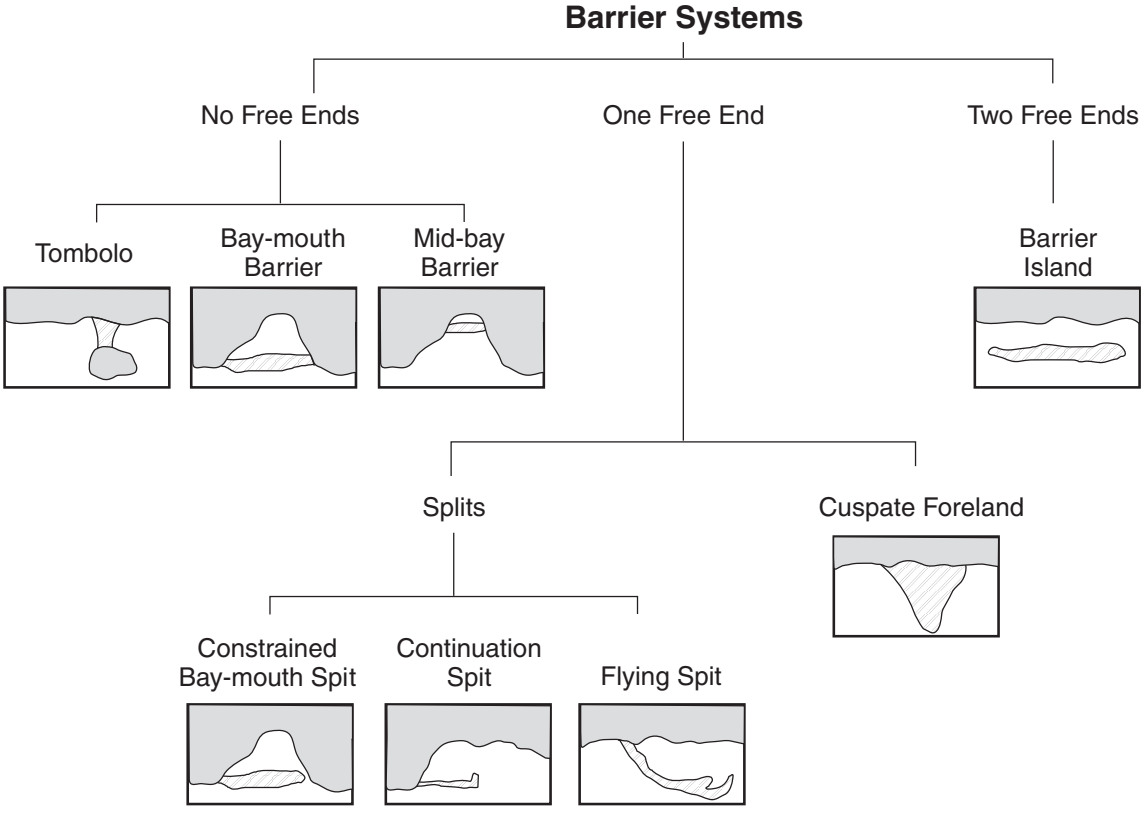

Figure 10.1 Classification of barrier systems based on morphology and geometry (after Ollerhead, 1993).

to assign barriers to one of the classes. In general, there is a tendency for stability of the barrier to increase from barrier islands with two free ends, to spits with one free end, to barriers that are attached at both ends.

No free ends

Barriers with no free ends include tombolos, and a variety of barriers built from one shore to the other across bays and estuaries (Figure 10.1). Natural tombolos are barriers that link islands to each other or to the mainland coast and they generally form because of wave refraction and diffraction around the island and the development of a littoral transport gradient that leads to deposition in the lee of the island or islands (Zenkovitch, 1967; Sanderson and Elliot, 1996; Flinn, 1997; Mariner *et al.*, 2008). Depending on the orientation of the barrier with respect to prevailing winds and waves, one side of the tombolo may be more sheltered than the other but in most cases one is subject to greater wave activity than the other, and this may include breaching and overwash. In many cases beaches on both sides are separated by a pond or marsh (Figure 10.2a), though this may be filled in over time by dune formation. On a much smaller scale, construction of an offshore detached breakwater may lead to the formation first of a beach salient opposite the breakwater, and this in turn may grow towards the breakwater to form a small tombolo (Silvester and Hsu, 1993; Bowman and Pranzini, 2004).

Baymouth and mid-bay barriers form in response to littoral sediment transport at the entrance to a bay or along the sides within the bay (Figures 10.2b, c). In some cases, where there is littoral transport from both sides, the barrier may build from both ends. However, there is often a net littoral transport from one side resulting in the building of a spit across the bay from the updrift end. Where a baymouth barrier forms early, it reduces wave action within the bay and a single barrier is formed. Where the entrance to the bay is comparatively deep, a midbay or baymouth barrier may develop first and subsequently a baymouth barrier forms, or there may never be sufficient sediment to form an outer barrier. If the area enclosed by the barrier is quite large there may be sufficient tidal flow to maintain an open entrance or inlet through the barrier, either permanently or episodically (Figure 10.2b).

One free end

This class includes quite a range of spit forms where there is a pronounced littoral drift from one direction, and cuspate forelands that form where there is a convergence of littoral drift from both directions. Cuspate forelands require that littoral drift from both directions be of the same order of magnitude (otherwise a spit would likely form) and thus they occur most often where there are features of the shoreline shape and orientation or fetch that are conducive to this (Sanderson *et al.*, 2000). They may form on the leeward coast of an island or reef as a result of wave refraction around the island (Figure 10.3a) or as an extension of a point where there is wave convergence (Figure 10.3b). They may also form on straight shorelines where the shore perpendicular fetch is restricted and there is substantial littoral drift from oblique waves from both the right and left. Point Pelee at the western end of Lake Erie is an example of this (Box 7.3 and Figure 7.21c). The large, complex sand and gravel barrier forming the Dungeness Foreland on the south coast of England is of comparable size and has also evolved over the past 5000 years (Long *et al.*, 2006). The resilience of these features can in part be traced to their location at zones of sediment transport convergence though there may be considerable change in form and appearance through reworking of the beach, dune and marsh complexes that make up the barrier (Coakley, 1976; Long *et al.*, 2006).

Spits are much more numerous than cuspate forelands and world-wide may be more significant than barrier islands. They are formed at the downdrift end of a littoral cell system where there is an abrupt change in shoreline orientation, for example where sediment builds across a bay. They also form where there is an obstruction such as a rock reef or a glacial moraine that initiates deposition and deflection of the littoral transport. It is useful to distinguish between continuation spits, where the direction of spit progradation is parallel to the updrift shoreline, and flying spits that leave the coast at an acute angle. Where continuation spits

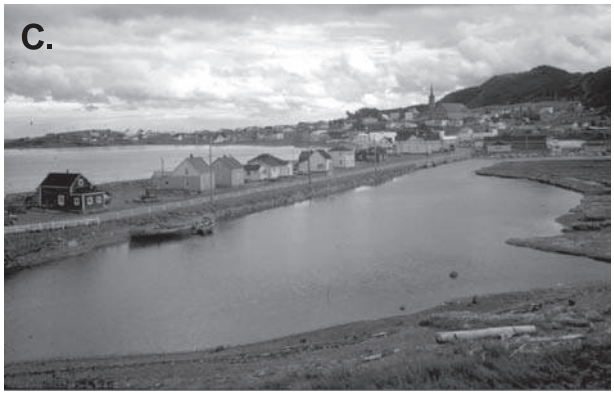

Figure 10.2 Examples of barrier with no free ends: (A) view south over the Friar's Bay tombolo connecting volcanic outcrops, SE Peninsula, St Kitts. The distant cloud covered peak is the volcanic peak on the island of Nevis; (B) baymouth barriers formed in gravel, Cape Breton, Nova Scotia. Note the small channel connecting the open ocean to the bay; (C) mid-bay barrier, Gaspe Peninsula, Quebec, Canada. The barrier provides road access across the bay as well as a small, sheltered harbour for fishing boats. Note the salt marsh in the protected bay to the right.

are built almost across a bay further progradation may be prevented by removal of sediment by strong tidal currents flowing into and out of the remaining opening so that closure to form a baymouth barrier is prevented. These are termed constrained spits (Figure 10.3c).

Spits can range in length from <100 m for small spits in estuaries and bays (Figure 10.3d) to features such as Long Point in Lake Erie which is about 40 km long and up to 5 km wide at the distal (downdrift) end. Wave refraction around the distal end of the spit leads to a pronounced curvature of the shoreline, and consequently of the foredune behind it. Migrating swash bars and sandwaves attach to the downdrift end and extend the spit both downdrift as well as normal to the shoreline. The result is to form a series of curved relic foredunes termed recurves, with

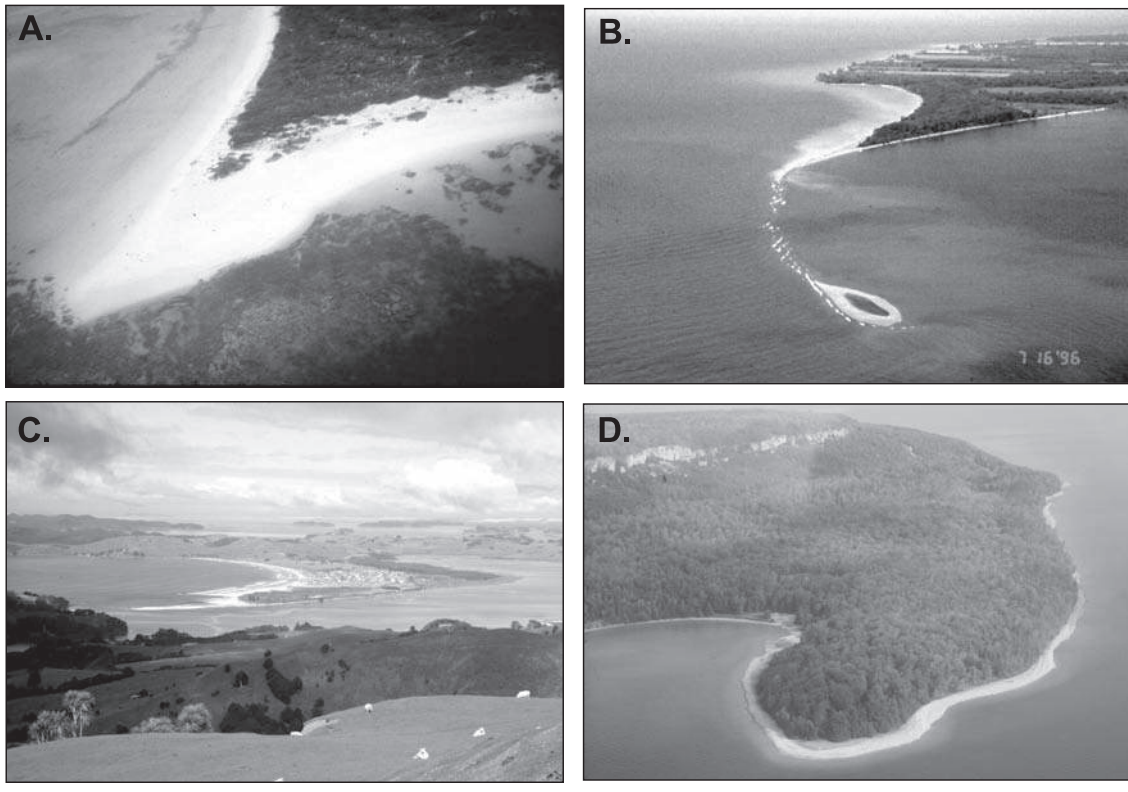

Figure 10.3 Examples of barriers with one free end: (A) oblique aerial view of a cuspate foreland on the south-west shore of Anguilla. Note the carbonate sands building over coral reef; (B) Fish Point, a cuspate foreland, formed primarily in sand and gravel, at the south end of Pelee Island, western Lake Erie; (C) view looking south across the inlet entrance to Omaha spit, on the east coast north of Auckland, New Zealand – an example of a constrained spit; (D) Cape Dundas spit, Georgian Bay, Ontario. This is a continuation spit built primarily in shingle supplied by erosion of sandy dolomite from a lower unit of the Niagara escarpment (see Figure 13.7). Ongoing isostatic uplift has resulted in preservation of the older shingle ridges at elevations up to 5 m above the present lake level.

interdune swales or marshes between them. Where water at the distal end is quite shallow, refraction is pronounced and the curvature can approach 90°. Where the spit builds into deep water the refraction becomes less pronounced and so do the recurves (see Box 10.3).

Two free ends

Barrier islands occur on gently sloping coastal plains in many parts of the world and tend to form chains of islands, separated by tidal inlets, that run parallel to the mainland coast and enclose a lagoon or bay that is typically 1–5 km wide. By strict definition they should have two free ends but some barriers in a chain may be attached to the mainland at one end or at a point where transgression has bridged the lagoon (Figure 10.4) and it is probably best to consider the whole chain as barrier islands rather than trying to separate some into the spit category. The barrier islands in Kouchibouguac Bay, shown in Figure 10.4, form part of a larger chain of barriers on the south-east coast of New Brunswick. In turn, this chain is one of four chains of barriers in the Gulf of St Lawrence that occur along the coasts of New Brunswick, Prince Edward Island and the Isles de la Madeleine (Owens, 1974; McCann, 1979). They exist in microtidal environments subject to storm wave activity, and where ice is present for several months of the year. The Gulf of St Lawrence barriers can be regarded as the northernmost extension of the barrier systems that extends southward along much of the east coast of the USA and into the Gulf of Mexico.

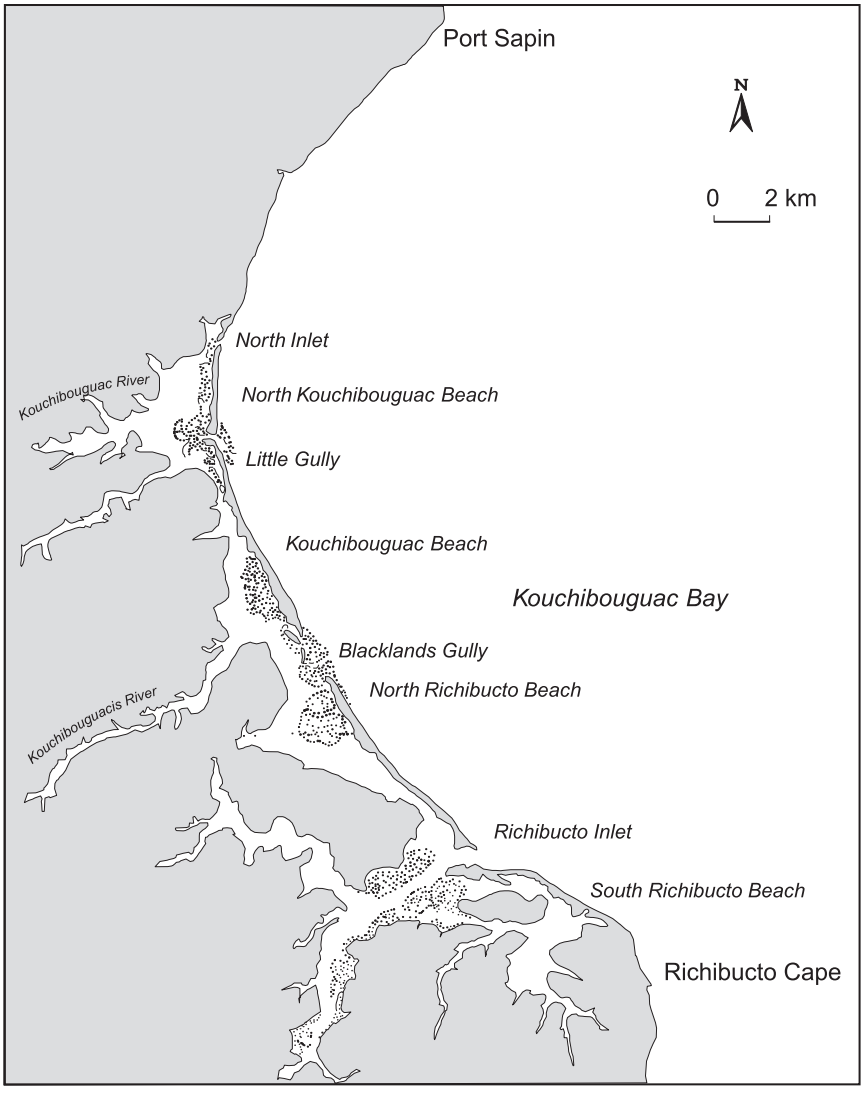

Figure 10.4 Map of the Kouchibouguac Bay barrier island system, New Brunswick. As a result of transgression the northern part of the barrier system has become fixed to the mainland forming a series of dune ridges backed by ponds and marsh. There are three permanent inlets opposite the major estuaries and occasionally a temporary inlet such as North Inlet is opened during a storm.

10.2.2 Structure and components of barrier systems

While there are some differences between the three major types of barrier recognised above, it is possible to recognise six major components or sub-environments (McCubbin, 1982; Oertel, 1985) most or all of which are common to all barriers (Figure 10.5). These include: (1) the mainland coast which is protected by the barrier and which may include bays and estuaries extending some distance inland; (2) the lagoon, bay or extensive marsh that separates the barrier from the mainland; (3) the subaerial barrier, including the beach, dune and backbarrier deposits; (4) the subaqueous platform of sediments which underpins the barrier and on which the subaerial portion of the barrier is built; (5) the shoreface extending offshore from

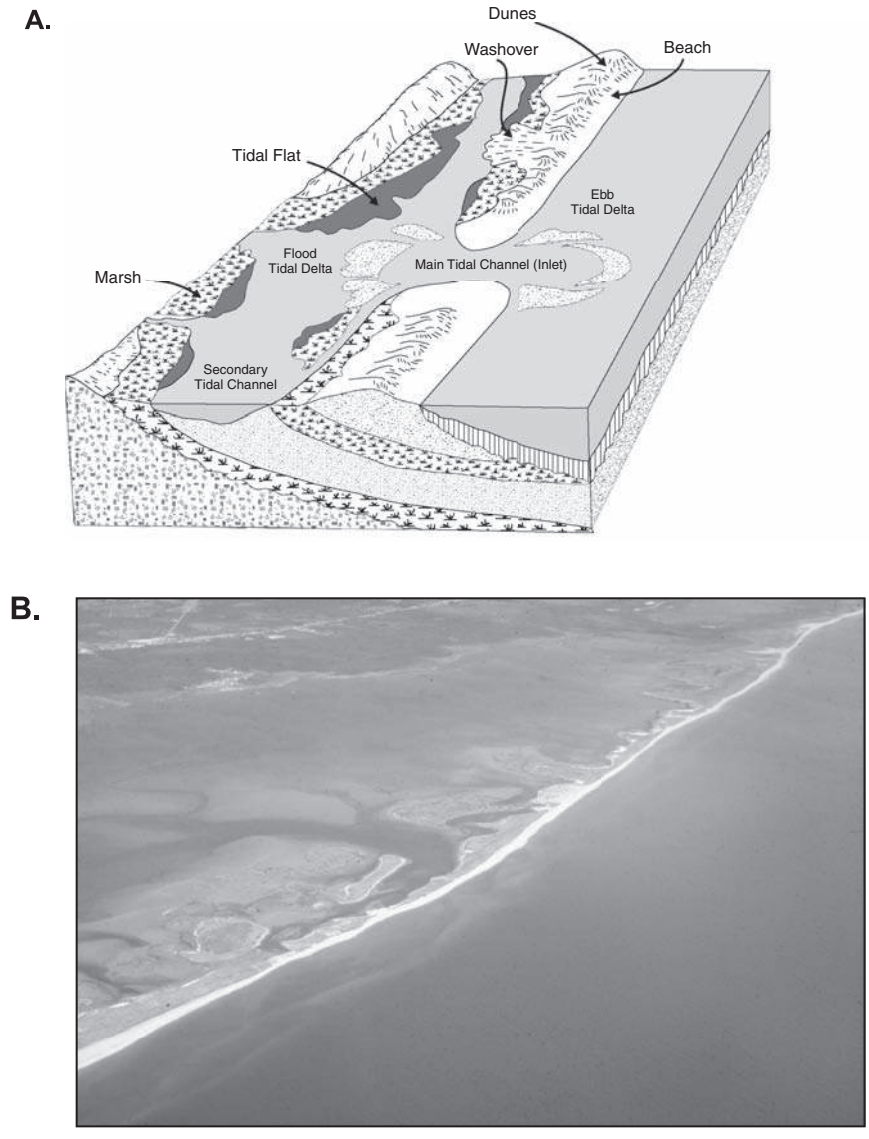

Figure 10.5 Components of a barrier island system: (A) plan view; (B) oblique aerial photograph of a portion of the Neguac barrier, northern New Brunswick.

the exposed beach; and (6) inlets and associated tidal deltas which are associated with barrier islands but may also be found, at least temporarily, on all of the other barrier types.

The mainland associated with barrier islands is generally a low-lying delta or coastal plain, often characterised by shallow bays and estuaries that have been drowned near the end of the Holocene transgression. Spits and baymouth barriers may form on much steeper coasts and often are attached to headlands at the entrance to a bay or along the sides. However, the bay itself must be shallow enough, relative to sediment supply, to permit the barrier platform to develop and the subsequent growth of the subaerial component. The mainland may have a range of protected sandy beaches, tidal flats or marshes. The other five components are

depositional environments characterised by a wide range of sediment types and sedimentary processes. There are frequent transfers of sediment from one component to the other and the evolution of the barrier results in changes to the direction and intensity of processes controlling erosion and sedimentation. As a result, most barrier systems are highly dynamic on a range of time scales from decades to centuries. Some features are common to more than one of the depositional environments (Figure 10.5). Beaches extend along the length of the seaward side of the barrier and are a major part of the attraction for recreational purposes. However, beaches are also found in places along the lagoon and on the mainland and estuaries, especially where the fetch is long enough to permit waves to remove fines. Tidal flats are formed on the ebb and flood tidal deltas of inlets as well as in the lagoon or bay. Marshes develop along protected shorelines on the lagoon coast of the barrier as well as on the mainland. Finally, dunes develop along both the exposed coast and onshore of the lagoon and mainland beaches, though the narrow beaches of the lagoon generally restrict the size of dunes that develop there.

10.3 Barrier dynamics: overwash and inlets

Overwash and inlet formation are characteristic features of most barrier systems as a result of the combination of large waves and surge associated with the passage of both tropical and mid-latitude storms. While overwash may occur on mainland dunes when the foredune is breached and sediment is carried into the landward swale, it is most characteristic of barriers where a single dune ridge or dune ridge complex exists and water can flow across the back-barrier deposits towards the lagoon shoreline. Overwash is particularly characteristic of transgressive barriers (or transgressive portions of barriers, such as the proximal (updrift) end of barrier spits) because they are relatively narrow and the volume of sand in dunes is more limited than stable or progradational barriers. The presence of the lagoon or bay on the landward side allows for the flow of water seaward when winds shift offshore and the resultant scouring can lead to the formation of an inlet. Both overwash and inlet formation during storms are important controls on the dynamics and evolution of barriers and they are key to the preservation of transgressive barriers because the landward transfer of sediment results in the rollover or landward migration of the barrier. This acts to preserve the barrier as a depositional landform through time while the location moves to accommodate reduced sediment supply or sea level rise. The focus here will be on sandy barrier systems but we will examine gravel barriers briefly at the end of the section.

10.3.1 Storm surge and overwash

Storm surge, erosion and overtopping

The process of overwash occurs when storm waves overtop low foredunes, or when erosion and scarping of the base of the foredune are so severe that a breach is formed, and water and sediments are carried inland. The resulting sedimentary deposit is termed a washover fan or washover terrace depending on the lateral extent. The general requirements for overtopping or breaching to occur are elevated water levels due to storm surge and high waves that erode and flatten the beach profile, thus allowing wave action to reach the dune. Storm duration is also important because it determines the number of high tides over which erosion can occur and coincidence with spring tides increases the potential for the combined surge and tidal elevation to exceed the threshold for generating overwash. Much of our basic understanding of the overwash process on barriers comes from studies in the 1960s and 1970s of overwash processes, documentation of volumes of erosion and deposition on the beach and on the barrier, and measurement of the sedimentary characteristics of washover deposits (e.g., Hayes, 1967; Pierce, 1970; Schwartz, 1975; Leatherman, 1976; Leatherman, et *al.*, 1977; Cleary and Hosier, 1979; Dolan and Hayden, 1981; Orford and Carter, 1984).

Recent papers have distinguished between two major overwash regimes (Morton *et al.*,

2000; Sallenger, 2000; Orford *et al.*, 2003; Donnelly *et al.*, 2006): (1) runup overwash where the storm surge level is below the level of the backshore ridge or dunes but wave run-up results in some swash overtopping the crest; and (2) inundation overwash where the elevation of the storm surge is above the backshore crest or foredune and water flows landward nearly continuously (Figure 10.6). It should be recognised that beach width and backshore ridge or dune elevation vary alongshore and at the same time the storm surge elevation will vary temporally with meteorological conditions and with the tidal cycle, as well as with the nearshore bathymetry (Figure 10.7). Increasing storm surge and wave run-up duration and elevation produces an increase in the extent and severity of overwash while increasing dune height and width, the extent of vegetation cover and the presence of shrubs, and the time since previous overwash events tends to decrease the potential for overwash. The result is that there is a continuum of overwash conditions (Claudino-Sales *et al.*, 2008; Matias *et al.*, 2008) beginning with occasional overtopping at low points and the reactivation of recent overwash channels through nearly continuous overtopping and washover fan formation at many places (Figure 10.8), to complete inundation along a substantial length of the barrier. Where there are relatively high, wide foredunes, overwash is confined to locations where the dune is vulnerable, usually pre-existing washover channels, points where the foredune is quite narrow due to erosion from earlier storms, and at 'hot spots' where locally the beach is quite narrow.

Routine mapping of barrier systems using LiDAR and extraction of DEMs from historical aerial photogrammetry has permitted mapping of pre- and post-storm topography along large sections of barrier coastline and documentation of the response of the coast to intense storms (Stockdon *et al.*, 2007; Leatherman, 2003; Morton and Sallenger, 2003; Robertson *et al.*, 2007). This is enabling quantification of the factors controlling the extent and severity of overwash and the development of predictive models of dune survival (Morton, 2002; Stockdon *et al.*, 2007; Claudino-Sales *et al.*, 2008; Price *et al.*, 2008; Houser *et al.*, 2008). Stockdon *et al.* (2007) tested the model developed by Sallenger (2000) on the impact of Hurricane Bonnie (August 27, 1998) and Hurricane Floyd (September 16, 1999) on a 50 km stretch of the North Carolina coast. The model was successful in predicting the overwash regime with an accuracy of 85–90% but tended to overestimate the impact and predicted inundation in many areas where it did not occur. There have been a number of attempts to develop models to predict the evolution of dune erosion and ultimately overwash (Kriebel and Dean, 1985; Larson *et al.*, 2004) and a variety of routines are now included in SBEACH (Donnelly *et al.*, 2006).

Overwash processes and washover fan characteristics

In the early stages of run-up, overwash waves may erode the top of the beach and cliff the embryo dune (Figure 10.9a) and occasional wave overtopping will generally result in the transport of some sediment over the crest with little impact on crest height. At higher storm surge levels wave overtopping is more frequent and the erosion occurs through the dune ridge, carving a channel and allowing surges of water to run through to the back barrier flats (Figure 10.9b). Deepening and widening of the channel produce a positive feedback because more surges flow through the channel and the flow is deeper. The greater volume and speed of these surges permit the water to flow much further across the backbarrier, perhaps aided by a raised water table or inundation from the lagoon side, and deposition rapidly increases the length and breadth of the fan (Figure 10.9c). An early example of pre- and post-storm surveys across a dune and washover channel (Leatherman *et al.*, 1977) illustrates nicely erosion of the beach and throat of the overwash channel (Figure 10.10). Some of this sediment is transported into the inner nearshore and returned to the beach during subsequent non-storm conditions.

Sediment deposited in the overwash fan comes both from erosion of the foredune and upper beach, and in the later stages of the storm it may also come from the beach. Much of the material is deposited as thin units of planar bedding dipping gently towards the lagoon.

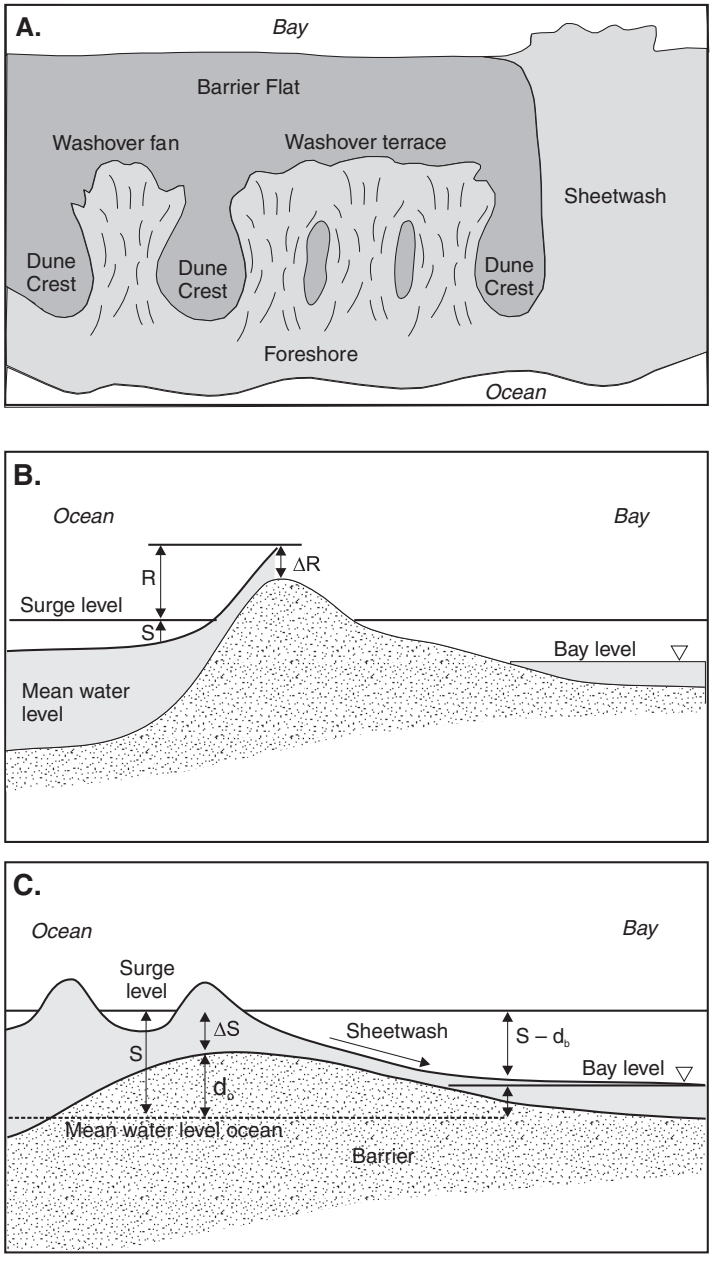

Figure 10.6 Overwash regimes: (A) definition sketch of the three principle forms of overwash morphology and sediments; (B) definition sketch showing overwash by wave run-up. *S* is the storm surge elevation and *R* the run-up elevation superimposed on this. The quantity *DR* is the amount by which the elevation *R* exceeds the dune or beach crest height d_c; (C) definition sketch showing overwash by inundation. The extent of inundation is indicated by the quantity *DS* which is the amount by which the storm surge elevation exceeds d_c (after Donnelly *et al.*, 2006).

In the throat where flow speeds are higher and erosion dominates, sediments are usually inversely graded, often with fine, heavy minerals at the base. On the overwash fans the beds are normally graded (Switzer and Jones, 2008) with coarse sediment at the bottom of each unit and fining upwards (Figure 10.11). The lower units are often disrupted by the effects of flow around or thorough vegetation on the backbarrier surface but continuity increases as this becomes buried. Foreset beds are formed where the fan progrades into ponds or standing water in marshes at the fringes of the barrier (Schwartz, 1975). Overwash fans are often reactivated by subsequent storms because of the absence of a protective dune and thus fans may contain

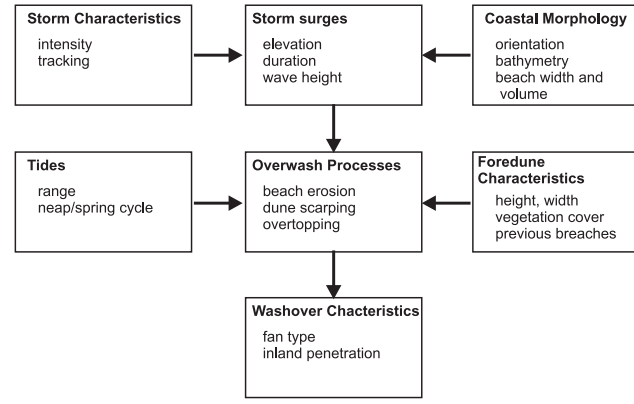

Figure 10.7 Schematic model of factors controlling the proportion of the shoreline overwashed and the severity and inland penetration of the overwash itself.

Figure 10.8 Extensive overwash, Cavendish Spit, Prince Edward Island generated by a storm on 28 December 2004. The spatial pattern of overtopping and erosion appears to reflect the alongshore spacing of rip cell/giant cusps with the dune remaining intact opposite the locations with a wider beach.

depositional units from more than one overwash event (Davidson-Arnott and Fisher, 1992; Sedgwick and Davis, 2003; Wang and Horowitz, 2007; Switzer and Jones, 2008). The bare sediments on the washover fan provide a source area for aeolian transport and thus the fan surface is often subject to deflation in the period between overwash events or the regeneration of vegetation. This often exposes and concentrates pebbles from the upper beach that may be dispersed within the general sandy matrix and acts to armour the surface. The sediment eroded from the fan surface is often trapped by vegetation around the margin of the fan, producing low dunes.

Washover healing and barrier recovery

Although some earlier work on barrier overwash and response to storms had touched on the evolution of overwash fans and barrier

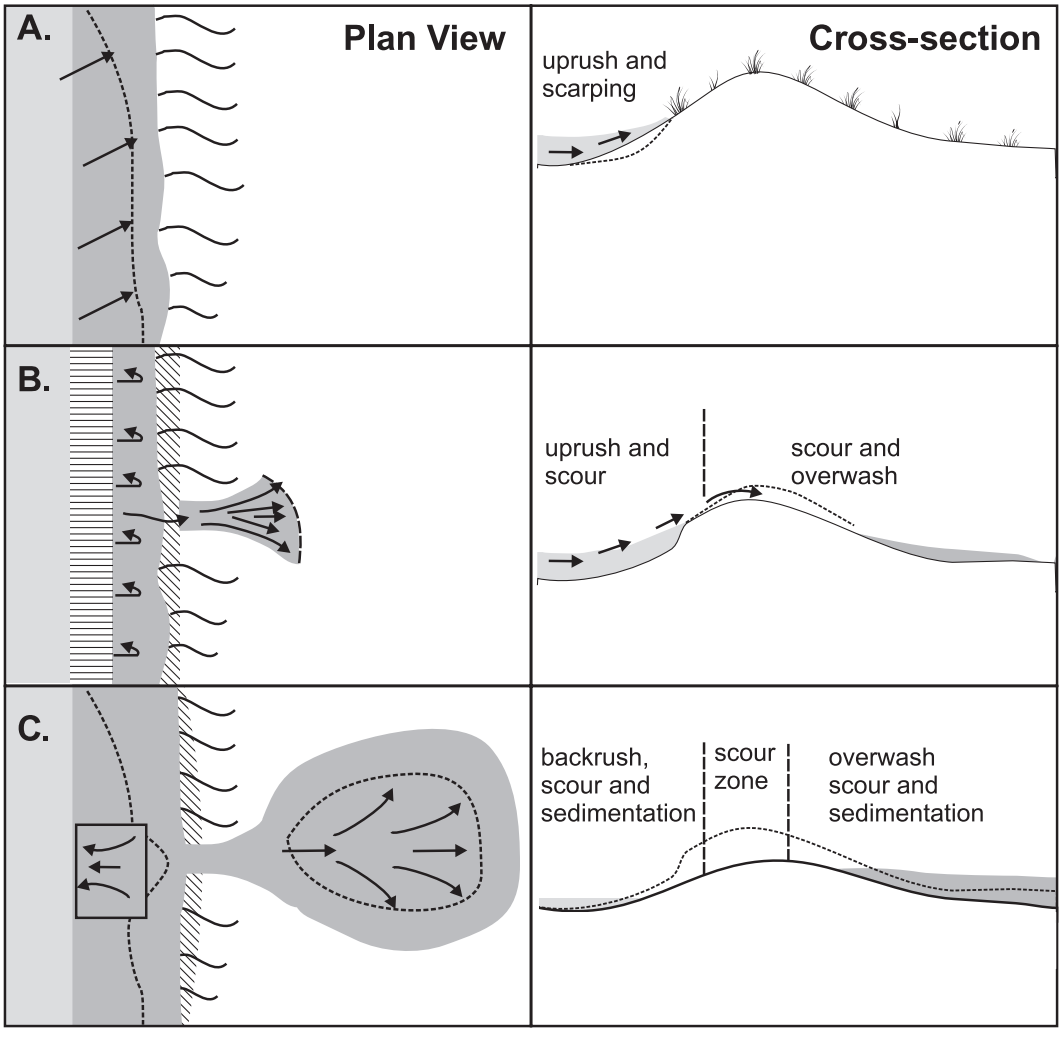

Figure 10.9 Plan and cross-sectional sketches of stages in the development of an isolated overwash fan: (A) initial erosion of the backshore and foredune with minor overtopping; (B) frequent overtopping leading to scour of the dune forming the inlet throat and initiating fan development at the edge of the backbarrier; (C) continued erosion of the overwash throat leading to deepening and widening with deposition on the backbarrier leading to landward and lateral extension of the fan.

island recovery from storms (e.g., Godfrey and Godfrey, 1973) it was the work of Cleary and Hosier (1979) that first clearly identified the concept of inlet and overwash healing. Based on extensive work on North Carolina barriers, both in the field and from the study of historical aerial photographs, they documented the history of overwash produced by tropical and extra-tropical storms, the form of overwash fans and the subsequent regeneration of vegetation and growth of new dunes. Cleary and Hosier recognised that the evolution of breaches through the dune line and the wash-over fans behind them followed recognisable patterns that were controlled by both physical factors, such as waves, aeolian sediment transport and sediment size, as well as biological factors determining the rate of colonisation of the bare surfaces and the distribution of species doing so.

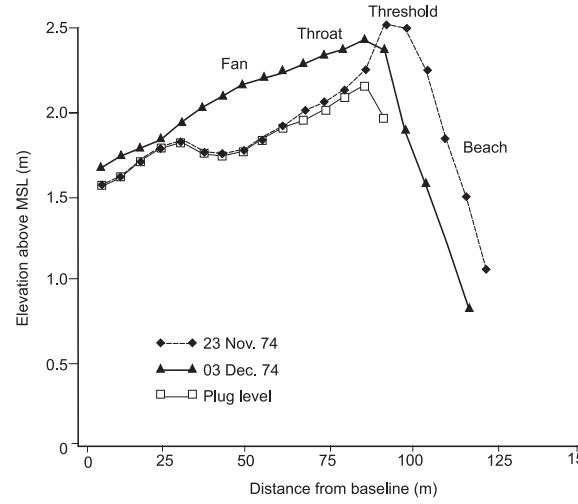

Figure 10.10 Pre- and post-storm survey of a washover throat showing beach erosion and deposition of sediment on the fan (after Leatherman *et al.*, 1977).

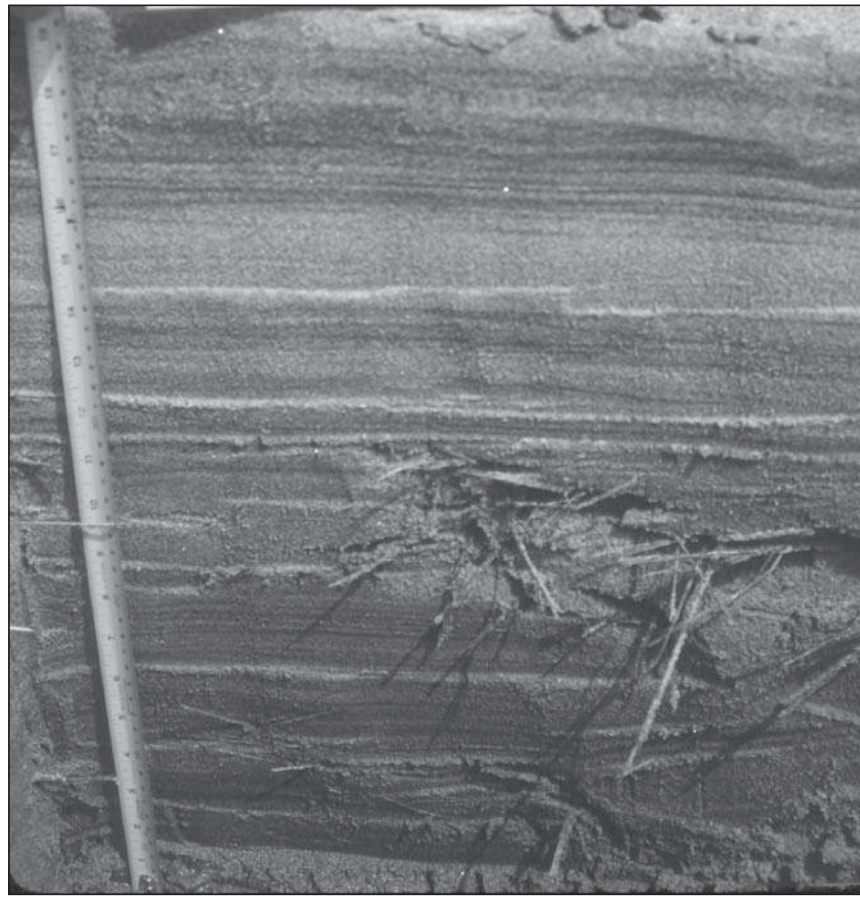

Figure 10.11 A small pit in an overwash fan, Long Point, Lake Erie showing about 40 cm of deposition from the overwash event of 2 December 1985. The sediments near the base initially buried grasses covering the backbarrier surface and are somewhat disturbed but overlying sediments are characterised by planar bedding on a nearly horizontal surface.

Cleary and Hosier (1979) identified two models of cyclic washover and recovery or healing – one related to fine-grained washovers and the other to coarse-grained washovers. While the models identified an ideal cycle from overwash to stabilisation and dune regeneration, it was recognised that the process of washover healing could be interrupted at any time by a new storm or storms that would then reset the recovery process. Subsequent work has shown that the process of washover healing is highly varied because of differences in the frequency and magnitude of overwash events, differences in barrier morphology, sediment budget and stability, and differences in the species composition of vegetation on the barrier. Where barriers, or sections of barriers, have a negative budget unvegetated washovers and active washover channels may always be present, and the barrier may be characterised by washovers at various stages of healing (Matias *et al.*, 2008). Following high-magnitude storm, large sections of the barrier may be subject to inundation overwash (Fritz *et al.*, 2007; Froede, 2008) and washover healing will likely take many years with all sections of the barrier passing through the healing stages at roughly the same time.

The width of the washover throat, the area and landward extent of the fan surface, elevation of the backshore and of the fan, both with respect to the potential for further overwash and proximity to the water table, will all influence the extent of aeolian sand transport and the development of dunes in the backbarrier region. Where the washover is quite narrow and the fan size is small, most aeolian activity will be limited to reworking of sediments on the washover fan and only small amounts of sand will be transferred through the throat from the beach (Figure 10.12a). Pioneer vegetation is quickly re-established from established dunes on either side and trapping of sediment and this quickly leads to the building of a foredune across the entrance to the washover (Figure 10.12a, b) cutting off further sand transport inland. Vegetation gradually becomes established on the washover fan surface and the process of healing may be completed within 6–10 years. Where the washover is much wider and a broad terrace is formed, the degree of aeolian activity as well as further overwash may restrict foredune development. Instead, isolated patches of vegetation become established on the surface forming small vegetated islands or nebka dunes. As these coalesce, overwash becomes restricted to a few well-defined channels and later these too become infilled (Figure 10.12c). It may take 10–15 years for healing to be completed. At Greenwich Dunes, Prince Edward Island a catastrophic storm in 1923 completely removed the foredune along a 5 km stretch of coast, forming a washover terrace that extended inland 100–400 m (Mathew, 2007). The absence of vegetation permitted large amounts of sand to be transported continuously from the beach across the washover terrace, leading to the formation of large transgressive dunes inland and hindering vegetation establishment. As a result it took several decades to establish a continuous foredune once more and about 70 years for complete stabilisation of the inland dunes.

10.3.2 Tidal inlets

Tidal inlets are openings that separate barrier islands, portions of a barrier spit, baymouth or mid-bay barrier, or lie between one end of a barrier and the mainland coast. Inlets provide a connection between the sea and the lagoon, bay or estuary landward of the barrier and therefore allow for the exchange of water between the two water bodies (Figure 10.16). In a tidal inlet this exchange is driven primarily by the rise and fall of the tides, with water flowing into the lagoon during the flood tide and out during the ebb (Seabergh, 2006). Where there is substantial freshwater input into the lagoon the volume of the ebb flow may be substantially enhanced over the flood. Inlets located opposite estuaries where the flow is directed by a channel incised in bedrock may be highly stable in location (Figure 10.16a) while others on barriers with a long shore-parallel lagoon may migrate rapidly downdrift or close off when a competing inlet opens. On some microtidal coasts where barriers close off a river mouth, inlets may only open seasonally when flooding from the river breaches the barrier, or sporadically as a result of an intense storm (Ranasinghe and Pattiaratchi, 1999). Many inlets provide an entrance to a safe

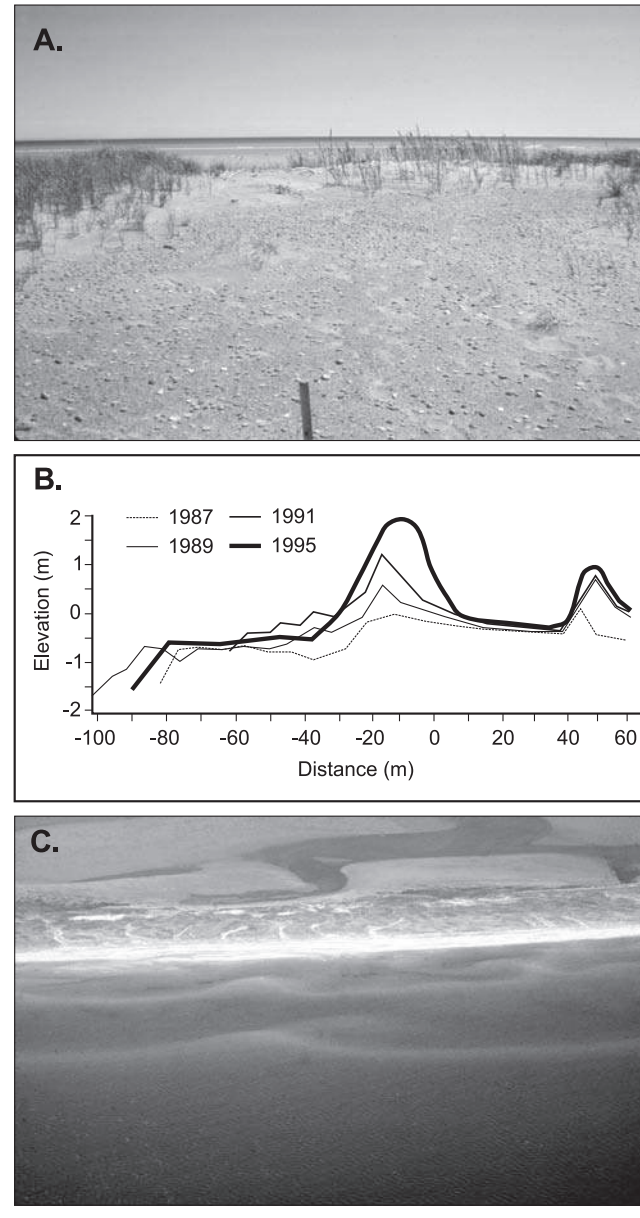

Figure 10.12 Washover healing: (A) view looking offshore of the throat of a small washover (the washover on the right side of the photo in Figure 10.14d,e) showing vegetation establishment at the top of the beach and growth of a foredune across the entrance. There has been some deflation of the fan surface leading to the development of a pebble lag; (B) profiles along the centre line of the washover fan showing growth of the foredune and of a small dune marking the landward edge of the fan; (C) oblique aerial photograph of a former inlet and washover fan surface, North Richibucto Beach, New Brunswick (Figure 10.4). Healing has progressed through the coalescence of small nebka dunes on the fan surface with washover channels remaining active over much of the healing period because of the low backbeach elevation.

harbour for recreational and fishing boats and in some cases for commercial shipping. Often this requires dredging the inlet channel and the entrance to it and installing jetties on one or both sides of the entrance in order to keep the dredged channel from silting up (Seabergh, 2006).

Tidal prism and flows through inlets

There is a continuous movement of sand into the inlet entrance by waves, littoral currents and tidal currents flowing into the inlet that acts to choke the inlet over time and close it off. This is opposed by the tidal currents into and out of the inlet opening, and the ability of these currents to keep the inlet open then depends on the volume and associated velocity of flow through the channel. Ignoring for the moment any freshwater inflows the volume of water flowing into the inlet on the flood tide generally equals the volume flowing out on the ebb and is termed the

Box 10.1 Overwash and lake level cycles

Long-term (years to decades) water level fluctuations in the Great Lakes impose a cyclical pattern on the timing of dune development and overwash activity (Olson, 1958; Davidson-Arnott and Fisher, 1992; Bray and Carter, 1992). In Lake Erie the range of lake level over several decades is on the order of 1 m, with high lake levels being experienced in 1952–53, 1972–73, 1985–86 and 1997–98 (Figure 10.13a). When intense storms occur around the periods of high lake level they produce extensive overwash on barriers around the lake and in the other Great Lakes. These washovers are frequently reactivated by less intense storms over the 2–4 year period that is characteristic of the high water phase. The susceptibility to overwash is also influenced by the local littoral sediment budget through its influence on beach width and dune volume.

A study of overwash on Long Point using historical aerial photographs and field measurements during and after the 1985–86 high water period (Davidson-Arnott and Fisher, 1992) illustrates the temporal and spatial patterns of overwash and washover healing. The long-term littoral sediment budget is negative in the proximal and central zones but positive at the distal end which is characterised by wide, progradational beaches (Figure 10.14). One or more intense storms occurred during each of the first three phases noted above and this is reflected in the high proportion of the spit occupied by active washover fans visible on historical aerial photographs and oblique photography flown each year from 1985–88 (Figure 10.13b). While overwash occurred over 30–50% of the shoreline in the proximal end in each of the three high water phases it occupied <5% of the 10 km stretch of the distal end. In 1985, overwash at the distal end was confined to a single location at the downdrift end of a longshore sandwave where the beach was very narrow (Figure 10.14d). Almost all of the washover formed in the proximal and central zones were reactivated during moderate storms in 1986 and 1987 but the wider beach resulting from longshore sandwave migration protected the two washovers at the distal end (Figure 10.14e).

Following the approach of Cleary and Hosier (1979) Davidson-Arnott and Fisher produced a schematic model relating of overwash occurrence and washover healing to long-term lake level cycles (Figure 10.15). There were no major storm events during the succeeding high-water phase of 1998 and as a result the healing cycle was completed over all sections of the spit. Similar temporal patterns can be associated with El Niño events on the west coast of the USA and with shifts in the tracks of major hurricanes and extra-tropical storms affecting the East and Gulf coast barriers of North America (Forbes *et al*., 2004).

tidal prism. The tidal prism is determined by the area of the lagoon, estuary or bay draining through the inlet and the tidal range:

$$Q_p = AR \tag{10.1}$$

where Q_p is the tidal prism, A is the area of the lagoon draining to the inlet and R is the tidal range.

Determining a value for A from a map is complicated because the basin sides are often very gently sloping, though an approximation can be obtained using the perimeter outlined by the mid-tide line. It will likely be complicated further where tidal conditions extend inland for some distance along estuaries because the tidal range will decrease with distance from the inlet

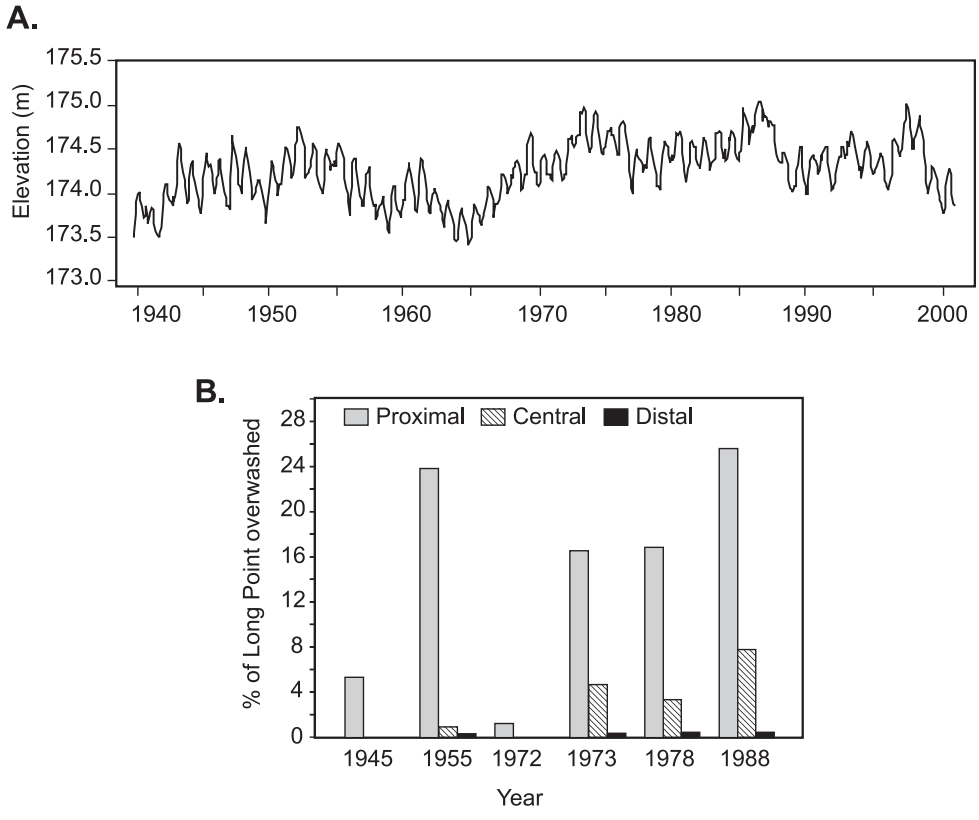

Figure 10.13 Washovers on Long Point in relation to lake level fluctuations in Lake Erie: (a) mean monthly water level in Lake Erie 1950–2000; (b) proportion of each zone occupied by washovers based on analysis of historical aerial photographs (after Davidson-Arnott and Fisher, 1992).

entrance. Finally, where there is more than one inlet entrance opposite the backbarrier lagoon, the ebb and flood flows may not be equal, and demarcating the drainage divide between inlets may be difficult. An examination of the map in Figure 10.4 will show that all of these complexities apply to the tidal prism of Little Gulley (Figure 10.16a).

Inlet morphology reflects the interaction between flows through the inlet entrance, sand transport by waves, and the evolution of the two ends of the barriers on either side of the entrance. The stability of an individual inlet depends on the relative magnitude of flows through the inlet to wave energy and littoral sediment transport. Where wave energy and littoral transport are high, more sediment is brought to the inlet entrance and greater flows, and hence a larger tidal prism, are required to flush sediment through and to keep it open. We should expect therefore to find the spacing between inlets to increase with increasing wave energy and to decrease with increasing tidal range, and this has been demonstrated for barrier island chains in a number of areas (Hayes, 1979; FitzGerald, 1996). Where chains of barrier islands extend over hundreds of kilometres it is possible to demonstrate the relationship between inlet spacing and the two controlling variables as has been shown for the Georgia Bight (FitzGerald, 1996 – see Figure 10.17).

The major feature of the inlet is a rectangular channel with the cross-section adjusted to the tidal prism that flows through it each tidal cycle. Flow speeds are highest in the channel between the islands and decrease once flow begins to spread out both on the lagoon side

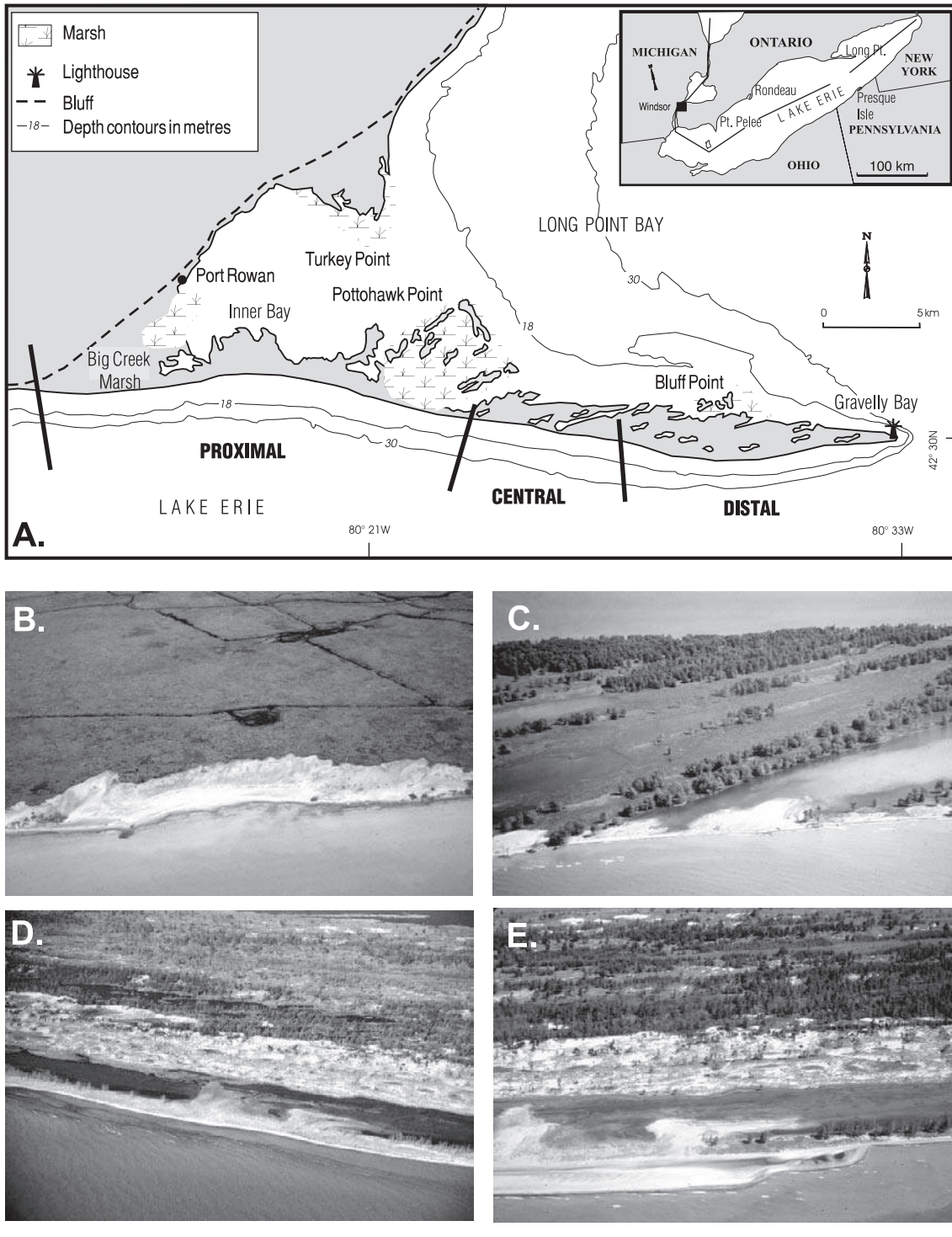

Figure 10.14 Overwash on Long Point, Lake Erie resulting from a storm on 2 December 1985: (A) map of Long Point spit showing the division into proximal, central and distal zones; (B) inundation overwash into marshes at the proximal end of Long Point spit following the 2 December 1985 storm; (C) overwash into ponds between old dune recurves in the central section; (D) oblique aerial photograph taken in June 1986 showing the formation of two small washover fans at the distal end. Note the narrow beach and the presence of a nearshore bar which is attached to the downdrift end of a longshore sandwave just off the picture to the left; (E) photograph taken 5 June 1987 showing migration of a longshore sandwave in front of the overwash areas. The wide beach associated with the sandwave prevented reactivation of these two fans during a severe storm on 15 December 1987.

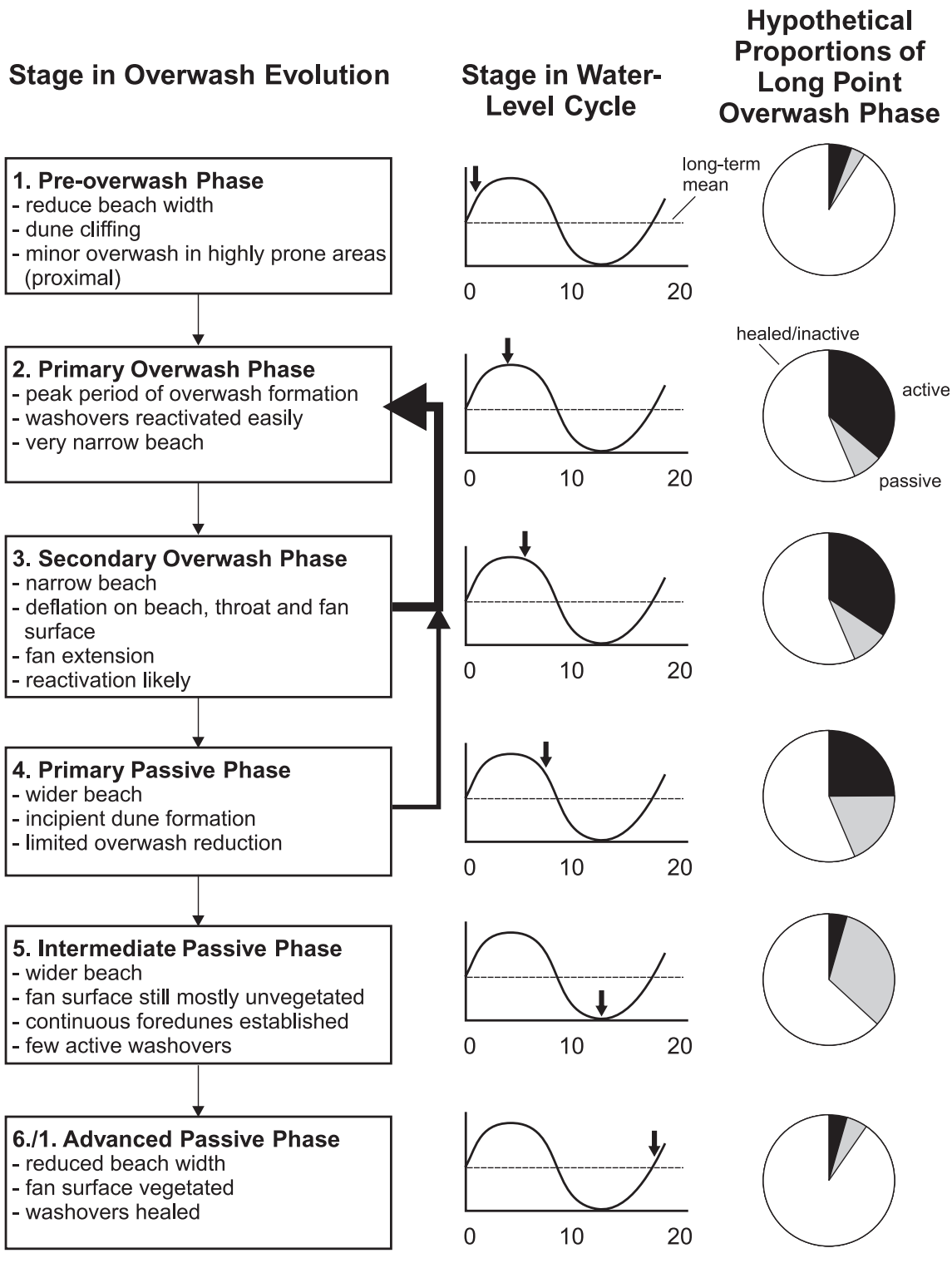

Figure 10.15 Schematic model of overwash occurrence and washover healing in relation to long-term lake level cycles on the Great Lakes (Davidson-Arnott and Fisher, 1992). Overwash potential is highest during the high water phase and the potential for washover reactivation decreases during the healing phases and water level declines.

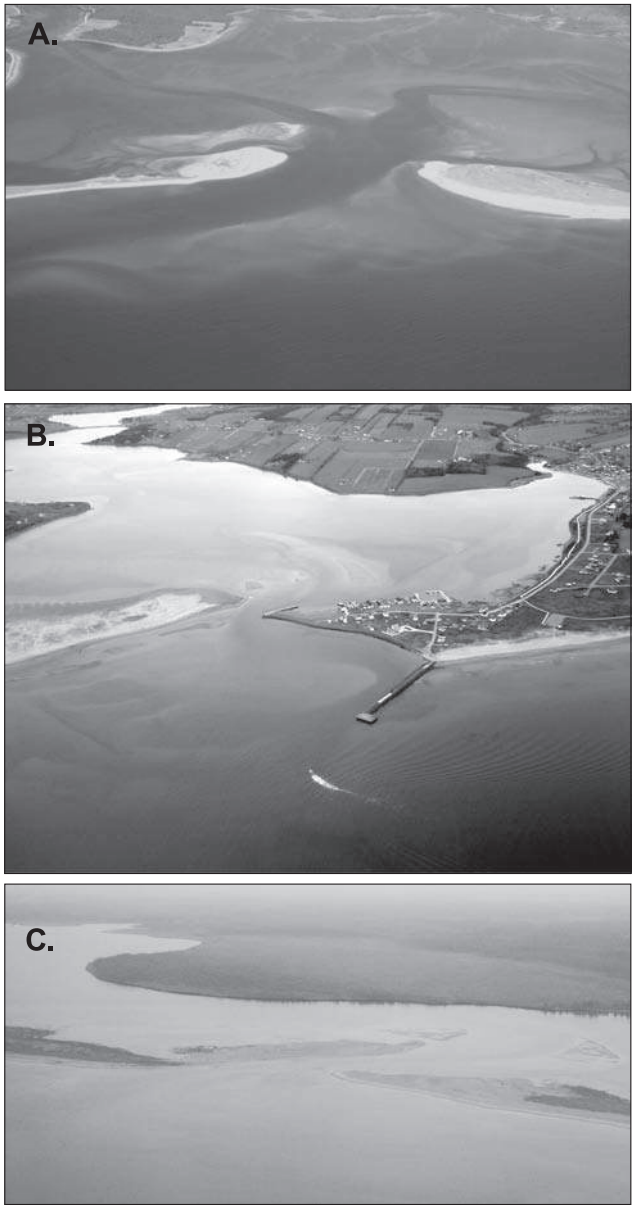

Figure 10.16 Tidal inlets: (A) Little Gulley inlet separating the North and South Kouchibouguac barrier islands (see Figure 10.4). The inlet location is highly stable because of its location opposite the drowned estuary; (B) North Rustico inlet on the north shore of Prince Edward Island. Like many of the small inlets through barriers on the shorelines of the Gulf of St Lawrence the inlet entrance is stabilised by jetties to protect small harbours for fishing boats; (C) North Inlet, a temporary inlet through the North Kouchibouguac barrier which was breached in 1970 and closed by 1976.

and on the ocean side. The channel is often scoured of fine sand leaving a lag of coarse sand and gravels, often mixed with clam and mussel shells. Sand is deposited at either end of the inlet entrance because of the increase in channel cross-section, decreased flow speed and, on the ocean side, the interaction of the ebb flow with waves. The result is the creation of two large depositional sand bodies – an ebb tidal delta on the seaward side of the inlet and a flood tidal delta on the landward side (Figure 10.18). Details of the morphology, channel patterns and size of the ebb and flood tidal deltas vary from inlet to inlet but there are a number of characteristics that are common to most or all (Hayes, 1980; Fitzgerald, 1996).

The primary component of the ebb tidal delta (Figure 10.18a) is the terminal lobe that extends seaward from the end of the main ebb channel and ideally has a curved form with a broad

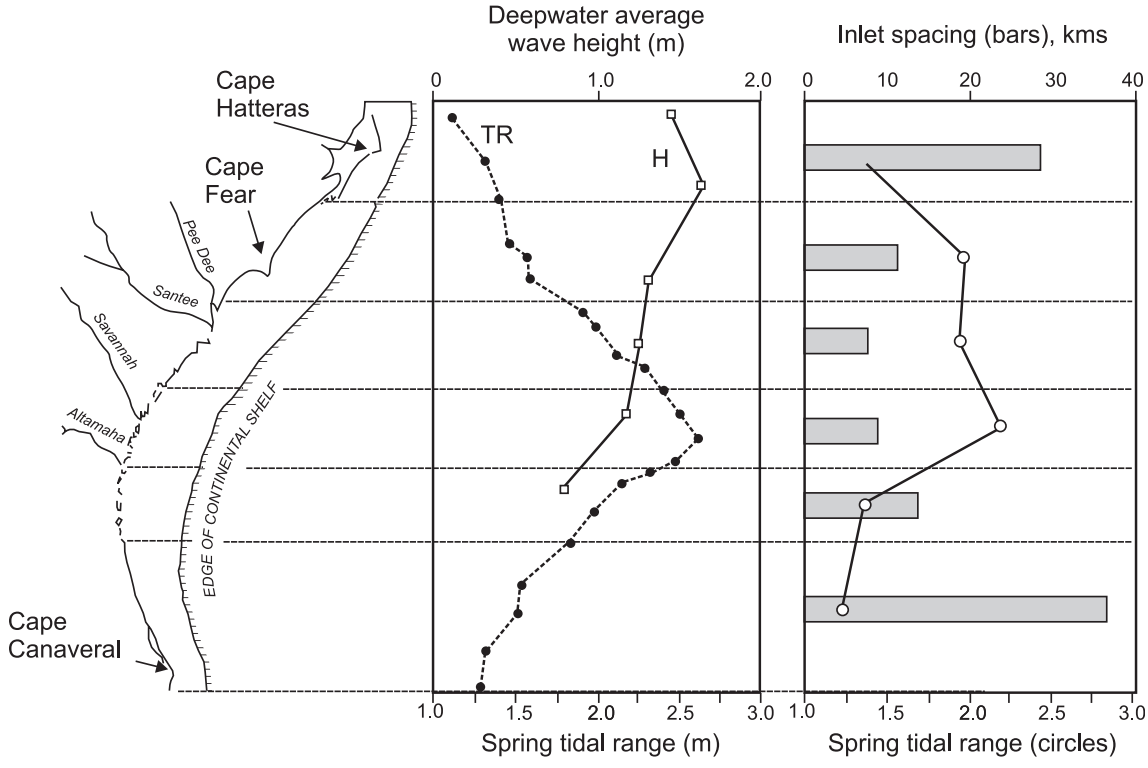

Figure 10.17 Patterns in the number and spacing of tidal inlets as a function of wave versus tidal energy along six lengths of shoreline in the Georgia Bight, USA (from FitzGerald, 1996).

shallow platform and a number of shoals or swash bars that are often emergent at spring low tide. The terminal lobe is built out over the barrier platform and extends some distance offshore beyond the beach and it has one or more channels across it. The speed of the ebb flow tends to be greatest close to low tide and continues while the tide is already rising on the ocean coast. As a result, the flood tidal waters are initially confined to marginal flood channels on either side of the main channel until water levels on the ocean side exceed those in the lagoon and flow into the lagoon is established over the entire inlet. The model shown in Figure 10.18a is typical of the mesotidal New England coast characterised by comparatively high wave energy conditions. Hayes (1980) suggests that the ebb tidal deltas become more elongate and more ebb-dominated in South Carolina because of reduced wave energy and perhaps larger tidal prism while ebb tidal deltas on the microtidal Gulf coast are much less developed. Where the tidal prism is large, for example because of an extensive estuary behind the inlet, both the ebb and flood tidal deltas may be large, though most of the area will be sub-tidal (Reinson, 1977).

Where the net littoral sediment transport is modest relative to tidal current discharge through the inlet, the terminal lobe is fairly symmetric (Figure 10.18a) but where there is a relatively large transport in one direction the ebb flow is deflected downdrift resulting in an extension of the swash platform parallel to the coast with the channel between it and the end of the downdrift barrier (Figure 10.16a). Sediment bypassing along the extended ebb tidal delta lobe results in the downdrift barrier becoming thinner at this location and increases the potential for overwash. At the same time the extended alongshore flow of the ebb tide becomes more and more inefficient and there is a tendency

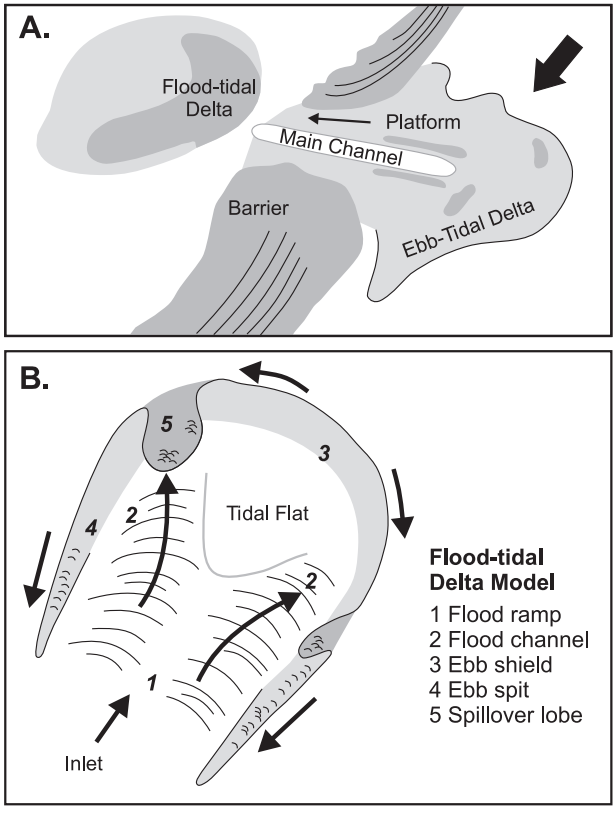

Figure 10.18 Schematic models of ebb and flood tidal deltas. Arrows indicate dominant direction of tidal currents: (A) ebb tidal delta with terminal lobe and swash bars that are exposed at low tide; (B) flood tidal delta showing bifurcation of inlet channels across the flood ramp (after Hayes, 1980).

for sediment deposition to block the end of the channel. Episodically when conditions are favourable, for example spring tides with offshore winds and low waves, the ebb tide flow may break through the ebb tidal delta opposite the inlet entrance thus restoring the shortest route seaward. The extended downdrift portion of the delta lobe may then be driven onshore, widening the beach and barrier at the updrift end and helping to stabilise it.

The flood tidal delta is similar to the ebb tidal delta in that it forms as a result of flow expansion and decrease in speed as the flood tidal currents spread out into the lagoon (Figures 10.16a, 10.18b). The flood ramp consists of lobes of sediment divided by bifurcation of the flood channels often with quite complex lobate shoals. Ebb flows tend to be concentrated in channels around the margin and along the landward sides of the barrier. The effects of wave action are generally much lower here than on the ebb tidal delta.

The spacing of inlets and their form in relation to tidal versus wave energy also influences the form of the barrier islands. Hayes (1979) found that barriers on microtidal coasts tend to be long and thin, with little variation in width along the length of the barrier (Figure 10.19a). In contrast, inlets on mesotidal coasts tend to be relatively short, narrow in the centre, with wider sections near the inlets due to progradation (Figure 10.19b). Being fond of his food, he labelled the microtidal barriers hot dogs and the mesotidal ones drumsticks – and these terms seem to have stuck. Barrier form is also influenced by other factors, including sea level history, sediment abundance and the area of the lagoon behind the barrier, but the relationship to tidal range and wave energy is an important one.

Inlet formation, stability and evolution

Inlets and the adjacent ends of barriers are dynamic features cut through sedimentary units and they respond relatively rapidly to changing

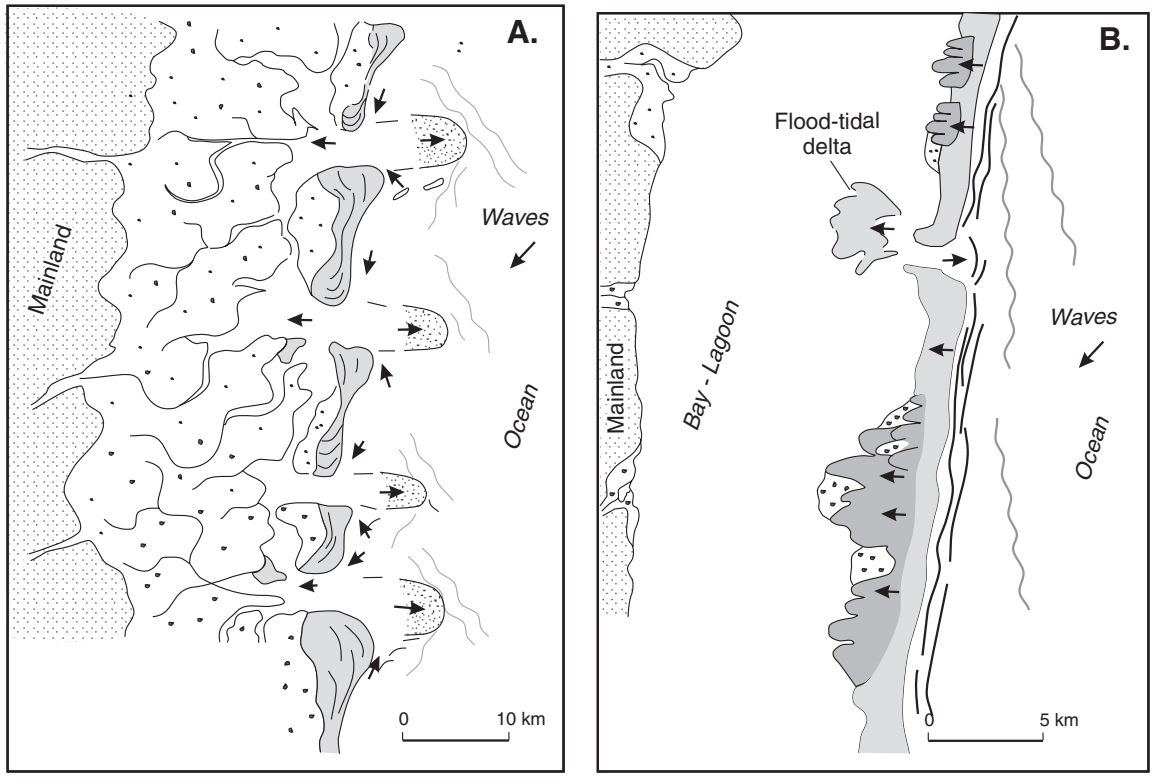

Figure 10.19 The general form of barrier islands as a function of tidal range: (A) microtidal coasts characterised by long, narrow hotdog-shaped barriers; (B) mesotidal coasts characterised by short, bulbous drumstick-shaped barriers (after Hayes, 1979).

sediment supply, storm events and wave regime as well as to factors that control the tidal prism. Inlets may form as downdrift extension of a spit building across a bay narrows the gap between the distal end of the spit and the downdrift coast. However, many inlets form as a result of the breaching of a barrier system during a storm. As we have seen in the previous section, overwash and breaching of the foredune is common on many barriers during intense storms. However, on the backbarrier the pulses of swash bore transport result in deposition and the building of a fan rather than erosion of a channel. Instead, inlet formation seems to occur primarily as a result of a coincidence of conditions that favour the generation of unidirectional flow from the lagoon side near the end of a storm event (Pierce, 1970; Greenwood and Keay, 1979). These conditions likely involve the generation of a large storm surge which elevates the water levels in the lagoon, a switch of winds from onshore to offshore coincident with a falling tide on the ocean coast which then produces a situation where the water level is much higher on the lagoon side and currents flow across a low-lying area driven by winds and the hydraulic head. These quickly scour a channel through the sand below mean sea level and the subsequent tidal current flows quickly erode a deeper wider channel. The long-term stability of these inlets then depends on the drainage area of the lagoon that the inlet can capture. If this is too small to be stable, given the wave energy and littoral sediment transport, then the inlet will close over a few years to decades (Greenwood and Keay, 1979; Ashley, 1987). Once the inlet is closed the ebb tidal delta is reworked by wave action and disappears but the flood tidal delta is preserved in the lagoon with

Box 10.2 Measurement of tidal prism and flows through an inlet

Studies of inlet stability and particularly modelling of inlet response to dredging and to stabilisation by navigational jetties requires information on the tidal prism and on the speed and duration of flows through the inlet channel (Bruun, 1978; Seabergh, 2006). Traditionally the simplest approach has been to treat the inlet channel as a reversing river channel and to apply standard stream gauging techniques to measure channel cross-section and flow speeds at vertical profiles spaced across the channel. In small streams this can be accomplished by stretching a rope across the channel and using this as a guide to the location of verticals. Measurements of flow speed and direction are made at one or more points in the vertical (depending on the depth of flow) using a mechanical current meter (cup, propeller, ducted impeller) electromagnetic current meter or acoustic doppler velocimeter. Because of the speed and depth of flow, especially at high tide measurements in tidal inlets are usually made from a small boat, rather than wading.

This approach was used for measurements made by Greenwood and Keay (1979) in the study of North Inlet (Figure 10.16c) where there was (at least most of the time) no boat traffic to be concerned about. Measurements of flow over a tidal cycle through Little Gulley (Figure 10.16a), which is too wide to stretch a rope across, were made by anchoring the boat along the transect, at points fixed by triangulation from shore. Care needs to be taken to ensure that flow direction is measured because even in small inlets flow may become stratified near the turn of the tide with, for example, warm water from the lagoon flowing seaward over cooler, denser water flowing landward near the bed after the tide has turned.

Simultaneous measurements of the tidal stage were made using temporary tide gauges set up on both the seaward and landward side of the inlet, and in the case of Little Gulley in the lagoon and up the estuary. Flow speed and discharge through Little Gully are shown in Figure 10.20 for one complete tidal cycle. Note that this is essentially diurnal during spring tides at this location (which makes for a very long measurement day!), and means that flow speeds are less than would be the case for a semi-diurnal tide. Ebb current speeds are slightly faster than those of flood currents but in this location the inequality is not as great as is often the case, and the highest speeds are recorded fairly early in the ebb tidal stage. The standardised tidal prism here is about 114×10^3 m^3 cm^{-1} and this can be compared to a maximum standardised tidal prism for North Inlet of about 11×10^3 m^3 cm^{-1} (Greenwood and Keay, 1979).

tidal channels meandering between saltmarshes occupying the former shoals (Moslow and Tye, 1985 – see Figure 10.21). Examples of former ebb tidal deltas can be seen in the lagoon in the left of the photo in Figure 10.5.

There have been extensive studies of tidal inlet geometry and stability, in particular related to design considerations for stabilisation of harbour entrances (O'Brien, 1969; Fitzgerald and Fitzgerald, 1977; Bruun, 1978; Pacheco *et al.*, 2008) and for the transport of sediment (Fiechter *et al.*, 2006). Inlets adjust their cross-sectional area over time in response to changes in tidal prism. The intertidal area in the lagoon may be reduced by sediment deposition, both naturally over a long time and through human intervention in the form of infilling and dyking (Kragtwijk *et al.*, 2004; Bertin *et al.*, 2005). The

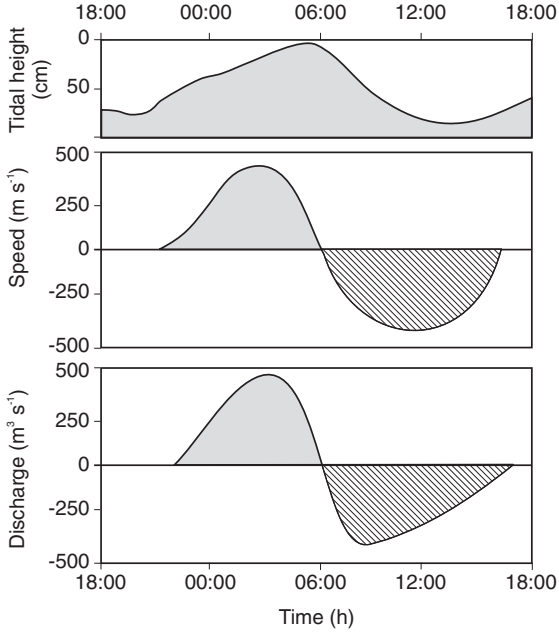

Figure 10.20 Tidal height, mean velocity and mean discharge through Little Gulley inlet over a spring tidal cycle.

resulting reduction in flow volume and speed through the inlet leads to infilling of the channel and reduction in the cross-sectional area until a new equilibrium is restored. Changes in the tidal prism may also result from the opening and closing of inlets in a multi-inlet system. These changes may occur naturally as a result of storm impacts, as was the case in the opening of North Inlet in 1970 (Greenwood and Keay, 1979). They may be the result of human intervention such as the large scale effects associated with the closure of the Zuiderzee in 1932 (Kragtwijk *et al.*, 2004) or the more limited impacts of artificial opening of small inlets such as one through the Ria Formosa barrier system (Vila-Concejo *et al.*, 2003. Where there is a loss of some of the tidal prism the inlet may be reduced in size or may silt up completely. Where there is an increase in the tidal prism the inlet may become completely unstable and migration of the inlet position may be initiated because of changes to flows within the lagoon and location of the inlet watershed.

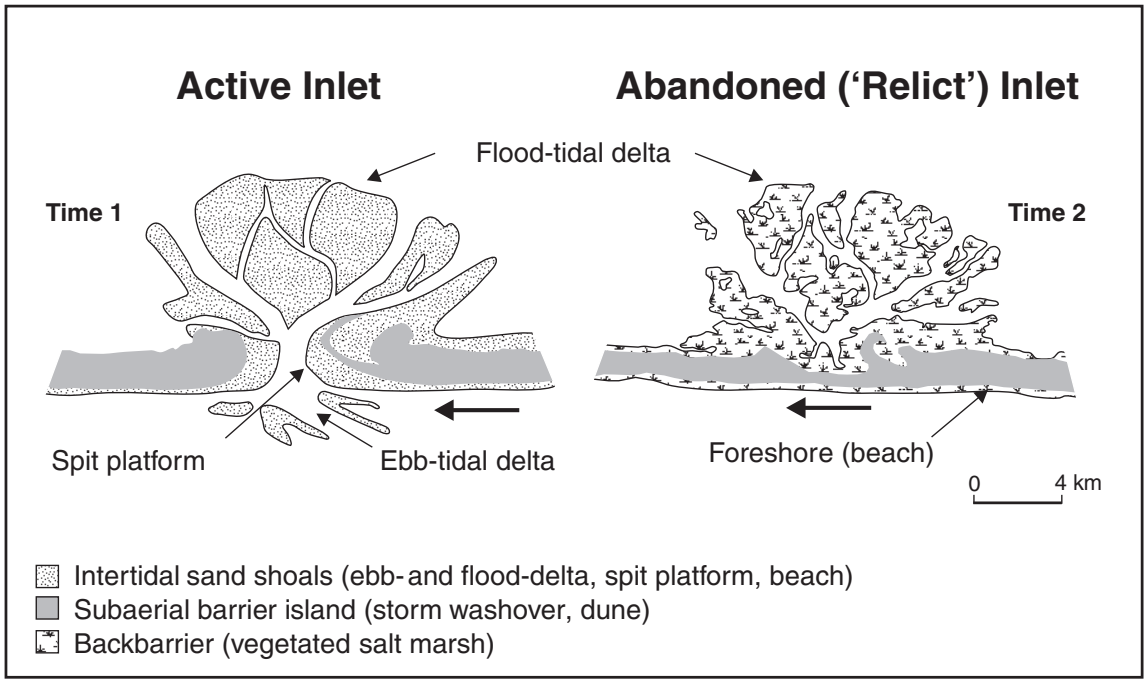

Figure 10.21 Morphologic evolution of a wave-dominated inlet following inlet closure. The inlet is closed through downdrift migration of the updrift barrier and gradual choking of the inlet entrance by swash bars. Flood tidal delta shoals become vegetated by saltmarsh leaving them as islands surrounded by old tidal channels. Arrows indicate the direction of longshore sediment transport (after Moslow and Tye, 1985).

Forbes and Solomon (1999) describe the effects of artificial closure of an inlet through a barrier island on Rustico Bay on the north shore of Prince Edward Island that provides a compelling cautionary tale of unexpected consequences on the stability and operation of the remaining inlet.

Inlets located opposite estuaries that extend inland for some distance and control the flow of a significant portion of the tidal prism tend to be relatively stable in position through time. The same is often true for inlets located between a headland or side of a large bay and the downdrift end of a spit. However, inlets may migrate downdrift on barriers where there is a strong net littoral drift in one direction, and where there are no features that tend to fix their position. Sediment entering the updrift side of the inlet entrance tends to build outward into the channel, constricting flow and leading to erosion of the end of the adjacent barrier. The result is to produce a depositional unit that is as thick as the depth of the inlet channel with the major bedding planes dipping in the direction of inlet migration (Kumar and Sanders, 1974; Hayes, 1980). The base of the unit is formed in the lag gravels and shells that make up the floor of the inlet channel fining upward through cross-bedded sand units and later capped by aeolian dune deposits.

10.3.3 Lagoons

Coastal lagoons are an important component of the barrier system. They are particularly rich ecologically because of nutrients brought into the system from both the land and the ocean and the production of organic matter in the lagoon (e.g. in beds of eel grass – *Zostera marinera* – and fringing salt marshes. Lagoon beaches, sand flats and mud flats provide food for migrating birds and the shallow waters are nurseries for many fish and shellfish. We can distinguish lagoons from estuaries on the basis of form and alignment, though there is some overlap between the two in all definitions. Estuaries extend inland for a considerable distance along a drowned river valley and are often oriented perpendicular to the coast, while lagoons generally have their long axis parallel to the coast and to the barrier. Estuaries are also distinguished by having a substantial freshwater input with mixing occurring downstream from the tidal limit. Lagoons too can have a considerable freshwater input, but it is not a condition of the definition. In many cases the tidal water bodies behind major barrier chains include both lagoons and estuaries, as is evident from Figure 10.4. It should also be recognised that similar lagoons exist behind coral reefs.

Kjerfve (1986) distinguished between three types of lagoons on the basis of the extent of water exchange between the lagoon and the ocean: (1) Choked lagoons are found along microtidal coasts where there is moderate to high wave energy and considerable sediment availability. They usually have only a single inlet and the inlet may be closed seasonally Ranasinghe and Pattiaratchi, 1999). As a result wind forcing is dominant and residence times may be weeks or months; (2) Restricted lagoons usually have two or more entrances. Circulation is controlled both by tidal currents and wind forcing and they are vertically mixed; (3) Leaky lagoons may stretch along the coast for tens of kilometres and have multiple inlets with relatively unimpeded exchange of water with the ocean. The waters of restricted and leaky lagoons usually range from brackish close to freshwater inputs to salinity close to that of the ocean, but hypersaline conditions may occur in choked lagoons in arid and semi-arid regions (Kjerfve and Magill, 1989).

Lagoons may expand in size and grow deeper under rising sea level, but they are primarily areas of net deposition and therefore their evolution is controlled by both rates of sediment infilling and sea level changes. Under present conditions whether lagoons expand or contract depends on the balance between the rate of net sediment input and the rate of sea level rise (Nichols, 1989; Cooper, 1994; Morton *et al.*, 2000). The main sources and pathways of sediment input to coastal lagoons are: (1) Littoral sediments – sand and gravel supplied from offshore and alongshore. These can reach the lagoon directly through transport by tidal currents into the inlet and deposition on the flood tidal delta or transport further into the lagoon by

Figure 10.22 Portion of a Landsat image of Jalisco, Mexico showing the Barra de Navidad lagoon and surrounding area. The delta of the Marabasco River has expanded rapidly as a result of increased sediment input from the surrounding hills. The El Tule lagoon near the top left of the picture is an example of a choked lagoon that is only open seasonally during the wet season.

waves and currents. Littoral sediments may also reach the ocean side of the lagoon through overwash, aeolian processes and through temporary inlets. (2) Fluvial sediments – fine to coarse sediments brought into the landward side of the lagoon primarily by rivers draining the uplands surrounding the lagoon and ephemeral streams acting on coastal bluffs. On relatively steep coasts the coarse sediment may be deposited directly in the lagoon, with fines being dispersed throughout the lagoon and possibly some through the inlet to the ocean. On gently sloping coasts much of the coarse material may be trapped some distance inland at the tidal limit on shallow estuaries and thus only silts and clays reach the lagoon proper; (3) Chemical and organic precipitates – carbonates primarily from shellfish growing within the sub-tidal and intertidal zones of the lagoon can be a significant input to the system and organic matter accumulation in salt marshes and sea grass beds may also be significant in some lagoons. While work on lagoons of the coastal plain of the USA suggests that rates of infilling on most of these are either roughly in equilibrium with sea level rise or not keeping pace with it (Nichols, 1989; Morton *et al.*, 2000) sedimentation on steeper coasts such as the west coast of Mexico (Moore and Slinn, 1984) and the east coast of South Africa often exceeds the rate of sea level rise (e.g. Cooper, 1994).

An example of this is provided by the Barra de Navidad, a choked lagoon in Jalisco, Mexico (Holland, 2005). This has an area of 3.6 km^2 with a single outlet and a large sediment input from drainage of the highlands behind it (Figure 10.22). Rates of fluvial sedimentation have been increased due to agricultural and logging activities in the surrounding river catchments and by clearing for urban and tourism development so that the lagoon now appears to have a net positive sediment budget (Holland, 2005; Méndez Linares *et al.*, 2007).

10.4 Barrier spit morphodynamics

All barrier systems are dynamic features that evolve rapidly in response to the processes controlling sediment supply, and to change in controlling variables such as sea level, wind climate and evolution of the mainland coast (Figure 10.23). As we saw in Section 10.3, morphodynamic processes such as overwash, inlet formation, inlet migration, and washover healing can result in significant changes to barrier systems over periods of years and decades. In response, many barrier systems, and particularly barrier spits and barrier islands, evolve rapidly and have a life span that may be only a few decades to a few thousand years. There is now considerable information on the sedimentary architecture and evolution of spits and other barriers from excavation of features preserved in former glacial and pluvial lakes (Gilbert, 1890; Jewel, 2007) or in areas of rapid isostatic uplift (Nielsen *et al.*, 1988; Mäkinen and Räsänen (2003). Extensive coring through modern features world-wide has provided many insights into barrier evolution and particularly the effects of the Holocene transgression (Dillon, 1970; Héquette and Ruz, 1991; Soons *et al.*, 1997; Anthony and Blivi, 1999; Otvos and Giardino, 2004; Harvey, 2006; Long *et al.*, 2006; Tomazelli and Dillenberg, 2007; Storms *et al.*, 2008) and the vertical stratigraphy of the core data may be extended through the use of seismic profiling and Ground penetrating Radar (van Heteren *et al.*, 1996; Jol *et al.*, 2003; Novak and Pedersen, 2006).

10.4.1 Spit progradation and recurve development

A clear feature of all spits is the existence of a significant volume of net longshore sediment transport from updrift of the point of attachment to the mainland to the downdrift or distal end of the spit. The transport direction is a reflection of local coastal orientation with respect to the wind and wave climate of the region and there must be a substantial source of littoral sediments from coastal erosion or fluvial sediment inputs updrift to provide for the initiation and continued evolution of the spit. Sand and gravel are transported along the ocean (or lake) shore of the spit by waves and currents operating in the nearshore and swash zones. There is usually a decreasing gradient of sediment transport towards the distal end (discussed further in the next section) and this is reflected by deposition leading to wide beaches, seaward progradation and the development of a succession of fore dune ridges and intervening swales or ponds (Figures 10.24a, b). The distal end of the spit is the zone where most or all of the active increase in spit size occurs through progradation normal to the shoreline and through extension of the spit and the spit platform (Meistrell, 1972) in the direction of net sediment transport.

At the terminus, sand in the nearshore is transported into increasingly deeper water

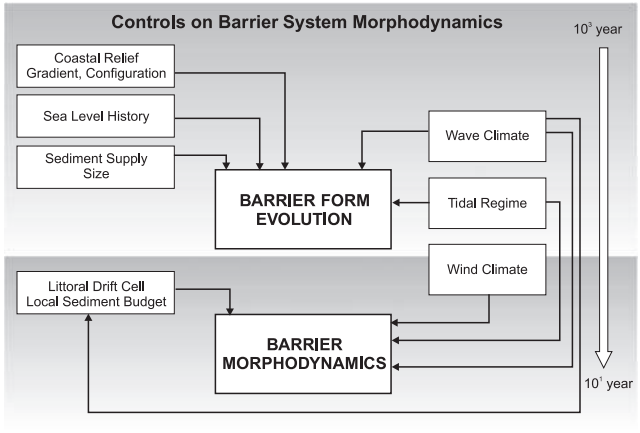

Figure 10.23 Schematic model of the factors controlling barrier system morphodynamics and evolution and the interactions between them.

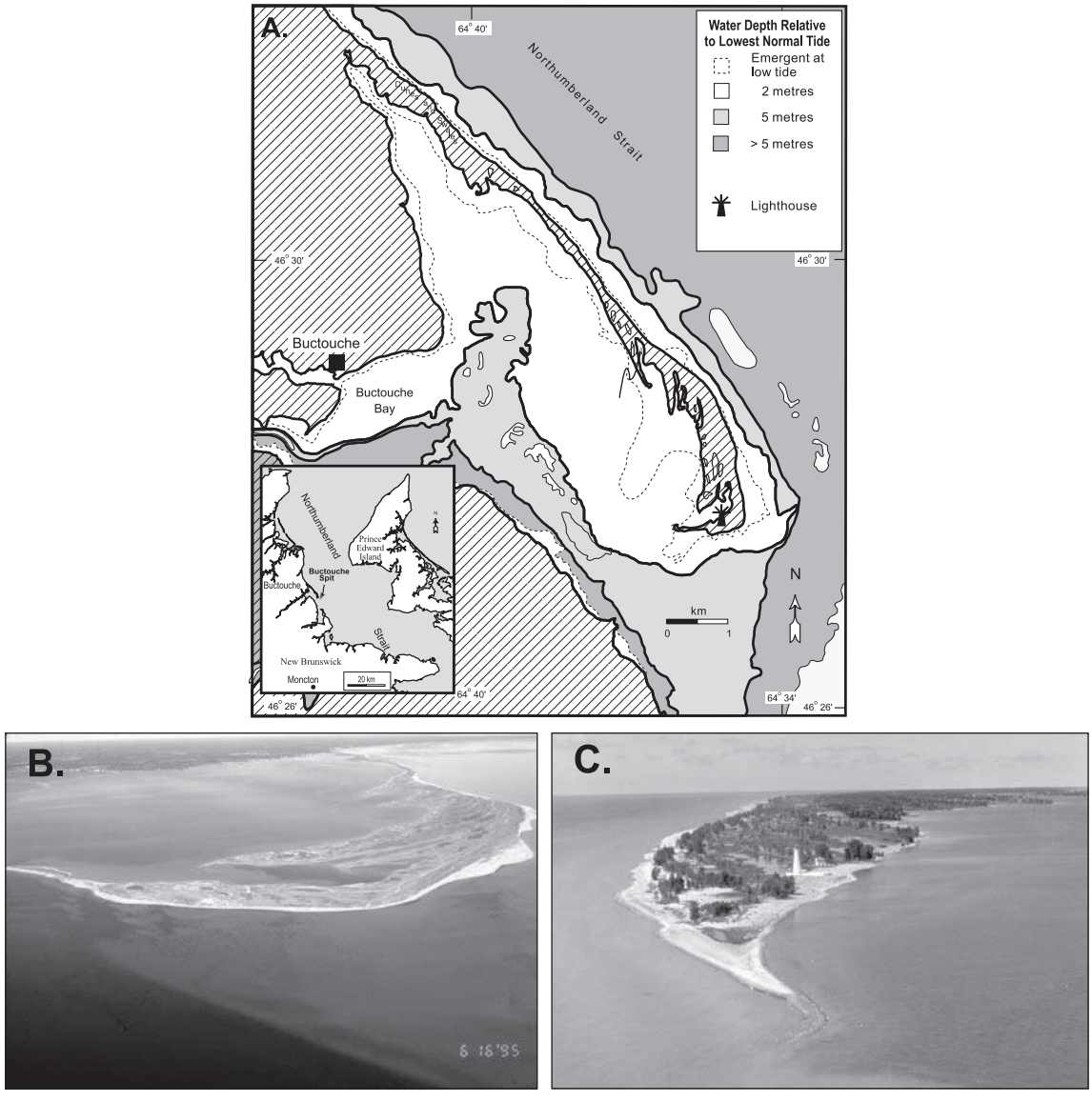

Figure 10.24 Examples of sandy spit development: (A) Map of Buctouche Spit, New Brunswick, Canada; (B) oblique aerial photograph of Buctouche Spit, The spit is about 14 km long from the downdrift end to the point of attachment near the top of the photo. The extensive shoals of the spit platform are evident at the downdrift end. The main tidal channel of the constricted entrance to Buctouche Bay can be seen at the lower left; (C) oblique aerial photo of the distal end of Long Point, Lake Erie. The progradational portion of the spit is about 10 km long.

leading to deposition and extension of the spit platform (Figure 10.24b). Refraction of the dominant waves over and around the platform results in the development of a curvature of the shoreline and transport of sediment towards the bay. Littoral sediment transport may be slowed further and the curvature of the shoreline enhanced by the effects of waves from the direction opposite to the direction of net littoral drift, sometimes producing an exaggerated 'hook'

Box 10.3 Comparison of Buctouche and Long Point spits

The role of refraction over the shallow platform in controlling shoreline and dune ridge curvature is illustrated by comparison of distal end of Buctouche spit with that of Long Point (Figures 10.24, 10.25a, b). Buctouche has built across the deepest part of Buctouche Bay and the platform is presently extending into water depths <6 m whereas Long Point is extending into a basin that is 30 m deep in the centre of Lake Erie (Figures 10.9a, 10.24c). The result is that wave refraction occurs for almost all waves affecting Buctouche (Ollerhead, 1993) but there is almost no refraction around the end of Long Point (Davidson-Arnott and Conliffe Reid, 1994). As a result, while the curvature of dune ridges on Buctouche has been increasing over the past few hundred years those at the distal end of Long Point have become less and less curved (Figures 10.25a, b).

The downdrift extension of the spit requires deposition of sufficient sediment to build the spit platform up to the surface and thus the rate of spit extension is a function of the littoral sediment transport rate and the depth of water into which the spit is building. There will be rapid extension when the sediment budget is large and the depth of the basin is small and vice versa. Sediment supply to Long Point has been estimated to be on the order of 1.0×10^6 m^3 a^{-1} though the actual supply of sand and gravel may be about half this. However, because the platform is building into about 30 m of water, a large volume of sediment is required to bring it to the lake surface and the rate of subaerial spit extension is about 4 m a^{-1} (Coakley, 1992). Sediment supply to Buctouche Spit is about 15 000 m^3 a^{-1} and spit extension over the past 150 years has also been about 4 m a^{-1} (Ollerhead and Davidson-Arnott, 1995) because the platform is only building into about 8 m of water.

shape to the end of the spit (Figure 10.24b). The shallow platform, and periodic downdrift extension by sandwaves and swash bars (Davidson-Arnott and van Heyningen, 2003; Park and Wells, 2007), often results in the enclosure of a large pond or runnel and the development of a new foredune ridge some distance from the next oldest one (Figure 10.24c). The result is to produce a series of elongate ponds facing the bay which over time become infilled through marsh development and the reworking of material by waves generated within the protected bay (Davidson-Arnott and Conliffe Reid, 1994).

10.4.2 Sediment budget and spit evolution

The overall growth of the depositional body forming the spit and its platform requires a net input of sediment from updrift and thus the overall sediment budget exercises an important control on both the size of the spit and its rate of growth. As the spit develops sediment budgets can be constructed for sub-units of the spit based either on spatial location – e.g., the proximal and distal ends of the spit – or on sub-environments such as the platform, beach, dunes and back barrier marshes. The evolution of a simple spit can be modelled theoretically by simulating wave refraction and the longshore sediment transport gradient (Petersen *et al.*, 2008). Similar modelling can be carried out for particular examples based on bathymetry and wave climate (Davidson-Arnott and Conliffe Reid, 1994; Park and Wells, 2007; Allard *et al.*, 2008). Semi-quantitative estimates of historical sediment budgets can be quantified from reconstruction of the evolution of the plan form of the spit from historic maps and aerial photographs along with some data on the thickness of the sedimentary unit from borehole data or seismic lines (Coakley, 1992; Soons *et al.*, 1997; Park and Wells, 2007; Allard *et al.*, 2008). The combination of sediment budget modelling and estimates of volumes of sediment accumulation

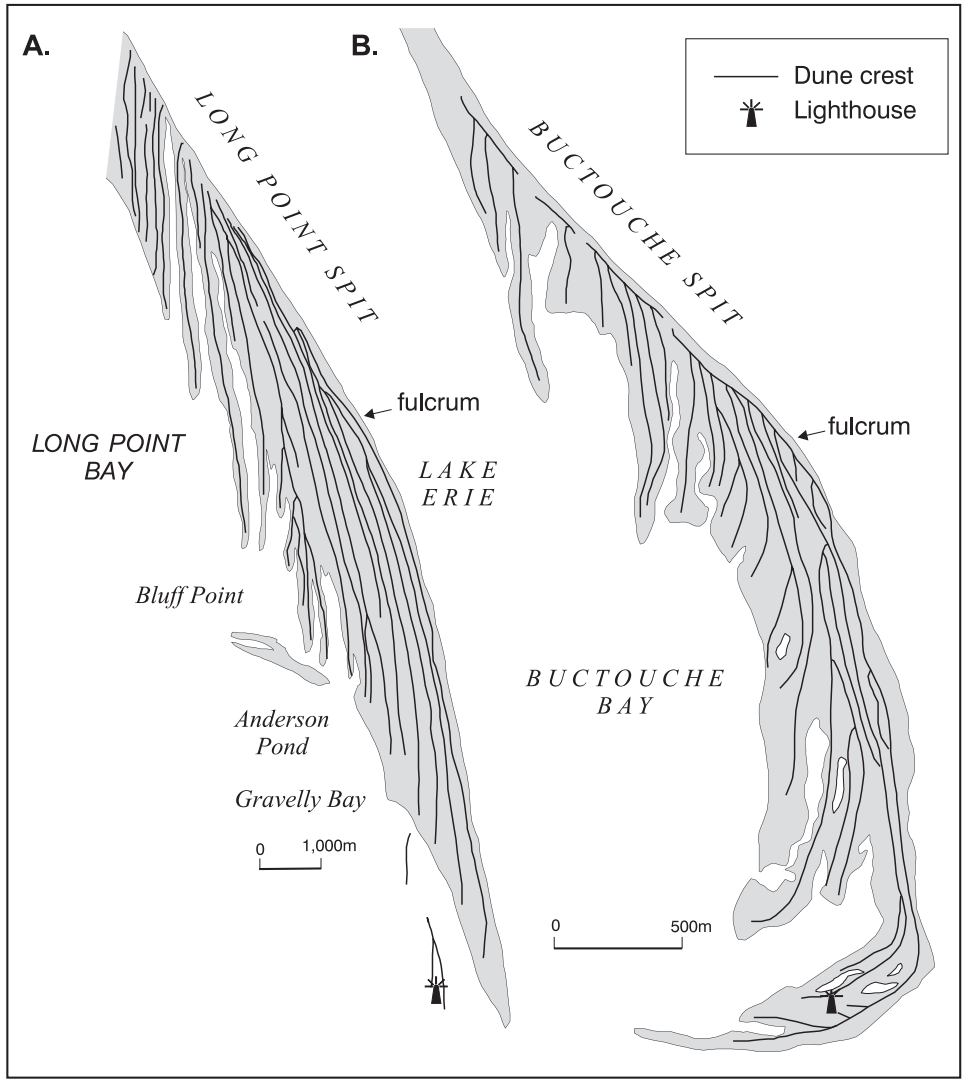

Figure 10.25 Comparison of the evolution of dune ridge curvature at the distal end of (a) Long Point and (b) Buctouche spits. The map of Long Point has been flipped so that the orientation of the two spits is the same. Note the differences in the scale of the two maps reflecting the much greater absolute size of Long Point.

at different locations from borehole data with littoral transport modelling can provide significant insights into the pattern of evolution determined from maps and aerial photographs.

However, there are a number of factors that also influence the local sediment budget both spatially and temporally, and which therefore have an impact on how the spit evolves. These include: changes to the volume of sediment supply from the updrift portion of the littoral cell; local changes resulting from the impact of storms such as overwash and the opening or closing of inlets; changes to the wave climate as a result of climatic factors or evolution of other coastal features; and sea level change. Changes to the sediment input from updrift may result from natural events, including the evolution of other barriers or changes to the locations of distributaries on a river delta. Changes may also result from human intervention such as the

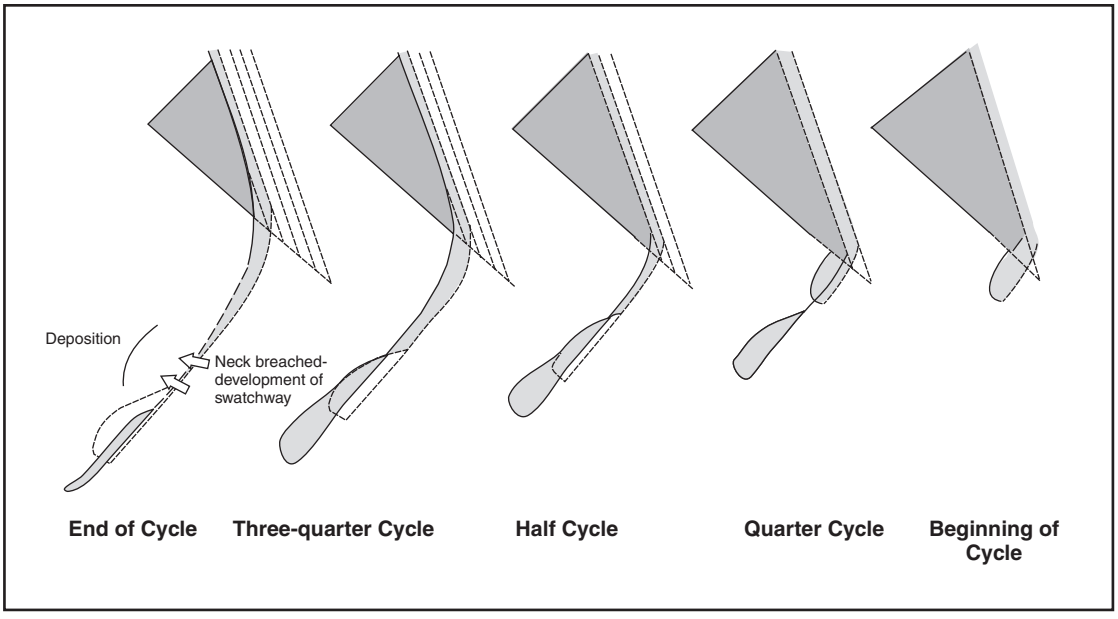

Figure 10.26 Schematic diagram of a cycle of accretion and erosion in the evolution of Spurn Head (after de Boer, 1964).

building of jetties at harbours updrift, or reduction in the sediment supply to the coast from rivers or cliff erosion because of dams or shore protection structures. Locally on the spit itself overwash can lead to sand transport through washovers onto the back barrier or into the lagoon, rather than being stored in the embryo dune and foredune system. Thus large volumes can be extracted from the beach until the foredune system is restored. Decadal scale shifts in wind patterns, storm tracks or ice cover can also produce significant variations in the littoral transport rate over a period of several years.

There is also a significant effect of the evolution of the spit itself on the sediment budget alongshore that is characteristic of almost all spits, and especially flying spits. Initially, when the spit first begins to grow, the entire spit likely has a positive sediment budget. However, as it extends, the proximal end of the spit often develops a negative sediment budget because of a change in the littoral transport gradient. This is brought about because the distal end begins to shelter the proximal end from waves from directions opposite to that of the dominant waves. The result is that the transport gradient at the proximal end increases – in effect more sand is moved towards the end of the spit than comes in from updrift. The result is that the spit becomes segmented into a transgressive proximal end characterised by overwash and temporary inlet formation (a process sometimes termed necking) and a progradational downdrift end characterised by wide beaches and the development of a relic foredune dunefield. The combination of transgression at the proximal end and progradation at the distal end results in the spit evolving into a distinct S shape. As transgression takes place in the proximal end, the original spit sediments are reworked until none of the original subaerial barrier remains. Within the transgressive portion of the spit there may be a transitional zone (the central zone in Figures 10.14a, c) where remnants of the original dune recurves are preserved as dune ridges at a distinct angle to the modern shoreline and foredune.

Transgression of the proximal end, overwash and instability are heightened when the spit is attached to an eroding shoreline as is the case for both Long Point and Buctouche spits. Erosion around the point of attachment results

in its downdrift migration. A breach of the narrow neck of the spit during a severe storm or series of storms can cut off sediment supply to the downdrift portion of the spit leading to the formation of a barrier island and potentially to the complete reworking and disappearance of that section. This appears to have happened on a number of occasions at Spurn Head, a small spit which is supplied with sediment from erosion of the bluffs along the Holderness coast and builds southward across the Humber estuary on the on the northeast coast of England (de Boer, 1964). The existence of historical maps and information going back several centuries enabled de Boer to reconstruct not only the shape and position of the spit over time but also some of the events that led to breaching. He was thus able to make a convincing case for a cycle of formation, extension and destruction (de Boer, 1964 – see Figure 10.26). Similar cycles of barrier overstepping have been postulated for a number of other areas including Buctouche spit (Ollerhead and Davidson-Arnott, 1995), the gravel barriers of Story Head, Nova Scotia (Forbes *et al.*, 1991) and Duxbury Beach spit, Massachusetts (Hill and Fitzgerald, 1992).

10.5 Barrier islands

Barriers that have one or both ends attached to the land are generally fed by longshore sediment transport and can occur on most coasts, including quite steep ones. Barrier islands, however, are generally restricted to comparatively wide, gently shelving coasts that permit the barrier to establish some distance offshore, enclosing a lagoon between it and the mainland shoreline. They are therefore found most commonly on trailing edge coasts in areas where there is an abundant supply of sand such as the east coast of North America, Western Europe between Holland and the Jutland Peninsula, and on the south-east coast of Africa from South Africa to Mozambique. Because they are not attached to the mainland, barrier islands migrate relatively rapidly in response to changing sea level and sediment supply, and in response to large storm events. Most barrier islands have formed under rising sea levels near the end of the Holocene transgression and few exist in the location where they were originally formed.

10.5.1 Origin and formation of barrier islands

Competing models of barrier island genesis led to some heated discussions in the 1960s and 1970s, and a plea by Schwartz (1971) to accept that there is evidence for barrier island formation through several different mechanisms. While there may still be disagreement over the origin of a particular barrier island or barrier island system, there is now general recognition that there are at least three valid mechanisms for barrier island formation; and in some cases barrier formation and evolution is quite complex, involving more than one mechanism. The three primary mechanisms are: (1) spit detachment or segmentation by inlet formation (Fisher, 1968); (2) nearshore aggradation of shoals (Otvos, 1981); and (3) detachment of a dune ridge complex through submergence and flooding of low-lying areas landward of the dune ridge (Hoyt, 1967).

Spit detachment

A simple scenario for barrier island formation through spit envisages a shallow headland bay complex in an area with a well-defined net longshore transport that leads to the formation of a drift-aligned spit. Extension of the spit across the bay leads to thinning of the neck of the spit which makes it susceptible to overwash and inlet formation during severe storms. If the spit has extended far enough, the inlet can capture a sufficiently large tidal prism to be self-sustaining and the detached downdrift portion of the spit now evolves into a barrier island (Fisher, 1968). The inlet and the barrier migrate downdrift while the spit begins a new phase of extension and progradation. This model of formation requires a relatively shallow embayment so that the newly formed barrier island continues to receive sediments through inlet bypassing. If the bay is too deep or tidal currents too strong, then the detached island quickly disappears, producing the cyclic model of spit development shown in Figure 10.26. Barrier islands on the Mozambique coast appear to have formed by this mechanism (Armitage *et al.*, 2006).

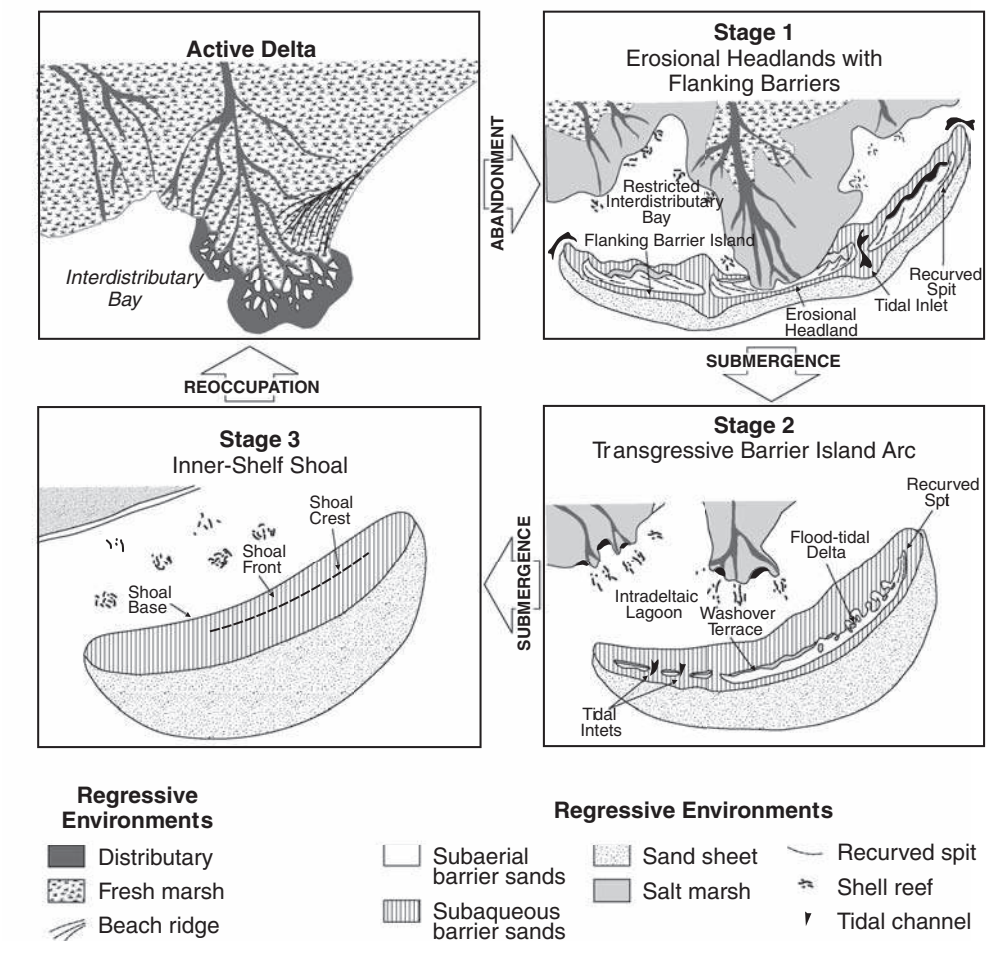

Figure 10.27 Model of transgressive Mississippi Delta barrier formation and evolution (Penland *et al.*, 1988).

Barriers may also evolve in a similar way through the erosion of delta lobes. This is the case for some transgressive barriers in the Gulf of Mexico associated with abandoned lobes of the Mississippi delta (Penland *et al.*, 1988), and similar spit and barrier island development have been observed at deltas such as the Rhone in France and the Po in Italy (Simeoni *et al.*, 2007). The model of Penland *et al.* (1988) begins (Stage 1) with the initiation of erosion and transgression, as active sediment supply through the distributary channels is reduced (Figure 10.27); it progresses (Stage 2) through the development of an erosional headland as the distributary channel recedes with accompanying spit and barrier island development; eventually (Stage 3), the barriers disappear as they are cut off from further sediment supply by transgression and submergence of the delta lobe and thinning of the barriers as they spread, leaving a relict shoal to mark the location of the barrier platform.

Shoal aggradation

An understanding of the dynamic nature of nearshore bars in relation to waves and water levels led to the discounting of early hypotheses of barrier island formation through the emergence of nearshore bars. However, where there is a large shoal area some distance offshore, it is possible for emergent intertidal features resembling swash bars to form and grow to the limit of

wave action forming a nucleus on which flotsam can accumulate. Colonisation by plants results in the trapping of sediment to form low dunes and the island may grow through further accretion in much the same way that coral cays develop on barrier reefs and carbonate platforms. Such an origin has been postulated for many of the Mississippi barrier islands (Otvos, 1981; Otvos and Giardino, 2004) and has also been shown to occur for isolated examples on other barrier shorelines (Oertel and Overman, 2004).

Davis *et al*. (2003) suggest a variant of this for development of barrier islands on the west side of the Florida Panhandle that occurred under stable or very slowly rising sea level near the end of the Holocene transgression. The Gulf coast here is a low gradient, low energy environment and they envisage the formation of a muddy mangrove or saltmarsh environment as the coastal plain was drowned. As the coastline position stabilised about 3000 years ago, reworking by waves separated increasing amounts of sand from the Pleistocene sediments, leading to the formation of offshore shoals that gradually accreted into the intertidal and finally supratidal with aeolian sediment transport and dune development (Figure 10.28a). Coring along nine transects shows a relatively simple stratigraphy for all the barriers (Figure 10.28b), with four major sedimentary units reflecting the transition from the organic rich mangrove or saltmarsh sediments through low-energy sea-grass-stabilised beds on the seaward or landward side of the barrier and then sand and shell deposits associated with shallow marine sediments, beach and dune sediments and coarser sediments associated with overwash and inlet formation. Where there is abundant sediment available progradation occurs, otherwise the barrier may be transgressive (Figure 10.28a).

Mainland beach detachment

Hoyt (1967) developed a theory of barrier island formation based primarily on sea level rise and transgression leading to the flooding of low-lying areas landward of a dune ridge on a gently sloping coastal plain. The theory was based primarily on work on barrier systems of the US east coast where transgression continued through much of the Holocene. The theory envisages the existence of substantial foredune ridges backed by a low coastal plain. Rapid sea level rise could lead to flooding of the area landward of the ridge to produce a lagoon while ongoing wave and aeolian processes act to maintain the ridge and associated beach. This was supported indirectly by the work of Swift (1975), though he noted that most contemporary barriers on this coast have migrated landward with the transgression and that the theory was likely more applicable to the early transgression. On a coastal plain this requires the rate of submergence to exceed the rate of dune transgression. Much of the logic for the theory is based on the apparent absence of open marine sediments landward of the barrier ridge; these should be present if the barrier was formed through shoal aggradation or spit detachment. Others have argued that the absence of these sediments in modern barriers reflects their destruction as they are overridden by barrier transgression.

The applicability of a particular model for barrier formation is clearly dependent on the general coastal morphology, shelf width, sediment sources and abundance, and the late Holocene sea level history. These factors likely account for differences in the amount of emphasis given to a particular theory in different coastal regions. Given the rapidity with which barrier systems evolve, the mode of formation probably is of limited significance in controlling barrier dynamics compared to the factors noted above and so less attention has been paid to it in the past couple of decades.

10.5.2 Barrier response to sediment budget and sea level change

Modern barrier islands and barrier systems generally continue to evolve in response to the factors that have controlled development towards the end of the Holocene. The major controls on this evolution are the local littoral and dune sediment budgets, and the effects of sea level change.

Sediment budget

When there is abundant sediment supply, the beach and nearshore will prograde. This leads to the development of new foredune ridges and

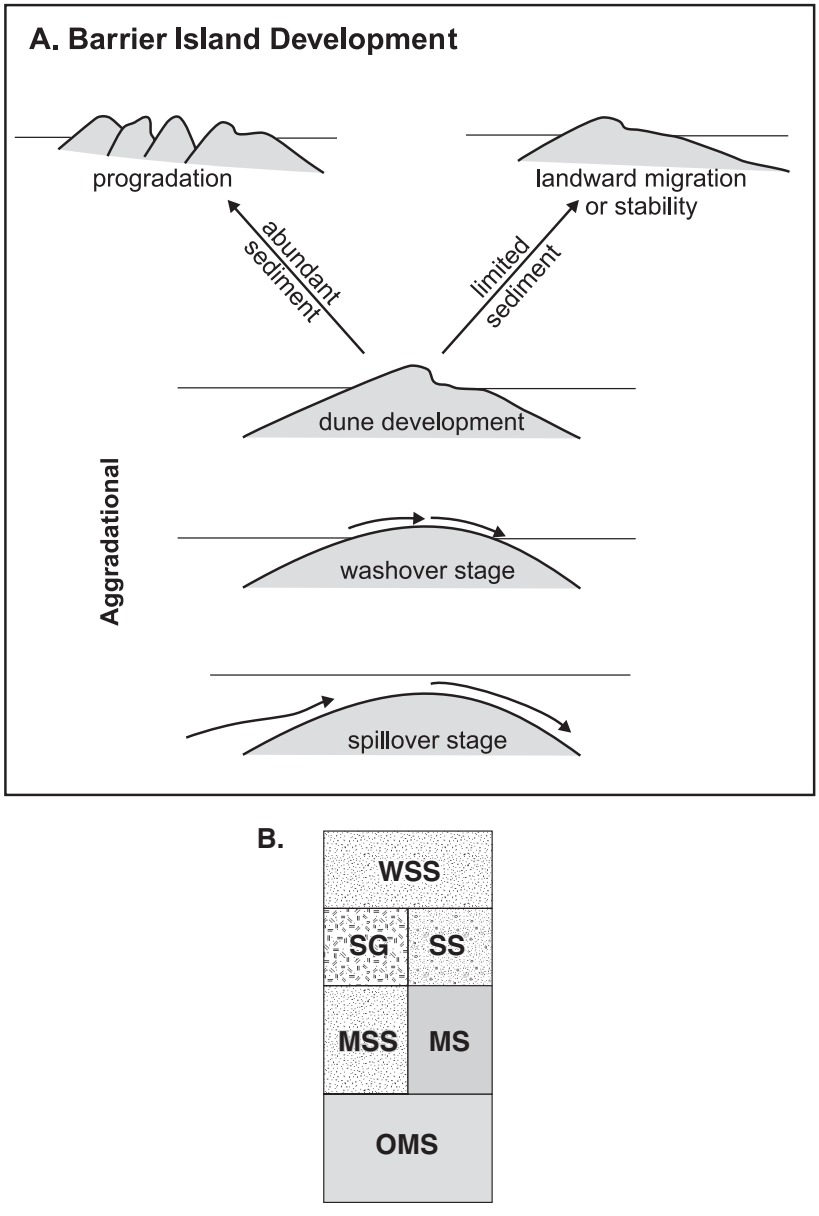

Figure 10.28 Stratigraphic model showing development of barriers on the west coast of the Florida panhandle by shoal aggradation: (A) stages in the evolution of the barriers; (B) simplified stratigraphy of the barriers based on the facies identified by Davis *et al.* (2003). WSS, well sorted sand – modern dune and beach sand. SG, shell gravel – washover channels and inlets; SS, shelly sand – beach and nearshore; MS, muddy sand – low-energy sea grass beds on either side of barrier; MSS, muddy shelly sand – low-energy sea grass beds on either side of barrier; OMS, organic muddy sands – basal Holocene unit with high organic matter content indicative of saltmarsh or mangrove.

increases the width of the barrier system (Figure 10.29). Backbarrier marsh and overwash deposits tend to be deposited in the early phase of progradation but as the island widens the potential for further overwash is diminished. However, disturbance to the relic dune system may lead to the development of migrating parabolic dunes that can cover the older back-barrier sediments and infill the lagoon. This is a characteristic feature of many of the Holocene barrier systems on the coast of New South Wales, Australia (Roy *et al.*, 1994; Hesp and Short, 1999; Harvey, 2006; Goodwin *et al.*, 2006) where evidence of several episodes of dune destabilisation and transgression can often be found. Progradation can occur relatively uniformly along the whole length of a barrier, and this is often the case for baymouth or mid-bay barriers anchored to headlands or the sides of large embayments. It may also be limited to particular

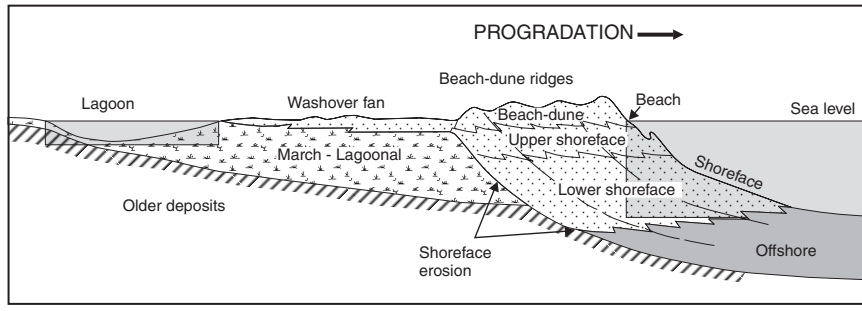

Figure 10.29 Progradation of a barrier island under stable sea level. Beach and dune sands build out across upper and lower shoreface sediments. Backbarrier marsh and washover fan sediments overly lagoonal sediments but development of new foredune ridges reduces the possibility of new overwash occurrence.

areas such as the updrift and downdrift portions of barrier islands adjacent to inlets or the distal portion of barrier spits.

The Holocene transgression resulted in the reworking of sediments deposited on the inner continental shelf by glaciers, rivers and by wave action during falling sea levels at the end of the Wisconsinan glaciation. Much of this is now stored in the form of beach and dune systems, including those associated with barriers, and large amounts are now stranded estuaries, in relic foredune plains and transgressive dune fields. As a result, the sediment supply to many barrier systems is now much lower than it was several hundreds to thousands of years ago and this has the effect of increasing the proportion of barriers that have a negative sediment budget over some or all of their length. The effect of a negative budget locally is to reduce beach width and ultimately to make that particular location more susceptible to overwash (Jiménez and Sánchez-Arcilla, 2004). Barrier islands such as the Isles Derniers and the Chandleur Islands off the Mississippi delta that are now largely detached from their sediment supply are rapidly thinning through loss of sediment at the margins of chain and divided into smaller and smaller islands through overwash and inlet formation (Penland *et al.*, 1988). Where barriers are supplied primarily through longshore sediment transport, reduced supply may lead to transgression across the backbarrier and lagoon, ultimately resulting in welding of the barrier to the mainland.

Sea level rise

Most modern barriers were initiated during the Holocene transgression somewhere on the continental shelf. Ideally, rising sea level leads to a continual transfer of sediments from the seaward side of the barrier to the landward side, building a base upon which the dune system can migrate inland and upward (Figure 10.30a). Sediment transfers can take place through three primary mechanisms: (1) transfers through the tidal inlets into the lagoon system through the building of flood tidal delta shoals and sedimentary deposits within the lagoon itself; (2) overwash of sediments onto the back barrier and into the lagoon; and (3) aeolian sediment transport either directly over the foredune crest onto the lee slope and beyond, or through the development of blowouts and parabolic dunes. All three mechanisms may occur within one barrier system but the relative contribution of each is highly variable from one barrier system to another. Infilling of the lagoon is counterbalanced by rising sea level, leading to flooding of the coastal plain landward and so all segments of the barrier migrate landward synchronously. There is some room here for dynamic equilibrium with the rate of sea level rise because a higher rate of sea level rise triggers greater erosion of the foredune ridge system and therefore increases the rate of landward transfers. Ultimately there may be limited recovery from overwash before another series of events occurs and this sets an upper limit for the ability of the system to adjust.

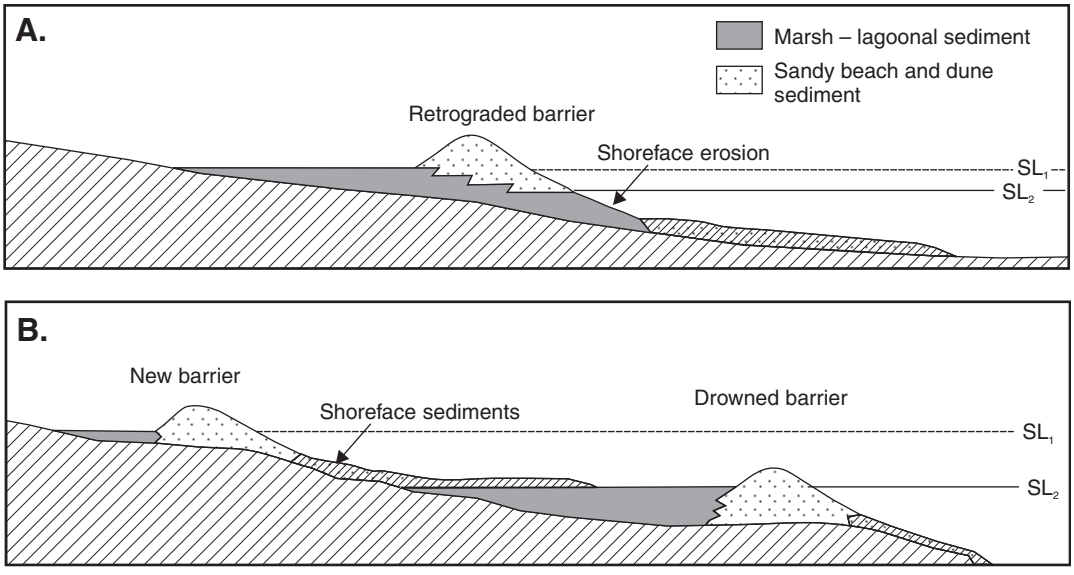

Figure 10.30 Transgression of a barrier island due to sea level rise: (A) rising sea level leads to landward migration of the beach and dune system and reworking of the inner shoreface. The barrier overrides marsh and lagoon sediments which are later eroded as they become exposed at the seaward side; (B) if sea level rises too quickly or there is insufficient sediment in the system then the barrier may be drowned leaving portions of the barrier and lagoon sediments stranded on the continental shelf.

If the rate of sea level rise is faster than landward transfer of sediment can occur, the barrier will become completely overwashed and the subaerial and inner shoreface sediments will be smeared across the marsh and lagoon sediments. These sediments are then preserved on the continental shelf (Figure 10.30b). There is evidence for drowned barrier sediments, rather than preserved barriers, in a number of areas including Australia (Roy *et al.*, 1994) and the east coast of the USA (Swift, 1975). Actual barrier overstepping as proposed by Rampino and Sanders (1980) among others, probably requires a very rapid sea level rise in order to preserve the subaerial components of the system intact but examples have been suggested, for example, for the northern Adriatic shelf off Italy (Storms *et al.*, 2008).

There is a growing body of literature on the potential acceleration of barrier erosion and migration as a result of increased rates of sea level rise and attempts to model this on a decadal scale (Dean and Maurmeyer, 1983; Dubois, 1995; Eitner, 1996; List *et al.*, 1997; Moore *et al.*, 2007; FitzGerald *et al.*, 2008). Dean and Maurmeyer adapted the Bruun Rule for the special case of a barrier island and their model allowed for overwash and inlet transfers. While some authors still favour this simple approach (Zhang *et al.*, 2004) others have suggested that response to sea level rise is more complex (Cooper and Pilkey, 2004). On a longer time-scale, the morphological behaviour model of Cowell *et al.* (1995) provides an alternative approach and this approach has been utilised in a number of recent papers (Stolper *et al.*, 2005; Moore *et al.*, 2007).

10.6 Management of barrier systems

Stable and progradational baymouth and midbay barriers in areas where there is sufficient sediment supply to counteract present rates of sea level rise pose relatively few problems for the management of human activities. The stability of the system means that there should be no need for shore protection, and the relatively simple setback and access restrictions designed for the management of coastal dunes (see Section 9.8.1) should be sufficient to prevent large-scale destabilisation and parabolic dune

development. Transgressive barrier islands and barrier spits pose much more of a problem for human activities, especially for the control of inlets for navigation purposes and development of housing, roads and other infrastructure.

We have touched on the problems posed by jetty construction and dredging at inlets in Section 7.4.1. Jetties tend to trap sediment on the updrift side and thus pose a problem for erosion of the downdrift side. Channel dredging below the level that can be maintained by tidal flow through the inlet results in rapid infilling by wave and tidal currents and necessitates ongoing dredging as well as the need for a plan for disposal of the dredged material.

Building of recreational homes, permanent residences, apartments and service facilities on barrier islands and barrier spits that are transgressive under rising sea level poses major problems for coastal managers. The greatest threat to property and human life comes from intense storms which result in significant storm surge and high wave activity. It is possible to stabilise portions of barriers for some period of time using seawalls and/or beach nourishment and this may act to protect property from flooding and overwash during some storms, but ultimately under a negative sediment budget or rising sea level the barrier needs to retreat. There are now numerous examples of the folly of building on transgressive barrier systems on the US east and Gulf coasts in the face of severe northeasters or hurricanes. Pictures of a section of barrier north of Galveston before and after Hurricane Ike struck the region on September, 2008 provide dramatic evidence of the extent of devastation caused by overwash, even to buildings constructed on stilts to allow water to flow beneath them (Figure 10.31). Similar destruction of houses on a barrier can occur with strong midlatitude storms. The storm on 2 December 1985 destroyed about 80 houses and cottages along a stretch of shoreline on the proximal end of Long Point (Figure 10.32).

Figure 10.31 Pair of oblique aerial photographs of a portion of the barrier north east of Galveston, Texas showing destruction in the wake of landfall by Hurricane Ike on 13 September 2008 (photographs courtesy of US Geological Survey).

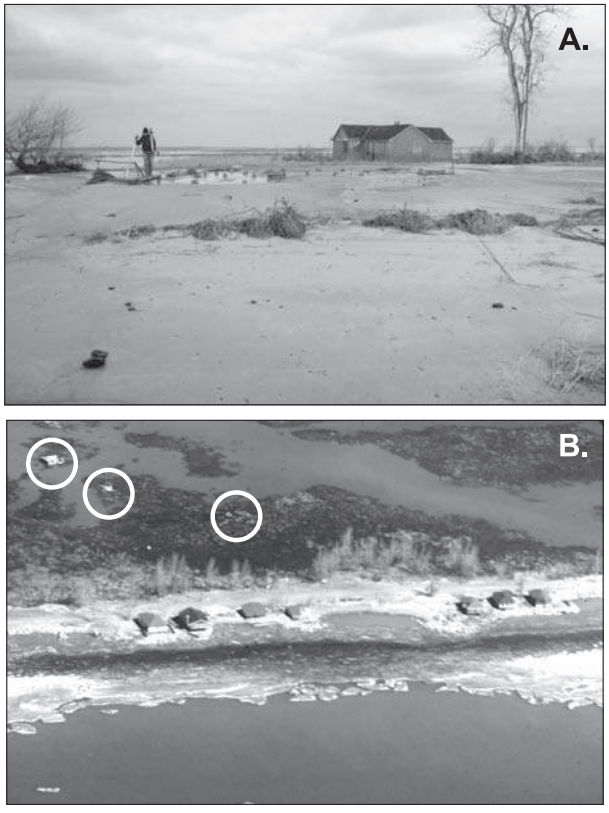

Figure 10.32 Destruction in the wake of an intense storm on 2 December 1985 along the proximal end of Long Point. (A) Overwash resulted in the destruction of the foredune. The cottage behind it was lifted off its foundations and carried it 75 m into the backbarrier marsh; (B) destruction of cottage along Hastings Drive. The circles indicate the location of houses that were transported into the marsh.

The US barrier coasts have been hit by a series of severe hurricanes in the past few years (e.g., Fritz *et al.*, 2007; Froede, 2008) and the extent of the losses has resulted in insurance companies refusing to insure against damage due to wave action and flooding associated with severe storms (H. John Heinz III Center for Science, Economics and the Environment, 2000). It has also resulted in changes to the operation of the Federal Emergency Measures Agency (FEMA) to attempt to force states to prohibit rebuilding within designated hazard zones by withdrawing funding to support this.

References

Allard, J., Bertin, X., Chaumillon, E. and Pouget, F. 2008. Sand spit rhythmic development: A potential record of wave climate variations? Arçay spit, western coast of France. *Marine Geology*, **253**, 107–131.

Anthony, E. J. and Blivi, A. B. 1999. Morphosedimentary evolution of a delta-sourced, drift-aligned sand barrier-lagoon complex, western Bight of Benin. *Marine Geology*, **158**, 161–176.

Armitage, S. J., Botha, G. A., Duller, G. A. T., Wintle, A. G., Rebêlo, L. P. and Momade, F. J. 2006. The formation and evolution of the barrier islands of Inhaca and Bazaruto, Mozambique, *Geomorphology*, **82**, 295–308.

Ashley, G. M. 1987. Assessment of the hydraulics and longevity of Wood End Cut (inlet), Cape Cod, Massachussetts, USA. *Journal of Coastal Research*, **3**, 281–295.

Bertin, X., Chaumillon, E., Sottolichio, A. and Pederos, R. 2005. Tidal inlet response to sediment infilling of the associated bay and possible implications of human activities: the Marennes-Oléron Bay and the Maumusson Inlet, France. *Continental Shelf Research*, **25**, 1115–1131.

Bowman, D. and Pranzini, E. 2004. Reversed responses within a segmented detached breakwater, the Tuscany coast, Italy – a case study. *Coastal Engineering*, **49**, 263–274.

Bray, T. F. and Carter, C. H. 1992. Physical processes and sedimentary record of a modern, transgressive, lacustrine barrier island. *Marine Geology*, **105**, 155–168.

Bruun, P. 1978. *Stability of Tidal Inlets: Theory and Engineering*. Elsevier, Amsterdam, 506 pp.

Claudino-Sales, V., Wang, P. and Horwitz, M. H. 2008. Factors controlling the survival of coastal dunes during multiple hurricane impacts in 2004 and 2005: Santa Rosa barrier island, Florida. *Geomorphology*, **95**, 295–315.

Cleary, W. J. and Hosier, P. E. 1979. Geomorphology, washover history, and inlet zonation: Cape Lookout, N.C. to Bird Island, N. C., In Leatherman, S. P. (ed.) *Barrier Islands: from the Gulf of St. Lawrence to the Gulf of Mexico*. Academic, New York, pp. 237–271.

Coakley, J. P. 1976. The formation and evolution of Pt. Pelee, western Lake Erie. *Canadian Journal of Earth Sciences*, **13**, 136–144.

Coakley, J. P. 1992. Holocene transgression and coastal landform evolution in northeastern Lake Erie, Canada. In Fletcher, C. H. lll and Wehmiller, J. F. (eds.), *Quaternary Coasts of the United States: Marine and Lacustrine Systems*. Society of Economic Paleontologists and Mineralogists, Special Publication 48, 415–426.

Cooper, J. A. G., 1994. Lagoons and microtidal coasts. In Carter, R. W. G. and Woodroffe, C. D. (eds.), *Coastal Evolution*. Cambridge University Press, Cambridge, pp. 219–265.

Cooper J. A. G. and Pilkey, O. H. 2004. Sea level rise and shoreline retreat: time to abandon the Bruun rule. *Global and Plantetary Change*, **43**, 157–71.

Cowell P. J., Roy P. S. and Jones R. A. 1995. Simulation of large-scale coastal change using a morphological behaviour model. *Marine Geology*, **126**, 46–61.

Davidson-Arnott, R. G. D. and Fisher, J. D. 1992. Spatial and temporal controls on overwash occurrence on a Great Lakes barrier spit. *Canadian Journal of Earth Sciences*, **29**, 102–117.

Davidson-Arnott, R. G. D. and Conliffe Reid, H. E. 1994. Sedimentary processes and the evolution of the distal bayside of Long Point, Lake Erie. *Canadian Journal of Earth Sciences*, **31**, 1461–1473.

Davidson-Arnott, R. G. D. and van Heyningen, A. 2003. Migration and sedimentology of longshore sandwaves, Long Point, Lake Erie, Canada. *Sedimentology*, **50**, 1123–1137.

Davis, R. A. Jr., Yale, K. E., Pekala, J. M. and Hamilton, M. V. 2003. Barrier island stratigraphy and Holocene history west-central Florida. *Marine Geology*, **200**, 103–123.

Dean, R. G. and Maurmeyer, E. M. 1983. Models for beach profile responses. In Komar, P. D. (ed.), *Handbook of Coastal Processes and Erosion*. CRC Press, Boca Raton, FL, pp. 151–166.

de Boer, G. 1964. Spurn Head: its history and evolution. *Transactions of the Institute of British Geographers*, **34**, 71–89.

Dillon, W. P. 1970. Submergence effects on a Rhode Island barrier and lagoon and inferences on migration of barriers. *Journal of Geology*, **78**, 94–106.

Dolan, R. and Hayden, B. 1981. Storms and shoreline configuration. *Journal of Sedimentary Petrology*, **51**, 737–744.

Donnelly, C., Kraus, N. and Larson, M. 2006. State of knowledge of modeling of coastal overwash. *Journal of Coastal Research*, **22**, 965–991.

Dubois R. N. 1995. The transgressive barrier model: an alternative to two-dimensional volume balanced models. *Journal of Coastal Research*. **11**, 272–286.

Eitner, V. 1996. Geomorphological response of the East Friesian barrier islands to sea level rise: an investigation of past and future evolution. *Geomorphology*, **15**, 57–65.

Fiechter, J., Steffen, K. L., Mooers, C. N. K. and Haus, B. K. 2006. Hydrodynamics and sediment transport in a southeast Florida tidal inlet. *Estuarine, Coastal and Shelf Science*, **70**, 297–306.

Fisher, J. J. 1968. Barrier island formation: discussion. *Geological Society of America Bulletin*, **79**, 1421–1426.

FitzGerald, D. M., 1996. Geomorphic variability and morphologic and sedimentologic controls on tidal inlets. *Journal of Coastal Research*, **S.I. 23**, 47–71.

FitzGerald, D. M. and FitzGerald, S. A. 1977. Factors influencing tidal inlet throat geometry. *Coastal Sediments '77*, ASCE, 563–571.

FitzGerald, D. M., Fenster, M. S., Argow, B. A. and Buynevich, I. V. 2008. Coastal impacts due to sea-level rise. *Annual Review of Earth and Planetary Sciences*, **36**, 601–647.

Flinn, D. 1997. The role of wave diffraction in the formation of St. Ninian's Ayre in Shetland, Scotland. *Journal of Coastal Research*, **13**, 202–208.

Forbes, D. L. and Solomon S. M. 1999. Inlet division and coastal instability following tidal prism diversion. *Proceedings Coastal Sediments '99*. ASCE, pp. 1418–1433.

Forbes, D. L., Taylor, R. B., Orford, J. D., Carter, R. W. G. and Shaw, J. 1991. Gravel-barrier migration and overstepping. *Marine Geology*, **97**, 305–313.

Forbes, D. L., Parkes, G. S., Manson, G. K. and Ketch, L. A. 2004. Storms and shoreline retreat in the southern Gulf of St. Lawrence. *Marine Geology*, **210**, 169–204.

Fritz, H. M., Blount, C., Sokoloski, R. and six others, 2007. Hurricane Katrina storm surge distribution and field observations on the Mississippi

Barrier Islands. *Estuarine, Coastal and Shelf Science*, **74**, 12–20.

Froede, C. R. Jr. 2008. Changes to Dauphin Island, Alabama, brought about by Hurricane Katrina (August 29, 2005). *Journal of Coastal Research*, **24**, 110–117.

Gilbert, G. K. 1890. *Lake Bonneville*. U.S. Geological Survey Monograph vol. **1**, 438 pp.

Godfrey, P. J. and Godfrey, M. M. 1973. Comparison of ecological and geomorphic interactions between altered and unaltered barrier island systems in North Carolina. In Coates, D. R. (ed.), *Coastal Geomorphology*, Publications in Geomorphology, SUNY, New York, pp. 239–258.

Goodwin, I. D., Stables, M. A. and Olley, J. M. 2006. Wave climate, sand budget and shoreline alignment evolution of the Iluka–Woody Bay sand barrier, northern New South Wales, Australia, since 3000 yr BP. *Marine Geology*, **226**, 127–144.

Greenwood, B and Keay, P. A., 1979. Morphology and dynamics of a barrier breach: a study in stability. *Canadian Journal of Earth Sciences*, **16** 1533–1546.

Heinz, H. John III Center for Science, Economics and the Environment 2000. *The Hidden Costs of Coastal Hazards*. Island Press, Washington, DC, 220 pp.

Harvey, N. 2006. Holocene coastal evolution: Barriers, beach ridges, and tidal flats of South Australia. *Journal of Coastal Research*, **22**, 90–99.

Hayes, M. O. 1967. Hurricanes as geological agents, south Texas coast. *American Association of Petroleum Geologists Bulletin*, **51**, 937–942.

Hayes, M. O. 1979. Barrier island morphology as a function of tidal and wave regime. In Leatherman S. P. (editor), *Barrier Islands: from the Gulf of St. Lawrence to the Gulf of Mexico*, Academic, New York, 1–27.

Hayes, M. O. 1980. General morphology and sediment patterns in tidal inlets. *Sedimentary Geology*, **28**, 139–156.

Héquette, A. and Ruz, M. H. 1991. Spit and barrier island migration in the Southeastern Canadian Beaufort Sea. *Journal of Coastal Research*, **7**, 677–698.

Hesp, P. A. and Short, A. D. 1999. Barrier morphodynamics. In Short, A. D. (ed.), *Handbook of Beach and Shoreface Morphodynamics*. Wiley, Chichester, pp. 307–333.

Hill, M. C. and Fitzgerald, D. M. 1992. Evolution and Holocene stratigraphy of Plymouth, Kingston and Duxbury Bays, Massachusetts. In Fletcher, C. H. lll and Wehmiller, J. F. (eds.), *Quaternary Coasts of the United States: Marine and Lacustrine Systems*. Society of Economic Paleontologists and Mineralogists, Special Publication 48, 45–56.

Holland, T. L. 2005. *Landscape Changes in a Coastal Lagoon System*, Jalisco, Mexico: Implications for Barra de Navidad Lagoon. *M.Sc. Thesis*, Universityof Guelph, 114 pp.

Houser, C., Hapke, C. and Hamilton, S. 2008. Controls on coastal dune morphology, shoreline erosion and barrier island response to extreme storms. *Geomorphology*, **100**, 223–240.

Hoyt, J. H. 1967. Barrier island formation. *Geological Society of America Bulletin*, **79**, 1125–1136.

Jewell, P. 2007. Morphology and paleoclimatic significance of Pleistocene Lake Bonneville spits. *Quaternary Research*, **68**, 421–430.

Jiménez, J. A. and Sánchez-Arcilla, A 2004. A long-term (decadal scale) evolution model for microtidal barrier systems. *Coastal Engineering*, **51**, 749–764.

Jol, H. M., Lawton, D. C., and Smith, D. G. 2003. Ground penetrating radar: 2-D and 3-D subsurface imaging of a coastal barrier spit, Long Beach, WA, USA. *Geomorphology*, **53**, 165–181.

Kjerfve, B. 1986. Comparative oceanography of coastal lagoons. In Wolfe, D. A. (ed.), *Estuarine Variability*. Academic, New York, pp. 63–81.

Kjerfve, B. and Magill, K. E. 1989. Geographic and hydrodynamic characteristics of shallow coastal lagoons. *Marine Geology*, **88**, 187–199.

Kragtwijk, N. G., Zitman, T. J., Stive, M. J. F. and Wang, Z. B. 2004. Morphological response of tidal basins to human interventions. *Coastal Engineering*, **51**, 207–221.

Kriebel, D. L. and Dean, R. G. 1985. Numerical simulation of time-dependent beach and dune erosion. *Coastal Engineering*, **9**, 221–245.

Kumar, N. and Sanders, J. E. 1974. Inlet sequence: a vertical succession of sedimentary structures and textures created by the lateral migration of tidal inlets. *Sedimentology*, **21**, 491–532.

Larson, M., Erikson, L. and Hanson, H. 2004. An analytical model to predict dune erosion due to wave impact. *Coastal Engineering*, **51**, 675–696.

Leatherman, S. P. 1976. Barrier island dynamics: Overwash processes and aeolian transport. *Proceedings of the Coastal Engineering Conference*, ASCE, pp. 1958–1974.

Leatherman, S. P. 2003. Shoreline change mapping and management along the US East Coast. *Journal of Coastal Research, SI* **38**, 5–13.

Leatherman, S. P., Williams, A. T. and Fisher, J. S. 1977. Overwash sedimentation associated with a large-scale northeaster. *Marine Geology*, **24**, 109–121.

List, J. H., Sallenger, A. H.Jr., Hansen, M. E. and Jaffe, B. E. 1997. Accelerated sea-level rise and rapid coastal

erosion: testing a causal relationship for the Louisiana barrier islands. *Marine Geology*, **140**, 347–365.

Long, A. J., Waller, M. P. and Plater, A. J. 2006. Coastal resilience and late Holocene tidal inlet history: The evolution of Dungeness Foreland and the Romney Marsh depositional complex (UK). *Geomorphology*, **82**, 309–336.

Mäkinen, J. and Räsänen, M. 2003. Early Holocene regressive spit-platform and nearshore sedimentation on a glaciofluvial complex during the Yoldia Sea and the Ancylus Lake phases of the Baltic Basin, SW Finland. *Sedimentary Geology*, **158**, 25–56.

Mariner, N., Goiran, J. P. and Morhange, C. 2008. Alexander the Great's tombolos at Tyre and Alexandria, eastern Mediteranean. *Geomorphology*, **100**, 377–400.

Mathew, S. 2007. *Quantifying Coastal Evolution Using Digital Photogrammetry*. Ph.D. Thesis, University of Guelph, 220 pp.

Matias, A., Ferreira, Ó, Vila-Concejo, A., Garcia, T. and Dias, J. A. 2008. Classification of washover dynamics in barrier islands. *Geomorphology*, **97**, 655–674.

McCann, S. B. 1979. Barrier islands in the southern Gulf of St. Lawrence. In Leatherman S. P. (ed.), *Barrier Islands: from the Gulf of St. Lawrence to the Gulf of Mexico*, Academic, New York, pp. 29–63.

McCubbin, D. G. 1982. Barrier-island and strand plain facies. In Scholle, P. A. and Spearing, D. (eds.), *Sandstone Depositional Environments*. American Association of Petroleum Geologists, Tulsa, Oklahoma, pp. 247–279.

Meistrell, F. J., 1972. The spit-platform concept: laboratory observation of spit development. In Schwartz, M. L. (ed.), *Spits and Bars*. Dowden, Hutchinson and Ross. Stroudsburg, PA, pp. 225–283.

Méndez Linares, A. P., López-Portillo, J., Hernández-Santana, J. R., Ortiz Pérez, M. A. and Oropeza Orozco, O. 2007. The mangrove communities in the Arroyo Seco deltaic fan, Jalisco, Mexico, and their relation with the geomorphic and physical–geographic zonation. *Catena*, **127**, 127–142.

Moore, N. H. and Slinn, D. J. 1984. The physical hydrology of a lagoon system on the Pacific coast of Mexico. *Estuarine, Coastal and Shelf Science*, **19**, 27–42.

Moore L. J., List J. H., Williams, S. J. and Stolper D. 2007. Modeling barrier island response to sea-level rise in the Outer Banks, North Carolina. *Coastal Sediments '07*, **ASCE**, pp. 1153–64.

Morton, R. A. 2002. Factors controlling storm impacts on coastal barriers and beaches – a preliminary basis for real-time forecasting. *Journal of Coastal Research*, **18**, 486–501..

Morton, R. A. and Sallenger, A. H. 2003. Morphological impact of extreme storms on sand beaches and barriers. *Journal of Coastal Research*, **19**, 560–574.

Morton, R. A., Ward, G. H. and White, W. A. 2000. Rates of sediment supply and sea-level rise in a large coastal lagoon. *Marine Geology*, **167**, 261–284.

Moslow, T. F. and Tye, R. S. 1985. Recognition and characteristic of Holocene tidal inlet sequences. *Marine Geology*, **63**, 129–151.

Nichols, M. N. 1989. Sediment accumulation rates and relative sea-level rise in lagoons. *Marine Geology*, **88**, 201–219.

Nielsen, L. H., Johannessen, P. N. and Surlyk, F. 1988. A late Pleistocene coarse-grained spit-platform sequence in northern Jylland, Denmark. *Sedimentology*, **35**, 915–937.

Novak, B. and Pedersen, G. K. 2006. Sedimentology, seismic facies and stratigraphy of a Holocene spit-platform complex interpreted from high-resolution shallow seismics, Lysegrund, southern Kattegat, Denmark. *Marine Geology*, **162**, 317–335.

O'Brien, M. P. 1969. Equilibrium flow areas and inlets on sandy coasts. *Journal of Waterways, Harbors and Coastal Engineering*, **15**, 43–52.

Oertel, G. F., 1985. The barrier island system. *Marine Geology*, **63**, 1–18.

Oertel, G. F. and Overman, K. 2004. Sequence morphodynamics at an emergent barrier island, middle Atlantic coast of North America. *Geomorphology*, **58**, 67–83.

Ollerhead, J. 1993. The evolution of Buctouche Spit, New Brunswick, Canada. Ph.D. Thesis, University of Guelph, 156 pp.

Ollerhead, J. and Davidson-Arnott, R. G. D. 1995. The evolution of Buctouche Spit, New Brunswick, Canada. *Marine Geology*, **124**, 215–236.

Olson, J. S. 1958. Lake Michigan dune development 3. Lake level, beach and dune oscillations. *Journal of Geology*, **66**, 473–483.

Orford, J. D. and Carter, R. W. G. 1984. Mechanisms to account for the longshore spacing of overwash throats on a coarse clastic barrier in southeast Ireland. *Marine Geology*, **56**, 207–226.

Orford, J. D., Jennings, S. and Pethick, J. 2003. Extreme storm effect on gravel dominated barriers. *Proceedings Coastal Sediments '03*, ASCE, 14 pp.

Otvos, E. G. 1981. Barrier island formation through nearshore aggradation–stratigraphic and field evidence. *Marine Geology*, **43**, 195–243.

Otvos, E. G. and Giardino, M. J. 2004. Interlinked barrier chain and delta lobe development, northern Gulf of Mexico. *Sedimentary Geology*, **169**, 47–71,

Owens, E. H. 1974. Barrier beaches and sediment transport in the southern Gulf of St. Lawrence. *Proceedings of the Coastal Engineering Conference*, ASCE, pp. 1177–1193.

Pacheco, A., Vila-Concejo, A., Ferreira, Ó and Dias, J. A. 2008. Assessment of tidal inlet evolution and stability using sediment budget computations and hydraulic parameter analysis. *Marine Geology*, **247**, 104–127.

Park, J. Y. and Wells, J. T. 2007. Spit growth and downdrift erosion: results of longshore transport modelling and morphologic analysis at the Cape Lookout cuspate foreland. *Journal of Coastal Research*, **23**, 553–568.

Penland, S., Boyd, R. and Suter, J. R. 1988. Transgressive depositional systems of the Mississippi Delta plain: a model for barrier shoreline and shelf sand development. *Journal of Sedimentary Petrology*, **58**, 932–949.

Petersen, D., Deigaard, R. and Fredsøe, J. 2008. Modelling the morphology of sandy spits, *Coastal Engineering*, **55**, 671–684.

Pierce, J. W. 1970. Tidal inlets and washover fans. *The Journal of Geology*, **78**, 230–234.

Price, A. J., Miller, D. L. and Branch, L. C. 2008. Identification of structural and spatial features that influence storm-related dune erosion along a barrier-island-island ecosystem in the Gulf of Mexico. *Journal of Coastal Research*, **24**, 168–175.

Rampino, M. R. and Sanders, J. E. 1980. Holocene transgression in south-central Long Island, New York. *Journal of Sedimentary Petrology*, **50**, 1063–1080.

Ranasinghe, R. and Pattiaratchi, C. 1999. The seasonal closure of tidal inlets: Wilson Inlet – a case study. *Marine Geology*, **37**, 37–56.

Roy, P. S., Cowell, P. J., Ferland, M. A. and Thom, B. G. 1994. Wave-dominated coasts. In Carter, R. W. G. and Woodroffe, C. D. (eds.), *Coastal Evolution*. Cambridge University Press, Cambridge, **517** pp.

Reinson, G. E., 1977. Tidal-current control of submarine morphology at the mouth of the Miramichi estuary, New Brunswick. *Canadian Journal of Earth Sciences*, **14**, 2524–2532.

Robertson, W. V, Zhang, K. and Whitman, D. 2007. Hurricane-induced beach change derived from airborne laser measurements near Panama City, Florida. *Marine Geology*, **237**, 191–205.

Sallenger, A. H. 2000. Storm impact scale for barrier islands. *Journal of Coastal Research*, **16**, 890–895.

Sanderson, P. G. and Elliot, I. 1996. Shoreline salients, cuspate forelands and tombolos on the coast of western Australia. *Journal of Coastal Research*, **12**, 761–773.

Sanderson, P. G., Eliot, I., Hegge, B. and Maxwell, S. 2000. Regional variation of coastal morphology in southwestern Australia: a synthesis. *Geomorphology*, **34**, 73–88.

Schwartz, M. L. 1971. The multiple causality of barrier islands. *Journal of Geology*, **79**, 91–94.

Schwartz, R. K. 1975. *Nature and Genesis of some Storm Washover Deposits*, US Army Corps of Engineers, Coastal Engineering Research Centre, Technical Memorandum 61, 67 pp.

Seabergh, W. C. 2006. Hydrodynamics of tidal inlets. Coastal Engineering Manual 1110–2–1100, US Army Corps of Engineers, Chapter II-6, 79 pp.

Sedgwick, P. E. and Davis, R. A. Jr. 2003. Stratigraphy of washover deposits in Florida: implications for recognition in the stratigraphic record. *Marine Geology*, **200**, 31–48.

Silvester, R. and Hsu, J. 1993. *Coastal Stabilisation: Innovative Concepts*, Prentice-Hall, Englewood Cliffs, NJ, 578 pp.

Simeoni, U., Fontolan, G., Tessari, U. and Corbau, C. 2007. Domains of spit evolution in the Goro area, Po Delta, Italy, *Geomorphology*, **86**, 332–348.

Soons, J. M., Schulmeister, J. and Holt, S. 1997. The Holocene evolution of a well nourished gravelly barrier and lagoon complex, Kaitorete 'Spit', Canterbury, New Zealand. *Marine Geology*, **138**, 69–90.

Stockdon, H. F., Sallenger, A. H., Holman, R. and Howd, P. A. 2007. A simple model for the spatially-variable coastal response to hurricanes. *Marine Geology*, **238**, 1–20.

Stolper D., List J. H. and Thieler, E. R. 2005. Simulating the evolution of coastal morphology and stratigraphy with a new morphological-behaviour model (GEOMBEST). *Marine Geology*, **218**, 17–36.

Storms, J. E. A., Weltje, G. J., Terra, G. J., Cattaneo, A. and Trincardi, F. 2008. Coastal dynamics under conditions of rapid sea-level rise: Late Pleistocene to early Holocene evolution of barrier–lagoon systems on the northern Adriatic shelf (Italy). *Quaternary Science Reviews*, **27**, 1107–1123.

Swift, D. J. P. 1975. Barrier island genesis: evidence from the central Atlantic Shelf, eastern U.S.A. *Sedimentary Geology*, **14**, 1–43.

Switzer, A. D. and Jones, B. G. 2008. Setup, deposition and sedimentary characteristics of two storm overwash deposits, Abrahams Bosom Beach, southeastern Australia. *Journal of Coastal Research*, **24**, 189–200.

Tomazelli, L. and Dillenburg, S. 2007. Sedimentary facies and stratigraphy of a last interglacial coastal barrier in south Brazil. *Marine Geology*, **244**, 33–45.

van Heteren, S., FitzGerald, D. M., Barber, D. C., Kelley, J. T. and Belknap, D. F. 1996. Volumetric analysis of a New England barrier system using Ground-Penetrating-Radar and coring techniques. *The Journal of Geology*, **104**, 471–483.

Vila-Concejo, A., Ferreira, Ó., Matias, A. and Dias, J. M. A. 2003. The first two years of an inlet: sedimentary dynamics. *Continental Shelf Research*, **23**, 1425–1445.

Wang P. and Horowitz, M. H. 2007. Erosional and depositional characteristics of regional overwash deposits caused by multiple hurricanes. *Sedimentology*, **54**, 545–564.

Zenkovitch, V. P. 1967. *Processes of Coastal Development*. Oliver and Boyd, Edinburgh, 738 pp.

Zhang K, Douglas B. C. and Leatherman, S. P. 2004. Global warming and coastal erosion. *Climate Change*, **64**, 41–58.

11

Saltmarshes and mangroves

11.1 Synopsis

Saltmarshes and mangroves are wetlands formed in the intertidal zone of sheltered coasts, notably in bays, lagoons and estuaries. The vegetation of the two environments is quite different: mangroves are composed of a number of tree species, while saltmarshes are dominated by grasses and herbs. Mangroves are confined to the tropics and the lower latitudes of the sub-tropics, and are the dominant intertidal vegetation in these regions. Saltmarshes are found throughout the mid- and high latitudes and may also occur in some areas in the tropics. Plants of both ecosystems are salt-tolerant because they are frequently inundated by salt water and they are also adapted to growing under anaerobic conditions. The stress imposed by frequent inundation and waterlogged soils generally produces a gradient with one or two species dominating at lower levels and species richness increasing towards the high intertidal and beyond as the frequency of inundation decreases.

The movement of tidal waters across both mangroves and saltmarshes results in the development of tidal creek systems which act to move water, sediments and organic matter into and out of the systems. The vegetation of mangrove swamps and saltmarshes act to reduce wave action and the speed of tidal currents, thus promoting deposition of fine material. Vertical accretion in both environments ranges from a few millimetres a year to several centimetres and includes both organic material and mineral grains. However, net vertical accretion over decades is generally much less because of compaction of sediments and loss of some of the carbon from roots and leaf litter.

Both ecosystems are highly productive and act to support a wide range of fish, shellfish, migratory birds and animals both within the environment and in the surrounding waters. While both ecosystems may be under stress from sea level rise, the greatest impact on them has come from a wide range of human activities, including dyking and drainage of saltmarshes for agriculture, which lead to physical destruction of the natural vegetation. The building of dykes and embankments may enhance the potential effects of sea level rise through inhibiting landward movement – termed coastal squeeze.

11.2 Saltmarsh and mangrove ecosystems

Saltmarshes and mangroves are types of halophytic wetland ecosystem that are found along marine coasts (Adam, 1990; Robertson and Alongi, 1992; Hogarth, 1999; Mitsch and Gosselink, 2000). They are found in the upper intertidal zone in areas that are sheltered from high wave action, which in turn permits the establishment of vegetation communities. Because they occupy a zone of transition between terrestrial and marine ecosystems, marshes and mangroves play a critical role in

Figure 11.1 View across a typical backbarrier saltmarsh, Skallingen Spit, Denmark showing the low surface gradient on the saltmarsh platform and a small tidal creek draining the marsh in the foreground. The marsh is about 1500 m wide at this location and the dunes marking the seaward margin of the barrier can be seen in the background. The marsh began forming about 100 years ago with colonisation of backbarrier overwash sediments and the development of a tidal creek network (Bartholdy *et al*., 2004). Herbaceous vegetation that characterises the low marsh is dominantly *Pucinellia maritima* and *Suaedia maritima*.

sediment exchange with adjacent mudflats, estuaries and open coastal waters and with sediments transported from uplands to the coast. Fine sediment accretion is not necessary per se for the establishment of mangrove or saltmarsh communities, but standing biomass leads to the rapid attenuation of waves and currents capable of importing coarse sediment (sand and gravel) and thus it promotes the deposition, and particularly the retention of fine sediment and organic matter. Saltmarshes and mangroves thus act as sinks for fine sediments that are brought in by the tidal waters and for the accumulation of organic matter (Gordon *et al*., 1985; Woodroffe, 1992). As a result, they also act as a sink for contaminants (Scrimshaw *et al*., 1996; Kostaschuk *et al*., 2008).

Rapid vertical accretion can occur in locations where there is an abundant supply of fine sediment (e.g. in estuaries and river deltas), producing a dominantly minerogenic deposit. However, where there is much less fine sediment available, accretion is predominantly from organic material such as roots, leaves and stems, and the resulting deposit is dominantly organogenic. Both saltmarshes and mangroves develop on nearly horizontal or gently sloping platforms with tidal creeks providing a conduit for the flow of water into and out of the zone (Figure 11.1). A significant fraction of inundation may occur from water coming across the marsh or mangrove margin, and in some cases this may be more important than that supplied from tidal creeks. Drainage may be restricted over portions of the surface while some areas near the landward margin may be inundated only a few times a year during extreme astronomical tides and/or storm surge events.

Saltmarshes are vegetated by grasses, herbs and small shrubs and are found throughout the middle and high latitudes Figure 11.2a). Mangroves, in contrast, are primarily woody trees and shrubs that are almost exclusively tropical (Figure 11.2b) though their range does extend into the sub-tropics (Hogarth, 1999). Mangrove communities are the predominant intertidal plant association in tropical intertidal zones, though small areas of saltmarsh may also be found. Areas of saltmarsh and mangrove development include river mouths, estuaries, drowned river valleys and deltas, back barrier lagoons and bays, natural embayments, and sheltered areas behind islands and coral reefs (Kelley *et al*., 1995; Allen and Pye, 1992; Woodroffe, 1992; Luternauer *et al*., 1995; Hogarth, 1999). Mangroves in particular may develop on open coasts where wave energy is dissipated over a wide shallow nearshore along deltas and muddy shorelines such as those of Guyana and major river deltas in Asia such as those of the Ganges and Mekong.

The vegetation of both saltmarshes and mangroves is adapted to three major forms of stress: high levels of salinity; inundation for periods of hours (and sometimes days or weeks in the case of mangroves in some locations); and waterlogged and anaeorobic soils. In general, these stress levels are highest at the seaward margins of marsh or mangrove communities where inundation periods are longest and most frequent,

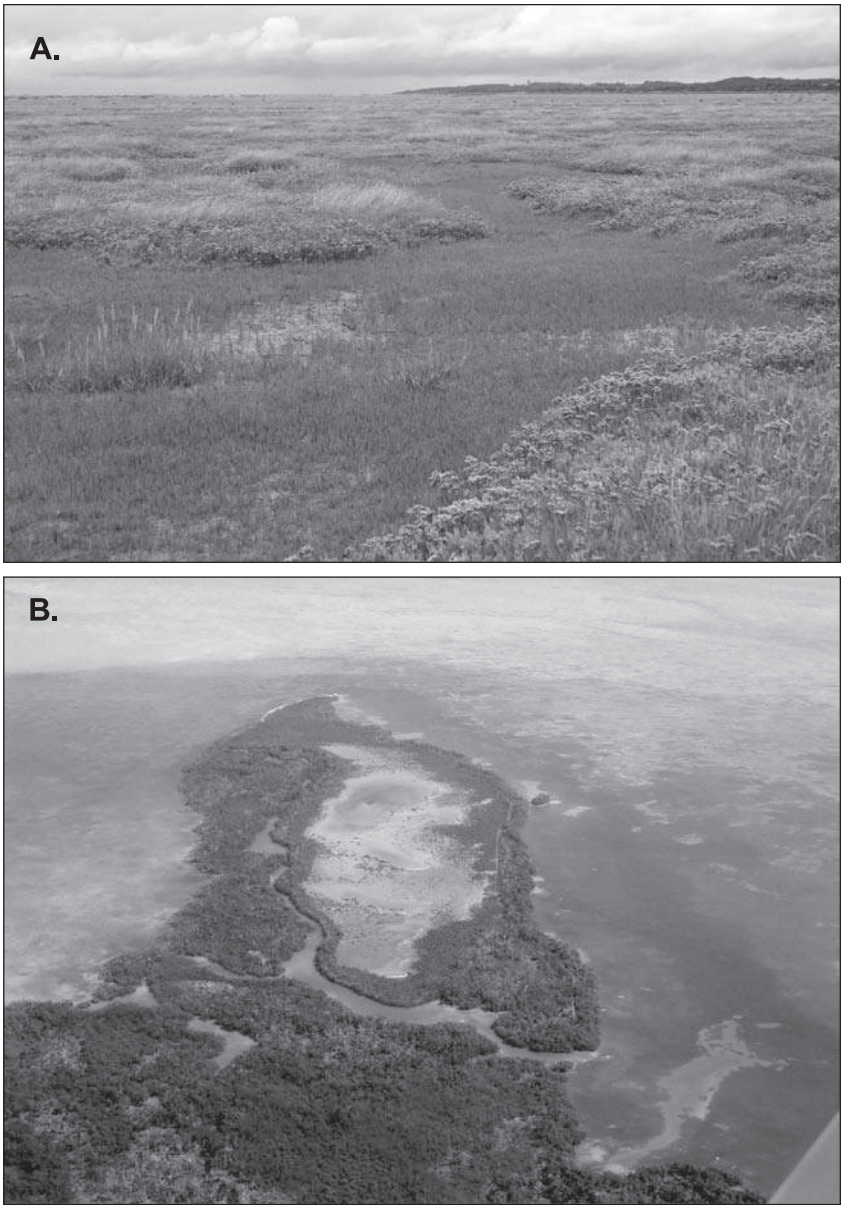

Figure 11.2 Vegetation of saltmarshes and mangroves: (A) view eastward with the sea to the left of the upper marsh at Stiffkey, North Norfolk. The elevation of the marsh platform here is about 2.7 m OD, which is close to MHWS. The lower areas are revegetated pans dominated by *Salicornia europaea*, with a few patches of *Spartina anglica*. The slightly higher areas around the panne are covered mainly by *Limonium vulgare* (purple flowers) and *Atriplex portulaciodes*, with some *Puccinellia maritima*. (photo Helene Burningham); (B) oblique aerial view of mangroves fringing the landward side of the lagoon behind the Belize barrier reef. mangroves occupy the mainland coast at the bottom of the picture and the margins of a small coral cay. The centre of the cay is largely bare of mangroves, possibly because of insufficient nutrient supply or excessive salinity.

and consequently there may be more waterlogging. This tends to produce a zonation of plant species parallel to the shoreline, with dominance of a few species close to the margin where stress levels are generally highest, and increasing diversity towards higher ground. However, evaporation of sea water from areas such as pannes on saltmarshes or enclosed

lagoons can produce salinities that are much higher than the 30–35‰ in seawater and local reversal of the zonation trend or the complete die back of vegetation can occur. At a small scale greater diversity is produced by small topographic irregularities that lead to improved or reduced drainage, by proximity to tidal creeks and by changes in local substrate or slope. Where saltmarshes and mangroves occur in the upper reaches of estuaries, along deltaic distributaries and in some closed lagoons, they may also be subject to periods where the water has a very low salinity. Saltmarshes can grade into tidal freshwater marshes inland or upriver and mangrove communities give way to other forest or herb communities that can survive inundation by fresh or brackish water.

Saltmarshes and mangroves are generally areas of high primary productivity. Decaying organic matter provides the beginning of a complex food chain that exists both within the marsh or mangrove community, and in the adjacent tidal flats and lagoon or estuarine waters to which organic matter is exported during ebb tides (Gordon *et al.*, 1985; Alongi, 1998). Most of the net primary productivity of mangroves comes from above the ground whereas the below-ground contribution of saltmarsh grasses may be 1.5 times that of the above-ground component (Alongi, 1998, p. 48). Mangroves and saltmarshes provide shelter for juvenile fish, and tidal mudflats (and some mangroves) support large populations of shellfish. Tidal creeks, and mudflats are staging and wintering habitats for a wide variety of shorebirds and waterfowl, and mangrove forests support a rich fauna. Both marshes and mangroves have supported a wide range of subsistence or harvesting activities and both have suffered destruction in the face of human actions such as drainage for intensive agriculture (including shrimp farming in tropical areas), construction of housing, port and navigation facilities, as well as utilities such as power plants. Recognition of the valuable role they play ecologically as well as their potential role as a buffer against storms and tsunamis, sea level rise and siltation of coral reefs has stimulated increased research into the biology and geomorphology of saltmarshes and mangroves and to the incorporation of their preservation as a significant component of integrated coastal management.

11.3 Salt marshes

Coastal saltmarshes form in the upper intertidal zone in latitudes ranging from the Arctic to the sub-tropics, and consequently they develop under a wide range of climatic conditions. There are extensive saltmarshes in the Arctic through Alaska, Canada, Russia and Scandinavia with the most extensive areas being in southern Hudson Bay and James Bay. They are found in the mid-latitudes throughout eastern and western North America, Western Europe and the Mediterranean, the East Asian coasts of Japan and Korea, as well as on the southern coasts of Australia, New Zealand, Argentina and Chile. Extensive saltmarsh systems on the east coast of North America and Western Europe are developed within shallow drowned river mouths and in the lagoons behind barrier islands and spits and a large proportion of the research on saltmarsh development has taken place in these environments.

11.3.1 Saltmarsh form, flooding and vegetation zonation

Morphologically saltmarshes consist of a gently sloping vegetated platform, dissected by a network of tidal creeks that increase in width and depth seaward (Pethick, 1992; Orme, 1993). The seaward margin (strictly speaking the margin bordering the ocean, bay, estuary or tidal creek from which tidal waters flood the marsh) may be gently sloping with no visible change in slope from the vegetated surface to the fronting mud or sand flat; or it may consist of a low cliff with an abrupt transition. An idealised cross-section shows a transition from the upland area with an elevation above that of inundation by marine waters, through the high-marsh zone, low-marsh zone and onto the tidal mud flats that often occupy the intertidal zone below the level to which saltmarsh vegetation can become established. An example of this zonation is shown for Allen Creek marsh, a macrotidal marsh on the Cumberland Basin, Bay of Fundy, Canada

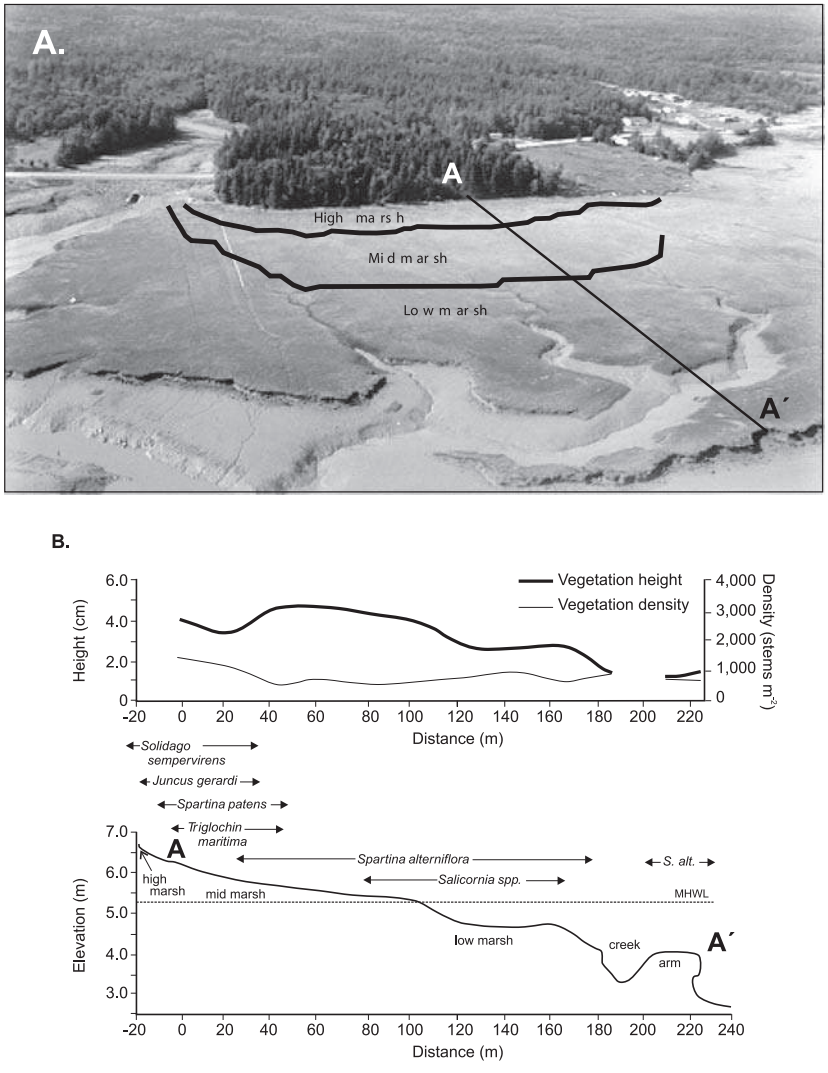

Figure 11.3 Allen Creek marsh, Cumberland Basin, Bay of Fundy: (A) oblique aerial photograph showing the main topographic features and approximate limits of vegetation zonation (van Proosdij *et al.*, 1999). The marsh is presently erosional so the margins bordering on the Cumberland Basin (bottom of photograph) are marked by a low cliff. Allen Creek is a small perennial stream which is tidal in its lower reach, while the marsh surface has a number of tidal creeks which only drain the marsh surface and which continue onto the fronting mudflats; (B) topographic profile, distribution of dominant plant species and vegetation characteristics along Line A A′ (after van Proosdij *et al.*, 1999).

(Figure 11.3). In the low marsh zone along the marsh edge and the banks of tidal creeks, vegetation is submerged on almost every tide and can be submerged for six hours or more depending on the tidal regime. Towards the high marsh zone the frequency and depth of inundation decrease and within the high marsh zone vegetation may be submerged only briefly during spring high tides. Close to the upland boundary, inundation only occurs during exceptional spring tides and as a result of high water levels associated with storm surge. In the first case the period of inundation is very short, but storm surge events may lead to submergence for hours and occasionally one or two days.

The depth and duration of submergence limit the amount of time that respiration and photosynthesis can take place, with the result that saltmarsh vegetation does not grow well much below the mean high tide level. This varies spatially with location on the profile and daily with the neap/spring tidal cycle, and it increases with increasing tidal range. Some portion of the leaves of grasses on the low marsh may be above the water for much of the time on microtidal marshes, but on macrotidal marshes the whole plant may be submerged for several hours (Figure 11.4). Growth of vegetation on the low marsh may also be affected by cold temperatures in the substrate that may take some time to warm

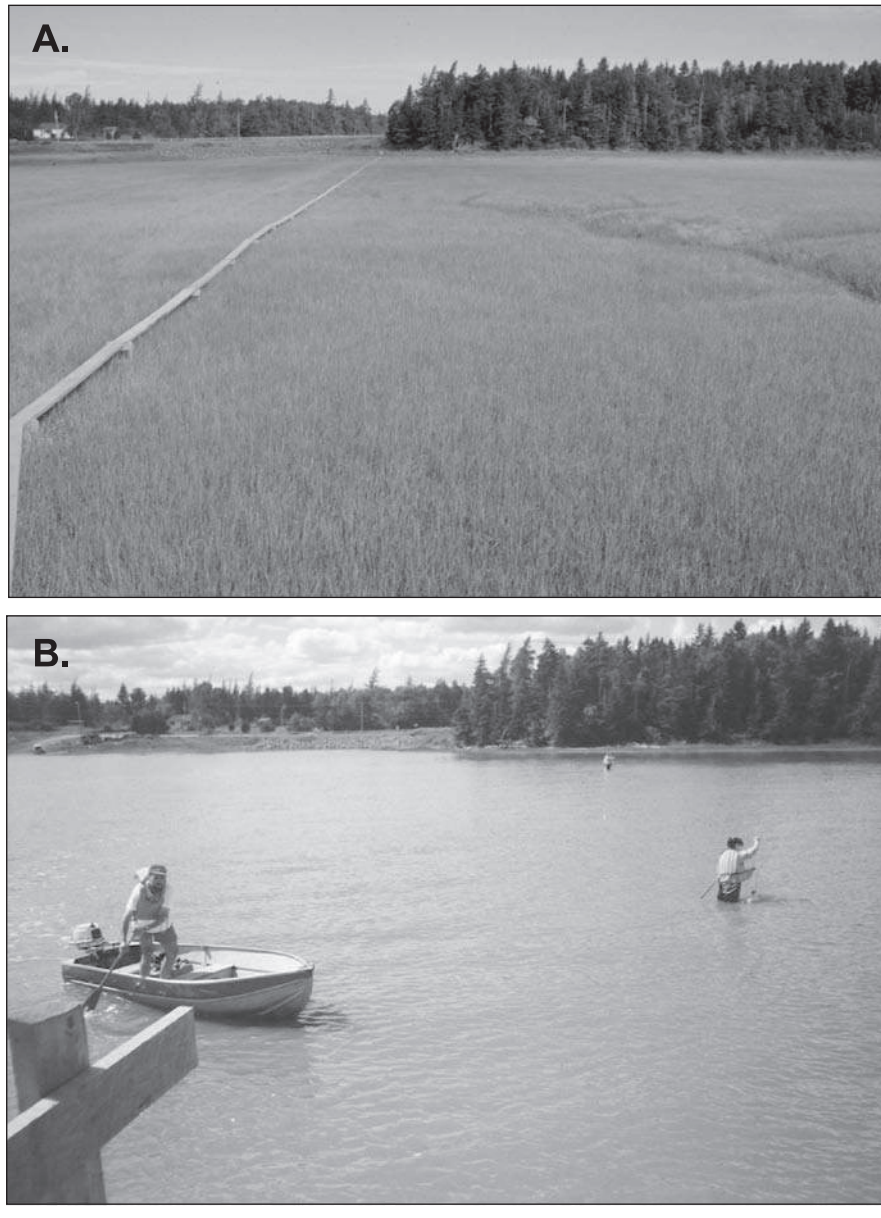

Figure 11.4 Photographs looking landward from a platform on Allen Creek marsh in late June at (A) low tide; (B) spring high tide. The vegetation in the foreground in (A) is *Spartina alterniflora* which is nearing its maximum height. This portion of the low marsh is submerged by water up to a metre deep on spring high tides.

up after flood waters recede. The result is that biomass productivity on the marsh is strongly influenced by location on the profile and thus the frequency and duration of submergence (Gordon *et al.*, 1985). Net primary productivity of saltmarshes can also be expected to decrease towards higher latitudes because of the decrease in growing season and is only about seven months in the Cumberland Basin (Gordon *et al.*, 1985).

Saltmarsh productivity and the zonation and abundance of species are also strongly influenced by salinity of the water and the substrate (Adam, 1990; Mitsch and Gosselink, 2000). In the low marsh, where plants are flooded once or

Table 11.1 *Dominant and subordinate species of the high-, mid-, and low-march at Allen Creek, Bay of Fundy (after van Proosdij* et al.*, 1999).*

Location	High marsh	Mid marsh	Low marsh
Elevation above datum	5.8–6.2	5.3–5.8	4.8–5.3
dominant species	Spartina patens	Spartina alterniflora	Spartina alterniflora
subordinate species	Atriplex sp	Triglochin maritime	Salicornia spp
	Dischilia spicata	Spartina patens	Suaeada maritima
	Elymus arenarius	Limonium nashi	Puchinella maritima
	Glaux maritime	Salicornia spp	Limonium nashi
	Hierochloe odorata	Suaeada maritime	
	Juncus gerardi		
	Limonium nashi		
	Plantago maritime		
	Puchinella maritime		
	Solidago sepmiverens		
	Triglochin maritima		

twice daily, salinity is similar to that of the ocean waters. Towards the upper marsh, salinity may increase as a result of a combination of moderate flooding frequency, poor drainage and greater evaporation, and this may limit both the species and their growth. In some very poorly drained areas salt pannes develop; salinity in them may exceed 80 ‰ and completely inhibit vegetation growth. Generally, the low marsh where stresses are highest is dominated by one or two species and species abundance increases in the high marsh zone where conditions are more favourable for a wider range of plants and competition becomes more important (Gray, 1992). Individual plant species commonly occupy quite a wide range here, but are abundant over a much narrower range (Figure 11.3b and Table 11.1). However, while elevation and distance from the creek margin may exercise some control on the occurrence of particular plant species, the resulting distribution is usually quite complex and reflects small topographic irregularities as well as historical and random factors (Silvestri *et al.*, 2005).

11.3.2 Controls on saltmarsh and tidal creek development

Saltmarshes

The characteristics and evolution of salt marshes (Figure 11.5) are determined by a wide range of physical and biological controls and processes, including: climate, shoreline configuration and wave climate, tidal range, sediment sources and volume of sediment input, sea level history, and vegetation characteristics and dynamics (Chapman, 1960; Beeftink, 1977; Adam, 1990; Allen and Pye, 1992; Orme, 1993; Luternauer *et al.*, 1995; Mitch and Gosselink, 2000). Climatic factors in middle and high latitudes control the occurrence and distribution of the species of vegetation that colonise the marsh as well as influencing physical processes such as marsh hydrology and salinity, wave climate and wave-induced sediment transport, and the occurrence of ice and factors associated with below freezing temperatures (Gordon and Desplanque, 1983; Dionne, 1989). The shoreline configuration influences the local wave climate, the slope and nature of the intertidal substrate, and the circulation pattern of tidal currents.

Tidal range and the tidal regime (semi-diurnal, mixed or diurnal) influence the hydrodynamics of flow in tidal creeks and over the marsh surface as well as the extent and duration of inundation (Healey *et al.*, 1981; French and Stoddart, 1992). In turn, all of these influence the vertical and horizontal extent over which salt marsh development takes place. The tidal range classes established in Chapter 3 can be used to divide saltmarshes into microtidal

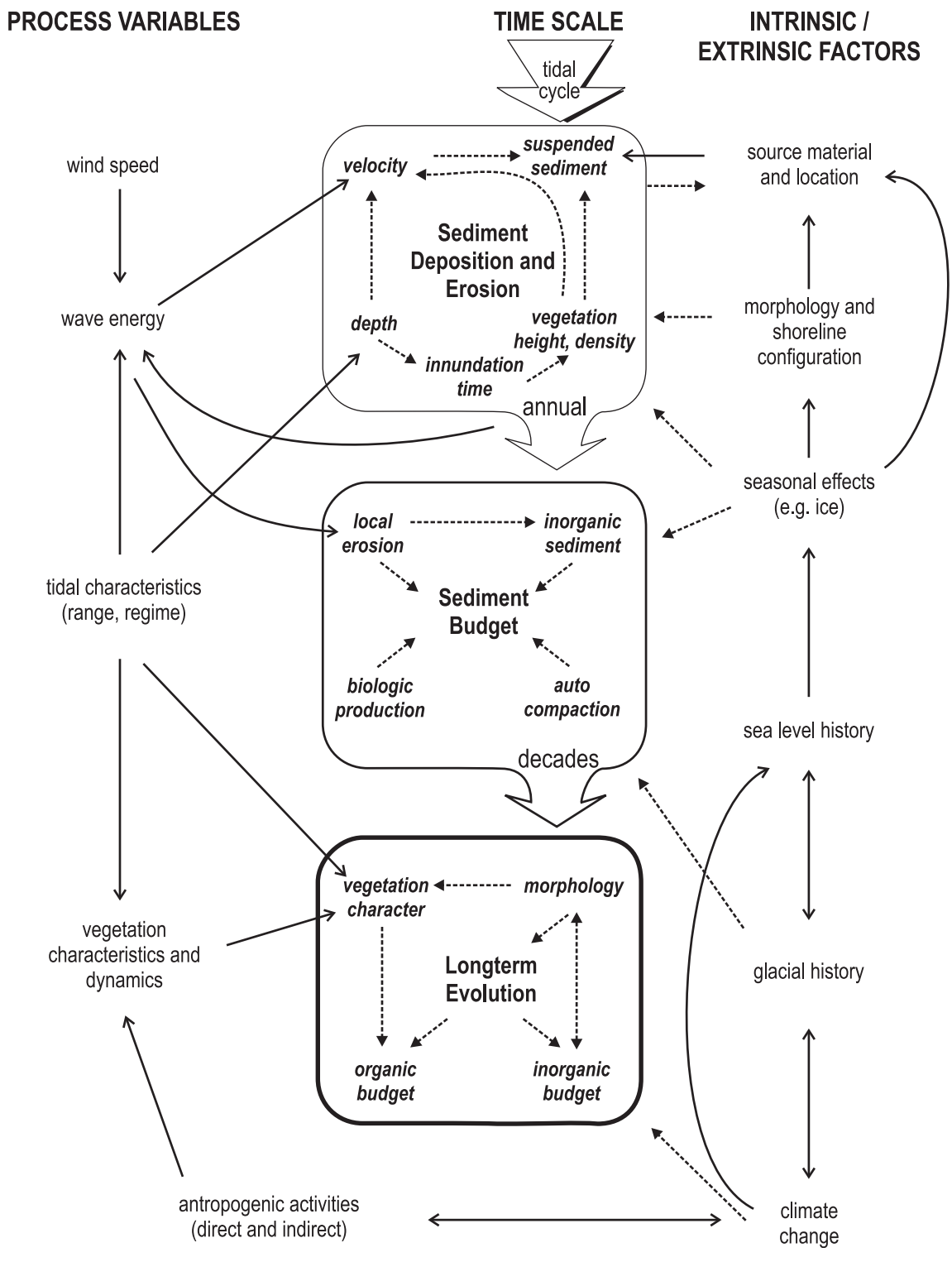

Figure 11.5 Controls on saltmarsh development at varying time scales (Davidson-Arnott *et al.*, 2002).

Figure 11.6 Colonisation of a tidal mudflat, Peck's Cove, Bay of Fundy by *Spartina alterniflora*. The marsh is about 15 years old and the vegetation front has advanced at 8–10 m a^{-1}. Note the fine sediments trapped by the vegetation which contrast with the coarse sand and gravel of the beach which is exposed to wave action only during spring high tides. The mudflats in the middle distance are up to 600 wide at low tide.

(<2 m), mesotidal (2–4 m); low macrotidal (4–8 m) and high macrotidal (>8 m).

The nature of sediment sources and the volume of sediment supply will influence the characteristics of the marsh substrate, sedimentation patterns and the potential rate of sediment accumulation, vertical accretion, and vegetation development. In estuaries, river mouths and deltas, sediments may be derived primarily from fluvial inputs, while in embayments and in barrier/lagoon systems they may be derived largely from shoreline erosion and alongshore and onshore sediment transport by waves. Sediment-laden waters may reach the marsh directly in the case of marshes located on open coast or embayments, or indirectly through estuaries and inlets. In some areas such as rocky coasts, or enclosed lagoons subject to infrequent overwash, the supply of mineral sediment may be very low and marsh accretion is largely by organic accumulation. In other areas such as the Bay of Fundy in Canada or the Wash in Great Britain, large volumes of sediment are supplied through coastal erosion of fine-grained rocks.

Saltmarsh development is commonly pictured as beginning with the colonisation of intertidal sand or mud flats by vascular plants that are both halophytic and tolerant of repeated submergence for periods of up to several hours (Figure 11.6). The establishment of plants then encourages the deposition of fine sediments and the accumulation of organic matter, leading to the vertical growth of the developing marsh surface and the integration of the tidal creek network into the saltmarsh tidal creek network (Redfield, 1972). Under a stable sea-level, vertical growth of salt marshes is limited by tidal range. The rate of upward growth of saltmarshes, and of minerogenic salt marshes in particular, has been shown, based on sampling of 14 saltmarshes in the UK, to be asymptotic, with rapid growth in the early phase and very low growth rates once a mature marsh surface is established near or above the mean high tide level (Pethick, 1981 – see Figure 11.7). The height of the marsh surface can thus be expressed as an asymptotic curve:

$$h = a - be^{-ct} \tag{11.1}$$

where h is the height of the marsh surface, t is the age of the marsh and a, b and c are constants.

The actual rate of growth will vary from marsh to marsh depending on the supply of sediment and rate of accumulation of organic matter. The model is based on the assumption that the rate of sediment deposition decreases rapidly as the marsh surface is above mean high tide because there is a rapid drop-off in flooding frequency, and thus the potential for sediment deposition, above this elevation. However, under rising sea-level, thick deposits can accumulate as long as the vertical growth can keep pace with the rate of sea-level rise (Allen, 1990b, French, 1993; Jennings *et al.*, 1995). The presence of ice during the winter may result in increased deposition at elevations near spring high tide as a result of stranding of ice floes and subsequent melt-out of sediment contained in the ice (van Proosdij *et al.*, 1999) and this will alter the pattern of saltmarsh development somewhat.

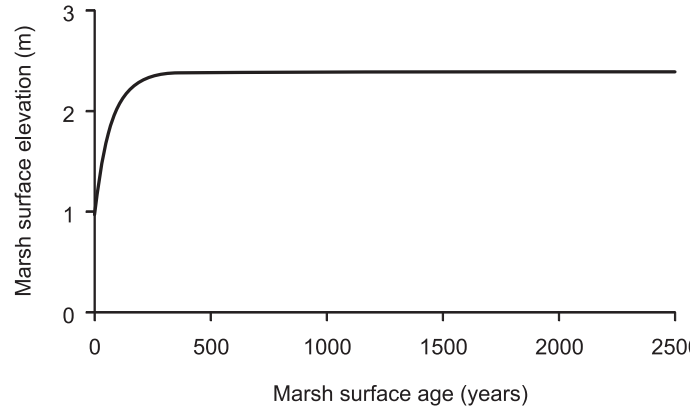

Figure 11.7 Conceptual model of the relationship between marsh height and age (Pethick, 1981).

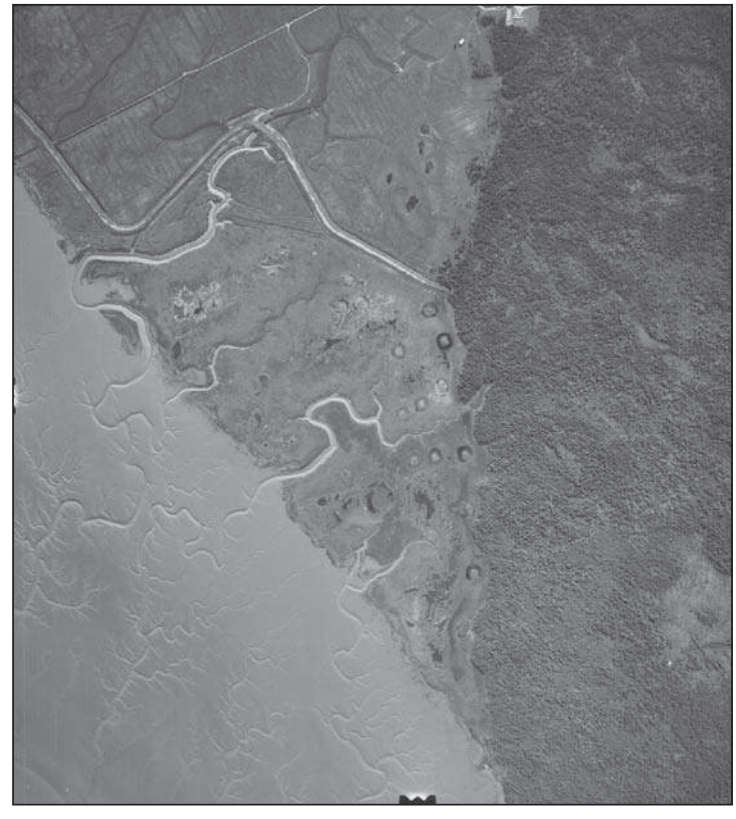

Figure. 11.8 Vertical aerial photograph of Minudie West saltmarsh in the Cumberland Basin showing the dendritic channel patterns on the marsh and mudflat and the link between the two.

Tidal creek networks

A characteristic feature of most saltmarshes is the development of a network of tidal creeks which resemble drainage basins of fluvial systems, with small tributaries forming near spring high tide and the depth and width of the creeks increasing towards the marsh margin (Pestrong, 1965; Steel and Pye, 1997). These creeks often continue out onto the intertidal mudflats in front of the marsh (Figures 11.4a and 11.8). The pattern of the creek networks is generally dendritic, but a range of other patterns can be identified, including reticulate, and complex patterns on poorly drained areas with numerous pannes or ponds (Steel and Pye, 1997). A major difference between the tidal creek system and

Figure 11.9 Two views of a tidal creek channel, Allen Creek marsh (A) near the marsh margin where the depth and width are greatest; and (B) near the mean high tide on the marsh platform where the channel is mostly vegetated and is likely being infilled as a result of accretion.

fluvial systems is that there are generally no topographic high points marking the drainage divides and when there is over marsh flooding the drainage into channels is controlled by hydraulic processes including winds and tides (Allen, 2000). It should be recognised that marsh platforms have little relief and that the total elevation difference on the platform will usually be less than half that of the spring tidal range. Flow is not driven by topographic slope, except at the end of the ebb, but rather by the hydraulic head resulting from the lag between tidal elevation in the bay or estuary and that on the marsh surface and by the total tidal prism over the marsh surface). The tidal range limits the maximum channel depth and thus channels on microtidal coasts will be very much shallower than those on macrotidal coasts.

Where saltmarshes develop through the growth of vegetation out onto tidal mudflats it is usually thought that the creek system on the marsh is inherited with very little change from the pre-existing tidal creek network on the mudflats. As vegetation becomes established, trapping of fine sediment leads to the vertical growth of the marsh and the channels become fixed in place because of bank stability. Under this condition, evolution of the channel network occurs very slowly (Allen, 2000). The bed and bottom portion of the channel banks on the lower portion of the tidal creek within the marsh may be free of vegetation, but the upper reaches are usually shallow and may be completely vegetated (Figures 11.9a, b). Once the landward portion of the marsh nears the upper limit of vertical growth and inundation is infrequent, the headwaters of the creek channels become silted up. This may also account for the infrequent occurrence of tidal creek networks in some Australian saltmarshes that may occupy the upper intertidal zone landward of a zone of fringing mangroves (Adam, 1997).

Where saltmarshes develop on backbarrier sands there may be no pre-existing channel network and drainage is often very poor, with many small ponds remaining on the surface after the

Figure 11.10 Poorly developed drainage and pans on the marsh surface of a backbarrier marsh, Culbin, Scotland.

Figure 11.11 The transition from flows in tidal creeks to overmarsh flow on Allen Creek marsh. The tide has overtopped the marsh margin and filled the lower tidal creek channel and is now advancing up the small creeks on the marsh surface.

tide has receded (Figure 11.10). In this case, the drainage system develops on the marsh surface after formation of the marsh and may result from the gradual connection of pans on the surface (Allen, 2000; Perillo and Iribarne, 2003; Bartholdy *et al.*, 2004 – see Figure 11.1). Spontaneous formation of a tidal creek network has been observed on the floor of a newly created marsh within the Venice lagoon (D'Alpaos *et al.*, 2007).

11.3.3 Saltmarsh hydrodynamics

The rise and fall of the tides generate flows first in the tidal creeks and then across the marsh surface as the level exceeds the creek banks and/or the marsh margin (Figure 11.11). Where the tidal creek channels are marked by levees, portions of the marsh surface may remain dry for some period during the rising tide until the levee is overtopped. At the same time, on wide marsh platforms, portions of the surface towards the landward end of the marsh may be flooded before others that are closer to the margin if there is a protective chenier, beach ridge or dune marking the transition to the tidal flats. In many cases, however, flooding of the marsh surface occurs nearly simultaneously from the

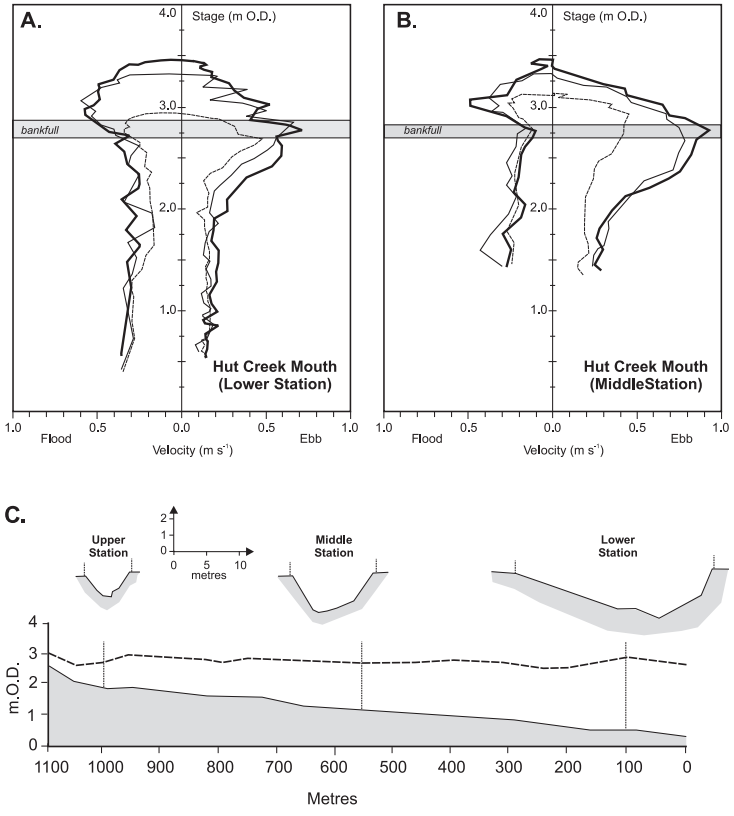

Figure 11.12 Flows speeds versus stage elevation for selected tides at two locations on Hut Creek, Scolt Head Island (A) middle station about 600 m from the mouth of the creek; and (B) lower station about 100 m from the mouth (from French and Stoddart, 1992).

margin and from overtopping of creek banks. We can thus distinguish between conditions during the early and late part of the tidal cycle when the waters are largely confined to the tidal creek network, and those near high tide when the marsh surface itself is covered and water movement may be influenced by tidal currents in the larger basin and by wind action in addition to hydraulic gradients due to the tidal rise and fall. These flows are critical to the import of siliclastic material to the marsh and the export of both siliclastic and organic materials from the marsh.

Tidal creeks

Where the marsh surface provides an extensive flat surface close to the creek channels there may be quite sudden large increases in the supply of water out of the channels on the rising tide and into the channel on the falling tide around the bankfull stage (French and Stoddart, 1992). An example of velocity-stage curves for gauging station near the mouth and in the middle section of a tidal creek developed in marshes behind Scolt Head Island, Norfolk, UK is shown in Figures 11.12a, b (French and Stoddart, 1992). These data show that flow speeds can reach nearly 1 m s^{-1} on the ebb tide when the stage crosses the bankfull elevation on the middle station (about 600 m from the creek mouth) and that speeds here are higher than at the lower station (about 100 m from the mouth). These speeds are high enough to erode the bank and to flush out sediments that might be deposited in the channel during neap tides. Both stations also show a distinct ebb asymmetry – higher speeds on the ebb than on the flow – which is commonly found in many tidal creeks (Bayliss-Smith *et al.*, 1979; Pethick, 1980; Allen, 2000). These findings contrast with measurements of flows in tidal creeks on Allen Creek marsh (Schostak *et al.*, 2000) where maximum flow speeds were generally <0.1 m s^{-1}. Despite the very large tidal range and the erosional appearance of the channel cross-section (Figure 11.9a), the short channel length and absence of levees produce a small tidal prism for an incremental change in stage

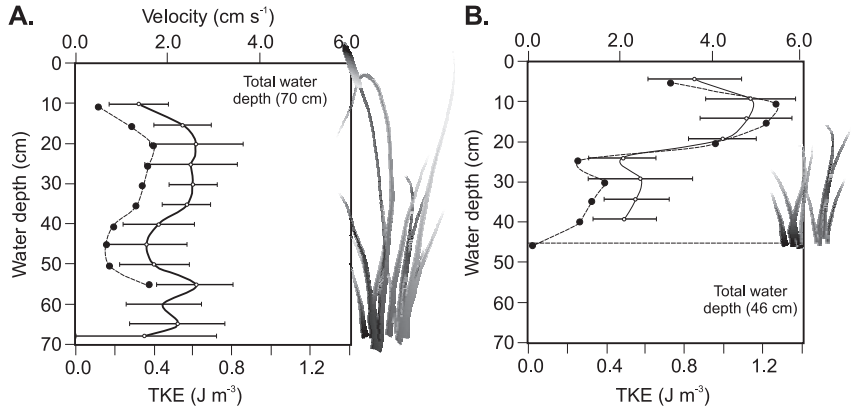

Figure 11.13 Velocity and Total Kinetic Energy profiles collected in emergent and submerged *Spartina alterniflora* canopies: (A) velocity and TKE profiles for the natural vegetation with leaves of the higher plants reaching the water surface; (B) the profiles after vegetation had been clipped to produce an average height of about 25 cm. Error bars show vertical turbulence intensity associated with each measurement. (Leonard and Croft, 2006).

elevation and serve to highlight the control of water surface slope and tidal prism on flow speeds.

Marsh surface

Flow over the saltmarsh surface is still driven primarily by the water surface slope but it is also influenced by winds and potentially by wave action. It is also greatly influenced by the presence of vegetation on the marsh surface which retards flow speeds and alters the velocity profile. Flow speeds are greatly dampened within the vegetation canopy and both vertical and horizontal eddies are reduced. The effects on mean flow speeds and turbulence intensity are greatly affected by the stem density, height and stiffness of the vegetation (Leonard and Luther, 1995; van Proosdij *et al.*, 2000; Christiansen *et al.*, 2000; Shi *et al.*, 2000; Leonard and Croft, 2006; Neumeier and Amos, 2006). As might be expected, flow and turbulence reduction are greater as the vegetation height increases (Figure 11.13), and the same kind of reduction occurs as the total vegetation biomass increases. Where the whole plant is submerged there is a rapid dampening of turbulence below the top of the canopy and this likely occurs because the ends of the leaves tend to curve and present a floating mat near the surface, particularly late in the growing season when the stems are longest and most flexible.

The effect of vegetation on flow varies with the depth of submergence of the plants and with the absolute and relative height of the plants. This will therefore vary through the tidal cycle, over the neap-spring cycle and with the tidal range (microtidal through macrotidal). In mid- and high latitudes it will also vary seasonally with the growth stage of the plants (Figure 11.14). Because the stems of most saltmarsh grasses are tightly bunched there are gaps around each plant close to the bed and flow speeds around each plant are generally faster at this level than a bit higher in the canopy where the leaves tend to spread out and occupy most of the space (Figure 11.15). Thus, some of the highest speeds over the marsh are measured soon after, and near the end of inundation. This may account for some of the rapid increases in flow in the tidal creek channels around these points. Flow speeds in the canopy are relatively slow until most of the plants are submerged and then flow speed increases dramatically in the area above the canopy and may be enhanced by skimming flow similar to wind flow over beach vegetation (Figure 11.15).

Saltmarsh vegetation also plays an important role in dampening wave action in marshes exposed to wave action (Knutson *et al.*, 1982; Allen, 2000). Waves may propagate from a bay or estuary across the mudflats in front of

Figure 11.14 New vegetation growth on Allen Creek marsh at the end of May. The last vestiges of dead leaves from the previous year are still visible. Contrast this with the absence of live vegetation in early spring (Figure 11.9b) and with the dense vegetation growth in early summer (Figure 11.4a). The photograph also shows a temporary platform built near the marsh edge for measuring suspended sediment concentration over a tidal cycle and a portion of the boardwalk system used to reach different parts of the marsh.

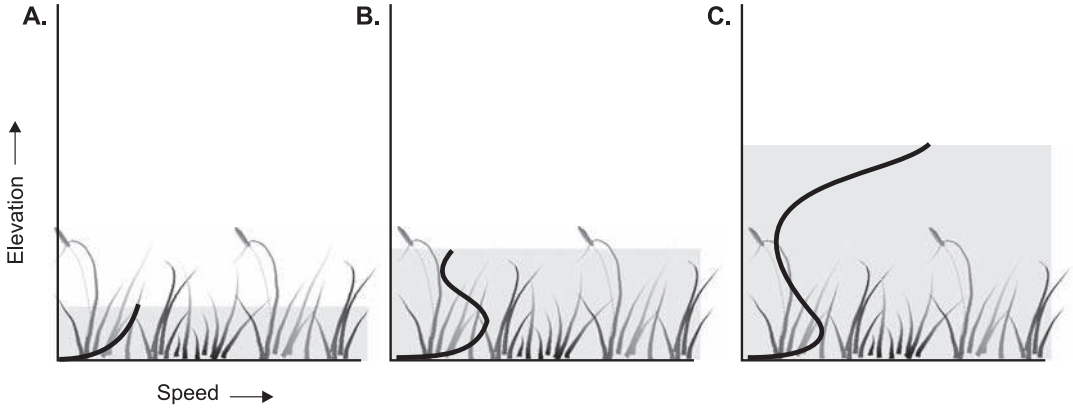

Figure 11.15 Schematic of the effect of depth of submergence on typical velocity profiles within saltmarsh grass canopies where: (A) water level is just above the marsh surface; (B) water level is near the top of the canopy; (C) water level is substantially higher than the vegetation canopy. Flow around the stems of individual plants within a few centimetres of the bed tends to be faster than that a bit higher because of the spread of the plant leaves. Once most plants are submerged flow speeds above the canopy are much higher.

the marsh or they may be locally generated at high tide, especially during storm surge events where the whole marsh surface is inundated. Measurements of attenuation across macrotidal saltmarshes show a 50% reduction in wave energy within 10–20 m of the edge of vegetation (Moller and Spencer, 2002; Moller, 2006 – see Figure 11.16). As is the case for unidirectional flows, the effectiveness of vegetation in dampening wave energy varies with plant species and with the height and density of the standing biomass (Moller, 2006). It is likely more effective for short-period waves than for long-period ones.

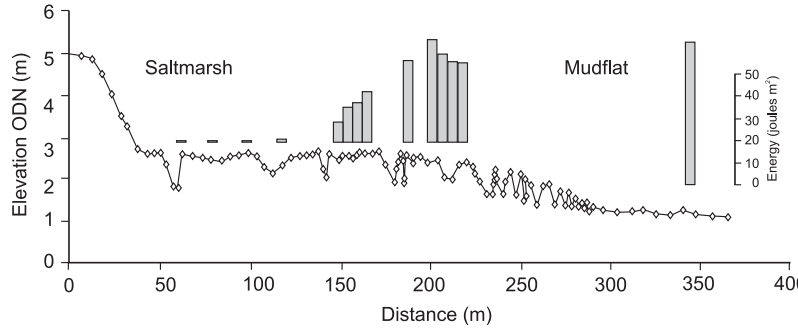

Figure 11.16 Change in significant wave height measured across the tidal flat and saltmarsh at Tillingham, UK. Vegetation height is shown for five locations on the marsh surface (modified from Moller and Spencer, 2002).

11.3.4 Saltmarsh sedimentation and dynamics

An understanding of the sedimentary dynamics of coastal salt marshes, particularly within the context of a sediment budget can be useful for examining the response of the salt marsh system to changes in one or more controlling variables such as sediment supply and sea level. These studies can also be seen as part of a broader effort to understand the complex interaction between the biotic and abiotic components of salt marsh ecosystems and of the patterns of energy flow, nutrient and sediment cycling within the marsh and between the marsh and coastal waters (Adam, 1990; Mitsch and Gosselink, 2000). Sediment deposition on the marsh surface can be seen as being a function of the availability of sediment and the opportunity for this sediment to be brought onto the marsh and to settle out on it (Reed, 1989; van Proosdij *et al.*, 2000). Both of these vary spatially and temporally. Sediment availability may reflect the passage of storms or cold fronts, storm surges, heavy rainfall events and river flooding all of which may act to increase the concentration of total suspended solids (TSS) in the water column. The opportunity for deposition depends on the frequency and duration of flooding of the marsh surface, which is controlled by the tidal regime, marsh elevation and storm surge effects. The potential deposition rate will also depend on the effects of vegetation on reducing current and wave energy as well as sediment size and flocculation. All of these factors will vary between marshes and spatially within a marsh.

Several different aspects related to the sediment budget and mass balance of coastal salt marshes can be recognised in recent studies, including: (1) measurements sediment dynamics (erosion, transport and deposition), and sediment budgets associated with individual tidal cycles and/or the biweekly spring-neap cycle in tidal creeks (Bayliss-Smith *et al.*, 1979; Reed *et al.*, 1985; French and Stoddart, 1992; Leonard *et al.*, 1995a) and over the marsh surface (Stumpf, 1983; Reed *et al.*, 1985; French and Spencer, 1993; Wang *et al.*, 1993; Leonard *et al.*, 1995b); (2) measurements of sediment accumulation and rates of vertical growth as well as changes in the areal extent of marshes and tidal creek networks over periods of 10^{-1}–10^{3} years using a variety of techniques for dating sediments and measuring the rate of growth (Jacobson, 1988; Williams and Hamilton, 1995; Pringle, 1995; Callaway *et al.*, 1997; and (3) development of simulation models to explore one or more aspects of the controls on salt marsh evolution (Allen, 1990a; French, 1993; Woolnough *et al.*, 1995; Callaway *et al.*, 1996b). In this section the focus is on deposition over individual tidal cycles and on seasonal patterns. The long-term mass balance and response to sea level change are considered in the following section.

Organic accretion

Much of the above-ground organic matter production is broken down on the marsh surface and exported to the surrounding tidal flats, estuary or bay, though the details of the operation of this process may be somewhat different to

Box 11.1 Measurement of accretion and surface elevation change

Sedimentary deposits are all subject to the process of autocompaction whereby the volume of the deposit decreases over time as a result of a set of physical, chemical and biological processes. A portion of this comes about from physical compaction leading to a rearrangement of the packing of mineral grains and concurrent reduction in the pore space (Long *et al*., 2006). A similar process can take place in plant organic matter, but in addition plant matter may decay through a number of biological processes. Chemical processes can lead to the dissolution of both plant material and carbonates, though some of these processes may add material through cementation (Allen, 2000). Autocompaction is especially important in saltmarshes because of the fine grained nature of many saltmarsh sediments, the significance of flocculation in inorganic sedimentation, and the initially high amount of organic matter in the root zone near the surface. One manifestation of this is a tendency for the bulk density of cores in saltmarshes to increase with depth and to reach a nearly constant figure at some depth on the order of 3–5 m. Alternately, the rate of autocompaction can be determined from the difference between the change in elevation of the marsh surface over time and the accretion on the surface (Cahoon *et al*., 1995, 2000; Turner *et al*., 2006).

Measurement of surface accretion on the marsh surface on an annual to decadal scale is most often determined using some form of subsurface marker horizon (Figure 11.17a). This may be a layer of sand, clay, brick dust or other readily identifiable sediment, or an aluminium plate which is buried a few cm below the surface (Steers, 1948; Wood *et al*., 1989; Cahoon *et al*., 2000). Distance to the marker horizon is commonly determined by taking short cores and measuring the depth below the surface. If an aluminium plate is used (Figure 11.17b), the distance to the plate can be measured by probing through the marsh surface with a thin rod. Seasonal or annual sedimentation is measured as a greater distance to the plate and vice versa for erosion.

The sedimentation erosion table (SET) is used to determine the net elevation change of the marsh surface by allowing for autocompaction (Boumans and Day, 1993; Childers *et al*., 1993). A pipe is driven into the marsh surface until it reaches a basal unit where compaction is minimal (Figure 19.17c). At Allen Creek this was a till or mudflat surface below the base of the marsh. Measurements were made by slotting the SET into the pipe and taking measurements of the distance to the bed at five points along three mutually orthogonal lines for a total of 15 points. The assumption is made that the pipe in the marsh is fixed and the elevation of the top of the pipe can be checked every two or three years using a total station or DGPS to ensure that this is indeed the case. The rate of autocompaction can then be determined by subtracting the surface elevation change measured by the SET from the accretion/erosion change determined from the aluminium plate or marker horizon.

that originally proposed by Teal (1962 – see Alongi, 1998; Mitsch and Gosselink, 2000). Small amounts of material from the above ground production can be incorporated into the saltmarsh sediments but the most significant contribution to increasing marsh elevation comes from root production at and below the ground surface (Nyman *et al*., 2006). Because the

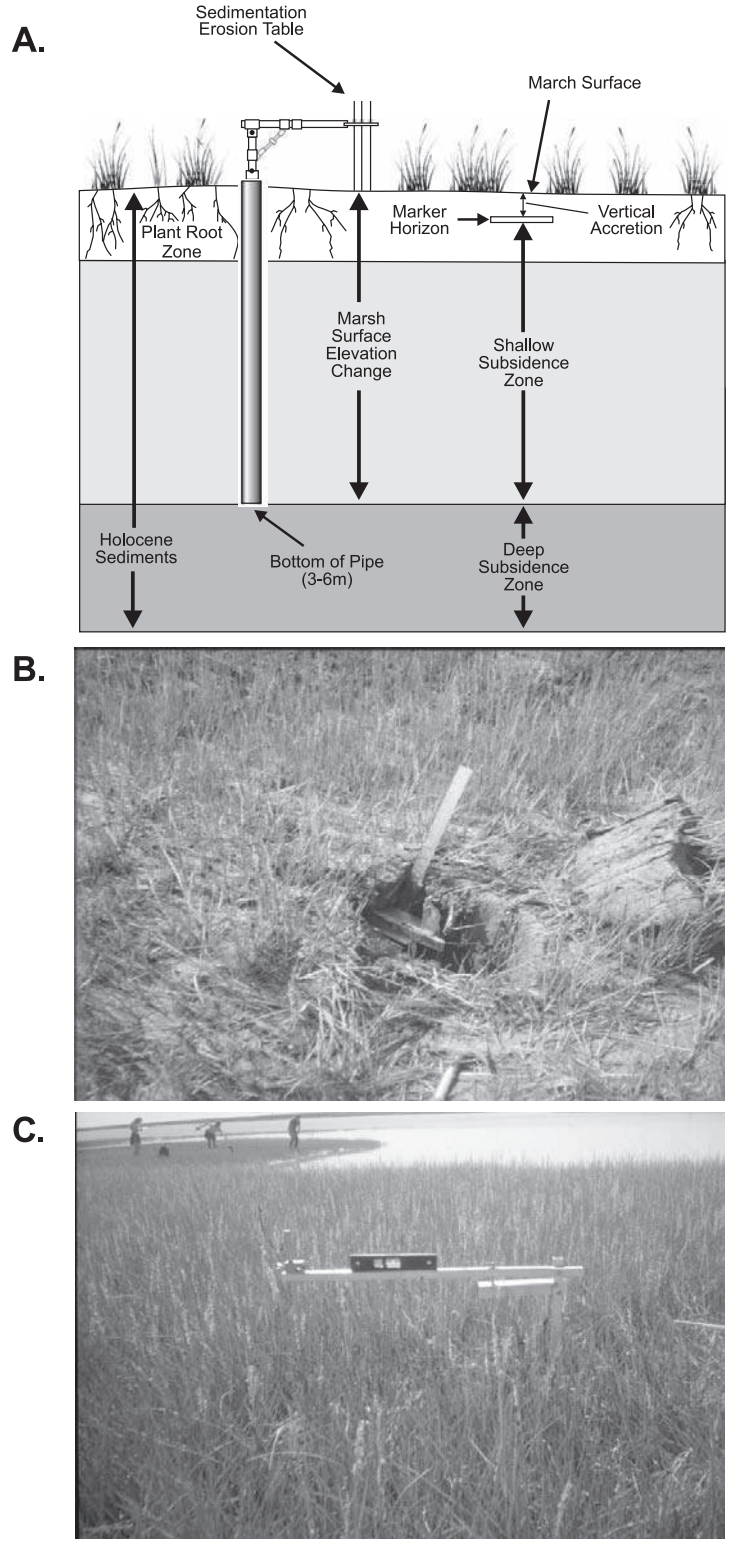

Figure 11.17 Measurement of vertical accretion and net elevation change in a saltmarsh: (A) schematic diagram showing saltmarsh zonation and the techniques used to measure accretion and elevation change (after Cahoon *et al*., 2000); (B) emplacement of an aluminium plate at a depth of 0.1 m below the surface. The turf is replaced following this and subsequently sedimentation/erosion of the surface is measured using a thin rod to determine the distance to the plate; (C) Sedimentation Erosion Table (SET) being used to measure elevation change on Allen Creek marsh. This version of the SET used a square aluminium tube which permitted it to be rotated in 90 increments so that a greater number of points could be used to determine an average.

saltmarsh soils are anaerobic beginning a few millimetres below the surface, the rate of breakdown of the organic matter tends to decrease rapidly after one or two years (Callaway *et al.*, 1996a) and substantial beds of peat can form where inorganic sediment input is low. Within the root zone, if inorganic sedimentation is low, pore space may account for 80% or more of the volume and this means that over time we can expect considerable compaction of the soil to take place. In many estuarine and deltaic marshes the inorganic input is much higher than the inorganic component, and the final contribution of the organic matter component to saltmarsh accretion is usually modelled as being quite small (e.g. French, 1993; Temmerman *et al.*, 2004). However, in areas such as coastal Louisiana, the supply of inorganic sediments is low and thus most of the accretion may come from organic production (Nyman *et al.*, 2006). In modelling saltmarsh evolution on a decadal time scale it is important to account for the organic matter contribution to the saltmarsh budget but modelling it directly is still difficult and is usually accomplished by making use of empirical data on compaction rates.

Sedimentation over tidal cycles

Sediments can reach the marsh surface through a variety of pathways, including runoff from upland areas, overwash of barriers and deposition of dust from atmospheric fallout (including radioactive elements from airborne testing of nuclear weapons which now provides a convenient dating horizon). In many marshes most of the mineral sediments are brought to the marsh as suspended sediment from the bay or estuary during periodic tidal flooding of the surface and episodically during storm surge events. This sediment is dominantly in the silt and clay size range though wave action may transport sand from adjacent intertidal sand flats if these are present. The focus here is on transport of the fine fraction. The amount and pattern of deposition over a tidal cycle will depend initially on the suspended sediment concentration of waters reaching the marsh through tidal creeks and over margin flows and then on factors that determine flow speeds and the settling of particles from suspension.

The concentration of TSS reaching the marsh surface averaged over a period of years will vary with the setting of the marsh and the available sediment sources. In relatively narrow estuaries measurements show a strong positive relationship between increasing tidal height (neap to spring tides) and increasing TSS (Allen and Duffy, 1998; Temmerman *et al.*, 2003; Murphy and Voulgaris, 2006), likely as a result of increased flow speeds and turbulence of tidal currents associated with the larger tidal prism. In other areas the correlation with tidal range is lower, with wind and wave action playing a much stronger role (Reed *et al.*, 1985; Leonard *et al.*, 1995b; van Proosdij *et al.*, 2006a) and rainfall events during low tide may also mobilise sediment on the surface of the marsh, tidal creeks and tidal flats (Mwamba and Torres, 2002; Murphy and Voulgaris, 2006).

Water flowing through the tidal creek network and over the marsh margin brings sediment in suspension onto the marsh surface. The TSS concentration tends to be highest initially because of remobilisation of sediment on tidal mudflats, in the tidal creeks and on the marsh surface, especially if there is some wave activity (Figure 11.18). Concentration decreases as flow depth increases and remains steady over much of the flood over the surface. It then decreases during the ebb as a result of deposition on the marsh surface (van Proosdij *et al.*, 2000; Christiansen *et al.*, 2000). There may be a short period of increased TSS near the end of the ebb, again because of sediment remobilisation in shallow flows (Figure 11.18).

It is not really feasible to calculate net deposition based on changes in the TSS concentration either in a tidal creek or on the marsh surface over a tidal cycle. However, on marshes where wave action is restricted there may be a strong positive correlation between net deposition over a tidal cycle and the magnitude of TSS concentration in an adjacent tidal creek. Sediment brought onto the marsh surface in suspension is deposited on the surface of the marsh, on leaf litter and on the stems and leaves of the plants. The settling velocity of individual silt and clay particles is very small and much of the time, even with reduced flow speed and turbulence

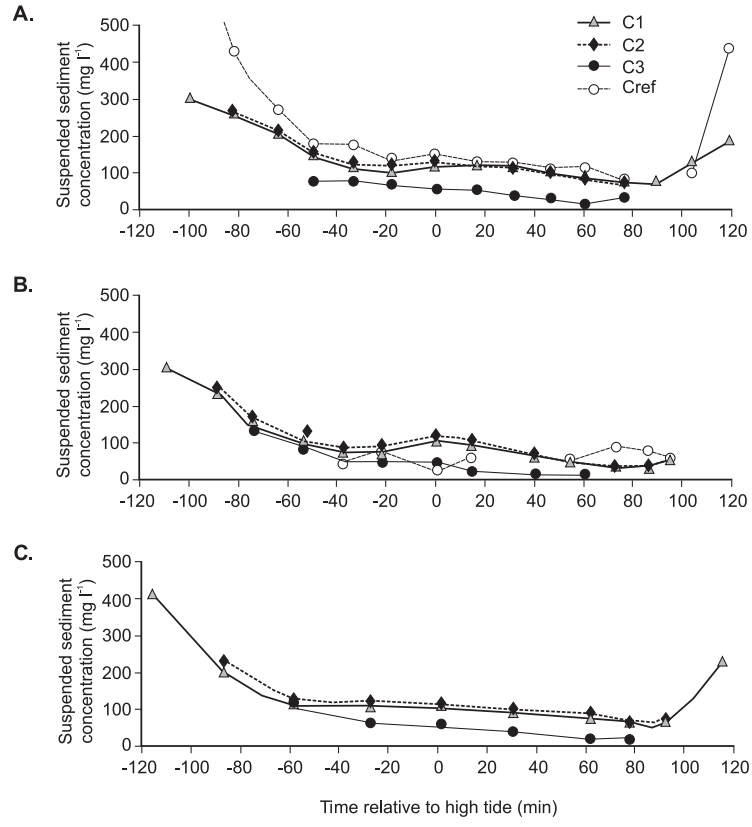

Figure 11.18 Suspended sediment concentration measured along a line from the main tidal creek and on the marsh surface at Allen Creek marsh over individual tidal cycles with increasing tidal range: (A) tidal range 6.95 m; (B) tidal range 7.15 m; (C) tidal range 7.35 m. (after van Proosdij, 2001).

within the marsh vegetation, there is insufficient time for sediments in all but the lowest few cm to settle. However, sediment can reach the marsh surface in a variety of ways other than settling of individual particles. A considerable proportion of the fine sediment making up the TSS is in the form of flocs that have a settling velocity less than a quartz particle of equivalent size but still much greater than that of the individual particles which make up the floc (Kranck *et al.*, 1992; Christiansen *et al.*, 2000). Thus a much greater mass of sediment can be deposited over a tidal cycle than would be predicted from the settling velocity of individual particles. Sediments may be deposited on, or adhere to litter on the marsh surface and to the stems and leaves of the vegetation and then reach the surface as a result of rainfall during low tide. Finally some sediments settle out of suspension within small pools remaining on the marsh surface at the end of the ebb tidal cycle. This tendency to fill in hollows is an important element in producing and maintaining the relatively flat marsh surface.

Sediment deposition on the marsh over a tidal cycle is commonly measured by collecting sediment on filter paper placed in a suitable container on the marsh surface. Reed (1989) used a simple modified Petrie dish placed over a layer of fine gravel and Brown (1998) used filter paper held in place by bent paper clips. These work well in low-energy environments but, where the traps may be subject to some wave action at high tide, a more robust frame is required (Figure 11.19a). These traps can be used to give an indication of relative rates of deposition over tidal cycles and used to test simple relationships between deposition rate and tidal range or spatial patterns related to distance from the marsh margin or a tidal creek (Cahoon and Reed, 1995; French *et al.*, 1995; Leonard, 1997; Allen and Duffy, 1998; Temmerman *et al.*, 2003, 2005; van Proosdij *et al.*, 2006a). However, they do not provide reliable measures of the true depositional mass.

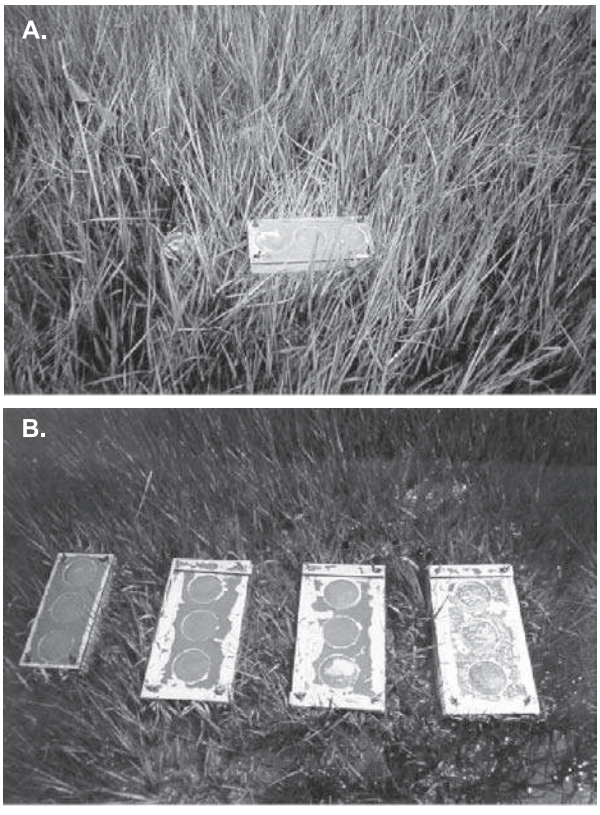

Figure 11.19 Measurement of sediment deposition on the marsh surface: (A) sediment deposition on a Petrie dish trap (after Reed, 1989) and the modified Guelph trap; (B) series of Guelph traps used for measuring deposition over various stages of the tidal cycle. The traps were fitted with lids and installed near a platform from which the lids could be lifted off at various stages of the tide. The trap on the left was exposed for the whole tidal cycle and the other three (from left to right) were exposed halfway through the flood, at the end of the flood, and halfway through the ebb.

Some early literature suggested that deposition occurred primarily at slack tide but more recent work suggests that it likely occurs over the whole tidal cycle (French *et al.*, 1993; Woolnough *et al.*, 1995; Christiansen *et al.*, 2000). Measurements at Allen Creek made use of traps with covers that could be removed during the period of inundation to determine the relative amass of sediment deposited at various tidal stages (van Proosdij *et al.*, 2000 – see Figure 11.19b). These showed that deposition tended to be highest near the beginning and end of the period of inundation and relatively steady during inundation (Figure 11.20). Under moderate wave conditions, sediment was deposited only at the beginning and end of inundation when water depth was too shallow to permit wave activity.

Studies of deposition at a number of marsh sites show that spatial and temporal patterns of deposition over tidal cycles are controlled by several interrelated variables including: tidal elevation, TSS concentration in waters of the tidal basin, relative roughness of vegetation, distance from the margin or tidal creek, and marsh topography. On Allen Creek marsh, where flow depth over the surface is often much greater than vegetation height and levees are poorly developed, distance from the marsh or tidal creek margin is an important control on the spatial pattern of deposition, but tidal elevation and wave activity are also significant factors (van Proosdij *et al.*, 2006a). On other marshes the pattern of decreasing deposition away from tidal creeks is much stronger (e.g. Reed *et al.*, 1999; Neubauer *et al.*, 2002; Temmerman *et al.*, 2003). Sediment deposition on most marshes decreases with decreasing inundation time – i.e. with elevation of the marsh surface – and there may also be a zone of low deposition near the marsh margin because of resuspension by wave activity.

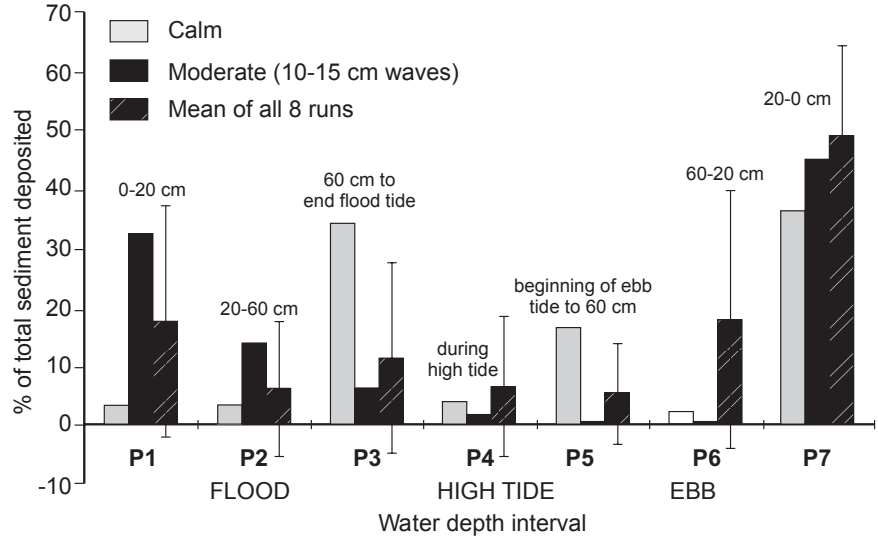

Figure 11.20 Variations in sediment deposition on the marsh surface through a spring tidal cycle under low and moderate wave conditions using the sequential traps illustrated in Figure 11.19b. The mean of measurements over eight tidal cycles is also shown (van Proosdij *et al.*, 2000).

Seasonal and annual variations in deposition and erosion on the marsh surface

Measurements of sedimentation and net accretion on the marsh surface over periods of months to a decade or more can be made with some version of the techniques described in Box 11.1. The advent of differential GPS has made relocation of marker horizons or plates and the pipes for SET stations much simpler and the techniques have been applied in a number of locations. Seasonal variations in accretion of the surface have also been evaluated indirectly by comparing levels of TSS, measured continuously at a station in a suitable location on a tidal creek or in the bay or estuary, in conjunction with measurement of deposition over individual tidal cycles at intervals during the same period (Murphy and Voulgaris, 2006).

Seasonal variations in sedimentation can be expected to reflect either variations in the TSS concentration of waters reaching the marsh (i.e. in the available supply of sediment) or variations in the factors controlling erosion and deposition on the marsh surface itself. Higher values for TSS usually reflect either periods of higher rainfall and runoff in rivers supplying sediment to estuaries or the coast, or strong winds and wave activity which mobilise sediments in the nearshore or on intertidal flats (Reed, 1989; Pethick, 1992; Childers *et al.*, 1993; van Proosdij *et al.*, 2000; Temmerman *et al.*, 2003). Reduced vegetation cover due to dieback in winter months might be expected to reduce deposition on the marsh surface, or at least result in increased remobilisation by currents and wave action. However, in the absence of significant wave action it seems that considerable deposition can occur on the marsh surface even with greatly reduced vegetation cover.

Whether there are strong seasonal signals in accretion on the marsh surface will therefore vary with the physical marsh setting (estuary, bay, back barrier) and with the climatic factors controlling rainfall and wind and wave action. Measurements over 2.5 years at two sites in North Inlet, South Carolina (Childers *et al.*, 1993), which are influenced by freshwater sediment inputs, illustrate the spatial variability in response both between marshes in different locations and between upper and lower marsh stations on the same marsh (Figure 11.21). At Oyster Landing deposition occurs in all seasons except winter. At South Town Creek erosion

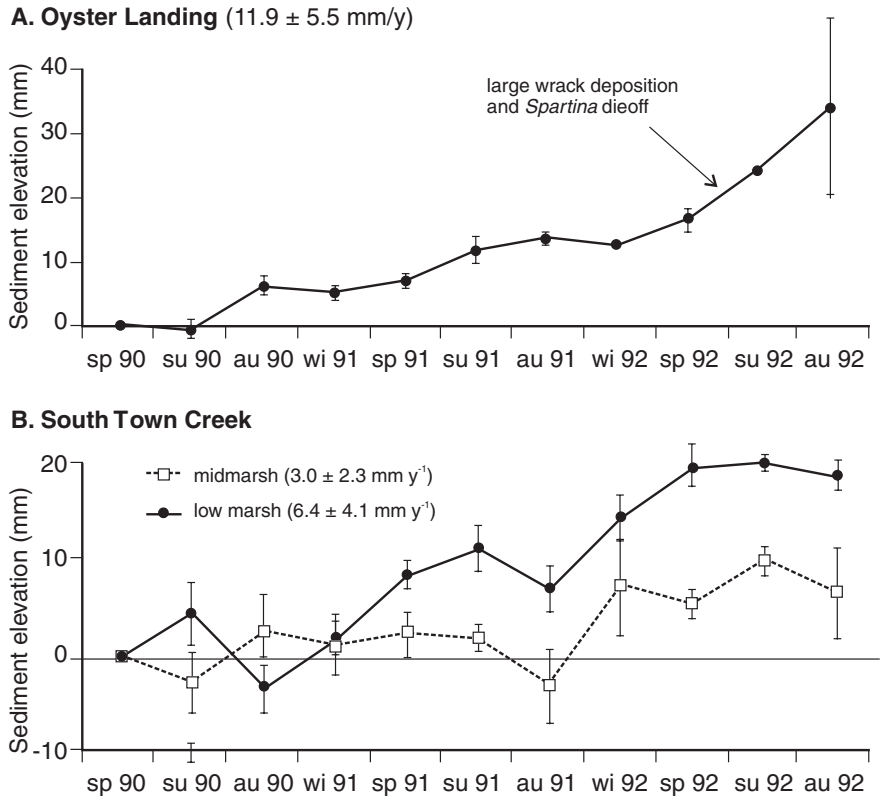

Figure 11.21 Changes in the elevation of the marsh surface over time at two marshes in North Carolina (after Childers *et al.*, 1993). Sediment input is chiefly from river sources with Oyster landing being closer to a source and therefore having higher inputs.

occurred in the autumn. Deposition was often greatest in the winter, with the high marsh site showing much greater variability. Temmerman *et al.* (2001) also found higher deposition in the winter months, but a number of studies in the US have found higher deposition in the summer (Leonard *et al.*, 1995a; Murphy and Voulgaris, 2006). Neubauer *et al.*, 2002 found highest rates of deposition during the summer months along creek margins in a tidal freshwater marsh but no seasonal pattern in the interior away from the streams. At Allen Creek marsh deposition is highly variable seasonally, but the pattern is different between high marsh and low marsh sites (Figure 11.22). Here deposition on the mid and high marsh is high in the autumn when TSS concentration is highest because of stronger wind and wave action and wave energy is dampened by vegetation on the low marsh. It is also high in the winter, in part for the same reason, but also because of the stranding of blocks of ice near the spring high tide limit and subsequent deposition of sediment from the ice due to melting in late winter (see Box 11.2). Deposition on the low marsh tends to be lower during this time because of hindered deposition and possibly erosion of the surface by waves coming over the marsh margin. In the late spring and summer deposition is higher here because of the reduced wave energy levels and greater vegetation height and density. Most seasonal studies that are carried out over just a few years have found considerable variability from year to year, e.g. because of the effects of one storm or a mild winter.

While deposition over tidal cycles and seasonally is highly variable, measurements made over a period of several years tend to show a more consistent spatial pattern. Deposition rates decrease with elevation on the high marsh

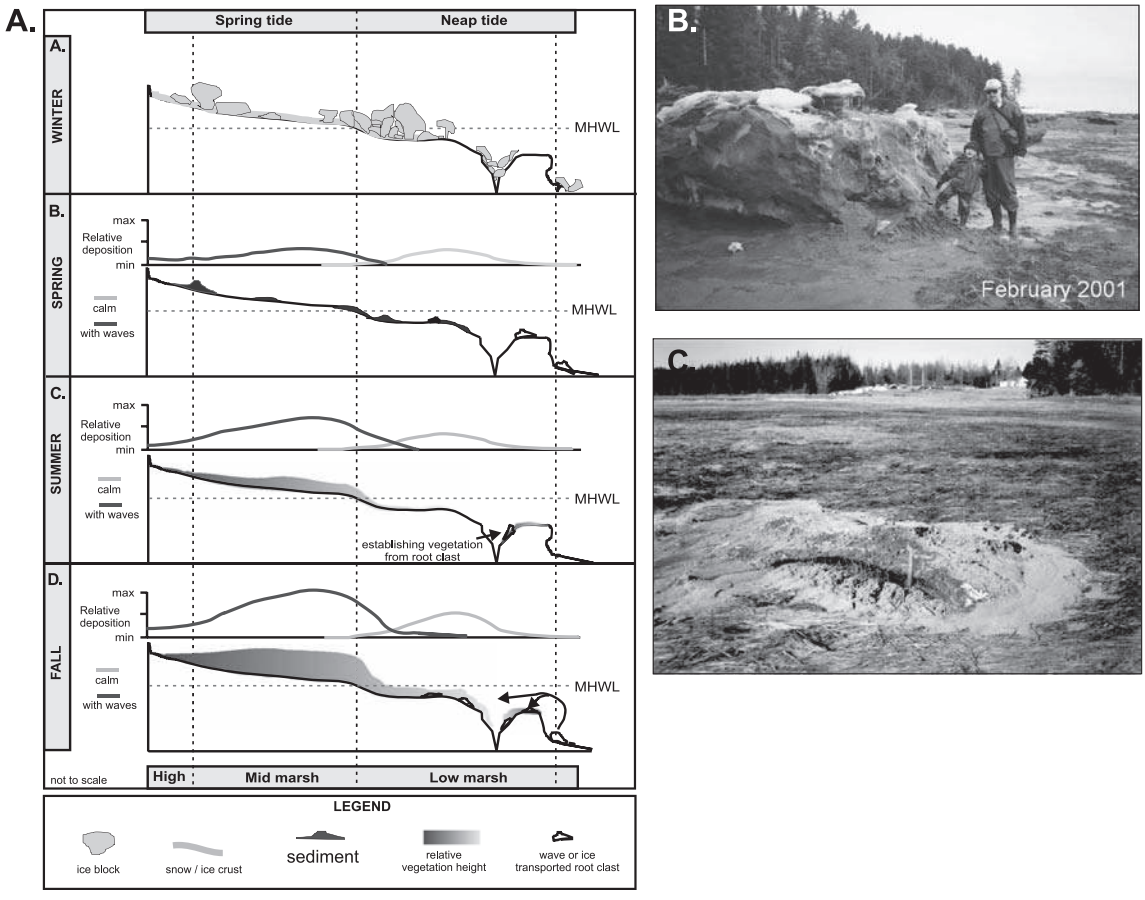

Figure 11.22 Controls on annual deposition on Allen Creek marsh: (A) schematic diagram showing seasonal patterns of sediment deposition across Allen Creek marsh and the influence of seasonal vegetation changes and ice (van Proosdij *et al.*, 2006b); (B) blocks of ice stranded near the spring high tide line; (C) sediment melting out of a remnant ice block at the end of the winter.

reflecting the lower frequency of inundation and this is consistent with the aymptotic model of saltmarsh evolution (Figure 11.7). Measurement of deposition on Hut marsh by Steers between 1935 and 1947 (Figure 11.23a), and subsequent measurements by Stoddart *et al.*, (1989) show a consistent trend and it is notable that the scatter decreases with increasing period of measurement (Figure 11.23b). This pattern is best developed on the high marsh where inundation occurs only on extreme spring tides or during storm surges. At Allen Creek marsh, which lies mostly below the spring high tide line, the decrease in deposition with elevation is much less pronounced and deposition from ice near the landward margin may offset the lower deposition from tidal inundation (Figure 11.24). The average rate of accretion on the marsh surface ranges from about 9 mm a^{-1} to about 1.3 mm a^{-1} and this is consistent with an average rate over about 50 years of about 1.0 mm a^{-1} obtained by Kostaschuk *et al.* (2008).

11.3.5 Decadal scale sedimentation and response to sea level rise

There are a few studies where marker horizons have been used to measure sedimentation for periods exceeding a decade (Steers, 1948; Bartholdy *et al.*, 2004; Goodman *et al.*, 2007) but most studies of saltmarsh dynamics over decades to centuries are based on analysis of historical aerial photographs to map changes in areal extent and

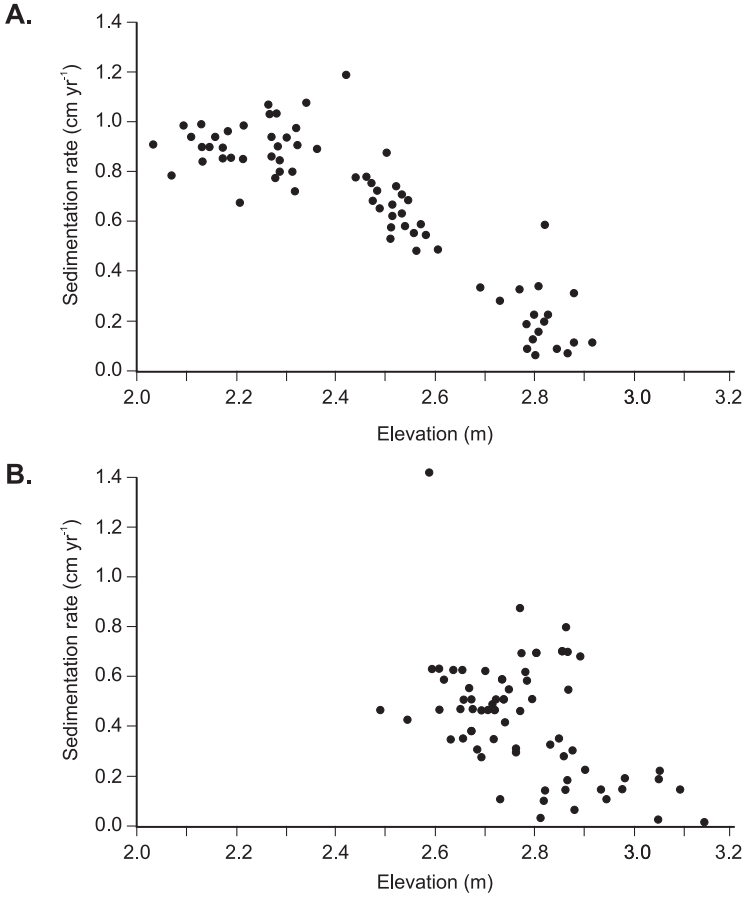

Figure 11.23 Relationship for sedimentation rate and elevation: (A) Missel and Hut marshes from 1935–47 (data from Steers, 1948); and (B) Hut marsh using the same locations as those occupied by Steers for 1983–87 (Stoddart *et al.*, 1989). Note the greater scatter in the data collected over a shorter time period. No distinction is made in (A) between samples taken from different parts of the marsh.

stratigraphic approaches where suitable dating material is available. In addition to the tradition al methods of stratigraphic dating the accumulation of ^{210}Pb and ^{137}Cs from airborne testing of nuclear weapons has been used to provide a marker horizon in a number of studies (Kearney and Ward, 1986; Orson *et al.*, 1998; Marshall *et al.*, 2007; Kostaschuk *et al.*, 2008). At a decadal to century scale, sedimentation is also influenced by relative sea level rise and particularly its influence on shoreline displacement and the accommodation space available for sediment deposition. In some regions, such as the eastern Canadian Arctic, northern Scotland and Scandinavia, isostatic uplift results in shoreline advance and a reduction in the accommodation space at any point on the marsh. Marsh deposits therefore tend to be quite thin but may be preserved over a considerable width normal to the shoreline. In Australia and parts of the Pacific, many marshes (and mangrove swamps) have developed under relatively stable sea level during the late Holocene. In much of North America and Western Europe marsh development has occurred under rising sea levels and there is considerable preoccupation today with the potential effect on marsh survival of an increasing rate of sea level rise relative to historic accretion rates (Stevenson *et al.*, 1986; Reed, 1995).

Decadal scale rates of accretion and response to sea level rise

Accretion rates measured over decades to a few centuries from sites in North America and western Europe typically show accretion rates ranging from 1–2 mm a^{-1} to 10–15 mm a^{-1} (Stoddart *et al.*, 1989; Ward *et al.*, 1998; Roman *et al.*, 1997; Callaway *et al.*, 1997b; Orson *et al.*, 1998; Bartholdy *et al.*, 2004; Temmerman *et al.*, 2004; Goodman *et al.*, 2007; Madsen *et al.*, 2007;

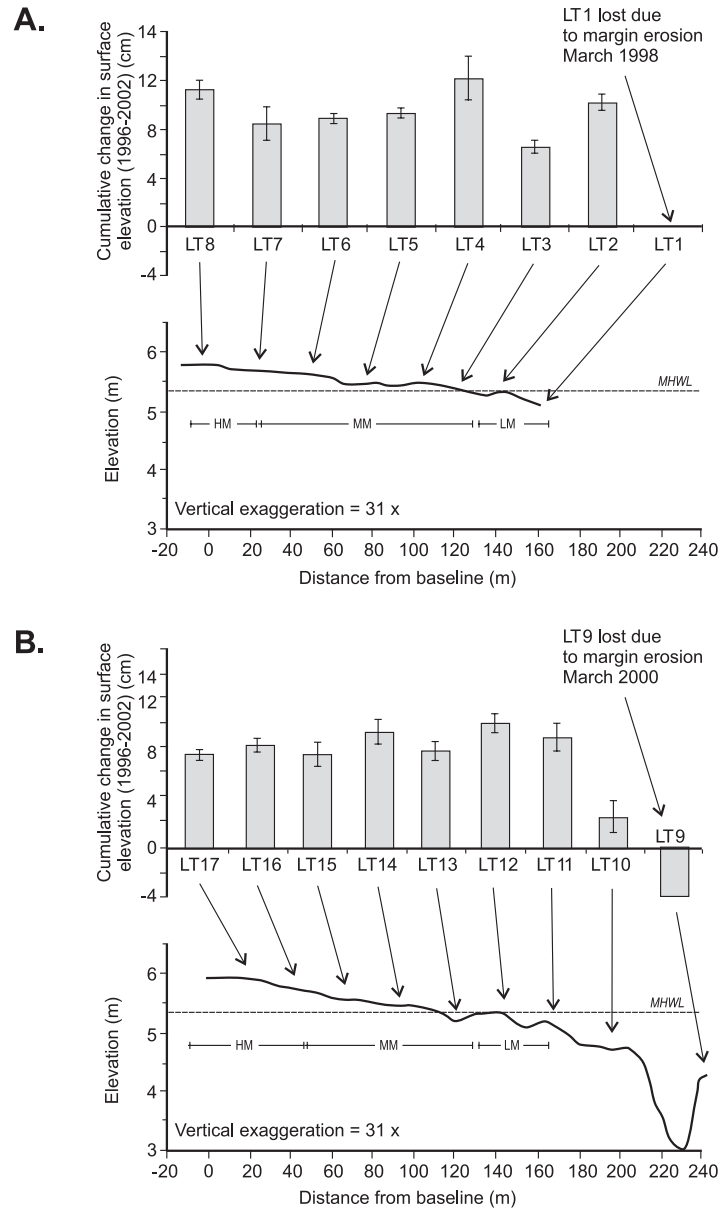

Figure 11.24 Sedimentation along two transects on Allen Creek marsh 1986–2002: (A) west transect; (B) east transect. The east transect is shown as line AA′ in Figure 11.3 and the west transect is parallel to it and 100 m to the west. At this site there is very little relationship between elevation and deposition because most of the marsh surface lies below the spring high tide limit and because of the effects of ice (van Proosdij *et al.*, 2006b).

Kostaschuk *et al.*, 2008). The wide range of accretion rates reflects the variety of locations for saltmarsh growth and thus differences in the supply of sediment and rate of organic matter accumulation. It also reflects differences in rates between low marsh sites, where deposition is usually highest, and high marsh sites where, as we saw earlier, the reduced number of flooding cycles ultimately reduces the rate of accumulation. It has been suggested that the marsh can be expected to drown gradually if the rate of accretion on a marsh is less than rates of sea level rise predicted for the next 50–100 years (e.g. Stevenson *et al.*, 1986; Temmerman *et al.*, 2004; Goodman *et al.*, 2007).

Examination of saltmarsh accretion over centuries to several thousands of years suggests that accretion rates change over time both in response to changing environmental conditions controlling sediment supply and plant growth, but also in response to fluctuations in sea level

and rates of sea level rise (Allen, 2000; Madsen *et al.*, 2007). In part this may reflect variations in the number of flooding cycles accompanying sea level change and the feedback relationship between flooding frequency and elevation relative to sea level at a point on a marsh. The result is that accretion rates tend to decrease during periods of stable or falling sea level and to increase during periods of rising sea level. In some cases rising sea level and transgression may be accompanied by increased sediment supply to the marsh. There is also some evidence from Louisiana marshes, where subsidence produces very high rates of relative sea level rise, that marshes may be able to accrete at rates up to 10 mm a^{-1} (Reed *et al.*, 2009). The response of marshes to sea level rise has been explored in a number of simulation models (e.g. French, 1993; Allen, 1995; Callaway *et al.*, 1996; Temmerman *et al.*, 2004; Kirwan and Murray, 2008). These offer some insights into the range of potential responses but their predictive ability is generally limited by fairly crude assumptions that make application to a particular site difficult.

The survival of salt marshes in the face of sea level rise much greater than the present does not depend on the ability of marshes to keep pace through vertical accretion. Saltmarsh vegetation can become established within a period of a few years and new saltmarshes develop rapidly whenever new opportunities exist within intertidal areas. Saltmarshes, like coral reefs, did not simply survive the Holocene transgression, but were a significant coastal feature throughout, with new marshes developing as estuaries were drowned and as barriers transgressed or developed anew. As sea level rises, flooding extends farther inland and in most cases we could expect the same thing to happen in the face of climate-change-induced sea level rise (Reed, 1995). The major problem with this comes not from the operation of the natural ecosystem, but from the effects of hardening of the coast. This could restrict the potential for inland migration of marshes, a concept termed 'coastal squeeze' (Pethick, 2001). The danger here is that hard structures such as dykes, seawalls and road embankments may simply prevent transgression of a natural shoreline and thus prevent this form of natural response. There is a need therefore to recognise these in coastal management planning, and indeed it is explicitly recognised within programmes of 'managed retreat' (see Section 11.5). Nevertheless, saltmarsh loss due to infilling, reclamation and a range of other human activities is still a much more significant threat than the effects of sea level rise.

Saltmarsh cycles and evolution

Some saltmarshes develop in areas where they expand to occupy much of the space in a lagoon behind a barrier system or areas protected by levees from wave action in the main bay or lagoon. The marsh margin especially in sandy intertidal systems may be marked by a narrow beach and small dune system that acts to protect the marsh behind from major erosional events or there may be a transitional zone of sparse vegetation that is occasionally pushed landward during storm events. In some lagoon and estuarine situations where fetch lengths are long enough in some directions to produce significant wave action the marsh margin may be eroded during storms leading to the formation of a marsh margin cliff that then recedes over time leading to a reduction in marsh area and ultimately to a net loss of sediment from the marsh (Allen, 1989; Ke and Collins, 2002; van der Wal and Pye, 2004). Recession of the cliff occurs as a result of wave action and erosion of the toe of the cliff which leads to undercutting and eventual toppling of material from the crest of the cliff (Figure 11.25). Cliff erosion takes place through all the mechanisms detailed in Chapter 13, but in this case the cliff may be completely overtopped at high tide. Direct wave attack may dislodge large blocks from near the crest where the sediments are strongly bound by roots of the vegetation and these can be deposited on the platform in front of the cliff (Figure 11.25b). Blocks of material from the crest can also be deposited on the marsh surface during periods of high waves when the water level is near the level of the cliff top and the process can also occur as a result of ice action under similar water level conditions.

Since marshes are generally areas of net deposition it is possible to determine the mass

Figure 11.25 Erosion of saltmarsh cliffs, Allen Creek marsh: (A) photograph of wave action on the cliff on the rising tide; (B) view of the marsh margin cliff at low tide showing notching and the accumulation of blocks of eroded material on the erosional platform; (C) Minudie marsh, Bay of Fundy showing an old marsh cliff now protected by the establishment of vegetation in front of it and beginning of a progradational cycle. The old cliff will be preserved for a number of years until the new marsh buries it beneath new deposits.

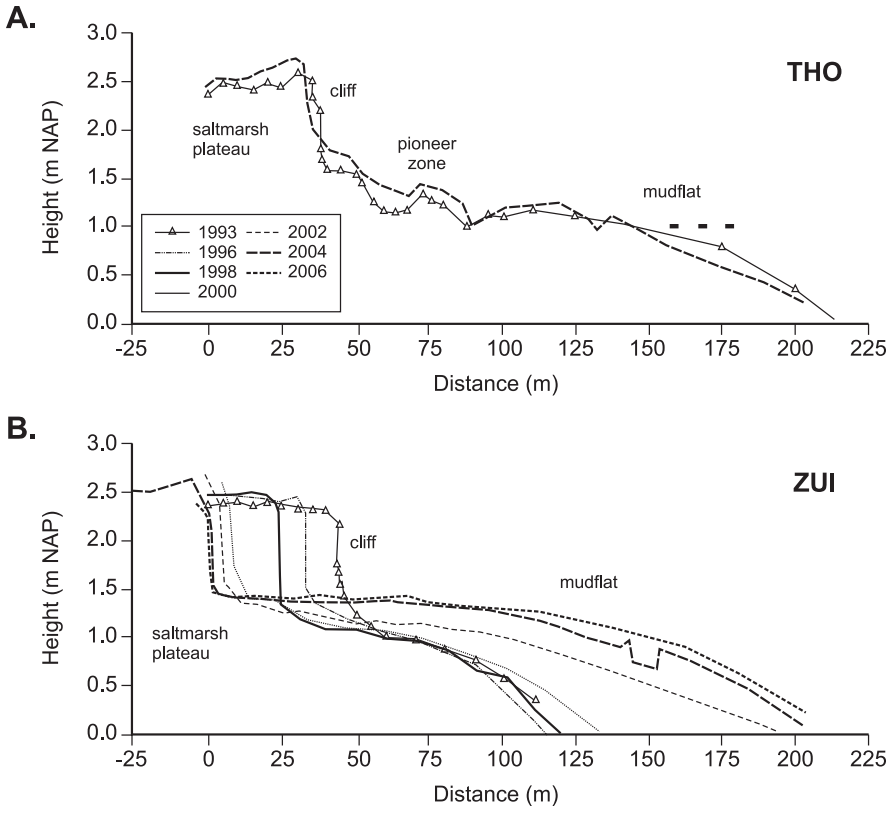

Figure 11.26 Examples of profile evolution on (A) an accreting marsh and (B) an eroding marsh in the Westerschelde, The Netherlands (van der Wal *et al.*, 2008).

balance of the marsh on an annual or longer time scale. Where the marsh is mature with few changes in the areal extent, the annual mass balance can be determined from measurement of accretion over the marsh surface. However, the expansion of vegetation onto previously bare intertidal areas and the existence of an erosional cliff both complicate the assessment of the mass balance and, while both change the area of the marsh, the loss of sediment associated with marsh cliff erosion is likely to be a lot higher than the addition of a similar area through extension of vegetation (Moreira, 1992; van Proosdij *et al.*, 2006b). Where vegetation extends onto the intertidal flats, the thickness of sediment added per unit area will be only a few millimetres. However, erosion of the cliff will produce a loss per unit area equal to the height of the bluff – this may be a metre or more in some marshes. In this circumstance, determination of the mass balance requires careful surveying of the marsh margins to determine areas of advance and retreat and the determination of the height and bulk density of sediments making up the marsh cliff. Because the marsh surface continues to accumulate sediment even while the areal extent is decreasing due to cliff erosion it is possible for the mass balance to be positive for many years after erosion is initiated.

A saltmarsh cycle can be defined as a period of seaward extension of the marsh, followed by development of a marsh cliff and a period of erosion as the cliff retreats landward until it is stabilised by recolonisation of vegetation in front of the cliff (Figure 11.26). They have been recognised and described from a number of saltmarshes world-wide (Yapp *et al.*, 1917; Allen, 1989, 2000; Pringle, 1995; Ollerhead *et al.*, 2005; van der Wal *et al.*, 2008). The cycles of accretion and erosion can be initiated by a number of

factors, including extrinsic ones such as changes in winds and storm intensity (Schwimmer, 2001) or changes in the position of estuary channels (Pringle, 1995). In some areas the marsh cycles may result from intrinsic factors reflecting feedback between vertical growth of the marsh surface and the establishment of a steep section at the outer edge of the marsh that evolves into a cliff and initiates a period of recession while the saltmarsh surface continues to accrete. One of the earliest reports of such an 'intrinsic-effect' cycle comes from Yapp *et al.* (1917) who worked in the Dovey estuary in Wales (cited in Allen, 2000). Cycles reported from the Westerscheldte estuary (van der Wal *et al.*, 2008) and from the Cumberland Basin (Ollerhead *et al.*, 2005) also appear to reflect a form of self-organisational feedback.

In the Cumberland Basin the process of seaward extension of marsh vegetation across tidal mudflats is rapid initially but slows as vegetation is established lower in the tidal frame where growth is restricted by longer periods of immersion and greater exposure to wave action (Figure 11.27). A cliff may form as a result of vertical accretion on the marsh over a period of several years, or it may be initiated by a major storm event. Once established wave reflection from the cliff face prevents the re-establishment of vegetation in front of the cliff until it has retreated to the point where energy dissipation over the erosional mudflat ramp is sufficient to permit revegetation (Figures 11.25c and 11.27). The cycle then begins again, with the residual cliff being preserved and eventually largely buried beneath new saltmarsh deposits (Ollerhead *et al.*, 2005).

Saltmarsh cliffs and sedimentation erosion cycles may also reflect the effects of sea level changes and fluctuations on a scale of hundreds to thousands of years (Schwimmer and Pizzuto, 2000). Marsh evolution on this time scale will reflect the effects of the Holocene transgression as well as local sea level fluctuations. Sea level rise increases the accommodation space for vertical growth of saltmarshes, permitting thick units of sediments, including peat beds, to develop. A range of possible scenarios can be envisaged, reflecting different sea level curves (e.g. fluctuation around a steady level or fluctuation within a general trend for sea level rise) and the local geomorphic setting within which the marsh develops (e.g. transgressive barrier lagoon system, stable barrier lagoon system and estuary). These have been documented extensively in the marshes of the Severn Estuary (see Allen, 2000 for a summary) and for marsh systems in many other parts of the world. One possible stratigraphic scenario, which takes into account both the simultaneous evolution of the marsh surface and that of the tidal creek network, is depicted in Figure 11.28.

11.4 Mangroves

Mangrove wetlands are the dominant coastal ecosystem of tidal salt and freshwater areas in the tropics and, where they are protected from cold outbreaks, they can extend into the sub-tropical zone. In terms of species they can be divided into the Old World, including East Africa and the Indo-Pacific region, and the new World including North and South America and West Africa. In North America they are well established in southern Florida in the Everglades but further north and along the Gulf coast into Texas their range fluctuates in response to the impact of freezing temperatures during cold air outbreaks (Stevens *et al.*, 2006). Black mangroves can survive lower temperatures than red mangroves and therefore tend to be found at the northern limit (Mitsch and Gosselink, 2000). On the west coast they grow as far north as Baja, California. In South America they extend as far south as 30° on the east coast but on the west coast they are limited to about 5° because of the effects of the cold Humbold current. Mangroves are not found in the Mediterranean but occur throughout most of the Pacific coast of Asia and along the north and east coasts of Australia and parts of North Island, New Zealand.

11.4.1 Mangrove swamp form, flooding and vegetation zonation

Mangroves can occur as a thin fringe along the borders of bays and lagoons or salt ponds, as well

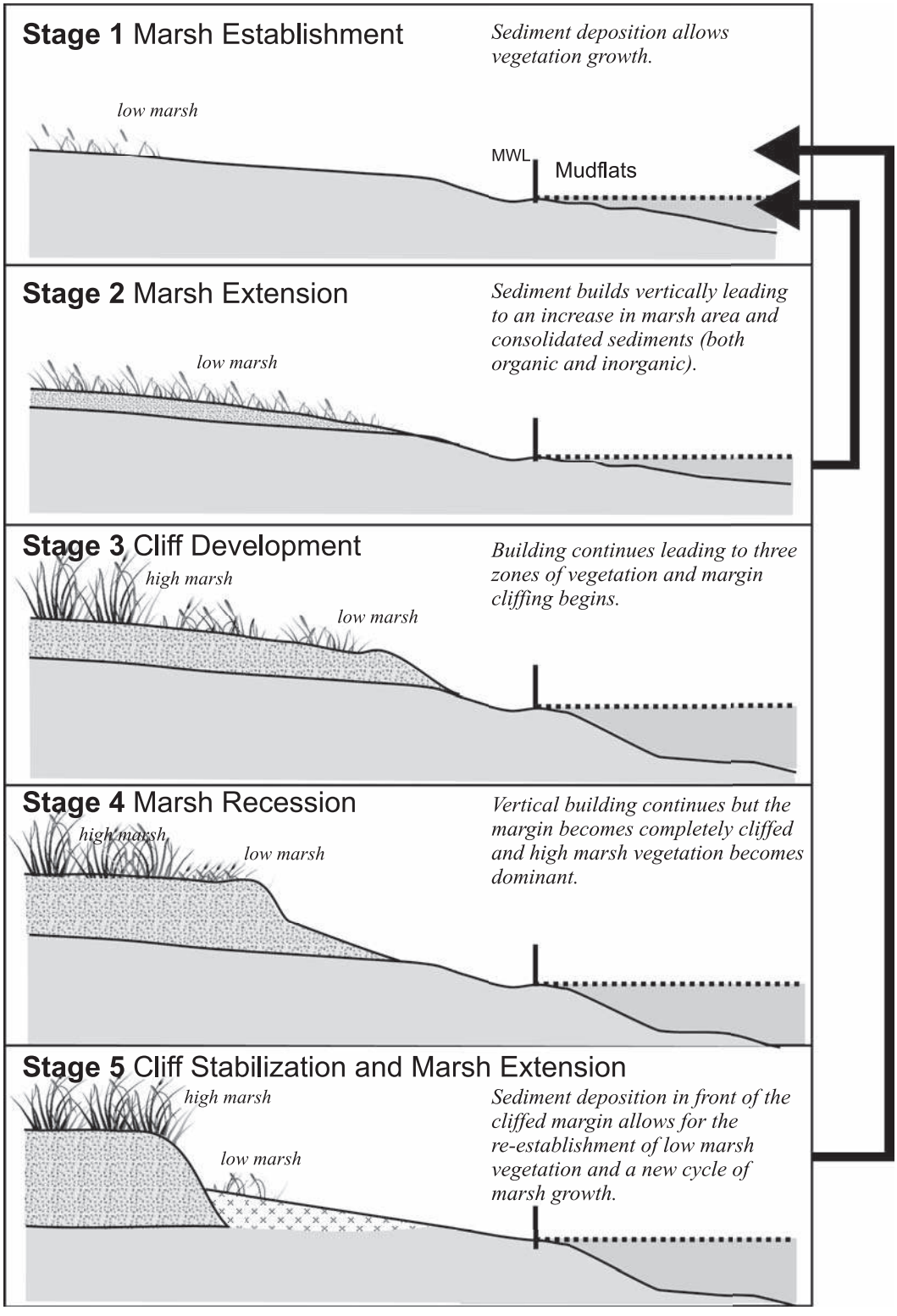

Figure 11.27 Schematic model of the stages in a cycle of accretion and erosion of marshes in the Cumberland Basin (Ollerhead *et al.*, 2005).

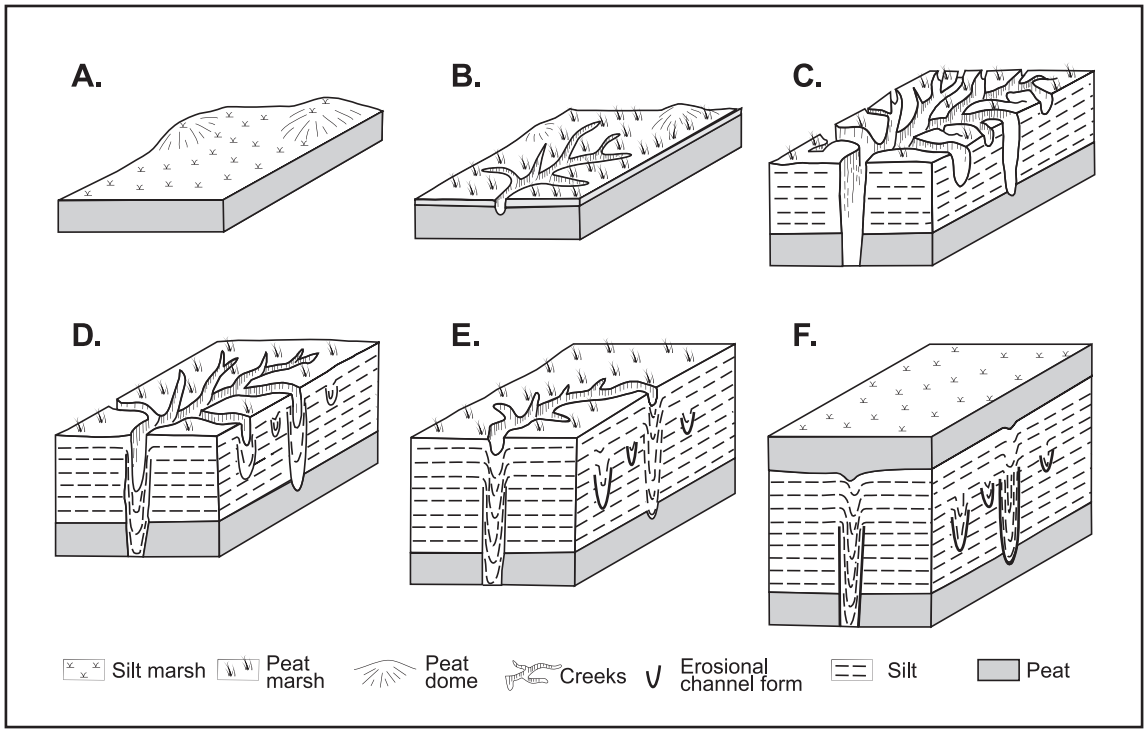

Figure 11.28 Conceptual morphostratigraphic model for the evolution of established coastal marshes in response to one fluctuation of an unsteadily rising sea level. The vertical scale and the cross-sectional scale of the tidal creeks are greatly exaggerated (after Allen, 2000).

as in a belt hundreds of metres to kilometres in width in prograding deltaic environments such as the muddy deltas of rivers in Malaysia, Indonesia, Vietnam and northern Australia. Mangrove establishment requires shelter from high wave energy conditions and so the geomorphological settings in which they are found are similar to those of saltmarshes (Thom, 1982; Woodroffe, 1992; Augustinus, 1995 – see Figure 11.29). They can be found on open muddy coasts such as French Guiana where wave energy is dissipated over a wide nearshore zone (Allison and Lee, 2004) and on muddy deltaic coasts such as the Red River in Vietnam (van Santen *et al.*, 2007) fringing active delta lobe mudflats, behind wave worked cheniers and along the banks of estuaries and distributary channels. They also occur in estuaries and embayments (Woodroffe *et al.*, 1989; Anthony, 2004; Knight *et al.*, 2008) and in salt ponds and areas sheltered by sandy barriers (Méndez Linares *et al.*, 2007) and coral reefs (Woodroffe, 1981, 1995; Fujimoto *et al.*, 1996).

Mangrove forests may also be characterised on the basis of the dominant physical processes controlling exchanges of water and sediment (Woodroffe, 1992 – see Figure 11.30). Tide-dominated mangroves are generally close to the sea or to a tidal creek that permits continuous connection to ocean tides (Figure 10.29a). As a result, flooding occurs daily and salinity is relatively stable and is close to that of sea water. There is also a continuous exchange of organic and inorganic matter between the mangroves and the sea.

River-dominated mangroves occur in deltas and estuaries and water level fluctuations due to river flows may be more important than tides. Mangroves may be flooded for periods of weeks or months during the rainy season and there is a strong flow through of sediment and organic matter to the sea. Nevertheless, sedimentation tends

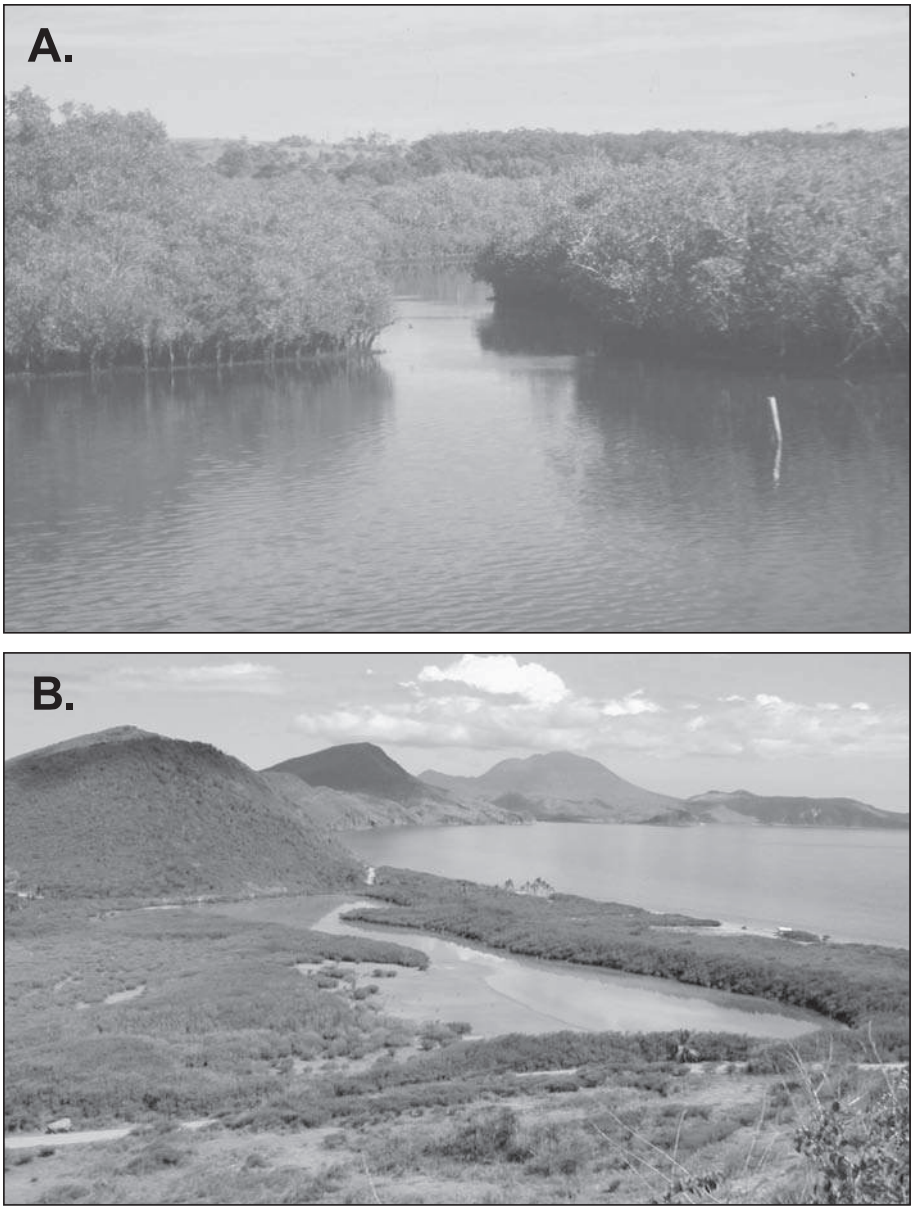

Figure 11.29 Examples of mangrove habitats: (A) estuarine mangroves, Myall River, NSW, Australia; (B) mangroves in a salt pond, South Friar's Beach, St Kitts.

to be quite rapid and inorganic sediments generally dominate over organic accumulation.

Interior mangroves such as the Florida Everglades occur in low-lying areas some distance from the sea and from tidal influence. They also tend to be cut off from river flooding and so salinity fluctuates with rainfall and evaporation. In the absence of inputs of mineral sediments, accumulation is dominantly organic, leading to the development of thick peat units. Mangroves in salt ponds where there is no permanent connection to the sea (Figure 11.29b) may be subject to similar water level and salinity fluctuations as riverine mangroves in areas with a pronounced dry season. Rainfall and runoff from the surrounding slopes produce high water levels and

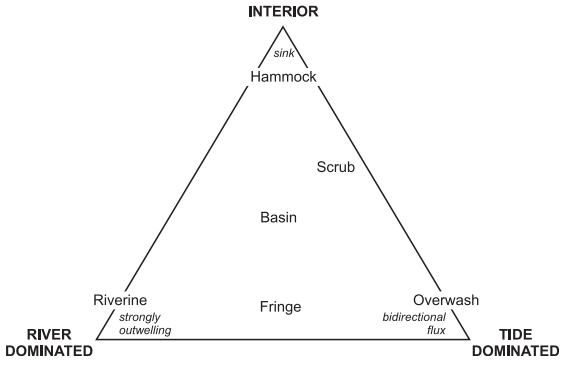

Figure 11.30 The relation between functional type of mangrove forests and the dominant physical processes. Riverine dominated habitats are characterised by strong outflow of sediments and organic material, tide-dominated mangroves have bi-directional fluxes and interior habitats are sinks largely for organic materials (after Woodroffe, 1992).

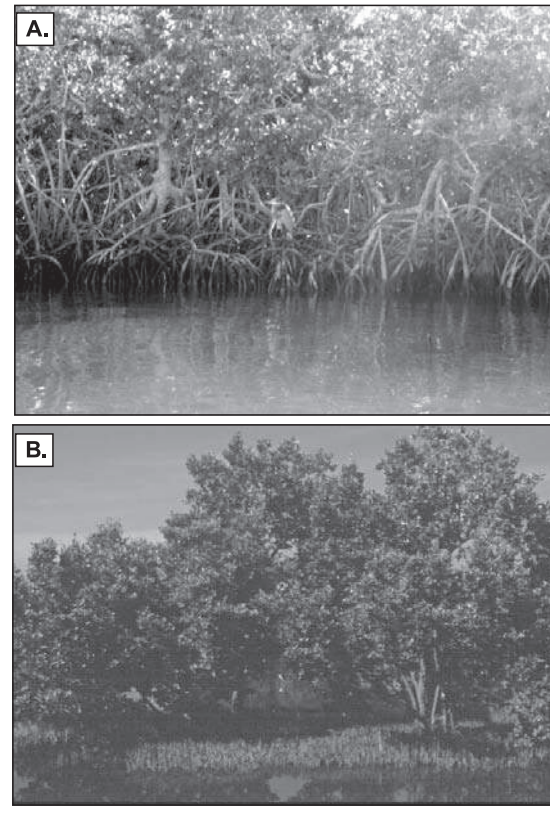

Figure 11.31 Adaptation by mangroves to waterlogged conditions: (A) red mangrove (*Rhizophora mangle*) showing the extensive aerial prop root system (photo M. Puddister); (B) pneumatophores of black mangrove.

reduced salinity during the rainy season, and evaporation leads to reduced water levels and increased salinity during the dry season. Like interior mangroves, they are cut off from regular tidal exchanges with the sea and there is considerable accumulation of organic material. However, run-off from the surrounding hill slopes can bring in considerable amounts of inorganic sediment. In a number of the Caribbean islands storm surge, associated with close passage of hurricanes, can result in overwash of the low barriers and the deposition of sandy beds over the organic-rich silt and clay beds that accumulate during most of the time.

There are about 54 species of true mangroves (those found only in wet, saline environments) with about half found in two families, Avicienniaceae and Rhizophoraceae (Hogarth, 1999). Mangroves are not only halophytic but they have adapted to growing in waterlogged soils where oxygen for respiration is difficult to obtain by special developments of the root forms. Roots of Rhizophora diverge from the trunk some distance above the soil forming a branching network of prop roots (Figure 11.31a) with air entering the portions of the roots above the water level. Because of this Rhizophora can grow down to the low-tide level and even just below, with the result that mangroves can occupy the whole intertidal zone, rather than just the upper half as is the case for saltmarshes. Species of *Avicennia* have roots that spread out just below the surface with pneumatophores that grow upward above the soil in a dense network of spikes (Figure 11.31b). In a mature Avicennia forest the pneumatophores can become so dense that they retard water flows to the extent that the depth of ponded waters is increased (Knight *et al.*, 2008) thus changing the hydrology of the whole area. Mangroves can spread to other sites rapidly because all species can disperse by water and most can survive long periods of transport. They are aided in this by a long period of development of the seed on the tree with the result that what is dispersed on the water is a seedling that can establish itself rapidly once it comes to rest on a suitable substrate.

Like saltmarsh and dune vegetation, there is a tendency for zonation of mangrove species, especially where there is a distinct gradient in flooding frequency or salinity. In the Friar's Bay salt pond (Figure 11.29b), red mangrove occupy most of the portions of the pond that are flooded frequently, with a border of black mangrove (*Avicennia germinans)* in the zone near the upper limit of flooding and some white mangrove (*Laguncularia racemosa*) at the edge of higher ground. Similar zonation is found in much of the Caribbean, Florida and Mexico.

Mangrove zonation is not as sensitive to flooding frequency as are saltmarsh plants. In part this is because of the adaptation of their root system to waterlogged conditions and in part to the fact that the canopy is always above the level of tidal inundation and thus respiration and photosynthesis can occur continuously even if the root system is flooded for days or months. In large basins where there is little topographic relief there may be little evidence of zonation and dominance by a single species (Knight *et al.*, 2008). Zonation may also be complicated in areas such as deltas where there are rapid variations in riverine flows and in sediment supply which influence mangrove distribution in addition to tidal effects (Méndez Linares *et al.*, 2007).

11.4.2 Flows and sediment deposition in mangroves

Conditions for measuring flows, TSS concentration and short-term deposition are not logistically as easy as for saltmarshes and the result is that there are fewer measurements of hydrodynamics and sedimentation than there are for saltmarshes (Augustinus, 1995). As is the case with saltmarshes, flow in tidal creeks and through the mangrove forest is driven by tidal water elevation changes and by the tidal prism (Wolanski *et al.*, 1992) The dense prop roots, pneumatophores and tree trunks of the mangrove forest act as very significant roughness elements with much of it extending beyond the water surface through tidal and riverine flows (Furkawa and Wolanski, 1996; Kobashi and Mazda, 2005). The result is that there is a marked reduction in flow speeds along the edge of tidal creek channels and away from the channels into the forest, and similar reductions for flows driven by riverine flooding (van Santen *et al.*, 2007). Furukwa and Wolanski (1996) report that flows beyond the margin seldom exceed 0.1 m s^{-1}, and similar observations have been found in other studies (Anthony, 2004; van Santen *et al.*, 2007).

The roots and trunks of mangroves similarly act to produce a rapid dissipation of wave energy away from the margin. The relatively small locally-generated waves in found in embayments, salt ponds and estuaries are quickly reduced in height to the point where the orbital motion is below that capable of causing sediment entrainment (Quartel *et al.*, 2007). Height reduction does depend somewhat on tidal stage and on the physical structure of the mangroves. Thus, Mazda *et al.* (2006) found that the rate of reduction of *Hs* was initially large in *Sonneratia* sp. which possess pneumatophores, but decreased as the tide rose because of the tapering nature of the pneumatophores spikes. At high tide, wave energy was again reduced because of the drag imposed by the trunks and branches. Similarly, Massel *et al.* (1999) measured changes in the energy spectra away from the bank of Cocoa Creek, near Townsville, Australia at different tidal stages (Figure 11.32). The first station was located on the mud flat in front of the mangroves and stations 2–4 were located in Rhizophora forest with dominant prop roots (Figure 11.32a). Station 5 was only flooded to a shallow depth around high tide and was located in a zone dominated by Aegiceras and Ceriops mangroves which do not have prop roots.

Mangroves thus act to encourage deposition of sediment in suspension and to reduce the potential for scour of sediments once deposited. Measurements of sediment deposition over tidal cycles or a few days can be carried out in a similar fashion to measurements on marshes, but where there is waterlogging, simple filter paper traps will not work and more robust surfaces such as canvas (Anthony, 2004; van Santen *et al.*, 2007) are deployed. As is the case with saltmarshes, the TSS concentration can be expected to decrease away from the mangrove margin as material is deposited on the surface and, in a simple tidally driven system, deposition can be expected to be

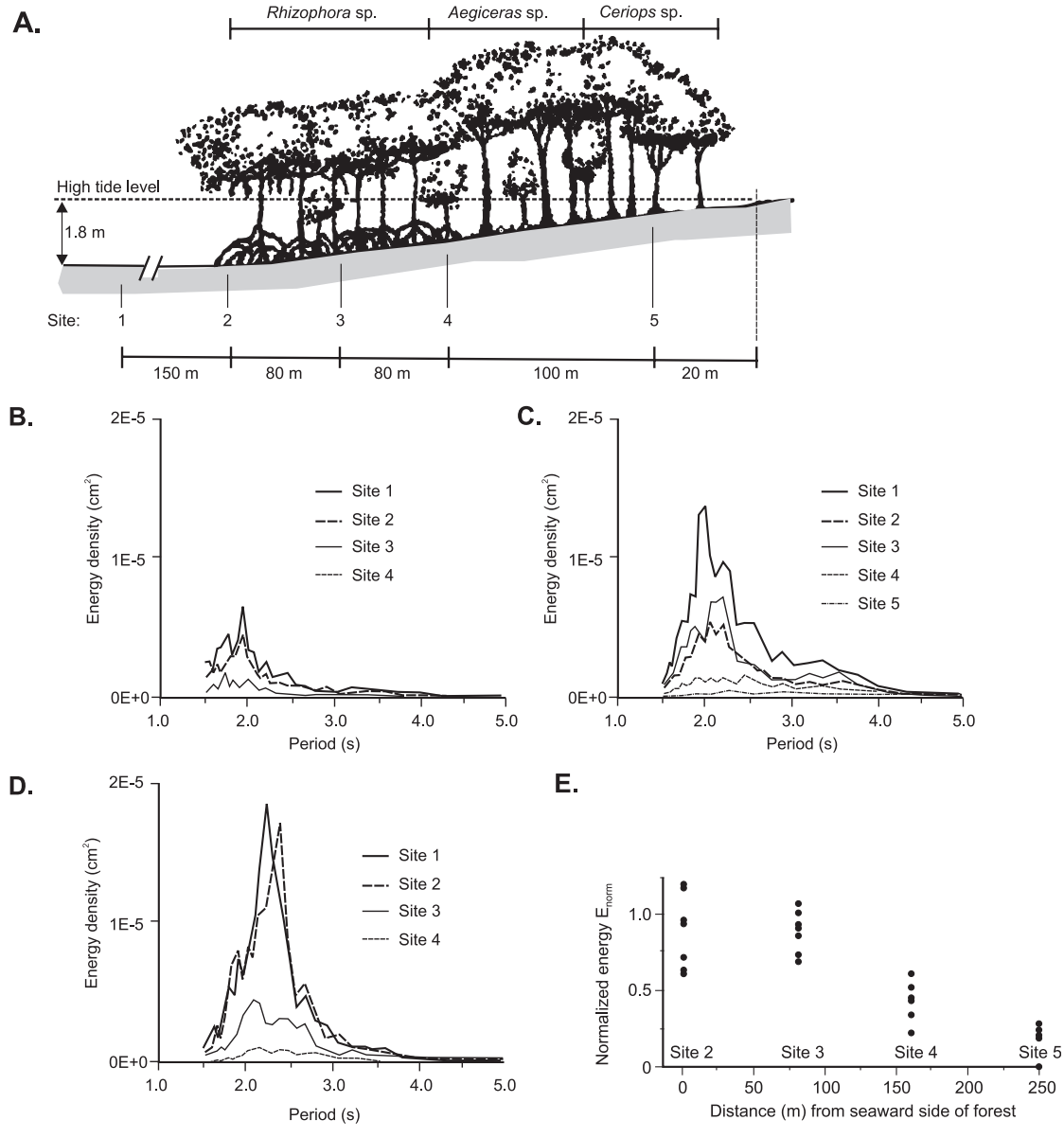

Figure 11.32 Measurements of wave attenuation in a mangrove community along a tidal creek at different tidal stages: (A) sketch of the transect showing instrument locations and dominant mangrove species; changes in wave spectra along the transect (B) on the rising tide (C) at high tide; and (D) on the falling tide; (E) normalised wave energy versus distance for all measurements (Massel *et al.*, 1999).

at a maximum near the tidal creek bank and to decrease away from it (Figure 11.33).

In addition to sediment imported from the bay, estuary or river, there is a steady supply of organic matter from leaf and stem litter and ultimately from the trunks and roots of the mangroves. The result is that mangrove sediments often contain large quantities of organic matter and the bulk density is initially quite low. Thus autocompaction is a problem here in the same way as it is for saltmarshes with the result that long-term estimates of sedimentation must be obtained from stratigraphic coring and dating (Woodroffe, 1981; Lynch *et al.*, 1989; Cahoon

Box 11.2 Mangroves and protection against tsunamis

Following the 26 December 2004 tsunami there have been several studies that have suggested that destruction in areas protected by a belt of mangroves was much less than in exposed areas (e.g. Danielsen *et al*., 2005; Kathiresan and Rajendran, 2005; Iverson and Prasad, 2007). The thesis is a simple one based on the known attenuation of wave energy within mangrove forests and it leads to a logical conclusion that planning for rebuilding of settlements in these vulnerable areas should include the potential for developing buffer zones of mangroves. Some of the studies have been criticised for misuse of statistical tests or for drawing conclusions from data that are not justified by the sampling strategy (e.g. Kerr *et al*., 2006; Baird and Kerr, 2007; Iverson and Prasad, 2007). It is clearly a multivariate problem and it is not easy in retrospect to provide reliable tests of the hypothesis.

Alongi (2008) provides a thoughtful review of some of the discussion, and makes the important point that the hydraulic characteristics of the tsunami waves are quite different from those used to measure wave attenuation (Massel, *et al*., 1999; Mazda *et al*., 2006). There is therefore a need to model the effectiveness of different mangrove species in attenuating tsunami waves and to assess the relative effectiveness of these versus, for example, other tree species or artificial shore protection in highly vulnerable areas.

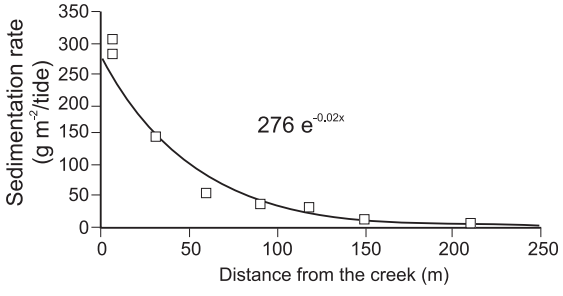

Figure 11.33 Observed and predicted sedimentation rate with distance from the tidal creek for one spring tidal cycle for measurements carried out at Cairns, Queensland, Australia (Furukawa and Wolanski, 1996).

and Lynch, 1997; Anthony, 2004; Ramcharan, 2004). Rates of accretion are similar to those reported for saltmarshes and like them vary with the geomorphic setting.

11.5 Conservation and management of saltmarshes and mangroves

The extent of both saltmarshes and mangrove ecosystems has been severely affected by human activities and there is now increasing awareness of the potential impact of these losses on other components of the marine ecosystem (Boorman, 1999; Adam, 2002; Alongi, 2002). In particular, the critical role of both within bays and estuaries as nurseries for fish and shell fish and for a wide range of birds and animals is well recognised. Saltmarshes have been subject to dyking and drainage for agricultural purposes for millennia, initially on a very small scale, but at an increasingly rapid rate since the eighteenth century in Western Europe (Doody, 2004). The Dutch landscape with its dykes and windmills probably represents the epitome of human impact on saltmarshes. Dutch technology was exported to many other areas including the Bay of Fundy where initial drainage by the Acadians in the 17th and the early 18th century was greatly expanded by English settlers with about 400 km^2 (about 85%) of high marsh presently dyked (Gordon and Cranford, 1984). The widespread destruction of mangrove forests is a more recent phenomenon, driven by a number of factors, including wood harvesting, aquaculture, port development and an expanding coastal tourism industry.

Recognition of the threats posed by human actions is relatively simple but addressing them

is a complicated task. Ideally these ecosystems can be protected within some form of coastal management policy (Morris, 2008). This may take the form of integrated coastal management that attempts to address the needs of all of the stakeholders, including the biotic ones (e.g. Clark, 1995; Kay and Alder, 2005; Christiansen *et al.*, 2008). Implementation requires considerable political will, often in the face of strong opposition from some of the groups most affected economically.

In a number of countries, including the UK, an end to large-scale conversion of saltmarshes to agricultural lands has come about partly because of environmental and conservation arguments, and also increasingly as a result of reduced economic benefits from the conversion and increasing costs of maintaining sea defence structures in the face of storm events and rising sea level (Doody, 2004). The concept of coastal squeeze now fits well with the recognition that saltmarshes may provide a flexible and low cost approach to protecting low-lying areas such as the Wash on the east coast of England from sea level rise and has given rise to trials of a policy of managed realignment in which some dyked agricultural fields are allowed to revert to saltmarshes through breaching of the sea defences in the hope that natural sedimentation on the saltmarsh will prove to be a more cost-effective method of providing coastal protection (Boorman, 1999; McGlashan, 2003; Doody, 2004; French, 2006; Turner *et al.*, 2007). Similar thinking has taken place in the Bay of Fundy, Canada where the costs of maintaining dykes is generally higher than the economic returns from agriculture and there are now small steps being taken towards testing managed realignment (Byers and Chmura, 2007). There is also broader support for saltmarsh protection and restoration within the Gulf of Maine Council that embraces both US States and Canadian Provinces along the Gulf of Maine and Bay of Fundy (e.g. Taylor, 2008).

While direct human impacts through drainage and infilling continue to be the most significant threat to saltmarshes and mangroves world-wide, the problem is a relatively simple one to identify. The indirect impacts of human activities manifested in global climate change (warming) and sea level are harder to predict and therefore to accommodate within management strategies. Global warming and climate change will likely bring changes to plant populations and these in turn may have an impact on the functioning of marsh and mangrove ecosystems (Woodruffe, 1990; Adam, 2002; Reed, 2002; Alongi, 2002; Reed *et al.*, 2009). Both saltmarsh and mangrove ecosystems are adapted to a wide range of natural stresses, including the impacts of major storms (Paling *et al.*, 2008) and to sea level rise, as is evident from their response to the Holocene transgression (e.g. Fujimoto, 1996; Allen, 2000). The threat comes not so much from the physical impacts of climate change and sea level rise but whether human activities will constrain in some way the ability of these ecosystems to migrate landward or to different locations.

Further reading

Mitsch, W. J. and Gosselink, J. G. 2000. *Wetlands*. Wiley, New York, 920 pp.

This is a classic text on the biology and dynamics of all wetlands.

Allen, J. R. L. 2000. Morphodynamics of Holocene saltmarshes: a review sketch from the Atlantic and Southern North Sea coasts of Europe. *Quaternary Science Reviews*, **19**, 1155–1231.

This is an excellent review of all aspects of the physical dynamics of saltmarshes.

References

Adam, P. 1990. *Saltmarsh Ecology*. Cambridge University Press, Cambridge, 461 pp.

Adam, P., 1997. Absence of creeks and pans in temperate Australian salt marshes. *Mangroves and Salt Marshes*, **1**, 239–241.

Adam, P. 2002. Saltmarshes in a time of change. *Environmental Conservation*, **29**, 39–60.

Allen, J. R. L. 1989. Evolution of salt-marsh cliffs in muddy and sandy systems: A qualitative comparison of British west-coast estuaries. *Earth Surface Processes and Landforms*, **14**, 85–92.

Allen, J. R. L. 1990a. Salt marsh growth and stratification: A numerical model with special reference to the Severn Estuary, southwest Britain. *Marine Geology*, **95**, 77–96.

Allen, J. R. L., 1990b. The formation of coastal peat marshes under an upward tendency of relative sea-level. *Journal of the Geological Society of London*, **147**, 743–745.

Allen, J. R. L. 1995. Simulation models of salt-marsh morphodynamics: some implications for high-intertidal sediment couplets related to sea-level changes. *Sedimentary Geology*, **113**, 211–223.

Allen, J. R. L., 2000. Morphodynamics of Holocene salt-marshes: a review sketch from the Atlantic and Southern North Sea coasts of Europe. *Quaternary Science Reviews*, **19**, 1155–1231.

Allen, J. R. L. and Pye, K. 1992. *Saltmarshes: Morphodynamics, Conservation and Engineering Significance*. Cambridge University Press, Cambridge, 184 pp.

Allen, J. R. L. and Duffy, M. J. 1998. Medium-term sedimentation on high intertidal mudflats and salt marshes in the Severn Estuary, SW Britain: the role of wind and tide. *Marine Geology*, **150**, 1–27.

Allison, M. A. and Lee, M. T. 2004. Sediment exchange between Amazon mudbanks and shore-fringing mangroves in French Guiana. *Marine Geology*, **208**, 169–190.

Alongi, D. M. 1998. *Coastal Ecosystem Processes*. CRC Press, Boca Raton, FL, 419 pp.

Alongi, D. M. 2002. Present state and future of the world's mangrove forests. *Environmental Conservation*, **29**, 333–349.

Alongi, D. M. 2008. Mangrove forests: Resilience, protection from tsunamis, and responses to global climate change. *Estuarine, Coastal and Shelf Science*, **76**, 1–13.

Anthony, E. J. 2004. Sediment dynamics and morphological stability of estuarine mangrove swamps in Shebro Bay, West Africa. *Marine Geology*, **208**, 207–224.

Augustinus, P. G. E. F. 1995. Geomorphology and sedimentology of mangroves. In Perillo, G. (editor), *Geomorphology and Sedimentology of Estuaries*. Elsevier, Amsterdam, pp. 333–357.

Baird, A. H. and Kerr, A. M. 2007. Landscape analysis and tsunami damage in Aceh: comment. *Landscape Ecology*, **23**, 3–5.

Bartholdy, J., Christiansen, C. and Kunzendorf, H. 2004. Long term variations in backbarrier salt marsh deposition on the Skallingen peninsula – the Danish Wadden Sea. *Marine Geology*, **203**, 1–21.

Bayliss-Smith, T. P., Healey, R., Lailey, R., Spencer, T. and Stoddart, D. R. 1979. Tidal flows in salt marsh creeks. *Estuarine Coastal and Shelf Science*, **9**, 235–255.

Beeftink, W. G. 1977. Salt-marshes. In Barnes, R. S. K. (ed.), *The Coastline*. Wiley, Chichester, 93–121.

Boorman, L. A. 1999. Saltmarshes – present functioning and future change. *Mangroves and Salt Marshes*, **3**, 227–241.

Boumans, R. M. and Day, J. W. Jr. 1993. High precision measurements of sediment elevation in shallow coastal areas using a sedimentation-erosion table. *Estuaries*, **16**, 375–380.

Brown, S. L. 1998. Sedimentation on a Humber saltmarsh. In Black, K. S., Paterson, D. M. and Cramp, A. (eds.) *Sedimentary Processes in the intertidal Zone. Geological Society of London*, Special Publication 139, 69–83.

Byers, S. E. and Chmura, G. L. 2007. Salt marsh vegetation recovery on the Bay of Fundy. *Estuaries and Coasts*, **30**, 869–977.

Cahoon, D. R. and D. J. Reed. 1995. Relationships among marsh surface topography, hydroperiod, and soil accretion in a deteriorating Louisiana salt marsh. *Journal of Coastal Research*, **11**, 357–369.

Cahoon, D. R., Reed, D. J. and Day, J. W. Jr. 1995. Estimating shallow subsidence in microtidal salt marshes of the southeastern United States: Kaye and Bighoorn revisited. *Marine Geology*, **128**, 1–9.

Cahoon, D. R. and Lynch, J. C. 1997. Vertical accretion and shallow subsidence in a mangrove forest of southwestern Florida, USA. *Mangroves and Salt Marshes*, **1**, 173–186.

Cahoon, D. R., French, J. R., Spencer, T., Reed, D. J. and Möller, I. 2000. Vertical accretion versus elevational adjustment in UK saltmarshes: an evaluation of alternative methodologies. In Pye, K. and Allen, J. R. L. (eds.), *Coastal and Estuarine Environments*. Journal of The Geological Society Special Publication, **175**, pp. 223–238.

Callaway, J. C., DeLaune, R. D. and Patrick, W. H. Jr., 1996a. Chernobyl ^{137}Cs used to determine sediment accretion rates at selected northern European coastal wetlands. *Limnology and Oceanography*, **41**, 444–450.

Callaway, J. C., Nyman, J. A. and DeLaune, R. D., 1996b. Sediment accretion in coastal wetlands: a review and simulation model of processes. *Current Topics in Wetland Biogeochemistry*, **2**, 2–23.

Callaway, J. C., DeLaune, R. D. and Patrick, W. H. Jr. 1997. Sediment accretion rates from four coastal wetlands along the Gulf of Mexico. *Journal of Coastal Research*, **13**, 81–191.

Chapman, V. J. 1960. *Salt Marshes and Deserts of the World*. 1st edn. Leonard Hill, London.

Childers, D. L.; Skalar, F. H.; Drake, B. and T. Jordan. 1993. Seasonal measurements of sediment elevation in three mid-Atlantic estuaries. *Journal of Coastal Research*, **9**, 986–1003.

Christiansen, S. M., Tarp, P. and Hjortso, C. N. 2008. Mangrove forest management planning in coastal buffer and conservation zones, Vietnam: a multi-methodological approach incorporating multiple stakeholders. *Ocean and Coastal Management*, **50**, 712–726.

Christiansen, T., Wiberg, P. L. and Milligan, T. G. 2000. Flow and Sediment transport on a tidal salt marsh. *Estuarine, Coastal and Shelf Science*, **50**, 315–331.

Clark, J. R. 1995. *Coastal Zone Management Handbook*. CRC Press, Boca Raton, FL, 694 pp.

D'Alpaos, A., Lanzoni, S., Marani, M., Bonometto, A., Cecconi, G. and Rinaldo, A. 2007. Spontaneous tidal network formation within a constructed salt marsh: Observations and morphodynamic modelling. *Geomorphology*, **91**, 186–197.

Danielsen, F, Sorensen, M. K., Olwig, M. F., and nine others. 2005. Asian tsunami: a protective role for coastal vegetation. *Science*, **310**, 643.

Davidson-Arnott, R. G. D., van Proosdij, D., Ollerhead, J. and Schostak, L. E. 2002 Hydrodynamics and sedimentation in saltmarshes: Examples from a macrotidal marsh, Bay of Fundy. *Geomorphology*, **48**, 209–231.

Dionne, J. C. 1989. An estimate of shore ice action in a Spartina tidal marsh, St. Lawrence Estuary, Quebec, Canada. *Journal of Coastal Research*, **5**, 281–293.

Doody, J. P. 2004. 'Coastal Squeeze' – an historical perspective. *Journal of Coastal Conservation*, **10**, 129–138.

French, J. R. 1993. Numerical simulation of vertical marsh growth and adjustment to accelerated sea-level rise, North Norfolk, UK. *Earth Surface Processes and Landforms*, **18**, 63–81.

French, J. R. and Stoddart, D. R. 1992. Hydrodynamics of salt marsh creek systems: implications for marsh morphodynamic development and matter exchange. *Earth Surface Processes and Landforms*, **17**, 235–252.

French, J. R. Spencer, T. 1993. Dynamics of sedimentation in a tide dominated backbarrier salt marsh, Norfolk, United Kingdom. *Marine Geology*, **110**, 315–331.

French, J. R, Spencer, T., Murray, A. L. and Arnold, N. S. 1995. Geostatistical analysis of sediment deposition in two small tidal wetlands, Norfolk, UK. *Journal of Coastal Research*, **11**, 308–321.

French, P. W. 2006. Managed realignment – the developing story of a comparatively new approach to soft engineering, *Estuarine, Coastal and Shelf Science*, **67**, 409–423.

Fujimoto, K., Miyagi, T., Kikuchi, T. and Kawana, T. 1996. Mangrove habitat formation and response to Holocene sea-level changes on Kusrae island, Micronesia. *Mangroves and Salt Marshes*, **1**, 47–57.

Furukawa, K. and Wolanski, E. 1996. Sedimentation in mangrove forests. *Mangroves and Salt Marshes*, **1**, 3–10.

Goodman, J. E., Wood, M. E. and Gehrels, W. R. 2007. A 17-yr record of sediment accretion in the salt marshes of Maine (USA). *Marine Geology*, **242**, 109–121.

Gordon, D. C. and C. Desplanque. 1983. Dynamics and environmental effects of ice in the Cumberland Basin of the Bay of Fundy. *Canadian Journal of Fisheries and Aquatic Sciences*, **40**, 1331–1342.

Gordon, D. C. and Cranford, P. J. 1984. Export of organic matter from macrotidal saltmarshes in the upper Bay of Fundy, Canada. In Mitsch, W. J. (ed.), *Global Wetlands: Old World and New*. Elsevier, Amsterdam, pp. 257–264.

Gordon, D. C., Cranford, P. J. and Desplanque, C. 1985. Observations on the ecological importance of salt marshes in the Cumberland Basin, a macrotidal estuary in the Bay of Fundy. *Estuarine, Coastal and Shelf Science*, **20**, 205–227.

Gray, A. J. 1992. Saltmarsh plant ecology: Zonation and succession revisited. In Allen, J. R. L. and Pye, K. (eds.), *Saltmarshes, Morphodynamics, Conservation and Engineering Ssignificance*. Cambridge University Press, Cambridge, pp. 63–79.

Healey, R. G., Pye, K., Stoddart, D. R. and Bayliss-Smith, T. P. 1981.Velocity variations in salt marsh creeks, Norfolk, England. *Estuarine, Coastal and Shelf Science*, **13**, 535–545.

Hogarth, P. J. 1999. *The Biology of Mangroves*. Oxford University Press, Oxford, 228 pp.

Iverson, L. R. and Prasad, A. M. 2007. Using landscape analysis to assess and model tsunami damage in Aceh Province, Sumatra. *Landscape Ecology*, **22**, 323–331.

Jacobson, H. A., 1988. Historical development of the saltmarsh at Wells, Maine. *Earth Surface Processes and Landforms*, **13**, 475–486.

Jennings, S. C., Carter, R. W. G. and Orford, J. D. 1995. Implications for sea-level research of salt marsh and mudflat accretionary processes along paraglacial barrier coasts. *Marine Geology*, **124**, 129–136.

Kathiresan, K. and Rajendran, N. 2005. Coastal mangrove forests mitigated tsunami, *Estuarine, Coastal and Shelf Science*, **65**, 601–606.

Kay, R. C. and Alder, J. 2005. *Coastal Planning and Management*. 2nd edn. Taylor and Francis, London, 380 pp.

Ke, X. and Collins, M., 2002. Saltmarshes in the West Solent (southern England): their morphodynamics and evolution. In Healy, T., Wang, Y. and Healy, J. A. (eds.), *Muddy Coasts of the World: Processes, Deposits and Functions*. Elsevier, Amsterdam, pp. 411–440.

Kearney, M. S. and Ward, L. G. 1986. Accretion rates in brackish marshes of a Chesapeake Bay estuarine tributary. *Geological Marine Letters*, **6**, 41–49.

Kelley, J. T., Gehrels, W. R. and Belknap, D. F. 1995 Late Holocene sea-level rise and the geological development of tidal marshes at Wells, Maine, USA. *Journal of Coastal Research*, **11**, 136–153.

Kerr, A. M., Baird, A. H. and Campbell, S. J. 2006. Comments on 'Coastal mangrove forests mitigated tsunami' by K. Kathiresan and N. Rajendran. *Estuarine, Coastal and Shelf Science*, **67**, 539–541.

Kirwan, M. L. and Murray, A. B. 2008. Ecological and morphological response of brackish tidal marshland to the next century of sea level rise: Westham island, British Columbia. *Global and Planetary Change*, **60**, 471–486.

Knight, J. M., Dale, P. E. R., Dunn, R. J. K., Broadbent, G. J. and Lemckert, C. J. 2008. Patterns of tidal flooding within a mangrove forest: Coombabah Lake, southeast Queensland, Australia. *Estuarine, Coastal and Shelf Science*, **76**, 580–593.

Knutson, P. L., Brochu, R. A., Seelig, W. N. and Inskeep, M. 1982. Wave damping in Spartina alterniflora marshes. *Wetlands*, **2**, 87–104.

Kobashi, D. and Mazda, Y. 2005. Tidal flow in riverine-type mangroves. *Wetlands Ecology and Management*, **13**, 615–619.

Kostaschuk, R.A, Chen, Z, Saito, Y. and Wang, Z. 2008. Sedimentation rates and heavy metals in a macrotidal salt marsh: Bay of Fundy, Canada. *Environmental Geology*, **55**, 1291–1298.

Leonard, L. A. 1997. Controls of sediment transport and deposition in an incised mainland marsh basin, southeastern North Carolina. *Wetlands*, **19**, 617–626.

Leonard, L. A., Hine, A. C., Luther, M. E., Stumpf, R. P. and E. E. Wright. 1995a. Sediment transport processes in a west-central Florida open marine marsh tidal creek; the role of tides and extra-tropical storms. *Estuarine, Coastal and Shelf Science*, **41**, 225–248.

Leonard, L. A., Hine, A. C. and Luther, M. E. 1995b. Surficial sediment transport and deposition processes in a Juncus roemerianus marsh, West-central Florida. *Journal of Coastal Research*, **11**, 322–336.

Leonard, L. A. and Luther, M. E. 1995. Flow hydrodynamics in tidal marsh canopies. *Limnology and Oceanography*, **40**, 1474–1484.

Leonard, L. A. and Croft, A. L. 2006. The effect of standing biomass on flow velocity and turbulence in Spartina alterniflora canopies. *Estuarine, Coastal and Shelf Science*, **69**, 325–336.

Long, A. J., Waller, M. P. and Stupples, P. 2006. Driving mechanisms of coastal change: Peat compaction and the destruction of late Holocene coastal wetlands, *Marine Geology*, **225**, 63–84.

Luternauer, J. L., Atkins, R. J., Moody, A. I., Williams, H. F. L. and Gibson, J. W. 1995. *Salt Marshes*. In Perillo, G. M. E. (ed.), *Geomorphology and Sedimentology of Estuaries*. Elsevier, Amsterdam, pp. 307–332.

Lynch, J. C., Meriweather, J. R., McKee, B. A., Vera-Herrera, F. and Twilley, R. R. 1989. Recent accretion in mangrove ecosystems based on ^{137}Cs and ^{210}Pb. *Estuaries*, **12**, 284–299.

Madsen, A. T., Murray, A. S., Andersen, T. J. and Pejrup, M. 2007. Temporal changes of accretion rates on an estuarine salt marsh during the late Holocene – Reflections of local sea level changes? The Wadden Sea, Denmark. *Marine Geology*, **242**, 221–233.

Marshall, W., Gehrels, W. R., Garnett, M., Freeman, S. H. T., Maden, C., and Xu, S. 2007. The use of 'bomb spike' calibration and high-precision AMS 14C analyses to date salt-marsh sediments deposited during the past three centuries. *Quaternary Research*, **68**, 325–337.

Massel, S. R., Furukawa, K. and Brinkman, R. M. 1999. Surface wave propagation in mangrove forests. *Fluid Dynamics Research*, **24**, 219–249.

Mazda, Y., Magi. M.Ikeda, Y, Kurokawa, T. and Asano, T. 2006. Wave reduction in a mangrove forest dominated by Sonneratia sp. *Wetlands Ecology and Management*, **14**, 365–378.

McGlashan, D. J. 2003. Managed relocation: an assessment of its feasibility as a coastal management option. *The Geographical Journal*, **169**, 6–20.

Méndez Linares, A. P., López-Portillo, J., Hernández-Santana, J. R., Ortiz Pérez, M. A. and Oropeza Orozco, O. 2007. The mangrove communities in the Arroyo Seco deltaic fan, Jalisco, Mexico, and their relation with the geomorphic and physical–geographic zonation. *Catena*, **127**, 127–142.

Mitsch, W. J., and Gosselink, J. G. 2000. Wetlands. Wiley, New York, 920 pp.

Möller, I. 2006. Quantifying saltmarsh vegetation and its effect on wave height dissipation: Results from a UK east coast saltmarsh. *Estuarine, Coastal and Shelf Science*, **69**, 337–351.

Möller, I. and Spencer, T. 2002. Wave dissipation over macro-tidal saltmarshes: effects of marsh edge typology and vegetation change. *Journal of Coastal Research*, SI **36**, 502–521.

Moreira, M. E. S. A. 1992. Recent saltmarsh changes and sedimentation rates in the Sado Estuary, Portugal. *Journal of Coastal Research*, **8**, 631–640.

Morris, R. K. A. 2008. English Nature's estuaries initiative: A review of its contribution to ICZM. *Ocean and Coastal Management*, **51**, 25–42.

Murphy, S. and Voulgaris, G. 2006. Identifying the role of tides, rainfall and seasonality in marsh sedimentation using long-term suspended sediment concentration data. *Marine Geology*, **227**, 31–50.

Mwamba, M. J. and Torres, R. 2002. Rainfall effects on marsh sediment redistribution, North Inlet, South Carolina, USA. *Marine Geology*, **189**, 267–287.

Neubauer, S. C., Anderson, I. C., Constantine, J. A. and Kuehl, S. A. 2002. Sedimentary deposition and accretion in a mid-Atlantic (USA) tidal freshwater marsh. *Estuarine, Coastal and Shelf Science*, **54**, 713–727.

Neumeier, U. and Amos, C. L., 2006. The influence of vegetation on turbulence and flow velocities in European saltmarshes. *Sedimentology*, **53**, 259–277.

Nyman, J. A., Walters, R. J., Delaune, R. D. and Patrick Jr., W. H. 2006. Marsh vertical accretion via vegetative growth. *Estuarine, Coastal and Shelf Science*, **69**, 370–380.

Ollerhead, J., Davidson-Arnott, R. G. D. and Scott, A. 2005. Cycles of saltmarsh extension and contraction, Cumberland Basin, Bay of Fundy, Canada. In Sanjaume, Eulalia and Mateu, Joan F. (eds.), *Geomorphologia Littoral I Quaternari: Homentage al Professor V. M. Rossello I Verger*, Publicacions Universitat de Valencia, pp. 293–305.

Orme, A. R. 1993. Wetland morphology, hydrodynamics and sedimentation. In Williams, M. (ed.), *Wetlands: A Threatened Landscape*, Blackwell, Cambridge, pp. 42–94.

Orson, R. A., Warren, R. S. and Niering, W. A. 1998. Interpreting sea level rise and rates of vertical marsh accretion in a southern New England tidal salt marsh. *Estuarine, Coastal and Shelf Science*, **47**, 419–429.

Paling, E. I., Kobryn, H. T. and Humphreys, G. 2008. Assessing the extent of mangrove change caused by cyclone Vance in the eastern Exmouth Gulf, northwestern Australia. *Estuarine, Coastal and Shelf Science*, **77**, 603–613.

Pestrong, R. 1965. *The Development of Drainage Patterns on Tidal Marshes*. Stanford University Publications in Geological Sciences, 10, 87 pp.

Pethick, J. S. 1980. Velocity surges and asymmetry in tidal channels. *Estuarine, Coastal and Marine Sciences*, **11**, 331–345.

Pethick, J. S. 1981. Long term accretion rates on tidal salt marshes. *Journal of Sedimentary Petrology*. **51**, 571–577.

Pethick, J. S. 2001. Coastal management and sea level rise. *Catena*, **42**, 307–322.

Pethick, J.S 1992. Saltmarsh geomorphology. In Allen, J. R. L. and Pye, K. (eds.), *Saltmarshes: Morphodynamics, Conservation and Engineering Significance*, Cambridge University Press, Cambridge, pp. 41–62.

Pringle, A. W., 1995. Erosion of a cyclic saltmarsh in Morecambe Bay, North-west England. *Earth Surface Processes and Landforms*, **20**, 387–405.

Quartel, S., Kroon, A., Augustinus, P. G. E. F., Van Santen, P. and Tri, N. H. 2007. Wave attenuation in coastal mangroves in the Red River Delta, Vietnam. *Journal of Asian Earth Sciences*, **29**, 576–584.

Ramcharan, E. K. 2004. Mid-to-late Holocene sea level influence on coastal wetland development in Trinidad. *Quaternary International*, **120**, 145–151.

Reed, D. J. 1989. Patterns of sediment deposition in subsiding coastal salt marshes, Terreborne Bay, Louisiana: the role of winter storms. *Estuaries*, **12**, 222–227.

Reed, D. J. 1995. The response of coastal marshes to sea-level rise: survival or submergence? Earth *Surface Processes and Landforms*, **20**, 39–48.

Reed, D. J. 2002. Sea-level rise and coastal marsh sustainability: geological and ecological factors in the Mississippi delta plain. *Geomorphology*, **48**, 233–243.

Reed, D. J., Stoddart. D. R. and Bayliss-Smith, T. P. 1985. Tidal flows and sediment budgets for a salt-marsh system, Essex, England. *Vegetatio*, **62**, 375–380.

Reed, D. J., Spencer, T., Murray, A. L., French, J. R. and Leonard, L. 1999. Marsh surface sediment deposition and the role of tidal creeks: implications for created and managed coastal marshes. *Journal of Coastal Conservation*, **5**, 81–90.

Reed, D. J., Davidson-Arnott, R. G. D. and Perillo, G. M. E. 2009. The future of coastal systems: from estuaries to dunes. In Slaymaker, O. (ed.), *Landscape Changes in the 21st Century*. Cambridge University Press, Cambridge.

Redfield, A. C. 1972. Development of a New England salt marsh. *Ecological Monographes*, **42**, 201–237.

Robertson, A.I. and Alongi, D.M. (editors), 1992. *Tropical Mangrove Ecosystems*. American Geophysical Union, Washington, DC,

Roman, C.T., Peck, J.A., Allen, J.R., King, J.W. and Appleby, P.G. 1997. Accretion of a New England (USA) salt marsh in response to inlet migration, storms, and sea-level rise. *Estuarine, Coastal and Shelf Science*, **45**, 717–727.

Schostak, L.E., Davidson-Arnott, R.G.D., Ollerhead, J. and Kostaschuk, R.A., 2000. Patterns of flow and suspended sediment concentration in a macrotidal saltmarsh creek, Bay of Fundy, Canada. In Pye, K. and Allen, J.R.L. (eds.), *Coastal and Estuarine Environments*. Journal of The Geological Society Special Publication 175, pp. 59–73.

Schwimmer, R.A. and Pizzuto, J.E. 2000. A model for the evolution of marsh shorelines. *Journal of Sedimentary Research*, **70**, 1026–1035.

Schwimmer, R.A. 2001. Rates and processes of marsh shoreline erosion in Rehoboth Bay, Delaware, USA. *Journal of Coastal Research*, **17**, 672–683.

Scrimshaw, M.D., Bubb, J.M. and Lester, J.N. 1996. Organochlorine contamination of the UK Essex coast salt marsh sediments. *Journal of Coastal Research*, **12**, 246–255.

Shi, Z., Hamilton, L.J. and Wolanski, E. 2000. Near-bed currents and suspended sediment transport in saltmarsh canopies. *Journal of Coastal Research*, **16**, 909–914.

Silvestri, S., Defina, A., and Marani, M. 2005. Tidal regime, salinity and salt marsh plant zonation. *Estuarine, Coastal and Shelf Science*, **62**, 119–130.

Steel, T.J. and Pye, K. 1997. The development of salt-marsh tidal creek networks: evidence from the UK. *Proceedings of the Canadian Coastal Conference*, CCSEA, pp. 267–280.

Steers, J.A. 1948. Twelve years' measurement of accretion on Norfolk salt marshes. *Geological Magazine*, **85**, 163–166.

Stevens, P.W., Fox, S.L. and Montague, C.L. 2006. The interplay between mangroves and saltmarshes at the transition between temperate and subtropical climate in Florida. *Wetlands Ecology and Management*, **14**, 435–444.

Stevenson, J.C., Ward, L.G. and Kearney, M.S. 1986. Vertical accretion in marshes with varying rates of sea level rise. In Wolfe, D.A. (ed.). *Estuarine Variability*. Academic, Orlando, FL, pp. 241–259.

Stoddart, D.R., Reed, D.J. and French, J.R. 1989. Understanding salt-marsh accretion, Scolt Head Island, Norfolk, England. *Estuaries*, **12**, 228–236.

Stumpf, R.P. 1983. The process of sedimentation on the surface of a salt marsh. *Estuaries, Coastal and Shelf Science*, **17**, 495–508.

Taylor, P.H. 2008. *Salt Marshes in the Gulf of Maine: Human Impacts, Habitat Restoration, and Long-term Change Analysis*. Gulf of Maine Council on the Marine Environment. www.gulfofmaine.org.

Teal, J.M. 1962. Energy flow in the saltmarsh ecosystem of Georgia. *Ecology*, **43**, 614–624.

Temmerman, S., Govers, G., Wartel, S. and Meire, P. 2003. Spatial and temporal factors controlling short-term sedimentation in a salt and freshwater tidal marsh, Scheldt Estuary, Belgium, SW Netherlands. *Earth Surface Processes and Landforms*, **28**, 739–755.

Temmerman, S., Govers, G., Wartel, S. and Meire, P. 2004. Modelling estuarine variations in tidal marsh sedimentation: response to changing sea level and suspended sediment concentration. *Marine Geology*, **212**, 1–19.

Temmerman, S., Bouma, T.J., Govers, G., Wang, Z.B. and De Vries, M.B. 2005. Impact of vegetation on flow routing and sedimentation patterns: Three-dimensional modelling for a tidal marsh. *Journal of Geophysical Research*, **110**, F00019–F00031.

Thom, B.G. 1982. Mangrove ecology: a geomorphological perspective. In Clough, B.F. (ed.), *Mangrove Ecosystems in Australia; Structure, Function and management*. Australian National University Press, Canberra, pp. 3–17.

Turner, R.E., Milan, C.S. and Swenson, E.M. 2006. Recent volumetric changes in salt marsh soils. *Estuarine, Coastal and Shelf Science*, **69**, 352–359.

Turner, R.K., Burgess, D., Hadley, D., Coombes, E. and Jackson, N. 2007. A cost–benefit appraisal of coastal managed realignment policy. *Global Environmental Change*, **17**, 397–407.

van der Wal, D. and Pye, K. 2004. Patterns, rates and possible causes of saltmarsh erosion in the greater Thames area (UK), *Geomorphology*, **61**, 373–391.

Van der Wal, D., Wielemaker-Van den Dool, A. and Herman, P.M.J. 2008. Spatial patterns, rates and mechanisms of saltmarsh cycles (Westerschelde, The Netherlands). *Estuarine, Coastal and Shelf Science*, **76**, 357–368.

van Proosdij, D. 2001. *Spatial and Temporal Controls on the Sediment Budget of a Macrotidal Saltmarsh*. Ph.D. Thesis, University of Guelph, 314 pp.

van Proosdij, D., Ollerhead, J., Davidson-Arnott, R.G.D. and Schostak, L., 1999. Allen Creek Marsh, a macrotidal temperate saltmarsh. *Canadian Geographer*, **43**, 316–322.

van Proosdij, D, Ollerhead, J. and Davidson-Arnott, R. G. D. 2000. Sedimentation on a macrotidal saltmarsh. In Pye, K. and Allen, J. R. L. (eds.), *Coastal and Estuarine Environments*. Journal of The Geological Society Special Publication 175, 43–57.

van Proosdij, D., Davidson-Arnott, R. G. D. and Ollerhead, J. 2006a Controls on spatial patterns of sediment deposition across a macro-tidal salt marsh surface over single tidal cycles. *Estuarine, Coastal and Shelf Science*, **69**, 64–86.

van Proosdij, D., Ollerhead, J. and Davidson-Arnott, R. G. D. 2006b Seasonal and annual variations in the volumetric sediment balance of a macro-tidal salt marsh. *Marine Geology*, **225**, 103–127.

van Santen, P., Augustinus, P. G. E. F., Janssen-Stelder, B. M., Quartel, S. and Tri, N. H. 2007. Sedimentation in an estuarine mangrove system. *Journal of Asian Earth Sciences*, **29**, 566–575.

Wang, F. C., Lu, T. and Sikora, W. B. 1993. Intertidal marsh suspended sediment transport processes, Terrebone Bay, LA, USA. *Journal of Coastal Research*, **9**, 209–220.

Ward, L. G., Kearney, M. S. and Stevenson, J. C. 1998. Variations in sedimentary environments and accretionary patterns in estuarine marshes undergoing rapid submergence, Chesapeake Bay. *Marine Geology*, **151**, 111–134.

Williams, H. F. L. and Hamilton, T. S., 1995. Sedimentary dynamics of an eroding tidal marsh derived from stratigraphic records of ^{137}Cs fallout, Fraser delta, British Columbia, Canada. *Journal of Coastal Research*, **11**, 1145–1156.

Wolanski, E., Mazda, Y. and Ridd, P. 1992. Mangrove hydrodynamics. In Robertson, A. I. and Alongi, D. M. (eds.), *Tropical Mangrove Ecosystems*. American Geophysical Union, Washington, DC, pp. 43–62.

Wood, M. E., Kelley, J. T. and Belknap, D. F. 1989. Patterns of sediment accumulation in the tidal marshes of Maine. *Estuaries*, **12**, 237–246.

Woodroffe, C. D. 1981. Mangrove swamp stratigraphy and Holocene transgression, Grand Cayman Island, West Indies. *Marine Geology*, **41**, 271–294.

Woodroffe, C. D. 1992. Mangrove sediments and geomorphology. In Robertson, A. I. and Alongi, D. M. (eds.), *Tropical Mangrove Ecosystems*. American Geophysical Union, Washington, DC, pp. 7–41.

Woodroffe, C. D. 1990. The impact of sea-level rise on mangrove shorelines. *Progress in Physical Geography*, **14**, 483–520.

Woodroffe, C. D. 1995. Response of tide-dominated mangrove shorelines in northern Australia to anticipated sea-level rise. *Earth Surface Processes and Landforms*, **20**, 65–85.

Woodroffe, C. D., Chappell, J., Thom, B. G. and Wallensky, E. 1989. Depositional model of a macrotidal estuary and floodplain, South Alligator River, northern Australia. *Sedimentology*, **36**, 737–756.

Woolnough, S. J., Allen, J. R. L. and Wood, W. L. 1995. An exploratory numerical model of sediment deposition over tidal salt marshes. *Estuarine, Coastal and Shelf Science*, **41**, 515–543.

Yapp, R. H., Johns, D. and Jones, O. T. 1917. The salt marshes of the Dovey estuary. II. The saltmarshes. *Journal of Ecology*, **5**, 65–103.

12

Coral reefs and atolls

12.1 Synopsis

Coral polyps are simple animals that form large colonies with rich varieties of forms and adaptation to differences in wave energy levels, light and other environmental conditions. Modern coral reefs contain a wide variety of hard and soft corals, but it is the fixing of calcium carbonate by the sceleractian corals to form a hard external skeleton that provides the basis for reef development as the coral structures grow over decades and centuries and as the breakdown of corals, coralline algae and other organisms that live in and on the reef supplies sediments to back reef and lagoon areas. Hard corals that grow fast enough to fix large amounts of calcium carbonate are found primarily in warm, tropical waters and exist in a symbiotic relationship with single-cell algae which remove waste and provide a large proportion of the nutrients that the corals need. They also give the corals their distinctive colour.

Coral growth is most rapid close to the surface where there is circulation of food by waves and currents and light for the symbiotic algae. Living corals reefs have a characteristic zonation that reflects the adaptation of individual species to particular levels of light, wave energy and food sources. The topography of the reef in a cross-section from the land oceanward can be divided into three zones: the reef flat which is a shallow area sheltered from direct wave action and an area of sediment accumulation; the reef crest is the shallowest part of the reef and is subject to high wave action and frequent damage to coral colonies; the forereef extends seaward into increasing water depths and decreasing light and wave energy with rapid coral growth in the portion above 20 m and a wide diversity of species.

Coral colonies are highly dynamic and resilient and because coral larvae are dispersed by waves and currents they can quickly colonise new substrate or areas damaged by high storm waves. As sea level fluctuated during the Pleistocene the location of reefs migrated seaward and downward and then landward and upward. During periods of rising sea level, such as the Holocene transgression, there were times and places when the rate of sea level rise exceeded the rate at which corals on many reefs could build upward and so individual reefs were drowned. However the establishment of coral reef communities always kept pace with sea level change. Most modern reefs were established about 5000–7000 years BP as the pace of sea level rise slowed and many of them are built on a framework of older reef deposits that may have been exposed subaerially during glacial periods.

Coral reefs are dynamic ecosystems that are continually evolving and changing in response to disturbances. These disturbances may be biological, such as those resulting from disease or predation, or they may be physical such as those resulting from sea level change or hurricane impact. Coral reef environments also evolve in response to the redistribution of sediment supplied by the break-up of coral colonies and other

reef organisms. These infill lagoons, and extend the shorelines of reef islands, and in places may bury reef substrate. Human activities also disturb reef ecosystems, either directly through activities such as dredging and overfishing, or indirectly through the effects of pollution, suspended sediment runoff due to land clearance or climate change. While all of these disturbances can have an impact on individual reefs and even reefs world-wide, the reef ecosystem is a resilient and persistent one, especially when viewed from a geomorphological or geological perspective.

12.2 Corals and reef formation

12.2.1 Coral organisms

Corals are anthozoans, a class that includes sea fans and anemones, and they form the largest class of organisms within the phylum Cnidaria. Corals may be divided broadly into soft and hard or stony corals (scleractinians) with the hard corals having an external skeleton of calcium carbonate within which the coral polyp lives. Most corals are colonial organisms containing thousands to hundreds of thousands of individuals, termed polyps, and each genera has a characteristic form or structure dictated largely by their growth form and by external forces such as wave energy. Coral polyps are simple organisms and most species consist primarily of a gastrovascular cavity which is open at the top to form the mouth and tentacles which form an extension of the body wall and surround the mouth opening. The tentacles act to capture food in the form of plankton and to clear away debris. The tentacles also contain stinging cells that kill their prey and which can give unwary divers and snorkelers a nasty rash.

The hard, scleractinian corals are the chief architects of coral reef formation along with a number of calcareous algae and minor inputs from other organisms such as molluscs. The majority of the scleractinian corals live symbiotically with zooanthelate single cell algae which inhabit the endothermal tissue of the stomach of the coral polyp. The role of the algae in the symbiotic relationship is to remove metabolic waste and to provide the coral polyp with additional nutrients, in some cases the majority of its nutrients, while the coral polyp in turn provides a protected environment for the algae to establish and to photosynthesise. The presence of the algae greatly enhances the rate of precipitation of calcium carbonate and hence the rate of reef building. The algae also give the corals distinctive colours, and it is the expulsion of the algae during periods of elevated water temperatures that produces coral bleaching.

Individual coral polyps are only a few mm in diameter. The calcium carbonate secreted by the polyp forms a basal plate and surrounding wall in which the polyp sits and which is connected to the other polyps in the colony. This provides protection to the polyp which extends itself to feed and withdraws completely within the walls for protection. The colonies of polyps making up a coral unit divide asexually and as older polyps die their skeletons are incorporated in the coral form – the coral thus consists of an interior calcium carbonate skeleton of dead polyps and an outer layer of living polyps. Corals also reproduce sexually and the resulting coral larvae disperse through the reef and beyond, dictated by wind and tidal currents and wave action. This is the primary source of evolution of the existing reef colonies and the establishment of new colonies.

Colonies of reef building corals take on a wide range of shapes including branching forms such as the large, flattened limbs of elkhorn coral (*Acropora palmata*) and the dense finger-like colonies of staghorn coral (*Acropora cevicornis*), ball-shaped and massive corals such as brain coral (*Diploria* spp.), and crustose forms which form thin layers over the substrate (Figure 12.1). Other corals such as sea fans have carbonate skeletons that do not contribute directly to the reef structure but do provide a source of carbonate sediment to the reef system. Branching colonies will grow at rates of up to 10 cm a^{-1} while the massive corals grow at half this rate or less. The branching corals are however more vulnerable to wave action as they grow larger and the impact of hurricanes can often be seen in the accumulation of large amounts of debris consisting of fragments of

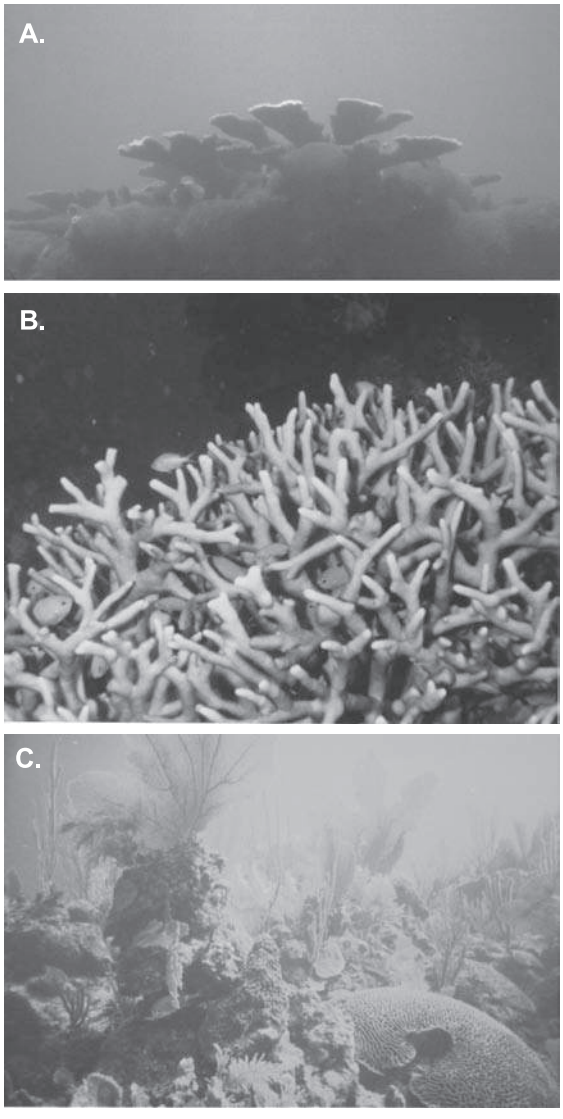

Figure 12.1 Examples of warm water corals: (A) flat, branching elkhorn coral (*Acropora palmata*) on the reef crest, Belize; (B) staghorn coral (*Aropora cervicornis*); (C) wide variety of hard and soft corals and sea plumes on the forereef at a depth of 20 m, Belize. Smooth brain coral (*Diploria strigosa*) right foreground and cavernous star coral (*Montastraea cavernosa*) centre foreground.

branches that have been snapped off. These may be cemented together by coralline algae and provide a substrate for new coral establishment and growth. Corals grow fastest in shallow water near the reef crest where there is plenty of available light for photosynthesis by the zooanthelates and a continuous supply of nutrients and food. The growth rate declines into deeper water down the front face of the reef and below 20–25 m depth the main reef building forms are largely replaced by soft corals, sea fans and other scleratinous corals that are adapted to lower light and slower growth. Thus, reef building takes place largely in shallow water close to land or on shallow continental shelves.

Actual rates of calcium carbonate accumulation are highly variable and not easily measured. Extreme rates may range from 1–35 kg $CaCO_3$ m^{-2} a^{-1} (Alongi, 1998). Corresponding rates of accretion are 1–7 mm a^{-1} with a mean of about 3 mm a^{-1}. These numbers indicate that coral reefs would not have been able to maintain themselves simply by vertical accretion during periods of rapid sea level rise during the Holocene transgression and that horizontal (landward) transgression through establishment of new colonies would have been the primary process of preservation of coral colonies.

12.2.2 Coral reef divisions

There is a wide range of reef planform which we will examine in greater detail in the next section. However, most reefs can be divided into a typical set of divisions along a transect from the shore across the reef flat, the reef crest, and the forereef to deep water (Figure 12.2a). The reef flat or back reef is the most landward zone and is sheltered from high wave action by the reef crest. It may be only a few metres in width or up to several km. It is generally very shallow with portions close to the reef crest that may be emergent at low tide and often a lagoon that may be a few metres deep between this and the shore. Portions of the reef flat may contain solidified reef material and there will be isolated coral heads consisting of both dead and live corals. Much of the reef flat however consists of fragments of coral as well as sand and fine sediments produced by the comminution of dead coral material, molluscs and other organisms which are washed landward across the reef by waves and currents. Bare sand areas will occupy considerable portions of the reef flat and may build above sea level to form beaches and sand cays.

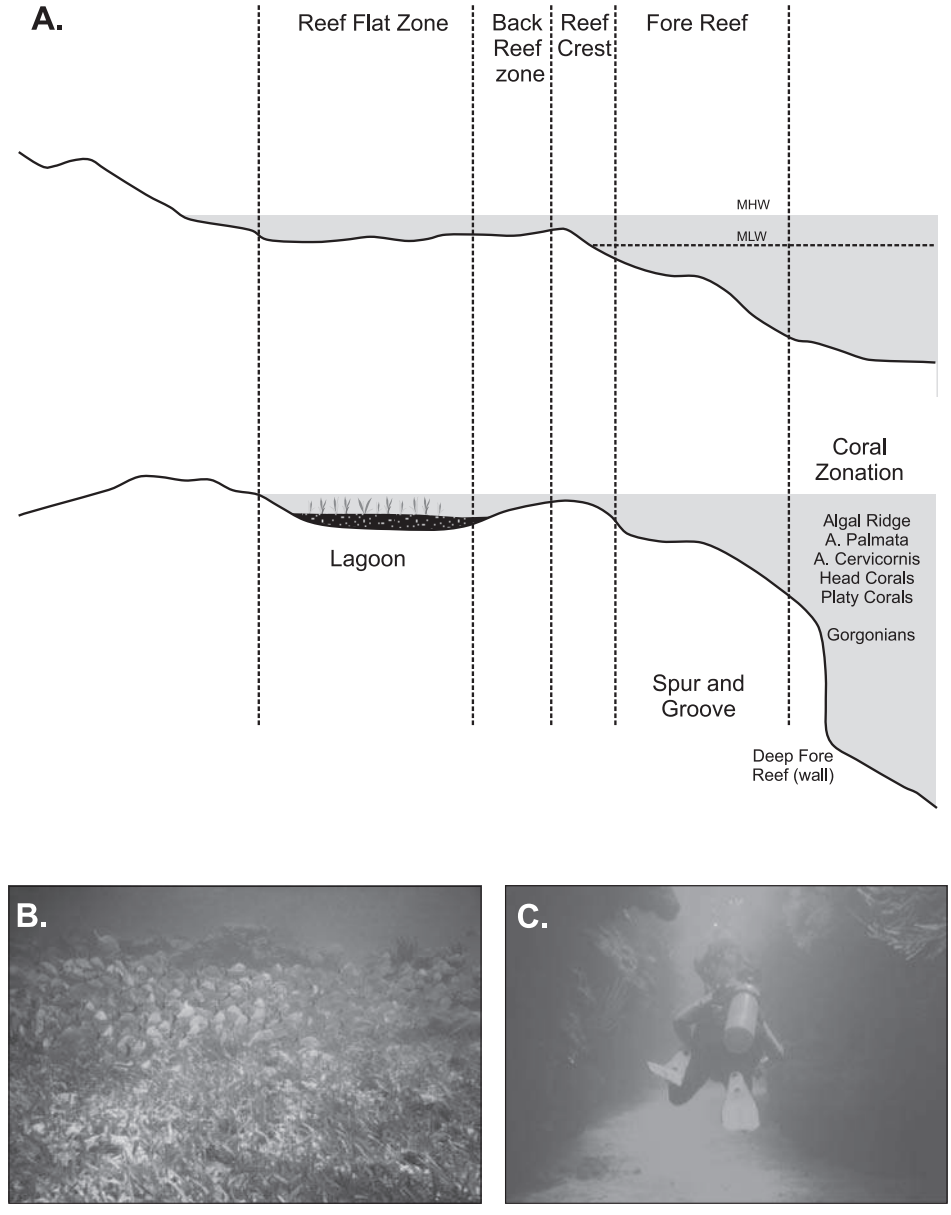

Figure 12.2 Morphological zones of Caribbean coral reefs; (A) schematic cross-sections across the reef from the shoreline to deep water showing the four main divisions of the reef (based on MacIntyre, 1988; Hubbard, 1997). The upper panel shows a shallow reef flat which dries at low tide and relatively shallow nearshore. The lower panel shows a lagoon with sea grass beds and a steep nearshore with reef wall grading at depths below 100 m into a carbonate slope. The zonation of corals reflects decreasing wave energy (based on Adey and Burke, 1977); (B) photograph of the reef flat Ambergris Caye, Belize showing sea grass beds on sandy deposits with corals of the backreef in the background. (C) spur and groove topography at a depth of about 15 m – note the steep sides of the 'canyon' and the sand and rubble on the bottom which is being transported downslope into deeper water.

The shallow lagoon floor is often covered by extensive area of sea grass accompanied by various algae and this in turn provides a rich habitat for a wide variety of small fish, molluscs and worms and in deeper lagoons for larger organisms such as turtles and manatee (Figure 12.2b).

The reef crest is the highest point of the reef and parts of it will be exposed at spring low tide. It is subject to wave shoaling and breaking and in the most exposed areas only some species of calcareous algae will survive. In slightly deeper or protected areas the crest will be dominated by strong branching corals such as *Acropora* which grow rapidly in the shallow water because of high rates of photosynthesis and strong circulation which supplies large quantities of food. Damage to colonies during high-wave events is thus quickly repaired and the dead broken pieces add to the structure of the reef. The reef crest provides protection for a wide range of small fish, crabs and crustaceans and thus is a prime area for snorkeling.

The seaward slope or forereef zone is marked by decreasing wave intensity and decreasing light with increasing distance and depth from the reef crest. The upper portion of the zone down to about 20–25 m is termed the buttress and is characterised by the presence of massive and branching corals as well as coralline algae all of which are well suited to withstand high wave energy levels. Conditions are ideal for rapid growth because of the shallow, generally clear water which permits maximum light penetration and photosynthesis, and the rapid turnover of water which brings fresh food to the coral polyps. This front face of the reef often develops a spur and groove topography with coral formations dominating the sides and crests of the spurs and narrow, flat floored channels separating them. Sand and broken coral are transported into the bottom of the channels and then work their way downslope to the base of the reef (Figure 12.2c). Reduced wave action often leads to the greatest diversity of coral types at depths of 15–30 m but below this the reduced light leads to a decline in the growth rate of scleratinous corals, and a variety of soft corals, sea whips and sea fans become dominant. Where the drop off is very steep the reef face may be a wall lined with corals to depths greater than 50 m. Alternatively, if the slope becomes more gentle sand flats develop and the reef becomes very patchy. A schematic summary of the distribution of dominant reef-building corals and coraline algae for high and moderate energy reefs in the Indo-Pacific tropics is shown in Figure 12.3.

12.2.3 Distribution of coral reefs

The reef-building hard corals and their symbiotic zooanthelates flourish in warm waters with temperatures above 18 °C and they generally do not survive when water temperatures exceed 30 °C for lengthy periods. Consequently they are found primarily in a band across the equator and extending to about 25 degrees latitude. The greatest proportion of reefs world-wide occurs in a band stretching from the east coast of Africa across the Indian and Pacific oceans to Central America, with the highest concentration in the region around Indonesia, Papua New Guinea and Australia (Figure 12.4). This includes the Australian Great Barrier Reef which extends over 15 degrees of latitude northward from Bundaburg in Queensland at about 24.5 degrees S into the Torres Strait between Australia and Papua New Guinea (Hopley *et al.*, 2007). In Australia the southernmost area of reef development is on Lord Howe Island in the Tasman Sea at latitude 31° 40′ south. The second, much smaller area of reef development is in the Caribbean region extending from the Florida Keys and the Bahamas through Mexico and Central America and the islands of the Caribbean south to Trinidad. The most northern occurrence of reef development here is associated with the islands of Bermuda at about 32 ° N, where the waters are warmed by the North Atlantic Drift. The second largest barrier reef in the world occurs along the coast of Belize.

Reef development is curtailed on the west coast of South America and to some extent North America by upwelling and the presence of cold currents and this is also a factor in the scarcity of reefs on the west coast of Africa in the Atlantic Ocean. Reef development is also curtailed by high levels of turbidity and/or sedimentation and thus reef development does not occur near the mouths of large rivers such as the Amazon and Orinoco on the NE coast of South America and other major river systems in the Pacific and Indian Ocean systems (McLaughlin *et al.*, 2003). Coral growth is also inhibited when salinity falls below 27‰ and this is also associated with large rivers reaching the coast. It may also account for gaps in reefs near the mouths of smaller rivers. Finally, coral reefs

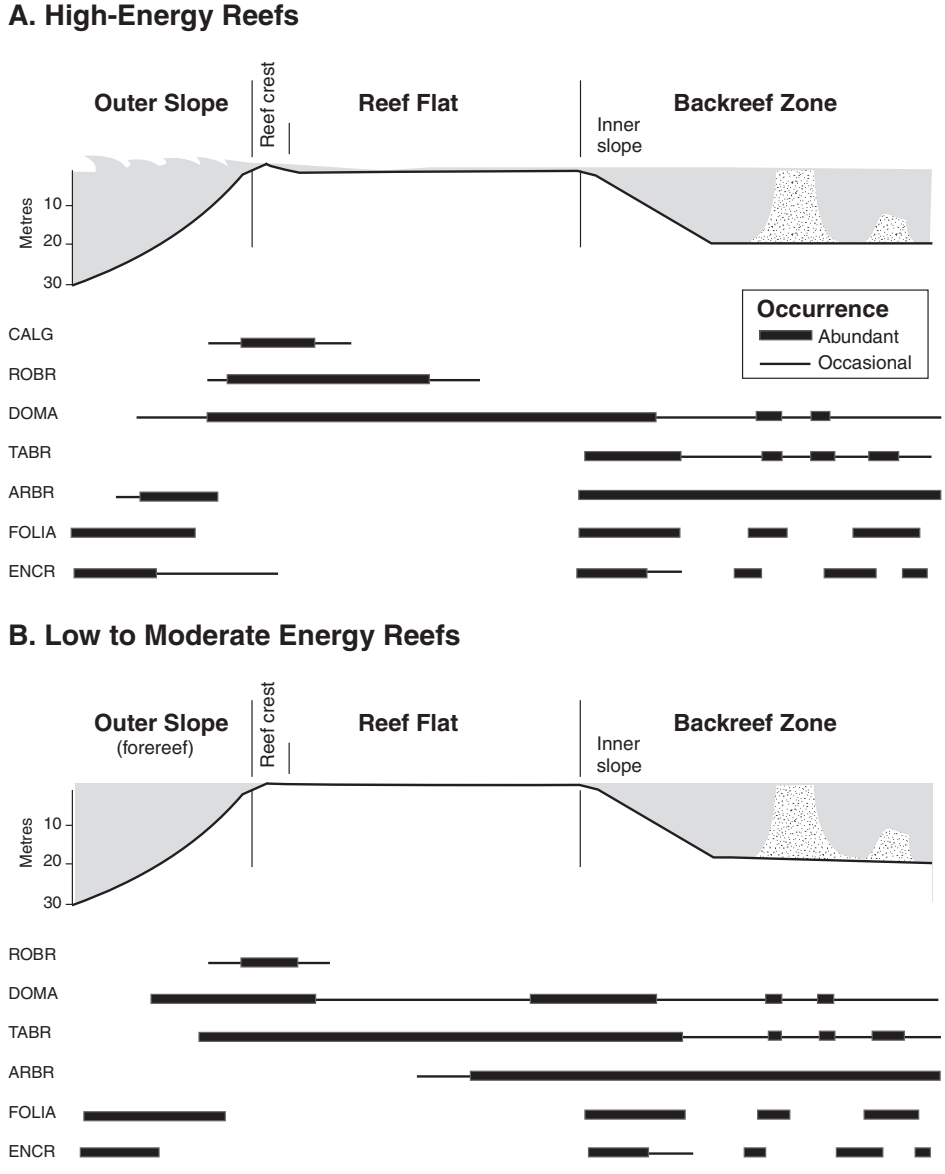

Figure 12.3 Schematic summary of the distribution of dominant reef-building coral (and coralline algal) forms and assemblages in the Indo-Pacific tropics, from deep outer slopes to backreef zones in relation to wave energy and water depth: (A) reef systems located in higher energy (outer shelf) settings; (B) reef systems located in lower energy settings (inner shelf and protected settings). CALG = coralline algae; ROBR = robust, branching corals; DOMA = domal coral; TABR = tabular branching; ARBR = arborescent corals; FOLIA = foliaceous corals; ENCR = encrusting coral (Montaggioni, 2005).

generally do not establish well on muddy sediments and so development is inhibited also in coastal plains with abundant fine sediment in shallow water.

12.2.4 Cold water corals

Most attention over the past 200 years in the study of corals and coral reefs has been on those that are associated with shallow tropical

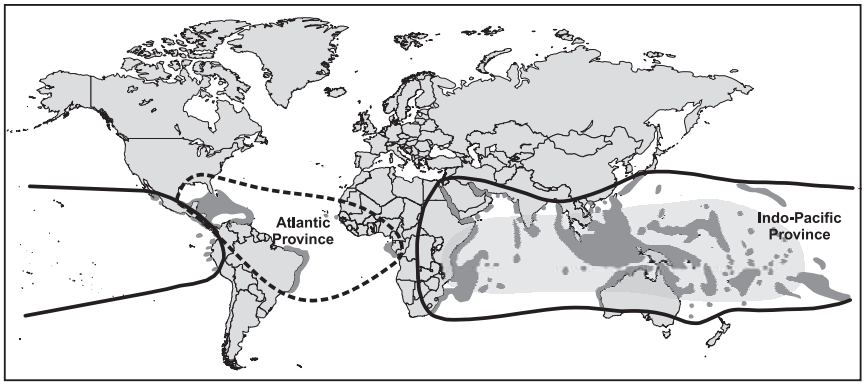

Figure 12.4 Global distribution of coral reefs. The shaded region indicates the area of most prolific reef development, almost all known coral atolls and the greatest number of reef building coral genera (Davies, 1980).

seas. It has been known for some time that a wide range of corals can be found in cool and cold waters, extending even into the polar seas. However, it is only in the last couple of decades that the great variety of cold water corals (similar in numbers to the warm water corals) has come to be appreciated. These corals include soft corals and sea fans, as well as black corals and varieties of scleratinous corals which are capable of producing large colonies in water depths up to 2000 m which can be compared to the reefs of shallow, tropical seas. The rate of formation is much slower than for tropical reefs because of the absence of the symbiotic zooanthelates but it is this absence that permits them to inhabit such cold and deep water. The deep water reefs are important habitat for a variety of commercial fish and shrimp and they are very vulnerable to destruction by trawl nets used to catch these. Because of the depth at which they tend to occur, these cold water reefs have little influence on coastal processes so we will focus only on the tropical shallow water reef dynamics in the remainder of this section.

12.3 Geomorphology and sedimentology of coral reefs

Tropical coral communities are vulnerable to a variety of natural and human stresses, including the effects of overgrazing by organisms such as the crown of thorns starfish, bleaching due to elevated sea surface temperatures, the impacts of hurricanes, disturbance from construction dredging, etc. Thus, there is a tendency from an ecological perspective to regard coral reefs as fragile environments. On the other hand, reefs are complex geomorphological and sedimentological features that have existed for hundreds of millions of years and are common features of the sedimentological record. Furthermore, coral reefs world-wide have been subject to large and relatively rapid changes in sea level throughout the Pleistocene, particularly in the past 600 000 years, and have not only survived but flourished. From this perspective reefs are robust and highly adaptive features of the tropical coast.

Coral reefs influence the geomorphology and sedimentology of tropical coasts both directly and indirectly, and they are the dominant control on the form and dynamics of many thousands o km of coasts in the two regions where the majority of reefs occur. The upward growth of the coral reef towards the low water line results in the development of a physical barrier which acts to reduce wave energy and thus leads to the development of extensive relatively sheltered areas of reef flat and lagoon, and low-energy shorelines where sediment accumulation and island development can occur. Reef sediments are produced by mechanical disintegration of reef corals and other $CaCO_3$ fixing organisms found in the reef and in the lagoon and reef flats behind the reef front as well as by

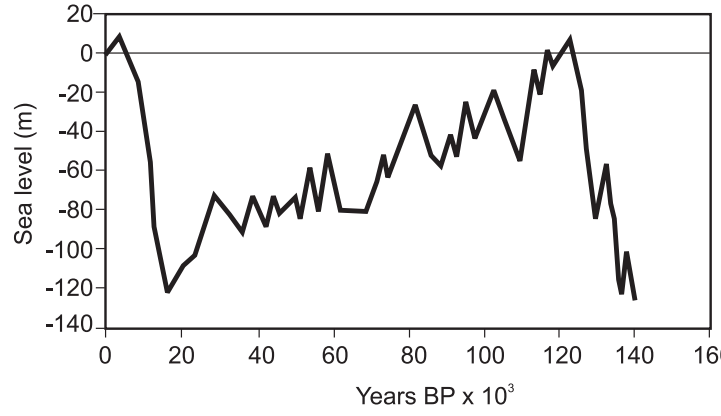

Figure 12.5 Generalised sea level curve for the Pacific over the past 140 000 years encompassing the last interglacial maximum, the last glacial period and the post- glacial transgression (based on Chappell *et al.*, 1996). The curve is based on data from rates of uplift of terraces in the Huon Peninsula, New Guinea and on $\delta^{18}O$ deep-sea core data. The original data points have been removed for clarity.

the activities of grazers such as parrot fish. Passages through the reef, and complex topography within the reef flat, result in spatially complex wave and current conditions. Temporal variation in energy levels and sediment transport occur as a result of tidal fluctuations, as well as seasonal variations in wave climate and the impact of major storms such as hurricanes. Thus the primary reef structure which results in the building up of the forereef towards sea level ultimately produces a much larger and more complex coastal form than the initial reef itself. The geomorphology of modern coral coasts is further complicated by the residual effects of the Holocene sea level rise and the relatively stable sea level of the past 5000 years as well as by the inheritance of the effects of fluctuating climate and sea levels over the Pleistocene.

12.3.1 Sea level fluctuations and coral reef evolution

Over the past three million years sea levels have fluctuated through a range of over 100 m in response to the growth and decay of upper latitude glaciers and ice sheets and shorelines have migrated seaward during periods of falling sea level and landward during periods of rising sea level. Coral communities have of necessity had to accommodate these changes. The generalised sea level curve for the past 130 000 years is shown in Figure 12.5 and it shows five features that are significant for coral reef development: (1) a period lasting about 12 000 years of relatively stable sea level during the last interglacial at about the same elevation as the present sea level; (2) a period of about 80 000 years during the early and middle Wisconsinan glacial period which is characterised by sea level fluctuations on the order of 20–40 m superimposed on a gradual fall in mean sea level to about 50 m below the present level; (3) a rapid decrease in sea level during the late Wisconsinan glacial maximum to a low level about 130 m below the present; (4) a rapid rise in sea level beginning about 25 000 years ago reaching the present sea level about 5000 years ago; and (5) the modern period with sea levels close to their present level – likely a decline of 1–2 m in Pacific areas and perhaps a small increase in Atlantic/Caribbean regions.

The regions of coral reef growth are outside the areas affected directly by glacial loading and unloading but there will be varying local response to oceanic loading and unloading of the continental shelf during these fluctuations that reflect the morphology and width of the shelf. Relative sea level will also be affected by local tectonics during the period such as the ongoing subsidence of atolls on the Pacific plate or the well-documented uplift of the Huon Peninsula in New Guinea. What were the changes to the coastal environment during this time and how did reefs change in response to this?

During the last interglacial (1) we can expect reef distribution somewhat similar to the present though with some differences in the detail – e.g. there is evidence that much of the Australian Great Barrier reef only developed at the end of the Holocene transgression (Hopley *et al.*, 2007). It can also be inferred from a study of modern reefs that the pace of new reef development

would have slowed considerably by the end of this relatively long period of stable sea level – i.e. that reefs would have colonised almost all of the places favourable places for reef development – and that much of the available accommodation space would have been filled by sediments generated by corals and other carbonate producing organisms that make up the reef community.

The second period is one of gradually declining sea levels but with fluctuations reflecting alternations in ice sheet growth and decay. Sea level fluctuations are small enough that in many areas we can expect the active coral communities to migrate landward and seaward in response to the sea level fluctuations over the reef substrate. Reef flat zones built at high sea level stands would become exposed and subject to reworking by subaerial processes including solution and karstification of the exposed carbonates that form the internal structure of the reef. On continental shelves there would be local coastal changes reflecting both the operation of coastal processes as well as the extension of rivers onto the exposed continental shelf bringing changes in the location of freshwater inflows and terrigenous sedimentation. Changing coastal configuration as well as changes in wind patterns and storm tracks will influence energy levels and nutrient supply and thus ability of the reef communities of any particular location to fluctuations in sea level. The impact of these in particular on the fast growing, reef-building corals that are crucial to the rapid development of the reef may have been an important determinant of whether individual reefs maintained themselves or died off.

The third period began around 25 ka BP when there was a rapid sea level drop to the low stand of about 130 m below the present level. On wide continental shelves reef activity was confined to the outer shelf and subaerial drainage extended over much of the shelf. On islands and atolls reefs likely formed at the base of existing reef fronts. Ongoing solutional processes on the former interglacial reefs lead to the formation caves and collapse features, exemplified by the famous blue hole of the Belize barrier reef. Evidence for these reefs is not widely available because they are for the most part submerged below 100 m and can only be explored by submersibles and deep drilling (Beaman *et al*., 2008).

The rapid melting of ice sheets beginning around 20 ka BP signals the start of the fourth period – the Holocene transgression. The rapid and nearly continuous rise in sea level to about 5 ka BP at rates of 5–10 mm a^{-1} is punctuated by at least three major meltwater pulses at 19, 14 and 11.5 ka BP with associated rates of accelerated sea level rise of 30, 40+ and 25 mm a^{-1} (Montaggioni, 2005). Each of these pulses is associated with a major period of non-reef construction or reef drowning. However, while there was insufficient time for reef building to occur, reef communities continued to exist and they kept pace with rising sea level through the continued recruitment of individuals to new substrates. Montaggioni (2005) recognises four reef generations beginning with RGO during the low stand, and RGI, RGII and RGIII following each of the meltwater pulses (Figure 12.6). Since about 11 ka BP the rate of sea level rise has been slow enough for many reef communities to persist to the present time, though some may occur well below the surface because of a slow growth rate (Harris *et al*., 2008).

The vertical accretion of reefs during sea level rise, particularly during the past 11 ka, has been characterised (rather anthropomorphically) as falling into three categories – keep-up, catch-up and give-up (Neuman and MacIntyre, 1985). In the first case the rate of vertical accretion keeps pace with rising sea level; in the second, accretion is initially slower than sea level rise but catches up either because of increased carbonate production or a slowing of sea level rise; and in the third scenario accretion is less than the rate of sea level rise over an extended period with the result that the reef is submerged to a depth where the reef generating corals can no longer survive and the reef is drowned. Each of these conceptual scenarios is associated with a different facies assemblage that should be recognisable in cores through reef sediments. There is some question as to whether these exist in reality or are an artefact of coring (Blanchon and Blakeway, 2003). Apart from the danger of thinking of these scenarios as reef 'strategies', it

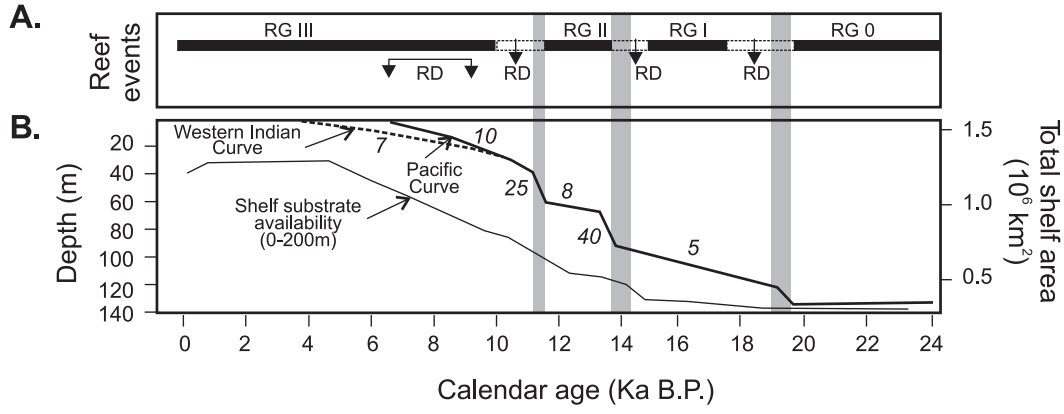

Figure 12.6 Post-glacial reef growth events in the Indo-Pacific province: (A) schematic reconstruction of reef evolution showing reef growth phases (RG) and reef drowning (RD) events; (B) late glacial and Holocene sea level curve for the western Indian Ocean and Pacific Ocean and associated area of shelf substrate available for reef growth (Montaggioni, 2005).

probably simplifies too much the complex set of biological and physiological factors that control the development of reef facies assemblages in space and time.

12.3.2 Geomorphic and sedimentologic characteristics of coral reefs

In the broadest sense we can distinguish between coral reefs developed on shallow continental shelves in relatively close proximity to land masses (characterised by fringing and nearshore reefs and complex reef assemblages associated with barrier reefs) and those developed on volcanic platforms or isolated volcanic islands in oceanic settings (notably the coral atolls of the Indo-Pacific region). Many mainland and large island coasts with a fairly steep nearshore and narrow continental shelf will be characterised only by the development of fringing reefs in favourable locations. In contrast, wide continental shelves or extensive shoal areas give rise to the development of reefs that are isolated from the mainland coast and evolve primarily in response to the interaction of reef building coral communities with controls such as sea level change, wave climate and coastal currents. Barrier reefs such at the Great Barrier Reef in Australia and the Belize Barrier Reef will contain some fringing reefs as well as a complex set of submerged or patch reefs, and emerged reefs and islands which may be located in on the exposed outer zone or in more sheltered central and inshore portions of the continental shelf.

Fringing reefs

Fringing reefs are common on mainland coasts as well as the coasts of islands on the continental shelf and on large oceanic islands Figure 12.7). They are relatively simple in morphology and occur as either shore-attached features or features very close to the shoreline (Kennedy and Woodroffe, 2002). Reefs may develop in a number of areas including rocky headlands, bayheads, along narrow linear sandy beaches and as nearshore shoals some distance offshore from a range of coastal forms (Hopley *et al.*, 2007). While there is a tendency to think of reef colonisation as being largely restricted to rock or rubble substrates, there is now much evidence that reefs can colonise sandy substrates equally well. The simplest reefs have a reef crest some distance offshore and a nearly horizontal reef flat that extends right to the shoreline and is generally exposed at spring low tides (Kennedy and Woodroffe, 2002). In much of the Indo-Pacific region reef flats may be completely emergent at low tide and these may reflect the small late-Holocene fall in sea level postulated for this region. Lagoonal fringing reefs on the other hand have a shallow lagoon between the reef flat and the shoreline that is typically 1–3 m deep. This may reflect simply the establishment of the reef

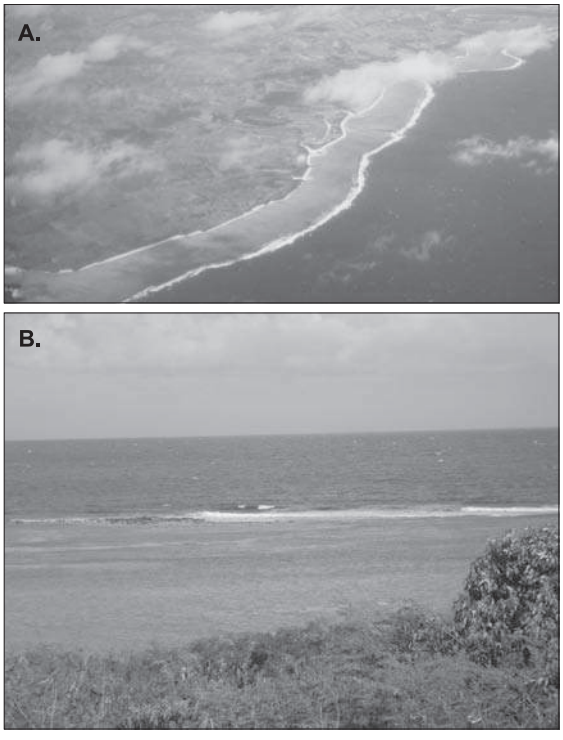

Figure 12.7 Fringing reefs: (A) fringing reefs on Fiji; (B) small fringing reef off the north coast of Antigua at low tide showing the reef crest and backreef with shallow, sandy lagoon landward of the reef.

front some distance offshore and limited coral growth close to shore, or the influence of runoff from the land inhibiting coral growth in this location. The shallow lagoon may also result from scour by strong currents produced by waves coming over the reef front which acts to inhibit deposition of carbonate detritus brought onshore from the reef front or from the reef flat.

As with all coral reefs, the evolution of fringing reefs over the past 20 ka has been controlled by the Holocene transgression and by local tectonics. Fringing reefs can evolve by growing upward at the same rate as sea level rise, but they can also backstep by colonising available terrestrial substrate as the land surface is drowned. As the rate of sea level rise slows, progradation of the reef front may occur. The result is a fairly complex set of potential scenarios for fringe reef development in the Holocene (Kennedy and Woodroffe, 2002 – see Figure 12.8). Coring in fringing reefs of the Great Barrier Reef of Australia indicates that many of them experienced rapid growth in the period around 7000–5000 BP when sea level rise slowed sufficiently to allow established reef communities to build upward into the available accommodation space (Hopley *et al.*, 2007). This growth slowed markedly after 5 000 BP in many fringing reefs coincident with establishment of a stable sea level and most fringing reefs today while they have healthy coral communities show either little evidence of progradation or progradation rates that are very much slower than in the mid-Holocene (Hopley *et al.*, 2007).

Clearly, the establishment of a stable sea level and then a slight sea level fall marks the end of a continuously increase in vertical accommodation space, but seaward progradation of fringing reefs also appears to have slowed markedly. In many cases this may simply reflect the fact that the reef has prograded rapidly over a gently sloping surface terrigenous surface and the reef front is now over a relatively steep seaward slope or even a 'wall'. Further progradation requires a greater supply of rubble to build the substrate platform up towards the optimum water depth for coral growth and with the steep slope much of this may be carried into considerable depth down the channels on the forereef (Figure 12.1d). It is also possible that increased turbidity and runoff from mainland coasts resulting from human activities as well as from dredging and construction on the coast, and in some cases on the reef itself, has reduced the optimum conditions for coral growth in some areas. Hopley *et al.* (2007) also argue that, with a relatively stable sea level, fringing reefs may now occupy most of the optimum areas for reef colonisation and growth and that the opportunities for establishment of new reefs or rapid growth of established reefs are now very much reduced.

Reefs of shallow continental shelves

On extensive warm water banks such as the Bahamas Bank and shallow continental shelves a wide range of reef forms and associated emerged islands can be found. Because of the considerable control imposed on reef growth and sediment

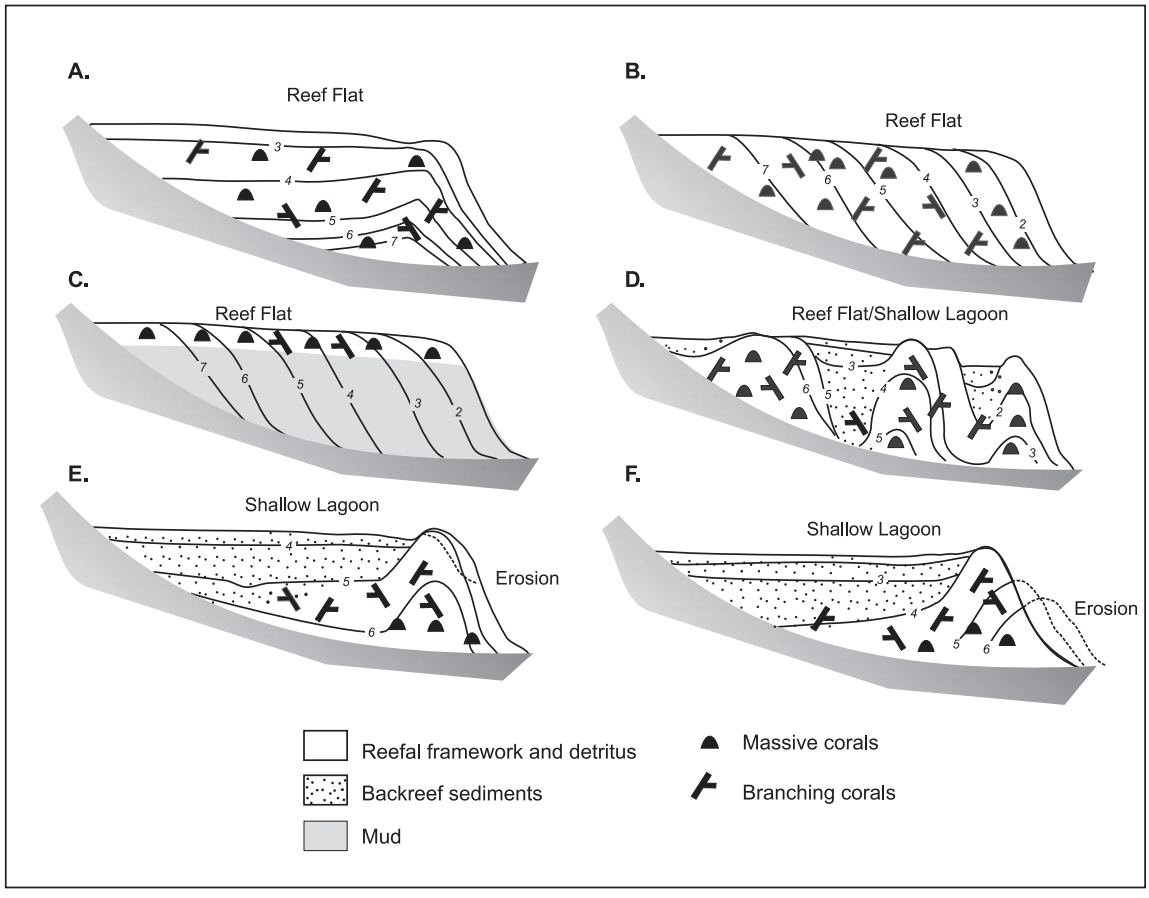

Figure 12.8 Generalised models of fringing reef development. (A) Vertical reef accretion keeping up or catching up with sea level rise; (B) lateral (offshore) accretion associated with stable sea level; (C) lateral accretion over non-reefal mud in the forereef zone; (D) episodic progradation model; (E) offshore accretion and gradual infilling of lagoon; (F) offshore reef structure formed primarily as a rubble pile by storm processes which may be reworked landward by large storm events (Kennedy and Woodroffe, 2002).

reworking by sea level change since the mid-Holocene it is possible in many cases to associate reef form with stages in an evolutionary scheme such as that outlined for reefs on the Great Barrier Reef of Australia (Figure 12.9). Rapid submergence of the shoal or continental shelf platform would have occurred during the early phases of the Holocene transgression with sea level rising too quickly to permit upward reef building to keep pace. However, as the rate of sea level rise slowed after 7000 BP vertical accretion of reefs establishing on the recently drowned terrigenous substrate could exceed that of sea level rise and initiate the upward building of the reef relative to sea level. As portions of the reef reach the surface, the form of the reef front and the development of areas of carbonate sediment accumulation are influenced by exposure to waves, by wave refraction, and by tidal-, wind- and wave-generated currents. Reef growth tends to be most vigorous on the high-energy windward or exposed side of the reef where there is a constant supply of nutrients and food for the polyps and species of rapidly growing branching corals are most likely to be found. Emergence of the reef crest provides protection for shallow lagoon or lagoons and sandy sediment derived from the reef or from organisms in the lagoons can be reworked by waves to form sand cays. Colonisation by vegetation can lead to some aggregation of these islands due to

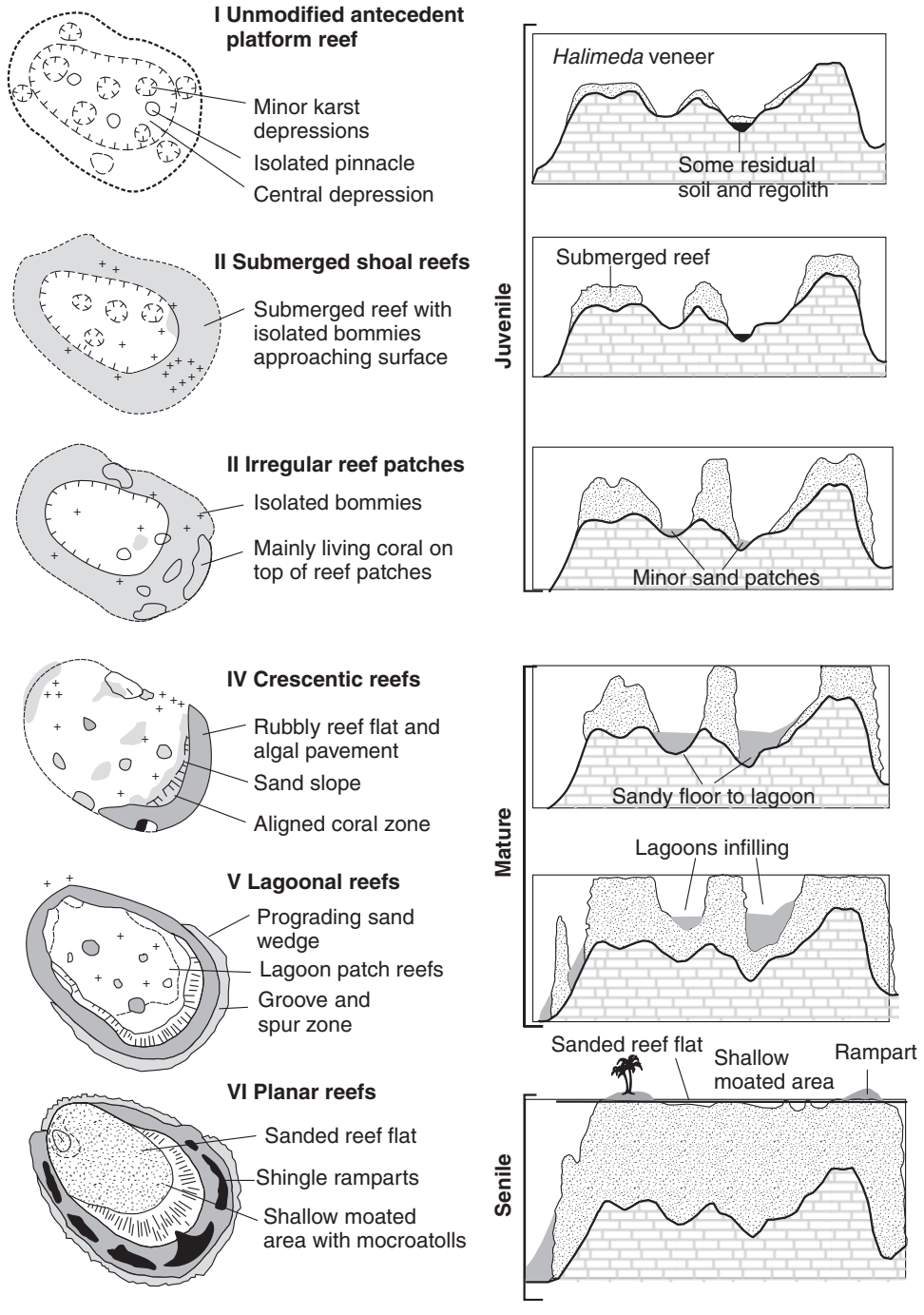

Figure 12.9 Schematic depiction of planform and profile changes associated with the evolution of coral reefs of the Great Barrier Reef, Australia (Hopley *et al.*, 2007).

Figure 12.10 Oblique aerial photograph of a portion of an Indo-Pacific atoll, Bairiki (South Tarawa) looking south. The lagoon is in the foreground and the oceanic reef in the background (photo courtesy Don Forbes).

trapping of sediment washed onshore during storm surges or blown inland by wind action.

Coral atolls

Atolls are reef complexes found in mid-ocean far from the continental shelves and large islands. They are characterised by an annular reef rim which encloses a central lagoon or lagoons and a variety of small islands which are mainly located on the margins of the atoll (Figure 12.10). Almost all atolls are found in the Indo-Pacific zone on the Pacific Plate and most seem to be associated with volcanoes that form at hot spots within the plate, rather than at convergent or divergent boundaries where volcanic activity is predicted by plate tectonics theory. Whatever the origin of the hotspot, magma reaching the surface of the ocean floor can build up to form a volcano which in many cases will reach the ocean surface and build a volcanic island that may be hundreds of metres above sea level (Figure 12.11). Movement of the Pacific plate carries the volcanic island away from its magma source. Gradual subsidence of the plate, at rates of 2–3 m per ten thousand years, as well as subaerial erosional processes, result in the volcanic island sinking below sea level and the transformation of fringing reefs into an atoll with central lagoon. If circumstances are favourable reef growth can keep up with the rate of plate subsidence leading to the construction of a carbonate platform of increasing thickness over the underlying volcanic core (Figure 12.11). If the atoll migrates towards higher latitudes coral growth may become restricted and the reef may die out leaving the top of the seamount to subside further and further below the wave surface.

The association of Pacific atolls with subsidence of volcanic islands and continued upbuilding by reef communities goes back to Charles Darwin and the voyage of the Beagle in 1836. Partial support for Darwin's theory came from drilling on Funafuti atoll between 1896–98 which showed the presence of shallow carbonate deposits down to a depth >300 m. Subsequently drilling on Bikini and Eniwetok atolls after World War ll reached the volcanic basement on which the carbonates were built (Guilcher, 1988; Woodroffe, 2008). As with all coral reefs, the modern atoll reefs have been greatly influenced by sea level fluctuations in the last few hundred thousand years. During the last interglacial we can expect a range of atoll forms similar to those existing today. As sea levels fell during the glacial

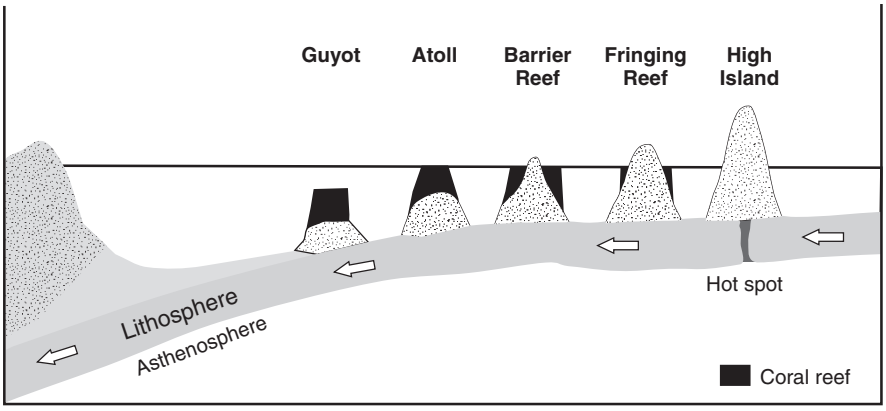

Figure 12.11 Schematic depiction of the development of a Pacific ocean atoll through subsidence of a volcanic island formed over a mid-oceanic hotspot. Once the volcanic island moves away from the hotspot, erosion reduces the sub-aerial relief and ongoing subsidence of the cone leads to the transformation of fringing and barrier reefs into an atoll. The atoll can be maintained as long as the rate of coral growth keeps up with subsidence of the volcanic core – if the atoll moves into waters with cooler temperatures then growth will fall below the subsidence rate leading to drowning.

period the active reefs would have migrated down the flanks leaving the upper sections exposed to subaerial processes (Figures 12.12a, b). As sea level rose at the end of the glacial period the response of reefs would have been similar to that in other areas, with some of the fringing reefs being drowned during periods of rapid sea level rise and others building upward along the flanks of the atoll platforms. The final stage came with relatively stable sea level and the building of the modern carbonate cap over underlying Pleistocene limestone (Figure 12.12c) and ongoing development of reef islands and lagoon systems.

Reef islands

Atolls, barrier reefs and carbonate platforms are characterised by the development of reef islands which are built up above the mean high tide level. The platform on which the island develops is usually late-Holocene back-reef and fore-reef conglomerates and sandy sediments and the islands themselves have developed as a result of accretionary processes driven largely by wave action. In parts of the Pacific and on the Australian Great Barrier reef, islands may have an emergent fossil reef platform resulting from a slight fall in sea level and this may be overlain by beachrock produced by cementation of carbonate sediments on the reef platform. In areas where reefs have built up to sea level more recently, the emergent part of the island may contain rubble and rubble ridges resulting from storm wave activity as well as carbonates sands and finer material deposited as sand sheets by overwash. Ridges are generally higher on windward coasts and build up to two or three metres above mean sea level. Portions of reef islands may be built above the limit of wave activity as a result of aeolian processes wherever there is abundant sand and sufficient wind energy. On some Caribbean islands (e.g. Anguilla) lithification of pre-Holocene dunes occurred during periods of lower sea level and this provides greater stability to the island. Islands generally grow by accretion vertically and especially seaward and lagoonward. The size and shape of the island will depend on the supply of sediments from the reef, the time since the reef platform reached sea level and the detailed local history of wave and current processes controlling sediment movement. A wide range of possible scenarios for island development can be envisaged (Woodroffe *et al.*, 1999) depending on the relative significance of seaward and lagoonward accretion, vertical accretion and island migration. They also document the history of accretion on West Island, Cocos (Keeling) Island with seaward

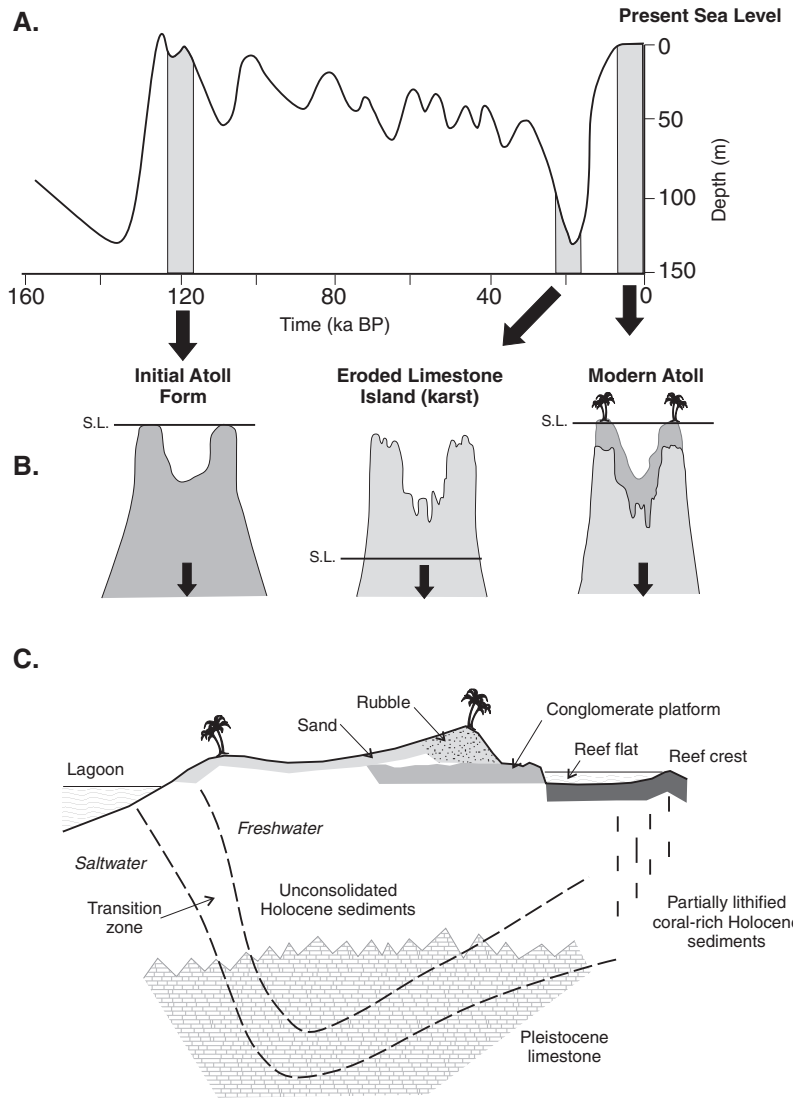

Figure 12.12 Schematic illustration of the late-Quaternary history of an atoll with respect to (A) changing sea level and (B) ongoing gradual subsidence, which together produce the idealised cross-section (C) of the rim of an atoll showing a reef island, its geomorphology, lithology and sediments, and typical configuration of the freshwater lens (Woodroffe, 2008).

growth dominant in the central section over the period 4000–2000 BP and more gradual accretion since then with sedimentation focused more on the ends of the island. In general, we should expect island accretion to continue as long as the biological productivity of the reef remains high and the island is the main sink for sediments.

Sedimentary facies of coral reefs

The general pattern of reef environments and associated sedimentary facies along a transect from reef flat and lagoon, across the reef crest and down the slope of the forereef is given added complexity by the range of reef forms and degree of exposure. In turn, the sedimentary unit that reflects accumulation over periods of thousands of years will reflect the influence of changing sea level, wind and wave climate, and terrigenous sediment input as well as changes in the biotic communities. Coring through modern reefs provides an opportunity to examine the interior structure of reefs and, together with dating of materials, to determine the growth history in response to changing environmental conditions and sea levels

(e.g. Gischler *et al.*, 2008). This information in turn provides improved understanding of sea level change in the Holocene as well as indirect evidence of changing climate and sea surface temperatures. Finally, we can use information from modern reefs to help in the interpretation of ancient reef deposits.

There were some notable early attempts to core reefs, such as the Royal Society sponsored drilling on Funafuti Atoll in 1896–1898 and the first drilling on the Great Barrier Reef in 1926 (Hopley *et al.*, 2007). However, it was the development of lightweight drilling rigs in the late 1960s that could be set up on emerged reef flats or mounted on pontoons to drill in shallow lagoons that resulted in an explosion of coring both in the Caribbean (e.g. MacIntyre *et al.*, 1982) and throughout the Indo-Pacific region, including an extensive programme on the Great Barrier Reef (Hopley *et al.*, 2007). This coring has provided much of the evidence for interpretation of reef evolution in response to sea level rise discussed earlier but the identification of facies in the cores also provides information on the various modes by which reefs are constructed, the nature of the contribution by different coral species as well as species of coralline algae, and the relative importance of secondary sand and muddy deposits in lagoons, reef flats and forereef.

Montaggioni (2005) on the basis of an extensive review of cores from the Indo-Pacific region identified ten major sedimentary facies composed of seven varieties of growth framework and three detrital facies (Table 12.1). Interpretation of the facies is based on comparison with the modern reef zones shown in Figure 12.3. The framework facies are considered the primary foundation of the reef structure but cores, particularly those from back reef areas, may be dominated by detrital facies. The sequence of facies encountered within an individual core will reflect the location on the reef and the evolutionary history of the reef – e.g., vertical growth, seaward progradation or backstepping (Kennedy and Woodroffe, 2002).

Coral facies may also be mapped in uplifted coral reefs and the sequence found on the coral reef terraces of Barbados has been extensively studied, both in terms of the characteristics of the ancient reef sediments, and because dating of the uplifted reefs has made a significant contribution to sea level chronology through the mid- to late-Pleistocene (Mesolella *et al.*, 1970; Blanchon and Eisenhauer, 2001; Schellmann and Radtke, 2004). Continued uplift of the Barbados ridge provides a sequence of uplifted reefs reaching an elevation of over 300 m and spanning much of the Pleistocene. Portions of the reef platform and reef flats are preserved landward of notches or cliffs cut in the uplifted reefs during high stands of sea level (Figure 12.13).

12.3.3 Wave and current dynamics on reefs

Waves and wave-generated currents influence reefs and reef dynamics in several ways and in turn the presence of fringing and barrier reefs has considerable influence on the amount of wave energy reaching the shoreline. Differences in wave energy and in exposure to intense storms have been used to explain broad differences in reef morphology, while energy gradients with depth down the forereef zone or across the reef crest and reef flat have been recognised as exerting an important control on both the biological zonation of coral reefs and on sediment dispersal and deposition. Wind and wave generated currents influence the transport of sediment over the reef and reef flats, and they are the primary control on the supply of nutrients and food for corals and other organisms of reef communities.

Broad relationships between reef zonation and wave climatology – specifically wave energy levels and the frequency of hurricanes – have been recognised for Caribbean coral reefs (Geister, 1977; Hubbard, 1997). Hubbard (1997) divides the Caribbean into three groups: (1) areas such as the eastern shores of the Windward Islands which are characterised by high wave energy and moderate-to-high frequency of impacts from hurricanes either directly or through high-swell waves generated by hurricanes passing within 100 km; (2) areas of high wave energy but infrequent disruption by hurricane impacts such as the north shore of St Croix and other protected sites in the Florida Keys; and

Table 12.1 *Facies identified in cores through reefs in the Indo-Pacific region. The distribution of the dominant coral forms and assemblages associated with the framework facies is shown in* **Figure 12.12**. *(Based on descriptive summary in Montaggioni, 2005, pp. 14–24).*

Facies type	Facies name	Description
Framework	Coralline algal	reef crests and reef flats – cm to decimetre thick laminated crusts binding in-place or reworked corals
Framework	Robust branching coral	reef crest and proximal reef fronts – open to cavernous interlocking framework formed by branching corals with infilling by rubble and sandy matrix
Framework	Domal coral	outer reef slope, crest and reef flats – coral heads encrusted with coralline algae or scattered colonies separated by skeletal sands and silts
Framework	Tabular branching coral	semi exposed or sheltered forereef and reef flats – rigid structure of tabular corals either in situ or reworked and mixed with silty sands
Framework	Arborescent coral	lower to middle parts of forereef and backreef – framework of encrusted corals or fragments of reworked branches
Framework	Foliaceous coral	sheltered areas with high turbidity – platy corals encrusted and often buried in muddy fine sands
Framework	Encrusting coral	high energy reef crests less than 10 m – coral components contained within matrix of carbonate and terrigenous mud
Detrital	Skeletal rubble	sub-tidal to intertidal reef flats – corral rubble consisting of broken coral and coralline algae in a matrix of fine to coarse sand. may make up to 60% of a core
Detrital	Carbonate sand	inner reef flat and backreef – sand and gravel derived from wide range of corals, coralline algae, mollusks and green algae. make up 10–50% of cores.
Detrital	Carbonate mud	sheltered inner reef flats and backreef zones, sea grass beds – may be inorganically precipitated or breakdown of skeletal material

(3) areas of low wave energy but subject to frequent hurricane impacts such as many parts of the Bahamas. Type 1 reefs are characterised *Acropora palmata* colonies which are frequently broken down by hurricane wave impacts with subsequent colonisation of the rubble by coralline algae. Type 2 reefs are dominated by *A. palmata* which thrive in the absence of hurricanes. Finally, Type 3 reefs have only isolated *A. palmata* colonies and relatively low diversity, but long periods of relatively low energy conditions encourage grazing which inhibits the growth of thick algal crusts (Hubbard, 1997).

Recent work has also focused on seasonal variations in wind and wave climatology and the effect of this on both physical processes and biological activity. In the Caribbean, in addition to the potential for hurricanes during the period from July through November, the strength of the trade winds, water surface temperatures and runoff from the land also vary seasonally. Reef island shorelines in the Maldives showed large changes in area in response to seasonal reversals in wind and wave conditions associated with west-northwest and north-east monsoons (Kench and Brander, 2006b). Similarly, measurements by Storlazzi and Jaffe (2008) on a fringing reef on West Maui, Hawaii over a 15 month period showed that there were considerable seasonal variations in wave energy levels and in the extent of turbidity in the water column, and this had significant effects on mixing and on the transport of both sediments and larvae in the water column. Because coral spawning occurs primarily during conditions dominated by trade winds (June to September) they speculate that the location of the reef with

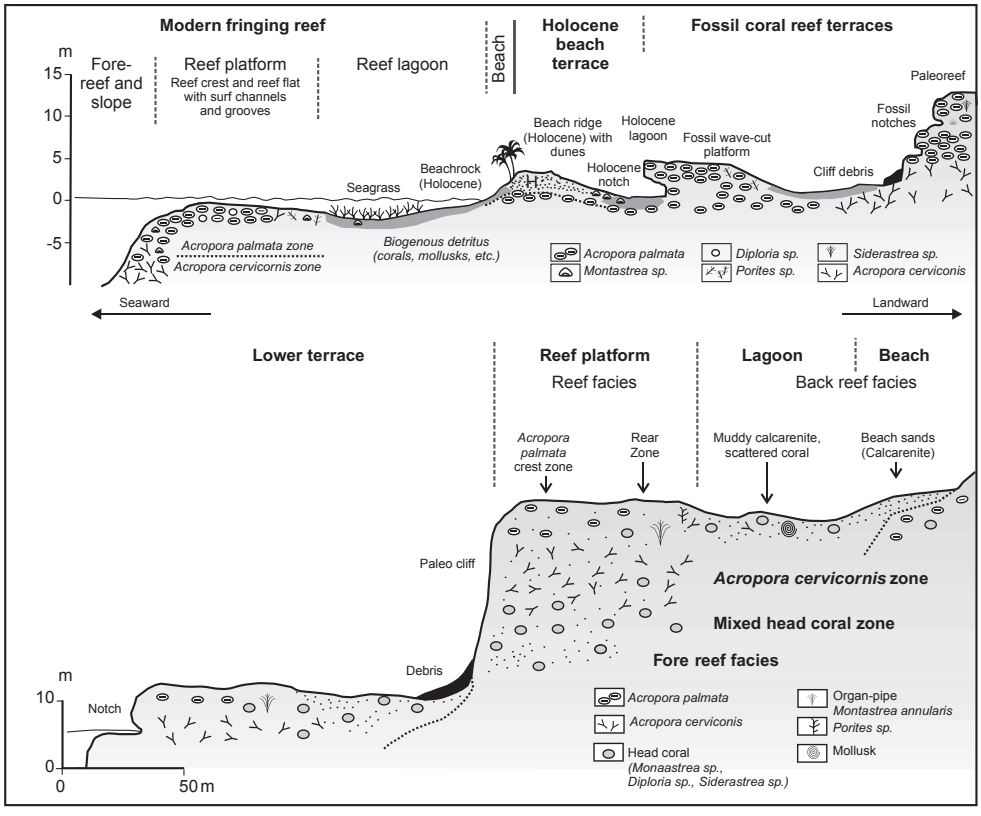

Figure 12.13 Sketch of the morphology and coral reef zones of fossil coral reef terraces on Southern Barbados (Schellmann and Radtke, 2004).

respect to currents would lead to dispersal of coral larvae to nearby downdrift island, thus increasing diversity of corals in these areas (Storlazzi and Jaffe, 2008). In contrast, fish communities on reef flats of reefs on Reunion Island in the SW Indian Ocean exhibit a strong spatial pattern related to geomorphological zones on the fringing reefs and showed little response to seasonal changes in winds and waves (Letourner *et al.*, 2008).

Recognition of the key role played by waves in controlling wave energy levels on the reef crest and currents over the reef flat and within atoll lagoons has led to an increasing number of field measurements as well as to attempts to generate models to predict set-up, wave transmission and currents (Gourlay, 1994; Lugo-Fernàndez *et al.*, 1998; Brander *et al.*, 2004; Gourlay and Colleter, 2005; Kench and Brander, 2006a; Kench *et al.*, 2006; Callaghan, *et al.*, 2006; Storlazzi and Jaffe, 2008). On simple fringing reefs with relatively gentle forereef slope the reef crest acts somewhat like a nearshore bar with the extent of wave set-up and transmission dependant on the crest elevation and tidal stage. Wave breaking on the crest transmits large volumes of water onto and across the reef flat and may drive strong alongshore currents close to the beach. This water then escapes from the lagoon through channels in the reef. Because the reef crest is irregular and because of the existence of channels through the reef waves may be refracted and focused in places, and the resultant set-up gradients and wave generated currents will determine areas of transport and deposition of sediments.

While both short-period wind waves and long-period swells are attenuated rapidly over the reef flat, long-period swell waves may

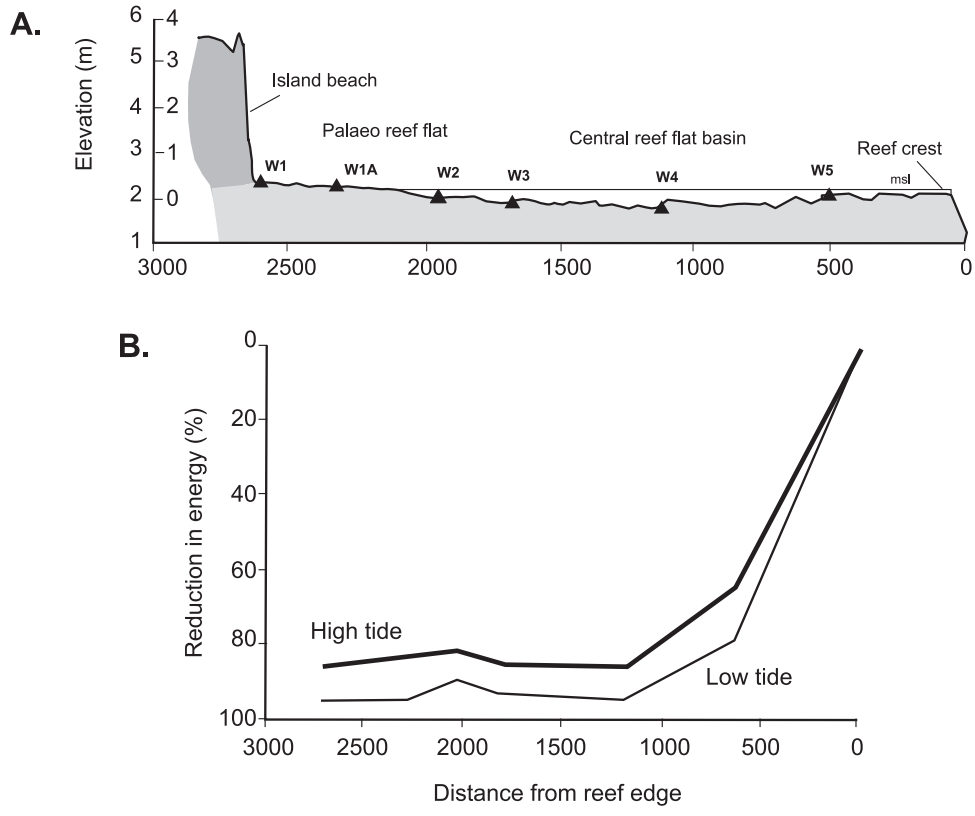

Figure 12.14 Wave energy dissipation across the windward reef flat, Warraber Island, Torres Strait, Australia at high and low tides: (A) profile showing reef zones and location of pressure transducers used to measure waves; (B) reduction in wave energy relative to offshore significant wave height at high and low tide (Kench and Brander, 2006a).

propagate through channels in the reef and they may also be the dominant waves on the leeward side of reefs (Kench and Brander, 2006a). On wide reef flats and shallow lagoons, locally generated wind-waves may become the dominant process influencing island beaches. In general wave attenuation is greatest for wide, shallow reefs and least for narrow, relatively deep reefs and is greater at high tide than at low tide when more of the reef crest is exposed or close to the surface (Figure 12.14). Kench and Brander (2006a) combine the effects of water depth at spring high tide and reef width to produce a reef energy window index (Ψ) which can be used to facilitate comparison of expected wave energy propagation across different reefs:

$$\Psi = \frac{d}{RW} \tag{12.1}$$

where d is mean water depth over the reef flat at spring high tide; RW is reef width.

This can provide some insight into the relative potential for sediment transport across the reef flat, in combination with the proportion of time over the spring-neap cycle that water depth on the reef flat exceeds a critical depth for wave propagation. It may also reflect the amount of sedimentation that has already occurred.

Wave set-up and subsequent inflow of water across the reef flat is an important source of mass and energy transfer driving transport of nutrients into the backbarrier and lagoon areas and contributes to the overall circulation in the lagoon. On windward coasts the effects of wind stress on the water surface will be added to that of waves and may also be a significant contributor on shallow reef flats. The relative importance of wave set-up

and winds will vary with incident wave height and with the tidal range at a particular site as well as with the depth of the lagoon and the spacing and depth of connections to the sea. Flushing due to tidal action is also very important, but since almost all coral reefs occur in areas of micro- to low mesotidal range, waves usually are a significant factor and may be the primary factor in microtidal areas.

On atolls where wide reef flats and reef islands may greatly constrain direct connection to the ocean through inlet channels, flushing by waves and wind becomes very important for maintaining water quality in the lagoon. In their study of water levels and flows across reef flats on two virtually enclosed micro-tidal atolls in the South Pacific Callaghan *et al.* (2006) found that wave breaking produced a nearly continuous super-elevation of the water surface on the exposed reef flat which drove an outflow of water across the leeward side of the atoll. In a neat applied study they used analytical modelling of flow over the reef to show that enhanced flushing of the lagoon to reduce the impact of oyster cultivation could be accomplished better by removing obstacles to wave pumping across the reef rim than by tidal pumping through artificial channels dredged through the reef (Callaghan *et al.*, 2006).

12.4 Impacts of disturbance on coral reefs

Coral reefs, like all ecosystems, consist of a biotic component of plants and animals and an abiotic component which includes the reef substrate the surrounding ocean and atmosphere and the physical and chemical processes that take place within the abiotic component. As such we can expect reef ecosystems to be diverse and dynamic, with diversity reflecting both the diversity of the abiotic habitat (e.g. Aronson and Precht, 1995; Cassata and Collins, 2008) and the dynamics (competition, opportunistic replacement) of the biotic component (Paulay, 1997). Reef dynamics includes both evolutionary processes, such as the upward growth of the reef towards the sea surface, and the response to disturbances produced by both biological and physical causes (Bythell *et al.*, 1993; van Woesik, 1994; Hubbard, 1997; Smith *et al.*, 2008). Disturbances to coral reefs can be grouped into those that result from natural processes, such as bleaching, predation, hurricanes and sea level change, and human activities such as runoff, nutrient loading, dredging and fishing (Brown, 1997).

12.4.1 Natural disturbance

As part of the larger reef ecosystem, coral organisms are subject to a wide range of potential natural disturbances that may affect individual organisms over a wide area or many organisms in a more restricted area. These disturbances can be biological in nature or result from physical processes such as wave action or temperature change.

Biological causes of disturbance

Coral organisms are subject to disease and to the effects of invasions by predators in the same way that land-based forests or animal populations are. In the Caribbean, populations of the dominant framework reef builder elkhorn coral (*A. palmata*) have declined drastically since the 1980s, primarily because of an outbreak of a bacterial disease termed white-band (Aronson and Precht, 2001). In the short term this has implications for continued reef building and for the dynamics of the reef crest but in the long term new disease-free colonies may establish as a result of recruitment from surviving areas and possibly selection of disease-resistant forms (MacIntyre et al., 2007).

One of the most studied coral reef predators has been the crown-of-thorns starfish (*Acanthaster planci*) which affected large areas of the Australian Great Barrier Reef in the 1960s and 1980s (Moran, 1986; Brown, 1997). The starfish, which is 10–15 cm in diameter, has multiple arms and a dense covering of mildly poisonous spines, feeds directly on live coral colonies. At low densities the impact is relatively small and recovery is rapid. During outbreaks the density of starfish in places can be 10–15 adults a square metre and coral mortality can exceed 90%. Recovery in this case may take 20 to 50 years depending on

recruitment patterns and on the growth of algae on dead coral. Several species of fish, notably the group of butterfly fish (*Chaetodontidae*), feed directly on coral (Hixon, 1997) though there does not seem to be the same potential for large-scale mortality as is associated with the crown-of-thorns starfish.

The dynamics of corals and coral reefs are also affected indirectly by the activities of herbivores such as parrot fish (*Scaridae*) and surgeon fish (*Acanthuridae*) which usually occur in schools on coral reefs. They feed largely on algae and can consume a very large proportion of the total annual growth (Hatcher 1982). These activities act as an important control on the spread of algae and the recruitment of new coral colonies. Large declines in the populations of another herbivore, the sea urchin *Diadema antillarium*, has led to a large reduction in the abundance of coral and an increase in algae on many Caribbean reefs since the 1980s (Brown, 1997).

Bleaching of corals results from the expulsion of the zooanthellae and is triggered by thermal stress from high water temperatures or exposure. Bleaching leading to death of corals occurs on the reef crest and back reef area when corals become exposed at low tide, a consequence of the vertical growth of the reef, and may be triggered by seasonal or decadal sea level fluctuations.

Physical causes of disturbance

Bleaching due to high sea surface temperatures may affect corals on the fore-reef as well as those on the reef crests and back-reef. It can be a consequence of climate patterns such as El Niño (Glynn, 1993; Smith *et al.*, 2008) and bleaching episodes are expected to increase as a result of climate change (Hughes *et al.*, 2003; Baker *et al.*, 2008). Response to thermal stress varies among individual species of coral and some species show little effect over a wide range of temperatures. The recovery of coral communities from bleaching events may occur through recovery of remnant colonies and through recruitment with the rate and extent to which this occurs being influenced by location as well as the extent to which damaged corals are replaced by other species such as algae (Golbuu *et al.*, 2007). Recent work suggests that there is a range of tolerance to thermal stress within a single species and that this may change through time through genetic adaptation and selection. As a result, the resilience of coral organisms and coral reefs to climate variation and climate change may be much greater than initial scenarios for climate change effects have portrayed (Hughes *et al.*, 2003).

In many areas of the tropics the most significant physical disturbance to reefs is caused by the passage of tropical storms (hurricanes, cyclones, typhoons) which bring with them several different types of disturbance, including the direct mechanical effects of wave action, burial by transported debris, high turbidity due to wave actions and runoff from mainland areas and changes in salinity (Harmelin-Vivien, 1994). The direct impact of large waves breaking on the reef crest is responsible for the breakage of coral, especially of branching corals such as *Acropora sp.*, while domal forms suffer much less (Woodley *et al.*, 1981; Hubbard *et al.*, 1991; Lugo *et al.*, 2000; Bries *et al.*, 2004). Some damage to coral colonies also occurs because of the impact of large fragments being transported in the waves and abrasion from sand. Hurricane damage should increase with increasing storm intensity but local sheltering, refraction and shoreline orientation as well as the reef profile generally produces quite a lot of variability in the impact. Recovery from hurricane damage is facilitated by three processes (Glynn, 1990; Harmelin-Vivien, 1994): (1) regrowth of surviving coral fragments; (2) regeneration of damaged colonies; and (3) the settlement of coral larvae on damaged reef surfaces. The first two processes appear to be most important where hurricane damage is relatively light. Recruitment of new colonies is most important where damage is severe (Harmelin-Vivien, 1994; Coles and Brown, 2007) and the rate of recovery through this process will depends in part on availability of suitable substrate, on competition with algae and on sources of recruitment.

While hurricane impacts have a damaging effect in the short term from a biological perspective, they can be regarded as simply part of the dynamics of the reef system which will have influence the overall diversity and structure of the reef ecosystem (Hubbard, 1997; Edmunds,

Box 12.1 Vulnerability of ocean atoll reef islands to sea level rise

Over the past two or three decades there has been considerable speculation that human-induced climate change is threatening the existence of Pacific atoll island communities such as the Maldives and Vanuatu. The major threats is seen as vulnerability to salt water intrusion into the freshwater lenses under the islands, increased erosion and flooding during cyclones and possibly increased frequency of large-magnitude cyclones. As is the case with any natural hazard, there are two components to consider – the nature of the physical process or processes that forms the hazard, and the ability of humans to adjust/adapt to the threat. Given our understanding of processes operating on coral reefs and reef islands, how real is the threat? How will reef and island processes change/adjust to increased sea level rise and possibly greater frequency of storms? How can our understanding of these processes aid in the development of adaptive measures that will mitigate the potential impact on human populations?

Most Pacific atolls have a ring of islands formed on reef flats that surround some form of central lagoon. Cross-sections of islands generally show a high ridge on the exposed side of the island that is generally 2–4 m above present sea level (Woodroffe, 2008) though some islands may have higher spots as a result of dune building where there is abundant sand. Less prominent ridges may occur on lagoon shores where there is sufficient fetch for moderate wave generation or ridges may be the result of agricultural activities in swampy areas. Some portion of the present height above sea level may reflect slight sea level fall since the Holocene maximum (Dickinson, 2001) but the significance of this varies regionally across the Pacific and will also vary locally depending on the history of the accretion of individual atolls and islands.

In most instances much of the accretion above sea level results from the impact of large storms which produce storm surge and wave run-up that leads to sediment being washed inland – as we have seen this may be in the form of rubble ridges where this reefal material is available, and these form the most stable ridges (Scoffin, 1993). We can expect that the frequency of water levels above a critical height will increase as a result of rising sea level, but this will be superimposed slowly on higher-frequency changes due to tides and seasonal and decadal sea level oscillations. Increased water depth will provide additional space for upward reef growth and continued supply of sediment to the reef flat (Woodroffe, 2008). Geomorphologically, it would seem that sea level rise due to global warming will have a limited impact on coral atolls and their islands and the ongoing process of reef building and sediment dispersal by waves and currents will continue to be the primary control.

As is the case with barrier islands, humans occupying atoll islands have chosen to live in a dynamic environment and may need to find a way to permit processes that lead to building up of the islands to continue while adapting human activities to minimise the risk posed by storm overwash and flooding. In cases such as Funafuti atoll, Tuvalu, human vulnerability to the threats posed by sea level rise has been increased by building on low-lying lands that are most threatened by flooding (Yamano *et al*., 2007). Adaptation to the threat of increased overwash and flooding therefore requires an understanding of the physical process posing the threat and the full range of adaptive strategies that are available (Solomon and Forbes, 1999). A key component of any management plan must however be the recognition of the significance of all the processes controlling island evolution and adaptation to sea level rise must be seen within the context of a much broader management and environmental strategy that must include the threats posed by human activities as well. In this respect, integrated coastal management for coral atoll islands is no different than for any dynamic coastal environment.

2002). The impact of hurricanes from a geomorphological or geological perspective can be regarded as largely constructive, since these high-magnitude events are important for shaping the reef crest, for providing large quantities of rubble for further reef growth and for transporting large quantities of sand and fines landward across the reef flat and seaward down the reef face. The characteristics of coral rubble deposition may vary with storm intensity and exposure and this in turn will influence the character of the reef substrate and the process of coral recovery (Perry, 2001). In some cases extreme storms produce large ridges of cobbles and boulders which may be 1–4 m in height and be built-up at the shoreline or on the reef flat (Richmond and Morton, 2007; Spiske *et al.*, 2008).

Similarly, while tsunamis can have a devastating impact on human populations on exposed coral atoll islands, the geomorphological impact appears to be relatively minor (Kench *et al.*, 2008). Kench *et al.* (2008) were able to repeat pre-tsunami profiles and vegetation line surveys on a number of uninhabited islands on South Maalhosmadulu atoll in the Maldives atoll chain and to examine both erosional and depositional features left by the tsunami impact. At this location the first wave overtopped all but the highest portions of the ridge along the outer rim of the islands but subsequent waves did not. The first wave flooded across the crest and deposited a relatively thin sheet as a washover fan with sediments ranging in thickness from 0.1–0.3 m near the ridge crest but rapidly tapering to a few cm inland. Subsequent waves produced small scarps and eroded the vegetation line. In most areas erosion of beach sediments and of the vegetated portion of the island was small (<4% by area). The tsunami impacts varied spatially depending on local relief, sources of sediment and configuration of the reefs and channels. Kench *et al.* concluded that most evidence of the tsunami would quickly disappear as a result of ongoing coastal processes and the most significant effect on island evolution was probably the addition of sediments to the central portion of the islands. Thus, like hurricanes, tsunamis may be viewed geomorphologically as generally having a positive impact on reef and atoll islands.

Human causes of disturbance

There is considerable evidence of a decline in the extent and biodiversity of coral reefs world-wide (Gardner *et al.*, 2003; Bell *et al.*, 2006; Mora, 2007). Much of this has been attributed to the direct and indirect impact of human activities, though there is still some difficulty in determining the impact of individual stresses in a system that is increasingly subject to multiple stressors (Hughes *et al.*, 2003; Aronson and Precht, 2006).

Locally human impacts on coral reefs include (Brown, 1997): sedimentation and high turbidity resulting from increases in soil erosion inland and from dredging and construction activities in the waters around coral reefs. Often this may be associated with tourism infrastructure; oil pollution from oil spills or chronic leakage in areas around oil refineries and harbours; and from mining of coral reefs for building materials and for making lime. Tourism development is often a major source of local threats both from the construction of facilities near the shoreline or in shallow water, and from the accompanying pollution from untreated or poorly treated sewage and runoff from fertilisers and other chemicals used to maintain hotel grounds and golf courses. Coastal development may result in destruction of mangroves and salt marshes and the infilling of small lagoons and salt ponds leading to reduced trapping of fines before they reach coastal waters. Anchor dragging (Maynard, 2008) and tourism diving and snorkelling can have severe local physical impacts on reefs though recognition of this has led to the training of dive masters and the adaptation of simple solutions such as the deployment of buoys along highly frequented reefs. Physical damage may also result from destructive fishing techniques such as blasting or the use of cyanide (Souter and Linden, 2000). Finally, overfishing, particularly of herbivores that feed on algae has been cited as one form of human impact, though the validity of this has been challenged by Aronson and Precht (2006).

There is considerable concern also over the potential impact of human-induced climate change on coral reefs, particularly through higher sea surface temperatures, increased rates of sea level rise and possibly increased intensity of tropical storms. As noted earlier, coral reef

communities show considerable resilience in the face of these types of stresses and the impact of climate change may be to produce changes in the diversity and make-up of reef communities rather than a decline in the reefs themselves (Hughes *et al.*, 2003). It seems that the more immediate destructive threats are the local and regional ones, and these will require a diverse suite of approaches and measures to produce a significant reduction in them (Souter and Linden, 2000; Bell *et al.*, 2006). It may also require a much more concerted effort on the part of scientists and social scientists to develop a robust framework for addressing the crisis and a convincing public relations effort to get it implemented (Risk, 1999).

Further reading

Barnes, R. S. K. and Hughes, R. N. 1999. *An Introduction to Marine Ecology*, 3rd edn.. Blackwell, Oxford, pp. 117–141.

One of several texts that provide useful background on the biology of reefs.

Birkeland, C. (ed.) 1997. *The Life and Death of Coral Reefs*. Chapman and Hall, New York, 536 pp.

This is a good compilation of chapters by some of the experts on coral reefs.

Hopley, D., Smithers, S. G. and Parnell, K. E. 2007. *The Geomorphology of the Great Barrier Reef*. Cambridge University Press, Cambridge, 532 pp.

This is an excellent book that brings together a wealth of information on the barrier reef and provides a strong geomorphological perspective.

Montaggioni, L. F. 2005. History of Indo-Pacific coral reef systems since the last glaciation: development patterns and controlling factors. *Earth-Science Reviews*, **71**, 1–75.

An excellent review of the stratigraphic history of coral reefs in the region in response to post-glacial sea level changes.

References

Adey, W. H. and Burke, R. B. 1977. Holocene bioherms of Lesser Antilles: Geographic control of development. In Frost, S. H. Weiss, M. P. and Saunders, J. B. (eds.), *Reefs and Related Carbonates: Ecology and Sedimentology*. American Association of Petroleum Geologists, Studies in Ecology 4, pp, 67–81.

Alongi, D. M. 1998. *Coastal Ecosystem Processes*. CRC Press, Boca Raton, FL, pp. 139–182.

Aronson, R. B. and Precht, W. B. 1995. Landscape patterns of reef coral diversity: A test of the intermediate disturbance hypothesis. *Journal of Experimental Marine Biology and Ecology*, **192**, 1–14.

Aronson, R. B. and Precht, W. B. 2001. White band disease and the changing face of Caribbean reefs. *Hydrobiologia*, **460**, 25–38.

Aronson, R. B. and Precht, W. B. 2006. Conservation, precaution and Caribbean reefs. *Coral Reefs*, **25**, 441–450.

Baker, A. C., Glynn, P. W. and Riegl, B. 2008. Climate change and coral reef bleaching: An ecological assessment of long-term impacts, recovery trends and future outlook. *Estuarine, Coastal and Shelf Science*, **80**, 435–471.

Beaman, R. J., Webster, J. M. and Wust, R. A. J. 2008. New evidence for drowned shelf edge reefs in the Great Barrier Reef, Australia. *Marine Geology*, **247**, 17–34.

Bell, J. D., Ratner, B. D., Stobutzki, I. and Oliver, J. 2006. Addressing the coral reef crisis in developing countries. *Ocean and Coastal Management*, **49**, 976–985.

Blanchon, P. and Eisenhauer, A. 2001. Multi-stage reef development on Barbados during the last interglacial. *Quaternary Science Review*, **20**, 1093–1112.

Blanchon, P. and Blakeaway, D. R. 2003. Are catch-up reefs an artefact of coring? *Sedimentology*, **50**, 1271–1282.

Brander, R. W., Kench, P. S. and Hart, D. 2004. Spatial and temporal variations in wave characteristics across a reef platform, Torres Strait, Australia. *Marine Geology*, **207**, 169–184.

Bries, J. M., Debrot, A. O. and Meyer, D. L. 2004. Damage to the leeward reefs of Curaço and Bonaire, Netherlands Antilles from a rare storm event: Hurricane Lenny, November, 1999. *Coral Reefs*, **23**, 297–307.

Brown, B. E. 1997. Disturbances to reefs in recent times. In Birkeland, C. (ed.), *Life and Death of Coral Reefs*. Chapman and Hall, New York, 354–385.

Bythell, J. C., Gladfelter, E. H. and Bythell, M. 1993. Chronic and catastrophic natural mortality of three common Caribbean reef corals. *Coral Reefs*, **12**, 143–152.

Callaghan, D. P., Nielsen, P., Cartwright, N., Gourlay, M. R. and Baldock, T. E. 2006. Atoll lagoon flushing forced by waves. *Coastal Engineering*, **53**, 691–704.

Cassata, L. and Collins, L. B. 2008. Coral reef communities, habitats and substrates in and near sanctuary

zones of Nongaloo Marine Park. *Journal of Coastal Research*, **24**, 139–151.

Chappell, J., Omura, A., Esat, T., McCulloch, M., Pandolfi, J., Ota, Y. and Pillans, B. 1996. Reconciliation of late Quaternary sea levels derived from coastal terraces at Huon Peninsula with deep sea oxygen isotope records. *Earth and Planetary Science Letters*, **141**, 227–236.

Coles, S. L. and Brown, E. K. 2007. Twenty-five years of change in coral coverage on a hurricane impacted reef in Hawaii: the importance of recruitment. *Coral Reefs*, **26**, 705–717.

Davies, J. L. 1980. *Geographic Variation in Coastal Development*. Longman, London, 2nd edn., 212 pp.

Dickinson, W. R. 2001. Paleoshoreline record of relative Holocene sea levels on Pacific islands. *Earth-Science Reviews*, **55**, 191–234.

Edmunds, P. J. 2002. Long-term dynamics of coral reefs in St. John, US Virgin Islands. *Coral Reefs*, **21**, 357–367.

Gardner, T. A., Cote, I. M., Gill, J. A., Grant A. and Watkinson, A. R. 2003. Long-term region-wide declines in Caribbean corals. *Science*, **301**, 958–960.

Geister, J. 1977. The influence of wave exposure on the ecological zonation of Caribbean reefs. *Proceedings of the 3rd International Coral Reef Symposium*, Miami, vol. **1**, pp. 23–29.

Gischler, E., Hudson, J. H. and Pisera, A. 2008. Late Quaternary reef growth and sea level in the Maldives (Indian Ocean). *Marine Geology*, **250**, 104–113.

Glynn, P. W. 1990. Coral mortality and disturbances to coral reefs in the tropical eastern Pacific. In Glynn, P. W. (ed.), *Global Ecological Consequences of the 1982–83 El Niño–Southern Oscillation*. Elsevier Oceanography Series, vol. **52**, pp. 55–126.

Glynn, P. W. 1993. Coral reef bleaching: ecological perspectives. *Coral Reefs*, **12**, 1–17.

Golbuu, Y., Victor, S., Penland, L. *et al*. 2007. Palau's coral reefs show differential habitat recovery following the 1998-bleaching event. *Coral Reefs*, **26**, 319–332.

Gourlay, M. R. 1994. Wave transformation on a coral reef. *Coastal Engineering*, **23**, 17–42.

Gourlay, M. R. and Colletter, G. 2005. Wave-generated flow on coral reefs – an analysis for two-dimensional horizontal reef-tops with steep faces. *Coastal Engineering*, **52**, 353–387.

Guilcher, A., 1988. *Coral Reef Geomorphology*. Wiley, Chichester, 228 pp.

Harmelin-Vivien, M. L., 1994. The effects of storms and cyclones on coral reefs: a review. *Journal of Coastal Research*, SI **12**, 211–231.

Harris, P. T., Heap, A. D., Marshall, J. F. and McCulloch, M. 2008. A new coral reef province in the Gulf of Carpentaria, Australia: Colonisation, growth and submergence during the early Holocene. *Marine Geology*, **251**, 85–97.

Hatcher, B. G. 1982. The interaction between grazing organisms and the epilithic algal community of a coral reef: a quantitative assessment. *Proceedings Fourth International Coral Reef Symposium*, Manilla, **2**, 515–524.

Hixon, M. A. 1997. Effects of reef fishes on corals and algae. In Birkeland, C. (ed.), *Life and Death of Coral Reefs*. Chapman and Hall, New York, 230–248.

Hopley, D., Smithers, S. G. and Parnell, K. E. 2007. *The Geomorphology of the Great Barrier Reef*. Cambridge University Press, Cambridge, 532 pp.

Hubbard, D. K. 1997. Reefs as dynamic systems. In Birkeland, C. (ed.), *Life and Death of Coral Reefs*. Chapman and Hall, New York, 43–67.

Hubbard, D. K., Parsons, K. M., Bythell, J. C. and Walker, N. D. 1991. The effects of Hurricane Hugo on the reefs and associated environments of St. Croix, U.S. Virgin Islands: a preliminary assessment. *Journal of Coastal Research*, **8**, 33–48.

Hughes, T. P., Baird, A. H., Bellwood, D. R. *et al*. 2003. Climate change, human impacts, and the resilience of coral reefs. *Science*, **301**, 929–933.

Kench, P. S. and Brander, R. W. 2006a. Wave processes on coral reef flats: implications for reef geomorphology using Australian case studies. *Journal of Coastal Research*, **22**, 209–223.

Kench, P. S. and Brander, R. W. 2006b. Response of reef island shorelines to seasonal climate oscillations: South Maalhosmadulu atoll, Maldives. *Journal of Geophysical Research*, **111**, F01001, 1–12.

Kench, P. S., Brander, R. W., Parnell, K. E. and McLean, R. F. 2006. Wave energy gradients across a Maldivian atoll: Implications for island geomorphology. *Geomorphology*, **81**, 1–17.

Kench, P. S., Nichols, S. L., Smithers, S. G., McLean, R. F. and Brander, R. W. 2008. Tsunamis as agents of geomorphic change in mid-ocean reef islands. *Geomorphology*, **95**, 361–383.

Kennedy, D. M. and Woodroffe, C. D. 2002. Fringing reef growth and morphology: a review. *Earth-Science Reviews*, **57**, 255–277.

Letourner, Y., Gaertner, J-C., Durbec, J-P. and Jessu, M. E. 2008. Effects of geomorphological zones, reefs and seasons on coral reef fish communities of Réunion Island, Mascarene Archipelago, SW Indian Ocean. *Estuarine, Coastal and Shelf Science*, **77**, 697–709.

Lugo, A. E., Rogers, C. S. and Nixon, S. W. 2000. Hurricanes, coral reefs and rainforests: resistance, ruin and recovery in the Caribbean. *Ambio*, **29**, 106–114.

Lugo-Fernàndez, A., Roberts, H. H. and Wiseman, J. W. 1998. Tide effects on wave attenuation and wave set-up on a Caribbean coral reef. *Estuarine, Coastal and Shelf Science*, **47**, 385–393.

MacIntyre, I. G. 1988. Modern coral reefs of Western Atlantic – new geological perspectives. *American Association of Petroleum Geologists Bulletin*, **72**, 1360–1369.

MacIntyre, I. G., Burke, R. B. and Stuckenrath, R. 1982. Core holes in the outer forereef off Carrie Bow Cay, Belize: a key to the Holocene history of the Belizean barrier reef complex. *Proceedings Fourth International Coral Reef Symposium, Manilla*, **1**, 567–574.

MacIntyre, I. G., Glynn, P. W. and Toscano, M. A. 2007. The demise of a major *Acropora palmata* bank-barrier reef off the southeast coast of Barbados. *Coral Reefs*, **26**, 765–773.

Maynard, J. A. 2008. Severe anchor damage to *Lobophyllia variegata* colonies on the Fujikawa Maru, Truk Lagoon, Micronesia. *Coral Reefs*, **27**, 273.

McLaughlin, C. J., Smith, C. A., Buddemeier, R. W., Bartley, J. D. and Maxwell, B. A. 2003. Rivers, runoff, and reefs. *Global Planetary Change*, **39**, 191–199.

Mesolella, K. J., Sealy, H. A. and Mathews, R. K. 1970. Facies geometries within Pleistocene reefs of Barbados, West Indies. *American Association of Petroleum Geologists Bulletin*, **54**, 1899–1917.

Montaggioni, L. F. 2005. History of Indo-Pacific coral reef systems since the last glaciation: development patterns and controlling factors. *Earth-Science Reviews*, **71**, 1–75.

Mora, C. 2007. A clear human footprint in the coral reefs of the Caribbean. *Proceedings of the Royal Society B*, doi:10.1098, 1–7.

Moran, P. J. 1986. The *Acanthaster* phenomenon. *Oceanography and Marine Biology Annual Review*, **24**, 379–480.

Neuman, A. C. and MacIntyre, A. G. 1985. Reef response to se level rise: keep up, catch up or give up. *Proceedings of the 5th International Coral Reef Congress, Tahiti*, **3**, 105–110.

Paulay, G. 1997. Diversity and distribution of reef organisms. In Birkeland, C. (ed.), *Life and Death of Coral Reefs*. Chapman and Hall, New York, pp. 298–353.

Perry, C. T. 2001. Storm-induced coral rubble deposition: Pleistocene records of natural reef disturbance and community response. *Coral Reefs*, **20**, 171–183.

Richmond, B. M. and Morton, R. A. 2007. Coral-gravel storm ridges: examples from the tropical Pacific and Caribbean. *Proceedings Coastal Sediments '07*, ASCE, pp. 572–583.

Risk, M. J., 1999. Paradise lost: how marine science failed the world's coral reefs. *Marine and Freshwater Research*, **50**, 831–837.

Scoffin, T. P. 1993. The geological effects of hurricanes on coral reefs and the interpretation of storm deposits. *Coral Reefs*, **12**, 203–221.

Schellmann, G. and Radtke, U. 2004. A revised morpho- and chronostratigraphy of the Late and Middle Pleistocene coral reef terraces on Southern Barbados (West Indies). *Earth-Science Reviews*, **64**, 157–187.

Solomon, S. M. and Forbes, D. L. 1999. Coastal hazards and associated management issues on South Pacific Islands. *Ocean and Coastal Management*, **42**, 523–554.

Souter, D. W. and Linden, O. 2000. The health and future of coral reef systems. *Ocean and Coastal Management*, **43**, 657–688.

Spiske, M., Böröcz, Z., and Bahlburg, H. 2008. The role of porosity in discriminating between tsunami and hurricane emplacement of boulders – A case study from the Lesser Antilles, southern Caribbean. *Earth and Planetary Science Letters*, **268**, 384–396.

Storlazzi, C. D. and Jaffe, B. E. 2008. The relative contribution of processes driving variability in flow, shear, and turbidity over a fringing coral reef: West Maui, Hawaii. *Estuarine, Coastal and Shelf Science*, **77**, 549–564.

van Woesik, R., 1994. Contemporary disturbances to coral communities of the Great Barrier Reef. *Journal of Coastal Research*, SI **12**, Coastal Hazards, 233–252.

Woodley, J. D., Chornesky, E. A., Clifford, P. A. *et al.* 1981. Hurricane Allen's impact on Jamaican coral reefs. *Science*, **214**, 749–755.

Woodroffe, C. D., Mclean, R. F., Smithers, S. G. and Lawson, E. M. 1999. Atoll reef-island formation and response to sea-level change: West Island, Cocos (Keeling) Islands. *Marine Geology*, **160**, 85–104.

Woodroffe, C. D. 2008. Reef-island topography and the vulnerability of atolls to sea level rise. *Global and Planetary Change*, **62**, 77–96.

Yamano, H., Kayanne, H., Yamaguchi, T., Kuwahara, Y., Yokoki, H., Shimazaki, H., and Chikamori, M. 2007. Atoll island vulnerability to flooding and inundation revealed by historical reconstruction: Fongafale islet, Funafuti Atoll, Tuvalu. *Global and Planetary Change*, **57**, 407–416.

13

Cliffed and rocky coasts

13.1 Synopsis

The focus of this chapter is on coasts where the shoreline is largely developed in rocks, or in sediments that possess some strength due to cohesion and thus are able to offer resistance to wave action. Beach material is generally scarce and is found primarily as a thin layer fronting the cliff toe, or in isolated pocket beaches. The term cliff is used where the slope angle >40° and thus cliffed shorelines are those characterised by steep slopes rising abruptly from the water or from the back of a platform that is narrow enough for the toe of the slope to be affected by wave action during storms. Cliffed shorelines develop in sedimentary rocks ranging from recent deposits with some cohesion due to the presence of clays or to overconsolidation due to glacial loading, through weakly cemented shale and sandstone. The most resistant cliffs are found in rocks such as limestone, where chemical bonding is important, and in massive igneous and metamorphic rocks such as basalt or granite that possess strength due to crystallisation from melt and high pressures. Unlike sandy coasts where erosion may be reversed by deposition and progradation, erosion of bedrock coasts destroys the bonding that provided strength and thus there is no reversal of the erosion process – cliffs remain stationary or they recede.

On hard, strong bedrock coasts rock strength greatly exceeds the erosional forces of individual waves and erosion takes place very slowly – perhaps millimetres to a few centimetres per century. Since sea level has been at the present level in most parts of the world for <5000 years, cliffs in these materials reflect the operation of both coastal and subaerial processes operating over 10^3–10^5 years and often the shoreline merely reflects the position of the sea against a pre-existing topography. The spectacular cliffs of fjords associated with glaciated highlands are a good example of this. Coastal processes act to modify the shoreline but most of the coastal morphology is inherited.

On soft coasts, such as those developed in glacial till and shale, wave action is able to erode the toe of the cliff relatively rapidly and to remove the eroded debris. Recession of the cliffs can be on the order of decimetres to metres per year and thus the cliff form is controlled by modern coastal processes and is not an inherited feature. Because of their relatively high rates of recession, these coasts offer an opportunity to study the controls on cliff erosion and profile evolution, and to extrapolate the results of these studies to hard rock coasts. Studies of soft rock coasts are also timely because the high recession rates may result in threats to houses and infrastructure located on the cliff top and lead to calls for intervention in the form of shore protection.

13.2 Cliffed coast morphology

13.2.1 Cliff form and occurrence

While cliffed coasts are occasionally formed in cohesionless sands where plant roots and soil moisture provide some strength, most cliffed

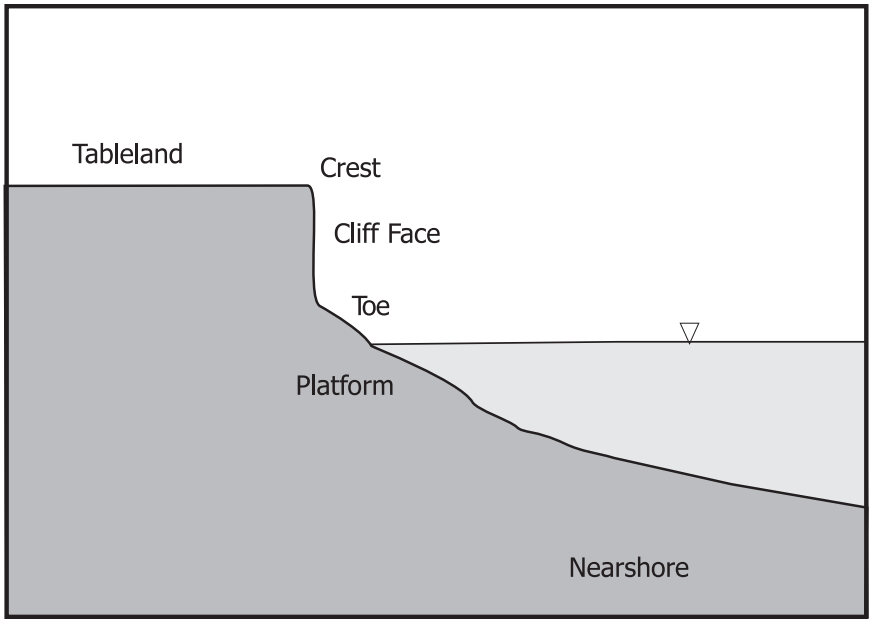

Figure 13.1 Major components of the coastal cliff system.

shorelines develop in material that possesses strength due to cohesion provided by the bonding of clay minerals, cementation by chemical precipitates or the crystal bonding of igneous and metamorphic rocks. The term cliff is used here for all shorelines with a steep subaerial slope – strictly speaking some portion of the slope should exceed 40°. The height of the cliff should exceed the maximum height of wave run-up and overtopping (though wave spray may reach the top of the cliff). If the cliff is so low that wave overtopping can occur then the shoreline feature is termed a bank. The term bluff can be used interchangeably with cliff, but here its use is restricted to describing cliffs formed in unconsolidated or weakly consolidated sediments, including sand, silt, clay and till. These cliffed coasts are termed cohesive coasts to distinguish them from coasts formed in much stronger bedrock where coastal processes modify the shoreline relatively slowly. While the terminology is a bit ambiguous because muddy coasts (e.g., estuarine mudflats) are also cohesive and because cohesion can equally apply to crystalline rocks, practically it is useful to make the distinction between them.

The presence of a cliffed shoreline reflects the existence of relatively high ground near the coast and this in turn may reflect tectonic forces on a continental scale, local folding and faulting, fluvial or glacial erosion, water level change, or simply recession due to coastal erosion on a gently sloping plain. Thus, the height of the coastal cliff is controlled primarily by the relief of the coastal zone and secondarily due to the operation of coastal processes.

In examining the processes and components that make up the coastal cliff recession system it is useful first of all to describe the morphological components of the system in a profile normal to the shoreline (Figure 13.1) Not all features will be present on all cliffed coasts. The major components are:

(a) The tableland or area inland from the cliff top.
(b) The cliff top that marks the change in slope from the tableland to the cliff face and is the transition zone to the area that slopes down to the water.
(c) The subaerial cliff face that extends from the cliff top to the toe of the slope where it

intersects the beach or platform. This area is dominated by erosion due to processes resulting from mass wasting as well as overland flow and gullying. In the case of plunging cliffs the face extends below the water level.

(d) The cliff toe that is the transition area between the subaerial cliff and the beach and shore platform. The upper limit of the cliff toe is marked by height to which wave action (not including spray) can reach and the lower limit by the junction with the more gently sloping shore platform. It also marks the transition from the cliff face which is dominated by subaerial erosional processes leading to horizontal recession, and the shore platform and nearshore profile which are dominated by processes resulting in vertical lowering.

(e) The shore platform that extends from the base of the cliff offshore to a point at, or just below spring low tide. The shore platform may be overlain by varying amounts of surficial sediments. The platform itself is subject to wave action as well as weathering processes during subaerial exposure.

(f) The nearshore slope that forms the subaqueous extension of the intertidal platform, and is a zone of shoaling and breaking waves extending offshore to the limit of wave erosion and transport of sediment.

13.2.2 Cliff coast classification

Two major types of cliffed coast can be recognised on the basis of the profile form normal to the shore and sea level (Figure 13.2). Plunging cliffs occur where the cliff extends below the water line to some considerable depth (Figures 13.2a, 13.3a, b). Waves break directly against the cliff face, and there is no beach, ramp or platform that would lead to wave breaking offshore and to the accumulation of sediments. Plunging cliffs usually occur in resistant bedrock where the slope and relief are determined by tectonic events (e.g., folding or block faulting) or where erosion by glaciers or rivers, and subsequent drowning due to sea level rise, has produced a steep cliff with deep water at the cliff base. Over time, jointing and vertical weaknesses may be exploited by wave action to produce chimneys and small pocket beaches, and irregularities in the cliff face may be enhanced by runoff and gully development. However, erosional processes are generally very slow on these coasts so these features form slowly. Plunging cliffs are not generally found on cohesive coasts because the cliff material is too weak to withstand direct wave attack for very long and cliff recession soon leads to the formation of a sloping platform and beach.

Where the overall slope of the inherited coastal morphology is less steep the toe of the cliff face will be located in or above the intertidal zone. Erosion of the cliff toe will occur, leading to recession and the generation of a platform as the cliff face recedes. Weaknesses such as jointing, bedding planes and beds of varying lithology and strength in the rock making up the lower part of the cliff will lead to spatially uneven rates of erosion and the development of a variety of erosional forms such as notches, blowholes, caves, arches and stacks (Figures 13.3c, d). The coastline tends to become highly irregular and the inner nearshore is often rocky with a variety of shallow reefs and emergent boulders (Figures 13.3c, d). These features are absent on cohesive coasts where rapid erosion on the beach and shallow nearshore quickly removes any irregularities.

Horizontal erosion is focused at the toe of the cliff, and recession of the cliff itself will tend to produce a quasi-horizontal erosion surface or platform. However, erosional processes in the intertidal and sub-tidal zones also act on the platform leading to vertical lowering of the surface. This in turn generates a profile with an intertidal zone that slopes away from the base of the cliff and grades into the underwater nearshore profile without any abrupt transition (Figure 13.2b). Type A platforms (Sunamura, 1992) are the most common form of platform on cliffed shorelines, particularly in rocks of moderate to low strength and in areas where sand and gravel are present in the intertidal zone. However, in some areas vertical erosion of the platform in the intertidal and shallow sub-tidal zone is relatively slow compared to horizontal recession of the cliff toe. This leads to the development of a Type B shore platform that has a nearly horizontal surface away from the

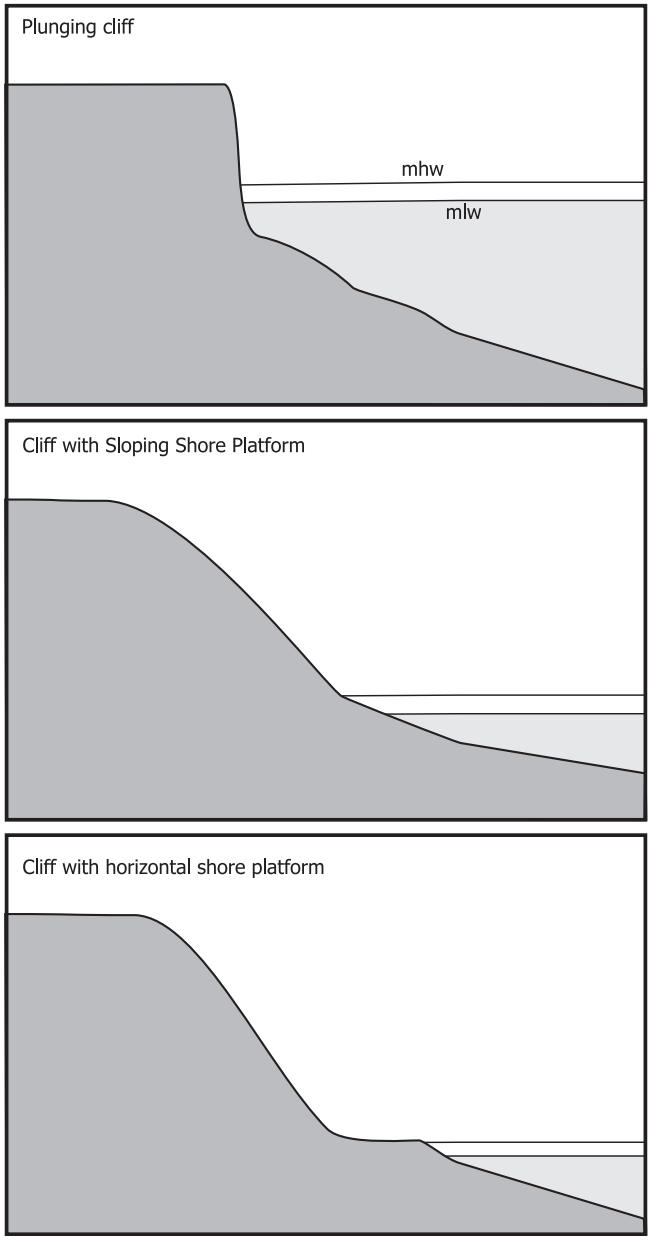

Figure 13.2 Profiles associated with the major types of cliffed coast.

base of the cliff, and then terminate abruptly in a seaward drop to the nearshore (Figures 13.2c and 13.3e). The elevation of the platform may be close to the high-tide level, the low-tide level, or somewhere in between. Type A platforms reflect conditions where vertical lowering of the platform in the intertidal area is similar to that in the inner nearshore and keeps pace with horizontal retreat of the cliff toe. The development of the nearly horizontal platform associated with type B must therefore reflect much slower vertical lowering of the intertidal platform compared to the recession of the cliff toe. The quasi-horizontal Type B platforms have generated much interest and there is considerable debate about the processes operating on them and the controls on their origin. We will examine this problem at the end of the chapter after we look at cliffed coast processes

generally, and at processes operating on cohesive and rock coasts.

13.3 Cliffed coast erosion system

Unlike coasts dominated by sedimentary deposits, where the beach and nearshore can be altered continuously but maintain a long-term equilibrium form and location, the dominant focus in cliffed coasts is on erosional processes. Thus, while on a sedimentary coast erosion can be balanced by subsequent accretion, on a cliffed coast erosion results in the breakdown of the constituent material forming the cliff and it is a process that cannot be reversed. Attention is

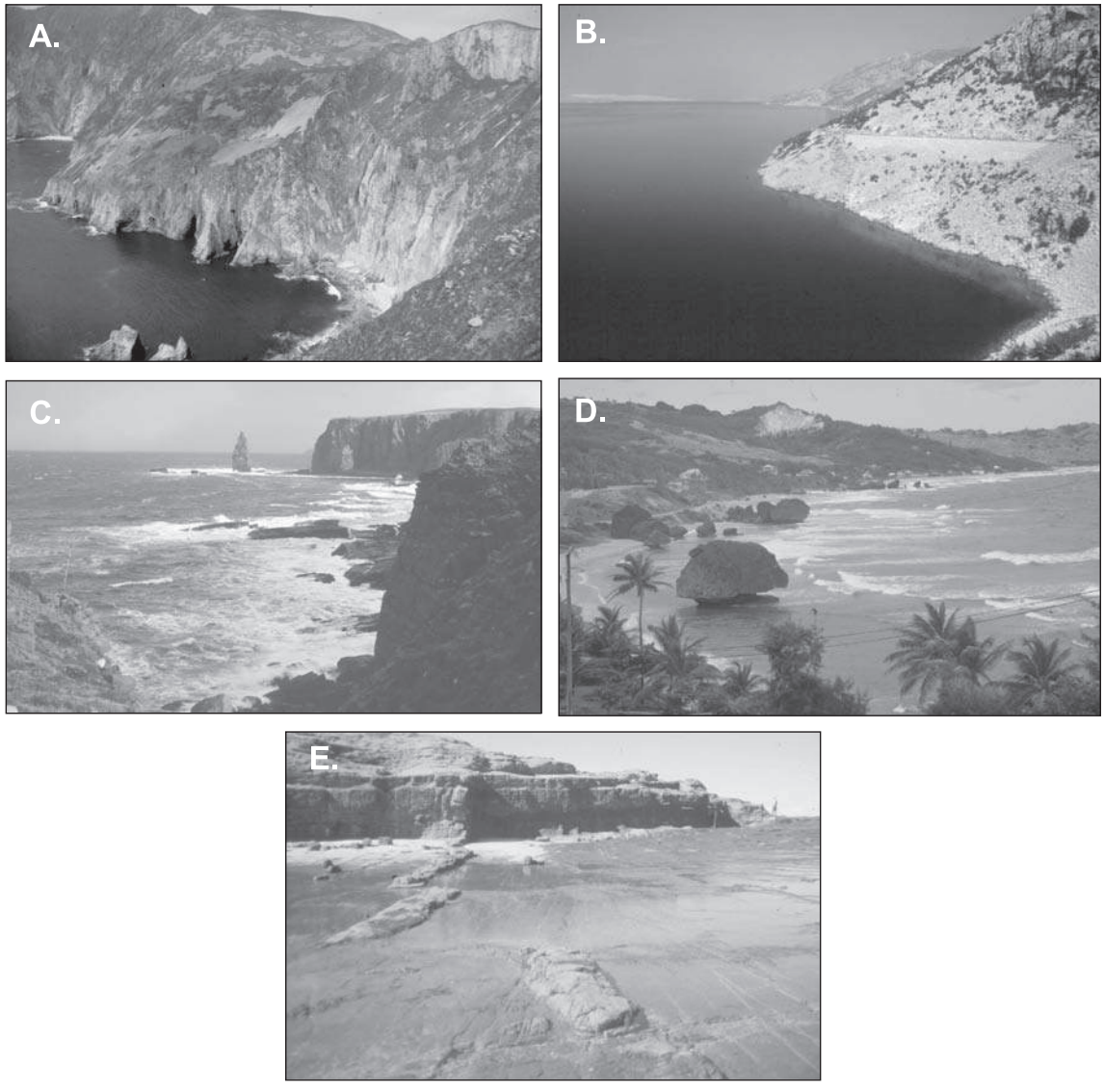

Figure 13.3 Photographs of cliffed and rocky coasts: (A) plunging cliffs West coast of Ireland; (B) plunging cliffs Yugoslavia; (C) cliffed coast NW Scotland with Type A platform, stacks, caves; (D) cliffed coast with Type A platform in uplifted coral limestone and old hat rocks, east coast Barbados; (E) cliffed coast with Type B shore platform near Wollongong, Australia.

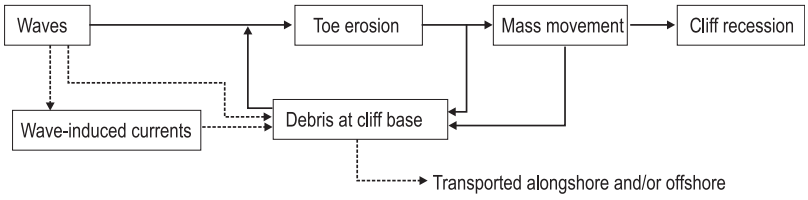

Figure 13.4 Coastal cliff recession system (Sunamura, 1983; 1992).

focused, therefore, primarily on rates of recession (retreat) and the processes leading to this. As is the case for clastic shorelines, it is useful to distinguish clearly between recession and erosion. Recession is used here as a measure of the horizontal retreat of a reference point on the cliff face – for example, the cliff toe or the cliff top. It can be expressed in absolute terms over a defined time period, or as a rate such as m a^{-1}. Erosion, strictly speaking, refers to the mass of rock material brought to the toe of the slope by subaerial processes or removed from the toe by processes such as waves and currents. Ideally it should be expressed as a mass or mass per unit length alongshore (e.g., Kg m^{-1}), though for some purposes it is useful to measure it as a volume. Vertical lowering of the platform and nearshore through erosion is a linear term equivalent to horizontal recession and likewise is expressed in absolute terms, or as a rate.

13.3.1 Coastal cliff recession system

Sunamura (1983; 1992) summarises the major controls on recession of coastal cliffs (Figure 13.4). The primary processes result from the action of waves reaching the bluff toe which lead directly to erosion and recession of the toe. Toe erosion in turn increases the slope angle of the cliff and is an important control on the relative importance and significance of a suite of subaerial processes acting on the cliff slope. These include mass wasting processes (creep, falls, slumps, slides and flows) as well as those resulting from unchannelled and channelled water on the slopes (splash, overland flow, rills and gullies). Material eroded from the cliff face by these processes will be transported by gravity down slope and accumulate temporarily at the cliff toe. The material brought to the cliff toe provides protection to the base of the cliff from wave action and if sufficient debris accumulates then toe erosion may cease altogether. Continued recession requires that the debris is removed offshore and/or alongshore by waves and wave-generated currents – hence the feedback loop shown in Figure 13.4. Where this removal does not occur, or where sediment is brought in from updrift, the toe eventually becomes protected and recession of the bluff by subaerial processes will continue only until a stable angle has been achieved. This explains why, for example, cliffs are so prominent at headlands, because net sediment transport will almost always be into the bay. This simple schematic model is true for all cliff systems, including those on land where toe erosion and debris removal may be triggered by impingement of a river channel or simply the result of overland flow in semiarid areas.

Coastal cliffs and bluffs exhibit the full range of mass wasting and slope removal processes from the movement of individual particles, to shallow slumps and slides, to spectacular deep-seated failures. The relative importance of a particular process will depend on the nature of the material making up the cliff (lithology, stratigraphy, jointing), climatic factors such as precipitation and temperature, vegetation and groundwater hydrology, and of course the slope angle. The form of the coastal cliffs is directly related to the interplay between these subaerial processes and the stratigraphy and strength of the rock material or sediments making up the cliff, as well as to local geomorphological or tectonic forces. The rich variety of coastal cliff scenery is a reflection of this complexity (Figure 13.3). Where human infrastructure (roads, buildings) encroach on the cliff top the form of mass wasting and cliff failure becomes of vital interest for determining appropriate planning setbacks based on the factor of safety and for engineering stabilisation solutions (see Section 13.7).

However, it can be argued that toe erosion and removal of sediment at the cliff toe are the primary controls on the rate of coastal cliff recession and that, while the subaerial processes of mass movement and water acting on the cliff face are interesting, they are irrelevant in determining the long-term (decadal to century) recession rate. In effect, the balance between erosion due to subaerial processes on the cliff face and erosion at the cliff toe acts primarily to influence the short-term pattern of recession of the cliff top and the slope angle of the cliff. If the rate of toe erosion is faster than the slope processes, undercutting will occur, leading to an increase in the slope angle and, therefore, to an increase in the rate of operation of the slope processes. Ultimately, this may result in the creation of a notch or overhang and the complete undercutting of the slope support, leading to massive slope failure. If the rate of erosion on the cliff face is faster than the rate of toe erosion, then the slope angle will decrease, leading to a reduction in the rate at which the subaerial cliff processes operate and bringing them into balance with the rate of toe erosion. Thus, while coastal cliffs provide fruitful sites for the study of slope processes, such processes can largely be ignored in developing a deterministic process-response model for predicting long-term rates of coastal cliff retreat.

13.3.2 Wave-induced cliff erosion model

The schematic cliff system model shown in Figure 13.4 can be expanded to incorporate a more detailed examination of the interrelationship among the processes and factors controlling erosion of the cliff toe (Sunamura 1983, 1992 – see Figure 13.5). The approach here is a mechanical, deterministic one with toe erosion being controlled by the relative magnitude of two groups of factors: (1) those determining the erosional forces produced by waves reaching the toe of the cliff – the assailing force; and (2) those controlling the strength of the material forming the lower cliff – the resisting force. Conceptually this is nice and relatively simple; and it does point to the need to quantify the processes of erosion in terms of forces. Note that in this model there is no consideration of subaerial processes on the cliff face and that there is the explicit assumption that material is removed alongshore and therefore does not provide any substantial protective role.

The schematic model outlined by Sunamura (Figure 13.5) is divided into two components: the wave system and the cliff system. Offshore wave energy (determined by the wave climate) is transformed through shoaling, refraction and breaking over the nearshore profile towards the beach/platform (if present) and cliff toe. The characteristics of the waves at the cliff toe then depend on the nearshore and intertidal morphology, mean sea level and short-term fluctuations due to tides and storm surge, and the effects of these operating together on wave shoaling and breaking transformation.

Wave action at the toe produces both hydraulic and mechanical forces, which make up the assailing force of waves F_W. Hydraulic forces include those resulting from compression due to the collision of the wave with the face of the cliff, tension as the water recedes from the cliff, and shearing from water moving upward or downward over the cliff face. The compressive force is greatest when the wave breaks directly against the cliff face with the plunging jet producing a nearly horizontal force into the cliff. This direct impact is termed water hammer and the shock of large waves breaking against a rock cliff can produce low-frequency oscillations throughout the cliff (Adams *et al.*, 2005). Much of the time a small layer of air is trapped between the breaking wave and the cliff face and the rapid compression of this develops high pressures within joints and cracks in the rock. Repeated impacts from waves and the forcing of water or air into spaces in the rocks results in the expansion of cracks, dislodgement of rock material and can produce blowholes that spurt a mixture of air and water high up onto the cliff. The recession of water in the wave trough and the downward drainage of water generate tension on the face. As material is loosened by repeated wave impacts it may be pulled or pushed off the face in a series of processes termed plucking or quarrying. Most of the dislodged rock material ends up at the base of the cliff, but some can be transported right onto the

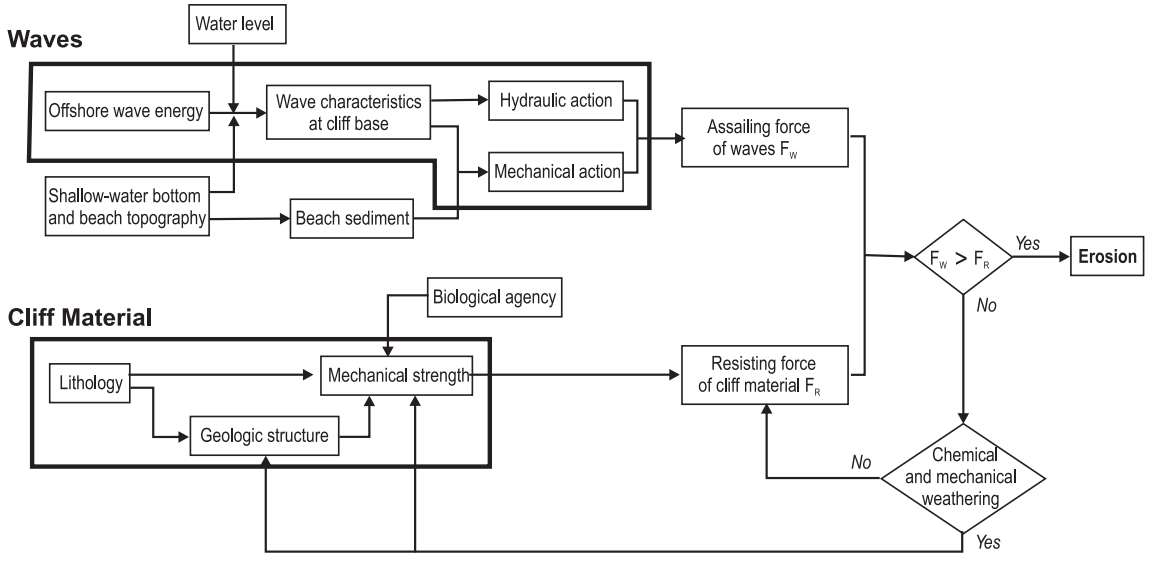

Figure 13.5 Wave-induced cliff erosion system (Sunamura, 1983).

cliff top by the vertical component of wave breaking to produce cliff-top storm deposits (Hall *et al.*, 2006).

Where the mean water level is quite high up the cliff face hydrostatic pressures are exerted on the cliff and there are fluctuations in these as a result of wave action, and especially the development of standing waves (clapotis). The hydrostatic pressures are greatest near the foot of the cliff while pressures generated by wave breaking tend to be focused at, or just above the mean water level. Wave impact forces against vertical or sloping structures as well as hydrostatic forces can be measured in laboratory studies and modelled semi-theoretically. However, it is much more difficult to apply this to real cliffs where wave breaking is often chaotic, the cliff face is irregular and the angle of wave approach often varies significantly from cliff perpendicular. Shearing forces are produced by two different mechanisms. Waves may break on the beach or platform and swash run-up reaching the toe of the cliff can run up for some distance, producing a shearing force right at the toe. Alternatively, where the mean water level is above the cliff toe a portion of the wave breaking on the cliff is usually directed upwards, producing shearing and tensional forces up the cliff face.

In addition to the hydraulic forces generated by the waves, mechanical forces are generated by entrained sand, gravel and rock particles. The impact of rocks and boulders hurled or rolled against the cliff face can be impressive at a point. However, abrasion by sand and gravel is probably more significant because it operates over a greater area and for a greater proportion of time. Abrasion and rock impact are most important at mean water levels ranging from just below the toe, when swash bores frequently reach the toe, to just above the toe where turbulence from wave breaking and orbital velocities at the bed can entrain material. As the water depth at the toe gets large there is less mobilisation of sediment and hydraulic forces become dominant. Thus, wave-induced forces will vary with the form of the platform and nearshore, as well as with the depth of water at the cliff toe and the availability of clastic material for impact and abrasion. They will also vary temporally as incident wave conditions and water levels change.

The significance of each of the hydraulic and mechanical forces associated with wave action can be related to four scenarios that reflect increasing water depth at the cliff toe (Figure 13.6):

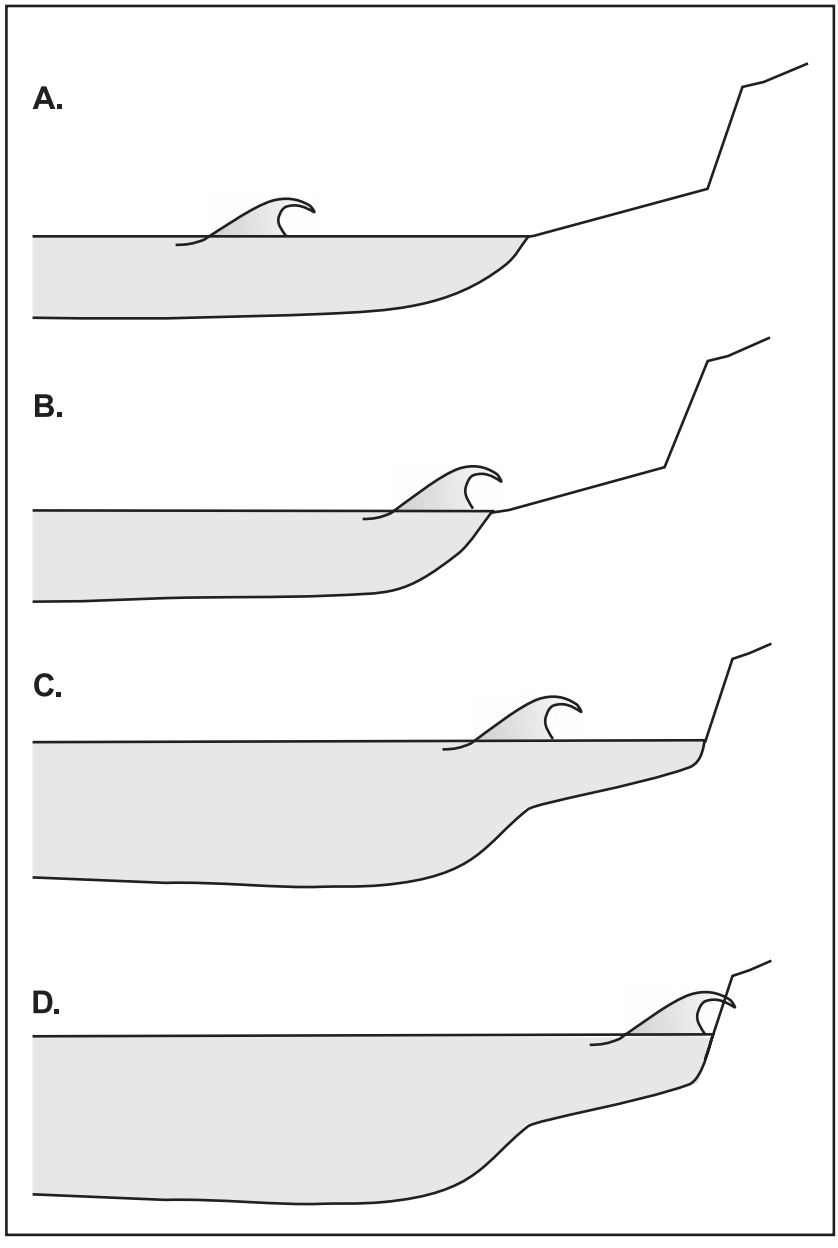

Figure 13.6 Effects of changes in mean water level relative to the elevation of the cliff toe on the relative significance of hydraulic and abrasional forces leading to toe erosion: (A) mean water level far below cliff/platform junction – waves do not reach cliff toe; (B) mean water level below cliff/platform junction – swash run-up reaches the cliff toe; (C) mean water level just above cliff/platform junction – broken waves reach cliff toe; (D) mean water level considerably above cliff/platform junction – waves break against the cliff face.

(1) In the first scenario the mean water level is well below the bluff toe. Waves shoal and break across the nearshore and beach or platform dissipating their energy in these zones and no waves reach the cliff toe. Erosion by waves is focused on the platform and nearshore, and subaerial processes continue on the cliff.

(2) Where water level is below the cliff toe, but wave run-up can reach the toe as swash

bores, the dominant erosional processes result from turbulence in the bore, shearing as the wave runs up on the toe, and abrasion from sediments entrained by the swash bore.

(3) Where the water level is above the toe of the cliff, but water depth is relatively shallow, wave compressional forces are produced from wave impacts. Most waves will begin breaking seaward of the cliff face, so impact forces are moderate. Hydrostatic forces are also significant, but still relatively small because of the shallow water depths. Abrasion remains significant where there is sand and gravel present on the platform.

(4) When the water at the cliff toe is quite deep, wave breaking frequently takes place right at the cliff face producing maximum water hammer and compressive forces. Hydrostatic forces also become more significant because of the greater water depth, while abrasion is greatly reduced because of the reduction in turbulence and oscillatory motion near the base.

The strength of the cliff system is designated the resisting force F_R (Figure 13.5). This is determined by intrinsic properties such as lithology, which determine the hardness of the rock material, and by the structure of the rock, including bed thickness and dip angle, joints and fractures and the relative strength and position of interbedded units – see Box 13.1. Qualitatively it is easily understood that relatively hard rocks such as granite, basalt and limestone are much more resistant to wave erosion than soft shale or cohesive till. Similarly, massive sandstone and chalk are likely to be much more resistant than thinly bedded sandstones because there are few weaknesses that can be exploited by water hammer, and compression of air by waves breaking against the cliff face. However, where resistant rock units are interbedded with weaker units such as shale, failure usually results from exploitation of the weaker beds, so the stratigraphic position of beds relative to mean sea level is important (Figure 13.7).

In the short term, seconds to days, if $F_R > F_W$ then no erosion will occur. However, over a longer period it is likely that the value of F_R at points on the cliff toe will decrease as a result of weathering thus producing the feedback loop in Figure 13.5. In this model, the term weathering is used here to include chemical weathering which may reduce cementation of sandstones of the breakdown of rock crystals through hydrolysis, oxidation, etc., mechanical weathering due to wetting and drying, freezing and thawing, growth of salts and the effects of a variety of biological agents, including plants and boring organisms. In the broader sense it also includes various forms of mechanical weakening due to loading and unloading or fatigue failure. This may result from repetitive flexing due to impact pressure fluctuations, the effects of air compression in joints, and hydrostatic pressure fluctuations produced by fluctuating water depths.

Erosion of the cliff occurs if $F_W > F_R$. This should not be envisioned as a threshold that applies to the cliff as a whole but rather it may be better to think of it as applying to a point on the cliff toe. There will be an infinite number of points on the cliff toe each with its own F_R value which together produce a characteristic probability distribution. In turn, because we are dealing with random seas, complex nearshore topography and varying breaker characteristics, there will be a range of instantaneous F_W values also characterised by a probability distribution. Over time F_W may vary systematically with tidal stage and less predictably with changing incident wave conditions. At an instant in time, wherever $F_W > F_R$, erosion will occur. If the mean value of F_W is small and the mean value of F_R is large, there may be long periods of time where there is no overlap between the two probability distributions or only a small area (Figure 13.8).

The increase in the probability of erosion is likely to be a function of increasing F_W, e.g., because of increasing storm intensity and/or tidal height. Thus the upper end of the F_W distribution represents conditions that exist for some time in an intense storm, perhaps coinciding with spring high tides, but then do not recur for several months or years. The lower end of the F_R distribution reflects the effects of weathering and fatigue failure on rock strength and it may be truncated after a severe storm when much of the weathered material is removed. The strength of hard rock

Box 13.1 Measurement of rock strength

Intuitively from Figure 13.5 it is evident that the rate of erosion of the cliff toe (and by extension, of the beach and nearshore platform) should be controlled by the resistance of the material making up the lower cliff – i.e., some measure of its strength in relation to an applied force or stress. More importantly, if we are to be able to develop some kind of numerical model for predicting toe erosion and cliff recession it is important to be able to quantify this strength. Since we have a variety of techniques for measuring the strength of rock and cohesive materials and quite an extensive set of theory and empirical data related to soil and rock mechanics, it would seem relatively simple to produce good estimates of the strength of materials making up a cliff. However, the task is complicated by two sets of factors: (1) strength of material must be measured as a response to an applied force; however erosion processes at on the cliff coast profile, and particularly at the cliff toe produce several types of applied force (e.g., compressive forces, tensional forces, shear forces, and forces due to impact and abrasion). Thus, ideally we should measure the strength in response to all of these. The task is further complicated by the effects of structural weaknesses from bedding planes and jointing, which are difficult to quantify but which may be extremely important where wave breaking produces cavitation and compression of entrapped air; (2) the intrinsic strength of the material may change over time as a result of a variety of weathering processes, which means that any model must account for these effects.

The mechanical strength of materials can be evaluated using a variety of tests used in soil and rock mechanics and described in standard engineering soil mechanics and rock mechanics texts and in documents from the American Society for Testing and Materials (ASTM) and ASTM International. For cohesive materials compressive strength may be measured using an unconfined compression test. Shear strength and compressive strength may be measured in a triaxial compression test with the results plotted as a family of Mohr circles. Shear strength may also be measured using a shear box or directly in the field using a shear vane. The unconfined compressive strength of rocks can also be estimated using a Schmidt Hammer (Aydin and Basu, 2005). When examining erosion of the platform and nearshore profile, resistance to abrasion may be more important. Ultimately many of the strength properties may be correlated with compressive strength (Sunamura, 1992; Budetta *et al*., 2000) and thus much of the work to date has attempted to relate erosion rates to some measure of this.

coasts made up of massive igneous or metamorphic rocks is much greater than wave impact forces, even from very large waves and there is almost no overlap between the two probability distributions – erosion here proceeds very slowly. Such rocks are usually also very resistant to weathering and so cliff retreat over many centuries may be a couple of metres or less. In softer rocks, especially those where thin bedding or jointing provides weak points to be exploited by wave pressure forces, the overlap of the two distributions will be greater and recession may be measured in cm or even metres per year.

There are numerous published cliff recession rates from individual sites and studies and some attempts to compile these systematically for regions or the world (Sunamura, 1983; Hampton and Griggs, 2004). However, direct measurement through surveying is often difficult, especially where it is desirable to collect the data over some alongshore length rather than at a few profiles. A relatively simple measurement of bluff

Figure 13.7 Erosion of shale at the cliff toe leading to undercutting and failure of blocks of relatively resistant sandy dolomite, Cape Dundas, Georgian Bay, Ontario. The shale is one of the lower units in the Niagara Escarpment. Note the rectangular jointing pattern in the overlying rocks which controls the size of the failure blocks.

crest recession over a small area can be carried out by setting up stakes on the bluff top and measuring the distance to the edge on a monthly, seasonal or annual basis (Bernatchez and Dubois, 2008). However, over the short term this is driven primarily by subaerial weathering and mass wasting processes and there is a disconnect from the processes controlling toe erosion. The compilation of a data set involves carrying out measurements over a number of years and there are few programs anywhere in the world that do this systematically over periods of decades. Most measurements of long-term recession rates have made use of rectified aerial photographs and measured change over the interval between photographs (Buckler and Winters, 1983). Recent advances in digital photogrammetry and the use of DGPS to collect ground control points have made the task easier (Lantuit and Pollard, 2008) and likely improved accuracy. Recession of top of bluff is generally the easiest to measure on aerial photographs, but it is subject to much greater temporal variability than is the toe of bluff. However, the bluff toe, which provides a better estimate of bluff recession rates related to wave energy, may be difficult to discern because of overhanging vegetation, slumps and shadow. This is especially true for high bluffs. Errors associated with mapping the bluff toe from aerial photographs are also greater because it is generally difficult to make use of ground control points below the bluff top. The advent of airborne and now land based LiDAR has made it more easy to collect areal data (Gulaeyev and Buckeridge, 2004; Young and Ashford, 2006).

In order to operationalise and test the predictive capability of the schematic model illustrated in Figure 13.5, we would need to have data for F_W, F_R, and recession rates from a variety of sites. Clearly, the difficulties noted above in measuring all three of these parameters make this task a daunting one and there is as yet no practical model available to test. Nevertheless, empirical studies do provide insights into the operation of some of the parameters discussed above. Thus, they allow us to get a sense of how the parameters control the type of equilibrium form, and the long-term recession rate that might be predicted to develop at a particular location. Before we examine this, it is useful to consider the time

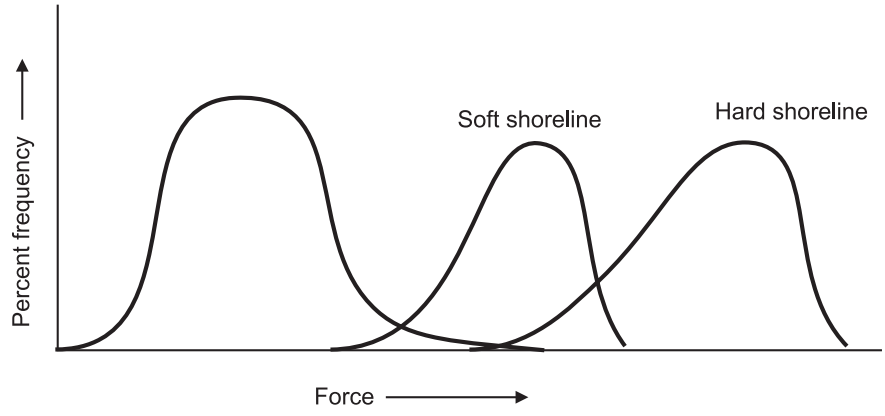

Figure 13.8 Schematic depiction of hypothetical average probability distribution functions for F_W and F_R. Erosion occurs only for the area of overlap between the two distributions and the greater the extent of overlap the more frequent is erosion.

scale over which modern coastal cliffs have evolved in relation to cliff recession rates.

Because of the eustatic sea level rise in the Holocene, most coastal cliffs and the nearshore profiles in front of them have been evolving with respect to a (relatively) stable sea level for only 3000–5000 years. As a first step, coastal cliffs can be divided into three groups on the basis of the cliff recession rate: (1) weak cliffs with recession rate $R > 0.05\,\text{m a}^{-1}$; (2) moderately resistant cliffs with $R = 0.005 < R > 0.05\,\text{m a}^{-1}$; and (3) strong cliffs with $R < 0.005\,\text{m a}^{-1}$. Recession of weak cliffs will be more than 300 m over the time period available, and thus the form of the cliff, shore platform and nearshore is likely to reflect modern sea level and wave conditions. Recession of moderately resistant cliffs will be on the order of 30–40 m in the time available and thus they may be evolving toward some form of equilibrium with modern conditions but have not yet achieved this. Finally, strong cliffs will show little measurable recession since sea levels stabilised, and thus the form is an inherited one. All that can be said about these coasts is that $F_R >> F_W$.

As was noted earlier, while it is evident from Figures 13.4 and 13.5 that the immediate control on cliff recession is erosion at the toe, consideration of the long-term evolution of cliffed profiles where there is a platform present suggests that the ultimate control on the cliff recession is the rate of lowering of the platform and nearshore profile. This is shown in the process-response model for cohesive shores (Davidson-Arnott, 1990) which is modified from the original system of Sunamura (Figure 13.9). This model introduces the effects of wave action and water level fluctuation on vertical erosion of the nearshore profile, in addition to consideration of wave-induced forces at the bluff toe. Of particular importance are the feedback relationships shown by dashed lines. If the rate of horizontal retreat of the bluff toe exceeds the vertical lowering of the nearshore, this leads to an extension of the platform profile and a reduction in the amount of wave energy reaching the bluff toe. This may be aided by the protective effect of sediment supplied from the upper bluff. Conversely, if bluff recession lags behind vertical lowering of the profile, then the nearshore profile deepens, permitting more wave energy to reach the bluff toe rather than being dissipated by bottom friction and wave breaking. It should be noted also that water level changes act in the opposite direction in the nearshore system compared to that at the bluff toe. Thus, a rise in water level tends to increase wave forces at the bluff toe and the platform immediately adjacent to the bluff. Conversely, a fall in water level tends to increase the wave forces on the lower platform and on the nearshore profile. In the Great Lakes, to which the model was initially applied, water level fluctuations are driven by seasonal

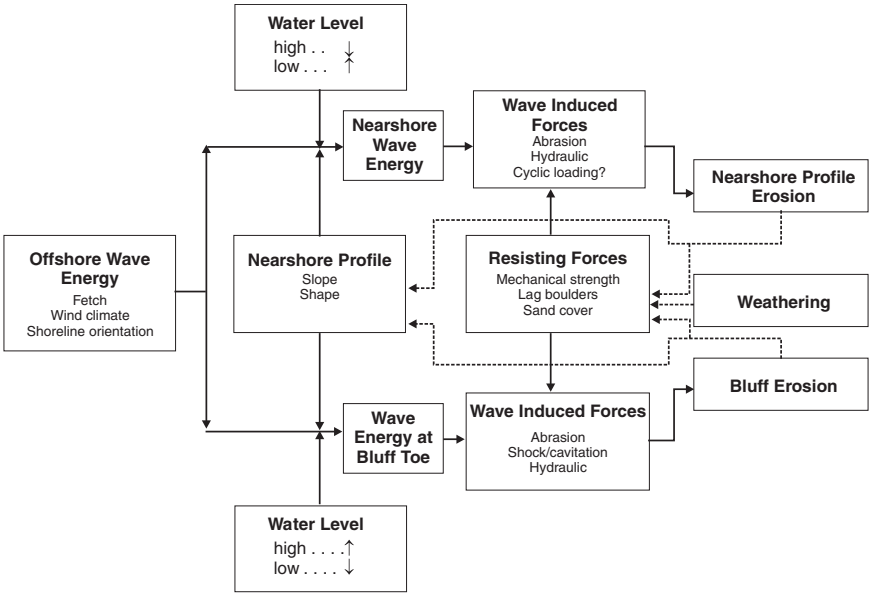

Figure 13.9 Cohesive shoreline process response model. Note the explicit inclusion of erosion of the nearshore profile as well as the inverse effects of water level fluctuations on nearshore erosion and toe erosion (Davidson-Arnott, 1990).

and multi-year variations in precipitation in the basins, as well as short-term fluctuations due to storm surge and seiching. On oceanic coasts daily and fortnightly tidal fluctuations act in a similar fashion in addition to the meteorological and wave-induced changes.

The focus of this section has been largely on establishing a conceptual basis for measurement and modelling of coastal cliff erosion and retreat. We can now turn to examining the results of field and laboratory studies of cliffed coast morphodynamics. The next section details the results of studies conducted on weak or soft coasts – coasts where the recession rate is typically tens of centimetres per year. The reasons for choosing to examine this before resistant rock coasts is that the high rate of recession makes it much easier to measure recession rates over short time periods, and because the cliff coast profile is much more likely to be in equilibrium with contemporary water levels and coastal processes. Following this we can see how an understanding of processes on these rapidly eroding soft coasts can be applied to studies of resistant rock coasts and the debate over shore platforms.

13.4 Cohesive bluff coasts

13.4.1 Cohesive coast characteristics

The term cohesive shoreline is used to describe cliffed coastlines in which the profile is developed in relatively non-resistant sediments with a high silt and clay content (Hutchinson, 1973, 1986; Prior, 1977; Quigley *et al.*, 1977; McGreal, 1979; Edil and Vallejo, 1980; Bryan and Price, 1980; Carter and Guy, 1988; Hequette and Barnes, 1990; Amin and Davidson-Arnott, 1995, 1997; Brew, 2004). These shorelines are characterised by steep, subaerial bluffs, narrow beaches of mixed sand and gravel, and a moderate to steep, concave intertidal and nearshore profile. Rates of bluff recession typically range from 0.3–2 m a^{-1}, and in places may exceed this. The high rates of recession can lead to very high economic costs through erosion of agricultural land, destruction of roads and buildings, and through efforts to stabilise the shoreline. These shorelines are found extensively in mid- and high latitudes where they are formed in glacial till, glaciofluvial and glaciolacustrine sand, silt and clay, and Holocene mud. In Western Europe they are

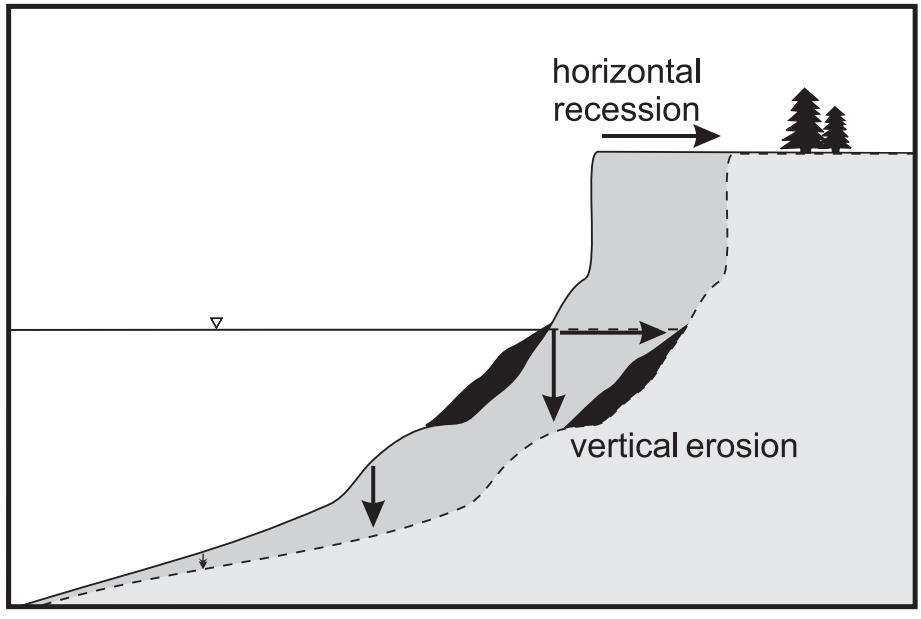

Figure 13.10 Equilibrium profile development on a cohesive coast (Davidson-Arnott and Ollerhead, 1995).

common on many stretches of the east and south coast of England (e.g., the Holderness coast of Yorkshire), parts of Ireland, and on the Baltic coasts of Denmark and Germany. They are also found on all three marine coasts of Canada (the Pacific, the Arctic and the Atlantic) and on the NE coast of the USA. They make up about 40% of the shoreline of the lower Great Lakes in Ontario (Canada) and the United States and because of the impact of coastal cliff recession on housing and infrastructure along these shorelines, they have been studied extensively here. Together with coasts characterised by cliffs developed in weakly cemented sediments, they make up the group of soft cliff coasts. The focus here is primarily on cohesive coasts, though much of it also applies to the other soft rock coasts.

The high rates of recession mean that along most of these coasts the modern nearshore profile has evolved over a period of a few thousand years and thus under a relatively stable water level and wave climate. Under these circumstances the rate of horizontal recession of the bluff is in dynamic equilibrium with the rate of vertical lowering of the nearshore profile (Davidson-Arnott and Askin, 1980; Davidson-Arnott, 1986a; Davidson-Arnott and Ollerhead, 1995 – see Figure 13.10). A simple check on the rate of lowering of the nearshore platform can be done by determining the depth of water for a location where the historical position of the cliff is known or by extrapolating the position from measured cliff retreat rates. Thus on a coast where recession rates average $1\,ma^{-1}$ the bluff toe from 1000 years ago will be located 1 km offshore. Together with the schematic model shown in Figure 13.9 this forms the conceptual basis for understanding the controls on soft coast erosion and the evolution of the coastal profile.

13.4.2 Bluff toe erosion

Recession of the bluff is initiated by wave action at the base (Figure 13.4; 13.11a, b). In low- energy environments, recession is slow and large amounts of sediment are supplied to the base by mass wasting and surface runoff. In these environments waves act primarily to remove the material offshore and alongshore, and subaerial erosion processes dominate (Wilcock *et al.*, 1998; Greenwood and Orford, 2008). These processes will also be significant where there is a wide platform and wave action on the bluff toe occurs only

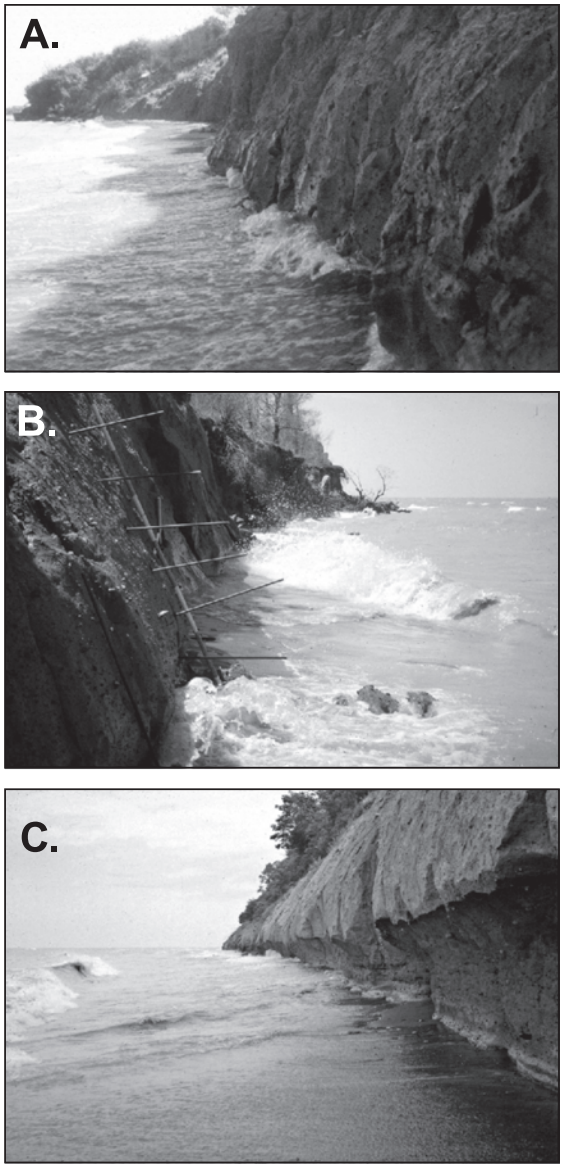

Figure 13.11 Photographs of toe erosion: (A) wave impact during a small storm with water level at the toe of the bluff (St Catharines); (B) waves breaking at the bluff toe, south shore Lake Erie (Amin and Davidson-Arnott, 1995). Note the rods sticking out of the face of the bluff. In this study they were later replaced with smaller pins; (C) notch formed in till from toe erosion (photographs (B) and (C) courtesy Shahalam Amin).

during intense storm events. Fine materials tend to be dispersed offshore into deep water, while sand and gravel remain on the beach and inner nearshore, and are transported alongshore to a sink. The slumped material may protect the toe of the bluff for a short while, but on these coasts it has little strength and is generally removed very quickly. On exposed coasts such as those on the Great Lakes and the Holderness coast of Yorkshire, recession rates are generally >0.3 m a^{-1} and direct wave attack at the toe occurs frequently – often several times a month. On the Great Lakes, this is dependent somewhat on lake level cycles that occur on a time scale of several years to one or two decades. During periods of rising and high lake level, beaches are very narrow and waves of even minor storms can reach the toe (Quigley *et al.*, 1977; Carter and Guy, 1988; Amin and Davidson-Arnott, 1995). During periods of falling lake level the cliff toe may be protected for several years by a wider beach and platform, but continued downcutting of the platform leads to renewed wave attack within a few years.

Erosion rate measurement

Wave erosion takes place by both hydraulic forces (impact, compression and cavitation, shearing) and by abrasion, as detailed in Section 13.3. On cohesive coasts developed largely in glacial till, sand and gravel are generally present in appreciable amounts and thus abrasion is likely to be the most significant process. Toe erosion associated with individual storms or periods of a few weeks, has been measured in several studies (McGreal, 1978; Carter and Guy, 1988; Amin and Davidson-Arnott, 1995; Greenwood and Orford, 2008). Carter and Guy measured the distance to the cliff face at a single height from a rope stretched alongshore and fixed to pipes hammered into the beach foreshore at five sites at the west end of Lake Erie – 4 sites in till or clay and 1 in weak shale. The other three studies were all in glacial till and used pins hammered into the bluff face at various heights above the beach (Figure 13.11b). The frequency of wave attack varied with site exposure (fetch length) and the number of erosional events depended on the magnitude of storms and storm surge. In the Great Lakes, the number of events was also closely related to long-term lake level fluctuations. Carter and Guy (1988) found that the number of events decreased from 1976 to 1980 as lake level decreased.

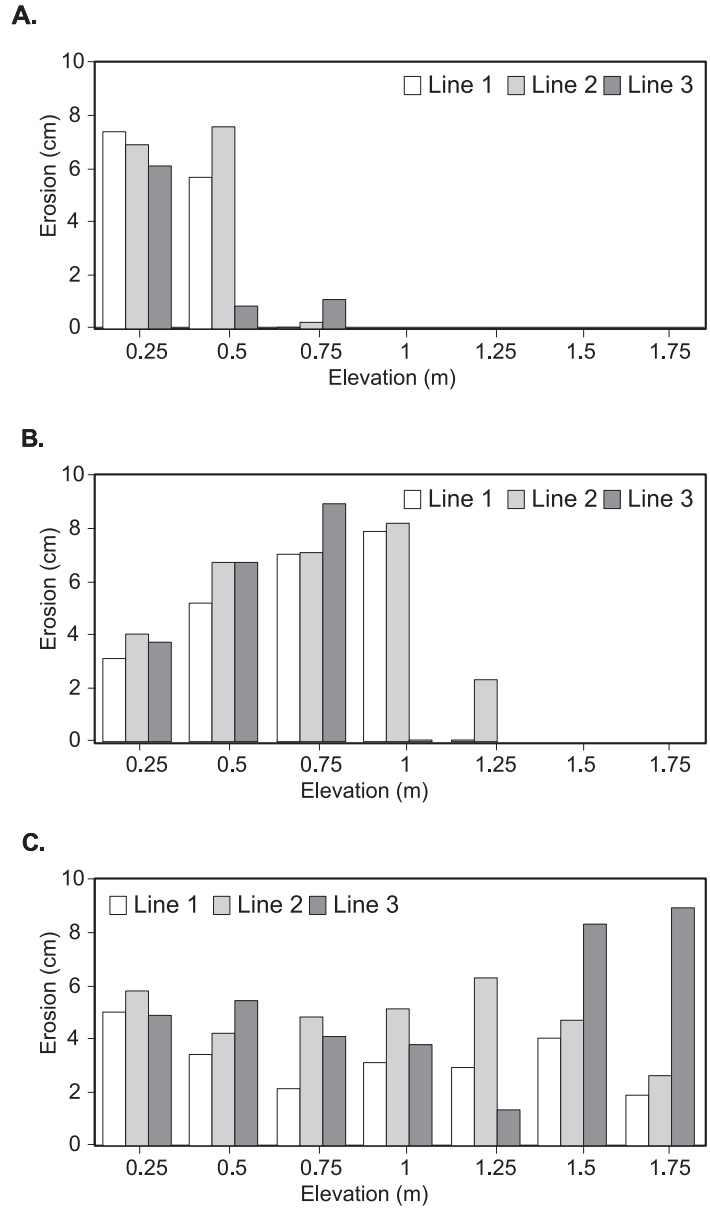

Figure 13.12 Variations in horizontal erosion during a single storm with height above the bluff/toe junction for a site (site 3) on the south shore of Lake Erie (based on data from Amin, 1991). The periods are chosen to illustrate the effects of increasing storm intensity (significant wave height and maximum water level) on the amount of erosion and height above the beach up to which erosion occurs: (A) low magnitude storm July 24–August 5, 1986; (B) moderate magnitude storm August 17–28; and (C) intense storm November 2–16. Data are for three lines of erosion pins spaced 2 m apart and show that there is considerable variation for each individual storm and for closely spaced points on the bluff face.

Amin and Davidson-Arnott measured toe erosion at four sites near Erie, Pennsylvania during 1986, at the peak of a high water phase when waves reached the bluff toe frequently. Erosion of the toe during individual storms produced recession ranging from <1 cm to as much as 10 cm (Figures 13.12a, b, c), but differences between measurement lines and between different elevations above the bed were much smaller when averaged over six months (Figure 13.13). Wave erosion reached as high as 4 m up the cliff face during intense storms (Amin and Davidson-Arnott, 1995), however measured recession was not much greater for intense storms than for moderate ones. This can be attributed to two factors: (1) the impact of larger waves is spread over a greater height and thus the actual intensity of attack is dissipated over a much larger

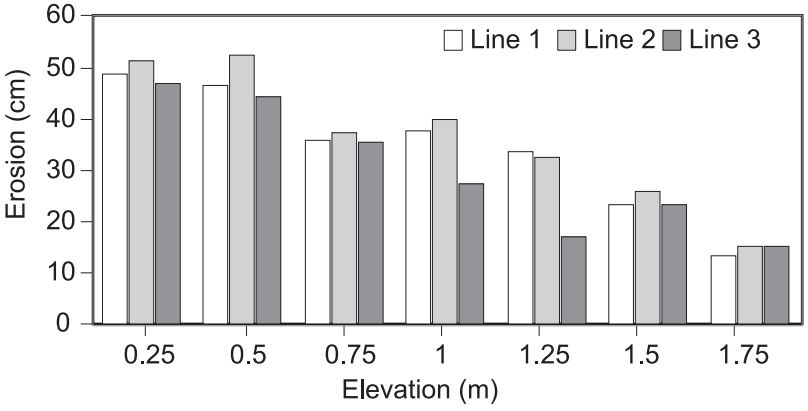

Figure 13.13 Variations in horizontal erosion of the bluff toe over the period July 15–December 9, 1986 at site 3 (based on data from Amin, 1991). Note that maximum erosion here occurs close to the toe and that the differences between the three lines are not significant when averaged over the whole period compared to individual storm events shown in Figure 13.12.

area. When water level is quite high and waves break directly against the bluff face, there is a partitioning of the erosional forces such that the upper section is subject primarily to wave impact forces while the lower section is affected most by abrasion; (2) the unweathered till has a compressive strength of about 16 MPa and is thus relatively resistant to compressive forces. During the interval between storms, a shallow layer a few cm thick weathers through wetting and drying or freezing and thawing and this is manifested in an increase in the moisture content from about 8% to more than 12%. The reduced strength of this layer means that it can be removed readily by even moderate wave action (Figure 13.11b). As this weathered layer is stripped away, the underlying unweathered till is exposed and the erosion rate is slowed considerably. Thus weathering during inter-storm periods may be as significant a control on the recession associated with an individual storm event as the absolute wave energy.

While the total erosion can be measured, conditions at the bluff toe during major storms make it difficult to determine the actual process of erosion, and the relative efficacy of impact versus abrasion. The surface of the bluff toe after a storm event tends to be relatively smooth, which could be indicative of either process. The massive nature of the clay till on the south shore of Lake Erie means that there are relatively few planes of weakness or fractures that can be exploited by cavitation or air compression and erosion produces a smooth notch or overhang (Figure 13.11c).

Prediction of erosion

These studies, as well as others such as McGreal (1978), Wilcock *et al.* (1998) and Manson (2002), suggest that the general framework of the controls on bluff toe erosion outlined in Figure 13.9 is reasonable. While we cannot test a physical model of the processes because of the dearth of such measurements at the toe during a storm, several studies have used correlation and regression to explore the contribution of factors thought to control the wave energy reaching the bluff toe with measured erosion rates (McGreal, 1978; Carter and Guy, 1988; Amin and Davidson-Arnott, 1997; Greenwood and Orford, 2008). We can expect the erosion during a single storm or over a few months would be some function of significant wave height and total wave energy over the period, and of the strength of the material at the toe. Wave energy can be derived from a direct measure of offshore waves, for example from a buoy, or it can be an indirect one based on hindcasting from winds and fetch lengths. However, energy actually reaching the toe of the bluff also depends on water levels and the width and height of the beach in front of the bluff, so some or all of these may be incorporated in the correlation analysis. In the Great Lakes during high water phases even small storms may cause significant erosion because of the associated narrow beach while during periods of falling lake level only extreme storms lead to significant erosion (Gelinas and Quigley, 1973; Carter and Guy, 1988; Amin and Davidson-Arnott, 1995).

The results of these studies all show a significant correlation between some measure of wave

energy at the bluff toe and the rate of toe erosion. However, the most significant parameter in an individual study might be some measure of wave height, storm surge or wind speed. The effect of the height and width of the beach in front of the bluff also varied. Amin and Davidson-Arnott found that it was not significant, but this was likely because beach width was always small during the high-water phase over which their measurements were made. Carter *et al.* (1986) and Lee (2008) found it to be significant. On marine coasts erosion may be greater during spring tides, and on the California coast Sallenger *et al.* (2002) showed a much higher rate of erosion associated with an El Niño period when water levels were elevated beyond seasonal norms. Sallenger *et al.* (2002) also documented a negative correlation between erosion rates and beach width and found that beach width was more effective in sheltering the bluff toe than the beach elevation. Similar results were reported from Wales (Jones and Williams, 1991). A study by Greenwood and Orford (2008) in Strangford Lough, Northern Ireland found a much weaker relationship between wave energy and recession rates, likely because of the small fetch lengths in the loch and generally lower wave energy both of which enhance the role of weathering and debris removal as compared to active wave erosion. Thus, the relative contribution of these factors to predicting toe erosion is quite variable from site to site and through time. In addition, each is likely associated with a particular threshold below which no erosion takes place.

However, it is notable that long-term measurements (5–10 decades) generally show quite uniform rates (e.g., Jibson *et al.*, 1994) and this may in part reflect the controlling influence of nearshore downcutting which is subject to much smaller variability on an annual basis.

In summary, field observations and measurements indicate that on exposed sites waves are able to erode the toe of the bluffs by both hydraulic and mechanical forces. Wave energy at the toe is moderated by the slope of the nearshore profile and by water levels, which in turn vary with the extent of storm surge, tides and seasonal and long-term water level variations. Actual erosion during a storm can exceed 10 cm in places, but is moderated by the removal of weathered sediments and exposure of more resistant unweathered till or clay. Toe erosion leads to steepening of the bluff face and can produce notches and overhanging sections that cause failure along planes parallel to the slope. Rapid weathering of till is important for reducing the strength of the bluff toe materials. This likely introduces some hysteresis in the rate of measured erosion relative to incident wave energy, so that the erosion should increase as the time interval between storms increases. It also means that differences in the strength of the unweathered till play a smaller role than might be expected from our model.

13.4.3 Subaerial bluff processes

Wave erosion at the toe of the bluff on most cohesive shorelines occurs frequently, leading to very steep cliff profiles. As a result of this, mass movement and water erosion also occurs frequently. All forms of mass wasting failures occur on cohesive bluffs (Hutchinson, 1973, 1986; Wilcock *et al.*, 1998; Hampton *et al.*, 2004, Collins and Sitar, 2008). On low bluffs and bluffs with simple stratigraphy most of the retreat results from shallow slides, slumps and mudflows, especially where there is ongoing wave erosion at the toe. Grain-by-grain removal also occurs as a result of overland flow and rill development on slopes that are largely bare of vegetation (Figure 13.14a). On high bluffs (>6 m) the path length is long enough for rills and gullies to develop, and headward erosion of gullies may complicate crest line retreat and the delivery of sediment to the bluff toe. High bluffs such as the 60 m high Scarborough Bluffs on the north shore of Lake Ontario are more likely to have complex stratigraphy with interbedded units of sand and clays. Failure here is often associated with seepage along the junctions of sand units with underlying units of lower permeability and complex failures may occur (Figure 13.14b). Occasionally deep-seated failure occurs, producing large rotational slides (Quigley *et al.*, 1977), but on most cohesive coasts bluff recession by shallow slides and running water is usually so rapid that deep-seated failures are rare.

Figure 13.14 Subaerial processes on cohesive bluffs: (A) shallow slumps and slides as well as water erosion on the bluff face, Holderness, England; (B) shallow slide and mudflow triggered by piping, Scarborough Bluffs, Lake Ontario.

13.4.4 Vertical erosion and platform evolution

As noted earlier, recession of soft cliffs, and particularly bluffs on cohesive shorelines occurs rapidly and this is accompanied by vertical lowering of the profile seaward of the base of the bluff. As a result, we can postulate the development of an equilibrium profile, with the horizontal retreat of the bluff tracking the vertical lowering of the profile (Figure 13.11). If this assumption holds, it is possible to predict the rate of vertical lowering of the nearshore from the local slope and the recession rate of the bluff toe using (Zenkovitch, 1967; Philpott, 1986; Sunamura, 1992)

$$\frac{dy}{dt} = \frac{dx}{dt} \tan \alpha \tag{13.1}$$

where: dy/dt is the rate of vertical lowering at a point y on the profile, dx/dt is the rate of horizontal recession of the cliff toe and $\tan \alpha$ is the nearshore profile slope at a point.

Ideally bluff recession and lowering of the nearshore profile exist in dynamic equilibrium and the rate of lowering anywhere on the nearshore profile can be predicted simply from shifting the profile or from the local slope (Figure 13.10). Evaluation of bluff recession and nearshore profile change along the north shore

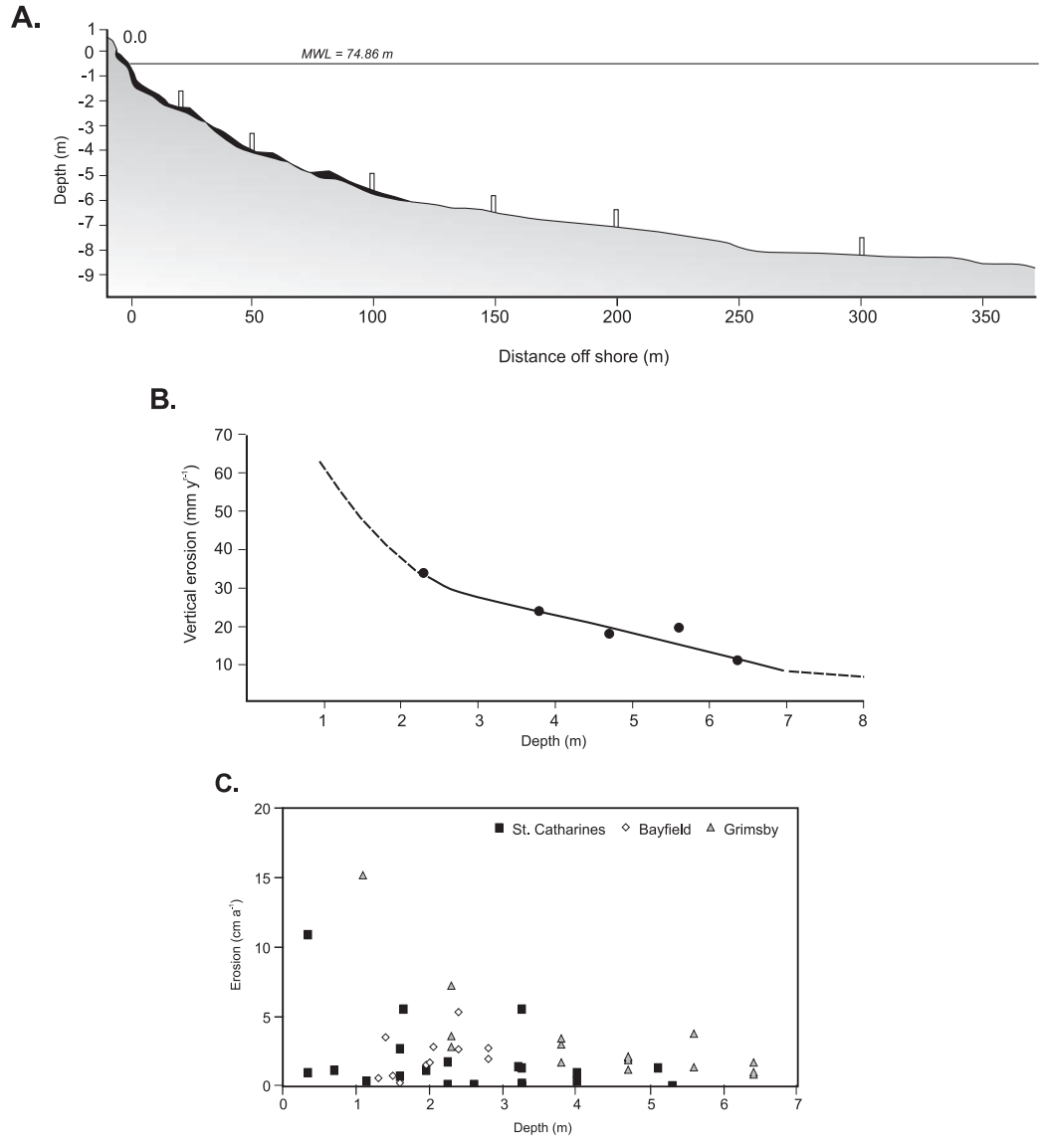

Figure 13.15 Variation of erosion rates with water depth over the nearshore on a cohesive coast: (A) beach and nearshore profile on a cohesive coast, Grimsby, Lake Ontario (from Davidson-Arnott, 1986a); (B) weighted average annual measurements at Grimsby based on MEM data from two profiles 1980–84 (from Davidson-Arnott, 1986a); (C) annual erosion for individual stations at Grimsby, St Catharines (Lake Ontario) and Bayfield (Lake Huron). Grimsby data are from Davidson-Arnott (1986a) and data from the other two sites from Davidson-Arnott *et al.*, (1999).

of Lake Erie over an 80 year period (Philpott, 1986) showed average downcutting rates ranging from about 0.5 cm a^{-1} in a water depth of 6 m to about 5–6 cm a^{-1} in a water depth of 1 m. Similar magnitudes were determined for profile erosion at a site on SW Lake Ontario based on recession over a 35 year period (Davidson-Arnott, 1986b). Healy *et al.* (1987) estimated the average long-term erosion rate for Kiel Bay over the past 5800 years to be 0.06 – 0.15 cm a^{-1} out to a depth of about 10 m. The much lower average rates here reflect much slower rates of erosion in deep water compared to shallow water and indicate that erosion in depths below about 6 m is indeed quite slow. These

studies all show that (13.1) is a good predictor of nearshore erosion and that the profiles at these locations were in dynamic equilibrium.

The shape of many cohesive profiles is concave, with steeper slopes close to shore and the gradient decreasing into deeper water (Figure 13.15a). This indicates in turn that erosion is greater close to shore and that the rate of erosion decreases exponentially offshore (Philpott, 1986; Sunamura, 1992). This is reasonable if we assume that the erosion rate is correlated with some measure of the bed shear stress under waves. This can be expected to decrease with increasing water depth for any given wave conditions. The erosion rate should also decrease with increasing water depth when evaluated over periods of several years because of the decreasing frequency of high magnitude events capable of eroding the bed in a depth of 6 m or more.

Short-term field measurements of erosion of the nearshore profile in till in Lake Ontario and Lake Huron provide some insight into the erosional mechanisms and the factors controlling their temporal and spatial pattern (Davidson-Arnott 1986a; Davidson-Arnott and Ollerhead, 1995; Davidson-Arnott *et al.*, 1999; Davidson-Arnott and Langham, 2000). The measurements were made using a modified micro-erosion meter (MEM) which measures the distance to the till surface at stations consisting of three pins set into the till (Askin and Davidson-Arnott, 1981 – see Box 13.2). Measurements made along two profiles on Lake Ontario between 1980 and 1984 in water depths ranging from about 1 m to just over 6 m showed average rates of erosion of 3–7 cm a^{-1} in water depths <2 m with rates decreasing to about 1 cm a^{-1} in depths greater than 6 m (Davidson-Arnott, 1986a – see Figure 13.15b). These weighted average annual values conceal quite high variability from year to year (Figure 13.15c). There is considerable variation in the length of time over which the data were collected (from a few months to three years) and this accounts for some of the variability. Measurements made in shallow water are under-represented because of loss of stations due to the high erosion rate, or because the steel pins were damaged or plucked from the surface by ice action over the winter. Vertical erosion rates predicted from the slope of the nearshore profile at Grimsby (Figure 13.15a) using (13.1) with a long-term cliff recession rate of 1.1 m a^{-1} are very similar to the short-term

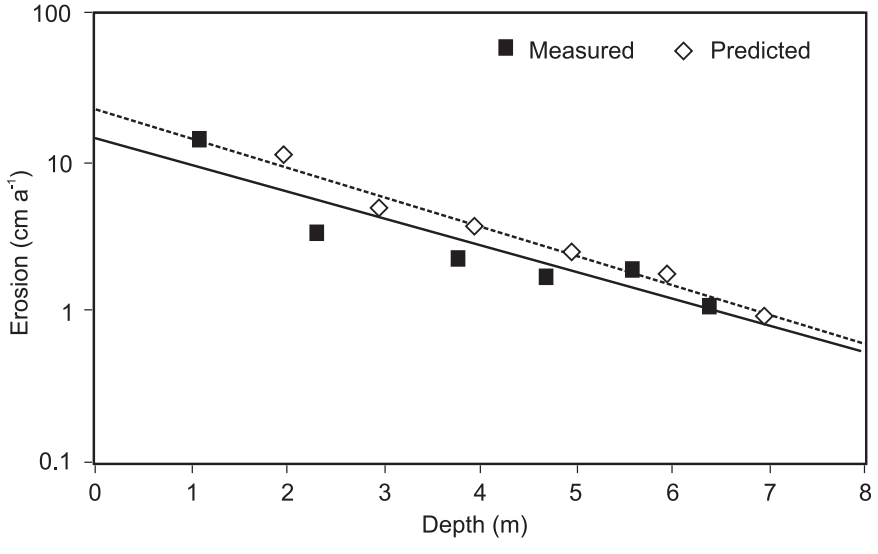

Figure 13.16 Predicted vertical erosion rate based on (13.1) and bluff recession rate of 1.1 m a^{-1} for Grimsby, Lake Ontario compared to measured erosion rates (Davidson-Arnott, 1986a).

Box 13.2 Measurement of vertical erosion

Successful modelling of the morphodynamics of erosion of the intertidal and nearshore platforms on cohesive or bedrock coasts requires measurements of profile change or rates of vertical lowering. Because the rate of erosion is measured in millimetres, standard surveying along profiles is not practical. Instead, this requires repeated high precision measurements be taken at points along the profile. This has been done almost exclusively through the use of some form of micro-erosion meter (MEM). The original design was used first for monitoring solution rates in limestone bedrock (High and Hanna, 1970) and was modified by Robinson (1976) for use on intertidal platforms. It has been used successfully for measuring erosion of intertidal rock platforms (Kirk, 1977; Robinson, 1977a, b; Stephenson and Kirk, 1996). The instrument consists of a triangular base that is constructed to fit onto three metal pins or studs that are drilled into the rock surface and the tops levelled. A high-precision engineer's dial gauge is mounted vertically on a platform that is secured to the base. In some models the base can be rotated to permit measurements in the centre of each side of the triangle, but simpler models move the whole instrument. In making measurements the MEM is brought to the measurement point, fitted over the metal studs and measurements of the distance to the surface are made in the middle of the three sides of the triangle to a precision of < 0.1 mm.

A simpler version of this was used to measure erosion underwater on cohesive profiles (Askin and Davidson-Arnott, 1981). Because erosion rates on the cohesive profile are mm to cm per year, the high precision required for measurements in rock was unnecessary. The engineers gauge was replaced by a simple metal ruler with a mm scale and the rotating assembly was dispensed with in favour of simply lifting the instrument off the pins and rotating it 120 degrees (Figure 13.17a). Metal pins were hammered into the relatively soft till and the surfaces levelled to provide a horizontal surface on which to place this modified MEM. The instrument proved robust and easy to use underwater often under low visibility and with a full wet suit (Figure 13.17b).

MEM measurements (Figure 3.15b) and provide support for the equilibrium profile concept (Figure 13.16). Note that Figure 13.16 is similar to one produced by Sunamura (1992, Figure 6.2) but he used an incorrect recession rate of 1.4 m a^{-1} that produced an offset between measured and predicted data.

Measurements of vertical erosion at intervals of 2–4 weeks were made in 1992 at 16 stations in water depths of 0.5–3 m at St Catherines on Lake Ontario (Davidson-Arnott and Ollerhead, 1995). A total of 94 measurements was obtained over six intervals (Table 13.1). Erosion was recorded at some stations in each interval and altogether erosion was measured 80% of the time. Only four records had erosion greater than 1.0 cm. These data show that even modest wave events are able to produce some measurable erosion and that erosion of the platform is nearly continuous, in contrast to the episodic events that are characteristic of bluff recession.

We can apply the same conceptual approach as for erosion of the bluff toe by envisaging a set of 'assailing forces' F_W and 'resisting forces' F_R which control erosion of the nearshore profile (Davidson-Arnott and Askin, 1980; Sunamura, 1983; Davidson-Arnott and Ollerhead, 1995). In the nearshore zone, erosion of cohesive materials has been related primarily to fluid stresses associated with wave orbital motion and nearshore currents, and to the effect of abrasion by coarse sediment rolling over the cohesive surface (Davidson-Arnott and Askin, 1980; Amos and Mosher, 1985; de Vries, 1992; Skafel and

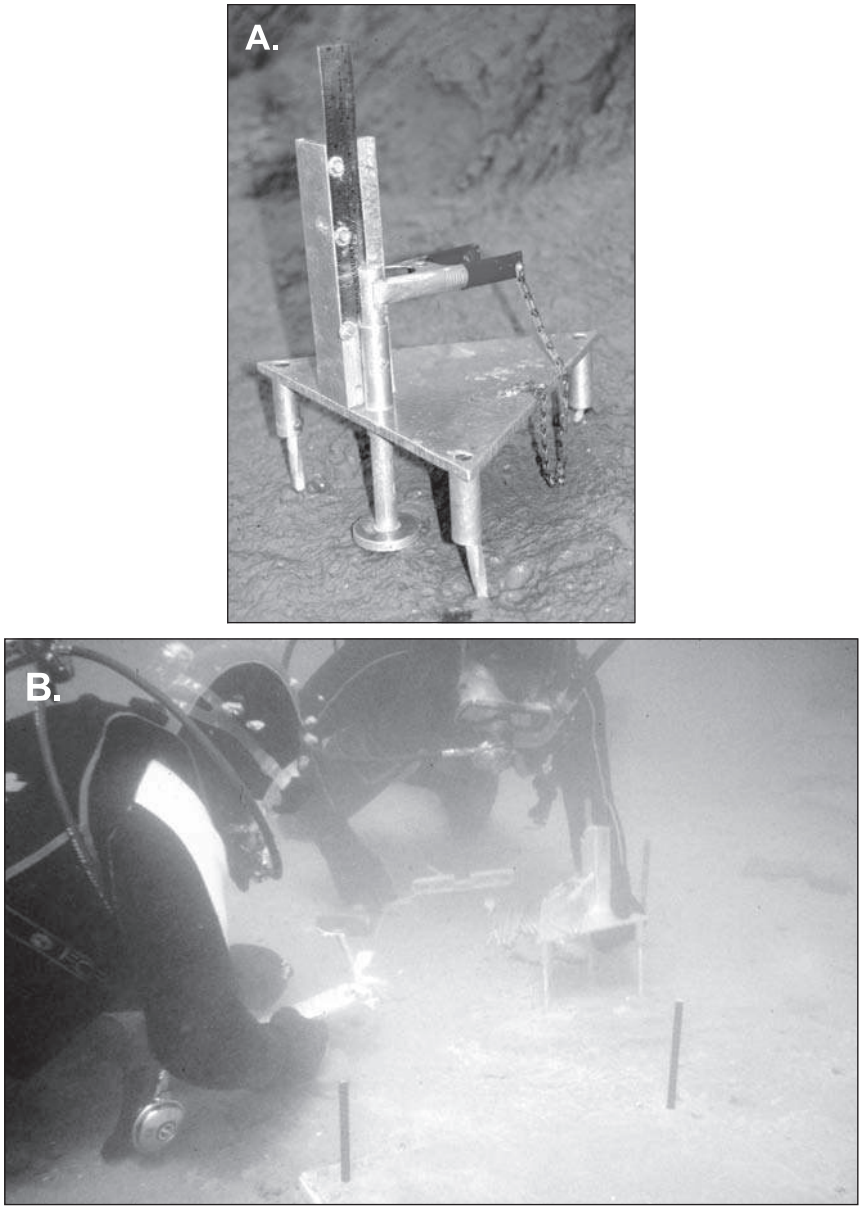

Figure 13.17 The modified Micro Erosion Meter developed for measurement erosion underwater on a cohesive coast: (A) photograph of the MEM taken on the foreshore sitting on the aluminium nails which are driven into the till at each measurement point. The rod used to measure distance to the bed slides in a vertical tube and, in contrast to the point measurement used for subaerial bedrock measurements, has a 2 cm diameter foot on it to prevent penetration in the softened upper layer of till; (B) Installation of a MEM station underwater. The three pins that mark the station have been hammered into the till surface using a template. The diver at the top of the photograph is about to use the carpenter's level floating below him to check that the MEM is level in all directions and the diver at the left is waiting to make the initial set of measurements for the station. The station was set up as part of the study by Davidson-Arnott and Langham (2000) and the frame that is partially visible at the bottom of the photograph was used to protect the surface from wave action in order to assess the role of pressure fluctuations in softening the till surface.

Bishop, 1994; Davidson-Arnott and Ollerhead, 1995). In the breaker zone, erosion may be accelerated by turbulence and the impact of plunging jets in breaking waves (Skafel and Bishop, 1994; Skafel, 1995). Erosion of fluid mud (vane shear strength <0.5 Pa) and soft cohesive sediments (vane shear strengths 4–25 kPa) can be modelled simply (Parthenaides, 1965; de Vries, 1992) by some form of the equation:

$$E = M\left(\frac{\tau_b - \tau_c}{\tau_c}\right) \tag{13.2}$$

where E is the rate of surface erosion (kg m^{-2} s^{-1}); M is the erosion rate coefficient (kg m^{-2} s^{-1}); τ_b is the bed shear stress (N m^{-2}); and τ_c is the critical shear stress (N m^{-2}).

The critical shear stress τ_c is some complex function of the shear strength, clay content, structure and other geotechnical properties (Kamphuis and Hall, 1983; Pachure and Mehta, 1985; Amos and Mosher, 1985).

The cohesive material forming the substrate of many of the cohesive coasts in mid-latitudes is frequently glacial till that has been overconsolidated and that may have a vane shear strength on the order of 40–80 kPa. Laboratory studies of the erodibility of till under both unidirectional and oscillatory flows (Kamphuis and Hall, 1983; Zeman, 1986; Kamphuis, 1990; Skafel and Bishop, 1994; Skafel, 1995) show that the critical shear stress for unweathered till is on the order of 10–20 Pa. This is much higher than the shear stress associated with wave orbital motion alone, though they do also identify the significance of weakness associated with discontinuities and micro-fissures. The laboratory experiments of Skafel and Bishop in a 100 m long wave tank did show erosion in a narrow zone associated with plunging breakers, while erosion was much reduced with spilling breakers. Observations underwater of scour around individual cobbles and boulders on the till surface (Davidson-Arnott (1986b) indicate that turbulence associated with flow around the obstacle can enhance erosion locally. There is also some evidence of the erosion of small flakes of the till matrix along micro-fissures.

However, both field and laboratory studies show that fluid processes by themselves can only account for a small portion of measured erosion in shallow water (depths <6 m). Laboratory experiments with unidirectional flow (Kamphuis and Hall, 1983; Zeman, 1986; Kamphuis, 1990) showed that erosion by fluid forces alone was generally small, but increased rapidly with the introduction of small amounts of sand. The wave tank experiments of Skafel and Bishop (1994) showed that the introduction of a thin layer of sand produced erosion of about 4 mm h^{-1} inside the surf zone and that, except for the location of plunging breakers, erosion was negligible in the absence of sand. Field studies (Davidson-Arnott and Askin, 1980; Healy and Wefer, 1980; Nairn, 1986; Davidson-Arnott, 1986a; Davidson-Arnott and Ollerhead, 1995; Davidson-Arnott and Langham, 2000) all point to abrasion as the primary mechanism of erosion of cohesive platforms wherever there is some sand and gravel available – and there almost always is some sand on cohesive shorelines developed in glacial, glaciofluvial and glaciolacustrine sediments.

The thickness of sand at points along the nearshore profile is shown in Figure 13.18 for profiles at three locations on the Great Lakes. There is clearly considerable variation along an individual profile, and between profiles. This raises the question of how does the efficacy of abrasion vary with the thickness of the surficial sediment cover? Conceptually we can expect that abrasion under given wave conditions should increase rapidly as surficial sediment thickness increases because the greater mass and larger number of contacts should speed up the process. Beyond this, erosion should decrease quickly to 0 as the sediment becomes thick enough for all movement to take place in the sand layer above the contact with the cohesive platform. Skafel and Bishop (1994) found that this occurred in the wave tank with a sand thickness greater than about 1 cm. In the field, with larger waves and the development of bedforms, a more realistic cut-off is likely to be on the order of 5–10 cm. However, this applies to conditions at a point on the profile and we also need to consider the fact that as wave conditions change, the type of bedform changes. On a larger scale, areas of accumulation, such as bars in the

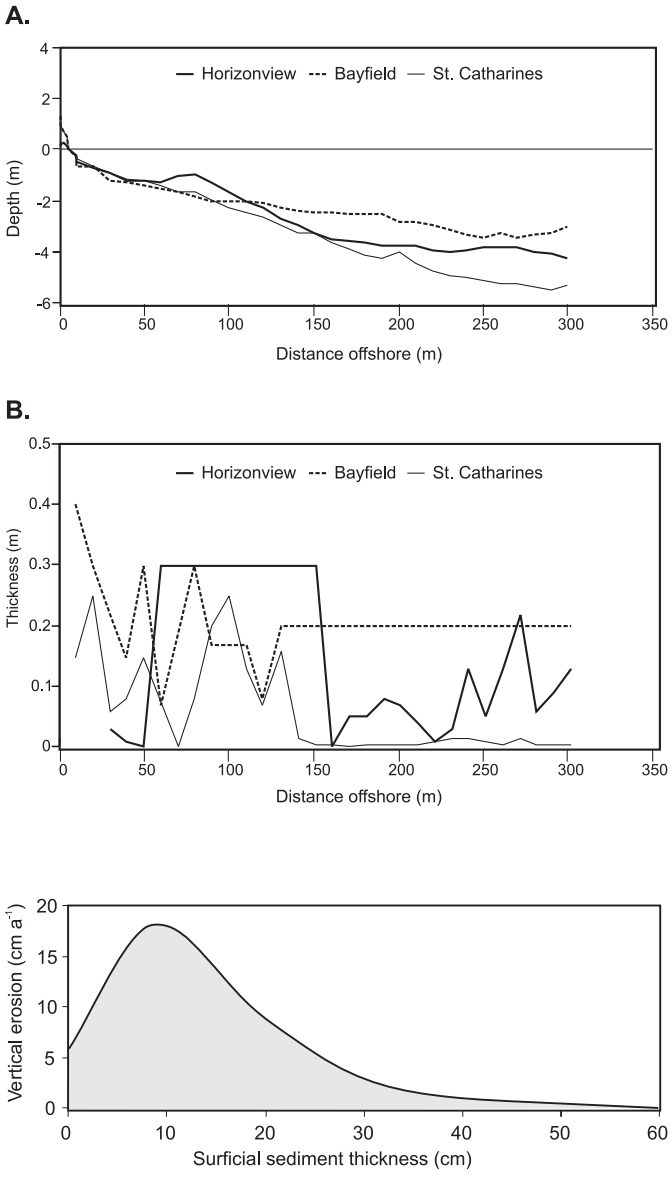

Figure 13.18 Measured thickness of surficial sediment on cohesive profiles at Horizon View and Bayfield (Lake Huron) and St Catharines: (A) profiles; (B) surficial sediment thickness. Note that the profile at Bayfield is completely armoured by cobbles and boulders beyond 130 m.

Figure 13.19 Hypothetical sketch of annual erosion rate versus sand cover thickness for the beach and nearshore area on a cohesive coast.

nearshore and berms on the beach, migrate onshore or offshore and this movement exposes new areas of cohesive substrate while other areas become protected. Some direct evidence of the effect of the mobility of sediment close to shore on abrasion is provided by Davidson-Arnott and Ollerhead (1995) and this work showed that erosion took place during periods of high wave activity even in areas where the surficial sediment cover during low waves was 30 cm or more. As sediment cover increases there are fewer locations and times when exposed areas are subject to abrasion and thus the overall rate of vertical lowering of the platform is reduced. Averaged over time and along the profile, the relationship between abrasion rate and surficial sediment thickness probably looks something like that shown in Figure 13.19. Support for

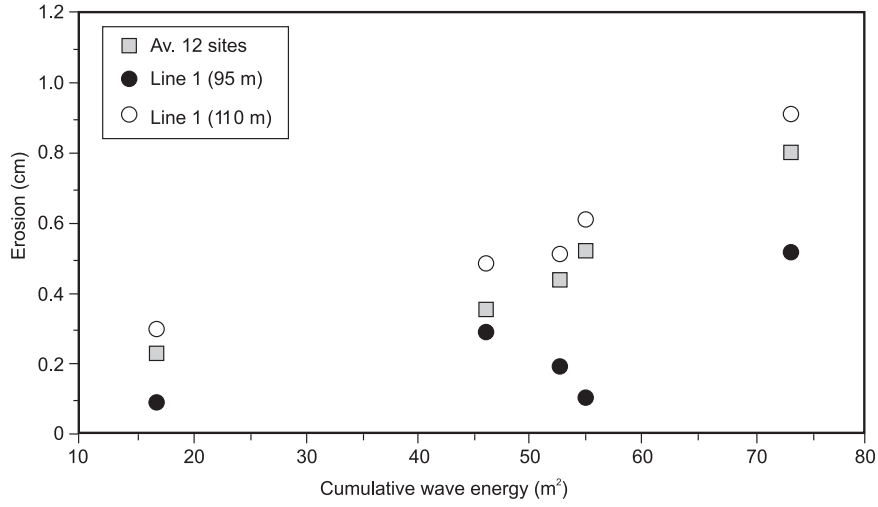

Figure 13.20 Relationship between wave energy and short-term erosion of the nearshore platform at St Catharines, Lake Ontario (Davidson-Arnott and Ollerhead, 1995).

this also comes indirectly from studies of alongshore sediment transport gradients on cohesive coasts that show a strong relationship between high recession rates and increasing rates of predicted longshore transport (Davidson-Arnott and Amin, 1985; Amin and Davidson-Arnott, 1997; Lawrence and Davidson-Arnott, 1997).

As is the case for erosion of the bluff toe, vertical erosion of the platform through both fluid stresses and abrasion should increase with increasing wave energy. This can be shown relatively easily in laboratory experiments (Zeman, 1986; Skafel and Bishop, 1994) and it has also been demonstrated for short-term field measurements (Davidson-Arnott and Ollerhead, 1995; Davidson-Arnott and Langham, 2000 – see Figure 13.20).

The conceptual model of the controls on vertical erosion of the platform, like that for toe erosion, should also include the resisting forces – the strength of the material making up the cohesive substrate. As noted earlier, where this is overconsolidated till, it is highly resistant to fluid forces alone and we would expect the rate of abrasion to decrease with increasing strength. As is the case with subaerial bluffs, weathering of the cohesive surface may reduce its strength, and thus enhance the potential for erosion by both fluid and abrasional processes. Observations showed the presence of a thin layer of softened till on the till surface in places underwater (Figure 13.21a). Detailed measurements in the field, and in the laboratory, of till from the site at St Catharines showed that softening of the upper layer does occur in response to cyclic loading and unloading by waves (Davidson-Arnott and Langham, 2000). This is manifested as an increase in the moisture content and decrease in shear strength of a layer up to a few cm thick (Figure 13.22). They also documented swelling of the till surface during periods of low wave activity. Similar measurements at sites with different clay mineral content suggest that the extent of this weathering will depend on the clay mineralogy. The degree of weathering depends on the time interval between storms and the measurements documented in Table 13.1 suggest that erosion of the weathered material occurs rapidly, but then slows down as the underlying harder, unweathered material is exposed. The extent of weathering also depends on the sheltering effect of surficial sand cover so that till remains hard under a

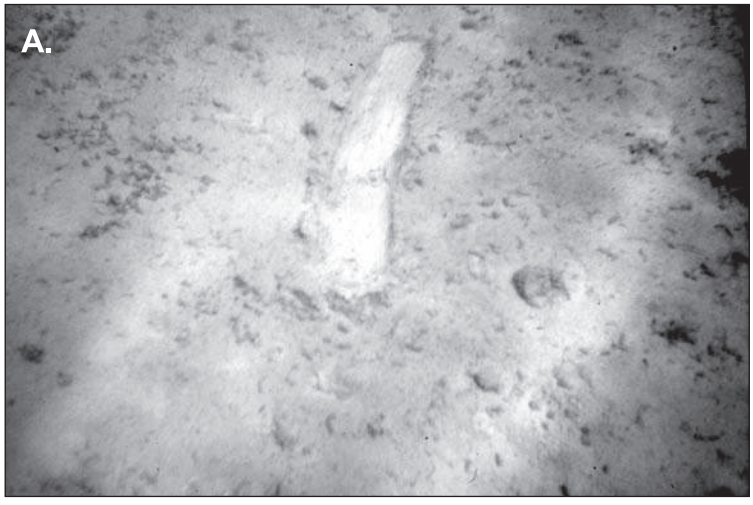

Figure 13.21 Weathering of till underwater: (A) till surface underwater showing removal of a thin layer by dragging a finger along the surface; (B) variations in shear strength of the till surface along the nearshore profile (Davidson-Arnott and Langham, 2000).

B. Surficial Sediment and Shear Strength

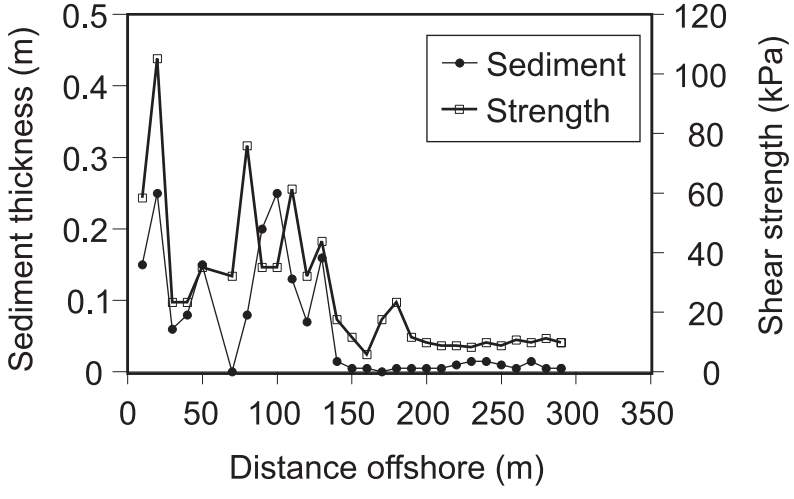

thick layer and may even undergo reconsolidation (Davidson-Arnott and Langham, 2000). The variability of shear strength of the till surface in the nearshore thus reflects the interaction of surficial sediment cover and water depth, as well as the frequency and magnitude of storms leading to erosion of the weathered material (Figure 13.21b).

The shape of the equilibrium profile generally indicates that the erosion rate is high close to shore and decreases rapidly offshore. Erosion does continue in depths greater than 6 m, though it is very slow (Healy *et al.*, 1987). It is driven by abrasion under large waves produced by the occasional intense storm, perhaps aided by continued softening of the till surface. Evolution of the profile may be affected by the accumulation of surficial sediment that can act to reduce erosion or shut it down. On stony till the accumulation of cobbles and boulders over time may act to armour the surface and drastically slow the rate of erosion (Figure 13.18b). A thick layer of sand and gravel will have the same effect. The result is that the profile is much flatter and, ultimately, there is a reduced rate of toe erosion (Davidson-Arnott *et al.*, 1999).

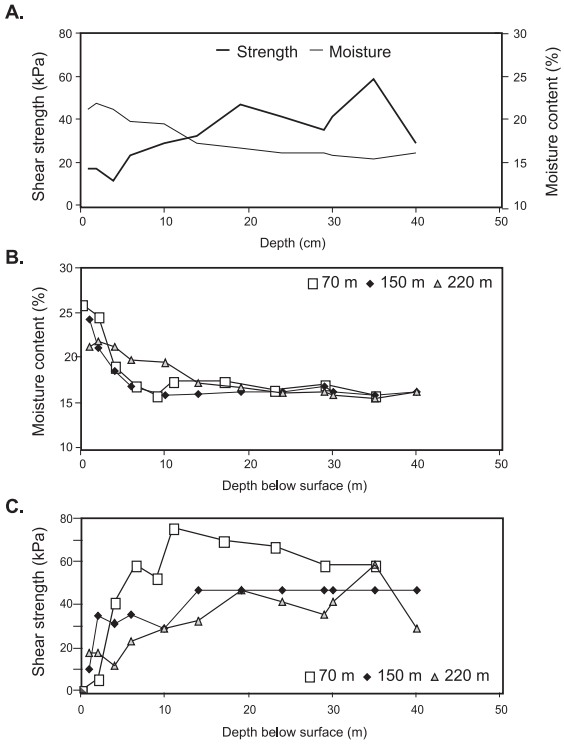

Figure 13.22 Variations in shear strength and moisture content with depth below the till surface in 5 cm diameter cores taken at St Catharines, Lake Ontario: (A) shear strength and moisture content variation in a core at 220 m offshore; (B) variations in moisture content for cores taken at 70 m, 150 m and 220 m offshore; (C) variations in shear strength for the same cores. The profile is shown in Figure 13.20b.

13.5 Rock coasts

The processes leading to toe erosion of rock cliffs are the same as those eroding cohesive shorelines and similarly their relative significance will vary with the height of the still water level relative to the cliff toe. Differences in the rate of toe erosion, the characteristics of subaerial mass wasting features and the form of the cliff and platform therefore can be attributed largely to structural and strength differences between cliffs in rock and those in cohesive materials. The 'hardness' or strength of the material forming a rock cliff is usually expressed in terms of the compressive strength and this has been found to be highly correlated with other measures of strength such as cohesive strength, shear strength and tensile strength (Sunamura, 1983 – see Box 13.1). However, the resistance of rock cliffs to erosion is influenced greatly by the presence of planes of weakness formed by bedding planes, joints and fractures as well as by the strength of bonding at the level of individual crystals or grains. Expansion of these joints by direct wave impact and by compression of air, as well as by weathering leads to direct quarrying of blocks of material that can then be disintegrated through abrasion and impact. Thus, it is necessary to produce a modified measure of rock strength that accounts for these weaknesses such as the Rock Mass Index of Budetta *et al.* (2000) or the rock mass strength of Tsujimoto (1987).

Based on this modified strength factor, we can expect to see a decrease in rock cliff recession rates, measured over periods of decades or longer, with increasing rock strength. There are few studies that have done this, but the data plotted in Figure 13.23 give an indication of how these rates may vary (Sunamura, 2004). These data show that weakly cemented sedimentary rocks such as sandstones and shales can have recession rates that are comparable to those of cohesive coasts, putting them into the category of soft coasts. Rapid cliff recession of uplifted sandstones and siltstones of Pleistocene and Tertiary age has been documented for large sections of the California coast (see reviews in Griggs and Trenhaile, 1994 and Griggs and Patsch, 2004) and this relatively rapid recession has resulted in loss of roads and buildings (Figure 13.24a). More strongly cemented sandstone and shales have a recession rate between 10^{-1} and 10^{-2} m a^{-1} and are therefore of intermediate strength. Cliffs in andesite, basalt and dolerite, which have a high compressive strength and relatively few planes of weakness, have recession rates that are too small to measure over a few decades and we can expect similar response for cliffs formed in, e.g., massive limestone and crystalline rocks of shield areas (Figure 13.24b).

Studies of soft rock cliffs show that, like cohesive bluffs, they respond rapidly to short-term

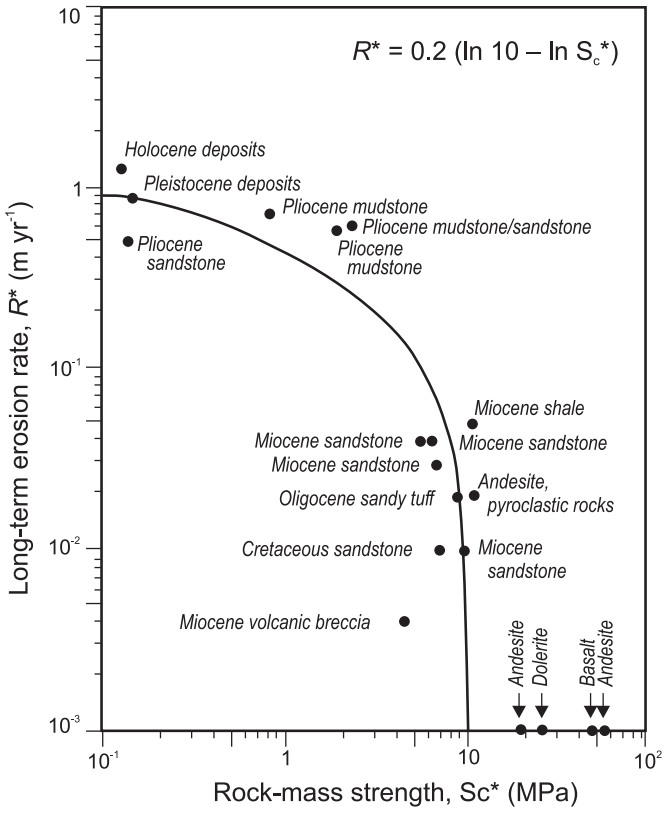

Figure 13.23 Relationship between long-term cliff recession rate and cliff-forming rock-mass strength of cliffs on open coasts of Japan. Rocks with recession rates that are too low to be measured are indicated by arrows (Sunamura, 2004, based on data from Tsujimoto, 1987).

increases in wave energy at the cliff. Such increases may result from large waves and storm surge associated with an intense storm or the effect of several storms during periods of elevated water levels, e.g., associated with El Niño events (Sallenger *et al.*, 2002). In these instances elevated water levels and erosion of the beach reduce the protection afforded by a wide, high beach. Similar reductions in beach width may result from interruption of longshore transport by groynes and harbour breakwaters; and by the extraction of sand and gravel, as has been documented for Cran Poulet on the on the northern Boulonainais coast of France (Pierre, 2006). Rapid subaerial cliff retreat may also be triggered by events on the land, particularly the effects of changing groundwater (Pierre and Lahousse, 2006).

As with cohesive bluffs, we can expect some correlation between wave energy levels and rates of bedrock cliff retreat over long time spans. There are few studies of this, but results from the early work of Sunamura (1983) and the more recent work of Mano and Suzuki (1999) provide some support for this association (Figure 13.25).

On soft rock cliffs, erosion is relatively rapid and the junction of the cliff toe with the shore platform is relatively straight producing a fairly smooth coastline (Moore and Griggs). 2002). However, it is likely that rapid toe erosion of sandstone cliffs is promoted by the availability of sandy material at the cliff/platform junction which enhances abrasion. With increasing rock strength, the character of the cliff toe and of the complexity of the coastline is increasingly influenced by the response of the rock material to different forms of erosion and by the exploitation of zones of weakness produced by varying lithology or fracture patterns. Undercutting of the cliff toe by abrasion produces a notch and visor form because the hard rock is able to maintain an overhang (Figure 13.24c) and failure eventually results from the development of

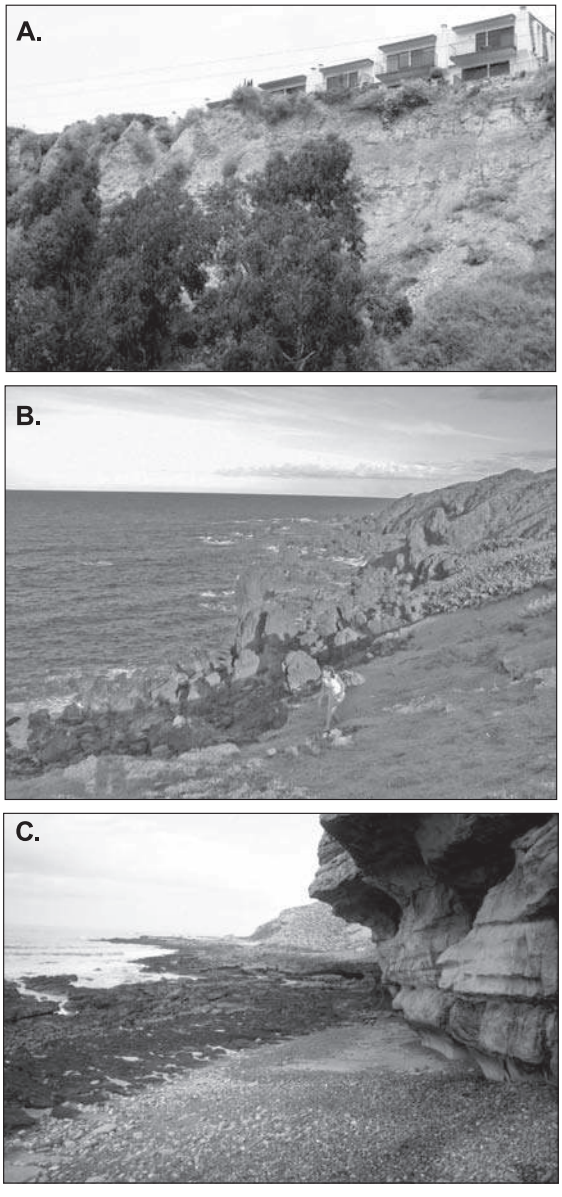

Figure 13.24 Features of erosion of bedrock coastal cliffs: (A) erosion of sandstones and siltstones on the California coast producing a sheer cliff and relatively straight coastline. Note the threat to cliff top housing produced by the cliff retreat; (B) irregular coast in resistant basalt lava flow, St Kitts; (C) notch and visor in resistant sandstone, Scotland.

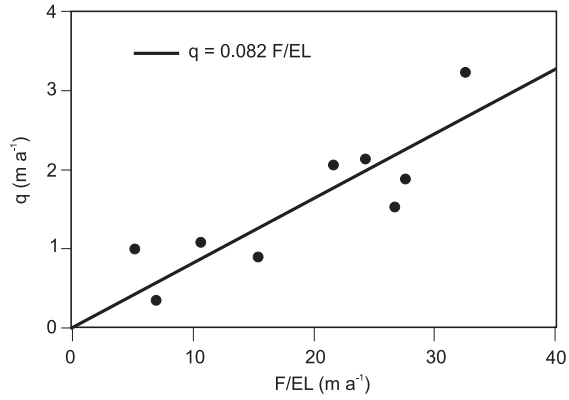

Figure 13.25 Correlation between *F*/*EL* (where *F* is the wave energy flux at the breakpoint, *E* is Young's modulus and *L* is cliff height) and the rate of cliff recession *q* for nine measurement points on the Fukashima coast, Japan (Mano and Suzuki, 1999).

tension cracks (Kogure *et al.*, 2006). Fractures and fissure may be exploited to produce indentations, caves and blow holes. The result is a rocky coast with a highly irregular shoreline and rapid variations in character, reflecting varying response of differing lithologies (Moura *et al.*, 2006). On a larger scale, joint patterns or alternating harder and softer rocks may result in the isolation of parts of the cliff producing stacks. Trenhaile *et al.* (1998) have documented the relationship of stacks at Hopewell Cape, Bay of Fundy, which are developed in arkosic sandstones and poorly sorted conglomerates of Carboniferous age, to the joint pattern in this location and produced a simple evolutionary model that probably can be extended to stacks in many other areas (Figure 13.26).

As with cohesive bluffs, toe erosion triggers mass movement failures on the cliff slope and these can take a wide range of forms. In some places massive failures occur through deep seated slides and the effect of this is to push the shoreline out for some distance. Such large-scale movements may lead to protection of the toe for years and even decades (Komar, 1998). However, most rock coasts are dominated by small failures, ranging from the detachment of individual blocks to topples, slumps and slides, which may only extend for some portion of the total bluff height and extend alongshore for metres or a few tens of metres (Andriani and Walsh, 2007). It is not easy to predict when and where this type of failure will occur, but where detailed mapping has taken place it is possible to calculate the statistical properties of mass movement hazards

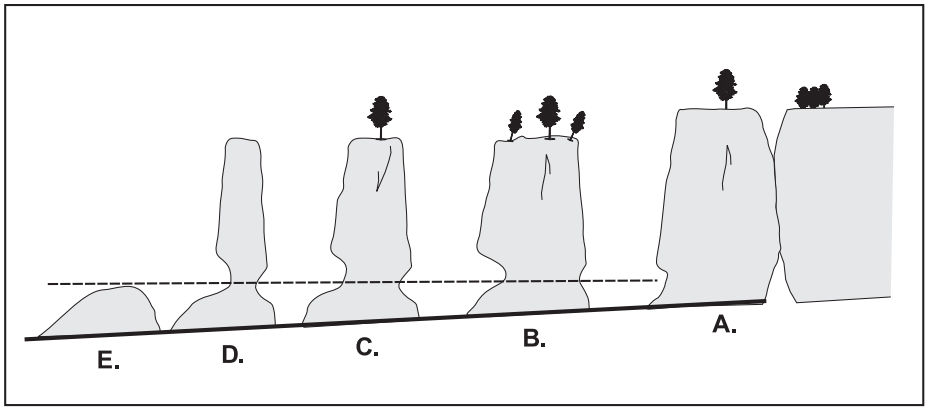

Figure 13.26 Schematic model for the evolution of stacks, Hopewell Rocks, Bay of Fundy, New Brunswick, Canada (Trenhaile *et al.*, 1999).

(Dong and Guzzetti, 2005; Teixeira, 2006). These data can then be used to predict the statistical probability of failure and thus aid in the development of management and setback schemes where it is difficult or too expensive to obtain the detailed measurements necessary for stable slope analysis. Mechanisms and controls on rock failure and cliff profile evolution over long time periods may be better explored with computer simulation models (Allison and Kimber, 1998).

On hard rock coasts, where recession rates are too small to measure adequately over a few tens of years, the presence of erosional features such as caves and shore platforms raises the question of how much of the coastal morphology is inherited from processes operating during previous interglacial periods (Trenhaile, 2002). Over the Quaternary sea levels have fluctuated over a range of 100 m or more and, while interglacial sea levels may have been similar to the modern period, the cumulative time at this level is relatively small compared to lower levels found during the much longer glacial periods. Some appreciation of the evolution of the whole coastal profile can be found in areas where uplift has raised the coast and nearshore allowing study of the erosional profile (Bradley and Griggs, 1976; Alvarez-Marrón *et al.*, 2008). In the example of uplifted terraces in western Asturias, Spain, the minimum age for the terrace is estimated to be 1–2 Ma. Thus, the nearshore slope has evolved over a large number of sea level cycles, of varying duration and magnitude, all the while subjected to slow uplift (Alvarez-Marrón *et al.*, 2008).

13.6 Shore platforms

Despite the title of Trenhaile's (1980) review (Shore platforms: a neglected coastal feature), there is a rich literature on shore platforms and no shortage of recent research. There is also no shortage of confusion over definition of the term and some controversy over the perceived importance of weathering versus marine processes in platform development (e.g., Stephenson, 2000). In this section we can make use of insights from the study of cohesive coast evolution to throw some light on the mechanisms that may be at work on hard rock coasts and which control the evolution of the profile following recession of the cliff toe.

Conceptually we can begin by defining a shore platform as the erosional surface in bedrock or other resistant material that extends from the cliff toe offshore to the limit of wave erosion. The platform is considered to be formed by recession of the coastal cliff toe and subsequently modified by wave action. However, a portion of it may lie seaward of the point at which cliff recession was initiated. The platform may have varying amounts of surficial sediments on it, but the thickness should not be great enough to

prevent exposure of the bedrock at least intermittently. In contrast to the steep face of the subaerial cliff, the platform slope is relatively gentle and parts of it may be nearly horizontal – hence the term platform. Shore platforms are usually portrayed as consisting of two types on the basis of the profile normal to the shoreline (Figures 13.2b, c) and much of the attention has been focused on Type B platforms that are marked a scarp or low cliff near the low-tide line, with a nearly horizontal component above this and a sloping component seaward of it.

While diagrams depicting platform types are usually drawn to include at least a part of the nearshore zone, the reality is that very little of the research carried out on platform processes on rock coasts has extended below the low-tide limit. This is in contrast to the work on cohesive coasts, where there has been a clear linkage established between the subaqueous and the subaerial processes, and to the rich literature on measurement of nearshore processes on sandy coasts. One result of this has been a tendency to limit the definition of the seaward boundary of the platform to the low-tide line (e.g., Palmara *et al.*, 2007) rather than viewing this as simply the portion of the platform which is intermittently exposed to subaerial processes in addition to wave action. This limited perspective is carried to the study of recent platform development in lake Waikaremoana, New Zealand (Allan *et al.*, 2002).

As we noted in Section 13.2, Type A platforms reflect conditions where vertical lowering of the platform in the intertidal area is similar to that in the inner nearshore and keeps pace with horizontal retreat of the cliff toe. The cohesive profiles described in Section 13.4 fall into this category and the conceptual model that we made use of to explore the concept of a dynamic equilibrium between horizontal retreat of the cliff toe and vertical lowering of the platform should be applicable to Type A profiles in bedrock. Where cliff retreat rates are comparatively rapid there has been sufficient time for an equilibrium to be established and we can expect platform profiles in areas such as the Bay of Fundy (e.g., Trenhaile *et al.*, 1998) and the California coast (Griggs and Patsch, 2004) to fit this model.

Since the time available for vertical lowering of the platform increases away from the cliff toe, the presence of the nearly horizontal intertidal portion of the platform associated with Type B platforms must therefore reflect very slow rates of vertical erosion in that zone compared to similar portions of Type A platforms. Measurements of vertical lowering of the intertidal areas of Type B platforms generally range between 0.5–1.5 mm a^{-1} (e.g., Table 1 in Stephenson, 2000). These are at least an order of magnitude less than those measured on cohesive coasts. The presence of the nearly horizontal platform and associated low rates of vertical erosion pose a number of research questions, including: (1) Why is the vertical erosion rate in this zone apparently much less than for similar zones on coasts with a Type A profile? Is it a function of the strength of the rock material (high F_R), reduced effectiveness of the erosive forces (low F_A) and/or low weathering rates? (2) Why is vertical erosion apparently much less effective than erosion of the cliff toe which produced cliff recession and widening of the platform? (3) How is the low tide scarp or the cliff formed? Is this a static feature or does it also recede, thus ultimately controlling the width of the horizontal component of the platform? (4) Are vertical erosion rates seaward of the low tide cliff similar to that of the intertidal, or are they higher and thus more comparable to Type A platforms?

As we noted in Sections 13.2 and 13.3, the mechanisms leading to vertical erosion have been identified as fluid forces associated with shoaling waves, breaking waves and surf bores, and mechanical forces resulting from abrasion by particles rolling across the bedrock surface. Quarrying may be important in some areas, especially where sedimentary rocks dip seaward (Trenhaile and Kanyaya, 2007). As is the case for cohesive profiles, weathering of the rock surface may reduce the surface strength so that wave action simply removes the weathered material. Stephenson and Kirk (2000a, b) have argued that wave action is relatively weak on the shore platforms of the Kaikoura Peninsula, New Zealand and that the dominant process of platform lowering is through subaerial weathering. They have also documented swelling of the bedrock surface (Stephenson and Kirk, 2001) which is similar to

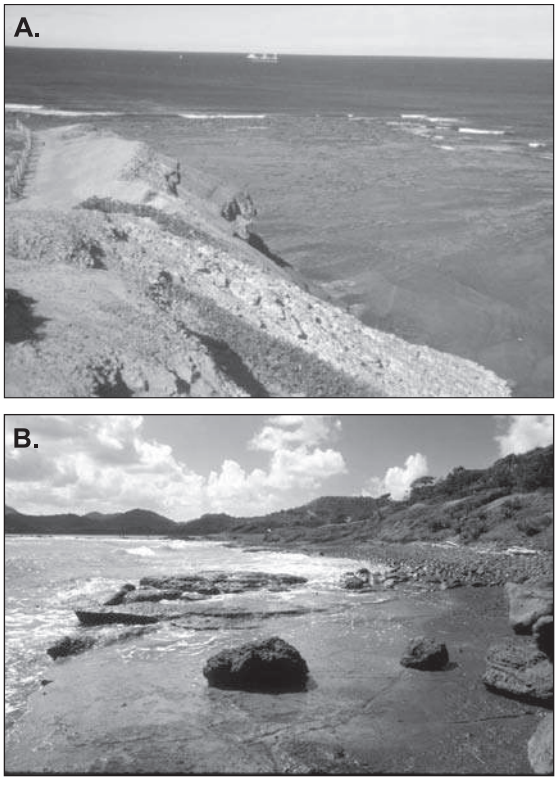

Figure 13.27 Photographs of the intertidal components of Type B shore platforms: (A) Sydney, New South Wales, Australia; (B) St Lucia, West Indies.

the swelling reported for the platform underwater by Davidson-Arnott and Langham (2000). On the other hand, in a series of papers reporting on laboratory and computer simulations Trenhaile and others have argued that weathering only plays a secondary role and that wave action is the dominant process (Trenhaile, 2006, 2008; Kanyaya and Trenhaile, 2005; Trenhaile and Kanyaya, 2007; Trenhaile and Porter,2007). It seems likely that the effectiveness of the two processes may vary with location (exposure), bedrock properties, the elevation of the intertidal platform and tidal range.

Whatever the relative effectiveness of wave action versus weathering, the problem still remains as to why the rates of erosion are so much lower in the intertidal zone than those associated with Type A platforms. Work on erosion of platforms on cohesive coasts detailed in Section 13.4 showed that abrasion was far more effective than fluid forces produced by waves alone. Thus, it is possible that the low rates of vertical erosion on Type B platforms reflect the scarcity of sand and gravel on the platform that would promote abrasion. This might arise because of limited rate of supply (e.g., very hard rocks and low recession rate, or rock types such as limestone or mudstone that do not supply much sand and gravel debris), and/or because the debris supplied is rapidly removed alongshore. Certainly, qualitative observations suggest that Type A platforms are associated with fairly abundant occurrence of sand and gravel over the bedrock surface while Type B platforms are mostly bare (Figure 13.27). The pioneering work of Robinson (1977a, 1977b) on the Northeast Yorkshire coast showed that areas where there was a substantial accumulation of sand and pebbles in front of the cliff had high rates of vertical erosion producing a ramp with a slope of 2.5°–15°. In contrast, areas where there was no surficial sediment over the shale bedrock had relatively low rates of vertical erosion producing a 'plane' with a slope of about 1°. The effectiveness of abrasion where there is a supply of material to do the work is supported by the study of Blanco-Chao *et al.* (2007) on the Galician coast of Spain as well as that of Thornton and Stephenson (2006) who noted lower platform elevations on platforms on the Otway coast, Australia, which were backed by a sandy beach.

The detailed morphology of Type B platforms, such as the form of the profile, platform width and elevation, and the nature and height of the low tide cliff, is quite variable even over quite a short distance alongshore. Some of these differences may reflect variability in processes such as wave exposure and weathering. Others may be attributable to differences in the strength of the bedrock and features such as lithology, the thickness of beds, angle of dip and the presence or absence of fractures and joints (Kennedy and Dickson, 2006).

Although the seaward cliff is a significant feature of the Type B platform there is very little information on its origin, its form, and erosional processes operating on it. Despite some speculation as to the origin of the cliff, and whether it retreats (Tsujimoto, 1987; Stephenson, 2000), none of the recent studies of these platforms seem to extend to the nearshore. Until we get

observations and measurements comparable to those carried out in the nearshore of coasts with Type A platforms, this will remain an important obstacle to modelling development and evolution of these platforms.

13.7 Management of coastal cliff shorelines

Recession of coastal cliffs results in loss of land, infrastructure such as roads and utilities, and buildings – private homes, factories and businesses – and it can pose a hazard to human life. This is particularly a problem in areas of soft cliffs where recession rates are >0.1 m a^{-1} and thus buildings constructed on the cliff top may be threatened within a few decades. High cliffs subject to deep-seated rotational slumps are also a problem, because a single event may result in cliff top recession of 10 m or more, even though the average recession rate is quite small. In general, areas of hard cliffs with recession rates <0.01 m a^{-1} pose few problems for human activities.

13.7.1 Zoning and regulation

As is the case in most other coastal areas, the preferred approach to managing the hazard posed by coastal cliff recession is to remove people and infrastructure from the hazard by the implementation of appropriate zoning regulations. Such regulations must take into account the stability of the cliff itself as well as ongoing recession of the cliff top. On the lower Great Lakes in Ontario about 40% of the shoreline consist of cohesive bluffs and recession rates exceed 0.3 m a^{-1} for much of this. As a result there was considerable incentive to develop a comprehensive approach to managing the hazard on these shorelines and to implementing setback regulations that would keep buildings and roads away from the threat for a 'lifetime' of 100 years. The components of these regulations provide a good example of the factors that need to be considered in zoning all cliff shorelines (Figure 13.28).

The first consideration is to establish the position of the toe of the bluff or cliff and to determine whether this is subject to toe erosion based on observation and mapping of the 100 year flood elevation plus an allowance for wave uprush. The second consideration is to establish a stable

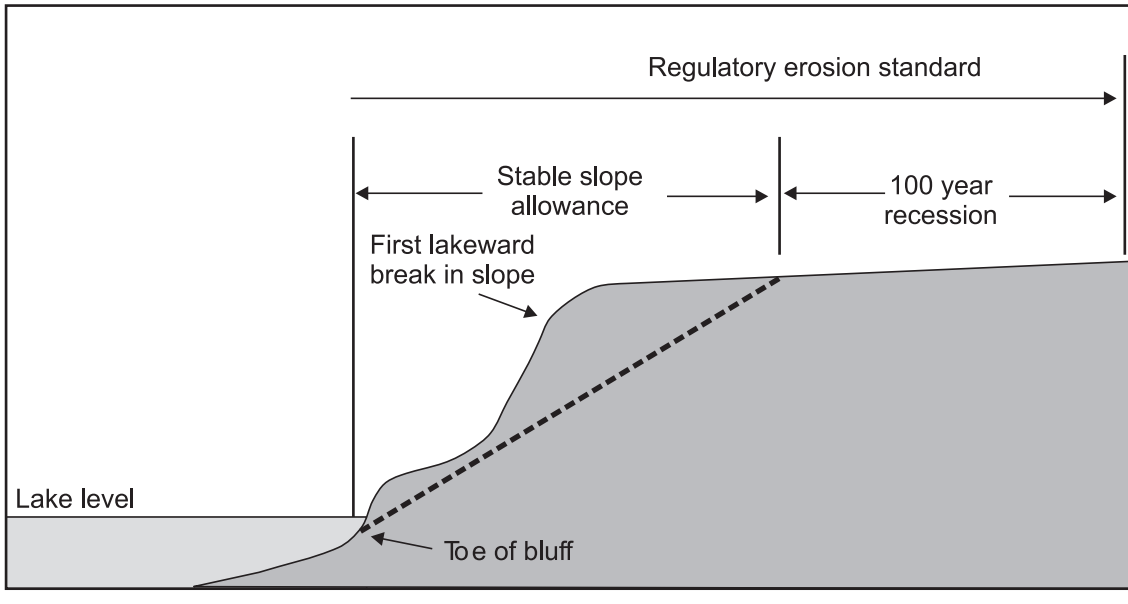

Figure 13.28 Schematic of the factors considered in setback on a cliff coast along the Ontario shoreline of the Great Lakes.

slope allowance – the portion of the top of the cliff that might be encompassed in any single mass movement event or closely-spaced series of events. This is designed to prevent loss of life as a result of a sudden event. In the absence of detailed geotechnical investigations at a specific site, the regulations specify a conservative setback based on a stable slope of 1:3 (Figure 13.28). The horizontal setback is determined as 3x the vertical distance between the first break in slope at the top of the cliff and the toe of the bluff, with the provision that the toe of the bluff may actually lie below the water line. This has been shown to exceed the measured factor of safety for almost all the cohesive shorelines on the Great Lakes, but there may be coastal cliffs in other areas where the stable slope angle is even less than this.

Under the Ontario regulations it is possible to reduce this allowance to permit building closer to the bluff edge but the developers have to undertake a detailed geotechnical study to demonstrate that, at the proposed location for development, the stable slope is <1:3. The cost of such a study has to be borne by the developer and these costs may also include funding the cost of an independent peer review of the study to ensure that the work is carried out satisfactorily and that the conclusions are warranted. The principle of putting the onus on the developer to provide evidence to support a reduction in the required setback, rather than having the authorities justify why it should not be allowed, has proved to be a significant factor in curbing the number of applications for reduction of the setback.

The second consideration is the fact that the bluff may be subject to erosion and recession and thus over time the line demarcating the stable slope limit may extend beyond the position of the building. The setback therefore has to include an allowance for cliff recession over the designated lifetime of the building. In Ontario this is set at 100 years but different jurisdictions – e.g., a number of the US Great Lakes states – may use a lifetime of 75 or even 60 years. Where the recession rate measured from historical aerial photography exceeds 0.3 m a^{-1} the additional setback is set at 100 × this average annual rate. Thus, if the long-term average annual recession rate is 1 m a^{-1}, the total setback would be 100 m + the stable slope allowance (Figure 13.26). Where the measured rate is <0.3 m a^{-1} it is difficult to determine an accurate recession rate because of limitations of the earliest aerial photographs. In this situation a conservative fixed setback of 30 m is used. It is possible to remove the allowance for cliff recession by installation of a seawall or revetment to prevent erosion of the cliff toe, but this approach is generally only permitted for key industrial or service installations where it is possible to guarantee maintenance of the structure over the 100 year lifetime.

An important element of the Ontario legislation is that the setback is not fixed but is determined on a property by property basis at the time an application is made for development or redevelopment. This avoids the need to have to redraw a fixed zone every decade or two.

13.7.2 Structural approaches

The threat to human infrastructure located close to the cliff edge (or in some cases on the cliff itself) can also be addressed through a variety of structural approaches. This has often been attempted in parts of North America and Europe though it is now recognised that it is expensive and often causes other problems along the shoreline. There are three general approaches used: (1) increase the stability of the slope itself and so reduce recession of the crest; (2) enhance the development of a protective beach in front of the cliff toe, most often through the construction of a groyne field; and (3) construct seawalls or revetments to protect the cliff toe from wave action.

Recession of the cliff crest occurs as a result of mass wasting and runoff on the cliff face and retreat of the crest may continue in the absence of toe erosion until a stable slope is established. Where slope instability has been triggered by increased runoff over the crest, by seepage from the cliff face where impervious layers outcrop, or by destruction of vegetation, it may be possible to enhance the stability and reduce recession. This can be accomplished by rerouting surface waters, installing drains in the cliff

face, building small retaining walls and planting vegetation. On cliffs where there is ongoing toe erosion this only provides protection for a matter of a few years to perhaps a decade or so. However, if toe protection has been installed then it has the effect of maintaining the stable slope at a higher angle than might otherwise be the case.

Where there is a wide protective beach in front of the cliff toe this acts to absorb wave energy and on a coast where there is a plentiful supply of sediment but high rate of longshore sediment transport it is possible to increase the width of the beach by slowing the rate of longshore transport. Traditionally this has been done through the construction of a groyne field that traps sediment and effectively widens the beach. If properly constructed, filled on completion, and properly maintained these can be effective, though there is always the threat posed to downdrift areas by the reduction in supply. Where there is limited sediment supply and ongoing erosion of the nearshore groynes are ineffective and their structural integrity is quickly compromised (Figure 13.29a). The life span of many structures put in by private landowners is only a few years (Davidson-Arnott and Keizer, 1982).

Direct protection of the cliff toe through the construction of a seawall (vertical structure) or revetment (sloping structure) can also be done. Construction of the robust structures necessary to provide long-term protection is usually too expensive for individual property owners and is usually only justifiable when the value of the land and buildings protected is very great. On soft cliff coasts vertical structures are particularly susceptible to failure through toe erosion resulting from the scour associated with wave reflection from the structure (Figure 13.29b). In the Great Lakes the most robust structure has been found to be an armourstone revetment (Figure 13.29c). The large armourstone blocks are heavy enough to provide their own stability and the sloped structure and high permeability promote efficient absorption of wave energy and minimise reflection and scour in front of the structure. The armourstone is also capable of some movement without losing structural integrity. However, the cost of a structure such as that shown in Figure 13.29c is very high.

Finally, erosion of cliffs provides sediment for beaches and dunes downdrift and thus successful cliff stabilisation may lead to a reduction in this supply. This may have the effect of accelerating cliff erosion downdrift and also poses a threat to sandy beach and dune systems that often form the downdrift sink.

13.7.3 Sea level rise and cliff recession

As is the case with other shoreline types, coastal managers are concerned over the potential impact of increasing sea level rise over the next 5–10 decades on coastal cliffs. In particular, there is concern that rising sea level will lead to an increase in toe erosion and cliff recession, with the effect of increasing management concerns over threats to properties located on the cliff top. There has, however, been much less focus on predicting and modelling this than, for example, sandy shorelines or saltmarshes. There is general recognition that rising sea level will have little impact on the recession rate on hard rock coasts where $F_R >> F_W$. Thus, at one extreme where waves break directly against a plunging cliff, increased sea level merely changes the elevation at which erosion takes place. On soft rock shores, where there is a platform in front of the cliff toe, rising sea level should lead to an increase in the frequency and magnitude of waves reaching the cliff and that should translate into an increase in the rate of cliff recession. This higher rate of recession could be sustained without any increase in the rate of downcutting of the nearshore profile because of the continued increase in water depth over the profile due to sea level rise.

One of the first attempts to model the effects of sea level rise on soft coasts was carried out by Bray and Hooke (1997). Their approach used a modification of the Bruun Rule and, while it pointed to the need for attention to be paid to the effects of sea level rise on this type of coast, the Bruun Rule is clearly inappropriate for this type of complex environment.

Nairn *et al.* (1986) developed a simple numerical model to simulate erosion of a cohesive profile and the approach was extended in the

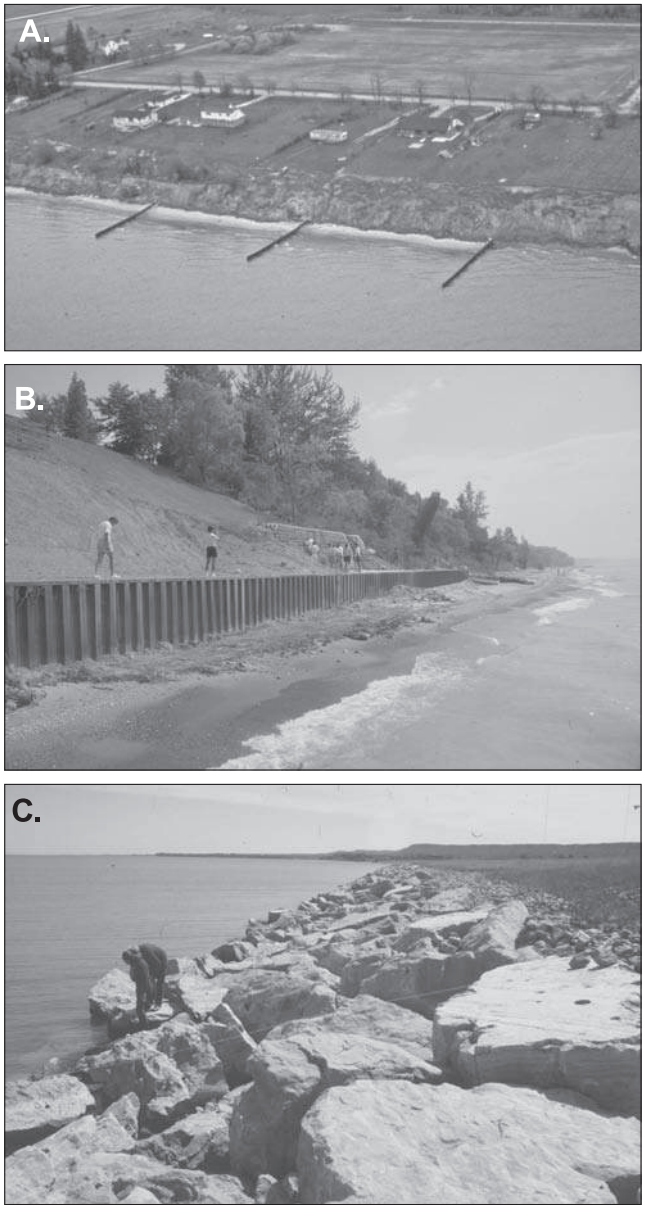

Figure 13.29 Examples of shore protection on a cohesive bluff shoreline: (A) oblique aerial photograph of the Lake Huron shoreline near Sarnia showing a small steel pile groyne field. There is limited sediment supply here and the groynes failed to capture much sediment. As a result they are largely ineffective; (B) vertical steel pile seawall being constructed along the Lake Huron coast near Goderich. Note the grading of the subaerial slope and construction of retaining walls to stabilise the slope. This form of structure is subject to rapid erosion of the toe due to wave reflection and has not proved successful; (C) armourstone revetment protecting low bluffs at Grimsby, Lake Ontario. The sloped surface and rough texture absorb wave energy and the structure can absorb some settlement and movement of the armourstone without losing structural integrity. The revetment has been in place for some 25 years and is still intact.

COSMOS 2D numerical model (Southgate and Nairn, 1993; Nairn and Southgate 1993). The latter included a module that permitted simulation of downcutting of the nearshore profile on a cohesive shoreline and this has been incorporated in various ways to assess the effects of a number of different scenarios, including water level variations, on the erosion of cohesive shorelines in the Great Lakes (e.g. Nairn *et al.*, 1999) and by extrapolation to predict the effects on bluff recession rates. It could be adapted to assessing the effects of sea level rise, though it requires considerable calibration for each site application.

Recently Walkden and Hall (2005) developed a simulation model for the erosion of soft rock shores and it has been applied to evaluating the effects of sea level rise on this coastline type (Dickson *et al.*, 2007; Walkden and Dickson, 2008). The model simulates erosion primarily as

a function of the relationship between breaking wave characteristics and rock resistance based on an equation from Kamphuis (1987):

$$E = \frac{H_b^{13/4} T^{3/2} \tan \alpha}{R} \quad (13.3)$$

where R is a function of the rock resistance and other factors that require calibration.

The inclusion of the slope angle is a bit problematic (as Walkden and Hall discuss in their paper). There does not seem to be any obvious physical rationale for erosion rate to depend on slope angle, especially for the small slope angles found in the intertidal zone. Rather, it reflects an empirical association between high recession rates and a steeper inner nearshore slope (concavity) on profiles in the Great Lakes. Walkden and Hall's model is also a bit restricted since it does not simulate erosion of the profile seaward of the breaker zone. Nevertheless, the modelling efforts provide some useful insights into the complexity of factors controlling recession of soft rock coasts and therefore the difficulty of isolating the effects of sea level rise from other controls.

Trenhaile (2009) describes a simulation model that makes use of a version of the excess stress approach (13.2) to predict erosion by waves across the nearshore and intertidal zone and also accounts for the presence of cohesionless beach material. It explicitly recognises the link between nearshore profile erosion and horizontal bluff recession and seems to offer the potential to explore a number of scenarios related to varying lithology, thickness of beach sediments and sea level rise.

Further reading

Brew, D. 2004. *Understanding and Predicting Beach Morphological Change processes Associated with the Erosion of Cohesive Foreshores Scoping Report*. Technical Report FD1915, Defra/Environment Agency, London, 73 pp.

This provides a comprehensive review of our understanding of erosional processes on cohesive shorelines.

Hampton, M. A. and Griggs, G. B. (eds.), 2004. *Formation, Evolution and Stability of coastal Cliffs-Status and Trends*. United States Geological Survey, Professional Paper 1693, 123 pp.

This contains a good review of cliff processes as well as regional reports from the US west coast and Great Lakes. It is available online as a PDF.

Sunamura, T. 1992. *Geomorphology of Rocky Coasts*. Wiley, Chichester, 302 pp.

Trenhaile, A. S., 1987. *The Geomorphology of Rock Coasts*. Oxford University Press, 384 pp.

Although getting a bit old now, these two books provide a wealth of material and somewhat contrasting approaches to the study of rock (or rocky) coasts.

References

Adams, P. N., Storlazzi, C. D. and Anderson, R. S. 2005. Nearshore wave-induced cyclical flexing of sea cliffs. *Journal of Geophysical Research*, **110**, F02002, 1–19.

Allan, J. C., Stephenson, W. J., Kirk, R. M. and Taylor, A. 2002. Lacustrine shore platforms at Lake Waikaremoana, North Island, New Zealand. *Earth Surface Processes and Landforms*, **27**, 207–220.

Allison, R. J. and Kimber, O. G. 1998. Modelling failure mechanisms to explain rock slope change along the Isle of Purbeck Coast, UK. *Earth Surface Processes and Landforms*, **23**, 731–750.

Alvarez-Marrón, J., Hetzel, R., Niedermann, S., Menéndez, R. and Marquínez, J. 2008. Origin, structure and exposure history of a wave-cut platform more than 1 Ma in age at the coast of northern Spain: A multiple cosmogenic nuclide approach. *Geomorphology*, **93**, 316–334.

Amin, S. M. N., 1991. *Bluff Toe Erosion: Magnitude, Processes and Factors Along a Section of Lake Erie South Shore*. Ph.D. Thesis, Kent State University, 235 pp.

Amin, S. M. N., and Davidson-Arnott, R. G. D. 1995. Toe erosion of glacial till bluffs, Lake Erie south shore. *Canadian Journal of Earth Sciences*, **32**, 829–837.

Amin, S. M. N., and Davidson-Arnott, R. G. D. 1997. A statistical analysis of the controls on shoreline erosion rates, Lake Ontario. *Journal of Coastal Research*, **13**, 1093–1101.

Amos, C. L., Mosher, D. C. 1985. Erosion and deposition of fine grained sediments from the Bay of Fundy. *Sedimentology*, **32**, 815–832.

Andriani, G. F. and Walsh, N. 2007. Rocky coast geomorphology and erosional processes: A case study along the Murgia coastline south of Bari, Apulia – SE Italy. *Geomorphology*, **87**, 224–238.

Askin, R. W. and Davidson-Arnott, R. G. D. 1981. Microerosion meter modified for use underwater. *Marine Geology*, **40**, M45–M48.

Aydin, A. and Basu, A. 2005. The Schmidt hammer in rock material characterization, *Engineering Geology*, **81**, 1–14.

Bernatchez, P. and Dubois, J-M. 2008. Seasonal quantification of coastal processes and cliff erosion on fine sediment shorelines in a cold temperate climate, north shore of the St. Lawrence Maritime Estuary, Québec. *Journal of Coastal Research*, **24**, 169–180.

Blanco-Chao, R., Perez-Alberti, A., Trenhaile, A. S., Costa-Casais, M. and Valcarcel-Diaz, M. 2007. Shore platform abrasion in a para-periglacial environment, Galicia, Northwestern Spain. *Geomorphology*, **83**, 136–151.

Bradley, W. C. and Griggs, G. B. 1976. Form, genesis and deformation of central California wave-cut platforms. *Geological Society of America Bulletin*, **87**, 43–449.

Bray, M. J. and Hooke, J. M. 1997. Prediction of soft-cliff retreat with accelerating sea-level rise. *Journal of Coastal Research*, **13**, 453–467.

Brew, D. 2004. *Understanding and Predicting Beach Morphological Change processes Associated with the Erosion of Cohesive Foreshores Scoping Report*. Technical Report FD1915, Defra/Environment Agency, London, 73 pp.

Bryan, R. B. and Price, A. G. 1980. Recession of the Scarborough Bluffs, Ontario, Canada. *Zeitschrift fur Geomorphologie, S.B.* **34**, 48–64.

Buckler, W. R. and Winters, H. A. 1983. Lake Michigan bluff recession. *Annals of the Association of American Geographers*, **73**, 89–110.

Budetta, P., Galieta, G. and Santo, A. 2000. A methodology for the study of the relation between coastal cliff erosion and the mechanical strength of soils and rock masses. *Engineering Geology*, **56**, 243–256.

Carter, C. H. and Guy, D. E. Jr. 1988. Coastal erosion: processes, timing and magnitudes at the bluff toe. *Marine Geology*, **84**, 1–17.

Carter, C. H., Monroe, C. B. and Guy, E. G.Jr. 1986. Lake Erie shore erosion: the effect of beach width and shore erosion structures. *Journal of Coastal Research*, **2**, 17–23

Collins, B. D. and Sitar, N. 2008. Processes of coastal bluff erosion in weakly lithified sands, Pacifica, California, USA. *Geomorphology*, **97**, 483–501.

Davidson-Arnott, R. G. D. 1986a. Rates of erosion of till in the nearshore zone. *Earth Surface Processes and Landforms*, **11**, 53–58.

Davidson-Arnott, R. G. D. 1986b. Erosion of the nearshore profile in till: rates, controls and implications for shoreline protection *Proceedings Symposium on Cohesive Shores*, National Research Council of Canada, Ottawa, Canada, pp, 137–149.

Davidson-Arnott, R. G. D. 1990. The effects of water level fluctuations on coastal erosion in the Great Lakes. *Ontario Geographer*, **10**, 12–25.

Davidson-Arnott, R. G. D.. and Askin, R. W. 1980. Factors controlling erosion of the nearshore profile in overconsolidated till, Grimsby, Lake Ontario *Proceedings Canadian Coastal Conference*, National Research Council of Canada, Ottawa, Canada, pp. 185–199.

Davidson-Arnott, R. G. D. and Keizer, H. I. 1982. Shore protection in the town of Stoney Creek, Southwest Lake Ontario, 1934–1979: Historical changes and durability of structures. *Journal of Great Lakes Research*, **8**, 635–647.

Davidson-Arnott, R. G. D. and Amin, S. M. N. 1985. An approach to the problem of coastal erosion in Quaternary sediments. *Applied Geography*, **5**, 99–116.

Davidson-Arnott, R. G. D. and Ollerhead, J. 1995. Nearshore erosion on a cohesive shoreline. *Marine Geology*, **122**, 349–365.

Davidson-Arnott, R. G. D. and Langham, D. R. J. 2000. The effects of softening on nearshore erosion on a cohesive shoreline. *Marine Geology*, **166**, 145–162.

Davidson-Arnott, R. G. D., van Proosdij, D., Ollerhead, J. and Langham, D. 1999. Rates of erosion of till in the nearshore zone on Lakes Huron and Ontario. *Proceedings Canadian Coastal Conference*, CCSEA, 627–636.

De Vries, J. W. 1992. Field measurements of the erosion of cohesive sediments. *Journal of Coastal Research*, **8**, 312–318.

Dickson, M. E., Walkden, M. J. A., and Hall, J. W. 2007. Systemic impacts of climate change on an eroding coastal region over the twenty-first century. *Climatic Change*, **84**, 141–166.

Dong, P. and Guzzetti, F. 2005. Frequency-size statistics of soft-cliff erosion. *Journal of Waterway, Port, Coastal and Ocean Engineering*, **131**, 37–42.

Edil, T. B., and Vallejo, L. E. 1980. Mechanics of coastal landslides and the influence of slope parameters. *Marine Geology*, **16**, 83–96.

Gelinas, P. J., and Quigley, R. M. 1973. The influence of geology on erosion rates along the north shore of Lake Erie. *Proceedings of the 16th Conference on Great Lakes Research*, 421–430.

Greenwood, R. O. and Orford, J. D. 2008. Temporal patterns and processes of retreat of drumlin coastal cliffs – Strangford Lough, Northern Ireland. *Geomorphology*, **94**, 153–169.

Griggs, G. B. and Trenhaile, A. S. 1994. Coastal cliffs and platforms. Chapter 11 in Carter, R. W. G. and Woodroffe, C. D. (eds.), *Coastal Evolution: Late Quaternary Shoreline Morphodynamics*. Cambridge University Press, Cambridge, 425–450.

Griggs, G. B. and Patsch, K. B. 2004. California's coastal cliffs and bluffs. In Hampton, M. A. and Griggs, G. B. (eds.), *Formation, Evolution and Stability of coastal Cliffs-Status and Trends*. United States Geological Survey, Professional Paper 1693, 53–64.

Gulyaev, S. A. and Buckeridge, J. S. 2004. Terrestrial methods for monitoring cliff erosion in an urban environment. *Journal of Coastal Research*, **20**, 871–878.

Hall, A. M., Hansom, J. D., Williams, D. M. and Jarvis, J. 2006. Distribution, geomorphology and lithofacies of cliff-top storm deposits: examples from high energy coasts of Scotland and Ireland. *Marine Geology*, **232**, 131–155.

Hampton, M. A. and Griggs, G. B. (eds.), 2004. *Formation, Evolution and Stability of coastal Cliffs-Status and Trends*. United States Geological Survey, Professional Paper 1693, 123 pp.

Healy, T. R. and Wefer, G. 1980. The efficacy of submarine erosion versus cliff retreat as a supplier of marine sediment in the Kieler Bucht, Western Baltic. *Meyniana*, **32**, 89–96.

Healy, T. R., Sneyd, A. D. and Werner, F. 1987. First approximation sea-level dependent mathematical model for volume eroded and submarine profile development in a semi-enclosed sea: Kiel Bay, Western Baltic. *Mathematical Geology*, **19**, 41–50

Hequette, A. and Barnes, P. W. 1990. Coastal retreat and shoreface profile variations in the Canadian Beaufort Sea. *Marine Geology*, **91**, 113–132.

High, C. J. and Hanna, F. K. 1970. A method for direct measurement of erosion on rock surfaces. *British Geomorphology Research Group*, Technical Bulletin 5, 1–25.

Hutchinson, J. N. 1973. The response of London Clay cliffs to differing rates of toe erosion. *Geologia Applicata e Idrogeologia*, **8**, 221–239.

Hutchinson, J. N. 1986. Cliffs and shores in cohesive materials: geotechnical and engineering aspects. *Proceedings Symposium on Cohesive Shores*, National Research Council of Canada, Ottawa, Canada, 1–44.

Jibson, R. W., Odum, J. K. and Staude, J-M. 1994. Rates and processes of bluff recession along the Lake Michigan Shoreline in Illinois. *Journal of Great Lakes Research*, **20**, 135–152.

Jones, D. G. and Williams, A. T. 1991. Statistical analysis of factors influencing cliff erosion along a section of the west Wales coast, UK. *Earth Surface Processes and Landforms*, **16**, 95–111.

Kamphuis, J. W. 1987. Recession rate of glacial till bluffs. *Journal of Waterway, Port, Coastal and Ocean Engineering*, **113**, 60–73.

Kamphuis, J. W. 1990. Influence of sand or gravel on the erosion of cohesive sediment. *Journal of Hydraulic Research*, **28**, 43–53.

Kamphuis J. W. and Hall, K. R. 1983. Cohesive material erosion by unidirectional current. *Journal Hydraulics Division*, ASCE, **109**, 49–61.

Kanyaya, J. I. and Trenhaile, A. S. 2005. Tidal wetting and drying on shore platforms: An experimental assessment. *Geomorphology*, **70**, 129–146.

Kennedy, D. M. and Dickson, M. E. 2006. Lithological control on the elevation of shore platforms in a microtidal setting. *Earth Surface Processes and Landforms*, **31**, 1575–1584.

Kirk, R. M. 1977.Rates and forms of erosion on intertidal platforms at Kaikoura Peninsula, South Island, New Zealand. *New Zealand Journal of Geology and Geophysics*, **20**, 571–613.

Kogure, T., Aoki, H., Maekado, A., Hirose, T. and Matsukura, Y. 2006. Effect of notches and tension cracks on instability of limestone coastal cliffs in the Ryukyus, Japan. *Geomorphology*, **80**, 236–244.

Komar, P. D. 1998. Wave erosion of a massive artificial coastal landslide. *Earth Surface Processes and Landforms*, **23**, 415–428

Lantuit, H. and Pollard, W. H. 2008. Fifty years of coastal erosion and retrogressive thaw slump activity on Herschel Island, southern Beaufort Sea, Yukon Territory, Canada. *Geomorphology*, **95**, 84–102.

Lawrence, P. L. and Davidson-Arnott, R. G. D. 1997. Alongshore wave energy and sediment transport on southeastern Lake Huron. *Journal of Coastal Research*, **13**, 1004–1015.

Lee, E. M. 2008. Coastal cliff behaviour: Observations on the relationship between beach levels and recession rates. *Geomorphology*, **101**, 558–571.

Mano, A. and Suzuki, S. 1999. Erosion characteristics of sea cliff on the Fukushima coast. *Coastal Engineering Journal*, **41**, 43–63.

Manson, G. K. 2002. Semi-annual erosion and retreat of cohesive till bluffs, McNab's Island, Nova Scotia. *Journal of Coastal Research*, **18**, 421–432.

McGreal, W. S. 1979. Marine erosion of glacial sediments from a low-energy cliffline environment near Kilkeel, Northern Ireland. *Marine Geology*, **32**, 89–103.

Moore, L. J. and Griggs, G. B. 2002. Long-term cliff retreat and erosion hotspots along the central

shores of the Monterey Bay National Marine Sanctuary. *Marine Geology*, **181**, 265–283.

Moura, D., Albardeiro, L., Veiga-Pires, C., Boski, T. and Tigano, E. 2006. Morphological features and processes in the central Algarve rocky coast (South Portugal). *Geomorphology*, **81**, 345–360.

Nairn, R. B. 1986. Physical modelling of erosion on cohesive profiles. *Proceedings Symposium on Cohesive Shores*. National Research Council of Canada, Ottawa, Canada, 210–225.

Nairn, R. B. and Southgate, H. N. 1993. Deterministic profile modelling of nearshore processes. Part 2. Sediment transport and beach profile development. *Coastal Engineering*, **19**, 57–96.

Nairn, R. B., Davis, J. E. and Thieme, S. J. 1999. A GIS-linked flood and erosion prediction system for Lake Michigan. Proceedings Coastal Sediments '99, ASCE, pp. 1978–1993.

Pachure, T. M., and Mehta, A. J. 1985. Erosion of soft cohesive sediment deposits. *Journal of Hydraulic Engineering*, **110**, 1308–1326.

Parthenaides, E. 1965. Erosion and deposition of cohesive soils. *Journal of the Hydraulics Division*, ASCE, **91**, 105–139.

Philpott, K. L. 1986. Coastal engineering aspects of the Port Burwell shore erosion damage litigation. *Proceedings Symposium on Cohesive Shores*, National Research Council of Canada, Ottawa, Canada, 309–338.

Pierre, G. 2006. Processes and rate of retreat of the clay and sandstone sea cliffs of the northern Boulonnais (France), *Geomorphology*, **73**, 64–77.

Pierre, G. and Lahousse, P. 2006. The role of groundwater in cliff instability: An example at Cape Blanc-Nez; Pas-de-Calais, France. *Earth Surface Processes and Landforms*, **31**, 31–45.

Prior, D. B. 1977. Coastal mudslide morphology and process, Eocene Clay, Denmark. *Geografisk Tidschrift*, **76**, 19–33.

Quigley, R. M., Gelinas, P. J., Bou, W. T. and Packer, R. W. 1977. Cyclic erosion-instability relationships: Lake Erie north shore bluffs. *Canadian Geotechnical Journal*, **14**, 301–323.

Robinson, L. A. 1976. The micro-erosion meter technique in a littoral environment. *Marine Geology*, **22**, M51–M58.

Robinson, L. A. 1977a. Marine erosive processes at the cliff foot. *Marine Geology*, **23**, 257–271.

Robinson, L. A. 1977b. Erosive processes on the shore platform of northeast Yorkshire, England. *Marine Geology*, **23**, 339–361.

Sallenger, A. H. Jr., Krabill, W., Brock, J., Swift, R., Manizade, S. and Stockdon, H. 2002. Sea-cliff erosion as a function of beach changes and extreme wave runup during the 199–1998 El Niño. *Marine Geology*, **187**, 279–297.

Skafel, M. G. 1995. Laboratory measurements of nearshore velocities and erosion of cohesive sediment (till) shorelines. *Coastal Engineering*, **24**, 343–349.

Skafel, M. G., Bishop, C. T. 1994. Flume experiments on the erosion of till shores by waves. *Coastal Engineering*, **23**, 329–348.

Southgate, H. N. and Nairn, R. B. 1993. Deterministic profile modelling of nearshore processes. Part 1. Waves and currents. *Coastal Engineering*, **19**, 27–56.

Stephenson, W. J. 2000. Shore Platforms: a neglected coastal feature? *Progress in Physical Geography*, **24**, 311–327.

Stephenson, W. J. and Kirk, R. M. 1996. Measuring erosion rates using the micro-erosion meter: 20 years of data from shore platforms, Kaikoura Peninsula, South Island New Zealand. *Marine Geology*, **131**, 209–218.

Stephenson, W. J. and Kirk, R. M. 2000a. Development of shore platforms on Kaikoura Peninsula, South Island, New Zealand: part 1, the role of waves. *Geomorphology*, **32**, 21–41.

Stephenson, W. J. and Kirk, R. M. 2000b. Development of shore platforms on Kaikoura Peninsula, South Island, New Zealand: part 2, the role of subaerial weathering. *Geomorphology*, **32**, 43–56.

Stephenson, W. J. and Kirk, R. M. 2001. Surface swelling of coastal bedrock on intertidal shore platforms, Kaikoura Peninsula, South Island, New Zealand. *Geomorphology*, **41**, 5–21.

Sunamura, T. 1983. Processes of sea cliff and platform erosion. In Komar, P. D. (ed.), *Handbook of Coastal Processes and Erosion*. CRC Press, Boca Raton, FL, 233–265.

Sunamura, T. 1992. *Geomorphology of Rocky Coasts*. Wiley, Chichester, 302 pp.

Sunamura, T. 2004. Cliffs, lithology versus erosion rates. In Schwartz, M. (ed.), *Encyclopedia of Coastal Sciences*. Kluwer, Dordrecht, pp. 241–243.

Texeira, S. B., 2006. Slope mass movements on rocky sea cliffs: A power-law distributed natural hazard on the Barlavento Coast, Algarve, Portugal. *Continental Shelf Research*, **26**, 1077–1091

Thornton, L. E. and Stephenson, W. J. 2006. Rock strength: a control of shore platform elevation. *Journal of Coastal Research*, **22**, 224–231.

Trenhaile, A. S., 1980. Shore platforms: a neglected coastal feature. *Progress in Physical Geography*, **4**, 1–23.

Trenhaile, A. S. 2002. Rock coasts, with particular emphasis on shore platforms, *Geomorphology*, **48**, 7–22.

Trenhaile, A. S. 2006. Tidal wetting and drying on shore platforms: An experimental study of surface expansion and contraction, *Geomorphology*, **76**, 316–331.

Trenhaile, A. S. 2008. Modeling the role of weathering in shore platform development. *Geomorphology*, **94**, 24–39.

Trenhaile, A. S. 2009. Modeling the erosion of cohesive clay coasts. *Coastal Engineering*, **56**, 59–72.

Trenhaile, A. S. and Porter, N. J. 2007. Can shore platforms be produced solely by weathering processes? *Marine Geology*, **241**, 79–92.

Trenhaile, A. S. and Kanyaya, J. I. 2007. The role of wave erosion on sloping and horizontal shore platforms in macro- and meso-tidal environments. *Journal of Coastal Research*, **23**, 298–309.

Trenhaile, A. S., Pepper, D. A., Trenhaile, R. W. and Dalimonte, M. 1998. Stacks and notches at Hopewell Rocks, New Brunswick, Canada. *Earth Surface Processes and Landforms*, **23**, 975–986.

Tsujimoto, H. 1987. Dynamic Conditions for Shore Platform Initiation. *Science Report*, Institute of Geoscience, University of Tskuba, Section A, **8**, 45–93.

Walkden, M. J. A. and Hall, J. W. 2005. A predictive mesoscale model of the erosion and profile development of soft rock shores. *Coastal Engineering*, **52**, 535–563.

Walkden, M. and Dickson, M. 2008. Equilibrium erosion of soft rock shores with a shallow or absent beach under increased sea level rise. *Marine Geology*, **251**, 75–84.

Wilcock, P. R., Miller, D. S., Shea, R. H. and Kerkin, R. T. 1998. Frequency of effective wave activity and the recession of coastal bluffs: Calvert Cliffs, Maryland. *Journal of Coastal Research*, **14**, 256–258

Young, A. P. and Ashford, S. A. 2006. Application of airborne LiDAR for seacliff volumetric change and beach-sediment budget contributions. *Journal of Coastal Research*, **22**, 307–316.

Zeman, A. J. 1986. Erodibility of Lake Erie tills. *Proceedings Symposium on Cohesive Shores*, National Research Council of Canada, Ottawa, Canada, 150–169.

Zenkovitch, V. P., 1967. *Processes of Coastal Development*, Oliver and Boyd, Edinburgh, 738 pp.

Index